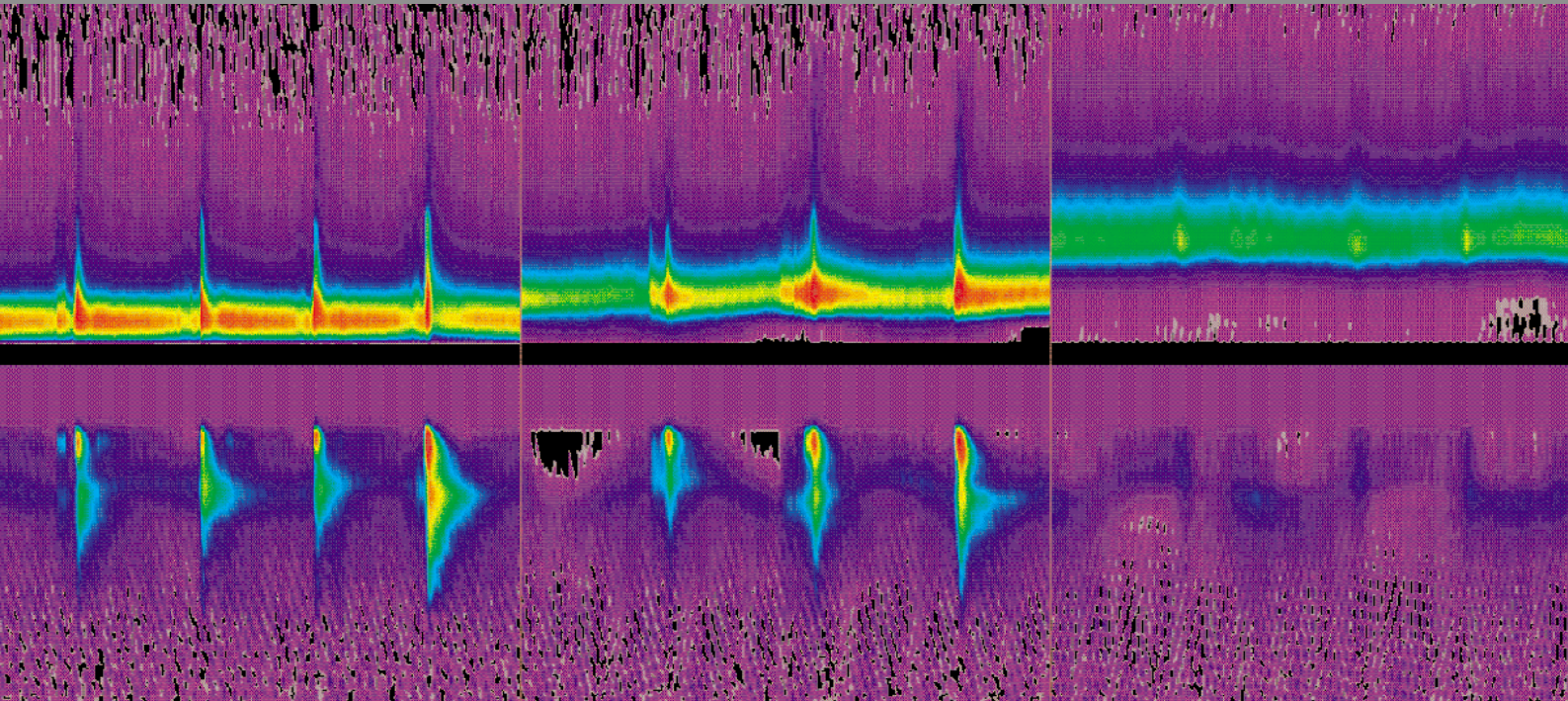




Max-Planck-Institut
für Plasmaphysik

Annual Report 2001



Foreword

Scientists at the Max-Planck-Institut für Plasmaphysik (IPP) investigate the basic physics underlying a future fusion power plant. This includes research on the two most advanced types of fusion device, the tokamak and the stellarator, as well as activities in plasma-surface interactions and materials. The work on the ASDEX Upgrade tokamak is directed towards the next step in fusion research, the International Tokamak Experimental Reactor (ITER). The geometry of ASDEX Upgrade is very similar to that of ITER and the experiment is thus particularly suitable for developing operating scenarios, testing control strategies and extrapolating these to ITER parameters. The WENDELSTEIN 7-AS stellarator in Garching has confirmed the basic optimisation principles of an “Advanced Stellarator”. Its successor, WENDELSTEIN 7-X, now being constructed at the Greifswald Branch of IPP, is aimed at demonstrating that the stellarator is a viable option for a demonstration reactor in the step following ITER. The Max-Planck-Institut für Plasmaphysik, as a EURATOM Association, is an important participant in the international effort to develop a fusion power plant. On the national level, the Institute is as an Associate Member of the Helmholtz-Gemeinschaft and coordinates its research activities with those of Forschungszentrum Karlsruhe and Forschungszentrum Jülich within the “Entwicklungsgemeinschaft Kernfusion”. It also collaborates with a number of German universities.

The ASDEX Upgrade tokamak programme is strongly motivated by possible ITER operating scenarios; in particular, the investigation of reactor-relevant plasma edge and bulk physics with a reactor-compatible divertor configuration plays a major role. After modification of the divertor structure of the machine, the experimental campaign was re-started in the spring of 2001. In close collaboration with theory, heat and particle transport in the basic ITER operating scenario, i.e. in the high-confinement, H-mode with edge-localised modes, was shown to be governed by “profile stiffness”. Power and particle exhaust in the ELMy H-mode could be achieved in a benign way by establishing small “type II” ELMs. Stability was improved by using the new capability to shape the poloidal plasma cross-section. Combination of these factors has led to a new operating scenario with tolerable ELMs, good confinement and superior stability properties.

Although numerous European institutions are already working on ASDEX Upgrade, IPP has recently increased its efforts to open up the experiment to more European fusion scientists. A new organisational structure has been established to facilitate participation of the EURATOM Associations. An international ASDEX Upgrade Programme Committee with equal representation of IPP and other Associations has been set up to determine the ASDEX Upgrade experimental programme in consensus with the European fusion community. In line with this development, facilities for remote participation are also being improved and expanded.

The joint European tokamak experiment JET is now being run under the terms of the European Fusion Development Agreement. IPP physicists have submitted over 40 proposals, several in collaboration with other EFDA Associates (the EURATOM Associations) and have made major contributions to the execution and analysis of specific experiments. The majority of these results are now being prepared for publication as full journal articles.

ITER is the next step in fusion energy research. Recent positive developments have been the first official offer of a site by Canada, the site proposals from France and Spain, the opening of international negotiations on a possible legal entity and the implementation of the international tokamak physics activity (ITPA). IPP continues its support for ITER physics research and development, in particular through contributions to the International Confinement Data Base, the International H-mode Threshold Global Data Base, the interval estimate for the global energy confinement time and design studies. Moreover, IPP plays an important role in research and development for ITER components, such as diagnostics and heating systems.

IPP has a strong tradition in stellarator physics: the WENDELSTEIN 7-A stellarator was first to demonstrate the stellarator principle with a hot plasma. Its successor, WENDELSTEIN 7-AS, will be shut down in summer 2002 after fourteen years of fruitful operation, after which IPP will concentrate on realisation of the WENDELSTEIN 7-X follow-up experiment. In 2001, a new regime of improved confinement at very high density, the “high-density H-mode”, was discovered on WENDELSTEIN 7-AS after installation

Foreword

of a so-called island divertor. The regime is characterised by significant reduction in the confinement of impurities and by a transition to good energy confinement. It is robust with respect to variations of the magnetic field geometry and heating power and allows long quasi-stationary discharges at high density and heating power, which was hitherto not possible. Improved control of plasma-wall interactions in WENDELSTEIN 7-AS has also allowed considerable improvement in high-beta discharges using a magnetic field configuration with high rotational transform and with the smoothest possible flux surfaces at the plasma boundary. Higher neutral beam heating power was accompanied by an increase in the maximum volume-averaged beta values. The higher beta values seem to be limited by the heating power, because there are no detectable instabilities. In contrast to previous high-beta discharges, which were terminated by a rapid increase of impurity radiation, quasi-stationary discharges are now possible in the presence of divertor modules although no divertor magnetic field configuration is used.

WENDELSTEIN 7-X is intended to demonstrate the reactor relevance of the advanced stellarator principle. It will have a five-period HELIAS configuration with an open island divertor and a superconducting coil assembly. Progress on production of the superconducting coils has been made and winding has started. Manufacture of the strands of superconductor is proving difficult, however, so that the coil production rate is slower than originally assumed. According to the latest projection, the first plasma in WENDELSTEIN 7-X will be obtained at the end of 2007. The Forschungszentrum Karlsruhe, which will provide the complete ECRH system, has successfully completed testing of a one-megawatt gyrotron developed jointly with CRPP Lausanne and European industry. The assembly of WENDELSTEIN 7-X has been worked out in detail and the special facilities necessary have been ordered.

The standard and scope of the research reports described in this volume testify to the many achievements at IPP in the past year. On behalf of the Directors and the Scientific Board I would like to take this opportunity of thanking all members of staff for their hard work and dedication to high-temperature plasma physics and fusion research.

Alexander M. Bradshaw

CONTENTS

Projects

ASDEX Upgrade Project

1. Overview
2. Operation with tungsten coated central column
3. Progress towards steady state advanced scenarios
4. Transport barriers
5. Electron heat transport
6. Main chamber edge transport and wall recycling
7. Technical systems
8. Characterization of DIV II B
9. Core plasma physics
10. Edge and divertor physics

International Co-operation

1. DOE-ASDEX Upgrade activities
2. CEA, Cadarache
3. Collaboration with Forschungszentrum Jülich, association KFA-EURATOM
4. Co-operation with Russian institutes
5. University of Cork
6. Centro de Fusao Nuclear, EURATOM IST Association, Lisbon, Portugal
7. TEKES (HUT and VTT), Finland
8. Institut für Allgemeine Physik, TU Wien und Friedrich Schiedel Foundation, Austria
9. National Institute of Laser Plasma and Radiation Physics,
EURATOM-NASTI Association, Bucharest, Romania

JET Co-operation Project

1. Overview
2. Pellet fuelling at JET
3. Task force S1
4. Task force S2
5. Task force E
6. Task force M
7. Task force H
8. Task force Ft

ITER Co-operation Project

1. Introduction
2. Performance analysis
3. Design studies

WENDELSTEIN 7-AS Project

1. Overview
2. Experimental and theoretical results
3. Diagnostic development
4. Neutral beam injection

WENDELSTEIN 7-X Construction

1. Introduction
2. Basic machine
3. Heating systems
4. Auxiliary systems

WENDELSTEIN 7-X Diagnostics

1. Overview
2. Status reports of subgroups
3. Technical coordination

CONTENTS

Stellarator Theory

1. Introduction
2. Configuration studies
3. Ideal MHD stability
4. MHD-stability with kinetic effects
5. Influence of kinetic electrons on Ion-Temperature-Gradient (ITG) driven instabilities
6. Drift waves in stellarators
7. Free boundary equilibrium calculations
8. Plasma edge theory

Stellarator System Studies

1. WENDELSTEIN 7-X
2. The Helias reactor

IEA Implementing Agreement

Plasma-facing materials and components

1. High-Z materials
2. Low-Z materials
3. Surface processes on plasma-exposed materials
4. Component related aspects
5. Migration of materials in fusion devices

Divisions and Groups

Scientific divisions of IPP

Experimental Plasma Physics Division 1

Experimental Plasma Physics Division 2

Experimental Plasma Physics Division 3

Experimental Plasma Physics Division 4

Experimental Plasma Physics Division 5

WENDELSTEIN 7-X Construction

Stellarator Theory Division

Tokamak Physics

1. Tokamak edge physics

Technology Division

1. Neutral injection heating
2. Ion cyclotron resonance heating
3. ECRH on ASDEX Upgrade

Surface Physics Division

1. Ion beam analysis methods
2. Surface science - SFB 338

Materials research division

Centre for Interdisciplinary Plasma Science

1. Plasma technology
2. Plasma theory
3. Data analysis

CONTENTS

Plasma Diagnostics Division

1. PSI-2 plasma generator
2. Electron Beam Ion Trap (EBIT)
3. UHV laboratory
4. Theory and modelling

VINETA

1. Introduction
2. Device and diagnostics
3. Experimental programme

Electron Spectroscopy Group, FHI Berlin

Garching Computer Centre

1. Major hardware changes
2. Data management
3. Development for high-end parallel computing
4. Vector computing
5. Multimedia
6. Developments in networking
7. Pilot projects for the German Gigabit science network
8. Data acquisition and data bases for plasma fusion Experiments

Central Technical Services

Office of the Director

1. Health and safety
2. Public information department
3. Library
4. Project planning
5. Equal opportunities
6. Energy studies

Administration

Publications

Publications and conference reports

Lectures

Laboratory reports

Author index

Teams

CONTENTS

University Contributions to IPP Programme

Lehrstuhl für experimentelle Plasmaphysik at Augsburg University

Plasma edge diagnostics

Lehrstuhl für Experimentalphysik III at Bayreuth University

Elementary reactions of hydrogen atoms with adsorbates and solid surfaces

Lehrstuhl für Experimentalphysik II at Greifswald University

Plasma deposition of metal-containing amorphous hydrocarbon films

Institut für experimentelle und angewandte Physik at Kiel University

1. The project TJ-K
2. Helicon wave studies
3. Turbulence studies

Lehrstuhl für Messsystem- und Sensortechnik at Technische Universität München

Speckle-interferometry in vibrating environments

Institut für Plasmaforschung (IPF) at Stuttgart University

1. Plasma heating
2. Plasma edge diagnostic

How to reach the Max-Planck-Institut für Plasmaphysik

How to reach Greifswald Branch Institute of the Max-Planck-Institut für Plasmaphysik

ASDEX UPGRADE PROJECT

(Head of Project: Dr. Otto Gruber)

Experimental Plasma Physics Division E1: U. Brendel, A. Carlson, P. Cierpka, T. Eich, H.U. Fahrbach, J.C. Fuchs, O. Gehre, A. Geier, J. Gernhardt, O. Gruber, G. Haas, A. Herrmann, J. Hobrik, L. Horton, T. Hül, D. Jacobi, E. Kaplan, M. Kaufmann, B. Kleinschwärzer, G. Klement, H. Kollotzek, G. Kölbl, P.T. Lang, P. Leitenstern, A. Lorenz, K. Mank, K.F. Mast, K. Mattes, D. Meisel, D. Merkl, V. Mertens, H.W. Müller, Y.-S. Na, J. Neuhauser, E. Oberlander, E. Posthumus-Wolfrum, G. Prausner, G. Reichert, V. Rohde, W. Sandmann, M. Sator, G. Schall, H.-B. Schilling, P. Schütz, G. Schramm, G. Schrembs, K.-H. Schuhbeck, S. Schweizer, J. Schweinzer, H.-P. Schweiß, U. Seidel, O. Sigalov, C. Sihler, A. Sips, J. Stober, B. Streibl, A. Tanga, W. Treutterer, M. Troppmann, T. Vierle, S. Vorbrugg, M. Wolf, R. Wolf.

Tokamak Physics Division: R. Arslanbekov, M. Apostoliceanu, G. Becker, A. Bergmann, R. Bilato, K. Borrass, M. Brambilla, D. Correa-Restrepo, D. Coster, K. Dimova, W. Feneberg, M. Götz, S. Günter, V. Igochine, F. Jenko, O. Kardaun, A. Kendl, J. Kim, R. Kochergov, P. Lauber, P. Martin, P. Merkel, R. Meyer-Spasche, Y. Nishimura, G. Pautasso, A.G. Peeters, G. Pereverzev, S. Pinches, E. Poli, S. Riondato, S. Schade, T. Schmidt-Dannert, W. Schneider, E. Schwarz, B. Scott, G. Spies, D. Strinzi, E. Strumberger, G. Tardini, H. Tasso, C. Tichmann, Q. Yu, H.-P. Zehrfeld.

Experimental Plasma Physics Division E2: C. Aubanel, H. Bauer, K. Behler, H. Blank, A. Buhler, G.D. Conway, R. Drube, K. Engelhardt, A. Gude, H. Hühnercker, M. Jakobi, A. Keller, S. Klänge, B. Kurzan, A. Lohs, M. Maraschek, H. Meister, R. Merkel, A. Mück, H. Murmann, G. Neu, G. Raupp, K.-H. Steuer, W. Suttrop, D. Wagner, D. Zäsche, T. Zehetbauer, H. Zohm.

Experimental Plasma Physics Division E4: K. Behringer, D. Bolshukhin, R. Dux, W. Engelhardt, J. Fink, J. Gafert, A. Kallenbach, C. Maggi, R. Neu, T. Peterich, R. Pugno, S.-W. Yoon, B. Waldmann, M. Zarrabian.

Technology Division: W. Becker, F. Braun, H. Faugel, P. Franzen, D. Hartmann, B. Heinemann, F. Hofmeister, K. Kirov, W. Kraus, F. Leuterer, F. Meo, F. Monaco, M. Münich, J.-M. Noterdaeme, S. Obermayer, F. Probst, S. Puri, R. Riedl, F. Ryter, W. Schöch, E. Speth, A. Stöckler, O. Vollmer, F. Wesner, R. Wilhelm. E. Wirsching.

Plasma Diagnostics (Berlin): D. Hildebrandt, M. Laux, W. Schneider, U. Wenzel.

Garching Computer Centre: K. Desinger, S. Groß, A. Hackl, C. Hennig, P. Heimann, S. Heinzl, H. Kroiss, J. Maier, M. Panea-Doblado, H. Reuter, A. Schott, M. Zilker.

Materials Research: M. Balden, B. Bensch, H. Greuner, H. Maier.

Surface Physics Division: X. Gong, K. Krieger, M. Mayer, J. Roth.

Central Technical Services: R. Ammer, H. Eixenberger, T. Franke, F. Gresser, E. Grois, M. Huart, C.-P. Kämmermann-Wilke, K. Klaster, M. Kluger, J. Perchermeier, G. Raitmeir, I. Schoenewolf, J. Stadlbauer, F. Stobbe, F. Zeus.

University of Cork, Ireland: M. Foley, P. McCarthy, E. Quigley.

IPF University of Stuttgart: G. Dodel, G. Gantenbein, E. Holzhauer, W. Kasperek, U. Schumacher.

Centro de Fusao Nuclear, IST Lisbon, Portugal: L. Cupido, M.-E. Manso, I. Nunes, T. Ribeiro, J. Santos, F. Serra, A. Silva, F. Silva, P. Varela, S. Vergamoto.

NCSR Demokritos, Athens, Greece: G. Kyriakakis, N. Tsois.

TEKES (HUT and VTT), Finland: O. Dumbrajs, J.A. Heikkinen, T. Kiviniemi, T. Kurki-Suonio, S. Saarelma.

University of Augsburg: U. Fantz, J. Günter, B. Heger.

IAP, Vienna, Austria: H. Falter, M. Proschek.

Guests: C.V. Atanasiu, G. Miron, Inst. of Atomic Physics, Romania;

S. Egorov, V. Rozhansky, I. Veselova, S. Voskoboinikov, Technical University, Plasma Physics Department, St. Petersburg, CIS;

A. Khudoleev, IOFFE, St. Petersburg, CIS;

P. Lalousis, IESL, FORTH, Heraklion, Greece;

S. Saarelma, Helsinki University of Technology, Finland;

G. Troumoulopoulos, University of Ioannina, Greece;

S. Sesnic, USA;

H. Weitzner, N.Y. University, USA;

A. Komarov, A. Kozachok, Kharkov Institute, Ukraine;

A. Savtchikov, Forschungszentrum Jülich, Germany;

J. Tataronis, University of Wisconsin, Madison, USA;

W. Pan, S.T. Wu, D. Yao, Academia Sinica, Hefei, China;

T. Bolzonella, R. Lorenzini, E. Martines, CNR Padua, Italy.

1. OVERVIEW

1.1 Scientific Aims and Operation

The ASDEX Upgrade non-circular tokamak programme has been largely focused to provide the physics basis for ITER, namely

- (i) confinement and performance-related physics in the ITER base-line scenario, the ELMy H-mode near operational limits, including ELM mitigation,
- (ii) investigation of scenarios and physics of advanced tokamak plasma concepts with both internal transport barriers ITB and improved H-mode scenarios leading to enhanced performance and possibly stationary operation,
- (iii) MHD stability and active stabilisation of β limiting instabilities as well as avoidance and mitigation of disruptions, and
- (iv) edge and divertor physics in these high-power, high-confinement regimes, with the aim of identifying and optimising power exhaust and particle control (ash removal) as well as testing of first wall materials.

The similarity of ASDEX Upgrade to ITER in its poloidal field coil system and divertor configuration makes it particularly suited to testing control strategies for shape, plasma performance, and MHD mode stabilization. Additionally, the similarity in cross-section to other divertor tokamaks is important in determining size scalings for core and edge physics. This collaborative work, including extrapolation to ITER parameters, was enhanced in the JET operation under EFDA during the last years. Furthermore, the ASDEX Upgrade programme is embedded in a framework of national (IPF Stuttgart, University of Augsburg, see also section on University contributions to IPP programme) and international collaborations (see section on International Co-operation).

With the increasing number of experiments proposed by collaborators within the EU fusion programme, the ASDEX Upgrade Programme Committee was opened to the associations to take more responsibility for the ASDEX Upgrade programme. This body defines the Task Forces responsible for the different elements of the ASDEX Upgrade programme and nominates the Task Force leaders. It also approves the experimental programme proposed by the Task Force leaders. By definition, every association involved in the ASDEX Upgrade programme has the right to nominate a member. At present, it comprises 9 members from the associations and 8 from IPP. Furthermore, the bodies that work out the programme proposals, are now open for external participants. In parallel, an initiative has been started to ease remote participation in these meetings. With this structure, we aim at a compromise between the increased international participation and the flexibility that has so far been typical for the ASDEX Upgrade programme.

The operation in 2001 was dominated by maintenance and hardware upgrades. In a 9 month shut-down till April this year one neutral beam line was reoriented for a more tangential

injection, which should provide 0.25 MA off-axis current drive. In parallel, the divertor structure of ASDEX Upgrade was adapted to maintain good divertor properties at high triangular plasma shapes putting the strike points on the vertical targets and increasing the pumping capability (DIV IIB). The studies of reactor-compatible materials was continued by a total tungsten coverage of the low field side LFS heat shield based on the positive experience with Tungsten on divertor and these inner heat shield tiles reducing carbon influx. The promising refuelling by pellet injection has led to a new high-field-side HFS pellet launcher, whose pellet-guiding system was finalized to allow injection velocities of up to 800 m/s for deep fuelling. Deeper particle deposition with pellet velocities of 560 m/s was confirmed. To get stationarity not only on the transport and MHD time scales but also on skin time, a flat-top time of 10 s will be provided step by step by an upgrading of the power supply systems, which is already available for 0.8 MA discharges. This allows steady state investigations for more than three current diffusion times, a unique feature for tokamaks with ITER plasma geometry.

During the 2001 experimental campaigns, ASDEX Upgrade operated routinely with NBI heating powers up to 20 MW and injection energies up to 100 keV, which allowed studies of the influence of heat deposition on energy and particle transport, stability and of fast particle effects. Minority heating with the ICRH system (up to 5.7 MW coupled) was used for central heating at high densities, and to study the influence of deep particle refuelling and toroidal rotation by substituting NBI. The ECRH system (four gyrotrons with a coupled power of 1.6 MW for 2 s) allowed pure electron heating and current drive, transport studies and feedback stabilisation of neo-classical tearing modes NTM. Provisions for current drive and for active control of current profiles in advanced scenarios were available with more perpendicular or tangential NBI and ECRF using remotely controlled mirrors (up to 0.35 MA driven on-axis).

The physics programme of 2001 was based on the conclusions and findings of the last years, ITER requirements and tokamak concept improvement (see section 1.2). High shaping capability with elongations $\kappa > 1.8$ and triangularities δ up to 0.45 at the separatrix allowed study of the influence of plasma shape on performance and operational limits. The present version of the closed DIV IIB (with vertical target plates including a roof baffle in-between and a cryopump), which is rather similar to the ITER-FEAT reference design, allows a strong reduction of heat flux to target plates and is capable of handling heating powers of up to 20 MW or P/R of 12 MW/m. The observed strongly reduced, distributed power flux to the surrounding structures during both ELM and ELM-free phases is in agreement with B2-Eirene simulations.

In the advanced scenarios characterized by a high fraction of bootstrap current and external current drive, emphasis was placed on performance enhancement and the extension of both internal transport barriers and improved H-mode scenarios using different heating and current drive methods (NBI, ECRF). Alignment of improved core confinement with the optimal magnetic and velocity shear profiles and the compatibility of this idea with stationary operation at high

power and, simultaneously, a cold divertor is one of the key elements of the ASDEX Upgrade programme.

1.2 Summary of Main Results

Both ion and electron temperature profiles in conventional L- and H- modes on ASDEX Upgrade are generally stiff and limited by a critical temperature gradient length $L_T = T/\nabla T$ normalized to the major radius R as given by ion temperature gradient ITG and trapped electron TEM driven turbulence. Electron cyclotron heating and modulation experiments both at ASDEX Upgrade and other EU tokamaks have confirmed that electron temperature profiles are also stiff with $R/L_T \approx 9$, as predicted by TEM turbulence. Accordingly, the core and edge temperatures are proportional to each other and the plasma energy is proportional to the pedestal pressure for fixed density profiles. Density profiles are not stiff, and confinement improves with density peaking. More triangular plasma shapes (up to $\delta \approx 0.4$) show strongly improved confinement up to the Greenwald density n_{GW} and, therefore, higher β -values, due to increasing pedestal pressure, and H-mode density operation extends above n_{GW} . Density profile peaking at n_{GW} was achieved with controlled gas puff rates and especially with off-axis heat deposition, while a balanced addition of central deposited ECRF or ICRF allowed control of density peaking. This is due to the increasing central anomalous transport of both energy and particles in combination with the neo-classical inward pinch. At these high densities with reduced edge temperatures small type II ELMs can provide good confinement combined with low divertor power loading. The operational regime of these type II ELMs was established at $q_{95} > 3.5$ and closeness to magnetic double null configuration.

In advanced scenarios the highest performance in terms of confinement improvement compared with L-mode plasmas and high β was achieved in high β_N H-mode discharges with $\delta = 0.4$ reaching transiently $H_{L-99P} \beta_N \approx 11.5$, limited by neo-classical tearing modes (NTM) at low central magnetic shear ($q_{min} \approx 1$). Still $H_{L-99P} \beta_N \approx 8$ was kept in steady state for 20 energy confinement times at line averaged densities of 90% of the Greenwald density and with type II ELMs. In the so-called improved H-mode discharges at $\delta = 0.3$ the highest performance in terms of $n_i(0) T_i(0) \tau_E \approx 10^{20} m^{-3} keVs$ was obtained for five confinement times. In both scenarios the T profiles are still governed by ITG/TEM turbulence, while by tailored NBI deposition the confinement is improved via density peaking connected with low central magnetic shear and fishbone activity.

Progress was also made in internal transport barrier discharges both in the ion heat (NBI in current ramp up) as well as the electron heat channel (central counter-ECCD). The ion barriers with reversed shear ($q_{min} \approx 2$) and L-mode edge achieved H-mode confinement level and $T_i(0) = 22$ keV and are limited to $\beta_N \leq 2$ by internal and external ideal MHD modes. Turbulence driven transport is suppressed in agreement with the ExB shear flow paradigm, and core ion transport coefficients are at neo-classical ion transport level. In comparison with the previous year, more stable discharges with central counter-ECCD and

reversed magnetic shear formation achieved electron cyclotron radiation temperatures of over 30 keV due to non-thermal electrons at low densities. The electron bulk temperatures are still at 20 keV connected with an electron ITB.

MHD instabilities limit the operational regime of conventional and advanced scenarios with positive magnetic shear (NTMs) and with reversed shear (double tearings, internal and external kink modes) scenarios. The onset β_N for NTMs is proportional to the normalised gyroradius ρ^* . Thereby the improved confinement scenarios with peaked density profiles are more susceptible for NTMs, as neo-classical theory predicts a stronger contribution from the density gradient to the missing bootstrap current in the islands. Using ECCD at the island position (10% of the total heating power) not only complete NTM stabilisation was demonstrated at $\beta_N > 2$, but also the β was enhanced compared with the pre-NTM phase. Disruption avoidance and mitigation (via strong Neon and Argon puffs) techniques have been further developed and can be used in real-time. For the future, disruptive MHD limits are expected to be extended using current profile control and wall stabilisation.

Finally, the plasma operation with a Tungsten coverage of a large wall area reduced the Carbon content, while the Tungsten concentrations remained below 10^{-5} . Only in discharges with improved core confinement and density peaking have increased Tungsten concentrations been observed. Central RF heating was used to control the impurity content by increasing the anomalous particle transport accompanied by only a modest reduction of energy confinement and electron density peaking.

1.3 ASDEX Upgrade Technical Enhancements and Programme in 2001

In 2002 the operation of ASDEX Upgrade in close connection with the JET programme and in co-operation with the EU Associations will continue. Core physics studies will emphasize the improvement of plasma performance (energy and particle transport, MHD-stability and β -limits, mode stabilization using stationary and AC ECCD) in both "conventional" H-mode and "advanced" tokamak scenarios. Main elements will be pressure and density profile as well as impurity control using tailored heat deposition forms ICRF, ECRF and NBI. Current profile control and sustainment in advanced mode operation with non-inductively driven currents in addition to the internal driven bootstrap current can be done in a flexible way by different deposition of NBI and the already available 1.6 MW coupled ECRF power to drive currents on-axis (up to 0.35 MA on-axis) or off-axis with remotely controlled mirrors. A further upgrading of the ECRF power to 4 MW at tuneable frequencies between 104 and 140 GHz is underway. To reach the ultimate ideal MHD limits the introduction of a stabilizing wall close to the plasma in combination with active feedback coils working on the resistive time scale of the wall are under consideration. The Tungsten coverage of the chamber walls will be extended towards the low field side and divertor entrance regions.

Sections 2- 6 are concerned with operation of the Tungsten coated central column, progress towards steady state advanced scenarios including type II ELMs and NTM stability and control, internal electron and ion transport barriers, electron heat transport experiments and comparison with theory, and main chamber edge transport and wall recycling. In section 7 the ASDEX Upgrade technical systems, control and data processing, and heating systems are described. Section 8 deals with the characterization of the new DIV IIb, and additional results concerning core plasma physics as shape control, core impurity measurements, HFS pellet injection and ELM control, density fluctuations and disruption physics are described in section 9. Section 10 is particularly devoted to the H-mode edge barrier and divertor physics, including modelling and Carbon layer deposition.

2. OPERATION WITH TUNGSTEN COATED CENTRAL COLUMN

Although the interaction of plasma and material is strongly concentrated in the divertor region, it has become evident in recent years that in all divertor devices with large areas of Carbon based wall components the Carbon impurity content is strongly influenced by the main chamber Carbon source. To avoid excessive co-deposition of Tritium with Carbon ITER will start operation with Be as the first wall material in the main chamber. However, in a later phase of ITER, or in a DEMO reactor, Tungsten seems to be the only material at hand to stand the fluences with acceptable erosion. Although W has large advantages over Be concerning thermo-mechanical properties, its use implies the risk of unduly high radiation losses in the central plasma.

The questions, how a Tungsten first wall influences plasma operation and performance and whether the amount of migrating Carbon can be reduced, were addressed in ASDEX Upgrade by coating the central column with tungsten in a step by step approach, starting with the experimental campaign 1999/2000. The tiles were coated commercially by plasma arc deposition to a thickness of $1\mu\text{m}$. Before the 2001 campaign a total Tungsten coverage of the central column was applied, except for regions which may be hit directly by the shine through of the neutral beam injection NBI or which are used as a limiter. Finally, starting from November 2001, the central part of the heat shield was W-coated leaving only the CFC tiles which are used as an NBI beam dump free of coating (see Fig. 2.1). At the limiter region each two neighbouring tiles were combined into a single one with a roof top, in order to minimize leading edges. The summer campaign began without preceding boronization or siliconization, to run the plasma discharges with the pure Tungsten surface. During this initial period the total radiation and the Z_{eff} were higher than for a well conditioned machine. This could be attributed to the high oxygen content (few percent), which led to the most challenging environment for the W-experiment: The W-source was potentially increased due to strong sputtering and obviously the anomalous transport was suppressed, similar to radiation enhanced regimes. After this initial phase, where most of the relevant scenarios had been performed, the vessel

was boronized twice during the remaining campaign. In summary the experiments showed that the operational space is somewhat more restricted than for a device having only low-Z PFCs and the Carbon content seems to be reduced by about 30%-50%.

The behaviour of W in the discharges was mostly monitored by spectroscopic means developed during the previous campaigns. The Tungsten influx stayed below the detection limit except for direct plasma wall contact or a reduced clearance in divertor discharges. Fig. 2.2 shows the behaviour of the W-influx and the W-concentration during the shift of the plasma towards the central column. From these observations a penetration factor in the order of 1% and effective sputtering yields of about 10^{-3} could be derived, pointing to a large contribution of light intrinsic impurities. Post mortem analysis of the W surfaces (see section on Plasma-Facing Materials and Components) strongly supports the evidence of dominant ion sputtering, but due to the very non-homogenous erosion patterns the above mentioned influx measurements may be hampered. The Tungsten concentrations ranged from below 10^{-6} up to a few times 10^{-5} in discharge scenarios without wall contact. In limiter discharges the concentrations were larger by about a factor of 10 and even higher in phases with internal transport barriers. Generally, in discharges with increased and/or evolving density peaking, a tendency for increased Tungsten concentrations or even accumulation was observed. Central heating (mostly) by ECRH led to a strong reduction of the central impurity content, accompanied by a very modest reduction of the energy confinement, thus providing an excellent tool to control the central impurity content. This is demonstrated in Fig. 2.3 for a high triangularity discharge with good confinement (H-factor above 1.1). From $t \approx 1.8$ s the W-concentration rises continuously and shortly after $t \approx 2.2$ s the soft-X ray measurement saturates. It has to be pointed out that this increase in the SXR brightness is not exclusively due to the increase of the W density, since the brightness of other impurity radiation (for example Fe) is also found to rise. From $t = 3.0$ s onwards, central ECRH is added. During the ECRH phase, T_{e0} is increased but no (or very minor) sawteeth appear and \bar{n}_e is slightly decreased similar to the so-called 'density pump out' effect. The stored energy remained almost constant, leading to a slight reduction of the H factor from 1.14 to 1.06. However, by far the strongest effect is found on the SXR brightness and the Tungsten concentration. Both drop on the timescale of the energy confinement time, leading to c_W below 10^{-6} . Once again after the heating phase, an increase of the SXR brightness and c_W is observed.

Since the edge parameters are unchanged throughout the discharge, a large variation of the W-source is very unlikely (in fact they are below the detection limit). Therefore the physical picture is as follows: Coupled to the low energy transport in these discharges, the anomalous particle transport is also decreased, even allowing a very small drift velocity as the Ware pinch leads to a density peaking of the background plasma. This density peaking together with the low anomalous transport and a moderate peaking of the temperature profiles provokes the neoclassical impurity accumulation. The central wave heating obviously counteracts this in several ways. The

Tokamak

anomalous particle transport is increased, leading to flatter density profiles of the background ions. At the same time T_{e0} and therefore also the gradient is increased. Assuming a fast equilibrium of T_e and T_i , this then leads to a strong reduction of the neoclassical inward drifts. Together with the increased anomalous transport this results in a strong reduction of the central impurity content. First impurity transport calculations support this physical picture and even a quantitative agreement with the temporal evolution and the amount of the W-reduction can be obtained, if the anomalous diffusion is moderately enhanced during ECRH. Concerning the high density ELMy H-Mode envisaged as the standard scenario in ITER, the situation concerning central impurity accumulation may be alleviated, since the Ware pinch will be smaller there and the central α heating may lead to higher central particle

diffusivity both resulting in flat density profiles of the background ions.

The two months of operation with the W coating at the central part of the heat shield, show very similar results to the previous campaign. In line with observations in preparatory experiments, the breakdown of the plasma discharges in contact with the W surface is not much different from the situation with the graphite limiters. This result further strengthens the perspective of using W in the main chamber in a later phase of ITER or in a Demo reactor.

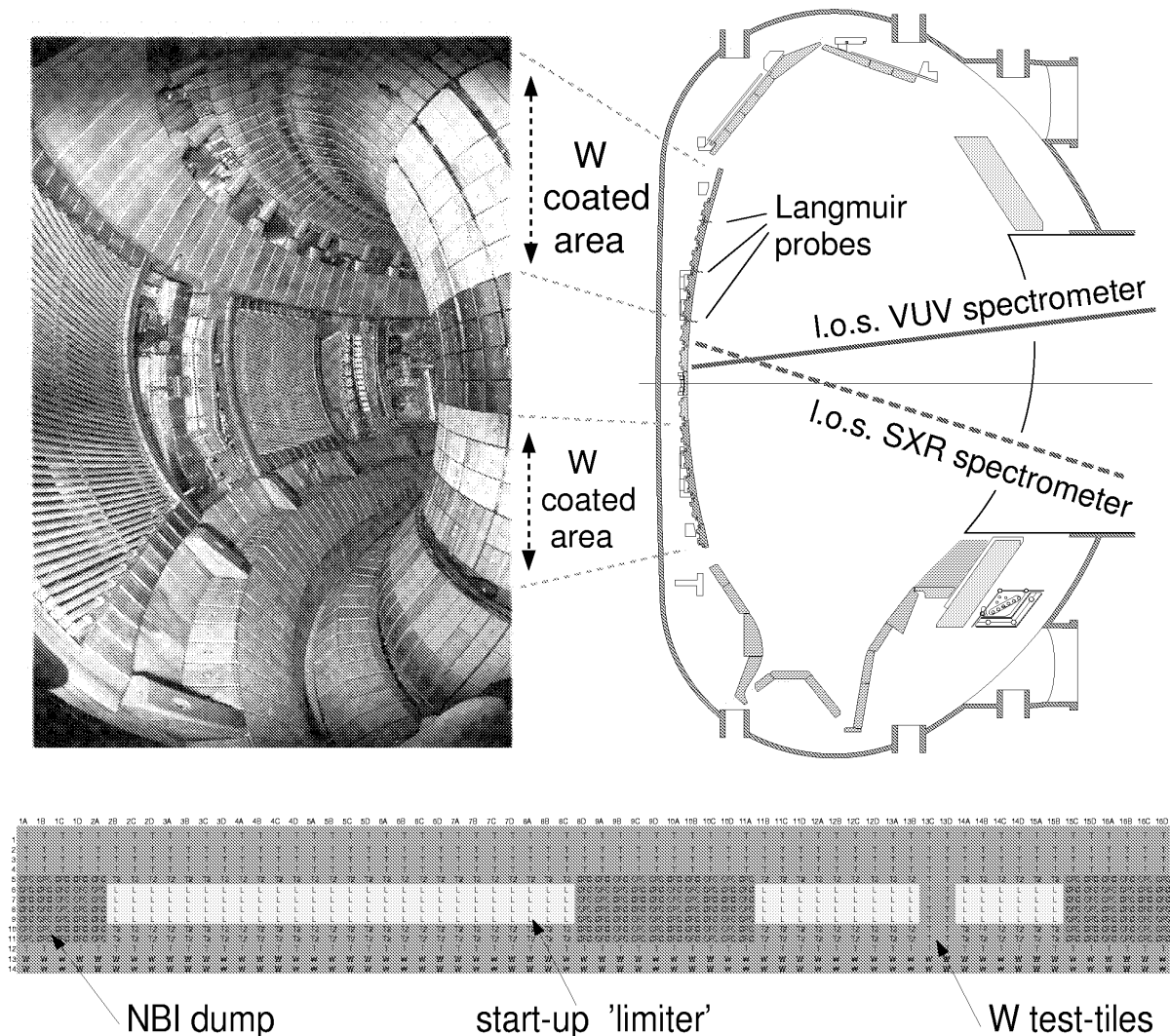


FIG. 2.1: Left side: Tangential view of the central column of ASDEX Upgrade with the tungsten coated tiles. The four rows in the equatorial plane are made of graphite and CFC and are used as limiter during plasma start up and in dedicated limiter discharges. Right side: Poloidal cross section, showing the line of sights of the two main diagnostics for the central W radiation, as well as Langmuir probe tips installed at the central column. Bottom: Schematic view of the unrolled central column: The light grey areas represent W coated tiles, the two lowest rows were already mounted in 1999. The dark grey tiles are manufactured from CFC because of potential shine through of the NBI. The white tiles are ordinary graphite tiles. This central region of heat shield is used as limiter during the start-up phase of the discharge.

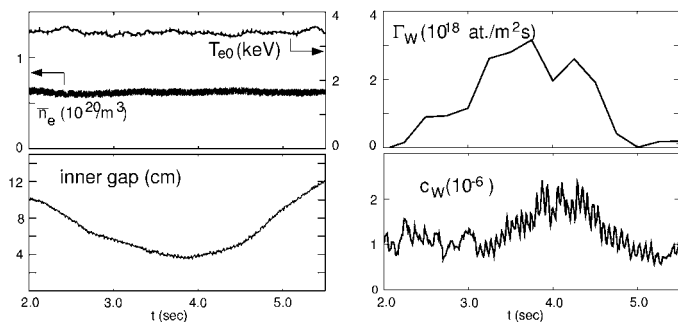


FIG. 2.2: W -influx Γ_W and W -concentration c_W during the radial shift of the plasma towards the central column (# 14186, $I_p = 1$ MA, $B_t = -2.3$ T, $P_{NBI} = 5$ MW, $\delta = 0.15$). On the top \bar{n}_e and T_{e0} are shown, to demonstrate that the main plasma parameters remain constant during the shift.

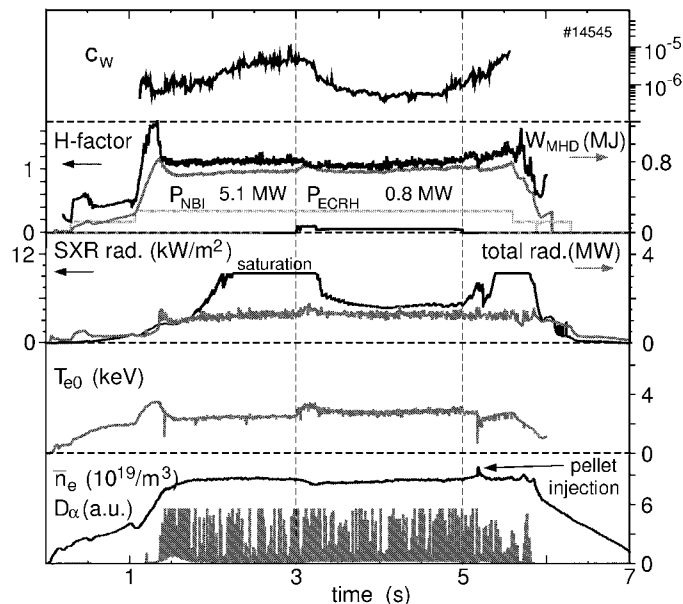


FIG. 2.3: Parameters during a moderately improved H-mode discharge at $I_p = 1$ MA, $\delta = 0.4$, showing enhanced c_W with NBI only, but a strong reduction of c_W during central ECRH.

3. PROGRESS TOWARDS STEADY STATE ADVANCED SCENARIOS

Plasmas with ITBs are proposed as a candidate for advanced scenarios. The transport barrier optimises the confinement and the non-monotonic q -profile allows for the current to be dominantly driven by off-axis bootstrap current. However, the central pressure that can be obtained in ITB discharges is limited by internal kink modes (infernal modes), keeping β_N well below 3. If on the other hand some central current is provided by electron cyclotron resonance current drive (ECCD) or the ohmic current, then reversed shear would not be required. This may give better MHD stability, is closer to the existing confinement data and would provide a conservative base-line for a steady state reactor.

At ASDEX Upgrade, research into advanced scenarios has concentrated on three main areas: (1) the formation of internal

transport barriers in discharges with reversed q -profiles, (2) full non inductive current drive scenarios at low plasma current (0.4 MA), with ECCD or neutral beam injection NBI in combination with the bootstrap current, and (3) on improved confinement H-modes in steady state, obtained in discharges with weak magnetic shear $s = (r/q)(dq/dr)$ in the centre, and q on axis close to 1. A summary of recent ASDEX Upgrade results is given in Figure 3.1. The best results have been obtained in plasmas without an ITB or without a reversed q -profile.

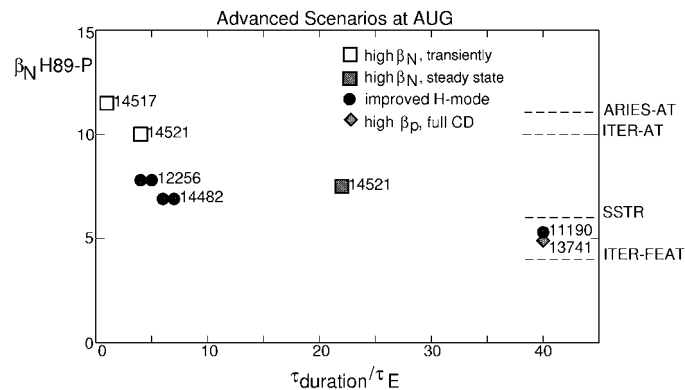


FIG. 3.1: Overview of advanced scenarios in ASDEX Upgrade. Plotted is $\beta_N \mathcal{H}_{89-P}$ versus the duration $\tau_{duration}$ normalised to τ_E . For the high β_N plasmas, points that are obtained transiently and in plasmas with near steady state conditions have been plotted. Reference values for the required $\beta_N \mathcal{H}_{89-P}$ are given for four reactor designs. The high β_N discharges come closest to the requirements for ITER-AT, the steady state reference scenario at $Q = 5$ for ITER.

3.1 High β_N discharges

The plasma configuration for these experiments has maximum shaping for ASDEX Upgrade, with triangularity $\delta = 0.42$ and elongation $\kappa = 1.65$. The plasma current is 0.8 MA, with toroidal fields from 1.7 to 2 T, giving edge safety factors in the range 3.6-4.1. Due to the high triangularity the plasma can be made near double null, with a separation between the two flux surfaces that define the two X-points of 0.009 m at the outer midplane. However, the lower X-point is still dominant with nearly all of the power flowing to the lower divertor target.

Pulse 14521, reaches the highest β_N , in conditions that approach steady state. In this discharge 10 MW of NBI is applied during the flat top of the plasma current. The neutral beams are injected tangentially by 4 sources, 2 of these sources deposit the power off-axis at $r/a = 0.5$. The electron density slowly increases to 88% of the Greenwald density limit. During this slow density rise, the stored energy decreases slowly. This is a combination of the loss of confinement generally observed for discharges approaching the Greenwald density limit and the slow reduction of the plasma inductance during the first part of the neutral beam heating phase. However, the confinement factor H_{89-P} over the ITER89, L-mode scaling remains at or above 2.2, while the enhancement factor compared to the

ITERH-98P(y,2) H-mode confinement scaling is 1.3 at the end of the heating phase. The edge safety factor q_{95} for this pulse is 3.6 at 1.7 T. Transiently and at lower density, higher values for β_N have been achieved in pulse 14517 with $\beta_N = 3.8$ and $H_{89-P} = 3$. Under these conditions a neo-classical tearing NTM mode is triggered by a sawtooth collapse.

High β_N has been obtained for a number of pulses at ASDEX Upgrade in discharges with similar conditions as for pulse 14521 and pulse 14517, emphasising that at high triangularity (up to 0.45), good confinement, high β_N and densities close to the Greenwald limit can be achieved simultaneously.

3.2 ELM activity at high β_N

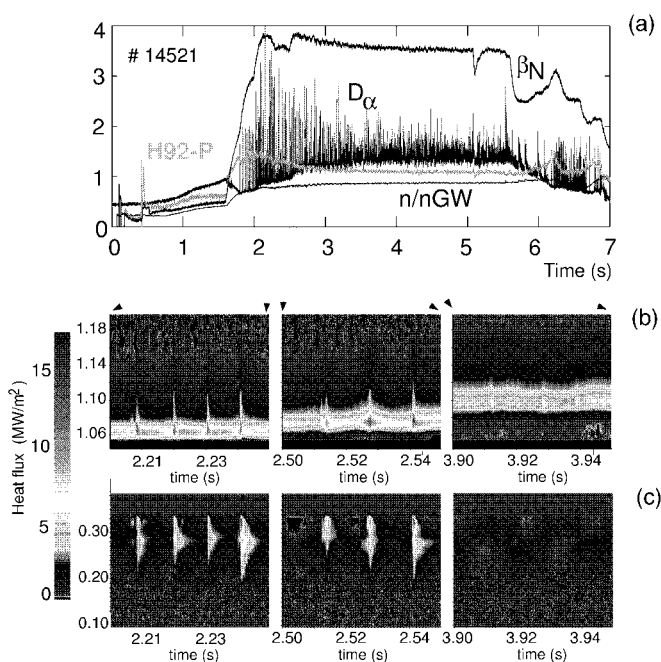


FIG. 3.2: A detailed overview of the ELM activity for pulse 14521 (a) for three short time intervals the infra red measurements of the outer lower (b) and inner lower divertor (c) are given.

In pulse 14521 (Figure 3.2) the line averaged electron density rises slowly to $9.1 \times 10^{19} \text{ m}^{-3}$ due to a combination of NBI and gas fuelling. Measurement of the density by interferometry, Thomson scattering and reflectometry indicate that the edge density is $6-7 \times 10^{19} \text{ m}^{-3}$. During the NBI heating phase, the ELMs reduce significantly in size as the density increases and the plasma configuration is moved up, closer to a double null configuration. This movement to a double null configuration is made deliberately and is completed at 3.2 seconds. Infra-red data shows that initially ELMs are observed on the outer target with a peak heat flux of up to 18 MW/m^2 . Towards the end of the heating phase (at 4.0 seconds) the maximum heat flux on the divertor has become steady, in the range of 6 MW/m^2 . For the inner target plate, the peak load is only observed during type I ELMs. However, during the double null configuration phase of the discharge, the heat flow to the inner divertor reduces to nearly zero. This is similar to what is observed for

type II ELMs at improved H-mode discharges. This implies that at heating powers well in excess (factor 5) of the H-mode power threshold and high gas fuelling rates, type II ELMs are observed at $q_{95} = 3.6$ in ASDEX Upgrade.

3.3 Modelling

For the pulses presented in this section, ASTRA code simulations have been performed. The calculations are started with an initial q -profile from the reconstruction using magnetic sensors only (no MSE data is available for these pulses). The simulations use a model for the NBI current drive, a model for the bootstrap current and use a transport model based on Weiland to simulate the evolution of the electron temperature and ion temperature. The measured density profile is used. The results of these simulations are generally in agreement with the experiments and can be used to calculate the non-inductive current drive contributions to the total current of 0.8 MA. The 10 MW of neutral beams (tangential injection angle), drive 0.13 MA (15%) of current, 5 MW of the beam power is deposited off axis, resulting in a broad current density profile provided by the neutral beams. Up to 0.46 MA (57%) comes from the bootstrap current using the model given in reference. This gives a total of up to $\approx 70\%$ non-inductively driven current at high density. Note that β_p for these discharges is 1.8-2.

3.4 Neo-classical tearing modes

The β_N achieved is limited by NTMs to 3.5 in conditions approaching steady state and limited to $\beta_N = 3.8$ transiently. High values for $\beta_p \sqrt{L_q/L_p}$ at the resonant surface ($q = 3/2$) are obtained before onset of the mode, compared to discharges at lower triangularity. The high density in these plasmas may partly explain this higher value for $\beta_p \sqrt{L_q/L_p}$ as may the increase in local magnetic shear due to the higher triangularity of these pulses. On the other hand, the confinement drop during the NTM is modest and $\beta_N = 2.9$ during the mode. The central temperature drops by 20%. At this β , the island at the $3/2$ q -surface in the plasma is expected to saturate to 20-25 % of the minor radius, which would give a much larger drop in stored energy or central ion temperature. In this respect, the NTM may be of the frequently interrupted 'FIR' type, where the growth of the mode is limited by other MHD modes.

3.4.1 NTMs in high β_N discharges

Onset behaviour of NTMs: In order to get a more robust prediction of the onset dependence of the achievable local β_p^{onset} from (3,2)-NTMs as a function of the local poloidal ion gyro-radius $\rho_{p,i}^*$ and the local collisionality $\bar{\nu}_{ii} = \nu_{ii}/(m\epsilon\omega_e^*)$ the range of these parameters has been extended.

Especially discharges with maximum shaping and high β_N and high H-mode factors, as described in the previous section,

extended the accessible range in \bar{v}_{ii} to much higher values. High densities near the Greenwald density limit together with still good confinement, made this high \bar{v}_{ii} and high $\rho_{p,i}^*$ range possible. In standard, less shaped cases, high densities lead to a reduction in confinement and hence also reduce $\rho_{p,i}^*$.

The observed density peaking in highly shaped discharges with beam heating alone, could explain the sometimes low threshold values for the NTM onset. A more detailed analysis revealed, that the $n_e \cdot \nabla T$ and the $T \cdot \nabla n_e$ terms need to be considered separately for calculating the driving bootstrap current for the NTM. Consistently with theory, the density gradient ∇n_e seems to contribute more to the bootstrap drive. A replacement of beam heating power by ICRH heating could reduce the probability for NTM excitation by reducing the density peaking.

3.4.2 NTM behaviour at high β_N FIR-NTMs

In discharges with strong heating power and hence high β_N values in the presence of NTMs the so-called frequently interrupted regime FIR could be observed. The NTM never reaches its saturated size in this phase, as the mode is repeatedly abruptly reduced on a very short timescale. This resulting reduced averaged amplitude decreases the loss in confinement caused by the mode in this FIR-phase. The abrupt reduction of the (3,2) NTM amplitude ($\approx 500 \mu\text{s}$ for ASDEX Upgrade) can be explained by a non-linear coupling to an additional fast growing burst-like ideal (4,3) mode. The additional presence of a (1,1) mode is required for this non-linear coupling with phase locked modes. Similar behaviour could be observed in general for (m,n) NTMs together with bursts of (m+1,n+1) modes.

The resulting confinement recovery in these NTM-phases may point to a regime of "acceptable" NTMs in a reactor (see Fig. 3.3)

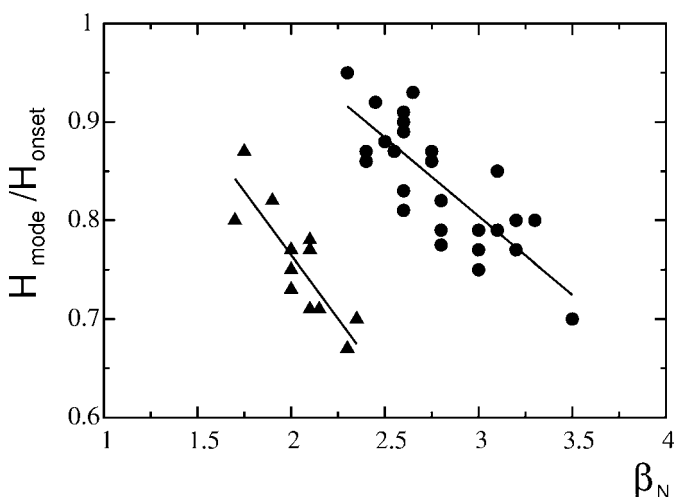


FIG. 3.3: H factor after (3,2) NTM saturation, normalised to the value at the NTM onset, versus β_N at the mode onset. For initial β_N^{onset} values above $\beta_N \approx 2.3$ the confinement loss is partially recovered.

3.4.3 NTM stabilisation with ECCD

The development of scenarios with a complete suppression of (3,2) NTM has been continued. By increasing the applied NBI power the stationary achievable β_N with a suppressed NTM could be raised to $\beta_N \approx 2.7$. An example of this is shown in Fig. 3.4.

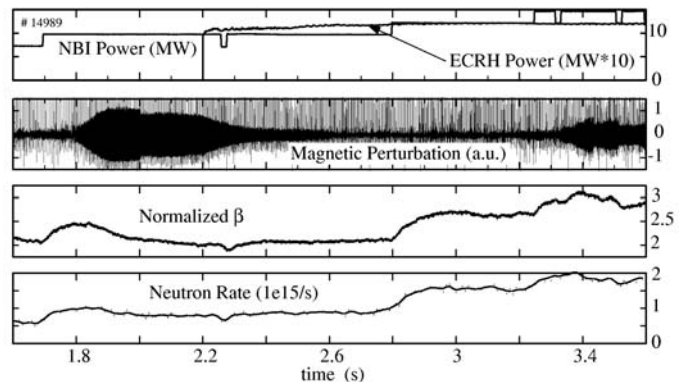


FIG. 3.4: The stationary achieved β_N with a suppressed (3,2) NTM could be raised to $\beta_N \approx 2.7$. Only with a maximum of 15 MW of NBI could the NTM be triggered again after the ECCD suppression.

4. TRANSPORT BARRIERS

In 2001 progress was made in the area of transport barriers. This included both the ion as well as the electron channel. They have, however, still been studied separately, the barriers in the ion heat channel through neutral beam heating in the current ramp up, and the barriers in the electron heat channel through counter electron cyclotron current drive ECCD in low density plasmas.

It was observed that the ion barrier formation correlated with density, appearing more frequently at low density. Since the neutral beams provide a particle source, the heating was applied at a later time point in the current ramp up. This new scheme has led to a new record for the central ion temperature of 22 keV (see Fig.4.1), and (in another discharge) to β_N values of 2 ($H_{99p} = 2$).

More important than the records, however, is that the new scenario is reproducible because it allows for more detailed physics studies. Variations of the plasma parameters can be made around this scenario sorting out the criterion for formation. So far, pre-heating of the electrons with electron cyclotron heating has been tried, in order to generate a larger region of reversed shear. The pre-heating has been shown to delay the barrier formation but does not affect the width of the barrier.

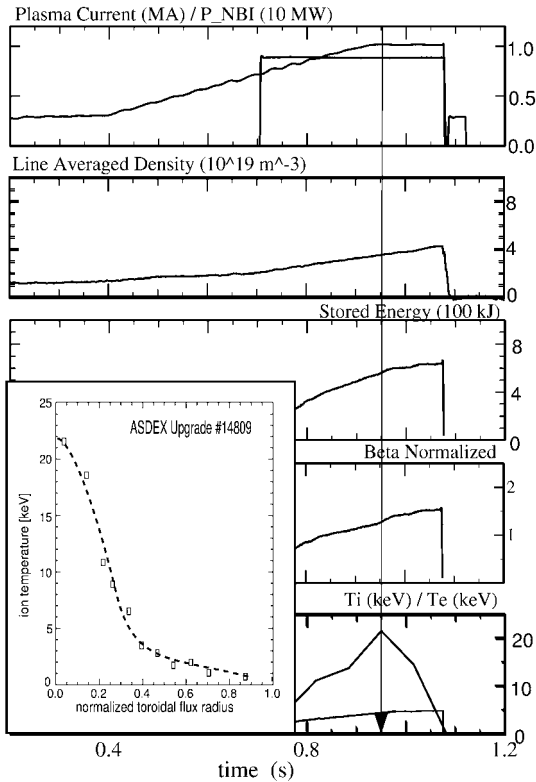


FIG. 4.1: Time traces and ion temperature profile of the internal barrier discharge #14809.

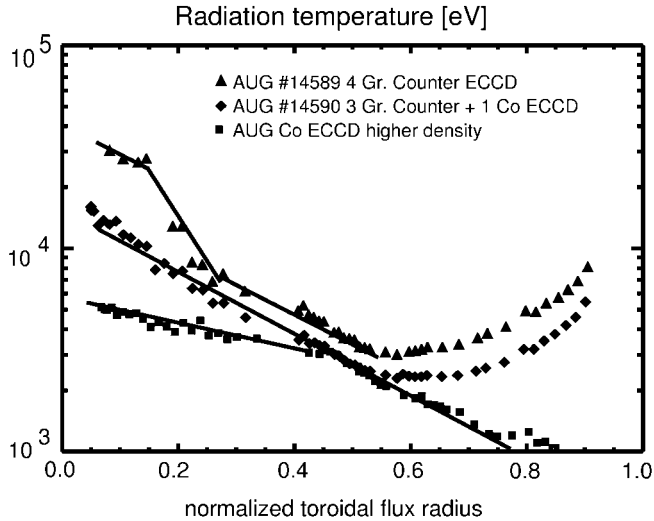


FIG. 4.2: Electron cyclotron radiation temperatures for discharges with different amounts of counter current drive

The electron barriers have, like the experiments in 2000, been generated with counter ECCD. In comparison with the previous year, more stable discharges have been obtained by going to larger currents or broader ECRH deposition profiles. At 0.6 MA electron cyclotron emission ECE radiation temperatures of over 30 keV (see Fig. 4.2) have been obtained at a central density of $1.2 \cdot 10^{19} \text{ m}^{-3}$ with 1.6 MW (4 gyrotrons) of counter ECCD. Changing one of the gyrotrons to co current drive, such that the deposition of power is the same but the driven current is reduced to 50% and the central radiation temperature decreases to 17 keV.

At these low densities, Fokker Planck calculations predict the existence of a significant non-thermal distribution which affects the ECE radiation as shown in Fig. 4.3, which shows the ECE measurements (#14589), the calculated radiation from a Maxwellian with a temperature profile equal to the measured one, and the calculated ECE radiation from the distribution obtained by the numerical solution of the Fokker-Planck equation using again the measured radiation temperature as bulk temperature. The simulations show that the radiation temperature is 30% larger than the bulk temperature which is estimated to be still 20 keV in the full counter current drive case. The 30% difference is insufficient to explain the difference in radiation temperature between full and half counter current drive. Furthermore, the heating power in the discharges with different amounts of current drive is the same and generates roughly the same non-thermal population. It is therefore concluded that the difference in central temperature must be due to a difference in electron heat transport.

A clear barrier is formed in the electron temperature in the case of full counter current drive, as can be seen from the comparison of #14589 and #14590. It is concluded that a sufficient amount of counter current drive leads to the formation of a strong barrier in the electron temperature, and that the formation is probably connected with the more inverted q -profile. Although no MSE is available for these discharges, a difference in the MHD mode behaviour is observed which supports this interpretation.

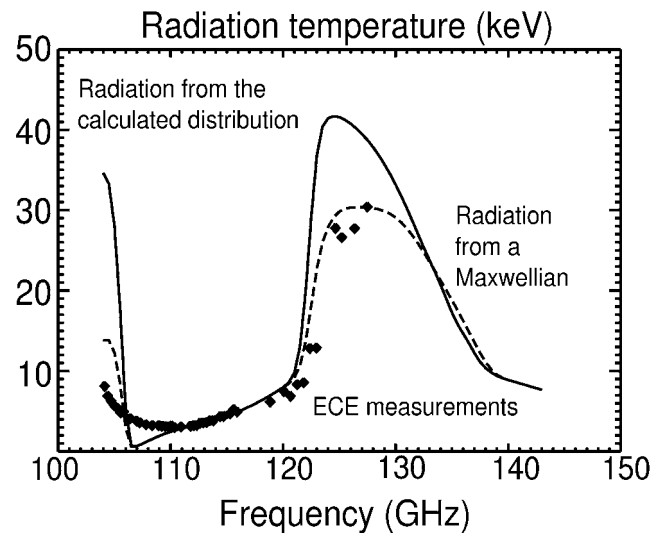


FIG. 4.3: ECE measurements (diamonds), the calculated radiation from a Maxwellian (dotted line), and the calculated radiation temperature from the non-thermal distribution function

5. ELECTRON HEAT TRANSPORT

5.1 Turbulent heat transport with $\nabla T/T$ threshold

For about 2 decades, the temperature profiles in conventional tokamak plasmas (without ITBs) have been observed to be

"resilient" or "stiff": their shape is almost independent of the heating deposition profile. The recent development of ECRH in several devices, and in particular in ASDEX Upgrade, allowed dedicated experimental studies of transport physics responsible for this behaviour. In addition, thanks to the intense development of numerical transport models for both ions and electrons made during the recent years, first-principle transport models are available for comparison with the experiment.

The stiff behaviour of both ion and electron temperature profiles in conventional scenarios is presently believed to be caused by anomalous transport driven by turbulence with a threshold in $1/L_T = \nabla T/T$, or when normalised R/L_T , where R is the major radius. According to theory, turbulence is likely to be driven by Ion Temperature Gradient ITG modes for ions, whereas it might be caused by Electron Temperature Gradient ETG and/or Trapped Electron Modes TEM for the electrons. These instabilities indeed have a threshold in $\nabla T/T$, with different respective values.

This behaviour is illustrated in Fig. 5.1 from calculations for ECRH heated plasmas. Here R/L_T at $\rho \approx 0.5$ was artificially varied to study its influence on electron transport. ρ is the normalized toroidal flux radius. In this figure the heat flux driven by transport clearly increases with R/L_T above a threshold. These results were obtained with the ITG/TEM Weiland model, which provides excellent agreement with the experiment as shown in the next section. The different behaviour of the two shots in Fig. 5.1 is attributed to the difference in collisionality: shot 13558 has low density and high temperature is believed to be in the collisionless regime for TEM whereas it is collisional for shot 12935.

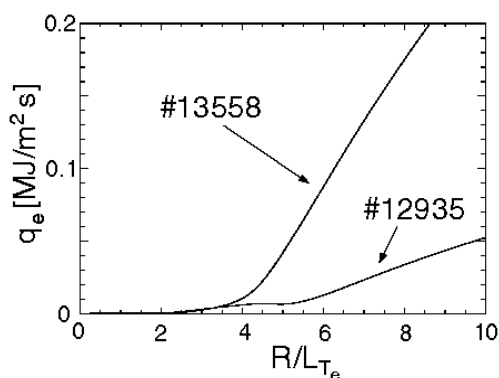


FIG. 5.1: Heat flux versus R/L_T calculated using the Weiland model for the electron heat transport in two cases. The analysis is made at $\rho \approx 0.5$.

According to these curves, at least for collisionless cases, above the threshold transport increases rather strongly with increasing heating power. This prevents in general the R/L_T values of the temperature profile from being larger than 2 or 3 times the threshold. In contrast, at low values of R/L_T , for instance in off-axis cases, transport is quite low. Therefore the R/L_T values of the temperature profile do not fall significantly below the threshold. In summary, this behaviour limits the excursion in R/L_T and provides a certain stiffness. Dedicated experiments carried out in ASDEX Upgrade with steady-state

and modulated ECRH in on-axis and off-axis heating scenarios, demonstrated without ambiguity the existence of the expected threshold for the electron heat transport (see annual reports 1999 and 2000).

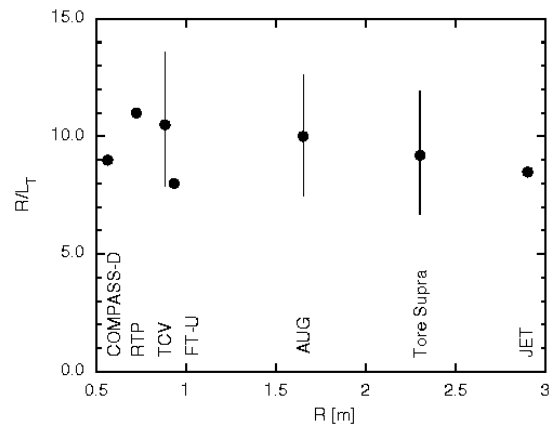


FIG. 5.2: Comparison of R/L_T measured at mid-radius in different tokamaks with central heating. The errors bars indicate the variation with plasma parameters when available.

In addition, the generality of the stiff character of the electron temperature profile has been documented in an inter-machine study including several tokamaks. The results, shown in Fig. 5.2, indicate that R/L_T from the experimental profiles has a very similar value around 10, for a large range in machine size at very different operation parameters. For instance, FTU and TCV have almost the same size but operate at densities which differ by almost one order of magnitude $\approx 10^{19} m^{-3}$ in TCV and $\approx 10^{20} m^{-3}$ in FTU, both heated with ECRH. This general behaviour strongly suggests that the same transport physics, probably with a similar threshold in R/L_T , governs the electron heat transport in the tokamaks considered here.

5.2 Agreement between experiment and theory

The ECRH experiments carried out in ASDEX Upgrade for transport studies have been successfully modelled with the ITG/TEM Weiland model. This is illustrated by modulation data from one discharge in an ohmic phase and in a phase with off-axis ECRH. As shown in previous annual reports, ECRH off-axis deposition determines radially two zones in the plasma with quite different transport. Inside the deposition ("inner region") the T_e gradient falls below the critical value of R/L_T and transport is low. Outside of the deposition ("outer region"), the profiles are driven strongly above the threshold and transport is high. This behaviour is revealed by power balance analyses and by the propagation of heat pulses excited at the edge and travelling toward the centre. The modelling reproduces the experiment with precision as illustrated in Fig. 5.3 for modulation data. The figure shows the modelled amplitude and phase profiles of the T_e modulation from both experiment and theory in the Ohmic case (left) and with off-axis ECRH (right). In the Ohmic case the propagation of the pulses does not exhibit any particular features and the rather slow propagation yields a transport coefficient close to that of power balance. However, the behaviour is quite different with off-axis ECRH. In the outer region the flat profiles indicate the

high transport experienced by the heat pulses. In contrast the steep slope of both amplitude and phase in the inner region are caused by the very low transport.

The good quantitative agreement of the amplitude and of the phase with respect to the modulated ECH demonstrates the ability of the model to reproduce the data with accuracy. It must be stressed that the model used here is derived from first principle physics without adjusting any transport-related parameters. The temperature at $\rho \approx 0.8$, which deals as boundary condition for the simulation, is taken from the experiment.

The good agreement between modelling and experiment suggests, in our ECR heated discharges at least, that the electron heat transport is dominated by TEM driven turbulence.

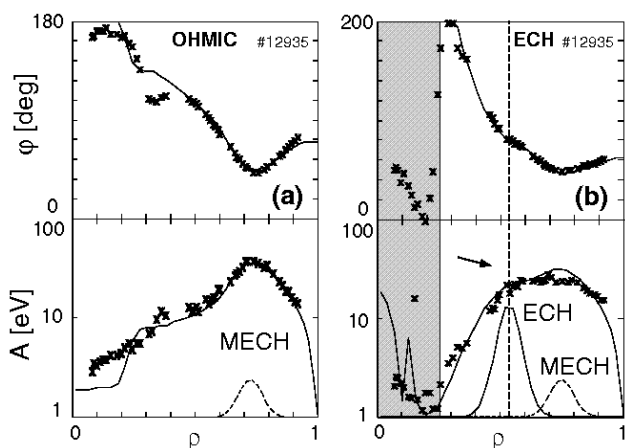


FIG. 5.3: Effect of off-axis ECRH on the propagation of heat pulses: simulation (lines) and experiment (points). Amplitude on logarithmic scale and phase profiles from Fourier transformation versus normalised flux radius. The signal to noise ratio is too low in the shaded region.

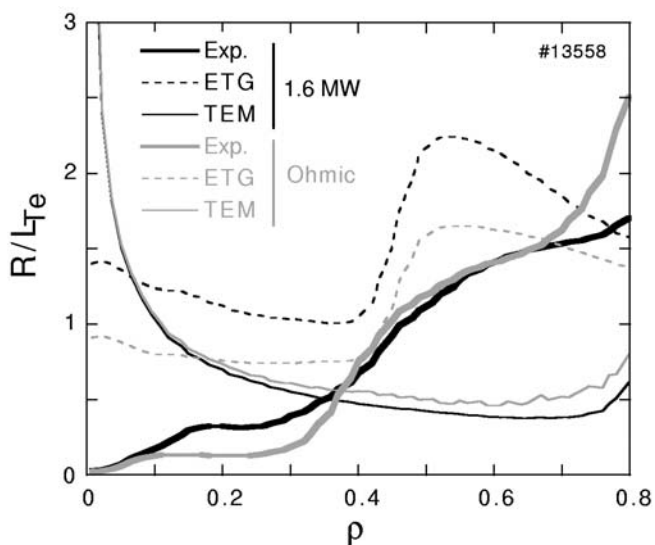


FIG. 5.4: Comparisons of the TEM and ETG R/L_T threshold with the experimental data.

A comparison of the experimental value of R/L_T with the threshold values for the TEM and ETG instabilities delivered by respective analytical formulae is shown in Fig. 5.4. Both the Ohmic phase and that with central ECH heating indicate that the experimental values of R/L_T are above the predicted threshold for TEM but below that of the ETG. Therefore ETG turbulence is not expected to be driven in these cases.

In our simulation with the Weiland model, R/L_T of the T_e profile is also significantly above the TEM threshold in the stiff region. Confirmation is provided by studies with an empirical transport model based on the assumption of a R/L_T : good results for both steady-state and modulated ECH are only obtained only when the R/L_T threshold is lower than that of the T_e profile.

6. MAIN CHAMBER EDGE TRANSPORT AND WALL RECYCLING

The edge plasma layer in the vicinity of the magnetic separatrix of a poloidal divertor tokamak has a surprisingly strong influence on the global plasma performance especially in H-mode type discharges. The steep gradient and pedestal region forming just inside the separatrix controls the global energy confinement at least in case of stiff core temperature profiles. Across the separatrix, this edge barrier region is coupled to the diverted scrape-off layer, which directs the power flow mainly to the divertor target plates (because of rapid parallel heat transport), while particles flow predominantly to, and recycle from main chamber walls. The latter seems to persist even for relatively large wall distance and may be related to the appearance of 'shoulders' and strongly enhanced cross field transport in the scrape-off layer wing as observed already in old ASDEX and in early ASDEX Upgrade experiments. In qualitative consistency with this picture, a clear correlation is routinely observed in experiment between core confinement and recycling flux in the extreme edge. Far edge transport and main chamber recycling has gained renewed interest recently in the fusion community because of its possible impact on first wall design and materials choice in next step experiments like ITER.

Based on high resolution edge diagnostics in combination with advanced analysis tools, this edge region has been analysed in detail. Fig. 6.1 shows electron density, temperature and pressure profiles in logarithmic scale from Thomson scattering (extending from the pedestal inside the separatrix out to the guard limiters) for a medium triangularity H-mode discharge in Deuterium with type-I ELMs (discharge #12200, $I_p = 1$ MA, $B_t = -2.5$ T, $q_{95} \approx 5$, $P_{NBI} = 5$ MW, $\bar{n}_e \approx 8.5 \cdot 10^{19}$ m⁻³ corresponding to about 67% of Greenwald density limit n_{GW} , cryo pump off). The spatial co-ordinate x measures the distance relative to the nominal separatrix position along a horizontal line through the magnetic axis. Actually, the profiles represent averages over a 2.8 s long time interval (including ELMs), during which the plasma is shifted horizontally by 2.2 cm, while keeping shape and plasma parameters as constant as possible. At each laser pulse, the temperature and density values measured in the respective scattering volumes are then

mapped onto the x-co-ordinate along the instantaneous equilibrium flux surfaces. The 'true' separatrix position derived from an analytic edge transport model fit is only 0.1 cm inside the nominal one for this specific shot, a correction which is nearly negligible. The black dots represent box car averages (2 mm box width) calculated on the basis of Bayesian statistics.

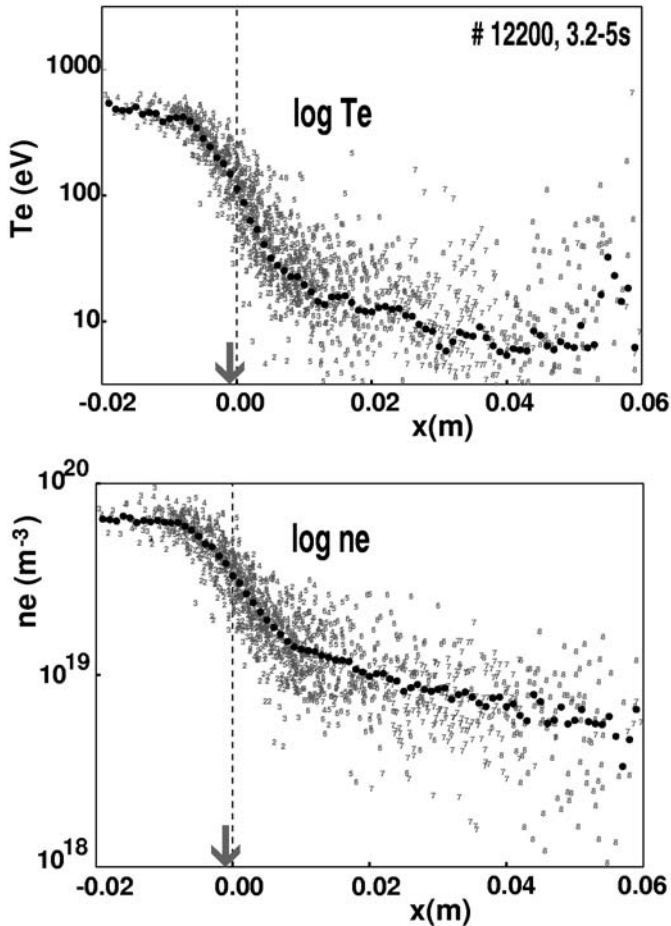


FIG. 6.1: Mid plane profiles of electron temperature and density for a medium triangularity H-mode discharge with type-I ELMs. The arrows indicate the separatrix position obtained from an analytic edge transport model fit. The black dots represent Bayesian averages over a 2 mm radial interval.

Obviously, we can distinguish several qualitatively different radial regions, which are likely to show rather different transport characteristics. The usual H-mode edge pedestal top is located near the inner end of the radial interval chosen. In outward direction it is followed by a steep gradient zone extending across the separatrix (about ± 1 cm), linking closed and open flux surfaces without any remarkable jump at the separatrix. Outside the hot scrape-off layer, the average temperature is low and the average gradients become much flatter again, but now with increasing relative scatter. There is also no clear signature of the second separatrix (at $x \approx 2.5$ cm) on the profiles.

Cross field transport in the steep gradient region shows the strong magnetic field dependence typical for ballooning modes as widely discussed in the H-mode pedestal literature. The smooth transition across the separatrix indicates that there is practically no change in anomalous cross field transport across the separatrix despite the transition from closed to open field lines. The similarity of the radial electron temperature and density profiles in this region suggests that, in parallel to a rather stiff pressure gradient, there is a correlation between the density and temperature decay lengths, making these profiles separately stiff in effect. In order to check this relation in more detail, we plot these profiles against each other (Fig. 6.2). While the individual data points still exhibit a strong scatter, the average profiles represented by the Bayesian mean values form essentially a straight line over a range extending from the pedestal top down to the outer edge of the hot scrape-off layer. The corresponding functional form is close to $T_e \sim n_e^2$, equivalent to $\eta_e = d(\ln T_e)/d(\ln n_e) \sim 2$, and could be consistent with a critical η_e behaviour typical for drift modes. About the same η_e value is obtained for all type-I ELMy H-modes looked at hitherto. Despite rather different plasma parameters, similar values are obtained for the low density phase of the L-modes, while the high density discharges closer to the empirical density limit shows somewhat higher values.

Transport in the scrape-off layer wing is strongly enhanced compared to that in the steep gradient zone. Taking average density profiles together with the corresponding measured particle recycling fluxes we get effective transport values far beyond Bohm diffusion in agreement with earlier findings. The strong scatter of density and temperature together with a statistical analysis of 'valid' data points in different radial channels indicates a highly turbulent structure in this region. A minority of hot filaments (not correlated with ELMs) seems to exist with temperatures comparable to those in the steep gradient zone.

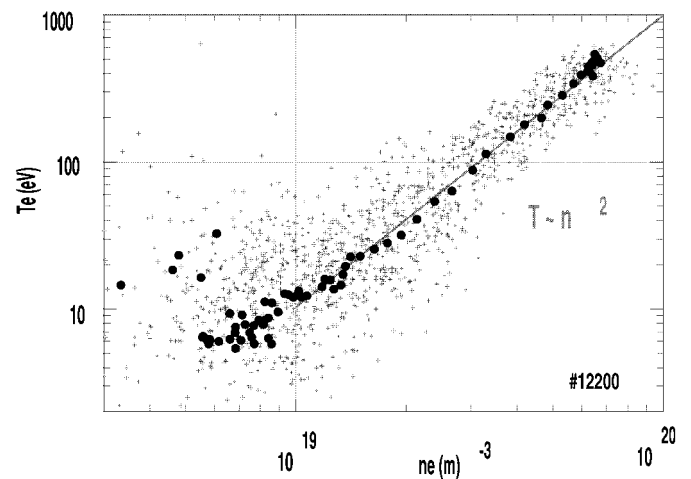


FIG. 6.2: Electron temperature and density data (including the Bayesian averages) for one the H-mode discharge as shown in the preceding figure are plotted against each other in double logarithmic scale. The straight line added corresponds to $T_e \sim n_e^2$, equivalent to $\eta_e = d(\ln T_e)/d(\ln n_e) \sim 2$. Remember that the separatrix corresponds to $T_e \sim 110$ eV and the flat scrape-off layer wing to $T_e > 20$ eV.

If these structures would, in fact, originate from this hot region and drift across open field lines, they would have to move fast enough to avoid electron cooling along field lines. Typically, an average radial ExB drift velocity beyond 1000 m/s is needed in order to survive, equivalent to a poloidal electric field of a few kV/m. This would be consistent with a potential drop of the order of kT/e over a filament diameter of a centimetre, consistent with the old ASDEX Langmuir probe analysis.

In effect, these results suggest that a local diffusive transport model is inappropriate to describe this region. Furthermore, this rapid scrape-off layer wing transport causes practically a short circuit between the hot barrier plasma in the separatrix vicinity and the outboard limiters, causing strong main chamber wall recycling even for fairly large wall distance. In contrast, the energy flux to the main chamber walls calculated from these data remains a small fraction of the heating power.

7. TECHNICAL SYSTEMS

After the rebuild of the lower divertor (DIV II \rightarrow DIV IIb) and the turning of the access port for the 100 keV neutral beam injector, starting in August 2000, the experiment resumed operation in April 2001. For the rest of the year, the experiment was in operation for 61 days performing 961 pulses in total. 56 of those days were dedicated to physics. The rest served for technical commissioning, calibration of diagnostics and servicing.

Lower divertor and NBI port: Two physical aims were driving the rebuild. The whole bandwidth of triangular plasma shapes should become consistent with a closed lower divertor. NBI should provide current drive at mid plasma cross section. To realise the new divertor in the plasma vessel, about 60.000 single parts had to be handled for pre- and main assembly. The required structural changes also entailed about hundred diagnostic modifications. Turning the NBI beam line required a partial rebuild of the poloidal field coil supports and a completely new access port. To be able to maintain the narrow tolerances required, the port cutting and welding operations were optimised on a spare vessel octant prior to their execution on the original vessel.

The summer opening, from August to mid October, was mainly dedicated to improvements on the inner heat shield and the upper inner target plates. The graphite tiles of the latter were also reshaped to reduce recycling also for upper Single Null configurations. The heat shield tungsten coating was extended to 6.5 m², leaving blank only the NBI dumps, made from fibre re-enforced graphite. A new heat shield tile design could be established by heat flux tests, withstanding even with standard graphite the NBI fault condition heat loads. In a first step, the new tiles were mounted on only two mid-plane rows of the start-up limiter, before covering them with the total heat shield next summer. The new tile design reduces the heat flux density both by doubling the toroidal length and improving the support precision. In addition, the clearance between toroidally adjacent tiles will be reduced for all poloidal positions from ≈ 20 mm towards 5 mm.

New helium supply circuit for the cryo pump: The helium consumption of the cryo pump could be reduced considerably. The modified He cryostat now effectively recovers the liquid leaving the cryo pump. A new LN₂ shielded feeder between the He cryostat and the 3000 l storage tank, together with a 80 m long shielded transfer line to the 5000 l liquifier vessel, further reduces the transfer losses. In addition, the capacity of He supply and He recovery were increased to cover continuous cryo pump operation. A TCF 50 liquifier is currently under commission. The He-recovery storage was doubled and is now consistent with the total tank inventory of 8000 l. The He recovery line with increased diameter now mitigates the pressure burst due to vessel glowing to an acceptable level.

Energy supply: Commissioning of the reactive power compensation RPC modules No. 3 ñ 8 for the EZ3 generator was completed in August. Since then the RPC system (8 x 15 MVar) has routinely been operated with the modules being

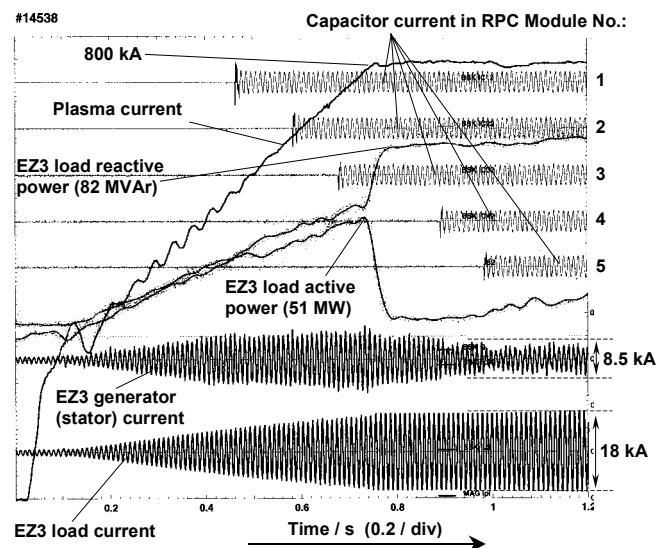


FIG. 7.1: Generator load reduction by RPC during a discharge

activated by feedback control. Fig. 7.1 shows the beneficial effect on the EZ3 stator current due to RPC. The reduction by a factor of two in current provides a significant increase of the plasma flattop duration. To further improve the energy supply conditions for the 10 kV grid, the technical design for paralleling EZ3 and EZ4 (hardware, multi-variable controller including interfaces to the existing controllers and supervision), has been elaborated in co-operation with industry to such an extent that a European call for tender could be envisaged for late 2002. The concept of paralleling synchronous flywheel generators is further pursued in co-operation with Rostock University. The aim is to achieve a stepwise extension of the flywheel energy by small generators existing on the market. Four of them are to be combined to a 36 MJ unit feeding into the 10 kV grid via a transformer. A feasibility study, completed in December, suggests this concept. The study results encourage carrying on with two prototype units, first being tested at the manufacturer's and then on site. It is envisaged to accompany these tests by further numerical simulations.

7.1 Optimisation of operation procedures and machine protection

A next-generation time system was developed for the new real-time plasma control and data acquisition. This novel approach makes time a unique measurable quantity throughout the experiment site. Timestamps are sampled with triggers for I/O of analog or digital signals or upon task scheduling. This eliminates problems of hidden delays in signal paths or a prior unknown real-time scheduling. A 64-bit time representation at 1 ns resolution outlasts the lifetime of the experiment. Entities of sampled data and associated timestamp simplify data archiving and naturally support steady-state operation schemes.

The PCI-based time system consists of a central time generator board, a unidirectional optical star network, and Time-to-Digital TDC convertor boards (similar to ADC boards) located at hosts or frontends. Once started, the central time generator (currently clocked with 50 MHz) periodically increments the 64 bit time counter. Clock and time count are broadcast and regenerated by all TDC boards, which sample timestamps upon external triggers (e.g. operated in parallel to ADC channels), or host access. Moreover, they output trigger pulse trains (e.g. to trigger ADC and TDC input) upon host command or external triggers.

To support ongoing experiments, the old plasma control system was again upgraded to feedback control divertor temperature with thermocurrents via gas puff, counteract excessive mode activity and monitor machine critical power thresholds of neutral beam injection. A vertical displacement event VDE reflex was added to plasma position control which upon VDE detection applies a radial field such that the disruption pending is pushed to the lower divertor. Especially for higher triangularity or close-to-double-null plasma configurations this shifts the mechanical stresses arising from a disruption to the more robust part of the vessel.

A tool for designing plasma shapes under the technical constraints of ASDEX Upgrade has been developed for public access. This offers to experimentalists the possibility to tune and check a proposal in advance. The interactive tool allows us to select equilibria from previous experiments as design starting points and to calculate the effects of modifications. Shape parameters can be set to definable values while the necessary PF coil currents are calculated. Scaling the plasma current or the toroidal field is also possible. The predicted results are checked against the constraints of power supply, coil suspension force, equilibrium stability and user-defined ranges for equilibrium variables. Violations are signalled and the user can adapt his demands until a feasible configuration is found.

7.2 Control room refurbishment

The new ASDEX Upgrade control room went into operation early in 2001. The old number of working desks for physicists and control staff were nearly doubled to achieve a total of 87 seats. Compliance with new statutory technical orders for workstation ergonomics was reached by using TFT instead of the old CRT screens. However, not only the seating and the

screens were changed but the whole information technology behind them was rebuilt to achieve maintainability and improved performance with respect to the increased number of users and tasks expected in the new environment.

- The whole control room has been covered with a fibre optic network emanating from a central patch field and providing two double connectors per table and per cupboard.
- A central Extreme Networks Black Diamond switch was set-up to integrate the control room into the ASDEX Upgrade GigabitEthernet backbone. Gigabit- and FastEthernet modules, as well as satellite switches distributed over the control room, now provide bandwidth which is gradually adaptable to the endpoint demands.

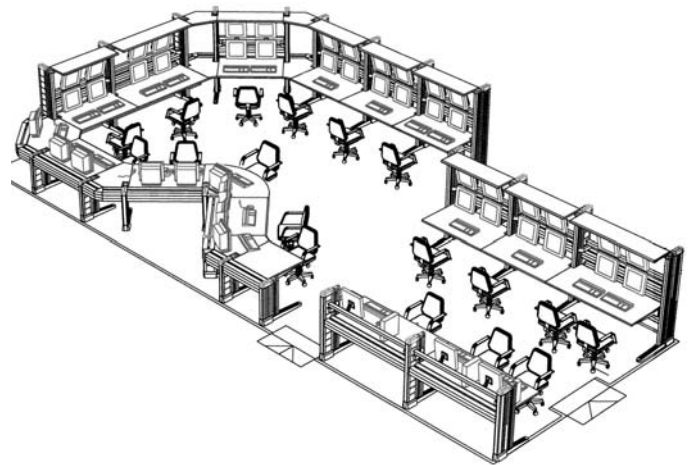


FIG. 7.2: The CAD drawing shows the workstation arrangement for the ASDEX Upgrade technical control booth.

- SunRay appliances (i.e. a zero administration thin client based on the SunRay software technology) have been chosen as workstation systems. Experience with this new platform is very satisfying especially with respect to the promised low administration overhead per installed system.
- The thin clients have replaced the former UNIX consoles of the diagnostic computers and in fact most of the diagnostic computers are now running screen-less or X-mote controlled via the network.
- At first two reasonable powered central servers (SunEnterprise 250) with 2 processors and 4 GB real memory each were foreseen to maintain performance and server backup facilities for a continuous experiment operation. At the end of 2001 further server capabilities became highly desirable.

7.3 Neutral Beam Injection

Following regular maintenance and a repair of the leaky gate valve, the first neutral beam injector (NI-1, 60 kV, 10 MW D⁰) was ready for injection at the end of the 2000/01 shutdown of ASDEX Upgrade and has operated reliably since then.

One of the major tasks to be completed during that shutdown was the re-orientation of the second injector (NI-2) as a whole towards a more tangential injection and the optimisation of its beam geometry with respect to off-axis NBI current drive; details were given in the previous Annual Report. The modified injector has been available for experiments since June 2001 and delivers, as expected, up to 10 MW of D^0 beams at 93 kV. In Fig. 7.2 the new beam geometry is illustrated and compared with the one of NI-1. During the phase of re-commissioning and initial injection into the plasma the functioning of the new parts of the system has been carefully monitored: The remote beam steering units necessary to change the vertical beam inclination between shots onto the calorimeter and into the plasma work reliably, the heat load of the magnetically deflected ions on the newly positioned ion dumps is well within the tolerances for all possible inclination angles and the geometrical transmission of the neutral beam through the new vessel port (see Fig. 7.2) is comparable to the one prior to the modifications. However, the internal C-tile protection of this new port against power loading from the re-ionised particles, deflected and focussed by the tokamak stray field, turned out to be insufficient. Melting traces have been discovered at unprotected surfaces far away from the neutral beam. In order to prevent the duct pressures from reaching too high a level, duct protection was extended and a more sensitive beam interlock has been operated since the summer shut down.

As part of the commissioning of the new tangential injector individual beams have been compared with respect to plasma heating with the corresponding beams of NI-1. Fig. 7.3 shows an H-mode discharge at "natural" density where a constant heating power (5 MW) is initially applied by the normal beams of NI-1, followed by the new off-axis tangential beams of NI-2 and, finally, by the more tangential, centrally heating beams of NI-1. Obviously, off-axis deposition of the heating power does neither affect the attained plasma energy content nor the density or other global parameters.

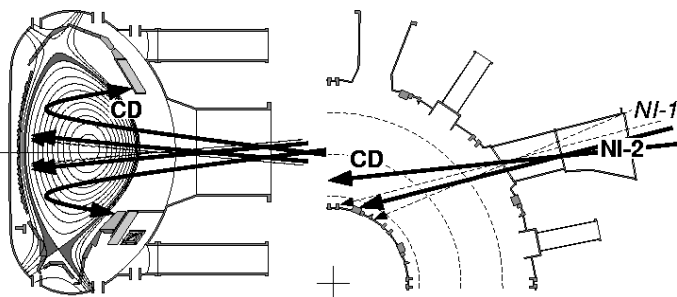


FIG. 7.2: Geometry of the four beams of the new tangential injector NI-2 (thick lines). For comparison the geometry of NI-1 is shown (broken lines).

However, the sawtooth behaviour, as illustrated by a central SX channel, or more generally, central MHD (also fishbones, (1,1) modes) is strongly influenced by the changes in beam power (and fast particle) deposition. Further experiments with the new tangential injector are described elsewhere in this report.

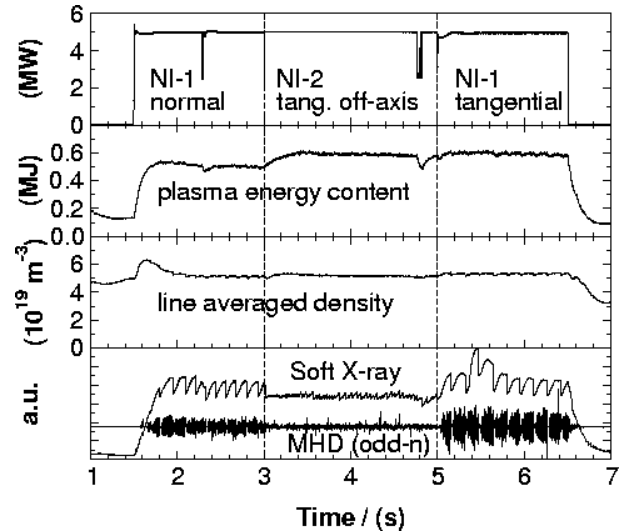


FIG. 7.3: Comparison of heating by off-axis tangential beams with beams of NI-1 at natural H-mode density.

7.4 Ion Cyclotron Resonance Heating

The power tetrodes are no longer manufactured commercially, however, three were successfully re-furbished by industry (mainly equipped with new cathodes and grids) and are now able to reach their original output power. Thus the lifetime problem of the 12 year old tetrodes seems to have been solved and a technically critical and expensive adaptation of the generators to another tetrode type can be avoided.

The ferrite matching system has been delayed but the main development efforts have been completed and delivery can be expected in 2002. As described in the last annual reports, this system will allow fast automatic matching of the antenna impedance, resulting in higher and constant heating power at plasma variations.

For feeding the RF probe for antenna breakdown studies (see Technology Division, Section 2.1) the RF system was supplemented by a feeding line and a resonator set-up at ASDEX Upgrade as well as by control and measuring devices required to operate the probe. It is fed by one of the ICRH generators and can be operated alternately to one of the two antenna systems.

7.5 Electron Cyclotron Resonance Heating

After the 9 month shutdown of ASDEX Upgrade, all four gyrotrons of the ECRH system were reactivated in rather a short time and without any problem. Thus all 4 gyrotrons have been available for most of the 2001 campaign. A transmission problem which occurred at the end of the year was due to an unexpected misalignment of one mirror, so that the quasioptical beams no longer entered the wave guides centrally and caused arcing with a subsequent switch off of the system.

A new ECRH system with target parameters 4 x 1 MW for 10 s is presently under construction. A particular feature of the new

gyrotrons will be the capability to work either at two frequencies, 105 or 140 GHz for which the diamond vacuum window is resonant, or at many frequencies in between making use of a Brewster angle gyrotron window. At the torus a Brewster angle window is inconvenient since it does not allow arbitrary polarisations to be transmitted. Here we think of developing a tuneable double disk window.

The launching mirrors inside the torus will allow a fast poloidal scanning to follow changes in the q-profile during a shot, and also a slow toroidal scanning to allow co- or counter ECCD. All four launchers will be in one A-port in sector 5. The fast mirror will be a radiation cooled copper coated graphite plate. The beam is designed to have a Gaussian profile with a power density diameter of < 50 mm anywhere in the plasma.

Due to our good experience with 87 mm HE-11 wave guides under atmospheric pressure and because of space limitations and safety considerations, the decision was made to use a wave guide transmission scheme again, with one line for each gyrotron. The gyrotrons will be located about 50 m away from the torus where we will not have any problems with stray magnetic fields like in the old system.

The arrangement of the gyrotrons will be crosswise with a central high power long pulse load serving as a dummy load. There will also be 1 s loads for each gyrotron allowing a quick start-up of the system each morning. At the end of the transmission lines we will again have 0.1 s loads to test the transmission before switching the beam to the plasma.

We will use the available thyristor controlled power supplies for the beam voltage, together with one tetrode modulator for each gyrotron, which will lead to more flexibility than we had with the old system, where two gyrotrons were fed from one modulator. A big advantage will be the use of depressed collectors. The beam voltage will be only 60 kV and we will need only one 70 kV module to run two gyrotrons (in the old system we had to use two such modules in series).

A first gyrotron is expected to come early in the summer of 2002. The installation of a first set of mirrors into the torus is planned for the end of summer 2002.

8. CHARACTERIZATION OF DIV II B

In 1997 the original 'open' AUG divertor DIV I was replaced by the rather 'closed' LYRA divertor DIV II. In support of ITER, this DIV II (see Fig. 8.1) had been designed for optimal divertor volume losses, high pumping efficiency etc., if used in connection with a narrow class of well-fitting low δ equilibria. These expectations were, in fact, nicely confirmed during a run period of several years. In parallel to these optimized divertor studies, there was increasing interest in strongly shaped, especially higher triangularity plasmas, because of their improved confinement at high plasma density and the possible access to type II ELM's etc. In DIV II geometry, these plasmas could be produced by positioning the outer divertor plasma leg on the top of the roof baffle located between the two curved vertical targets. Therefore some of the DIV II benefits were

degraded, especially the power load characteristics and the pumping capability of the cryo-pump placed in the outer divertor region. To overcome this, the roof baffle and the outer part of DIV II were reconstructed (DIV IIb) to accommodate a large variety of plasma shapes up to bottom triangularities of 0.48.

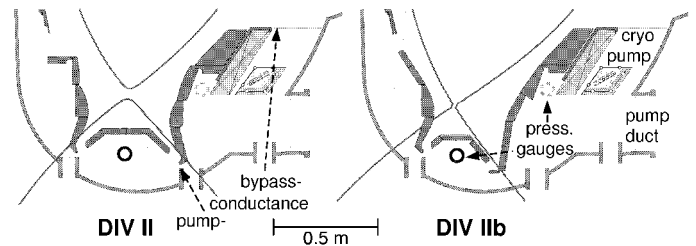


FIG. 8.1: DIV II and the new DIV IIb with low and high δ equilibria. The pressure gauges measure the neutral particle flux densities

According to the positive experience with the power handling in DIV II, ordinary grain graphite has been chosen for the outer strike point region. The tiles are, as in DIV II, slightly tilted in toroidal direction in order to hide the leading edges. In the poloidal cross section, the outer strike point module forms a straight line with larger poloidal angle to the flux surfaces. The resulting incidence angle of magnetic field lines therefore increased from values below 2° to $\approx 4^\circ$. The inner part of the divertor strike point module remained unchanged, but at the divertor entrance a smooth transition to the inner heat shield is provided to minimize local hydrogen recycling there. The roof baffle is diminished at the outer part to allow the outer divertor plasma leg to hit the strike point module even for the highest triangularities. The conductance to the cryo-pump is not affected by the new shape. The related diagnostics were adapted. Operation with DIV IIb started in April 2001. After the transition from DIV I to DIV II experiments suggested that the 'inward' reflection of neutrals at the vertical target was a key point for the reduction of the parallel heat flux by a factor of 2. Even shifting the strike points upwards by nearly 10 cm away from the V-shaped, narrow divertor corner to a region above the roof baffle had little effect on the heat flux profiles.

In DIV IIb the outer strike point of the low δ equilibria also lies clearly above the baffle region. Thermographic measurements show that the maximum heat flux perpendicular to the target is higher by 70% compared to DIV II for low density H-mode discharges. At least part of this increase is due to geometrical reasons because of the larger field line inclination hitting the targets. The total integrated power load increased also by almost a factor of 2. Fig. 8.2 shows the corresponding fractions of the divertor radiation. For comparison the values of DIV I and DIV II are included. The reduction of the load in DIV II was attributed to strong carbon radiation in the dense divertor plasma. This resulted also in a substantial increase of the total divertor radiation to values $\approx 40\%$ almost independent from the input power. Comparing DIV IIb and DIV II for low δ cases, similar radiation levels are found, although in DIV IIb the strike points are well above the baffled region. For medium to high δ discharges the outer divertor leg is now placed on the vertical target instead on the roof baffle. Since the radiation

levels are similar in this case, too, the lower values have to be attributed to more subtle effects like effective divertor depths than just the target modifications.

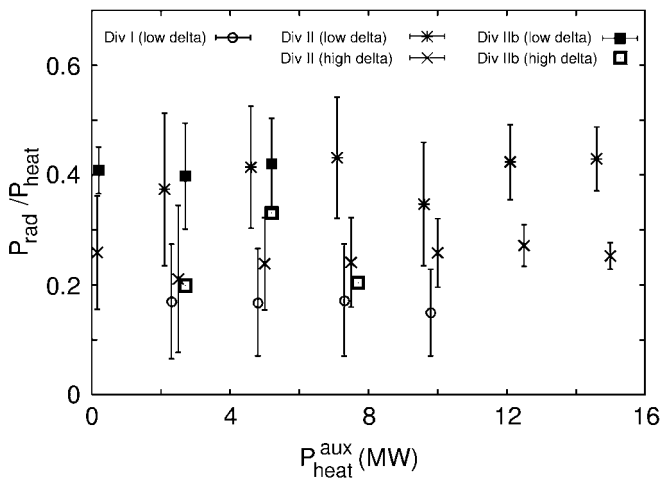


FIG. 8.2: Fraction of the divertor radiation over auxiliary heating power. The vertical bars indicate the typical ranges due to plasma parameter variations.

Experiences in AUG and JET show that the divertor geometry can strongly influence the plasma parameters in the divertor and to certain degree also in the plasma edge. This may diminish the operation window in terms of the formation of MARFE's, but early onset of detachment leads also to the desired strong reduction of the power flowing to the divertor plates. Whereas the maximum T_e at the separatrix is 10 eV higher in DIV IIb than in DIV II, it is quite similar in the SOL in both cases. Of special interest here is also the relation of the recycling fluxes in the divertor and the main chamber. Comparisons show that for the old low δ as well as for higher δ no distinct differences in the neutral particle pressures are found, in contrast to simulations with the B2-Eirene code. This might be explained by the fact, that the divertor pressure is mainly maintained by the colder inner divertor leg, the configuration of which remained unchanged, and that the plugging by the outer leg is still effective despite its larger distance to the gap. A key feature of DIV II was the high He compression accomplished by the narrow divertor leg which hindered effectively the back flow of neutral particles. This behaviour was reproduced by B2-Eirene calculations, which predicted also a degradation of the compression accompanied by the strong decrease of the hydrogen flux density in the pumping plenum. First results (see Fig. 8.3) confirm the trend predicted by the modelling, however the observed reduction is still much smaller than expected.

In parallel, a clear reduction (about 20%) of the L-H mode transition power threshold for low δ configurations has been found. First edge density measurements in the outer midplane indicate that the density at the separatrix and in the SOL is lower, pointing out the importance of local edge parameters, as already seen after the change from DIV I to DIV II, where an increase of the threshold power was found.

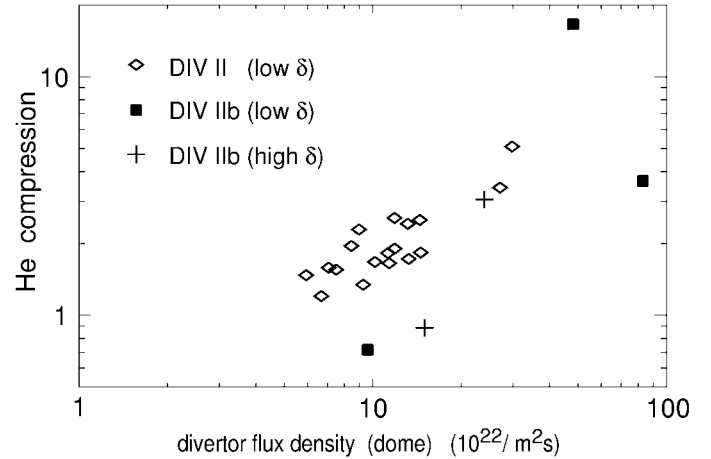


FIG. 8.3: He compression for 5 MW NBI heated H-mode discharges.

9. CORE PLASMA PHYSICS

9.1 Improvements of plasma position and shape control

New discharge scenarios with plasma shapes adapted to the new lower DIV IIb have been designed. These shapes have medium or high triangularity fitting the plasma legs deep in the divertor. An edge-optimised configuration EOC shape furthermore features an almost constant distance to the ICRH antenna in the midplane and optimal placement with respect to diagnostic laser beams for plasma edge investigations.

To improve and validate the magnetic plasma model used for feedback controller design a set of plasmaless experiments with multi-sine perturbation by PF coils has been executed in collaboration with CRPP (Lausanne). From the field and flux signals measured frequency transfer functions can be deduced and compared with the characteristics of a theoretic model. Investigations will be continued in the next experiment campaign with plasmas.

To evaluate the effects on the magnetic configuration and measurement signals exerted by ferromagnetic materials close to the experimental set up and by eddy currents induced in vessel and structures during dynamic phases, special FE-models are being developed and analysed with the ANSYS programme package.

9.2 MHD equilibrium identification

Function parametrization FP: To reflect the extended parameter range of ASDEX Upgrade, in particular higher triangularities, a new data base of equilibria was generated. The coefficients derived from this led to a new FP version which is in rather good agreement with interpreted equilibria using the CLISTE code. Development continued on a new FPJ algorithm to recover the q profile in real time using MSE data combined with equilibrium magnetic measurements.

CLISTE code development: The main avenue of code development in 2001 centred on the interpretation of kinetic

data, in particular high-resolution Thomson scattering profiles of the pedestal region. With the aid of a code provided by O. Sauter, CRPP Lausanne, a detailed comparison of the reconstructed pedestal current density profile with that expected from neoclassical calculations was carried out. The results showed reasonable agreement between interpreted and calculated plasma current profiles at the pedestal.

CLISTE fitting solely the magnetic measurements is run routinely for up to 100 equilibria per discharge. The results EQI and GQI (equivalent to FPG) are usually available within 1/2 hour after the discharge.

The interface between magnetic measurements and FP results on the one side and CLISTE on the other has been extended to be used also by DINA - the equilibrium package developed at the Kurchatov Institute.

9.3 NBI deformation of the electron velocity distribution

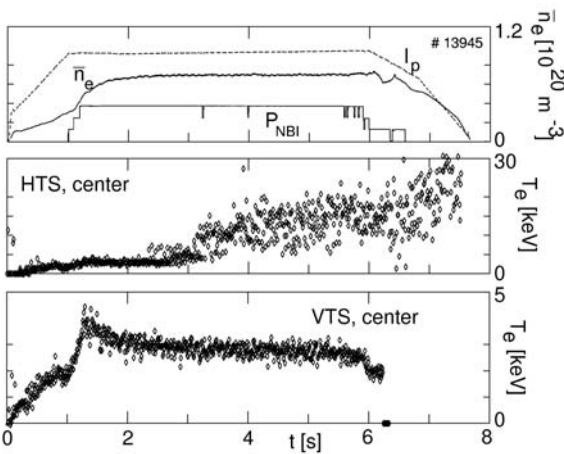


FIG. 9.1: The figure shows a typical example of diverging central electron temperature measurements, performed by the horizontal HTS and vertical VTS Thomson scattering systems.

On ASDEX Upgrade two Thomson scattering diagnostics are now installed, which are sensitive to different parts of the electron velocity distribution function: The Vertical Thomson Scattering VTS system analyses the velocity distribution mainly perpendicular to the magnetic field, and the Horizontal Thomson Scattering HTS system is sensitive to a segment of the velocity distribution which is centred around a pitch angle of 135 deg.

During H-mode discharges when the neutral beam injection is applied early in the discharge, during the current ramp up phase or directly after it, the apparent temperature observed with the HTS system increases in the centre of the plasma up to 20 keV after a delay of about 2 s with respect to the beginning of the NBI. The temperature measured with the VTS system, however, stays constant at about 3 keV in this phase (Fig. 9.1). This high apparent temperature measured with the HTS system usually relaxes again with a time constant of 1-2 s to the values measured by the VTS system after NBI is switched off.

9.4 Central Z_{eff} measurements and further applications with a new pulse height analysis diagnostic of soft x-ray spectra

With a newly introduced Silicon Drift detector allowing count rates up to 10^5 s^{-1} and a resolution of 160 eV at a quantum energy of 6 keV, a pulse height analysis diagnostic of the central soft x-ray emission in the energy range 1-20 keV was introduced. In most cases the line of sight crosses the centre of the plasma.

Impurity elements present in the plasma, like Si, Ar and Fe can be identified from the observed line radiation in the spectra and the electron temperature T_e of the central plasma ($\rho_p < 0.35$) which is obtained from the continuum deceleration radiation and recombination radiation.

The concentrations of the impurities, Z_{eff} and T_e can be obtained by fitting these quantities to the absolutely calibrated spectra. The obtained values of Z_{eff} and T_e are in good agreement with the values of Z_{eff} obtained from a line-of-sight averaged Bremsstrahlung signal in visible light and Thomson scattering measurements (see Fig 9.2). High energy electrons are observed often in coincidence with the horizontal Thomson scattering system. In these cases the soft x-ray spectra have to be fitted by a Bi-Maxwellian distribution.

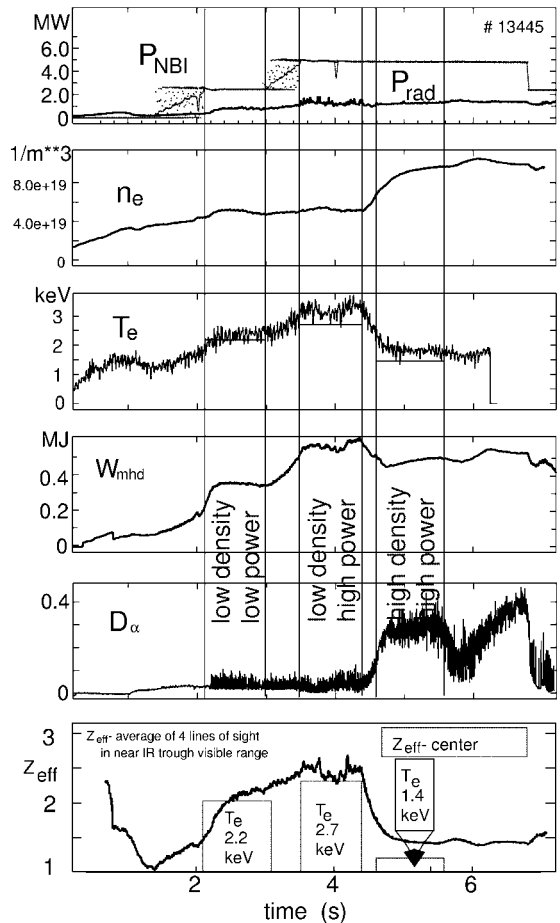


FIG. 9.2: Z_{eff} comparison of the central (from X-ray, denoted by boxes) and the average (from visible bremsstrahlung) values in a so called 'standard H-mode discharge'.

9.5 High speed pellet launch from the magnetic high field side and ELM effect mitigation

Increasing the penetration depths of pellets launched from the magnetic high field side HFS has been proven as a means for improvement of the refuelling performance. With the pellet born particle deposition profiles shifted towards the plasma centre, reduction of post pellet particle and energy loss rates takes place. Consequently, deeper pellet penetration reduces the required pellet flux to achieve a requested density enhancement and thus keeps confinement high. Density perturbations forming an upper limit for acceptable pellet sizes, thus the pellet launch velocity is the only parameter for penetration improvement in a given target discharge. To maximise available launch speeds but also maintaining high pellet delivery reliability, the preliminary "sprint" HFS launch looping set-up was replaced by the final, fully optimised system. With this system smoother pellet guiding paths are now possible. Moreover, an enlarged gas expansion dump as well as a strongly enhanced pumping capability reduce friction by the ablating gas in the guiding tube. In the final system reliable pellet delivery up to pellet speeds of about 900 m/s was achieved. However, it was found that the pellet size still undergoes some reduction during the transfer. These losses increasing with pellet launch speed can be drastically reduced when hardening the pellet ice, e.g. by doping with small amounts of Nitrogen. Best results have been obtained by adding about 0.5 vol % of Nitrogen to the Deuterium gas used for pellet production. At higher doping grades mechanical pellet stability starts to decline again. Even with the highest doping grades applied (2 % Nitrogen) no significant change of the plasma impurity content was observed. This way of pellet hardening is well suited to achieve enhanced refuelling performance.

Injection of small pellets at an adequately high repetition rate has been proposed for controlled release of ELMs in order to avoid occurrence of giant ELMs removing large fractions of particles and energy from the plasma and causing immense transient heat loads in the strike point regions. The first exploratory experiments were performed making use of the high available repetition rate of the pellet injection system up to 75 Hz. In the H-mode regime, every pellet was found to trigger at least one instant ELM. Regular pellets designed for refuelling purposes caused a density increase of about order of $\bar{n}_e \sim 1 \cdot 10^{19} \text{ m}^{-3}$, releasing a sequence of ELMs lasting longer than typical regular type-I ELMs. Reduction of the pellet mass down to about 1/5 of the regular size was achieved by launching "sliced" undoped pellets at high velocities. Reduced pellet mass and hence density increase resulted in a strong reduction of these post-pellet ELM losses while the initial ELM was still triggered. For the smallest pellets injected, still causing about 3 times the density perturbation of a regular type-I ELM, total induced energy losses imposed by the pellet had almost shrunk to the energy loss imposed by a regular type-I ELM. Experiments continuing this promising first approach will be conducted in 2002 aiming at a set-up allowing for controlled ELM release and mitigation of related losses.

9.6 Improved interpretation of density fluctuations

The output of a Landau-fluid turbulence code DALFTI has been successfully coupled to three different 2D reflectometer simulation codes: a finite-difference time domain full-wave code, a time invariant network full-wave code and a physical optics code. The purpose is to allow a direct comparison of numerical turbulence simulations and experimental measurements from a tokamak device, and hence provide a means of validating code predictions. Since real turbulence properties can only be inferred via diagnostics, the inherent diagnostic response function must first be modelled and then applied to the numerical data. For the edge and core regions of a tokamak the most appropriate diagnostic for measuring localised density fluctuations in the Ion Temperature Gradient and Trapped Electron Mode instability wavelength range ($\lambda_{\perp} > \text{few cm}$) is reflectometry. Using spectral and statistical data analysis techniques, real reflectometer signals from an L-mode edge discharge compare favourably with simulated density perturbations from the reflectometer kernels and DALFTI code modelled on the same discharge.

9.7 Disruptions

An accurate analysis of the halo current asymmetries and their physical origin (1), and the use of large fluxes of impurity gas for disruption mitigation (2) have been the main investigation points in the framework of disruption studies.

(1) The halo currents and the forces on the vessel are known to be toroidally asymmetric but the origins of these asymmetries has not been yet clarified. Several disruptions in flat-top in the shot range 13000-14050 of ASDEX Upgrade were considered with the aim of analysing the asymmetries of the halo currents and the correlation among the asymmetries and the MHD activity during the disruption and the plasma parameters. The halo currents in ASDEX Upgrade often exhibit an $(n=1, m=1)$ structure; the $n = 1$ structure is always clearly correlated with a reconnection phenomenon seen by several diagnostics and appears when q_{cyl} approaches or becomes smaller than 2 (see Figure 9.3). The SXR emission drops abruptly after a strong kink-like movement of the plasma centre, the D_{α} signal and the heat load measured by the thermography show a large flux of particles and heat to the structures and the Mirnov coils a strong positive voltage spike.

Several observations (not all reported above) are consistent with the following picture. The $(n = 1, m = 1)$ structure of the halo current has to grow on the $q = 1$ surface; at the time of the asymmetry growth the $q_{cyl} \sim 2$. It is not clear if the $q = 2$ surface plays a role in triggering the $(1,1)$ mode or if this mode is triggered by the interaction of the $q = 1$ surface with the wall. In any case, the dominant role of the $q = 1$ surface is consistent with parametric studies of the current profiles and with the following facts: when the toroidal plasma current profile is flat then the $q = 1$ surface is small or absent and therefore (a) after killer-pellet, (b) in turbulent post-disruption phases and (c) in plasmas with a fast current quench (no re-heating, no re-

peaking of the flat post-thermal-quench current profile, absence of SXR emission) the (1,1) structure is not seen.

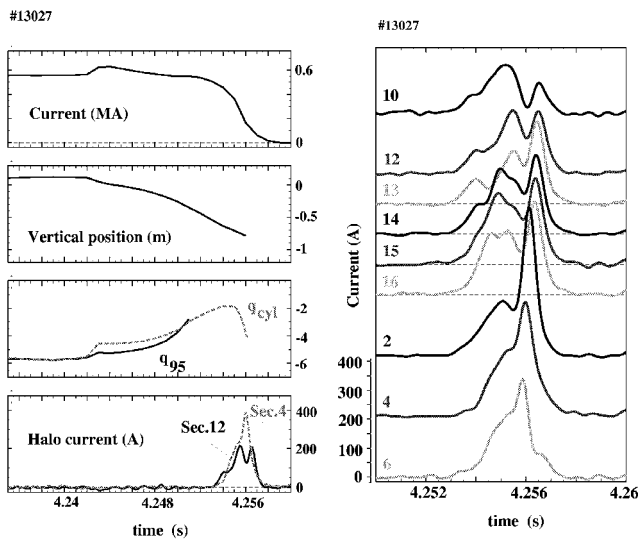


FIG. 9.3: (a) Time traces of several plasma parameters and of the halo currents measured at the DUAm tiles positioned in sector 4 and 12, 180 toroidal degrees apart. (b) Time traces of the halo current measured at the 8 tiles of the DUAm toroidal array in sectors 10, 12, etc...

(2) The injection of impurity gas or of impurity pellets into a plasma, which is going to disrupt, are the mitigation strategies which keep being improved. A fast valve system developed by the Forschungszentrum in Jülich was installed. The fast valve can inject up to 500 mbarl of impurity gas within one ms. Experiments were carried out with 180 mbarl ($= 4.5 \cdot 10^{21}$ particles) of Helium, Neon and Argon in limiter and divertor plasmas. Helium did not accelerate the current quench in limiter disruptions (0.8 MA in 30 ms) and was not used further. Neon and Argon accelerated the current quench in limiter disruptions with respect to the divertor ones (0.8 MA in 7 ms) and caused a reduction of the current quench duration and of the vertical displacement and the halo currents of a factor of two in lower X-point plasmas. Runaway electrons were not seen in these faster current quenches. The system is going to be further tested in the next shot period to find out the minimum amount of impurity gas necessary to mitigate the mechanical loads.

10. EDGE AND DIVERTOR PHYSICS

10.1 Improved edge density profiles from upgraded Lithium-beam

The neutral Lithium-beam emission spectroscopy is an established diagnostic tool for the measurement of edge electron densities at ASDEX Upgrade. To increase its penetration depth into the plasma and thus its useful range, an upgrade from 35 to 100 kV acceleration voltage has been implemented. A first comparison of edge electron density profiles measured with different Li beam energies of up to 60 keV showed excellent agreement, indicating the accuracy and suitability of the atomic data base used for the evaluation procedure.

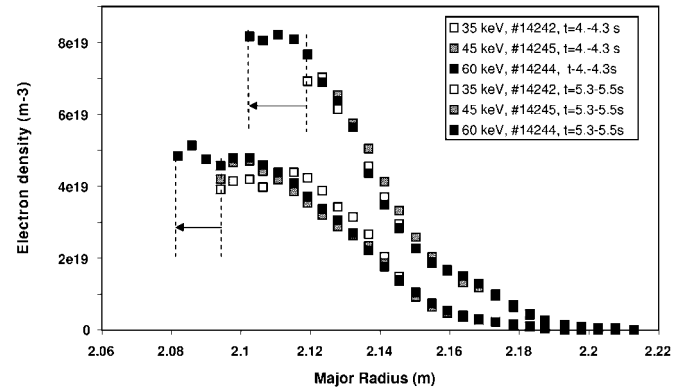


FIG. 10.1: Comparison of electron edge density profiles measured with 35, 45 and 60 keV Li-beam.

Figure 10.1 shows electron density edge profiles recorded in three similar shots (Standard H-mode discharges) with the Lithium beam set to 35, 45 and 60 keV, respectively. While there is hardly any difference in penetration depth for 35 and 45 keV (in agreement with predictions from beam attenuation calculations), the 60 keV beam delivers density profiles even reaching the pedestal.

Not only the higher acceleration voltage but also an optimised emitter geometry (developed in co-operation with the Institute of Plasma Physics, NSC 'Kharkov Institute of Physics & Technology', Ukraine) lead to higher current densities, required for the measurement of ion temperatures with Lithium-beam charge exchange spectroscopy. First ion temperature edge profiles could be obtained in low density discharges with a long flat top phase.

10.2 Impurity transport in the H-mode barrier

The radial impurity transport in the edge region of H-mode plasmas is temporally modulated when ELMs are present. ELMs expel impurities from the confined plasma and are essential to achieve stationary H-mode discharges without accumulation of impurities. The transport of Si and Ne in type-I ELMy H-mode plasmas was investigated by the modelling of soft X-ray measurements with the 1D impurity transport code STRAHL. Independent determination of inward drift velocity v and diffusivity D could be achieved by combining the analysis of supplementing transport experiments. In the first experiment, Neon was constantly puffed and the variations during an ELM cycle were measured on a dense spatial grid using a radial shift of the plasma column. In the second experiment, the decay of laser blow-off injected Silicon was measured for discharges with different ELM frequencies.

Both experimental situations could be simulated with the same 1D edge impurity transport model, whose features are shown in Fig.10.2.

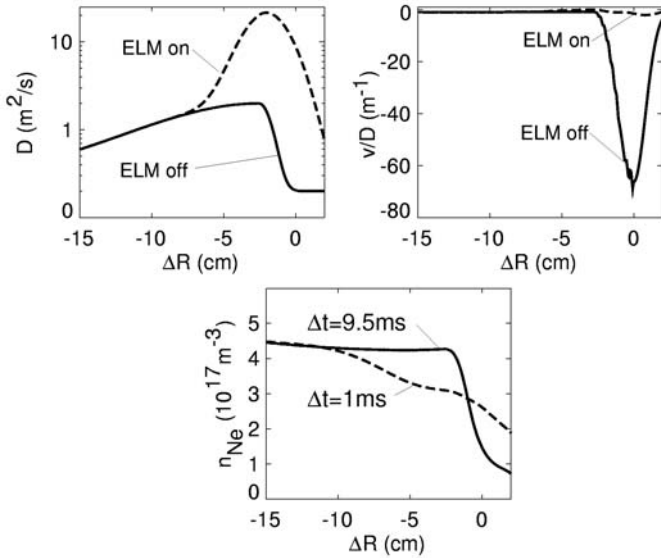


FIG. 10.2: Edge profiles of D and v used in the 1D model for the impurity transport during an ELM and in between ELMs and the resulting Neon density distribution before and after an ELM. R is the radial distance of the flux surfaces to the separatrix in the horizontal midplane.

In the quiet phase between ELMs, D is set to decrease from the edge to the centre for $R < -2.5$ cm as shown in previous experiments on impurity transport in ASDEX Upgrade H-mode plasmas. The maximum value is $D_{max} = 2 \text{ m}^2/\text{s}$. For $R > -2.5$ cm, a strongly decreasing diffusion coefficient is chosen which reaches the edge value $D_{edge} = 0.2 \text{ m}^2/\text{s}$ at $R \approx -1$ cm. For the drift velocity in between ELMs, an inward pinch is used, where the drift parameter v/D has a minimum value of -70 m^{-1} around the separatrix. At the start of the ELM a large diffusion coefficient with $D_{max} = 20 \text{ m}^2/\text{s}$ is switched on followed by a linear decrease to the pre-ELM values during 1.5 ms. This large diffusion coefficient causes a loss of the impurity content of $\approx 7\%$. Between ELM's the impurity profile evolves a strong negative gradient, which is flattened during the ELM.

10.3 Divertor plasma modelling

Two different codes have been used to model spatial profiles of various Carbon ionization stages in the divertor and main chamber. One code is the multifluid-Monte Carlo 'B2-EIRENE' code package and the second is the 2d-Monte Carlo code DIVIMP. Both 'DIVIMP' and 'B2-EIRENE' codes can treat impurities, however with different underlying physical models. 'DIVIMP' follows trajectories of impurity neutrals and ions in a given background plasma. 'EIRENE' calculates the particle sources with the resulting ion source rate transferred to B2, which treats the ion species as a fluid. In 'DIVIMP' the impurity source is calculated similarly to 'EIRENE', however without taking into account neutral hydrogen impact. The code results are compared with spectroscopic measurements of C^{III} obtained from arrays of lines of sight looking radially across the separatrix in the outboard divertor.

Fig. 10.3 shows the integrated intensity as a function of the cross-section co-ordinate S of the line of sight with the target

plate, assuming 3% constant chemical erosion yield for both 'B2-EIRENE' and 'DIVIMP' (using for this the corresponding 'B2-EIRENE' background plasma).

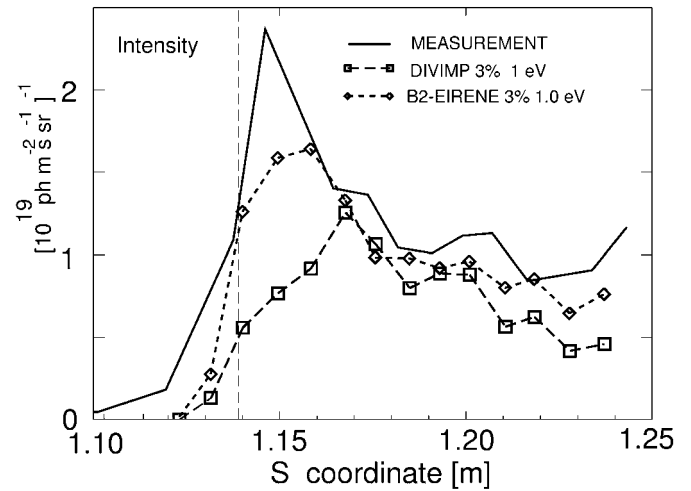


FIG. 10.3: Measured and calculated line of sight integrated C^{III} intensity (line at 465 nm) with 'DIVIMP' and 'B2-EIRENE'.

Similar results are obtained with 'B2-EIRENE' and 'DIVIMP' using the same background plasma and analog sputtering models but significant discrepancies arise approaching the separatrix position. A fairly good agreement is shown between divertor measurements and model predictions, both for the profile shape and the absolute value in the outboard divertor. 'B2-EIRENE' is able to reproduce the emission maximum near the separatrix better than 'DIVIMP'. This is explained with an important contribution to the Carbon influx from neutral particles sputtering, accounted for in 'B2-EIRENE' but not in 'DIVIMP'.

10.4 Carbon layer deposition

The use of Carbon as plasma facing material in a future fusion device is restricted due to the formation of a a-C:H layer, which will contain a significant amount of Tritium. Investigations on the growth of these Carbon layers were continued in DIV IIb. Although the divertor shape changes, very similar properties are found. The amount of Carbon deposited each second of plasma discharge is about $2 \cdot 10^{15} \text{ atoms/cm}^2$ (DIV II: $2.2 \cdot 10^{15} \text{ atoms/cm}^2$) and the ratio of the layer thickness in the inner divertor with respect to the outer divertor is again close to 3:1. At JET huge amounts of Carbon flakes are found even at the pump ducts. Additional monitors, mounted at the pump ducts, show that in ASDEX Upgrade only a negligible amount of Carbon is deposited at these positions.

The deposition pattern in DIV II indicates that charged ions and molecules play a role at the layer formation. To verify this a Langmuir probe was installed below the divertor structure. Although this position is not connected via field lines with the divertor plasma, electron densities up to $1 \cdot 10^{18} \text{ m}^{-3}$ are found.

INTERNATIONAL CO-OPERATION

In 2001 ASDEX Upgrade enjoyed fruitful collaboration with many national and international research institutes and universities. In addition the ASDEX Upgrade programme was opened to the EU Associations (see section 1.1 of ASDEX Upgrade Project). In the following some co-operations are described in more detail.

1. DOE - ASDEX Upgrade Activities

The collaborations in 2001 within this Agreement, were very beneficial to both sides. The primary area of collaboration is on Advanced Tokamak physics issues and divertor physics. The activities ranged from sharing data and carrying out theoretical studies and computations to joint work on RF physics and technology. About twelve scientists from each side were involved directly in personnel exchanges this year between the U.S. (DIII-D, C-MOD, ORNL, and PPPL) and the ASDEX Upgrade in experiments, theory and modelling. Some of the collaborative work in data analysis and modelling work is carried out off-site, at home laboratories. In addition there were five personnel exchanges from South Korea to U.S. Labs. Results from these exchanges have been presented at various international meetings and published in journals.

The ASDEX Upgrade programme is aimed at the physics basis of ITER-FEAT and tokamak concept improvement, while the U.S. Fusion programme aims at basic tokamak physics and burning plasma issues. Both of these goals have many common research interests. For example, both ASDEX Upgrade and DIII-D have been at the forefront of research on feedback stabilization using "Neoclassical Tearing" modes using Electron Cyclotron Heating (ECH) system, and ASDEX Upgrade and C-MOD share close interest on edge physics. All three tokamaks are keenly interested in plasma fuelling and density limits. This collaboration serves the interests of both the EURATOM/IPP and the U.S. programmes.

This year South Korea signed the IEA AUG Agreement in April 2001 and changed from an observer to full member. South Korea is building a superconducting Advanced Tokamak with divertor, KSTAR, which will enhance this collaboration by introducing long pulse physics and technology issues. KSTAR will begin operations in 2005. Several Korean scientists are participating in tokamak experiments in the U.S.

and at IPP Garching this year. The 16th meeting of the IEA Executive Committee (EC) was held at Mito, Japan on May 30, 2001 where physicists from South Korea were welcomed as full members of the Committee for the first time.

The collaboration is expected to continue in 2002 at a slightly higher level of activity resulting from the participation of Korean scientists.

2. CEA, Cadarache

During the transition from H to D on ASDEX Upgrade the mode conversion layer can be put close to the $3/2$ ion cyclotron harmonic resonance of the deuterium. Theory predicts that this results in a possible scenario to heat ions through the non linear damping at the $3/2$ cyclotron harmonic of the Ion Bernstein Wave (IBW), produced at the mode conversion layer: a self interaction of the wave with itself occurs, making a beat wave that can resonate with the bulk ions of the plasma. Clear indication of ion heating was indeed found from neutron signals as well as from NPA measurements. Ion heating scenarios are important for future machines in order to increase the fusion reactivity.

3. Collaboration with Forschungszentrum J, lich, Association KFA-EURATOM

A fast valve system developed at the Forschungszentrum in J, lich has recently been used on ASDEX Upgrade. The fast valve can inject up to a few 100 s mbarl of impurity gas within 1 ms. Experiments were carried out with up to 180 mbarl ($\approx 4.5 \cdot 10^{21}$ particles) of Helium, Neon and Argon in limiter and divertor plasmas; they showed a reduction of the current quench duration, of the vertical displacement and of the halo currents of a factor of two.

3. Co-operation with Russian Institutes

A fast valve for the injection of impurities and disruption mitigation has been commissioned by Dr. Egorov, Technical University in St. Petersburg. He also supported in the installation and operation of the impurity pellet injector.

The DINA code developed by V. Lukash and R. Khairoutdinov, Inst. of Nucl. Fus., Kurchatov Institute, Moscow, will be used for disruption investigations. Both authors installed the code at IPP and have started disruption simulations.

The co-operation with the Ioffe Institute, St. Petersburg, in the field of Neutral Particle Spectra analysis has been continued. A. Khudolev mainly studied the possibilities to derive ion temperatures from the neutral spectra above the NBI energy and the differences between H⁰ and D⁰ spectra in low density discharges.

5. University of Cork, Ireland

The collaboration with the University of Cork concerning MHD equilibrium identification using magnetic measurements was continued. The "CLISTE" interpretative equilibrium package and the FP real-time reconstruction now include information from magnetic probes, MSE diagnostics and kinetic data. This was further developed as described in Sec. 8.3, ASDEX Upgrade Project.

The second part of the collaboration was concerned with the correlation of internal transport barrier formation with plasma parameters just before the barrier formation.

6. Centro de Fusão Nuclear, EURATOM IST Association, Lisbon, Portugal

The collaboration with CFN on the measurement of density profiles and density fluctuations, using fast swept microwave reflectometers, has seen, during 2001 the substantial completion of several hardware upgrades. This has included an expansion of the data acquisition memory allowing the number of acquired profiles to be increased by a factor of four, leading to enhanced time resolution. This expansion was accompanied by improvements to the analysis, control and profile evaluation software. One notable consequence has been the regular use of "burst mode" averaging to reduce profile distortions. One of the fluctuation monitor channels was also converted to full heterodyne with in-phase and quadrature detection, the second channel should be converted shortly. The diagnostic hardware development has now reached a mature state and the emphasis of the collaboration is moving more towards exploitation of the diagnostic for physics studies. This year, studies have included the investigation of the effects of ELM perturbations on the reconstruction of profiles; estimation of edge pedestal density and width; the characterization of coherent edge plasma oscillations during type II ELMy H-mode discharges; and the demonstration of the potential use of reflectometers for plasma position control.

Studies have continued on density profile deformation during inboard pellet injection (specifically velocity dependence) and progress has also been made on the use of X-mode channels for improved initialisation of the density profile reconstruction.

7. TEKES (HUT and VTT), Finland

The collaboration between TEKES and IPP aims at describing kinetic effects using Monte Carlo techniques and the study of MHD instabilities. The ASCOT Monte Carlo code developed in Finland was used for the first of these investigations. In 2001, the energy distribution of neutrals emitted from the plasma was investigated. Above the neutral beam energy this distribution reflects the central ion temperature and can, therefore, be used as a diagnostic tool. A start has been made in analysing the fluxes at low energies to assess the accuracy of the edge ion temperature measurements. In the work on MHD, the ELMs have been investigated and a consistent interpretation of type I and type II ELMs based on the ballooning and peeling mode has been developed.

8. Institut für Allgemeine Physik, TU Wien and Friedrich Schiedel Foundation, Austria

Efforts continued into the investigation of the suitability of He-beam emission spectroscopy for plasma electron density and temperature determination. Various He-lines were measured using a helium-doped deuterium beam at ASDEX Upgrade and at JET. An improved collisional-radiative beam attenuation model yielded emission line profiles which are in good agreement with experimental data. The efficiency of the computer code was optimized allowing its implementation for recursive determination of electron density or temperature from measured He-emission line profiles. These activities were carried out within the EURATOM-OEAW Association and were supported by the Austrian Friedrich Schiedel Stiftung für Energietechnik.

9. National Institute of Laser Plasma and Radiation Physics, EURATOM-NASTI Association, Bucharest, Romania

The main topic of this co-operation is the interpretation and control of helical perturbations in tokamaks. As a first step, an equilibrium momentum code has been improved by using a new analytical function describing exactly the X-point singularity. The metric coefficients were checked on an analytical Solov'ev solver, describing a separatrix configuration. The influence of the triangularity on the stability Delta' parameter has been investigated for ASDEX Upgrade discharges. As a second step, plasma models for feedback control of helical perturbations were developed. With the plasma represented by a surface current model, the inductance of the modes and wall have been determined.

JET CO-OPERATION PROJECT

(Head of Project: Prof. Dr. Michael Kaufmann)

Long Term Secondments: A. Buhler, A. Lorenz, J. Schweinzer, R. Wolf, W. Zeidner.

Other Secondments: G. Conway, D. Coster, R. Dux, J. Gafert, S. Ginter, A. Herrmann, J. Hobirk, A. Kallenbach, K. Kirov, K. Krieger, P. Lang, M. Laux, M. Maraschek, K. McCormick, F. Meo, R. Neu, J.-M. Noterdaeme, G. Pereverzev, S. Pinches, R. Pugno, V. Rohde, F. Ryter, A. Stuber, J. Stober, W. Suttrop, R. Wolf.

1. OVERVIEW

The JET tokamak is exploited under the framework of the European Fusion Development Agreement. The facility is operated by the UKAEA under contract with the European Commission while the physics exploitation of JET is carried out by task forces from the Euratom Fusion Associates. In 2001, one experimental campaign (C4) of 58.5 experimental days was executed followed by a shutdown phase in which the divertor septum was replaced by a cover plate and the neutral beam power upgrade project was initiated (planned completion: October 2002). By the end of 2001, the shutdown had been successfully completed and the restart begun in preparation for three new experimental campaigns in 2002, totaling 100 experimental days.

Planning for the three experimental campaigns in 2002 (C5-C7) is now well advanced. IPP physicists made over 40 experimental proposals, several in collaboration with other Associates. All of these proposals have been included in the outline experimental programme for 2002. IPP participation is expected to be at a level similar to that of the first four campaigns. Already two new long term secondments, one to the Culham Close Support Unit and one as a Task Force Leader, are in place.

Detailed results of the first four EFDA-JET campaigns are now being reported. Eleven IPP physicists reported on JET and ASDEX Upgrade / JET comparison experiments at the 2001 European Physical Society meeting in Madeira. The majority of these results are now being prepared for publication as full journal articles.

The contributions of IPP scientists to the JET programme have been as part of the larger JET workprogramme, in collaboration with the other contributors to the JET workprogramme¹. Below are described some of the areas where IPP physicists have made major contributions to the execution and analysis of specific experiments on JET.

¹ See Annex to J. Pamela et al., *Overview of Recent Results and Future Perspectives*, Fusion Energy 2000 (Proc. 18th Int. Conf. Sorrento, 2000), IAEA, Vienna, 2001.

2. PELLETT FUELLING AT JET

Several approaches are used at JET to achieve operation at high density with good energy confinement. One of them is the injection of solid fuel pellets to realise efficient particle refuelling by deposition deep inside the plasma column. The new pellet launch system capable of launching from the torus magnetic high field side was investigated for its capability to fulfil this task in conventional ELMy H-mode discharges.

To achieve the best performance, target plasma discharges were chosen fully compatible with pellet refueling and an optimised pellet sequence developed. During this optimisation process it turned out that special attention had to be paid to three critical issues:

- prompt particle losses causing increase of neutral gas pressure and edge density
- trigger of central MHD activity by the pellet
- ELM bursts following pellet injection

as each one of these pellet-related effects can cause severe energy losses and must therefore be avoided or minimized.

Excessive increase of the edge density could be avoided by restricting the maximum pellet rate to 6 Hz. This prevented an increase of the neutral gas pressure in the main chamber beyond a level of 2×10^{-3} Pa found critical for the onset of confinement degradation.

Like many high performance operational modes, pellet refuelling scenarios suffer from magnetohydrodynamic (MHD) mode activity and especially neoclassical tearing modes (NTM) become a major obstacle for reaching high performance. Pellets driving up density accordingly reduce temperature. Reduction of the ion temperature causes a shrinking poloidal ion gyro radius $\rho_{p,i}$ reducing the critical pressure β_p^{onset} for the triggering of an NTM. Thus, if previous pellets have driven down the plasma temperature too far, strong local perturbations on resonant surfaces introduced by a further pellet can trigger an NTM. In order to improve this situation, it was necessary to keep the temperature above a critical level. This was achieved by increasing the heating power by using combined NBI and ICRH heating. Reduction of MHD activity was observed when approaching the maximum heating power of about 18 MW available in these experiments.

Mitigation of the confinement losses imposed by pellet-induced ELM activity was achieved by adapting the pellet fuelling cycle. Interrupting the pellet string allows a recovery of the plasma energy content while the particle inventory still remains elevated. The optimised pellet sequence consists of an initial density build up phase at a high repetition rate followed by a density sustainment phase with the pellet rate reduced to a

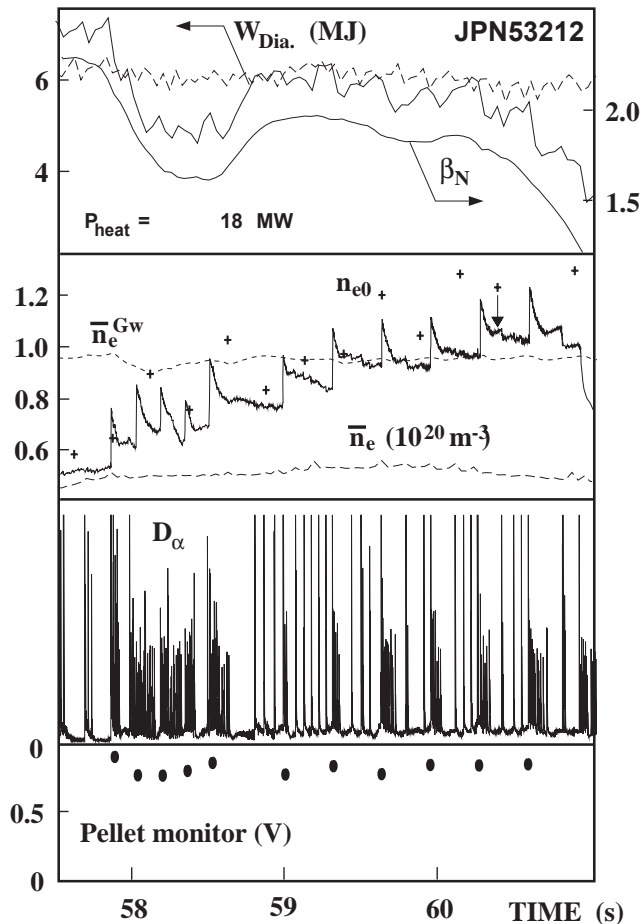


FIG 1: Optimised pellet fuelling for high performance, high density operation. Central density n_{e0} above the Greenwald level n_e^{GW} is achieved at the energy content W_{dia} of an unfueled reference discharge (dashed lines).

significantly lower value. Figure 1 shows an example for a discharge with 18 MW heating power. The initial 6 Hz pellet sequence causes an energy drop due to enhanced ELM activity. When entering the 2 Hz sequence the transient energy drop initiated by each pellet can be almost fully recovered before the next pellet arrives in the plasma. By the end of the high performance phase, densities above the Greenwald level are reached with about 6 MJ plasma energy content and β_N still above 1.8. In this discharge, the high performance phase is terminated by a pellet triggered (3/2) NTM.

3. TASK FORCE S1

Experiments of Task Force S1 during JET campaign C4 in 2001 aimed to further extend the performance at high density near the ITER target of 85% of the Greenwald density and developments towards an integrated scenario with tolerable Edge Localised Modes (ELMs). The main techniques employed to achieve high density are: (i) strong plasma shaping (triangularity $0.35 < \delta < 0.5$), (ii) deuterium pellet injection from the high-field side. (iii) impurity seeding. While plasma shaping aims to improve edge stability and consequently achieve a higher pedestal pressure and pedestal density, the two latter methods result in peaked density profiles with high central density. In addition, spontaneous peaking of

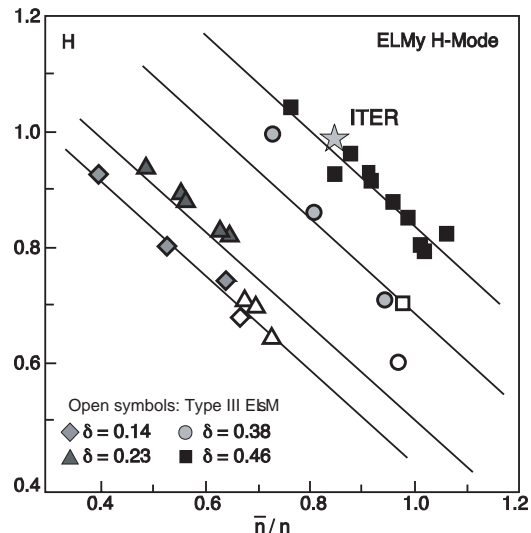


FIG 2: H-mode confinement enhancement factor $H_{98}(y,2)$ as a function of the density normalised to the Greenwald density for density scans with different triangularity (plasma current $I_p=2.5$ MA fixed).

the density profiles occurs on a slow time scale which has been further studied.

Figure 2 shows the confinement enhancement factor H_{98} as a function of the line-averaged density, normalised to the empirical Greenwald density limit scaling. With increasing density, both the stored energy and the H_{98} factor decrease in agreement with previous experiments in JET and ASDEX Upgrade. Strong plasma shaping, in particular increasing the triangularity δ , results in improved confinement at high density. In addition to plasma shapes with $\delta=0.14$, $\delta=0.28$, and $\delta=0.35$, a configuration with a cross section similar to that envisaged for ITER (ITER-like configuration, $\delta=0.46$) has been extensively studied during 2001. In this configuration, the ITER target parameters, $H_{98}=1$ at $n_e/n^{GW}=0.85$, are regularly achieved.

The reduction of confinement at high density is accompanied with a reduction of pedestal temperature at high pedestal density. Series of pulses with successively increased gas fuelling reveal a favourable property of ITER-like plasmas: At highest edge density approaching 80% of the Greenwald density the pedestal temperature does not drop further and the pedestal pressure recovers to values almost approaching that found without gas puff. The stored energy is proportional to the pedestal pressure. While usually the ELM frequency increases with increasing gas puff, ITER-shape plasmas show a reduction of type I ELM frequency at high edge densities. Power balance analysis at the edge indicates that only 10-15% of the heating power is lost during ELMs, compared with 30-40% in usual ELMy H-modes. Continuous broad-band MHD activity is seen in magnetic measurements. The contribution of this benign mode activity to edge transport is a topic of further investigation.

Impurity seeding experiments have been carried out with a lower single X-point inside the divertor septum. This configuration shows a reduced H-mode threshold and allows to keep H-mode with high fractions of radiated power. At the

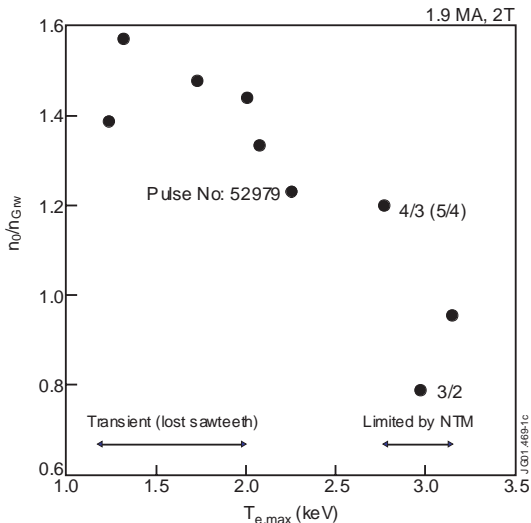


FIG 3: Central density (normalised to the Greenwald density) versus central temperature in a power scan. At low heating power the performance with peaked profiles is limited by loss of sawteeth and increased core radiation while at high heating power neoclassical tearing modes occur.

beginning of the H-mode flat top, a strong deuterium gas puff is applied to raise the H-mode density towards the Greenwald limit (puff phase). In addition, Ar gas is introduced. During this phase, a significant confinement deterioration is observed. The strong gas fuelling is stopped for the remaining flat top (after-puff phase), resulting in a recovery of H-mode confinement to near $H_{98}=1$. Without continued Ar seeding, the plasma density decays on a slow time scale. With small amounts of Ar gas puff, it is found that high densities between $n_e/n^{GW}=0.8$ and $n_e/n^{GW}=1$ can be maintained with much reduced deuterium fuelling compared with unseeded plasmas. Ar seeding results in peaked central densities with similar temperature profiles as in unseeded plasmas. Consequently the central plasma pressure is increased at increased density giving rise to the observed confinement improvement at higher densities. With Ar seeded plasmas, $H_{98}=1$ at n_e/n^{GW} has been achieved at low triangularity for the duration of the full after-puff phase (5 s or $12 \tau_E$).

While after transition to H-mode typically a flat density profile inside the H-mode pedestal area is found, often a slow peaking of the central density is observed, mainly with neutral beam heating and moderate external gas fuelling. The central density can rise to values above the Greenwald density while the pedestal density remains essentially constant. At low heating powers ($P_{NBI} < 8$ MW) the density peaking process is terminated by a radiative collapse of the plasma core after loss of sawtooth activity while at high heating power ($P_{NBI} > 8$ MW) neoclassical tearing modes (NTM) occur, usually starting with higher mode numbers, e.g. $n=3$, $m=4$. A power scan experiment reveals that the range of stable plasma conditions with peaked density profiles can be expressed as a function of the central temperature as shown in Fig. 3. Thermal collapse is avoided if the central temperature can be kept sufficiently high to avoid excessive radiation levels. This can be done effectively, for example, with central RF heating. At high heating power, the occurrence of NTMs limits the achievable

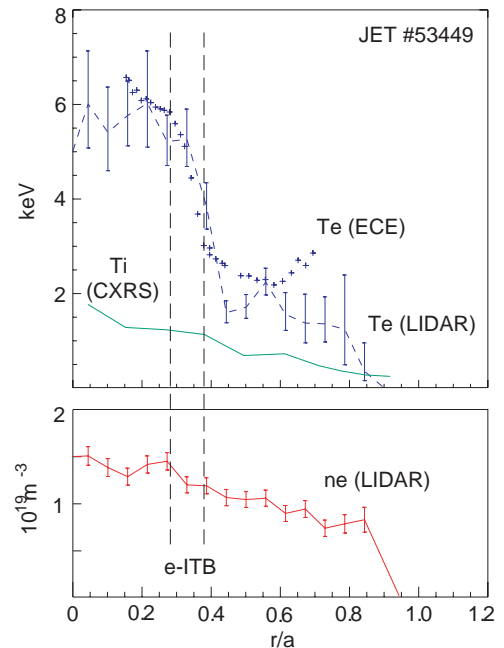


FIG 4: Example of an electron barrier in JET for a reversed shear configuration, obtained with dominant electron heating (LHCD) during the current rise phase of the discharge ($t = 2.8$ s).

central density and, for given plasma current and pedestal density, the density profile peaking factor.

4. TASK FORCE S2

Several scientists from IPP contributed to the programs of S2 at JET. The main contributions were in areas of operation support, scientific coordination of experiments and data analysis. The main topics of the scientific work in S2 concentrated on internal transport barriers (ITBs) under different heating conditions, impurity transport in ITB discharges and fluctuation measurements during the current rise phase of the discharge.

4.1 ITBs with ion and electron heating

The basic ITB scenario at JET uses a reversed shear configuration produced by off-axis lower hybrid current drive (LHCD) during the current ramp-up phase. The ITB can be obtained for the ions, or the electrons, or both, depending on the heating scenario used. Some of the experiments have ITBs obtained with dominant electron heating of ITBs (Figure 4). In other experiments, the effect of a variation of the electron heating on the confinement properties of ITBs has been studied, by comparing discharges heated by NBI alone to discharges heated with a combination of NBI and ICRH. In this case the heat flux to the ions remains constant, while the heat flux to the electron rises by 40%. Under these circumstances the ion confinement is not degraded and the transition to a strong ITB is independent of the partition between the ion and electron heat flux in the plasma. With the stronger electron

heating, the electron temperature increases slightly in the centre and the profile broadens.

4.2 Impurity accumulation in ITBs

Impurity behaviour in scenarios with an internal transport barrier is of special concern since neoclassical convection might cause strong inwardly directed drift velocities which are not suppressed by anomalous diffusion or MHD phenomena (sawteeth, fishbones etc.). In particular, the behaviour of metallic impurities in JET discharges with an internal transport barrier has been studied by using the intrinsic nickel impurity sources in the JET Tokamak. For transient ITB discharges where the high performance phase is terminated by MHD events, the impurity accumulation plays a minor role. However, in long pulse ITB discharges which are MHD stable, the impurities accumulate over several seconds. At some time in the discharge, the impurity radiation exceeds the power input to the electrons, leading to a radiative collapse of the core. In summary, in ITB discharges with reversed shear, metallic impurities accumulate in cases with too strong peaking of the density profile. The peaking increases with the impurity charge and is low for the low-Z elements C and Ne. This behaviour is in agreement with neoclassical convection.

4.3 Fluctuation measurements during the current rise phase

The formation of an electron thermal ITB (e-ITB) typically begins with the application of 2-3 MW of 3.7 GHz lower hybrid (LHCD) heating and current drive during the plasma current ramp up. The core electron temperature rises from < 2 keV (in the ohmic phase) to > 8 keV. The electron temperature profile is flat from the core out to around $r/a \sim 0.3-0.4$, nominally coincident with the broad peak in the LHCD deposition profile, where it then drops sharply, as shown by the radial profiles in Figure 4. The plasma density also remains low at $n_e \sim 1.5 \times 10^{19} \text{ m}^{-3}$ with only a moderate gradient. In the absence of significant ion heating from the LHCD the ion temperature profile (from charge exchange spectroscopy during a short phase of neutral beam injection) has no steep gradient, implying no corresponding ion thermal ITB. The presence of an e-ITB is also correlated spatially with the reversal in magnetic shear $s = r/q$ (dq/dr). The radial position of the e-ITB (maximum T_e gradient - marked by the vertical lines in the Figure 4) does not appear to be related to position of q_{\min} but to the maximum negative magnetic shear. Measurements of core and edge density turbulence using X and O-mode reflectometry show that low frequency ($f < 50$ kHz) fluctuations are reduced within the e-ITB volume, to levels below that measurable by the diagnostic. Figure 5 shows the radial profile of the RMS density fluctuation level together with frequency spectra from inside and outside the e-ITB. In the spectra the low frequency fluctuations are seen to rise sharply by more than an order of magnitude within 0.5 s (i.e. on a time scale short compared to the q profile evolution) as the cutoff enters the e-ITB region (shown by the hatched box in

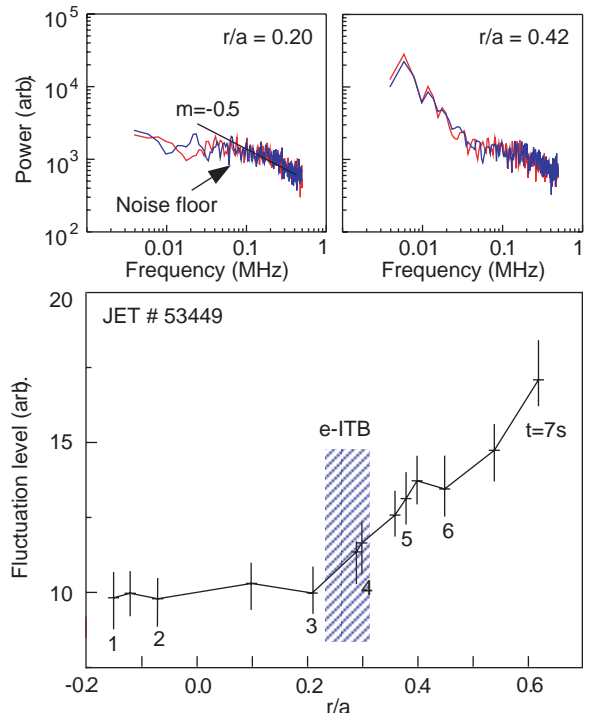


FIG 5: Turbulence spectra inside and outside e-ITB, plus profile of density fluctuation level vs normalized radius compiled from reflectometer cutoff layer sweeps.

Figure 5). Transport analysis also confirms the region of low RMS fluctuation level is correlated with reduced electron diffusivity χ_e . From the rotational spectral broadening during an NBI beam blip, turbulence phase velocities are estimated at $v_{ph} < 300$ m/s in the electron diamagnetic drift direction, and perpendicular fluctuation wavelengths $\lambda > 0.11$ m. This wavelength range is not consistent with electron temperature gradient (ETG) type turbulence. The suppression of this turbulence has been proposed as the principle mechanism for e-ITB formation. However, they are consistent with ion temperature gradient (ITG) and trapped electron mode (TEM) turbulence which can exist in the observed wavelength range, and have a propagation velocity in the v_e^* direction. In the plasma edge ($r/a > 0.6$) the turbulence is unaffected by the ITB. Moving away from the core, on the high field and low field sides, the turbulence spectra both broadens and rises in amplitude. As the edge current density falls during flat top phase of the discharge, the edge q profile steepens which increases the positive magnetic shear. When the shear exceeds unity, the turbulence amplitude and spectral index fall, indicating reduced wavenumber content. The observation that high magnetic shear, both positive and negative, reduce turbulence is consistent with ITG/TEM growth rate calculations which peak around $s = 0.5$, decreasing at higher positive shear and low or negative shear. Core turbulence is also reduced within an ion thermal barrier (i-ITB) generated by neutral beam injection. These discharges, however, are dominated by ion heating ($T_i > T_e$) and high momentum input with low (zero to slightly positive) central magnetic shear. In this case the turbulence reduction is dominated by plasma rotation shearing effects.

5. TASK FORCE E

TFE work at IPP in 2001 concentrated on data evaluation of the campaigns C1-C4, in particular Langmuir probe evaluation, Zeeman spectroscopy and modelling.

A technique was developed to coherently average signals from divertor Langmuir-probes (but possibly also other signals) during ELMs. The D_α emission was used to mark ELM events in a series of comparable ELMs and overlay and average the signals. The results obtained using the method are stable and exhibit a remarkable noise reduction. The coherently averaged traces of probe signals demonstrated that electron temperature and floating potential react earlier than the particle flux to the ELM. The derived plasma potential, nevertheless, exhibits a simple smooth temporal evolution. Depending on the time delay between the peaking of T_e and V_{float} on the one hand and I_{sat} on the other, the calculated convective power flux to the divertor plate may show one or two maxima. The same identification technique can be developed further to sort ramped single probe data and construct UI-characteristics for successive ELM-phases.

As the Zeeman pattern of a spectral line is determined by the local magnetic field vector, a highly resolved emission spectrum contains the information to identify the location of the emission, and the distribution of impurities between the inner and outer SOL in the main chamber can be obtained from a careful analysis of the Zeeman profile of the corresponding emission lines. Using an optical line of sight near the midplane in JET viewing the plasma radially from the outside of the vessel, the applicability of this technique has been explored in various discharges with gas puffing (CD_4 , D_2) from different valves and the significance of the results has been investigated. Another outcome was that in regular H-Mode discharges (with closed divertor configuration) the relative contribution of the CIII light from the inner and outer SOL varies between about $\sim 3:1$ and $\sim 6:1$, whereas in typical L-Mode plasmas, this ratio (inner:outer) is reduced and ranges between $\sim (2:3)$ and $\sim (2:1)$.

Support of SOLPS (B2-Eirene) for JET modelling has continued with Garching supplying coordination of Europe-wide JET edge modelling. A start to applying the interpretive version of B2.5 to JET was made, but instrumental resolution limitations of the edge diagnostics postponed this activity until 2002 when some hardware upgrades and operational changes should allow this program to continue.

6. TASK FORCE M

6.1 Onset behaviour of Neoclassical Tearing Modes (NTMs)

In order to get a more robust prediction of the onset dependence of the achievable local β_p^{onset} from (3/2)-NTMs as a function of the local poloidal ion gyro-radius $\rho_{p,i}^*$ and the local collisionality $\nu_{ii}^* = \nu_{ii}/(m_e \omega_e^*)$ this parameter range has been extended to lower $\rho_{p,i}^*$ and higher ν_{ii}^* . This goal has been achieved for the (3/2) mode by including low q_{95} discharges

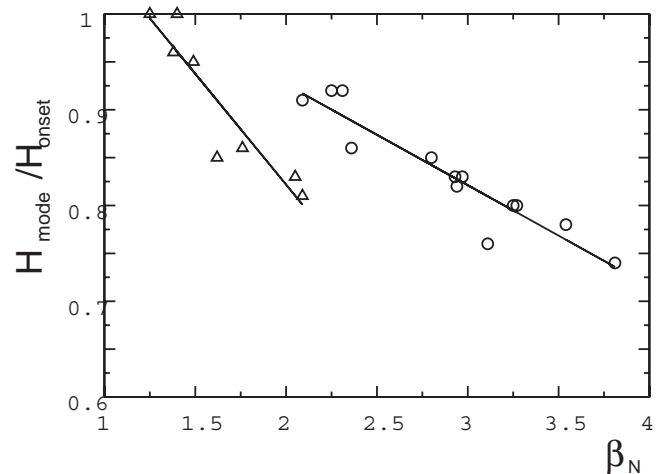


FIG 6: H factor after (3,2) NTM saturation, normalised to the value at the NTM onset, versus β_N at the mode onset for JET. For initial β_N^{onset} values above $\beta_N \sim 2$ the confinement loss is partially recovered.

and, for the lowest $\rho_{p,i}^*$ values, also including pellet triggered NTMs at high densities and hence high ν_{ii}^* . Under the assumption of comparable seed-island sizes the $\beta_p^{onset} \sim \rho_{p,i}^*$ dependence and a small increase of β_p^{onset} with ν_{ii}^* could be confirmed for JET. Similar experiments have been done for the (2/1) mode.

6.2 NTM behaviour at high β_N

Based on experimental observations on ASDEX Upgrade, the behaviour of (3/2) NTMs at high β_N has been analysed in detail. At high β_N the so-called frequently interrupted regime (FIR) is observed. Due to the FIR, the NTM never reaches its saturated size, as the mode is repeatedly and abruptly reduced on a very short timescale. The resulting reduced average amplitude decreases the loss in confinement caused by the mode in this FIR-phase. The abrupt reduction of the (3/2) NTM amplitude ($\sim 500 \mu s$ for ASDEX Upgrade) can be explained by a nonlinear coupling to an additional fast growing burst-like ideal (4/3) mode. The presence of an additional (1/1) mode is required for this nonlinear coupling. The resulting confinement recovery during NTM phases combined with the FIR may make operation with NTMs present in the plasma a tolerable regime for a reactor.

6.3 Influence of non-resonant fields on NTMs

Based on theoretical predictions and experimental hints from the suppression of (m/n) NTMs by modes with higher mode numbers (m+1/n+1), the influence of externally applied non-resonant magnetic fields has been studied. A reduction of the NTMs by external non-resonant fields is a promising candidate for decreasing the influence from NTMs in a reactor. Initial experiments suggest that the non-resonant external field might indeed be able to reduce the amplitude of a (3/2) NTM. In addition to the observed variations of the mode amplitude, a

yet not fully understood reduction of the rotation frequency was seen.

6.4 Theroretical contributions

The influence of fast ions on MHD mode has been modelled. One topic of interest was the role of fast ions for triggering the experimentally observed Alfvén modes, which appear in cascades. In addition to this type of specific analysis, general tools and support for the fast analysis of data from many experiments have been developed and improved where needed.

7. TASK FORCE H

The campaign at the beginning of 2001 was dominated by the use of different (majority/minority) gases which allowed presently less used ICRF heating scenarios to be investigated. These scenarios are either relevant for ITER or allow new possibilities of investigations on JET. The experiments produced a series of interesting new results.

The pinch effect on ^3He minority ions was clearly identified and the transition from ^3He minority heating to mode conversion heating was made. In mode conversion heating, the electrons are dominantly heated and the location of the power deposition layer can be set by the concentration of ion species and the choice of magnetic field and frequency. Experimentally, the power deposition layer was observed through modulation experiments and its location was controlled (Fig. 7). A strong synergy between JET and ASDEX Upgrade is present here, since similar experiments had been performed on ASDEX Upgrade and this prior experience was very beneficial to the successful conduction of the experiments on JET. In JET, the mode conversion scenario provides the basis for electron transport experiments which are foreseen in the future. Power has been coupled at the third harmonic of ^4He to ^4He beam ions, in a ^4He plasma. Alfvén eigenmodes were triggered by the ^4He beam ions accelerated to very high energies by the ICRF.

The analysis of the experiment on plasma rotation was continued and software in support of the CXRS diagnostic was developed.

Support was also provided for the TF-H physics of JET-EP and for the definition of the JET-EP antenna. We strongly emphasised the need to implement 3 dB couplers (which are used very successfully on ASDEX Upgrade to cope with the ELM transients in the coupling) on JET to improve the operation of the ICRF system. A study of the use of 3 dB couplers on JET was performed.

Improving the power capability of the ICRF system, in particular on type I ELMy plasmas is of utmost importance for improving the overall power available on JET and making JET even more ITER relevant. It is part of the task of TF-H to identify and propose measures that will improve the power capability of the ICRF system. However, the decision to implement those measures and their actual implementation (as

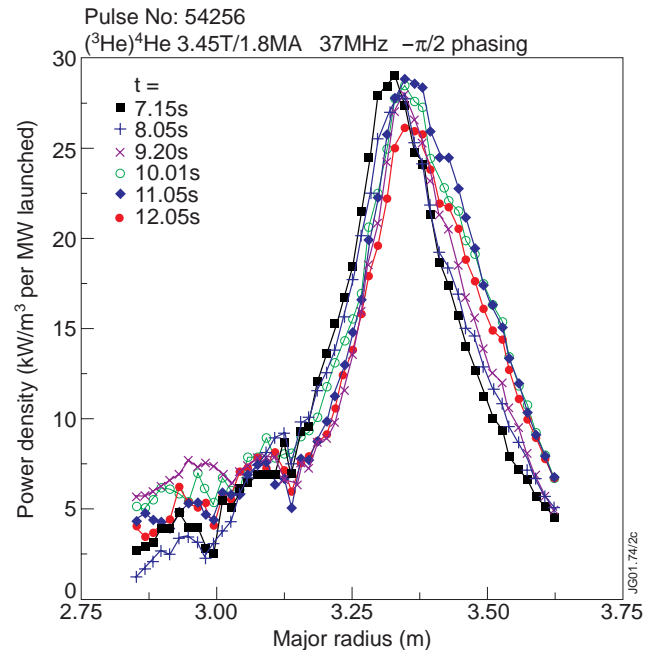


FIG 7: Power deposition through mode conversion to the electrons at different times, showing the rather narrow deposition profiles as well as the excellent control of the deposition through control of the concentration.

far as hardware is involved) is beyond its responsibility. We would like to emphasise here again that adding 3 dB couplers on as many ICRF antennas as possible is the best way to improve the power capability of the ICRF system.

8. TASK FORCE FT

The IPP is strongly involved in the determination of wall erosion, redeposition of eroded material, and hydrogen inventory trapped in redeposited layers at JET. These investigations are of crucial importance for the prediction of the tritium inventory in ITER. In order to determine material erosion at the inner JET vessel wall, long term samples (LTS) consisting of thin films of different materials on a carbon substrate were installed in 1999 and replaced in autumn 2001 by a new set of LTS, consisting of thicker films of Be, C, Ni and W. Due to the large anticipated erosion, new methods for the exposure and analysis of these thick films ($2.5 \mu\text{m}$ to $10 \mu\text{m}$) were developed. In order to identify the species of hydrocarbon radicals, which are responsible for the growth of redeposited layers in the divertor, two cavity samples for the measurement of the sticking coefficient of these radicals were installed in the JET divertor in 1999 and replaced in 2001. The deposition of different elements in the JET divertor is determined by the use of marker tiles, which were also installed in 2001. A full poloidal section of six JET divertor tiles were coated with a 20 mm wide and $3.5 \mu\text{m}$ thick tungsten stripe over the full tile length by DIARC Technology Inc. (Finland). The W layer was characterised by ion beam analysis methods prior to tile installation and allows the determination of material deposited on top as well as the identification of net erosion areas. All long-term samples and instrumented tiles will remain in JET until the next opening in summer 2004.

ITER COOPERATION PROJECT

(Head of Project: Prof. Dr. Hartmut Zohm)

1. INTRODUCTION

With the positive developments towards the realisation of ITER, such as the first official site offer by Canada and the implementation of the International Tokamak Physics Activity as an international expert system to advance the physics basis for burning plasma experiments, IPP continued its strong support for ITER Physics R&D. Many of the results achieved on ASDEX Upgrade (see previous chapter) are of course directly relevant for ITER. This chapter describes additional work that is done specifically in support of ITER.

2. PERFORMANCE ANALYSIS

2.1 ASDEX Upgrade contribution to the international confinement database

F. Ryter, L Horton

The available pedestal data of the ASDEX Upgrade shots already included in the International H-Mode Confinement Global Database have been given to the database group to allow an inter-tokamak study on the confinement interplay between edge and core.

A new subset of ASDEX Upgrade confinement data has been produced and contributed to the International H-Mode Confinement Global Database in June 2001. This dataset includes a variety of different plasma parameters such as triangularity, plasma current, magnetic field and density. The shots have been chosen such that a corresponding dataset with detailed pedestal and edge measurement is available and is contributed to the international pedestal database, allowing a meaningful merging of the 2 databases.

2.2 International H-mode Threshold Global Database

F. Ryter and International Database Working Group

The ASDEX Upgrade contribution to the International H-mode Threshold Global Database has been revised. Some of the time slices have been corrected and a few of the outlying ones have been deleted. These corrections reduce the RMSE of the threshold scaling for this tokamak from 20.2% to 18.8%.

Taking into account the 20% difference in power threshold observed between DV-I and DV-II, this further reduces the RMSE to 16.7%.

A similar work has been made for the other 9 tokamaks contributing to the database. The power threshold scaling obtained with this new version of the multi-machine database yields results similar to the previous ones but with significantly lower RMSE: 21.4% instead of 26.9%.

2.3 ITER oriented Confinement Database Analysis

O. Kardaun, (in co-operation with Y. Murakami, K. Thomsen and G. Bracco)

Interval estimation of the global energy confinement time in ITER FEAT based on global multi-tokamak confinement scalings has been further developed, and incorporated into a probabilistic framework for plasma performance assessment, specifically to estimate the 'epistemic' probability of reaching an energy multiplication factor $Q = P_{\text{fus}} / P_{\text{aux}}$ of at least 10 in ITER FEAT ($R=6.2$ m, $a=2.0$ m, $\kappa_a = 1.7$, $V=831$ m³, $I_p=15.0$ MA, $B_t = 5.3$ T, $n_{e,20} = 1.0$, $P_{LH}=88$ MW). The scaling ITERH-98(y,2), derived from a nine tokamak dataset (ITERH.DB3v5) in the ITER Physics Basis Document proved to predict reliably the enlarged confinement dataset (ITERH.DB3v10, July 2001) from 14 tokamaks, as long as the operational limits (Greenwald limit, beta limit, L-H transition power threshold) are respected, which is foreseen in standard inductive ITER FEAT scenario. On the basis of the additional data, the width of the interval estimate (1 technical standard deviation) could be reduced from 3.6 s times $2^{\pm 1/4}$ to 3.6 s times $\exp(\pm 0.14)$. Based on 0-D power-balance calculations this interval translates into the interval ($7 < Q < 50$) under more or less realistic estimates for Z_{eff} , dilution by helium and temperature profile shape. Allowing for a 10% confinement time difference between the nominal 1/2 and 1/6 quantiles of the confinement-time distribution at the ITER FEAT reference operating point, the epistemic probability to reach Q at least 10 (at $P_{\text{fus}} = 250$ MW) was estimated to be 3/4 for 'a large fraction' (nominally 50%) and 7/8 for 'a substantial number' (nominally 16%) of the ELMy H-mode discharges. These results are in agreement with ITER FEAT probabilistic performance assessment for which PRETOR 1-D model calculations have been used.

The new version of the international L-mode dataset (ITERL.DB2) was analysed and exhibits a significantly tighter simple power-law fit when the elongation $\kappa = b/a$ is replaced by $\kappa_a = \text{Vol} / 2\pi^2 R a^2$, an effect shown previously for ELMy H-mode and used in the ITERH-98(y,2) scaling. The updated pedestal dataset, with type I ELMy data from ASDEX Upgrade, DIII-D, JET and JT-60U and enhanced D- α from Alcator C-mod, was analysed and yielded a similar scaling of the pedestal energy as presented at the IAEA in Sorrento. It was found that the negative β dependence of the ITERH-98(y,2) scaling, is related to the scaling of the pedestal energy, rather than that of the core and that the edge gradient width scales rather weakly with the normalised Larmor radius.

3. DESIGN STUDIES

3.1 Design Study for an Alternative Ion Dump

P. Franzen, J. Sielanko (University of Lublin, Poland), B. Heinemann, R. Riedl, E. Speth, A. Entscheva

The scoping study on an alternative concept for the ITER residual ion dump has been continued. As a result of the previous studies, a magnetic deflection system (MIRS ñ magnetic ion removal system) with remote ion dumps is not possible, due to the geometric limitations of the ITER beam line. The new concept now includes magnetic deflection of the residual ions to in-line dump plates with an oblique incident angle (<14°). Two large plates (2 m long, 1.8 m high) are located beside the beam. Power loads depend on the beam divergence and do not exceed 15 MW/m² for the most critical value of 3 mrad. The concept is somewhat similar to the presently foreseen electrostatic in-line dump plates (ERID), however, there are no plates within the beam hit from both sides. Further advantages are the possibility of subdividing the dumps in larger dump panels (like Hypervaportrons) being water-fed from behind instead of using swirl-tubes as it is the case for ERID. These tubes have to be supplied with water from above and cannot withstand more than 6 to 8 MW/m². The detailed design of the MIRS dump plates is now in progress.

3.2 An RF Ion Source for Negative Ions

M. Bandyopadhyay (IPR Gandhinagar, India), A. Entscheva, B. Heinemann, Ch. Hu (ASIPP Hefei, China), W. Kraus, P. McNeely, R. Riedl, W. Schäch, E. Speth, O. Vollmer

Although the H- yields reported previously have not been exceeded, progress has been made in several areas. To protect the ceramic insulator of the driver from thermal stress an internal copper Faraday screen had been added some time ago. This has now resulted in reliable long pulse operation up to 15 s. Different grid materials have been investigated as potential options for cesium free operation. No clear-cut conclusion can yet be drawn from those experiments due to unexpected copper sputtering from the Faraday shield onto the plasma grid.

The effect of noble gases addition to the discharge has been investigated using a Langmuir probe. These measurements indicate that the enhancement of H- current may be caused by an increase in plasma density in the driver due to the addition of a noble gas. This would result in an increased density of vibrationally excited molecules, which in turn would raise the density of negative ions. Suitable diagnostics for the density of vibrationally excited molecules are presently being discussed. Another reason for the enhanced H- yield may be the ponderomotive ($j_{RF} \times B_{RF}$) forces in the driver, which cannot be neglected at those power levels. These forces are caused by the RF field and are always directed inwards, leading to enhanced energies of the plasma ions. An enhanced population of vibrationally excited molecules could be caused by direct collisions with those higher energy ions.

3.3 Plasma Divertor Modelling

H. D. Pacher (INRS-Energie et Matériaux), G. W. Pacher (Hydro-Québec, Varennes, Québec, Canada)

Under the contract "Plasma Divertor Modelling Support to the design of RC-ITER", INRS and Hydro-Québec have collaborated with ITER JCT and IPP in the ITER divertor studies. These showed the advantage of a V-shaped divertor configuration and the necessity of good gas conductance between the inner and outer divertors. A saturation of the separatrix density as function of the puffing rate was found, which accompanied the transition of the plasma in the inner divertor from a partially attached to a fully detached state. An operating window of the ITER divertor was determined. Steady state operation was found to give acceptable divertor parameters, and the inclusion of elastic collisions for helium was found to reduce significantly the helium concentration.

Zero-dimensional simulations were carried out to determine the performance of ITER under reactor-relevant wall loads. One-dimensional simulations of the core plasma of ITER were carried out with the purpose of developing a physics-based model for plasma confinement in the core and pedestal, calibrated on experimental results, for later extrapolation to ITER. Both a time-dependent and a time-averaged ELM model have been developed. Using the latter, the edge operational space of ITER has been traced out. It is a major conclusion that the fuelling rate required for high fusion power operation of ITER, if provided by edge fuelling alone, is almost an order of magnitude larger than that edge fuelling which can be supplied through the scrape-off layer according to B2-Eirene simulations, producing a large edge density gradient, high charge-exchange losses and a reduction of Q. Q exceeding 10 is recovered when the fuelling in the pedestal region (e.g. pellets) is at least equal to the edge fuelling.

Further work concerned a complete re-optimisation of the port startup limiter for ITER, yielding peak power loads of 6.7 MW/m², as well as sensitivity studies. In addition, a generic study of guard limiters for ITER in terms of the curvature mismatch between the plasma and the limiters was carried out.

WENDELSTEIN 7-AS

(Head of Project: Dr. Rolf Jaenicke)

Members of the W7-AS group: see section "Divisions and Groups, Experimental Plasma Physics Division 3".

1. OVERVIEW

The highlight of the past year was the discovery of a new regime of improved confinement at very high density. Access to the new regime was obtained after installation of divertor modules and in a well-conditioned torus vessel after applying boronization. For the future fusion reactor the newly found **High Density H-mode (HDH)** has decisive advantages over the "old" H-mode found in ASDEX in 1982. This conventional H-mode shows an increase of particle confinement times with density leading to accumulation of impurities and radiation collapse in the absence of ELMs. Furthermore it has low edge densities, which is not suitable for divertor action.

In contrast, the HDH-mode is connected with very high densities of up to $4 \times 10^{20} \text{ m}^{-3}$, a significant decrease in impurity confinement avoiding impurity accumulation, good density control even for neutral injection powers of up to 3 MW and high edge densities adequate to drive detachment. Furthermore, the HDH-mode is characterized by an evident reduction of fluctuations (partly ELM-like), by temperature profiles somewhat augmented over normal confinement and by very flat density profiles, which are responsible for the high energy confinement times of up to a factor of two above the ISS95 scaling. The new regime is robust with respect to, for example, variations of the magnetic field geometry and heating power, and it allows long quasi-stationary discharges hitherto impossible at high density and heating power.

It is assumed that access to the new regime is made possible primarily by the enlarged coverage of the plasma-wall interaction region by the divertor carbon tiles which screen the plasma more efficiently from unfavourable interaction with the metallic vessel wall. Above a threshold density the energy confinement time steeply increases with density at the transition into the HDH-mode. In contrast, impurity confinement times drop and then further decrease with increasing density. At still higher densities continuous transition to a detached plasma is observed in divertor magnetic field configurations. With increasing upstream edge

density, the energy and particle fluxes on the near-plasma part of the targets show rollover without passing through a high-recycling regime. The radiation stays peaked at the edge so that the bulk plasma is almost free of impurity radiation. Radiated power fractions are low to moderate in attached regimes and reach up to about 90% in detached plasmas.

The better control of the plasma-wall interaction also allowed considerable improvement in high- β discharges using a magnetic field configuration with high rotational transform and with flux surfaces at the plasma boundary as smooth as possible. Together with higher neutral beam heating power (due to rearrangement of all injectors in the co-direction) the maximum volume averaged β -values could be raised from 2% to more than 3%. Still no significant instabilities were found, so that these higher- β -values also seem to be heating power limited. In contrast to previous high- β discharges which were terminated by a rapid increase of impurity radiation, quasistationary discharges are now possible as long as the toroidal field is not too small. Radiation profiles are not so hollow as in divertor discharges, but they are broad and no longer centrally peaked as in discharges before installation of divertor modules.

Electron Bernstein wave heating by OXB-mode conversion with 70 GHz was previously demonstrated on W7-AS. The advantage of this heating scenario with respect to conventional ECRH is that no cut-off density or upper density limit exists. There is, however, a lower threshold density. For second-harmonic OXB heating at 140 GHz the density has to be well above $2.4 \times 10^{20} \text{ m}^{-3}$, a density hitherto not accessible in stationary discharges. Now, the HDH-mode with its steep density gradient and high central densities is very well suited to application of this heating method. Successful heating at 140 GHz could be demonstrated with a heating efficiency comparable to neutral beam heating.

The diagnostics was completed concomitantly with the divertor experiments. Theoretical work concentrated on interpretation of experimental data of W7-AS and development of codes necessary for W7-X.

2. EXPERIMENTAL AND THEORETICAL RESULTS

2.1 Divertor Experiments

2.1.1 Core plasma performance

W7-AS is now being operated with a modular, open island divertor (see Annual Report 2000) similar to that envisaged for W7-X. First studies were performed at $B = 2.5$ T and an edge rotational transform $t_a \approx 5/9$. The divertor allows access to a new NBI-heated, very high-density (up to $\bar{n}_e \approx 4 \times 10^{20} \text{ m}^{-3}$) operating regime with improved confinement properties (HDH-mode). Above a certain threshold density, which increases with NBI power, the energy confinement time τ_E steeply increases with density and exceeds τ_E^{ISS95} by a factor of up to two. In contrast, the particle and impurity confinement times dramatically decrease with increasing density (Fig. 1).

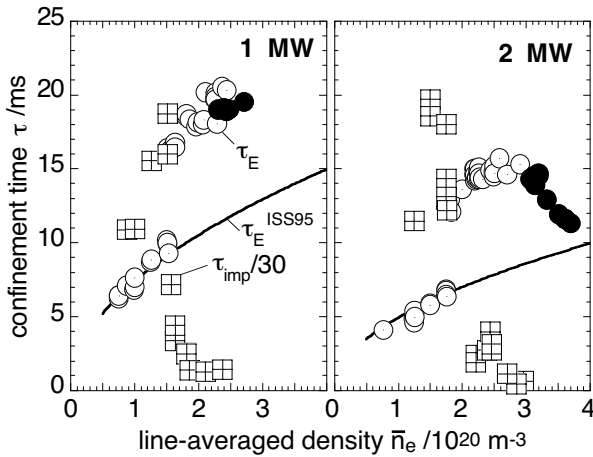


FIG. 1: Energy confinement times τ_E and impurity confinement times τ_{imp} (from laser blow-off injection of aluminium) as functions of the line-averaged density \bar{n}_e for NBI-heated discharges. $B = 2.5$ T, $t_a = 5/9$, minimum separation between x-points and targets $\Delta_x = 3.8$ cm. Solid symbols indicate partially detached discharges.

The HDH-mode is characterized by flat density profiles with steep gradients at the edge, significant radial E -field gradients at the edge, and strong suppression of turbulence similar to an ELM-free H-mode. In contrast to the 'conventional' quiescent H-mode scenarios previously observed in W7-AS, there is no impurity accumulation. These new features allow full density control and quasi steady-state operation even at the highest available NBI power of 3.5 MW, and also under conditions of partial detachment from the divertor targets (see further below). The plasma radiation mainly originates from lower ionization states of the intrinsic impurities, carbon and oxygen, and is always peaked at the edge. Radiated power fractions are moderate in attached regimes and reach up to 90% in detachment scenarios. The HDH-mode is rather robust against changes of the magnetic field configuration (Fig. 2).

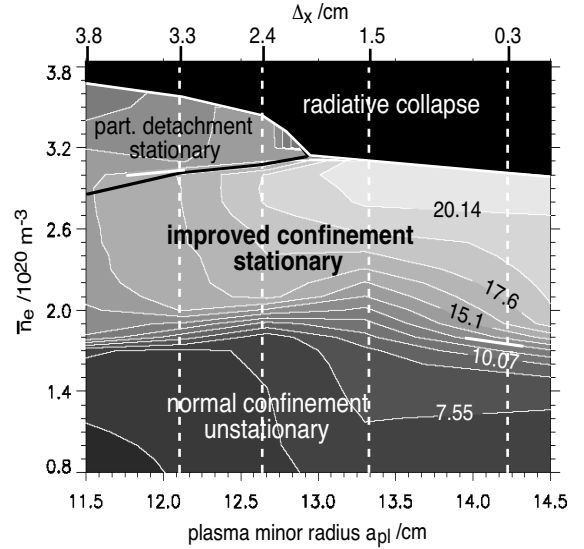


FIG. 2: Energy confinement times τ_E [ms] for NBI (2 MW) discharges as a function of the line-averaged density \bar{n}_e and the plasma minor radius a_{pl} (separation Δ_x between x-points and targets). $B = 2.5$ T, edge rotational transform $t_a \approx 5/9$. a_{pl} and, hence, Δ_x were varied by control coil currents affecting the size of the magnetic islands at the edge.

2.1.2 Divertor regimes

Stable detachment is observed in configurations with sufficiently large boundary islands, not too long field line connection lengths inside the islands, and distances Δ_x between x-points and targets ≥ 2.4 cm (Fig. 2). The threshold upstream density for the onset of detachment decreases with increasing Δ_x and decreasing power. The upstream density n_{es} increases steeply with \bar{n}_e up to a rather high level (e.g. $6 \times 10^{19} \text{ m}^{-3}$ for 2 MW of NBI), saturates above a certain \bar{n}_e value, which increases with power, and drops in detached regimes. The upstream temperature T_{es} and, hence, the upstream plasma pressure tend to decrease above the \bar{n}_e value where n_{es} becomes constant. Concomitantly with this, the energy and particle fluxes onto most of the target area show, with increasing \bar{n}_e , rollover already prior to detachment. A specific feature is that detachment is achieved without running through an intermediate high-recycling regime. Detachment is always partial: the plasma at a certain small target region, far from the main plasma but with steeper inclination to the field lines ('wing' region), stays attached (downstream temperature $T_{ed} > 20$ eV) even at highest density, but with reduced thermal load (Fig. 3). Detachment from the remaining, much larger area is also partial in the sense that the particle and energy fluxes stay finite ($T_{ed} > 2$ eV). With increasing detachment, the up/down parameters (thermal load, radiation from the divertors, neutral pressures in the divertor subvolumes) become increasingly asymmetric. Moreover, the radiation from the separatrix region becomes asymmetric, indicating a MARFE-like development. Nevertheless, these asymmetries do not prevent stable operation with acceptable energy confinement and significantly reduced power flux onto the targets.

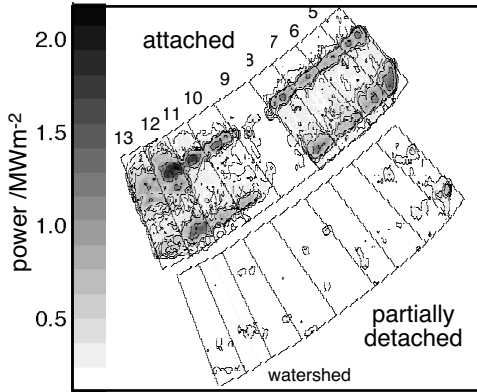


FIG. 3: Thermal load on a bottom target (from thermography) for attached and partially detached NBI (2 MW) discharges. The plasma at tile 5 stays attached, but at reduced thermal load.

2.1.3 Density limit

First attempts were made to compare the maximum line-integrated density \bar{n}_e in W7-AS divertor discharges with predictions by the density limit scaling law derived for W7-AS limiter discharges. For example, by assuming 0.70 MW of deposited power and a minor radius of 12 cm the scaling law predicts $\bar{n}_e = 2.6 \times 10^{20} \text{ m}^{-3}$ in comparison with the $\bar{n}_e = 2.0 \times 10^{20} \text{ m}^{-3}$ achieved. A summary of the maximum densities for various magnetic fields, input powers and plasma radii are compared with previous results in a limiter configuration of W7-AS in Fig. 4. The highest line-averaged densities have clearly been recorded in the last campaign. However, on the basis of the increased input power and reduced plasma radius the values achieved do not exceed that predicted by a scaling law based on previous density limit studies in a magnetic configuration with limiter.

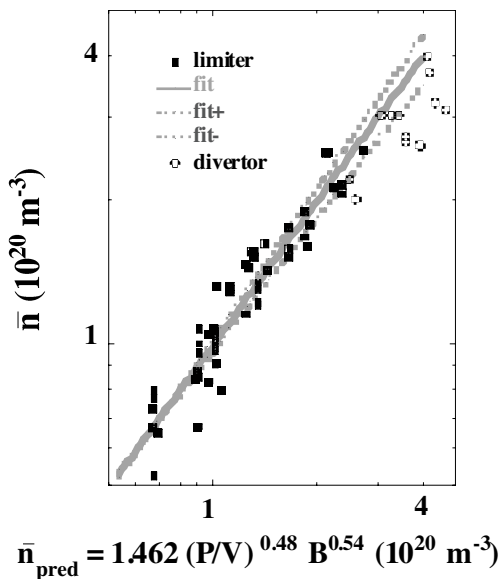


FIG. 4: Comparison of achieved and predicted values of line-integrated densities for density limit discharges in the divertor configuration.

The attractive property of the new divertor configuration lies in the ability to run steady-state discharges at higher NBI input powers compared with earlier limiter discharges. Previously, the line-integrated density would increase in an uncontrolled way. Above the density threshold for transition to the high-density H-mode, the reduction in impurity confinement time, and hence by inference the particle confinement time, allows density control to be attained in the divertor configuration. The radial profiles of radiated power are hollow and even at the highest densities the plasma no longer suffers radiation collapse. The radiated power fraction does not increase with time. Below the density threshold for the high-density H-mode the radiation profiles are peaked and the radiated power increases with time. This was also the case for the limiter discharges.

2.1.4 Edge transport study

Major EMC3-EIRENE code predictions, namely the absence of high recycling prior to detachment (Fig. 5), the additional momentum losses at low density, high temperature (Fig. 6) and the jump of the carbon radiation on transition to detachment (Fig. 7) were verified by the first W7-AS high-density, high-power divertor experiments. The first two effects are essentially due to the enhanced role of the cross-field transport related to the small field-line pitch and plasma-to-target distance in the island-divertor geometry; the third one was derived from the energy balance equation and is due to a thermal instability associated with the form of the impurity cooling rate function.

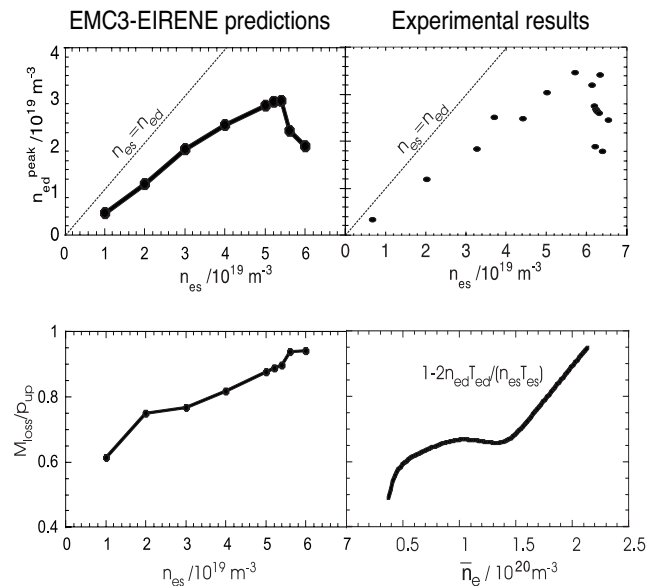


FIG. 5: Absence of high recycling prior to detachment (top) and momentum loss at low densities (bottom).

After the start of W7-AS divertor operation, a quantitative comparison of code simulations and measurements were made (Fig. 5). The code correctly reproduces the \bar{n}_e dependence of n_{ed} from Langmuir probes, including rollover and detachment.

The sharp increase of the ionization fraction in the core S_{core} at $\bar{n}_e > 2 \times 10^{20} \text{ m}^{-3}$ is considered to be the reason for the rollover and the drop of the measured upstream density on detachment.

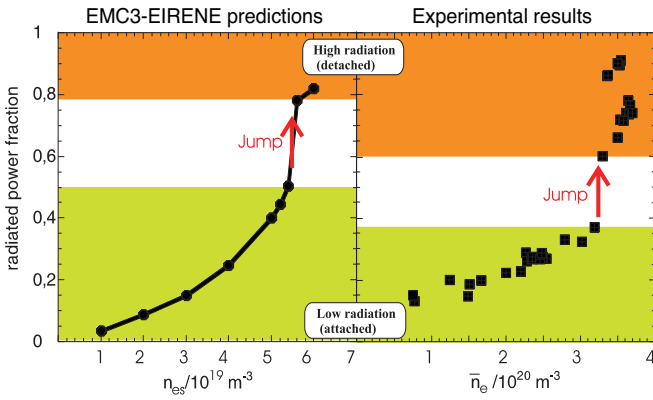


FIG. 6: Jump of carbon radiation on transition to detachment

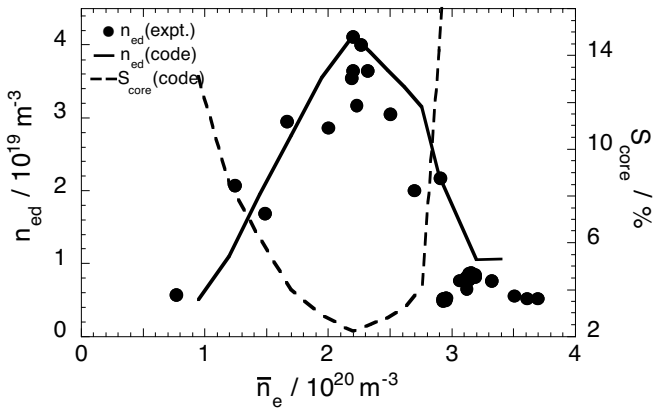


FIG. 7: Downstream densities from experimental data and code calculations, and simulated ionization fraction in the core.

Additionally, estimates for the transport coefficients D and χ were derived for ECRH discharges (normal confinement) by fitting the calculated density and heat flux profiles to the measured ones, yielding a roughly $1/n_e$ scaling. With this scaling, the calculated neutral pressure values agree with the manometer data.

2.2 New High- β Results

Previous experiments in the Wendelstein 7-AS stellarator, where volume-averaged β -values of up to $\langle\beta\rangle \approx 2\%$ could be achieved with ≈ 3.5 MW of balanced neutral beam heating, showed that the heating efficiency of the counter-injected beams was very poor particularly at the low magnetic fields of 0.7...1.25 T required to reach the maximum β -values. After rearrangement of all injectors in the co-direction and installation of the island divertor, a new attempt was made to increase the plasma performance in the high- β regime and explore the stability limits under the new experimental boundary conditions.

Although most of the experiments were not conducted with proper island divertor configurations, the divertor was found to have the beneficial effect of improving confinement and density control in combination with relatively low radiation losses. Flat-top times of ≈ 0.7 s could be achieved with average β -values of $\langle\beta\rangle \approx 2.5\%$. At the magnetic field of $B = 1.25$ T typical values of the central temperatures and the line-averaged density are measured in the range of $T_{e0} = 350\text{...}450$ eV and at $\langle n_e \rangle \approx 2.2 \cdot 10^{20} \text{ m}^{-3}$, respectively. At lower magnetic fields ($B = 0.8\text{...}0.9$ T) maximum beta values of $\langle\beta\rangle \approx 3.1\%$ could be achieved (Fig. 8).

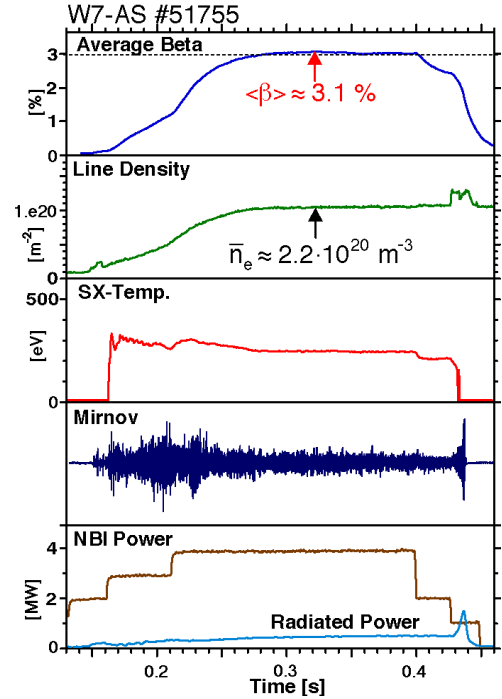


FIG. 8: Optimized quasi-stationary high- β discharge with $\langle\beta\rangle$ reaching 3.1 % (at 0.9 T and $t_{\text{ext}} = 0.52$). The (low) radiation losses are peaked at the plasma edge.

The divertor control coils were used to minimize the edge islands and establish smoothed flux surfaces at the edge in the range of $t > 0.5$, which is favourable in respect of plasma equilibrium.

The observed pressure-induced horizontal plasma axis shift is nevertheless very significant and has to be controlled by a vertical field. According to free boundary equilibrium calculations (NEMEC) the Shafranov shift stays below 40 % of the horizontal plasma radius. Reasonable agreement is found between X-ray tomography data and NEMEC calculations.

The MHD activity becomes noticeably more quiescent towards the highest β -values. In the intermediate β -range pressure-driven coherent modes at ≈ 10 kHz appear with mode numbers corresponding to low-order rational surfaces. X-ray tomography reveals a pronounced ballooning structure of these modes. In addition, global Alfvén gap modes with frequencies up to ≈ 300 kHz can be destabilized at lower densities where the drive by resonant fast ions is larger. Particularly in cases of low temperatures very short (≈ 100 μs) ELM-like MHD events can cause fast relaxations

of the electron temperature profile and significant drops of the plasma energy. These effects may be caused by resistive MHD modes, since they are absent in high-performance discharges, where the temperature can be maintained above a critical value.

The local MHD stability (Mercier and resistive interchange criteria and ideal ballooning mode stability) as well as the stability of ideal global modes were found to increase with β . This is in qualitative agreement with the experimental data and can be attributed to the deepening of the magnetic well and the increase of internal shear. The numerical results suggest that stable plasmas may be maintained in W7-AS up to the equilibrium β -limit expected in the range $\langle\beta\rangle = 3.5\text{...}4.5\%$, depending on the rotational transform.

2.3 Electron Cyclotron Resonance Heating

2.3.1 High power combined ECRH-NBI heating

The improved machine performance by the helical island divertor allows high power ECRH (2.2 MW) to be combined with high power NBI (2 MW) heating. At iota 1/2, which is the operational regime of the divertor, a discharge with a strongly peaked electron temperature profile, the so-called electron root regime, was established. The improved confinement in the centre is due to the creation of a positive radial electric field, which reduces the otherwise large neo-classical losses. The low heat transport was confirmed by the coherent analyses of heat wave propagation in the central region. The additional NBI heating did not greatly perturb the central high-temperature gradient region, but generates a second region of improved confinement at the plasma edge which was accompanied by a negative radial electric field (ion-root) as shown in Fig 9. By combination of ECRH and NBI, formation of an edge pedestal and a central temperature peak could be established.

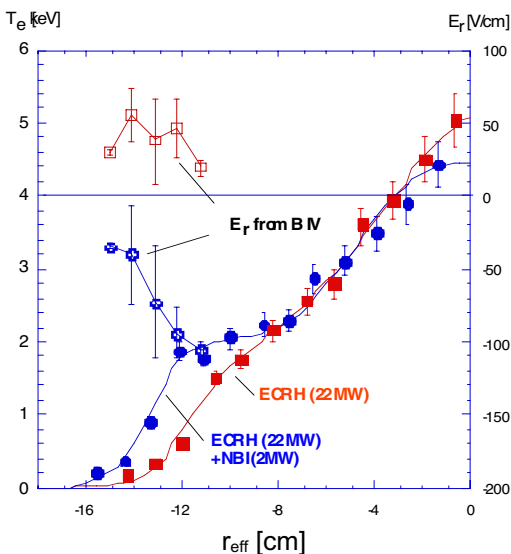


Fig.9: The generation of an edge pedestal in the electron temperature profile by combined ECRH and NBI heating (solid markers). The blank markers represent the accompanying radial electric field from BIV spectroscopy.

2.3.2 Electron Bernstein wave heating

Efficient electron Bernstein wave heating by OXB-mode conversion with 70 GHz has already been successfully demonstrated at Wendelstein7-AS. But second-harmonic OXB heating with 140 GHz has remained unexplored, since it requires a threshold density of $2.4 \times 10^{20} \text{ m}^{-3}$. The high-density H-mode regime (HDH) with its steep edge density gradient and peak density of up to $4.0 \times 10^{20} \text{ m}^{-3}$ attainable under stationary conditions allows efficient second-harmonic Bernstein wave heating with 140 GHz, which is the ECRH frequency designated for W7-X. The experiments showed that the heating efficiency is comparable with NBI (Fig. 10). The local power deposition of EBW's and the possibility of fast modulation qualify EBW heating for heat wave generation (see Fig. 10 and section 3.2), temperature profile shaping and fine tuning of power flow through the separatrix.

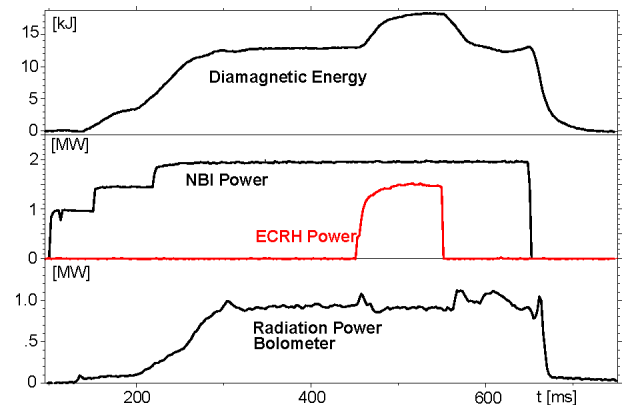


FIG. 10: Second-harmonic 140 GHz EBW heating at a constant density of $3.5 \times 10^{20} \text{ m}^{-3}$. The large increase of plasma energy indicates the good heating efficiency.

2.3.3 Electron Bernstein wave current drive

For the EBW's parallel refractive indices N_{\parallel} larger than 1 are possible. High efficiency is therefore predicted for EBW current drive (EBCD). At W7-AS successful current drive experiments were performed for the first time with 70 GHz first-harmonic EBW heating. Up to 1.8 kA of current in the co-direction was driven by 400 kW EBW's at a density of $1.4 \times 10^{20} \text{ m}^{-3}$ and a temperature of 500 eV (Fig.11). Since OXB-mode conversion requires an optimal launch angle, no angular scan was possible to investigate the driven current. However, to maximize the current drive efficiency, the N_{\parallel} component of the EBW's was varied by either reversing the magnetic field or changing the magnetic configuration.

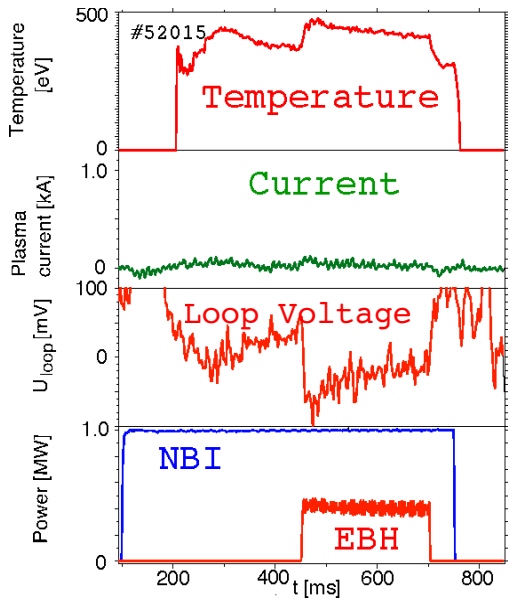


FIG. 11: First EBW current drive with 70 GHz. In a current-free discharge the EBCD-driven current was compensated by the inductively driven current, which is represented by the large change of the loop voltage.

2.4 Theory

2.4.1 EMC3-EIRENE code development

At present, the EMC3-EIRENE code is being extended to arbitrary edge magnetic structures, including closed and open island sections and ergodic regions as found in both low-shear and high-shear configurations. Standard magnetic coordinates are replaced by a finite flux tube system defined and stored over one field period. A new reversible field-line mapping (RFLM) technique is used which provides, in combination with the Monte Carlo integration method used in the EMC3 code, a very accurate treatment of both the parallel and cross-field transports. Several accuracy tests were carried out by the RFLM technique for W7-AS, W7-X, LHD, and TEXTOR-DED configurations. They show that the radial deviation of the mapped field lines from "exact" numerical integration (GOURDON code) for flux surfaces or islands, which is a crucial parameter for correct numerical distinction between the parallel and the cross-field transport, remains bounded at a very low level with an increasing number of mapping steps (see "mapping noise" in Fig. 12 for W7-AS). In other words, mapped field lines do not leave flux surfaces or islands for any relevant number of mapping steps if the grid chosen is sufficiently fine. Comparison of the linear RFLM technique with the linear "Interpolated Cell Mapping" (ICM) technique applied to W7-AS shows that the radial deviation of the same field line calculated with ICM exhibits a mapping noise of increasing amplitude drifting linearly away in the direction of increasing radius, with the drift velocity and the noise amplitude depending on the mesh size (Fig. 12).

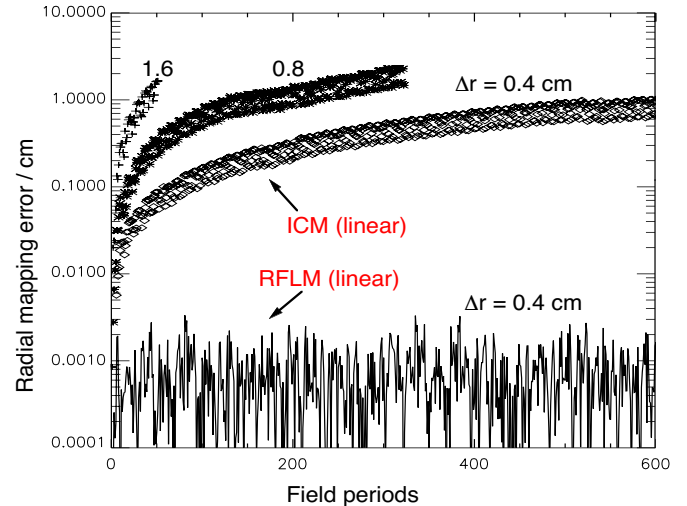


FIG. 12: Radial deviations of a mapped field line from its "exact" position for a W7-AS flux surface from the RFLM and ICM techniques. Starting position: $R=183$ cm, $z=0$ at triangular plane, Δr =average mesh width.

2.4.2 Validation of profile data

Integrated concepts for the systematic evaluation of Thomson scattering data were successfully applied and a comparison of different evaluation schemes was made (cooperation with R.Fischer and S. Gori (CIPS)). Transfer of the concept is currently done for different diagnostics. This diagnostics software development had an impact on diagnostics improvement due to the strong interaction of all parties participating in the process (experimentalist, theoretician, statistician, software developer). Software tools for data base access continued to be developed. Efforts on data consistency checks and data validation from different fusion laboratories were evaluated and investigated with respect to applicability on W7-AS and W7-X. A European workshop on data validation was held in summer 2001 at Greifswald. Data base-oriented checks on the consistency of the density diagnostics were performed on W7-AS. Detection criteria for malfunctioning diagnostics were defined and applied.

2.4.3 Equilibrium calculations for W7-X

Free-boundary NEMEC calculations for W7-X with non-vanishing toroidal current profiles were provided for the magnetic diagnostic development. This is of particular interest in minimizing the effect of stray fields in flux measurements due to toroidal currents.

2.4.4 HINT code

A version of the HINT code was adapted for equilibrium calculations in the high- t range of the W7-AS configurational space which is used for divertor experiments. The NEMEC code which is usually used assumes the existence of good nested flux surfaces; this ansatz fails when applied to these configurations due to their highly corrugated separatrix arising from the natural boundary islands.

Like the PIES code, HINT does not rely on the existence of flux surfaces, and its numerical algorithm seems at the moment to be computationally more efficient than PIES. Moreover, in contrast to PIES, HINT is an intrinsic free-boundary code which is necessary to get the finite- β equilibria correct. First calculations have been initiated to test HINT's general applicability.

2.4.5 *High- β equilibrium calculations for W7-AS at high ϵ*

Although NEMEC fails in calculating separatrix-bounded high- ϵ configurations for W7-AS, it is possible to apply it if the plasma boundary is smoothed. In the high- β experiments around $\epsilon = 0.5$, this is performed with the high vertical fields used in the experiments to compensate for the Shafranov shift. This reduces the vacuum field island widths at low β , leading to smoother plasma boundaries. Moreover, an appropriate choice of currents in the correction coils employed in the divertor experiments provides additional smoothing of the flux surfaces at higher β values, making the calculations quite reliable.

2.4.6 *NBCD Fokker-Planck calculations*

High-power NBI discharges at high temperatures (long slowing-down times) cannot be correctly described within the linear approach since the non-thermal ion fraction can be comparable to the thermal one. The friction of passing ions with respect to the locally trapped ones can be the dominant momentum sink for small Z_{eff} , an effect not present in tokamaks. An important deviation from the Maxwellian is obtained in the thermal range which reduces the neutral beam current drive (NBCD) efficiency in comparison with the estimate from linear theory.

The bounce-averaged Fokker-Planck code (FPTM) with the complete nonlinear collision operator is used for calculating the ion distribution function which is applied within a linear approach to estimate the electron Ohkawa current contribution.

2.4.7 *Kinetic instabilities driven by NBI*

The kinetic instabilities driven by the NBI at W7-AS are analyzed both theoretically (in collaboration with A. Shalashov, IAP, Nizhny Novgorod; International Max Planck Research School) and experimentally (WTZ collaboration with E. Suvorov and L. Lubyako, IAP, Nizhny Novgorod). For the different scenarios (tangential NBI, perpendicular diagnostic beam injection, and the new oblique NBI), broad-band cyclotron mode activity was measured (ICE), and the lower-hybrid (LH) activity in addition by the CTS diagnostic. The effect of the loss-cone width on the LH activity roughly corresponds with theoretical expectations. For a more detailed analysis, the fast ion distribution function will be modelled with respect to the loss-cone size, allowing numerical solution of the full dispersion relation.

2.4.8 *Monte Carlo code*

The applicability of the δ -f Monte Carlo technique used in tokamaks for improving the statistical convergence properties will be checked for stellarators. In the δ -f technique, the characteristic system (eqs. of motion) is inhomogeneous and the new "marker" equation leads to a weighting algorithm. With the radial gradient of the Maxwellian being taken as the inhomogeneity, the weight of particles deviating from flux surfaces is increased. As long as this particle motion is periodic (e.g. for tokamak bananas) the statistical properties are improved. For the radial drift of ripple-trapped particles in stellarators, however, the weight increases monotonically. First δ -f Monte Carlo simulations of the bootstrap current coefficient for W7-AS and W7-X indicate strongly degraded statistical properties (in collaboration with R. White, Princeton).

2.4.9 *International collaboration in neoclassical theory*

In the international collaboration in neoclassical theory, the following codes have been successfully benchmarked: MOCA and DCOM (both Monte Carlo codes), DKES (drift-kinetic eq. solver), GSRAKE (ripple-averaged eq. solver) and NEO (estimating the effective helical ripple by field-line integration technique). These codes have been applied to W7-AS, TJ-II, NCSX, and several LHD and W7-X configurations, and the lmfp confinement regimes known from classical stellarators were identified. However, some new features were found: e.g. a transition region between the $1/\nu$ and the $\sqrt{\nu}$ regimes for the "drift-optimized" LHD configuration (with $R = 3.60$ m), where the deeply-trapped particles are magnetically confined, shifting the transition to the $\sqrt{\nu}$ regime to larger values of the radial electric fields.

In the next step, the monoenergetic transport coefficients for all configurations of interest based on the classical lmfp-regimes must be described in a fast database which can be used for transport analysis as well as for predictive transport modelling. Finally, the benchmarking of DKES and Monte Carlo techniques with respect to the bootstrap current coefficient was started (collaborations with V. Tribaldos, CIEMAT; S. Murakami, NIFS; D. Mikkelsen and R. White, PPPL; W. Kernbichler and S. Kasilov; TU-Graz).

3 DIAGNOSTIC DEVELOPMENT

3.1 Ruby Thomson Scattering Diagnostic

After complete reconstruction the Ruby Thomson scattering diagnostic is now in operation to cover again the complete plasma cross-section. The total viewing chord (420 mm) is observed by means of two individual Littrow-type polychromator setups, with intensified CCD cameras for light detection. The section near the inner torus wall (120 mm) is covered by the edge system, which offers a high spatial resolution of 4 mm. Further on it can be optimized for measuring electron temperature and density profiles of the edge or gradient region of W7-AS plasma by exchanging the grating. The remaining part of the viewing chord (300 mm) is again observed by a new Littrow-type polychromator setup

which in fact replaces the former photomultiplier-based polychromator system. Here the spatial resolution is restricted to 20 mm as the original fibre guides were kept for observation, but they had to be reshaped to build the entrance slit of the new polychromator. In collaboration with members of CIPS, an additional evaluation of the diagnostic data was established by using Bayesian statistical methods to improve detailed knowledge of measurement uncertainties, including all calibrating procedures.

3.2 Electron Bernstein Emission Diagnostic

The diagnostic, whose setup was described in the last annual report, takes advantage of black-body emission and mode conversion of electron Bernstein waves (EBW) to provide electron temperature profiles at densities above the ECE cutoff (Fig.13).

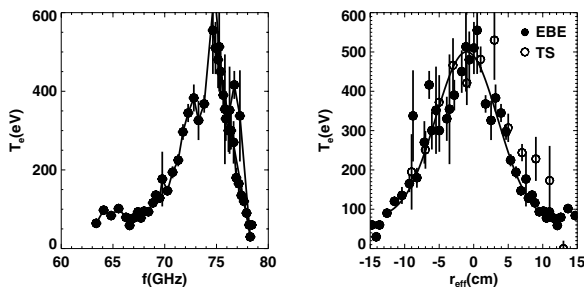


FIG.13: Left: Spectrum of EBW emission at 1st harmonic. Right: Temperature profile reconstructed with the aid of an EBW ray-tracing code (solid circles). Thomson scattering data are also shown for comparison (blank circles).

The heat wave propagation method for determining local heat transport coefficients was also extended for the first time beyond the ECE cutoff density by combining EBW emission measurements at the 1st harmonic (63-78 GHz) with modulated second-harmonic EBW heating at 140 GHz (Fig.14).

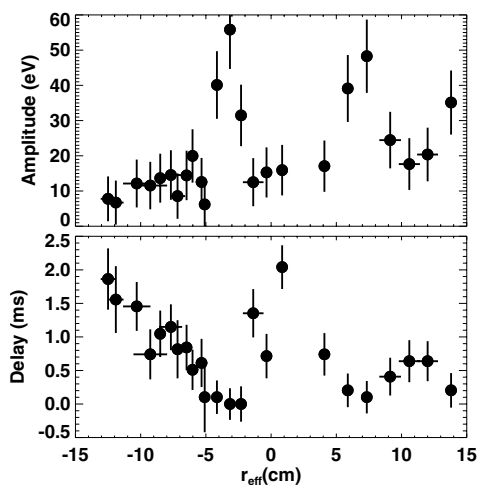


FIG. 14: Amplitude and phase of heat waves generated by off-axis EBW deposition ($r_{\text{eff}} \approx 5$ cm) and measured by EBW emission.

3.3 Li beam Diagnostic

3.3.1. Two-dimensional electron density fluctuations

Two-dimensional electron density fluctuation profiles were measured by means of the Lithium (Li) beam diagnostic with a poloidally deflected beam. From the fluctuation measurements the radial, poloidal, and temporal correlation of density fluctuations was determined. The results agreed well with Langmuir probe measurements in the scrape-off layer.

3.3.2 Ion temperature and poloidal rotation measured by CXRS

The Doppler shift and broadening of the C6+ charge exchange radiation (529 nm) with the high-energy neutral Li beam is measured with a 0.75 m imaging spectrometer. Spectra at 5 radial channels can be simultaneously collected with a frame transfer CCD camera. Typical operational limits are $n_e < 5 \times 10^{19} \text{ m}^{-3}$ and $T_e > 100$ eV with a time resolution of about 100 ms, necessary for signal averaging. Limits are imposed mainly by the attenuation of the Li beam. In high T_i discharges, ion temperatures between 40-700 eV and poloidal rotation velocities up to 30 ± 2 km/s were determined. The diagnostic is well suited to documenting the edge region and provides supplemental information to the hydrogen diagnostic beam.

3.4 Bolometer Camera for Tomography

Installation of a divertor in W7-AS necessitated extension of the present 32-channel gold foil bolometer camera used to measure radial profiles of radiated power. For measurements of the radiated power in the divertor, 3 bolometer cameras comprising 44 channels were recently installed. Radiated power measurements in the divertor chamber show that on detachment the radiating volume moves away from the divertor plate. Three-dimensional simulations of energy, particle, and impurity transport in the divertor magnetic configuration with magnetic islands at the plasma boundary support these observations. On detachment the radiating volume then moves to the separatrix.

Measurements of radiated power in the divertor were also made with photodiodes. Two unbiased AXUV 16 channel photodiode arrays with a bandwidth of 3 kHz are connected by 10 m of cable to the data acquisition system. Bursts in radiation power during the discharge are suspected to be carbon flakes from the divertor plates. This could be directly confirmed from spectroscopic measurements of carbon line emission. The value of a photodiode system measuring only radiation losses was demonstrated in detached discharges.

3.5 Divertor Diagnostics

3.5.1 2D divertor observation

The divertor camera observation system based on CCD cameras (12-bit dyn. range) equipped with interference filters has now been completed. The bottom divertor in module 1

can be simultaneously observed in the light of H_{α} , H_{β} and CII, the top divertor in module 2 in the light of H_{α} . The entire system can be remotely operated. First studies dealt with the up/down asymmetry and the degree of detachment across the entire divertor modules. A simpler, uncooled version of the CCD camera was installed in module 5. Two cameras with H_{α} interference filters observe the top and bottom module. This system allows the toroidal symmetry of the divertor plasma to be studied. A further camera with a CMOS detector was installed with a toroidal view. Due to its logarithmic response the dynamic range covers up to 6 decades, allowing faint signatures in the plasma edge region to be observed together with strong ones from the divertor without saturation. Moreover, each pixel can be individually read-out. A linescan camera with 2,048 pixels, 12-bit dyn. range views a radial section of the divertor at an image rate of 4.5 kHz.

3.5.2 Thermal He beam

A thermal He-beam diagnostic was installed in the W7-AS divertor in order to measure n_e and T_e profiles ($10 \text{ eV} < T_e < 200 \text{ eV}$, $2 \times 10^{18} \text{ m}^{-3} < n_e < 5 \times 10^{19} \text{ m}^{-3}$) with high spatial resolution (vertical 1-3 mm, radial 0.8-6 cm increasing with height above the target due to the beam divergence) in the zone between the target plate and separatrix. Two independently operating thermal He beam nozzles were integrated into the central part of the upper divertor in module 2. The nozzle and gas control system were supplied by FZ-Jülich. The He beam, formed by a 33 mm long, 8 mm diameter nozzle made of $340 \times 0.27 \text{ mm}$ inner-dia. micro-tubes, has a beam divergence of 42° FWHM. To avoid any influence on core plasma performance, the pressure in the gas reservoir for the nozzles was kept at less than 25 mbar. T_e and n_e are derived from intensity ratios of 3 spectral lines simultaneously recorded with an $f = 0.19 \text{ m}$, $f/3.9$ imaging spectrometer. The emitting zone is observed through a cut-out in the divertor baffle via two mirrors. A UV-VIS-IR achromat is used for direct imaging of the emission zone onto the entrance slit of the spectrometer, which is equipped with a magnetic-field-hardened water-cooled back-illuminated 2D CCD camera. The time resolution is limited by the readout time of the CCD and depends on the freely selectable vertical resolution (binning of lines), e.g. at 3 mm resolution the time resolution is limited to 25 ms.

3.5.3 Passive divertor spectroscopy

A spectrometer with a triple grating turret is being used in the He-beam observation system. Under conditions close to detachment (high n_e , low T_e), i.e. when the He beam technique can no longer be meaningfully employed, this allows one to record the Balmer series spectrum, from which line of sight averaged n_e and T_e profiles across the 9 cm region between target plate and separatrix can be derived for $T_e < 5 \text{ eV}$ and $n_e > 10^{20} \text{ m}^{-3}$. The system can also be used to monitor the movement of the carbon radiation zone towards the separatrix during detachment. This system is complemented by a higher-resolution imaging spectrometer of similar type ($f = 320 \text{ mm}$, $f/4.1$) equipped with the same

CCD detector. That system views a radial section across the divertor, e.g. at the location of the thermal He-beam nozzles, from a port on the opposite side of the torus via a row of 25 quartz fibres, giving a radial resolution of 7 mm. The system allows one to determine the emission from molecular bands, the radial distribution of the impurity radiation zones, and line of sight averaged radial electron density profiles across the target from Stark broadening of spectral lines.

3.5.4 Z_{eff}

Two PC plug-in card-based microspectrometers (resolution 1.5 nm, 25 μm entrance slit, 600 g/mm grating) with 2,048 pixel linescan detectors (time res. 7 ms), one for the UV-Vis and one for the IR region, together covering the spectral range 250 - 1175 nm, look toroidally via two optical fibres in the midplane through the plasma axis. As imaging optic a UV-Vis-IR achromat ($f = 50 \text{ mm}$, $f/4$) is used. The system has a time resolution of 7 ms. The great advantage of the system over an interference filter based one is that one can automatically select all truly spectral line-free regions over the entire range, which ensures very high reliability of such a system.

3.5.5 IR divertor observation

A second IR camera was put into operation and now permits one to measure the temperature distribution of the upper divertor target plates in module 2 with a spatial resolution of 2 mm. The new camera operates with a frame rate of up to 315 Hz.

3.6 2D ECE Correlation Measurements

3.6.1 Radial-poloidal correlation of temperature fluctuations

2D ECE correlation measurements were made, supplementing earlier temperature fluctuation measurements. The setup of the 2D ECE correlation diagnostics is already described in last year's Annual Report. Structures were found which are elongated in the radial and poloidal directions. These structures show a higher coherency in the poloidal than in the radial direction and are found to move in the electron diamagnetic drift direction. They are thought to be of the drift-wave type of fluctuations. Numerical simulations are under way in order to identify the type of fluctuation (ITG; TEM). Scaling experiments show that electron temperature fluctuations decrease with increasing ECRH heating power, in agreement with earlier studies. The vanishing of the structures can be attributed to increasing velocity shear which arises from higher radial electric fields with increasing heating power. This tears the structures apart to smaller scale lengths, then too small to be detected by the two-dimensional ECE correlation diagnostics.

3.7 Emissive Electrical Probes for Plasma Potential Measurements

Fluctuations of density (ion saturation current) and electric plasma potential and the correlation between these two fluctuating quantities has to be measured to calculate the fluctuation-induced (turbulent) particle transport, which was shown to account for the anomalous transport observed in the edge of fusion devices. Instead of the plasma potential, usually the so-called floating potential was measured by means of electrical probes (Langmuir probes). The floating potential deviates from the plasma potential by an amount which depends on the electron temperature and on several further quantities, which are experimentally hard to access. A hot probe which thermally emits a sufficiently high electron current density charges to an electric potential value much closer to the plasma potential than a non-emissive probe, which has been used for many years in laboratory plasmas. The aim of this project is to develop indirectly heated LaB₆ probe tips more capable of withstanding the thermal loads imposed on them in the edge of a fusion plasma than the thin tungsten filaments used in laboratory plasmas.

3.8 Fluctuation Measurements by Laser Blow-off

A repetitive laser blow-off system was put into operation on W7-AS. It has been used to inject lithium atoms as well as aluminium micropellets.

The micropellets have been observed with a two dimensional CCD camera to detect the cloud distribution of different aluminium ions that were formed during the ablation of the micropellets in the scrape-off layer and the edge plasma. The lithium was observed with a radial 8-channel photomultiplier array to investigate the electron density fluctuations as well as with a CCD camera to determine density profiles.

The aim of the fluctuation studies was to verify the results of similar investigations made with a high-energy lithium beam and to have a closer look at the changes that can be seen in the inner and outer vicinity of the separatrix.

It could be shown that the autocorrelation of the signals from the confinement region shows a wavelike structure that cannot be seen in the scrape-off layer. This is in agreement with the results from the high-energy beam.

Due to the better radial resolution of the laser blow-off (2 mm) compared with the high-energy beam (1 cm) a change in the apparent radial velocity can be seen at the separatrix which cannot be seen so clearly by other methods. One has to take into account, however, that this apparent radial velocity can be the result of the poloidal movement of structures that are inclined in the radial-poloidal plane. This kind of structure has been observed on W7-AS with Langmuir probes.

By reversing the magnetic fields, it could be seen that the apparent radial velocity in the scrape-off layer is reversed as well. This observation can give some hints on the formation process of the structures.

4.3 Neutral Beam Injection

The final stage of neutral beam injection at W7-AS has now been reached. A new co-injector and a new radial injector are operational. Co-injection on W7-AS affords better heating efficiency, especially at the low magnetic fields necessary for high-beta experiments. The radial injector with an almost perpendicular injection angle allows the possibility of studying both interaction of perpendicular injection and generation of a radial electric field.

4.3.1 Tangential co-injector

The new co-injector started with plasma operation in April. When W7-AS operates with reversed field there are now two tangential co injector boxes. Each box is equipped with four filament sources running at 50 kV/25 A (hydrogen) or 55 kV/23 A (deuterium). The total tangential NBI power is 3.4 MW.

Co-injection on W7-AS has better heating efficiency, especially at low magnetic fields. For example, for a B-field of 0.9 T and $n_e(0) = 2.1 \cdot 10^{20} \text{ m}^{-3}$ the efficiency for co-injection is in excess of 80 %, while for counter-injection it is less than 40 %. This increase in heating efficiency was used to improve the $\langle \beta \rangle$ obtained at W7-AS. A $\langle \beta \rangle$ of 3.1 % was obtained in a quiescent discharge with eight tangential co-NBI sources at 0.9 T. The old $\langle \beta \rangle$ value with co- and counter-NBI from 1997 was $\langle \beta \rangle = 2 \%$ at 1.25 T.

Since W7-AS has its new island divertor in operation a maximum density of $n_e(0) = 3.5 \times 10^{20} \text{ m}^{-3}$ is now possible with stationary plasma discharges and four NBI sources at 2.5 T and $T_e = 500 \text{ eV}$. Although the NBI deposition profile starts to become hollow, an efficiency of about 85 % is achieved with tangential NBI.

4.3.2 Radial injector

This injector is equipped with two new RF sources with a total power of 550 kW. Installation of the ion sources, their connection to the high-voltage supply, and the remaining electrical and mechanical work were finished in summer.

The radial injector has been in operation since November. It is not a "heating injector" but is intended for studying the interaction of radial injection and electric field generation. The injection angle of 15° is a compromise between optimum ion loss and transmission. High fast ion losses need a mirror magnetic field configuration, a sufficient density of $n_e(0) = 1 \times 10^{20} \text{ m}^{-3}$ to minimize shine through and high T_e to have low collisionality. The W7-AS fast ion loss detector finds the expected dependence of the fast ion loss rate on the magnetic field configuration. The first measurements of the change of T_i and the radial electric field with radial injection were also completed.

WENDELSTEIN 7-X CONSTRUCTION

(Head of Project: Dr. Manfred Wanner)

Members of the W7-X Construction team and contributors to the project: see section "Division and Groups, WENDELSTEIN 7-X Construction"

Assembly of the machine is being studied in detail and the tool for stringing the coils across the plasma vessel was delivered.

FZK contributes the complete ECRH system for W7-X. Joint development of a continuously working 140 GHz gyrotron by FZK, European industry, and CRPP Lausanne led to a first prototype, which was successfully tested. The design of the microwave transmission line was continued by IPF Stuttgart.

The Low Temperature Laboratory of Commissariat à L'Énergie Atomique (CEA) in Saclay started commissioning of the test facilities for the cryogenic acceptance tests of the coils.

The University of Rostock and the Universities of Applied Sciences at Stralsund and Neubrandenburg are supporting the project with specific tasks.

The project schedule is determined by production of the superconductor and winding and assembly of the coils. Since delivery of the superconductor is severely delayed, the acceptance tests at Saclay need to be accelerated and assembly of the stellarator re-organised to adjust the assembly to the new delivery dates of the coils. The date for commissioning W7-X and mapping the magnetic field will be moved to the end of 2007.

1. INTRODUCTION

The W7-X Construction project is responsible for the design, manufacture, and assembly of the W7-X stellarator, the heating systems, the power supplies, the cooling system, and the system control.

The main components of the stellarator are the superconducting magnet system to confine the plasma, the cryostat to insulate the cryogenic parts, the ports to observe and heat the plasma, and the plasma-facing components to control the energy and particle exhaust. Steady-state plasma heating is based on powerful ECR sources. In addition, the plasma temperature and density can be increased by pulses of ICR and NBI heating. The superconducting coils are energised with high current by dedicated supplies and kept at a temperature close to absolute zero by a helium refrigeration plant. The heating systems are supplied with high voltage. A total input power of about 48 MW is required to operate the magnet system, supply the heating systems, and provide power for cryogenic refrigeration. At a later stage NBI heating is to be upgraded to 20 MW to explore the high-density regimes and the β -limit of W7-X.

The R & D activities have been completed. These cover construction and testing of the DEMO coil, an original-sized superconducting magnet, the DEMO cryostat, a sector of the W7-X stellarator, and prototypes of the plasma-facing components.

Meanwhile most of the main components of the basic machine and the power supplies have been contracted to industry. Series production of the superconductor and winding of the coils has started. Several sectors of the massive coil support structure have been welded and machined. Manufacture of the plasma vessel, outer vessel and ports has started. The first module of the high-voltage power supply is being commissioned.

2. BASIC MACHINE

2.1 Magnet System

The detailed design of the magnet system was basically completed, taking into account the enhanced cooling requirements of the coil casings. The engineering groups of the Central Technical Services (ZTE) of IPP at Garching were involved in the design and construction of several components as well as in structural analyses of the coils and the coil support structure and in supervision of production in industry.

2.1.1 Superconductor

The superconducting cable is composed of 243 strands enclosed by an aluminium jacket. Strands with the required critical currents were manufactured by the VAC/EM consortium. The consortium encountered, however, unexpected difficulties with cabling the ropes, jacketing the cable, and verifying the specifications of the conductor. The strands manufactured by VAC and EM behaved differently during cabling. Several iterations to adjust the nozzle of the extrusion tool were required to keep the void fraction within the specified range and the minimum wall thickness at 2 mm. The tolerance band for the void fraction had to be relaxed to 35 – 39 %. Although the qualification lengths had already been manufactured at the end of 2000, series production could only be initiated in May 2001. At the end of 2001, about 30 lengths of conductor have been manufactured, but the output is still below the needs for coil manufacture and measures to speed up production are being implemented. The delay of the conductor has meanwhile had a serious impact on production of the non-planar and planar coils and hence on the overall project schedule.

2.1.2 Superconducting coils

The Babcock-Noell Nuclear (BNN)/Ansaldo consortium made progress on the design and manufacture of the fifty non-planar coils. In 2001, design of the coil casings was completed and several half-shells were successfully cast, heat-treated, and machined to the required accuracy by the Swedish subcontractor, Österby Gjuteri AB.

To wind the different types of coils, three parallel winding lines have been set up at Ansaldo and two parallel winding lines at BNN's subcontractor ABB. Winding starts with preparation of the conductor by straightening, sand-blasting, and insulating with glass tape. For each winding package 108 turns are wound to form six double layers electrically connected in series. One double layer is wound from one conductor length. Since all conductor terminals need to be located on one side of the winding package, winding starts midway of a double layer. For that purpose the conductor is first re-spooled on two hasps before it is wound and fixed by clamps. By the end of 2001 one winding package was completed by ABB. The first winding package from Ansaldo is expected in January 2002.

To improve cooling of the coil casings, the casings have to be coated by 2 mm thick copper. Sheet copper can only be applied to a fraction of the surface of the casings. To cover the more complicated areas economically with copper, spray technology was suggested and successfully qualified by BNN. The measured thermal conductivities of samples of spray copper were 38 W/mK at ambient temperature and 9 W/mK at 4 K. Since the conductivity of sprayed copper is considerably lower than that of sheet material, the number of cooling pipes around the casings was increased. By using a pre-series coil casing BNN was able to optimise the application of copper and fixture of the cooling pipes and to practise different steps of assembly of the coils.

Design of the twenty planar coils at Tesla Engineering has been largely completed and the winding line for manufacturing the winding packs was prepared. To check the winding process, a test layer was successfully wound and hardened using a test length of conductor. With the delivery of the first lengths of superconductor, production of the first winding package started in October.



FIG. 1: Two half-shells of a non-planar coil casing during final inspection (by courtesy of BNN)

The coil casings of the planar coils are manufactured from plate material. For each casing a U-shaped base part and a plane top plate are screwed together. As a consequence of structural analyses of the casing it was decided to fix the top plate additionally by local welding. After some reworking the first casing was manufactured according to specification.

The double layers of the coils need to be electrically connected in series by low-resistance joints. To limit the ohmic heat at cryogenic temperatures, the resistance of a single joint must be below 1 n Ω . Prototypes tested by Ansaldo and Tesla showed that this stringent requirement can be met.

In order to insulate the electric circuits of the windings against the helium pipes, special voltage breakers were designed and tested. For such joints two stainless-steel pipes are connected by an insulating piece of glass-fibre-reinforced epoxy. The voltage breakers have to withstand a maximum voltage of 13 kV and allow for the different thermal contractions of the dissimilar materials during cool-down. During multiple cool-down to liquid-nitrogen temperature the function of prototype voltage breakers was demonstrated.

At the Low Temperature Laboratory of CEA in Saclay two test cryostats were installed, the current supply was upgraded to 20 kA, and the data acquisition system was adopted for the tests. Support rings were manufactured and mechanically tested at IPP Garching to allow any combination of two coils to be tested in one cryostat. The facilities were successfully tested using the DEMO coil.

2.1.3 Coil support structure

The coil support structure consists of ten identical sectors with a total weight of 72 t which will be joined by screws to span a

central pentagon. Ten supports carry the structure and provide the thermal barrier between the cold parts and the machine foundation. The coil support structure is made from steel plates and precisely cast steel elements for the coil fixtures. Precise fitting of the flanges between the sectors without additional interlayers requires machining to a precision of a few tenths of a millimetre.

The coil support structure needs to be kept at the same low temperature as the coils. For that reason helium-cooling pipes are fixed to the surface of the structure. To enhance the heat transfer, both the steel pipes and the contact areas of the fixtures are copper-plated. The fixtures of the structure are coated by the same spray technique as used for the coil casings.

Uniform transmission of the forces at the screw connections between the coils and the coil support structure is achieved by epoxy fittings. Samples of epoxy were tested at 7 K by FZK. After 5,000 pressure cycles of up to 60 MPa the samples failed only at a static load of 300 MPa. This means that the material has a safety factor of five against the expected loads in W7-X.

The support elements which carry the coil support structure have to pass through openings of the outer vessel. To allow for thermal shrinking of the coil system against the outer vessel during cool-down, the support elements are equipped with bellows and gliding bearings. A special mechanism will ensure self-centring of the structure. The coil support structure is being manufactured by the Spanish contractor, Equipos Nucleares, S.A.

2.1.4 Magnet current supply

The five types of non-planar and two types of planar coils require seven power supplies which provide direct currents of up to 20 kA at voltages of less than 30 V. The Swiss contractor, ABB, selected the concept of twelve-pulse rectifiers to ensure that the currents will be stabilised to an accuracy of 2×10^{-3} .

Fast and reliable discharge of the superconducting magnets in case of a quench is realised by a fast circuit which short-circuits the coils and dumps the magnet energy to nickel resistors. These resistors feature a high heat capacity and a strong increase of the resistance with temperature. The switching voltages can thus be kept low. The results of tests with arc shoot breakers and a newly developed ignition device were in accordance with the specification. The proposed control concept of ABB was accepted, including the detection of defects in the grounding of the electric circuits.

A test facility was built at Greifswald to test electrical components in a magnetic environment of up to 100 mT.

2.1.5 Current leads

Fourteen current leads which are able to carry 20 kA are required to connect the seven groups of superconducting coils with the power supplies. A study conducted by the National

High Magnetic Field Laboratory at Tallahassee (USA) showed that conventional current leads designed for lower than nominal current, but operated under overload conditions, can be superior to leads based on high-temperature superconductors, which were considered as an alternative. The reason for this is that the magnet system of W7-X is energised to 2.5 T during only 10 % and to 3 T during only 1 % of the total operation time. Designing the current leads for lower current reduces the stationary heat conduction during the long idle current period at the expense of slightly higher heat loads during peak current operation. If the cold end of the current lead is allowed to warm-up during stand-by, the refrigeration power can be further reduced. Therefore, the lower heat losses of high-temperature superconducting leads during current operation do not warrant the development effort and higher investment costs.

2.1.6 Control coils

Ten copper coils will be installed in the plasma vessel behind the baffle plates to correct minor field errors, influence the extent and location of the magnetic islands, and allow the power deposition area to be swept across the target plates.

Each coil can be supplied with a direct current of 3 kA at a voltage of 30 V, which can be modulated at frequencies of up to 20 Hz by a dedicated power supply. Manufacture of the ten power supplies is nearly completed by the Spanish contractor, JEMA, and the first units have passed the specified works acceptance tests.

The basic design for the coils was finished. The coils, with dimensions of $2 \times 0.3 \text{ m}^2$, will be wound with 8 turns of a hollow copper conductor and cooled by water.

2.2 Cryostat

The cryostat provides the thermal protection of the coil system. Its main components are the plasma vessel, the outer vessel, the ports, and the thermal insulation. The German company, Deggendorfer Werft und Eisenbau GmbH (DWE), is responsible for manufacturing the plasma vessel and outer vessel.

The plasma vessel will be assembled from steel rings bent precisely to the required shape and carefully welded together to keep local tolerances of 3 mm. DWE has meanwhile determined bending edges and radii as well as the shrinkage of the welds. Water pipes around the outside of the vessel allow its temperature to be controlled during plasma operation and for bake-out. Tests for welding the thin-walled steel pipes to the vessel have started.

Design of the outer vessel is being detailed and envisages approx. 1,500 openings for ports, manholes, and feedthroughs. The structural design of the vessel is being checked. The results are required to design weldseams and the dimensions of flanges. The fabrication halls and tools for assembly of the vessels have been prepared.

Manufacture of the 309 ports is being done by the Swiss company, Romabau. Comprehensive tests showed that the material for the ports and bellows satisfies the outgassing requirements of W7-X. Manufacture of the first ports started at the end of 2001.

Efficient insulation of the superconducting coils requires careful reduction of heat conduction and shielding of thermal radiation by high vacuum and many layers of reflecting metallic foils. Efficiency of the thermal protection is further improved by metallic shields which additionally cover all areas which are at ambient temperature. These shields are kept at temperatures between 40 K and 70 K by circulating cold helium gas. Components which penetrate the shields, such as current leads, helium pipes and supports, need to be individually insulated. The call for tenders has been issued.

2.3 In-vessel Components

2.3.1 Divertor engineering

With respect to plasma interaction three different types of surfaces can be distinguished in W7-X: The divertor target plates are hit predominantly by hot particles from the plasma and have to withstand heat loads of up to 10 MW/m². Baffles, which influence the fluxes and density of neutralised particles in front of the target plates, need to be designed for heat loads of 0.5 MW/m². The wall protection of the plasma vessel is mostly interacting with neutral particles and radiation from the plasma boundary and has to withstand heat loads of up to 0.2 MW/m². To control the reflux of impurities to the plasma all plasma-facing surfaces have to be covered with low-Z material. For conditioning the target plates, baffles and wall protection need to be baked at a temperature of 150° C.

During a symposium international experts reviewed and discussed the present design of the W7-X divertor. They confirmed that the first divertor should already be designed for steady-state cooling since the expected time constants of the plasma, in particular the time to stabilise the bootstrap current and the time constant of the target plates, are of the order of several seconds. It was also agreed to design the first divertor already for maximum heat load. Because of the difficulties, experienced during construction of carbon fibre armoured limiter components for Tore Supra, it was recommended that the target plates be armoured with a new carbon fibre composite (CFC) material.

Modelling of the behaviour of the neutral particles in the boundary layer of the plasma and recycling of impurities near the divertor needs to be improved by taking into account the 3-dimensional geometry of the plasma boundary.

In summary, the divertor design was confirmed and considered to be sufficiently detailed to start with procurement of the components.

A divertor advisory board comprising members of EFDA, Tore Supra, and the Materials Research Division of IPP was established to monitor progress and advise the project.

2.3.2 Target plates

Appropriate positioning of target plates relative to the magnetic field lines allows the particle and energy flows from the plasma to be controlled. With two target plates per divertor unit, a total of twenty target plates will be arranged along the plasma column and cover an area of 30 m².

The target plates were designed in detail. The design considered that the exact position and shape of the target plates will intercept the particle flow from the plasma along the open flux bundles at the boundary at a maximum distance from the confinement region. To keep the local heat load to below 10 MW/m², the focus area is adjusted to achieve a small incidence angle of 1-3° at the target plates. In addition, the size of the target area was chosen large enough to allow operation throughout the accessible range of the rotational transform from 5/6 to 5/4.

The ideal shape of the target plates, which has to follow the 3-dimensional boundary of the plasma, is approximated by a series of planes. Five standardised plane target elements with dimensions ranging from 55x270 mm² to 55x500 mm² are sufficient to achieve a nearly constant angle of particle incidence. After assembly of the target elements, the plasma-facing surface is machined to the required 3-dimensional shape.

Each target element is composed of a water-cooled metallic support and flat CFC. Prototype target elements using SEPCARB® N11 were produced in combination with various heat sink materials. N11 tiles which were either brazed to TZM (titanium zirconium molybdenum) or welded to a Cu alloy structural support were successfully tested at heat loads of up to 12 MW/m². Similar elements using N11 and CuCrZr, which were manufactured for the Ciel project of Tore Supra, revealed, however, bonding defects after some time, which were attributed to excessive stresses in the bond between the support material and the N11 tiles. The project therefore decided to manufacture the cooled supports of the W7-X targets from copper alloy (CuCrZr) and the armour from 7 mm thick tiles of CFC of a new type NB31. This combination was successfully tested for ITER. The advantage of NB31 is its higher tensile stress property and its better heat conductivity perpendicular to the tile surface. Alternatively to brazing, bonding of the CFC tiles to the copper support can be accomplished by first applying a thin layer of copper to the tile (Active Metal Casting technique, patented by Plansee AG) and welding this layer to the support by an electron beam. The good heat conductivity of the copper alloy helps to keep the temperature of the divertor well below the tolerable limit of 1200° C. To enhance heat transfer to the cooling water by turbulence, the cooling channels are equipped with a twisted tape.

The call for tenders for the target plates started at the end of 2001. Due to the long delivery time of NB31 this material was ordered in advance from the French company, SNECMA.

To avoid misalignment of in-vessel components due to thermal expansion or contraction of the plasma vessel, the temperature of the plasma vessel will be stabilised by a water-cooling loop.

2.3.3 Baffle and wall

Baffles are installed in front of the target plates to enhance the concentration and improve pumping of the neutral particle fluxes. These baffles span a total area of 30 m² and will be covered by flat graphite tiles of approx. 150x100 mm². These tiles are clamped to water-cooled support structures made of copper alloy CuCrZr. Tubes which are brazed to cooling structures to get high cooling efficiency are used for the baffle and the highest-loaded parts of the wall elements. Prototypes of such elements were tested in the FIWATKA device at FZK. Sufficient heat transfer between the tiles and the support was achieved by fixing the tiles with TZM screws, Inconel washers, and a thin, flexible graphite interlayer. Exposure of the samples to stationary heat fluxes of up to 500 kW/m² and 500 cycles of 400 kW/m² lasting 200 s showed that the target value for the heat transfer of 2000 W/m²K was achieved. Meanwhile the design has been further detailed to start call for tenders.

The wall of the plasma vessel spans a total area of approx. 120 m². Two concepts will be used to provide protection of the plasma vessel: At critical areas where the distance between the plasma boundary and the wall is small the concept of clamped tiles as developed for the baffles will be applied. For the major part of the area, covering 70 m², a panel concept with an integrated cooling loop and a surface coating of B₄C is preferred. This approach allows us to reduce the number of tiles and the carbon inventory and simplify mounting within the plasma vessel. The arrangement of the different types of plasma-facing components of one module is shown in Fig. 2.

A design study showed that the complicated surface of the plasma vessel can be approximated by cylinder segments of different radii, which further simplifies production. A single embossed prototype made of stainless steel with an area of approx. 200x600 mm² with representative curvature was built by industry to the required accuracy.

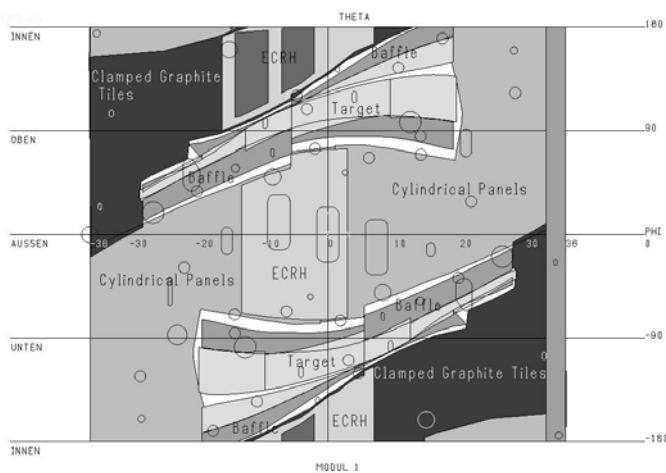


FIG. 2: Arrangement of the plasma-facing components using CFC (dark grey), graphite (middle grey) and B₄C (light grey)

B₄C is to be applied to the stainless-steel panels by the vacuum plasma spray technique. The Materials Research Division of IPP analysed the physical properties of several samples. Layers with a thickness between 0.2 mm and 0.5 mm were applied to stainless-steel samples and showed a smooth surface, good homogeneity and adherence under thermal loads, as well as sufficient heat conductivity and electrical resistivity (see section "Plasma-facing Materials and Components" for further details).

During a symposium experience at IPP, FZJ, and FZK on B₄C coating was exchanged. Arcing observed at limiter elements in TEXTOR was not considered critical to W7-X due to the larger distance of the wall from the plasma. The compatibility of the low electrical conductivity of B₄C with glow discharge conditioning still has to be investigated in more detail.

Removal of a maximum heating power of 15 MW from the divertor and the wall requires a water flow of 2750 m³/h. The water cooling of each divertor unit is divided into several circuits which can be independently controlled to allow economic distribution of the cooling water. The pressure in the water cycle will be kept above 10 bar to avoid boiling. Process design of the water cycles and routing of the pipes inside the cryostat as well as in the torus hall were continued.

2.3.4 Pumping

Vacuum pumps are required to evacuate the plasma vessel to a level of less than 10⁻⁸ mbar before plasma operation, to pump out neutral particles from the divertor chamber, and to control the density of auxiliary gases injected into the divertor chamber. Additional cryo-pumps allow the pumping capacity to be increased during high-density plasma discharges. In such cases particle fluxes of 5x10²¹ s⁻¹ have to be handled at pressures of about 10⁻³ mbar.

Turbomolecular pumps (TMP) will be connected to the 10 divertors in series with Roots and rotary pumps and will provide an effective pumping speed of 4200 l/s for H₂. The degraded performance of turbomolecular pumps in magnetic fields above approx. 5 mT made detailed examination of their positioning necessary.

The cryo-pumps will be designed for a total pumping capacity of 150,000 l/s in 2 hours.

2.3.5 Divertor diagnostics

The diagnostics required to operate and protect the divertor are designed by the Plasma Diagnostics Division, Berlin. The diagnostics include instruments for target thermography and thermometry, water flow control, and measurement of thermocurrents.

Other methods such as remote microscopy and analysis of acoustic emission from the target elements were tested but turned out to be not sensitive enough to diagnose potential target erosion. Supplementary diagnostics will be used to

provide physical data on the plasma boundary and interacting areas. They are described in detail in the section "Diagnostics for W7-X".

The thermography system will consist of 10 uncooled microbolometer cameras which can inspect all ten horizontal and vertical divertor targets in the wavelength range from 8 to 15 μm . Supervision of the whole target area requires a viewing angle of 107° of the camera optics. CAD studies have shown that this can be achieved with the optics being placed in either the F or B port. The infrared light will be transmitted through endoscopes and an optics with 24 lenses made from ZnSe or ZnS.

The proposed concept of cooling-water control requires analysis of signals from about 100 flow meters and some 2,000 Pt100 temperature sensors within cycle times of 1 s. A PROFIBUS system (SIMATIC) for real-time data processing was constructed and connected to an ET200S field bus system and a PC running WinCC. In order to store signals, sufficiently fast cycles with data block transfer are considered. Knowledge of the time required to transmit and process these data blocks allows to estimate the time needed to process all measured data with the system now in use. As a result of the data analysis the power to individual divertors and the total power absorbed will be visualised on a PC.

Experiments to investigate the electric currents to the target plates were continued and showed that the water-cooling pipes to the target plates have sufficiently high resistance for use as shunt resistors. Final layout of this diagnostic depends on the detailed design of the target plates and their electrical insulation.

2.4 System Control

The W7-X experiment will be controlled by a master control system with local controllers for all subsystems such as magnets, cryogenics, heating systems, diagnostics, and data acquisition. The local controllers will run automatically according to predefined routines and parameters, which will be set from the master control system whenever the units have to operate together. In order to structure operation of the experiment, machine, and related subsystems, all periods of operation will be divided into segments of variable duration. A "segment programme" defines the operational rules and parameters which determine the state and activity of each unit in use.

Programmable Logic Controllers (PLCs) will be used mainly to control those machine components and diagnostic systems which do not require short response times. Segment processing and fast feedback control, which require data processing in real time, will be performed by PCs running the VxWorks real-time operating system. Real-time information such as measured values will be shared between all units using a switched Ethernet. A network protocol has been developed which copies selected data structures from any computer which acts as data source into any other computer or PLC which is connected to the network and activated to receive these data.

Work on the software required for segment control was continued. This includes the technology of switching between segment control objects within the control units and accessing a central SQL data base from the VxWorks control units. A clear structure of the software making maximum use of common modules for the many computers required was defined. It will be further developed and a documented version will be controlled with the programmes SniFF+ and CVS.

A prototype of the TTE cards which provides trigger, time and event handling for each unit and which was developed in co-operation with the university of Rostock was manufactured and is being tested. A specification for the central TTE unit was prepared.

2.5 W7-X Assembly

Basically, assembly of the stellarator is performed by joining five prefabricated modules to a torus. Each module is composed of two half-modules which are mirror-symmetric to each other.

A paramount prerequisite for proper confinement of the plasma is exact fivefold symmetry of the magnetic field. As a consequence, errors in the shape of individual coils or deviations from their ideal position which break the symmetry must be smaller than 0.1 mm on a scale of one metre. Such small tolerances require high precision during manufacture of the components and assembly. Measurement and control of the positions of the major components to the required accuracy will be performed by computer-controlled theodolites and a laser tracker. The reference points in the assembly hall and appropriate measuring marks were defined with the support of the University of Applied Sciences at Neubrandenburg.

Studies were performed to avoid collisions between the complicatedly shaped components during assembly and to support the detail design of various handling devices.

Ultimate alignment and stiffness of the plasma vessel and the coil system will be achieved only after closing the torus. To keep the precise shape and alignment of these components during handling, assembly, and transport, several temporary supports were defined and designed.

The assembly sequence starts with pre-mounting and adjusting the coils of one half-module and preparing the inter-coil supports. Next the coils are strung across the plasma vessel. The small clearance between the coils and the plasma vessel means that the plasma vessel of each half-module has to be divided to allow the innermost coil to be strung across the vessel.

Next, the vessel is welded together, and part of the thermal insulation is mounted. A special handling tool was built and delivered by the German company, RST, to move and rotate the non-planar coils with masses of up to 6 t precisely according to the calculated path (see Fig. 3). A second coil-handling tool is required to handle the planar coils. Two assembly stands were

ordered from the Austrian company, Siempelkamp Nukleartechnik, to allow assembly of the half-modules.

Two half-modules are joined in a further mounting stand fabricated and delivered by the German company, AKB. Hydraulic cylinders allow precise alignment of the half-modules in three directions. The sectors of the coil support structure are bolted, the plasma vessel is welded, and electric bus and cooling lines are connected. Design of the electric bus was started. The design has to consider a bifilar routing of the conductor to avoid disturbance of the magnetic configuration, electric insulation against 13 kV, assembly of approx. 300 disconnectable low-resistance joints, and numerous mechanical supports. Tests of detachable electric joints have started at CEA Saclay.



FIG. 3: Coil-handling unit during tests using a coil dummy

After assembly of the modules the units are moved into the torus hall and lifted into the insulated lower half of the outer vessel. After integration of supports, the outer vessel is closed and some sixty ports and the in-vessel components are installed. Design of a device for module integration and assembly of the torus has started. Steel structures with a mass of about 55 t each and hydraulic actuators are used to move and align the modules with masses of 145 t on a steel ring resting on five supports.

After connection of the coil support structure is complete, the plasma vessel and the outer vessel are closed by welds. Finally, all temporary supports are removed, some remaining ports are mounted, the thermal insulation is completed, and the final bus connections are made.

Design of the distribution of the cooling water and helium started and has to consider routing of some 20 km of cryogenic and water pipes, with diameters of up to 600 mm, and installation of some 750 valves.

The high-quality requirements resulting from the accuracy of the magnetic field, low-temperature operation, and cleanness of the plasma-facing components call for stringent quality control after every step of assembly. Dedicated techniques which consider the restricted accessibility and complicated shape of the components tested are being developed.

3. HEATING SYSTEMS

3.1 Electron Cyclotron Resonance Heating

The electron cyclotron resonance heating (ECRH) system is being developed and built by FZK as a joint project with IPP, IPF Stuttgart, and CRPP Lausanne. The 'Projekt Mikrowellenheizung für W7-X' (PMW) at FZK co-ordinates all engineering and scientific activities in the laboratories and in industry.

ECRH is the main heating system in the first operation phase with 10 MW steady-state heating power at 140 GHz. Ten gyrotrons with 1 MW each will provide the required microwave power. A European R&D programme for the development of the W7-X gyrotrons was launched in 1998 as a joint effort of European industry, FZK, IPP, IPF, and CRPP Lausanne.

The first prototype ('Maquette') provided by the French company, Thales, was tested at FZK. A maximum RF output power of 1.15 MW was measured during short pulses of 1.5 ms. Operating the tube with a collector voltage depression of up to 33 kV recovered energy and increased the output efficiency to almost 50 %. At the beginning arcing in the RF load limited the pulse length to about 5 s at power levels of 840 kW. After improvement of the internal optics of the dummy load the arcing was shifted beyond 1 MW and an output power of 1 MW could be obtained during a pulse length of 10 s with an efficiency of almost 50 %. Pulse lengths were set to 45 s with 0.89 MW, 100 s with 0.74 MW, 140 s with 0.64 MW, and 180 s with 0.47 MW of output power. The pressure increase in the tube caused by outgassing, however, indicated that the pulse lengths were near the expected limits. Video images of the diamond window of the gyrotron showed light emission with a star-like spot distribution. Since these spots were detected only on the vacuum side of the disk, they were not considered dangerous for operation of the gyrotron. After completion of the tests the tube was sent back to the manufacturer. Visual inspection after dismantling showed a damaged collector and some melted spots in the mirror box, which could be explained by sweeping the magnets at a too low frequency or operating the gyrotron in wrong modes. Design was modified to improve the cooling, increase the absorption surface for the stray radiation, and add a relief window. These design changes are being implemented in the prototype tube. The Maquette tube was reassembled and is now used at FZK to optimise the behaviour of the long-pulse RF load.

IPF Stuttgart is responsible for the entire transmission system as well as the ECRH-specific HV system. After successful low-power testing of the prototype transmission line, work in 2001

concentrated on detailed design and specification of the mirrors. Two prototypes for the multi-beam mirrors were built and passed the acceptance test. The diameter of the cooling channels varies across the surface of the mirror and thus allows the local cooling to be matched to the Gaussian distribution of the power deposition on the mirror.

The temperature distribution of one of the cooling channels during a simulation with hot water and using thermography is shown in Fig. 4.

Several fabrication contracts were placed, and a large number of components, e.g. supports for the matching optics and the multi-beam mirrors, mirror substrates, and polarizers were delivered. Beam and power monitors and a calorimeter are being designed. Work on the final version of the acceleration voltage supply with modulator, cathode heater, and protection system was continued at IPF. A prototype of this HV equipment was extensively tested on the test stand at FZK. At Greifswald the HV cabins for the gyrotrons were built, and installation of the cables is under way. Several mirror supports

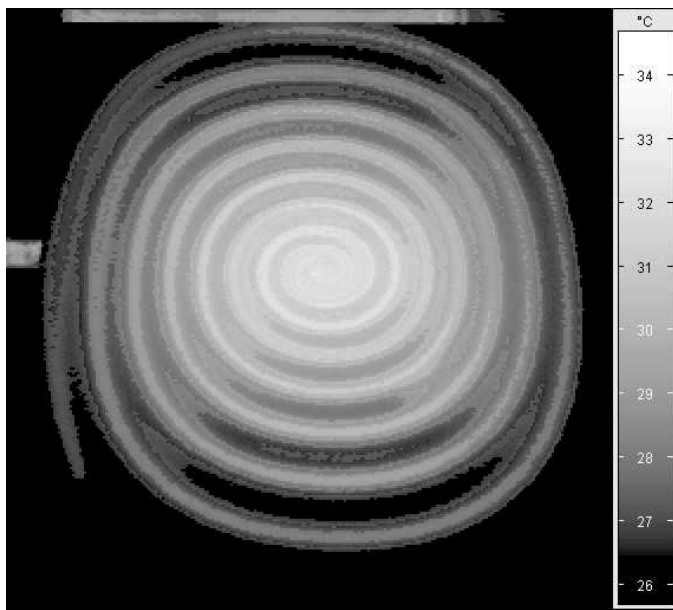


FIG. 4: Thermographic picture of the cooling channels of a Multi-Beam-Waveguide (MBWG) mirror. The channels are embedded in a SS-Cu sandwich

and the main water-cooling system for the transmission line and dummy loads were installed in the transmission duct.

RF background radiation at W7-X introduces additional heat load to the first wall, plasma-facing components, and plasma-exposed diagnostic parts. During particular heating scenarios some areas in the neighbourhood of the launching ports will be exposed to directed RF radiation. Samples of tungsten-covered graphite tiles were examined by the Materials Research Division of IPP and IPF to study their microwave properties. This kind of material is a good candidate for the inner-wall microwave reflectors due to its low microwave absorption. A low microwave absorption was also found for

molybdenum alloys, which are candidates for in-vessel structures.

The collaboration with CNR-Milano on experimental and theoretical investigations of non-absorbed ECRH stray radiation was continued. Due to their similar geometry the experimental results from W7-AS can be transferred to W7-X. Results from the experiments in W7-AS were used to benchmark the code modelling, thus improving the accuracy of the predictions on the expected radiation levels for W7-X.

3.2 Ion Cyclotron Resonance Heating

In view of the good results with ion resonance heating (ICRH) on W7-AS and on LHD a steady-state operating system is planned for W7-X. A frequency range of 25 to 76 MHz will, at different magnetic fields, allow ^3He and H minority heating in D plasmas, mode conversion heating in H/D mixtures, and second-harmonic heating of hydrogen. The system is to deliver a RF power of 2x2 MW using two double-loop antennas. Steady-state heating requires further development of the antennas, generators, RF transmission lines, and impedance-matching systems.

The layout of the ICRH system has been worked out in more detail. The antennas are located on either side of the kidney-shaped symmetry plane of the plasma. They are radially movable to facilitate launching of the RF power into differently shaped plasmas. Basic design principles of the antennas and a mechanism for installation and radial movement were developed.

Specification of a RF generator which would also satisfy the requirements of ITER and Tore Supra is being worked out in co-operation with other European ICRH groups. This approach helps to reduce the cost of upgrading the existing generator technology to steady-state operation.

A ferrite system matches the antenna impedance to the generator impedance for load variations slower than 0.1 ms. Such a system is now being developed and will be tested at ASDEX Upgrade. For faster load variations, e.g. during ELMs, the generators are passively protected by 3 dB couplers.

Active cooling of the coaxial transmission lines and other components has to be developed for steady-state operation. With a transmission line resonator designed for the ICRH test bed at Garching the 50 kW steady-state capability of an ASDEX Upgrade generator is sufficient to achieve locally the high voltages and currents occurring during full power operation in W7-X. Technologies for active cooling of components, movable contacts, and ceramic spacers can thus be tested.

3.3 Neutral Beam Injection

Neutral beam injection (NBI) is planned in W7-X for bulk heating of the plasma in the high-density, high- β regime. A neutral beam power of up to 20 MW will be available using

100 kV deuterium injection. This power will be available in two stages. Stage I, which is fully approved by EURATOM and is now being realised, comprises two injector boxes of the ASDEX Upgrade type with one neutral beam source each. This system will deliver up to 5 MW for 10 s using 60 keV deuterium injection. During Stage II the system is to be upgraded to 20 MW for 15 s by adding three more beam sources in each beam injector box and replacing the titanium evaporator pumps with cryo-pumps. The phase II application for preferential support has been submitted to EURATOM and is waiting for approval.

4. AUXILIARY SYSTEMS

4.1 Refrigeration System

The helium refrigeration system comprises a powerful helium refrigerator, a plant for helium purification, a subcooler, vessels for the storage of liquid and gaseous helium as well as for liquid nitrogen, cryogenic distribution boxes, and transfer lines between the refrigerator hall and stellarator.

The storage vessels for pure helium gas with a volume of 1000 m³ and the reservoirs for liquid helium and liquid nitrogen with capacities of 10,000 l and 30,000 l resp. were delivered and accepted.

The refrigeration concept was refined, taking into account the increased cooling requirements of the coil casings. Since the current leads are major consumers of refrigeration power during magnet operation, they are supplied directly from the liquid-helium storage reservoir. Peak withdrawal will be replenished overnight, which allows economic operation of the refrigerator.

Design of the coolant distribution within the cryostat was detailed and the interfaces between the refrigerator and the components were defined. A worst-case failure analysis showed that in case of a quench a total of 500 kg of helium could be expelled at a rate of up to 80 kg/s.

4.2 Gas Supply and Wall Conditioning

The gas supply for plasma discharges was built and installed by the German company, INTEGA. It allows local, remote, and automated controlled supply of the gases hydrogen, deuterium, helium, nitrogen, methane, and mixtures thereof. In addition diborane or silane mixtures can be provided for wall coating. Safety of the system is ensured by continuously venting the gas cabinets, by interlocks, and by safety alarms. To vent the plasma vessel after the experiments a high-purity nitrogen gas supply was built.

W7-X will ultimately require a method of cleaning the plasma vessel which works in a steady-state magnetic field. Although glow discharge cleaning is not compatible with magnet fields, its use during shutdown of the magnet system is for the time

being the only practicable method known. Experiments were run in the DEMO cryostat for the purpose of optimising the electrode geometry and discharge conditions. Tests with rod-shaped steel anodes mounted along the wall at a distance of a few centimetres allowed discharge breakdown without auxiliary ignitors and stable macroscopic discharges in the whole volume. It was observed that the discharge current oscillates with high amplitude at a frequency of a few 10 kHz. This phenomenon is also observed in other experiments but is not yet understood. Proper grounding and filtering will protect the power supply and reduce electromagnetic interference with other electronic systems in the vicinity of the machine.

The high-voltage anodes must resist the heat load during glow discharges and the radiation from steady-state plasma discharges. Graphite anodes which would resist these loads at high temperatures are technically feasible. It has to be checked whether the radiation emitted by the glowing anode is a serious disturbance for certain diagnostics. If necessary, water-cooled anodes need to be developed.

4.3 HV Power Supply

The power requirements of W7-X amount to approx. 48 MW and will be provided by the local 20 kV grid and a dedicated 110 kV junction of the Mecklenburg-Vorpommern grid. The ECR, ICR, and NBI heating systems will be supplied with DC power spanning the ranges 50-160 A and 18-130 kV. Ten modules are required to supply the heating units. They can be operated either in series to deliver high voltage or in parallel to deliver high currents. In a first step, eight modules using the advanced pulse step modulation (PSM) technique were ordered from the Thales/Siemens consortium.

Work in 2001 concentrated on the installation of the complete high-voltage switch-gear distribution, the load for full power tests, the control system, and the first two modules of the power supply. Commissioning started in autumn. Almost all parameters have met the specification. The overvoltage after fast turn-on and the ripple were larger than specified and need to be improved.

W 7-X DIAGNOSTICS

(Head of Project: Prof. Dr. Hans-Jürgen Hartfuß)

Experimental Division 3: T. Bindemann¹, H. Ehmler¹, F. Gadelmeier¹, J. Geiger, H. Hartfuß, R. Jaenicke, M. Kick, S. Klose¹, J. Knauer, G. Kühner, M. Otte, E. Pasch

Experimental Division 4: J. Baldzuhn, R. Burhenn, R. König

Experimental Division 5: M. Endler, L. Giannone, P. Grigull, M. Hirsch, K. McCormick, A. Weller, A. Werner

Plasma Diagnostics Division: C. Biedermann, D. Hildebrandt, M. Laux, R. Radtke, U. Wenzel

FZ Jülich: W. Biel, G. Bertschinger, A. Kreter, P. Mertens, A. Pospieszczyk, B. Schweer

1 Postdoc

1. OVERVIEW

On the basis of the generally accepted set of diagnostics for W7-X which has been discussed in detail with the International Diagnostics Advisory Board, the project's work concentrated on feasibility studies and on detailed front-end design especially of those diagnostics which share a common port and those to be integrated into cryostat or vessel components of W7-X. This work, carried out and conducted in the technically oriented group of the project, has almost been completed. Infrastructure requirements concerning vacuum, power, cooling etc. are being defined now. Concerning the scientifically oriented nine expert subgroups of the project, the Annual Report 2000 gave a concentrated summary of all diagnostics envisaged. In this present brief summary, progress and new developments of individual diagnostics are reported.

In various fields international collaborations are being established, contracts are being prepared.

2. STATUS REPORTS OF SUBGROUPS

2.1 Fluctuations

The emphasis in the preparation of the W7-X fluctuation programme was in collecting reference data on W7-AS and continuing the development and testing of a number of fluctuation diagnostics, specifically fast-swept Langmuir probes for the simultaneous measurement of density, electron temperature and plasma potential fluctuations in the plasma

edge, a 2D-resolving ECE system for the spatially resolved investigation of electron temperature fluctuations in the core, a Doppler-reflectometer for poloidal velocity measurements, two-dimensional beam emission spectroscopy measurements on a fast Li-beam in collaboration with KFKI-RMKI, Budapest and a CO₂ laser collective scattering system in collaboration with Risø National Laboratory, the last two for the observation of density fluctuations in the edge and in the core, respectively.

2.2 Plasma Edge

Activities continued to specify the individual diagnostic's viewing lines and to define and to design in more detail necessary breaks through baffle and target elements of the divertor. Of importance in this context is a probe manipulator. Design studies of such a device have been started.

It is planned to make those target elements of the divertor which need diagnostic instrumentation replaceable. In a later stage these elements can then be substituted by elements which are removable without braking the vacuum. They will be separately cooled and equipped with, for example, probe arrays or nozzles for atomic beams etc., adapted to special diagnostic needs.

2.3 Microwave Diagnostics

Diagnostics in the mm, sub-mm and IR wavelength regions are proposed. Work concentrated on the development of the laboratory version of a single channel prototype interferometer with vibration compensation. The system uses simultaneously two lasers in the infrared and the visible spectral regions respectively. The system operates in a heterodyne detection scheme. Since it is envisaged to install a ten-channel system at W7-X, sightlines through the plasma must be defined. In collaboration with the Technical University Helsinki a theoretical model is being developed to elaborate the optimum sightlines with respect to spatial resolution obtainable from Abel inversion particularly in the edge region of the density profile. In addition the development of new fluctuation diagnostic techniques in the fields of Doppler-reflectometry and 2D-ECE correlation radiometry continued at W7-AS.

2.4 Charge Exchange Diagnostics

To diagnose the local energy spectra of plasma ions, 5 neutral particle energy analyzers will be operated together with a neutral beam injector. 24-channel E//B analyzers are being developed in collaboration with the Ioffe-Institute, St. Petersburg. R&D work was started at the Budker-Institute of Nuclear Physics, Novosibirsk with the aim to develop the diagnostic injector and all and its subsidiary components.

2.5 Spectroscopy

The spatial requirements of the individual spectroscopic diagnostics have been estimated and their compatibility in shared ports investigated in detail. First contracts have been placed to investigate possible optical designs for divertor observation endoscopes. The detailed technical specifications required for an international tender of a double SPRED and a compact flat-field grazing incidence spectrometer system have been completed so that the tender procedure can be initiated early in 2002. Newly developed bolometer electronics for W7-X have been tested on W7-AS. A prototype of the planned 2D interference filter based divertor observation systems installed on W7-AS has been found to be adequate. For a single line of sight, a dual channel system of the proposed bremsstrahlung-based Zeff-profile diagnostic has been constructed and installed for testing on W7-AS. First results are promising while a detailed investigation of the concept will be performed in 2002. The suitability of a Li-beam as a source for edge CXRS measurements of the ion temperature, the impurity density and their velocity on W7-X was successfully demonstrated on W7-AS by a newly installed multi-channel observation system.

2.6 Thomson Scattering

Work concentrated on the bulk and on the edge Thomson scattering systems proposed. The scattering geometry at W7-X has been fixed. Contrary to an earlier proposal, the laser beam line and the observation sightline of the edge scattering system have been exchanged to reduce the demand on divertor break throughs. Design studies have been carried out to define in more detail the laser beam imaging system for guiding the laser beams from the peripheral diagnostic hall to the ports envisaged. In addition studies at W7-AS are continued with remote beam position recognition and alignment control. At W7-AS good progress was achieved with the high resolution edge scattering system employing CCD-cameras as preparatory work for the dedicated systems for W7-X.

2.7 Soft X-Ray and Electromagnetic Diagnostics

Detailed design studies have been started for the soft X-ray cameras to be installed inside the vacuum vessel as well as first tests of detectors, vacuum feedthroughs and different mechanical components.

The induction loops forming the set of electromagnetic diagnostics have been designed in more detail, in particular the

saddle coils and toroidal flux loops with most complex geometry. The paths and positions have been defined applying a specially developed software tool which includes W7-X magnetic field and vessel geometry. In this way optimal conductor geometry could be determined under the constraints of circumventing portholes in the vessel surface, meeting other optimization criteria as well, such as being as close as possible to given current filaments in the plasma.

2.8 Heavy Ion Beam Probe

The heavy ion beam probe is capable of measuring the local plasma potential and is therefore of great importance for W7-X transport studies. A primary beam of singly ionized gold with a maximum energy of 3 MeV is being considered. The accelerator can be installed outside the W7-X experimental hall. A beam line between the place of installation and W7-X has been designed and beam trajectories re-calculated within the vacuum vessel to study its compatibility with the divertor baffles.

2.9 Fusion Product Diagnostics

It was decided to concentrate on the development of 6 neutron detectors to be installed around the torus for total yield measurements. For detector design purposes calculations of the plasma as a neutron source under various heating scenarios as well as neutron fluxes and neutron transport calculations in the experimental hall and the near counter positions will be performed. All work will be done in close collaboration with the Alfvén Lab Stockholm and the PTB Braunschweig.

3. TECHNICAL COORDINATION

Before fixing the large number of proposals of the full diagnostic set for W7-X, detailed feasibility studies and front-end design investigations have been carried out. For this purpose CAD-drawings of the estimated outer envelopes of the different diagnostics were created and integrated into the port's design. Also place holders marking the spatial requirements behind the ports outside the vessel have been designed and included in the overall CAD-model of the machine. The set of place holders was employed to check their mutual compatibility and also the compatibility with subsidiary components of the machine. These checks so far include the divertor, the divertor cooling conduit as well as the plasma chamber lining. Necessary changes were initiated. The infrastructure for the W7-X diagnostics was further prepared by aiding the installation of cranes. In addition the definition and the design of a gas exhaust system to be installed in the experimental hall was started. Preparatory work begun to define the electrical grounding concept at the experiment and in the peripheral rooms. This concept includes also the definition of the electrical power lines for the diagnostics electronics and the data acquisition hardware. Closely related to these subjects is the discussion which has been started on the necessary emergency and safety systems for the planned diagnostic installations.

STELLARATOR THEORY

(Head of Project: Prof. Dr. J. Nührenberg)

X. Bonnin, M. Borchardt, M. Drevlak, S. Gori, R. Hatzky, R. Kleiber, A. Könies, V. Kornilov, H. Leyh, K. Matyash, N. McTaggart, P. Merkel, A. Mutzke, C. Nührenberg, J. Nührenberg, A. Pulss, J. Riemann, R. Schneider, S. Sorge, R. Zille.

Guests: J. Andersson¹⁾, K. Appert²⁾, A. Boozer³⁾, B. Braams⁴⁾, H. Dürr⁵⁾, T. Hayashi⁶⁾, M. Isaev⁷⁾, S. Kalvin⁸⁾, Y. Kolesnichenko⁹⁾, S. Kuhn¹⁰⁾, A. Kuyanov⁷⁾, P. Lalouis¹¹⁾, H. Majaniemi¹²⁾, J.-P. Matte¹³⁾, M. Mikhailov⁷⁾, D. Mikkelsen¹⁴⁾, K. Miyamoto¹⁵⁾, T. Rafiq¹⁾, T. Roglien¹⁶⁾, V. Rozhansky¹⁷⁾, A. Runov⁵⁾, I. Senichenkov¹⁷⁾, V. Siminos¹⁸⁾, F. Subba¹⁰⁾, A. Subbotin⁷⁾, D. Tskhakaya¹⁰⁾, M. Umansky¹⁶⁾, I. Veselova¹⁷⁾, S. Voskoboynikov¹⁷⁾, X. Xu¹⁶⁾, R. Zagorski¹⁹⁾.

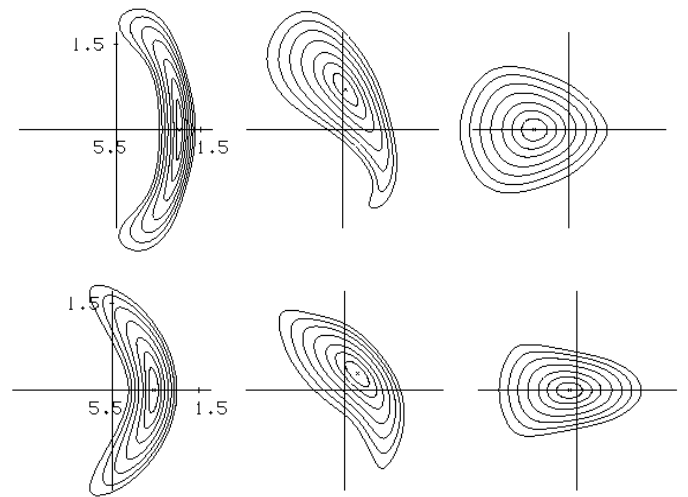


FIG. 1: Flux surface cross-sections of two 3-period stellarators: q_i (top), q_a (bottom). Shown are sections at the beginning, quarter of and half period. The scale has been chosen as the size of W7-X ($R = 5.5\text{m}$), the corresponding volumes are about 10^2 m^3 .

1. INTRODUCTION

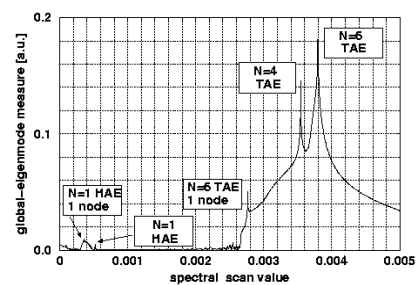
In 2001, the work of the Stellarator Theory Division was concentrated on widening the scope of the theoretical work at the Greifswald Branch Institute /4, 795/ and on further development of the stellarator concept /732/, notably for quasi-axisymmetric /302, 323/ and quasi-isodynamic configurations /701/.

2. CONFIGURATION STUDIES

3-period stellarators of the quasi-isodynamic and quasi-axisymmetric types were optimized with respect to a set of physics objectives with the help of computational tools more complete than those that had been available for the Wendelstein 7-X optimization. Fig. 1 shows a comparison between two such configurations²⁰⁾.

3. IDEAL MHD STABILITY

In 2001, the 3D global ideal MHD stability code CAS3D /297, 410, 298, 168, 683/ has further been generalized to offer



a response version²⁰⁾.

FIG. 2: Peaks indicate global eigenmodes of a high- β high-mirror W7-X-type equilibrium: TAEs (toroidicity-induced), and HAEs (helicity-induced) with one or no radial nodes and

¹⁾Chalmers University Göteborg, ²⁾CRPP&EPFL, ³⁾Columbia University, ⁴⁾New York University, ⁵⁾FZ Jülich, ⁶⁾NIFS, ⁷⁾Kurchatov Institute, ⁸⁾KFKI Budapest, ⁹⁾Institute for Nuclear Research Kiev, ¹⁰⁾Universität Innsbruck, ¹¹⁾IESL FORTH Kreta, ¹²⁾Universität Joensuu, ¹³⁾INRS Varennes, ¹⁴⁾PPPL, ¹⁵⁾Keio University Yokohama, ¹⁶⁾LLNL, ¹⁷⁾State Technical University St. Petersburg, ¹⁸⁾Universität Thessaloniki, ¹⁹⁾Institute of Plasma Physics and Laser Microfusion Warsaw, ²⁰⁾contributions to ISW 2001/2002 Canberra

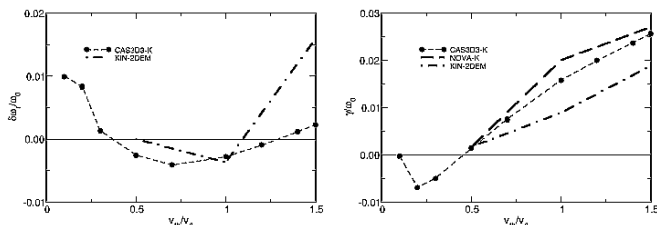
dominant toroidal Fourier indices of to the $N = 1$ mode family.

Now, the MHD spectrum of 3D equilibria may be studied in a more comfortable way, with the stable, global free-boundary eigenmodes being indicated by peaks in an appropriately chosen measure when performing a frequency scan.

5. MHD-STABILITY WITH KINETIC EFFECTS

Recently, a kinetic energy integral was constructed from the solution of the drift kinetic equation in three-dimensional geometry assuming zero radial orbit width.²¹⁾ This integral is formally similar to the MHD energy principle and allows a perturbative determination of growth rates and frequency shifts with MHD eigenmodes. The three-dimensional ideal MHD stability code CAS3D has been extended to include kinetic effects of hot particles using this theory. The particle orbits have been integrated along field lines using a Fourier transform technique in which particle drifts are approximated as bounce averaged drifts. The code keeps track of all possible orbits in this approximation and retains the complete field strength structure. Good agreement between the local approximation from the CAS3D3K code and analytical tokamak result has been found for the Landau damping rate (all drifts are neglected). The comparison with the NOVA-K code is shown in Fig. 3. The KIN-2DEM code includes gyrokinetic effects and therefore yields smaller growth rates /651/.

FIG. 3: Benchmark of growth rate and frequency shift for a



circular tokamak with $A = 4.4$, $\beta_{\text{pol-fast}} = 1$ and a Maxwellian distribution with $T(_) = \text{const}$ and $n(_) = n_0 \exp(-11_)$.

5. INFLUENCE OF KINETIC ELECTRONS ON ION-TEMPERATURE-GRADIENT (ITG) DRIVEN INSTABILITIES

ITG driven instabilities are likely to be one main mechanism to drive turbulence leading to transport in magnetic confined plasmas. For tokamaks, it is found that the growth of these modes is increased by the influence of trapped electrons due to the bad curvature on the outer side of the torus where they are located. In W7-X, their influence on the ITG modes is expected to be smaller than in a tokamak, because most reflected particles are located in smaller curvature regions.

The influence of the trapped electrons has initially been investigated in the configuration of a bumpy pinch as a simplified but reasonable model. The linear gyrokinetic particle-in-cell (PIC) code GYGLES (CRPP) for ITG modes in tokamak configurations²²⁾ and modified for the bumpy pinch

configuration at IPP²³⁾ has been modified by substituting the adiabatic response of the electrons by their gyrokinetic treatment. First test calculations lead to two results: For a straight pinch configuration, the results show a convergence to the results obtained with adiabatic electrons when the mass of the marker electrons is decreased sufficiently.

For a bumpy cylinder with a spatial variation of the magnetic field comparable to that of W7-X, the increase of the growth rate of the ITG modes due to the trapped electrons is much less than that found for typical tokamaks.

6. DRIFT WAVES IN STELLARATORS

The formerly developed global eigenvalue code for linear resistive electrostatic drift instabilities in general geometry was applied to a sequence of $\beta = 1, 2$ stellarators with aspect ratio $A = 10$, five field periods and ellipticity $\beta = 0.3$. The sequence parameter β is a measure for the excursion of the magnetic axis out of the plane. In the pure $\beta = 2$ case the most unstable mode shows a dominant toroidal ballooning structure modified by tiny helical variations and large radial structures /199/. Increasing β up to 0.5 leads to a slight variation of the growthrate, decreasing toroidal ballooning and a build up of a small scale radial structure. For $\beta = 0.6$ a mode which shows nearly no toroidal ballooning becomes dominant.

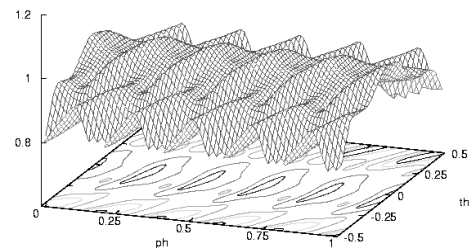


FIG. 4: Mode amplitude for the mode with poloidal wavenumber $M_F=5000$ in the $-\beta$ -plane, $\beta = 0.6$.

7. FREE BOUNDARY EQUILIBRIUM CALCULATIONS

Computation of 3D MHD equilibria for W7-X was pursued using the PIES code. The method of interfacing PIES to initial equilibria obtained with VMEC was applied, with an extended domain used in the VMEC computation providing extra clearance between the plasma boundary and the edge of the computation domain during the PIES calculation. These PIES calculations were taken to values of $\beta < 3\%$. An extension code was written to compute the magnetic field beyond the PIES computation domain. This allows investigation of the $\beta = 5/5$ islands without having to include the corresponding region in the computation domain of PIES.

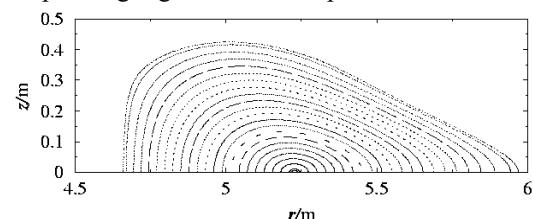


FIG. 5: Upper half of Poincaré plot for a free-boundary W7-X equilibrium at the triangle shaped cross section.

²¹⁾ A. Könies, Phys. Plasmas 7, 1139 (2000)

²²⁾ M. Fivaz et al. Computer Comm. 111, 27 (1998)

²³⁾ R. Hatzky et al. Eur. Conf. Abstr. 22C, 1804 (1998)

8. PLASMA EDGE THEORY

8.1 3D Edge Modelling

The 3D SOL transport code BoRiS was extended to solve /41, 826/, in addition to the electron and ion heat equation, the equations for the parallel momentum and the plasma density. In implementing the new equations, several tests were performed in different geometries from simple slabs to full 3D setups.

Fig. 6 shows the results for a simple 1D test case which was benchmarked against UEDGE and B2. At the left, the following boundary conditions were used: $T_e = T_i = 100$ eV, $n_i = 10^{19} \text{ m}^{-3}$, $u_p = 0.01$ sound speed. At the right, sheath conditions were assumed. While the temperatures show little variation, the parallel velocity approaches sound velocity being accompanied with a drop of plasma density by two orders of magnitude.

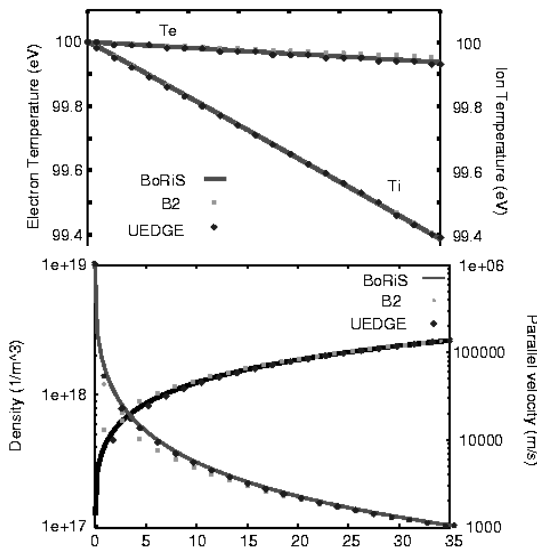


Fig. 6: Electron and ion temperatures along the magnetic field (top). The plasma density drops as the parallel ion velocity approaches sound speed (bottom).

In parallel to the development of the full 3D code, existing 2D codes are used to test numerical techniques suitable and necessary also for the 3D problem. Here, the B2-solps6.0 edge plasma multifluid code was developed. All equations are now solved for cell-centered grids (no longer using a staggered grid for the velocities) /58, 508/. By this, automatic local grid refinement is made possible. In contrast to experience with simplified problems solving only a single equation, the benefit of this for the complete set of equations (heat equations, continuity equation, momentum equations, potential equation) is not a large reduction in grid size (because the different equations have quite different locations of gradients requiring refinement) but an improved numerical stability.

To extend the transport models to ergodic configurations two different methods are used. The first model solves the transport equations with Monte-Carlo techniques making use of mappings. This code was benchmarked in a 2D-case with BoRiS and a standard-solver from NAG for the solution of the electron heat equation /763/. Successful applications to

TEXTOR-DED /336, 762/ and core transport barriers /617/ were done.

As an alternative ansatz a finite-difference discretization of the transport equations on a custom-tailored grid is used. This grid is generated by field-line tracing to guarantee an exact discretization of the dominant parallel transport (thus minimizing the numerical diffusion problem). The perpendicular fluxes are then interpolated on a 2-D plane (using local orthogonal coordinates), where the interpolation problem for a quasi-isotropic problem has to be solved. First successful tests on 3D slab geometries for the solution of the electron heat equation were performed.

8.2 Pellet Modelling

Numerous scenario calculations were performed for pellet-fuelled tokamak discharges of ASDEX-Upgrade. The measured pellet penetration depths were reproduced, both for LFS and HFS injection scenarios, within the error bars of the experimental data, by means of a single code and by ignoring the existence of possible grad(B)-caused drift effects /402/. The results indicate that, in the cases considered, the penetration depths were not affected by the grad(B)-induced drift of the pellet cloud. Apparently the drift trajectories of the ionized pellet particles did not interfere with the path of the injected pellets. The same code was used also for the stellarator W7-AS. Assuming Maxwellian energy distributions for the recipient (background) plasma particles, the measured penetration depths for the majority of the discharges considered were reproduced. In a number of cases, a distinct difference was observed between the calculated and measured penetration depths: the calculated ones being notably larger than the observed ones. In agreement with experimental hints, adding a small number of super-thermal electrons (approximately 1%, with energies of 15 to 20 keV) in the code to the peripheral region of the plasma reduced substantially the discrepancy between the calculated and measured penetration depths.

8.3 Plasma Surface Interaction

Modelling of ECR-heated methane plasmas is done to get a better understanding in the problem of carbon layer production and chemical sputtering in such plasmas, which serve as a model system of divertor plasmas being dominated by carbon sputtering, especially at detached conditions. A hierarchy of models is applied starting with 0-D particle balance rate equations (accounting for 171 reactions) and representing already quite well experimental observations. Improved understanding is hoped to be reached by using fully kinetic models (resolving also the sheath in front of the wall) including all relevant species and their reactions (neutrals, molecules, ions, electrons).

Also a new generalized version of the binary-collision codes TRIM and TRIDYN is developed to be used as a new master version using modern computing and code management techniques.

STELLARATOR SYSTEM STUDIES

(Dr. Horst Wobig)

T. Andreeva, C.D. Beidler, E. Harmeyer, F. Herrnegger, Yu. Igitkhanov, J. Kisslinger, Ya.I. Kolesnichenkoⁱ, V.V. Lutsenkoⁱ, I. Sidorenko, A. Wiczorekⁱⁱ, H. Wobig, Yu.V. Yakovenkoⁱ

1. WENDELSTEIN 7-X

In 2001, the Stellarator System Study Group performed some work for the Wendelstein 7-X device, which is under construction in Greifswald, Mecklenburg-Vorpommern. The magnetic field at the location of the current feeders to the coils has been calculated in view of special superconducting material in these regions. Furthermore, magnetic field calculations were made in the regions of the current feeders of the test arrangement of CEA-DAPNIA in Saclay, where the W 7-X coils will be tested individually.

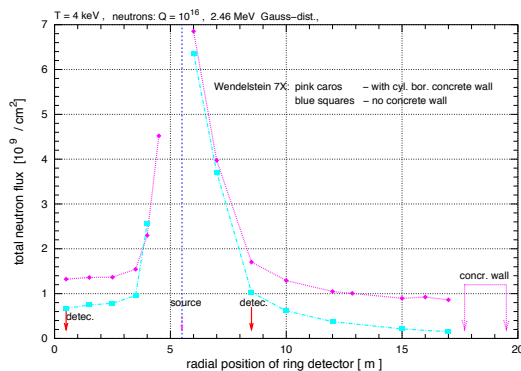


Fig:1. Wendelstein 7-X. The figure shows the total neutron flux density per cm^2s as function of the radial position of the ring detector. The neutron source (ring source) is at 550 cm. The envisaged positions of the neutron point detectors (in fact cylindrical boxes) and of the concrete wall are indicated by arrows. The concrete wall acts also as neutron reflector.

2. THE HELIAS REACTOR

The investigations on a Helias Reactor (HSR) were continued. Particular attention was devoted to a coil system of HSR4/18 with 4 field periods and 18 m major radius. This system comprises 40 modular coils with NbTi-superconducting cables. The reduction from 5 to 4 field periods and the reduction in size will also reduce the cost of the Helias reactor.

For performing the elastomechanic stress analysis of the coil system the ANSYS code was used. By means of shape functions the magnetic force density distribution is transformed into nodal forces of the finite elements. The coils are surrounded by strong stainless steel housings, in order to withstand the large value of the virial stress which characterizes the specific magnetic load of the coil system. The magnetic field at the coils is reduced by using a trapezoidal shape for the coil cross-section and splitting the winding pack into 8 double pancakes with a wedge between the two halves. By this method the maximum magnetic field at the coils can be reduced to about 10 T, sufficient for NbTi-technology at a temperature of 1.8 K. The coil pancakes are embedded in the coil housing with an epoxy layer between winding pack and housing. The coil housing is designed with a box-type profile having seven webs between the double pancakes for the reason of mechanical stiffening, as shown in Fig.2. The coil support is carried out as a common vault support; the coils of a field period are connected to a module. This intercoil structure is similar to that already applied in former 5-period systems, but some optimization work was done to achieve a more appropriate material distribution. For each individual

coil the cross-section of the double pancakes is subdivided into 32 elements and the coil housing 87 elements, resulting in a total number of 60151 elements with 72016 nodes for half a field period.

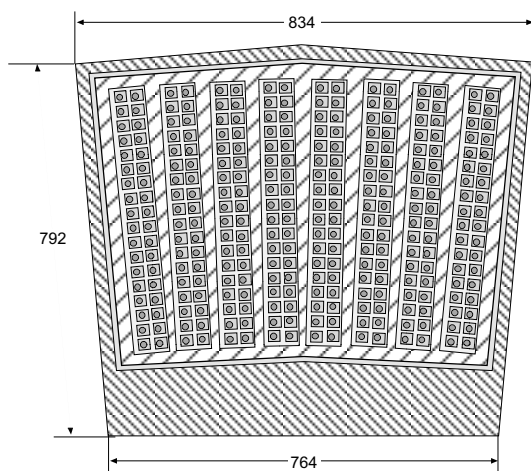


FIG. 1: Coil cross-section of HSR, showing the 8 double pancakes of the winding pack, the insulation and the housing. For the reason of stiffness this coil housing must be reinforced.

At the boundaries of the half period model the conditions of stellarator symmetry and the five-fold field periodicity of the system is taken into account, applying a coupled degree of freedom for congruent nodes. Maximum values of the equivalent stress (av. element solution) of about 750 MPa were found in the stainless steel structure.

In order to evaluate the stress and strain distribution inside the winding pack, the geometric nonlinear behaviour of the embedding of the double pancakes is taken into account. As one result of the computations a typical behaviour of strong compression at the outer radius of the pancake, which varies along the coil circumference was obtained, while the surface at the inner radius was detached. In the actual design, maximum radial compression stress values of about 70 MPa for the winding pack compound, and of about 94 MPa for the embedding layer were found in the winding pack of HSR4/18. A protection system for the coil system of HSR4/18 has been investigated.

The magnetic energy stored in the coil system of HSR4/18 at an operational current of 40 kA and 5 T on magnetic axis amounts to about 100 GJ. The classical method of protection is dissipating the stored magnetic energy of the coils via external resistors. A safety discharge must be initiated, disconnecting the magnet from the power supply by means of fast-acting switches. The current is fed into an external dump

resistor according to the system time constant. The dump resistor is composed of stainless-steel elements which absorb the magnetic energy, thus heating up to about $\delta\theta=700^\circ\text{C}$. Since the coils of HSR4/18 are magnetically coupled to each other, simultaneous dumping of currents in the entire coil system is necessary.

The proposed 40 kA superconductor has a dump time constant of about 12 s which ensures that the maximum temperature of the superconductor will stay below 100 K. On the other hand, the maximum voltage between windings and ground should not exceed 20 kV. For these reasons, the dump resistor of each coil group was subdivided into 4 units, connected to the 8 coils of this group. A heat production of 1.9 kW was estimated for these current leads. With a liquefaction factor of 1300 this results in a 2.5 MW electric input power for cooling of the current leads, which is an acceptable value of about 5% of the total power of the cryogenic system of HSR4/18.

2.1 Neoclassical transport.

The model magnetic field employed in the General Solution of the Ripple-Averaged Kinetic Equation (GSRAKE) has been extended to account for changes in local ripple topology due to non-zero rotational transform per field period. Such changes are critical to an accurate description of the radial transport processes in the high-mirror Helias configurations being considered as reactor candidates; an example is given in the figure.

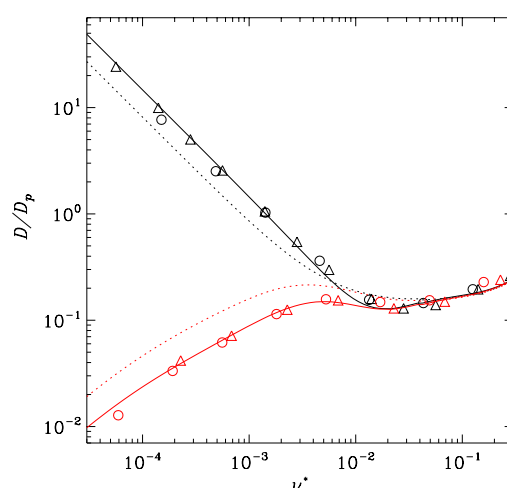


FIG. 3: The mono-energetic diffusion coefficient D , normalized by the plateau value of the equivalent tokamak, D_p , is plotted as a function of collisionality, $\nu^*=R\nu/l\nu$, for a reactor candidate with five field periods. Numerical results from a Monte Carlo simulation (circles), the Drift Kinetic Equation Solver

(triangles) and GSRAKE (solid curves) are compared, assuming normalized values of the radial electric field to be $E/vB_0=0$ (upper results) and $E/vB_0= 2 \times 10^{-3}$ (lower results). The dotted curves are obtained from GSRAKE when the ripple averages are simplified by using the common assumption that the rotational transform per field period is negligible.

2.2 Destabilization of Alfvén eigenmodes

A theory of Alfvén instabilities excited by circulating energetic ions in optimized stellarators of the Wendelstein line has been developed and the characteristic magnitudes of the growth rates of Alfvén eigenmodes (AE) of various types in a Helias reactor were calculated. It is predicted that several sideband resonances may considerably contribute to the instability growth rate in stellarators (in contrast to tokamaks). In particular, a significant role of the resonance associated with the helicity-induced drift motion of the energetic ions is revealed. An important practical consequence of the new resonances discovered is that tangential neutral-beam injection can destabilize Toroidicity-Induced Alfvén Eigenmodes (TAE) even when the velocity of the beam particles is less than one third of the Alfvén velocity (the latter is the case in, e.g., experiments on W7-AS).

Aimed at calculating the continuum damping of AEs, a set of resistive magnetohydrodynamic (MHD) equations, which generalize the ideal MHD Alfvén eigenmode equations obtained in 2000 [Physics of Plasmas **8** (2001) 491–509] was derived. The derived equations were solved numerically to investigate the damping of waves of global character in a Helias reactor.

A new set of reduced ideal MHD equations allowing for effects of the plasma compressibility, which are known to be of importance for the low-frequency part of the Alfvén spectrum, were derived. The equations are suitable for stellarator geometry and perturbations of arbitrary spatial scale. A new code COBRAS (COntinuum BRanches of Alfvén and Sound waves) was developed. The code is intended for numerical calculations of the low-frequency part of the MHD continuum in stellarators. Calculations of the MHD continuum in W7-AS with the new code were performed. It was found that because of the compressibility the TAE continuum gap is compressed and shifted upwards in frequency. In addition, coupling with sound waves produces new Alfvén-sound gaps in the Alfvén continuum.

2.3 Stochastic diffusion

Various mechanisms of stochastic diffusion were analysed: the orbit-transformation-induced diffusion of transitioning particles, the Goldston-White-Boozer diffusion of toroidally trapped particles, and the cyclotron-resonance-induced diffusion. It is concluded that the first mechanism, which was considered for the first time in C.D. Beidler, Ya.I. Kolesnichenko, et al. Physics of Plasmas **8** (2001) 2731–2738, dominates.

2.4 Concept of a breeding blanket

Neutronic calculations using the MCNP code have been made, in particular the effects of the 3-D geometry of the blanket on the tritium breeding ratio and on the activation of the structural material need to be investigated. The tritium breeding ratio has been computed as a function of the thickness of the breeding zone for a geometric model where the results can be benchmarked against results published in the literature. The model consists of a nested system of axisymmetric toroidal shells, the innermost contains the plasma followed by a vacuum region, the breeding zone (lithium or lithium-niobium) and some reflecting material (stainless steel of variable thickness or carbon). Within this model a tritium breeding ratio of 1.16 can be achieved for a breeding zone of 40 cm thickness and 5 cm steel on the backside acting as reflecting material. The impact of varying the Li-6-enrichment on the breeding ratio has been analysed.

A similar study has been done for various lithium-lead mixtures as breeding material but without a reflecting zone. In an eutectic lithium-lead mixture of 40 cm thickness (17 atomic % lithium) the tritium breeding ratio is 1.15 and is increased to 1.21 if the Li-6 content is increased from 6.4 % to 8.0% of weight. If the natural lithium content is increased to 30 atomic % (melting temperature about 350 °C) a breeding ratio of 1.47 can be achieved. The real 3-D geometry of the blanket of a Helias reactor has been prepared as input data for the MCNP code and the wall loading due to the 14 MeV fusion neutrons has been calculated. The wall loading is more inhomogeneous than in a tokamak reactor which underlines the importance of a careful investigation of the 3-D geometry.

ⁱ Scientific Centre “Institute for Nuclear Research”
03680 Kyiv, Ukraine

ⁱⁱ Fachhochschule Regensburg

IEA IMPLEMENTING AGREEMENT for Co-operation in Development of the Stellarator Concept

1. OBJECTIVES OF THE AGREEMENT

The objective of the Implementing Agreement, first concluded in 1985, is to "improve the physics base of the Stellarator concept and to enhance the effectiveness and productivity of research and development efforts relating to the Stellarator concept by strengthening co-operation among Agency member countries". To achieve this, it was agreed to exchange information, conduct workshops, exchange scientists, do joint theoretical, design and system studies, coordinate experimental programmes in selected areas, exchange computer codes, and perform joint experiments. In 2000 the Agreement was extended until June 2005. The contracting parties are EURATOM, the U.S. DoE, Japan, and Australia. In September 1994, Russia became an Associate Contracting Party. Also the Ukraine will join the Implementing Agreement. Signature of the contract is envisaged for spring 2002.

2. STATUS OF THE AGREEMENT

In 2001, there has been no meeting of the Executive Committee. The next meeting will be held at Canberra, Australia, in February 2002.

3. REPORT ON 2001 ACTIVITIES

In 2001, 16 physicists participated in the exchange of scientists.

O. Shishkin from the University of Kharkov, Ukraine, participated in the studies on the magnetic field of the Helias reactor on the basis of Gourdon codes from 7 January to 13 February. Y. Kolesnichenko from NUCRESI, Kharkov, Ukraine, investigated energetic ions in toroidal fusion devices during his stay from 17 February to 30 March. A short visit of L. Zakharov from PPPL Princeton in April was devoted to studies on the reference coordinate system for 3D equilibria. A. Kislyakov from Ioffe Institute, St. Petersburg, conducted neutral particle analyses during his stay at Garching from 6 May to 3 June. S. Murakami from NIFS worked on Monte Carlo and Fokker-Planck modelling from 6 to 17 June. From 8 July to 5 August, A. Shyshkin from the University of Kyiv,

Ukraine, worked on impurity transport studies on W 7-AS. At the same time, Y.V. Yakuvenko and V.V. Lutsenko, both from NUCRESI, Kharkov, Ukraine, studied energetic ions in toroidal fusion devices. During a 3-day visit to Garching in October, H. Yamamoto from NIFS held discussions about MHD instabilities. A short visit of H. Mikkelsen from PPPL in December was devoted to intensifying international collaboration in neo-classical theory, in particular the quasi-axisymmetric configuration of the NCSX.

M. Hirsch attended the 5th Reflectometry Workshop at NIFS, Japan, from 5 to 7 March. G. Michel participated in the 14th Topical Conference on Radio Frequency Power in Oxnard, USA, from 7 to 9 May. A 2-week stay of J. Geiger at NIFS in October was devoted to transferring the 3D-MHD equilibrium code of NIFS to IPP. A. Weller attended the 5th NCSX Programme Advisory Committee Meeting at Princeton from 13 to 16 November. P. Grigull and H. Wobig participated in the 12th International Toki Conference from 11 to 14 December.

4. CONFERENCES AND WORKSHOPS

From 5 to 7 March, the 5th Reflectometry Workshop was held at NIFS, Japan. A workshop on Innovative Concepts and Theory on Stellarators took place at Kyiv, Ukraine, from 28 to 31 May. The 13th International Stellarator Workshop, originally scheduled for September 2001 at Canberra, Australia, was postponed to 25 February to 1 March 2002. The 12th International Toki Conference took place at Toki City, Japan, from 11 to 14 December.

PLASMA-FACING MATERIALS AND COMPONENTS

(Heads of Project: H. Bolt, J. Roth)

During the operation of fusion devices the plasma facing materials are subjected to particle fluxes from the plasma (ions, electrons, atoms) and to electromagnetic radiation. This results in a multitude of complex processes termed as “plasma-wall interaction”. The understanding of these processes helps to improve the materials used for applications on the first wall of fusion experiments. It also leads to optimised operation conditions and thus to performance improvement during the plasma discharge. New materials with improved properties in terms of e.g. erosion behaviour and heat flux capability are to be developed and characterised under plasma interactive conditions. The integration of new materials into the plasma facing components also requires detailed work on interfacial engineering, since dissimilar materials with different functions have to be used. Within the project „Plasma Facing Materials and Components“ the areas of plasma wall interaction studies, material modification under plasma exposure, development of new plasma facing materials and their characterisation have been merged to form a field of competence at IPP. The work supports the exploration and the further development of the fusion devices of IPP and also generates basic expertise with regard to the PFC related questions in ITER and fusion reactors.

Starting from the analysis of loading and exposure conditions of plasma facing materials in the IPP devices, materials and model systems of plasma facing material surfaces will be tested under equivalent laboratory conditions. They are subjected to particle fluxes and to thermal exposure in laboratory experiments to quantitatively determine erosion, hydrogen desorption, and thermally induced chemical and physical surface processes. Based on this knowledge, new materials are being developed for experiments in ASDEX Upgrade and in W7-X. These materials which are firstly being synthesised on laboratory scale will be characterised with regard to their properties and may subsequently be further developed within an industrial environment. Results gained from the operation of these materials in ASDEX Upgrade and -later- in W7-X are of direct relevance also for ITER. Plasma material interaction processes in ASDEX Upgrade can be scaled to ITER conditions and the issues of stationary heat fluxes to plasma facing surfaces are a fundamental aspect of the stationary plasma operation of W7-X. The tasks of the project are:

• High Z materials, • Low Z Materials, • Surface processes on plasma exposed materials, • Component related aspects, • Migration of materials in fusion devices

1. Members: M. Balden, I. Beguiristain, B. Böswirth, K. Durocher, W. Eckstein, K. Ertl, M. Fußeder, X. Gong, H. Greuner, Q. Guo, E. de Juan Pardo, K. Klages, F. Koch, S. Kötterl, K. Krieger, S. Lessmann-Bassen, D. Levchuk, S. Lindig, Ch. Linsmeier, J. Luthin, H. Maier, K. Marx, G. Matern, P. Matern, M. Mayer, O. Ogorodnikova, W. Ottenberger, E. Oyarzabal, C. Popescu, O. Poznansky, S. Rolle, J. Roth, J. Schäftner, K. Schmid, H. Schmidl, D. Valenza, A. Weghorn, A. Wiltner, M. Ye, J.-H. You

2. Contributors: W. Bohmeyer, M. Laux, R. Neu, H. Renner, V. Rohde, S. Schweizer

1. HIGH-Z MATERIALS

1.1 Tungsten Coatings for the First Wall

Since the application of tungsten as a first-wall material in ASDEX Upgrade proved to be very successful, the central column was almost completely covered with tungsten-coated fine-grain graphite tiles in 2001. Further extension of the tungsten-coated first-wall portion may necessitate utilization of fibre-reinforced carbon materials (CFC). Since such materials are inhomogeneous and possess anisotropic thermal properties, e. g. thermal expansion and heat conduction, test coatings were

investigated. The coatings were manufactured by the same method as the bulk of the already installed coated fine-grain graphite tiles, e.g. plasma arc deposition by Plansee AG.

To study possible influence of the mentioned substrate anisotropy on the film properties, the residual stress state of the coatings was investigated by means of X-ray diffraction employing the newly installed device of the Materials Research Division. All films deposited were found to be in a state of compressive residual stress. In the case of a bidirectional CFC substrate this stress significantly depended on the orientation of the substrate fibre planes, see Fig. 1. In cooperation with Forschungszentrum Jülich thermal loading tests were performed

using an electron beam facility. In spite of the thermomechanical anisotropy of the substrates, no macroscopic cracking or delamination was observed. The only observed failure was melting. Using a power ramp-up time of 0.7s and a flat-top time of 2s this occurred at a thermal load of about 30 MW/m².

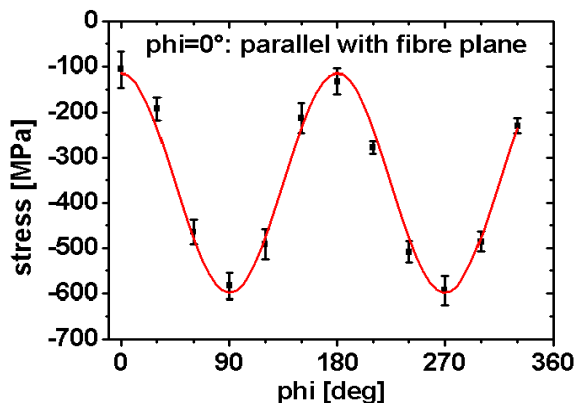


FIG. 1: Residual compressive stress in a W film on 2D CFC in various directions with respect to the fibre planes.

1.2 Erosion of W by C and H Isotopes

The complex erosion and deposition processes occurring during simultaneous bombardment of W by C and H isotopes were investigated both experimentally and in modelling calculations. In order to describe the transition from C layer deposition to W erosion under plasma conditions, controlled ion beam experiments were performed to determine temperature-dependent parameters such as the C diffusion coefficient and radiation-enhanced sublimation (RES). It was found that RES cannot be neglected for elevated temperatures and that C diffusion in W is strongly concentration-dependent and becomes pronounced above 1000 K. To model the simultaneous carbon bombardment and diffusion, the TRIDYN Monte Carlo code was coupled to the newly developed DIFFUSED C diffusion code. With this code package and the experimental information about C diffusion and RES it is possible to simulate the temperature-dependent erosion and deposition processes occurring during bombardment of W by C without any free parameters and compare them with experimental results. These calculations showed that for pure C bombardment and surface temperatures below 1073 K a shielding C layer builds up on the W surface, protecting it from further erosion. To model the simultaneous bombardment of W with C and D from a plasma, the chemical erosion of C due to D was added to the TRIDYN+DIFFUSED C code package. Taking into account the Maxwellian energy distribution and the acceleration of the incident C⁴⁺ and D⁺ in the sheath potential, we calculated the W sputtering yield due to a D plasma with varying C impurity concentration. These calculations showed that in contrast to pure C bombardment simultaneous bombardment of W with C and D leads to continuous erosion of the W for C concentrations below a concentration limit that depends on the plasma temperature and surface temperature. In Fig. 2 the results for the weight change of a W surface ($dW/d\Phi$) in equilibrium is shown as a function of the C concentration in the incident C/D

particle flux and the plasma temperature T_e . The weight change is a measure whether net erosion of W ($dW/d\Phi < 0$) or deposition ($dW/d\Phi > 0$) of C occurs. A weight loss of $-0.03 \mu\text{g}/10^{16}$ ions is roughly equivalent to a W erosion yield of 10^{-2} . One can see that for low C concentrations no shielding layer buildup is possible due to chemical sputtering and that net erosion occurs, whereas at larger concentrations a transition to C deposition occurs.

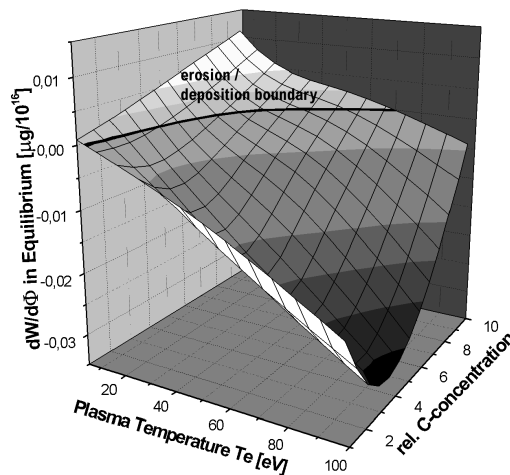


FIG. 2: Weight change in equilibrium of W surface under C/D irradiation as a function of C concentration and the plasma temperature.

2. LOW-Z MATERIALS

2.1 Low-Z Coatings for the First Wall of W7-X

On the outboard-side first-wall panels of W7-X the application of thick plasma-sprayed low-Z coating is envisaged. The use of such coatings on water-cooled stainless-steel panels should result in good plasma compatibility as well as a long erosion lifetime. The heat flux in these zones is estimated to be 100 kW/m² with local maxima of 200 kW/m². In collaboration with an industrial partner, Plansee AG, plasma spray coatings of both B₄C and Si-B-C were developed and deposited on stainless-steel AISI304 substrates, Fig. 3. Deposition was done by the vacuum plasma spray method without interlayer and with Mo or mixed steel/B₄C interlayers, and the thickness was varied in steps of 150 μm , 300 μm and 500 μm . Actively cooled specimens of 300 mm x 80 mm surface area were prepared for heat flux testing of the coatings. The tests were carried out in the FIWATKA facility at Forschungszentrum Karlsruhe. For all specimens the heat flux was increased in steps of up to 500 kW/m². During each of these steps stationary heat removal conditions were obtained. In addition the specimens were subjected to 100 thermal cycles. Except for one specimen, no change or damage was observed on the coatings.

Local failure, crack formation, and partial delamination took place on a predamaged zone of the directly bonded 500 μm thick B₄C coating. In a highly stressed edge zone pre-existing fissures grew in the heat load range of 200 to 500 kW/m² and led to delamination of approx. 2 cm² of the coating. B₄C and Si-B-C coatings with stainless-steel/B₄C interlayer were also

subjected to thermal cycling experiments at 500 kW/m^2 for 1,000 cycles. No change or damage occurred. It was concluded that coatings up to $500 \mu\text{m}$ thick with interlayer can be applied under the heat load conditions envisaged for W7-X.

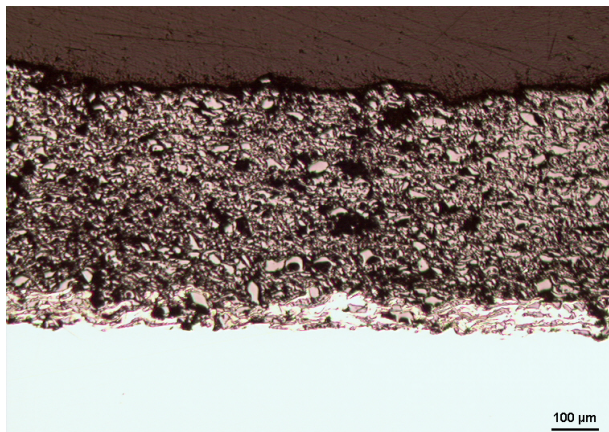


FIG. 3: Cross-section of B_4C coating ($500 \mu\text{m}$) with mixed B_4C -steel interlayer on stainless-steel substrate.

2.2 Reduction of Chemical Erosion of Carbide-doped Graphites

Chemical erosion by low-energy deuterium bombardment (tens of eV) of fine-grain graphites doped with SiC, TiC, VC, WC, and ZrC was investigated by weight loss measurement and mass spectrometry. The graphites were produced in cooperation with CEIT, San Sebastián, and characterised with respect to the catalytic effect of the dopant on the graphitisation, to the thermal conductivity, and to the mechanical properties. The highest thermal conductivity of 170 W/mK has been achieved with 4 at% ZrC doping.

Preferential erosion of the pure carbon phase of the doped graphite leads to enrichment of the dopant on the surface with fluence and subsequently to reduction of the erosion. Together with this enrichment a rough surface morphology is created.

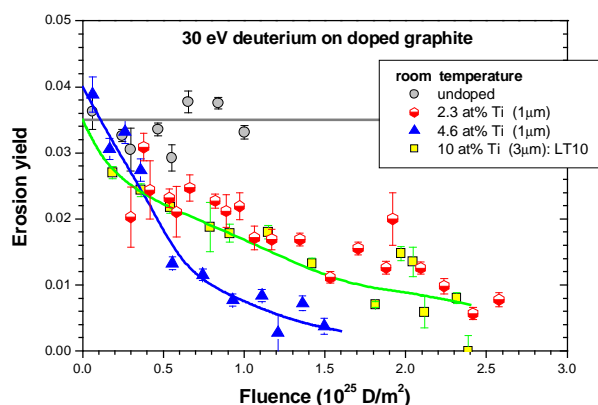


FIG. 4: The fluence dependence of the total erosion yield of TiC-doped graphite with different dopant concentrations and grain sizes.

For the low-energy low-temperature erosion regime a reduction of the erosion by one order of magnitude has been achieved at high deuterium fluences. Fig. 4 shows the fluence dependence of the total erosion yield of TiC-doped graphites. The decrease of the yield with fluence depends on the grain size as well as on the dopant concentration, as expected due to the enrichment. But the dopant enrichment does not exceed 25%. Therefore, in addition to the geometrical shadowing other mechanisms reduce the erosion: The enhanced re-deposition of the eroded hydrocarbons in the rough morphology could be important and the change in the chemical processes could make a small contribution.

3. SURFACE PROCESSES ON PLASMA-EXPOSED MATERIALS

3.1. Carbide Formation on Iron

Carbide formation at the interface of thin carbon layers on iron as a function of the annealing temperature was studied by X-ray photoelectron spectroscopy (XPS). Formation of carbides on Be, Si, Ti, and W, which is an exothermic reaction, could be explained by carbon diffusion governed by the carbide structures and the negative enthalpy of formation. Iron carbide, however, is an endothermic compound. First measurements of thin (1 and 2 nm) carbon films showed the reaction between carbon and iron to iron carbide already at room temperature. The surface carbon amount is stable up to $\sim 650 \text{ K}$, where carbon starts to diffuse into the bulk iron. Between 670 K and 770 K the integral C 1s intensity rapidly decreased to a few per cent of the initial value. The binding energy shift indicated a loss of elementary carbon and carbide formation. Further annealing up to 970 K did not change the amount of carbide in the surface region. No elementary carbon could be detected in this temperature regime.

3.2 D^+ Ion Bombardment of Mixed Materials

The effects of deuterium ion bombardment of elementary materials (highly oriented pyrolytic graphite (HOPG), polycrystalline W and Ti) as well as multi-component materials (vapour-deposited C layer on Ti) were studied at ion energies of 1 and 4 keV. The chemical composition and state of the surface were analysed by XPS. The D^+ bombardment led to shifts in the C 1s and Ti 2p peaks on the graphite and titanium samples, respectively. The C 1s shift on HOPG was -0.15 eV , whereas the Ti 2p signal shifted by $+0.2 \text{ eV}$. D^+ bombardment of a 2.9 nm carbon layer on Ti led to significant erosion of the surface which is not explained by physical sputtering, simulated by means of the kinematic TRIDYN code. This behaviour indicates chemical erosion of carbon by D^+ ions.

3.3 Deuterium Retention in W

The physical mechanism of hydrogen trapping and migration in tungsten is not yet completely understood. We investigate the retention of ion-implanted deuterium in polycrystalline tungsten as a function of (i) incident ion energy (between 100 eV and 3 keV), (ii) temperature (between 300 K and 600 K), (iii)

fluence (up to 10^{25} D/m²), and (iv) surface conditions. It is shown that the retention strongly depends on the tungsten structure, sample preparation, and pre-implantation history. An increase in the ion energy results in a slight increase of the retention. As a function of temperature, a maximum is found around 430-470 K. An increase of the fluence results in an increase of the deuterium inventory until saturation is reached at approximately 3×10^{24} D/m². The saturation value of the retained deuterium is about 3×10^{21} D/m² at room temperature and has a maximum of about 5×10^{21} D/m² at 470 K.

Calculations based on the diffusion including thermodesorption and the modified trapping equation show that most of the deuterium is trapped in W in two kinds of defects with trapping energies of about 1.0 eV and 1.4 eV. The first kind of trap is associated with natural traps (dislocation, some impurities, presence of bulk oxide), which are always present in polycrystalline W. Both the increase of the temperature and time of W pre-heating and pre-implantation of W by deuterium ions at high temperature strongly decrease the concentration of 1.0 eV defects owing to removal of residual stresses, impurities, vacancies, and dislocation near the surface and reduction of the dislocation content in the bulk. The concentration of 1.4 eV traps increases with fluence and incident energy of implanted deuterium, and has a maximum as a function of temperature. It seems that the second kind of trap is connected with the growth of hydrogen bubbles.

3.4 Recombination Coefficient of Hydrogen on a Clean Metal Surface

Knowledge of the recombination coefficient is necessary for estimating the hydrogen isotopes' behaviour in the metallic structures of a thermonuclear reactor. The recombination coefficient of hydrogen on a clean metal surface was derived. It is shown that the recombination coefficient is a function of the diffusion pre-exponential factor, D_0 , and the heat of solution, Q_s : $K_r^{clean} = D_0 \lambda^2 \exp(2Q_s / kT)$, where λ is the distance between two adjacent interstitial sites in the lattice, k is Boltzmann's constant, and T is the temperature.

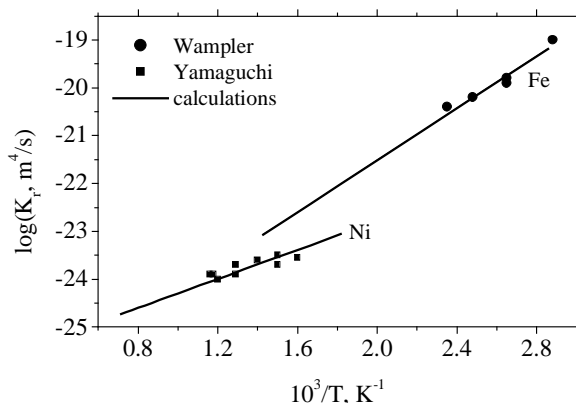


FIG. 5: Recombination coefficient of ion-implanted hydrogen for iron and nickel.

Comparison of the calculations of the recombination coefficient of hydrogen on a clean metal surface with experiments are in a good agreement (Fig. 5).

4. COMPONENT-RELATED ASPECTS

4.1 Metal Matrix Composites

Copper alloys and reduced activation martensitic steels (RAMS) have been considered as structural materials for the plasma-facing components of a future fusion reactor. Since such components will be subjected to high heat flux loads, sufficient mechanical strength at elevated temperatures is one of the crucial prerequisites. Component performance is expected to be significantly improved by applying ceramic fibre reinforcement due to the high strength and high temperature stability of the fibres.

To assess the feasibility of long SiC fibre-reinforced metal matrix composites (FRMMCs), the overall mechanical properties of two FRMMCs, each with a matrix of precipitation-hardened copper alloy and RAMS, were estimated by micro-mechanical methods.

In Fig. 6 the predicted mechanical properties of the RAMS composite are compared with those of the matrix steel and the oxide-dispersion-strengthened RAMS. The calculated values are given in relation to those of the RAMS composite with 40 % of the fibre volume fraction at room temperature. It is seen that most of the mechanical properties could indeed be improved by long-fibre reinforcement.

In addition to this theoretical work, galvanic coating experiments of SiC long fibres with Cu were carried out. It was found that thick and homogeneous Cu coatings could be deposited as a key step in the processing of Cu-SiC fibre MMCs. With this process SiC fibres of 140 μ m diameter were coated with a Cu coating to a total diameter of up to 500 μ m. Initial characterisation was done by metallography, scanning and transmission electron microscopy.

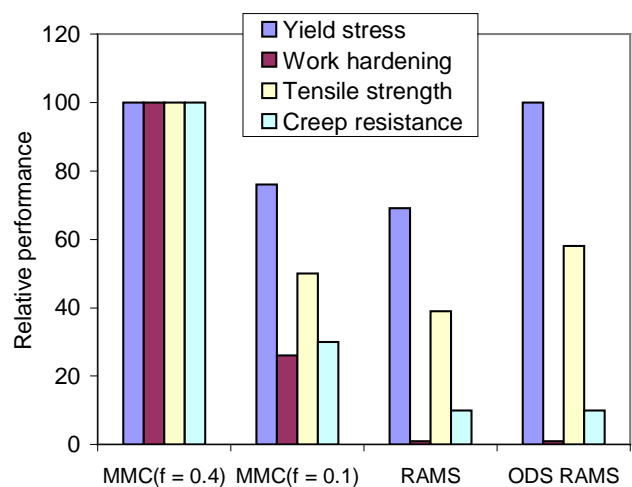


FIG. 6: Comparison of the mechanical properties of three steel-based candidate materials: fibre composites (SiC fibre content 40 % and 10 %), steel (Eurofer), ODS steel.

4.2 Al₂O₃ Coatings for Hydrogen Permeation Barrier Applications

Penetration of hydrogen isotopes into and through metallic structural materials will be an issue in the construction of fusion reactors. Surface coating with thin films acting as diffusion barriers is a promising approach for handling this hydrogen isotope migration problem. Films are deposited by a filtered vacuum arc from an aluminium/oxygen plasma.

In a first step the morphology and crystal structure of the films are investigated. Since deposition is performed from a plasma, a bias voltage can be applied to influence the kinetic energy of deposited particles. The newly installed X-ray diffraction device of the Materials Research Division was used to obtain a tentative phase diagram of crystal phases as a function of the bias voltage and substrate temperature. Deposition of the thermodynamically stable α -crystal phase was found to be possible at substrate temperatures below 400° C.

In a second step the hydrogen retention performance of the coatings is investigated in a custom-built permeation measurement setup. This setup has produced first data and the suitability of the employed sample mounting and sealing technique has been confirmed up to operating temperatures of around 500° C. In addition, cooperation has been initiated with the National Institute of Fusion Science (NIFS), Japan, where sample coatings prepared at IPP are being investigated with respect to their ability to withstand corrosive processes in a lithium-containing breeder environment.

4.3 HHF tests of PFC for ASDEX Upgrade and W7-X

During operation the plasma-facing components of fusion devices are subjected to heat loads from the plasma. Both for ASDEX Upgrade and for W7-X the thermomechanical behaviour of plasma-facing components was examined. In cooperation with ASDEX Upgrade high heat flux tests of the newly designed inner heat shield elements were carried out on the MARION ion beam facility at Forschungszentrum Jülich. The heat shield elements made of graphite (FP 479, Schunk) were loaded with transient heat pulses of 4 MW/m² for 5.5 s and 35 MW/m² for up to 300 ms. For the same type of element, but coated with a 1 μ m W layer, these experiments were repeated. The metallographic investigation of both types of sample revealed few fissures but no delamination or losses of W coating. The spatial and temporal temperature distributions for these transient loading conditions were simulated by FE methods. The calculated results are in good agreement with the recorded experimental data. These results support the application of such elements for the neutral beam dumps of the inner heat shield. For W7-X heat flux tests were performed on prototypes of baffle and first-wall components. These components were tested with stationary heat loads of up to 500 kW/m² on the FIWATKA facility at Forschungszentrum Karlsruhe. As a result, the thermomechanical basis of the component design was confirmed. (see section "W7-X construction")

5. MIGRATION OF MATERIALS IN FUSION DEVICES

5.1 Erosion and Migration of Tungsten Employed at the Central-Column Heat Shield of ASDEX Upgrade

In ASDEX Upgrade, tungsten-coated graphite tiles were employed as plasma-facing components at the central-column heat shield in the plasma main chamber. Within the frame of this experimental programme plasma-wall interaction studies were carried out. The technical setup of the tungsten tiles in campaign 2001 is described in section ASDEX Upgrade Project. In addition to the W-coated tile rows at the upper and lower edges of the heat shield, a complete poloidal column of tungsten-coated tiles with reduced layer thickness was introduced to analyse the spatial distribution of the tungsten erosion. The campaign-averaged W erosion flux was determined by measuring the difference of the W layer thickness before and after the experimental campaign by Rutherford backscattering spectroscopy. In addition, the small-scale distribution of the remaining tungsten layer after the experimental campaign was studied by scanning electron microscopy. From the observed strong lateral variation (see Fig. 6) and the measured total amount of eroded tungsten, erosion by impact of ions from the scrape-off layer plasma is identified as the predominant tungsten erosion mechanism.

Migration and redeposition of eroded tungsten were investigated by quantitative analysis of tungsten deposited on collector probes and on a complete poloidal set of divertor tiles. The maximum deposition is found on tiles in contact with the far periphery of the plasma scrape-off layer. This observation and the spectroscopically observed low tungsten plasma penetration probability indicate that a major fraction of the eroded tungsten migrates predominantly through direct transport channels in the plasma boundary region without entering the confined plasma.

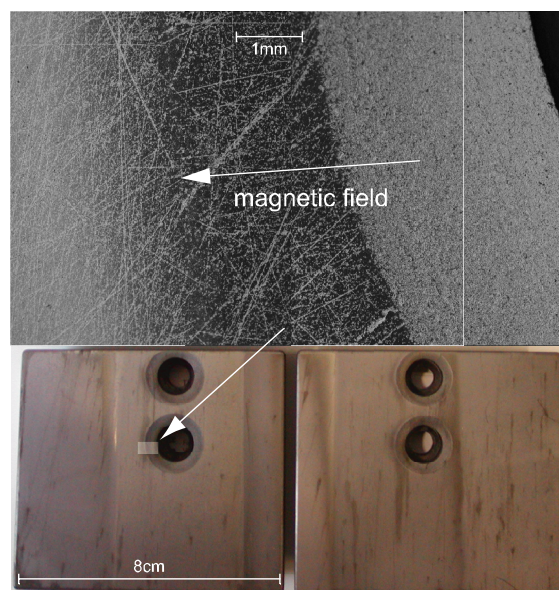


FIG. 7: Electron backscattering image of W-coated tile. The bright areas correspond to remaining W in scratches and shaded regions after exposure to plasma discharges. Dark areas correspond to the carbon substrate.

SCIENTIFIC DIVISION OF IPP

Experimental Plasma Physics Division 1

Director: Prof. M. Kaufmann

ASDEX Upgrade (Divertor Tokamak)

operation of ASDEX Upgrade
investigation of ITER plasma boundary in a reactor-relevant divertor
advanced tokamak studies
investigation of energy transport, MHD stability, beta limit, density limit and disruptions

JET collaboration

participation in experiments on JET under EFDA
operation of special discharge scenarios at JET
comparative studies together with ASDEX Upgrade

Experimental Plasma Physics Division 2

Director: Prof. H. Zohm

ASDEX Upgrade

MHD Stability studies
edge and pedestal physics
diagnostics

ITER

coordination of ITER-related activities at IPP

JET

contributions to Task Forces S1, S2 and MITER
coordination of ITER-related activities at IPP

Experimental Plasma Physics Division 3

Director: Prof. F. Wagner

WENDELSTEIN 7-AS (Advanced Stellarator)

- stellarator with improved magnetic characteristics
- Experiment-orientated stellarator Theory
- interpretation of stellarator experiments
- Stellarator power plant system studies
- development of the HELIAS power plant concept
- Preparation of the WENDELSTEIN 7-X diagnostics
- Preparation of ECRH for WENDELSTEIN 7-X
- Development of Greifswald site

Experimental Plasma Physics Division 4

Director: Prof. K. Behringer

Experimental and theoretical investigations of plasma boundary and divertor physics, impurity transport, chemical impurity production and plasma radiation in ASDEX Upgrade and WENDELSTEIN 7-AS

- spectroscopic diagnostics on ASDEX Upgrade
- spectroscopic diagnostics on WENDELSTEIN 7-AS laboratory experiments at the University of Augsburg, Experimental Plasma Physics

Experimental Plasma Physics Division 5

Director: Prof. T. Klinger

dynamical behaviour of stellarator plasmas physics of the plasma edge and divertor region stellarator magnetohydrodynamics data acquisition and control

WENDELSTEIN 7-AS

development and optimization of diagnostics

WENDELSTEIN 7-X

preparation of the experiment program

VINETA

basic behaviour of plasmas waves and plasma instabilities

INTERNATIONAL MAX-PLANCK RESEARCH SCHOOL "BOUNDED PLASMAS"

training of PhD students

Stellarator Theory Division

Director: Prof. J. Nührenberg

General stellarator theory

- Further development of the stellarator concept and computational as well as analytical methods to investigate equilibrium, stability and transport problems in three-dimensional toroidal configurations.

Plasma edge physics

- Theoretical work on 3D plasma edge physics

SCIENTIFIC DIVISION OF IPP

Plasma Diagnostics Division

Director: Prof. G. Fussmann

Edge plasma physics

- experimental and theoretical work relating to fusion devices

Plasma generator PSI-II

- basic plasma physics
- plasma interaction with solid surfaces
- development and testing of plasma diagnostics
Electron Beam Ion Trap (EBIT)
- production of highly charged ions
- X-ray spectroscopy and atomic physics measurements
UHV laboratory, arc physics, ITER collaboration

Materials Research Division

Director: Prof. H. Bolt

- Characterisation of fusion relevant properties of plasma facing materials; development and qualification of plasma facing materials for present fusion devices, esp. ASDEX Upgrade and WENDELSTEIN 7-X
- Design and development of materials for plasma facing components in fusion reactors

Surface Physics Division

Directors: Prof. V. Dose, Prof. J. Küppers

Surface physics

- atomistic characterisation of surfaces
Plasma-wall interactions
- interactions of atoms, ions and electrons with solid surfaces
- wall fluxes in the boundary layer of plasma devices
- limiter and wall analyses

Low temperature plasma physics

- preparation and characterisation of thin-film coatings for plasma devices

Data analysis*

- application of Bayesian techniques to experimental data
- * Part of Centre for Interdisciplinary Plasma Science

WENDELSTEIN 7-X Construction

Director: Dr. M. Wanner

WENDELSTEIN 7-X Construction

- engineering, construction and installation of the W 7-X device
incl. system control, plasma heating, in-vessel components, and auxiliary systems
- project control and quality management

Technology Division

Director: Prof. R. Wilhelm

Neutral injection

- development, construction and operation of the injection
- systems for WENDELSTEIN 7-AS, ASDEX Upgrade and W 7-X
- NBI development for ITER
- development of RF-driven negative ion sources for ITER

Electron cyclotron resonance heating

- construction and operation of an ECRH system for ASDEX Upgrade

Ion cyclotron resonance heating

- development, construction and operation of ICRH systems for WENDELSTEIN 7-AS, ASDEX Upgrade and WENDELSTEIN 7-X

Tokamak Physics

Director: Prof. S. Günter

Theoretical support for the tokamak activities of IPP as well as study of fundamental plasma physics in toroidal magnetic confinement devices:

- plasma edge physics
- nonlinear plasma dynamics and turbulence
- heat and particle transport in tokamaks
- large scale instabilities in tokamaks including MHD and kinetic effects
- wave propagation and absorption in inhomogeneous plasmas

EXPERIMENTAL PLASMA PHYSICS DIVISION 1

(Prof. Dr. Michael Kaufmann)

The activities of division E1 are concentrated on the ASDEX Upgrade related work and are reported in the section "ASDEX Upgrade Project".

The division E1 comprises:

1. Three diagnostic groups:

pellet injection, bolometer, neutral gas, neutron measurements, hard XRs, mass spectrometer, SABA databank, charge exchange neutrals in core and edge (LENA), DCN and CO₂ interferometer, calorimetry, Langmuir probes, Li-beam diagnostics, manipulators, electromagnetic measurements, plasma control, current density and radial electric field (MSE), halo current measurements, transport analysis, which are responsible for the development of plasma diagnostics as well as for plasma physics exploitation.

2. Three machine groups:

a. operation,
b. mechanical design,
c. assembly,
which are concerned with the operation and engineering developments of the tokamak experiment ASDEX Upgrade and its peripheral installation. These groups are supported by three workshops:
1. mechanical
2. electrical
3. electronic.

Division E1 is also devoted to collaboration on JET and to continue studies for ITER.

EXPERIMENTAL PLASMA PHYSICS DIVISION 2

(Head of Division: Prof. Dr. Hartmut Zohm)

Department E2 investigates the magnetohydrodynamic (MHD) stability of ASDEX Upgrade discharges. In addition to the pure analysis of instabilities, their effect on the reduction of the tokamak operational space is examined. In collaboration with the ASDEX Upgrade ECRH group (technology division), strategies are being developed which will increase the operational space via the active control of instabilities. In particular, this involves the planning of an extension of the present ASDEX Upgrade ECRH system to frequency tuning, fast beam steering and more power at longer pulse length. Further tasks within E2 at ASDEX Upgrade are the experiment specific data management as well as the real-time control of the experiment.

In addition, E2 staff take part in the work on JET under EFDA in Task Forces S1 (conventional scenarios) and M (MHD). Furthermore E2 co-ordinates the physical study for the planned ECRH system at JET.

Also, the ITER-related activities at IPP are co-ordinated by E2.

E2 comprises the following working groups:

Diagnostics IV

ASDEX Upgrade control group

ASDEX Upgrade data management group

Scientific staff: K. Behler, H. Blank, A. Buhler, G. Conway, R. Drube, K. Engelhardt, A. Gude, H. Hohenöcker, M. Jakobi¹, A. Keller², B. Kurzan, M. Maraschek, H. Meister¹, R. Merkel, A. Mück², H. Murmann, G. Neu, G. Raupp, K.-H. Steuer, W. Suttrop, D. Wagner, D. Zasche, T. Zehetbauer, H. Zohm

¹ Post-Doc
² PhD student

Technical staff: C. Aubanel, H. Bauer, J. Hausmann, H.-J. Jung, K. Klöss, J. Krippner, A. Lohs, U. Ortner, B. Pachur, T. Pirsch, E. Schmid, L. Scoones, T. Seth, G. Zimmerman

EXPERIMENTAL PLASMA PHYSICS DIVISION 3 (W7-AS)

(Head of Project: Prof. Dr. Friedrich Wagner)

The W7-AS group comprises Experimental Plasma Physics Division 3. The work is fully reported in the section "STELLARATOR Project", of which the members are as follows:

Experimental Plasma Physics Division 3

S. Baeumel¹⁸⁾, N. Basse²⁾, A. Bencze⁸⁾, M. Berta⁸⁾, T. Bindemann¹⁷⁾, R. Brakel, M. Bruchhausen⁶⁾, A. Dinklage, A. Dodhy, H. Ehmler¹⁷⁾, M. Endler, K. Engelhardt, Y. Feng, C. Fuchs, F. Gadelmeier¹⁷⁾, J. Geiger, L. Giannone, P. Grigull, O. Grulke¹⁸⁾, H. Hacker, H.J. Hartfuss, M. Hirsch, E. Holzhauer, K. Horvath¹⁸⁾, R. Jaenicke, S. Kalvin⁸⁾, F. Karger, M. Kick, A. Kislyakov¹¹⁾, T. Klinger, S. Klose¹⁷⁾, J. Knauer, G. Kocsis⁸⁾, Y. Kolesnichenko¹⁵⁾, A. Kreter⁶⁾, H. Kroiss, G. Kühner, A. Kus, J. Lingertat, R. Liu, V.V. Lutsenko¹⁵⁾, H. Maassberg, V. Marchenko¹⁵⁾, N. Marushchenko, K. McCormick, G. Michel, A. Mikkelsen¹⁶⁾, V. Mishagin¹³⁾, S. Murakami⁸⁾, R. Narayanan¹⁷⁾, S. Nica¹⁰⁾, S. Niedner¹⁸⁾, U. Neuner, M. Otte, M.G. Pacco-Duechs, E. Pasch, G. Petravich⁸⁾, E. Polunovsky¹⁷⁾, A. Pospieszczyk⁶⁾, N. Ruhs, J. Saffert, F. Sardei, V. Savkin¹³⁾, M. Schmidt¹⁷⁾, F. Schneider, M. Schubert¹⁸⁾, B. Schweer⁶⁾, A. Sengupta³⁾, A. Shishkin¹⁴⁾, O. Shishkin¹⁴⁾, J. Svensson¹⁷⁾, H. Thomsen¹⁸⁾, Y. Turkin, F. Volpe¹⁸⁾, F. Wagner, A. Weller, A. Werner, A. Wieczorek⁷⁾, E. Wuersching, Y. Yakovenko¹⁵⁾, H. Yamamoto⁹⁾, S. Yamazaki⁹⁾, D. Zimmermann, L. Yao¹⁾, S. Zoletnik⁸⁾

- 1) Guest from SWIP Chengdu (China)
- 2) Guest from Risoe Lab. Roskilde (Denmark)
- 3) Guest from University of Cork (Eire)
- 4) Guest from University of Kiel (Germany)
- 5) Guest from IPF Stuttgart (Germany)
- 6) Guest from FZ Juelich (Germany)
- 7) Guest from Profess. Univ.-College Regensb. (Germany)
- 8) Guest from KFKI Research Inst., Budapest (Hungary)
- 9) Guest from NIFS, Nagoya (Japan)
- 10) Guest from TU Kishinau (Moldova)
- 11) Guest from IOFFE Institute, St. Petersburg (Russia)
- 12) Guest from IAP Nizhny Novgorod (Russia)
- 13) Guest from Budker Inst., Novosibirsk (Russia)
- 14) Guest from IPT-NSC Kharkov (Ukraine)
- 15) Guest from NUCRESI Kyiv (Ukraine)
- 16) Guest from PPPL (USA)
- 17) Postdocs
- 18) Doctoral fellow

Technical Team W7-AS:

G. Abele, P. Ahlrep, J. Ahmels, D. Assmus, S. Bartsch, M. Bergbauer, P. Boehm, M. Braun, K.H. Brumm, H. Czich, K. Ewert, A. Fohr, M. Fusseder, H. Greve, U. Herbst, J. Hofner, H. Holitzner, F. Hollmann, H. Ibbach, A. John, P. Junghanns, K.H. Knauer, F. Kunkel, K. Lehmann, U. Neumann, F. Noke, F. Offenbaecher, I. Ott, R. Puff, F. Purps, S. Radau, A. Rahm, T. Richert, H. Rixner, H. Schmidt, H. Scholz, P. Schoetz, T. Schulz, W. Schulz, R. Semler, S. Siche, R. Singer, H. Speer, B. Stajminger, H.-J. Stresau, M. Steffen, H. Volkenandt, Chr. Wiechmann, G. Zangl, R. Zille, Do. Zimmermann

Experimental Plasma Physics Division – Reactor Studies

T. Andreeva, C. Beidler, E. Harmeyer, Y. Igitkhanov, F. Herrnegger, J. Kisslinger, I. Ott, H. Wobig

Experimental Plasma Physics Division 4

J. Baldzuhn, K. Behringer, R. Burhenn, K. Gresser, R. Koenig
ECRH (Electr. Cycl. Resonance Heating):
V. Erckmann (IPP Garching)
W. Kasperek, L. Empacher, G. Gantenbein, H. Laqua, G. Michel, P.G. Schueller, K. Schwoerer (IPF Stuttgart)
L. Lubyako, S. Malyguine, E. Suvorov (IAP Nizhny Novgorod)

ICRH (Ion Cycl. Resonance Heating):

W. Becker, F. Braun, H. Faugel, D.A. Hartmann, J.M. Noterdaeme, F. Wesner, E. Wuersching (Technology Division)

NBI (Neutral Beam Injection):

W. Ott, F. Probst, R. Riedl, N. Rust, W. Schaerich, E. Speth, R. Suess, (Technology Division),

Plasma Surface Interaction Group:

R. Fischer, V. Dose, J. Roth, E. Taglauer

Plasmadiagnostics (Berlin)

D. Hildebrandt, D. Naujoks, U. Wenzel

Computer Centre:

S. Heinzl, H. Lederer, M. Panea-Doblado, A. Schott

Central Workshop:

H. Eixenberger, Th. Franke, F. Gresser, C.P. Käsemann-Wilke, K. Klaster, J. Perchermeier, G. Raitmeier, I. Schoenewolf, J. Stadlbauer, F. Stobbe, K. Voigt, G. Wenzel

EXPERIMENTAL PLASMA PHYSICS DIVISION 4

(Head of Division: Prof. Dr.-Ing. Kurt Behringer)

Experimental Plasma Physics Division 4 (E4) consists of the ASDEX Upgrade and the W7-AS Diagnostics groups. Their work is described in the ASDEX Upgrade and W7-AS project reports. Experimental Plasma Physics at the Augsburg University is closely linked to E4, allowing physics students to participate in IPP's scientific programme or do basic research at Augsburg. Recent results in the Augsburg laboratories are given under University Contributions to IPP Programme.

ASDEX Upgrade: I. Altmann, D. Bolshukhin, R. Dux, W. Engelhardt, J. Gafert, A. Geier, S. Higashijima, A. Kallenbach, R. Pugno, R. Neu, C. Maggi, H. Meister, Si-Woo Yoon, M. Zarrabian. **W 7-AS:** J. Baldzuhn, R. Burhenn, R. König. **Augsburg:** U. Fantz, M. Biberacher, J. Günther, B. Heger, S. Meir, M. Kirch, T. Pütterich, S. Richter, J. Schabert, P. Starke, B. Waldmann, D. Wunderlich. **Technical Staff:** G. Daube, M. Hien, J. Fink, K. Grosser.

Co-operation: IPP Berlin, JET, FZ Jülich, TU München, University of Strathclyde (Scotland), Stuttgart University.

The E4 scientific programme deals with plasma boundary and divertor physics, with impurity transport and plasma radiation, and with low- and high-Z wall materials. Mainly spectroscopic diagnostics and analysis methods are being used in E4. Recent topics in ASDEX Upgrade were divertor plasma parameters, and chemical erosion of carbon and silicon. Impurity transport at the H-mode edge is being studied from silicon soft X-ray radiation. As an alternative to carbon, a successively higher part of the ASDEX Upgrade walls has been covered by tungsten and neoclassical high-Z transport is therefore being investigated. The interest in W 7-AS is focused on measurements of electric fields, neoclassical impurity transport, impurity pellet injection and magnetic field structures. Spectroscopic diagnostics for W7-X are also being developed.

Spectroscopic measurements of line or continuum intensities as well as molecular band radiation require interpretation on the basis of atomic physics and radiative transfer. To have access to the most up-to-date results, E4 is part of the ADAS international co-operation. Recently, an improved set of electron excitation rate coefficients for neutral helium has become available [1]. These data are very important, since helium line intensities or line ratios are being used for plasma edge diagnostics (thermal helium beam). High energy helium beams are being discussed for main plasma diagnostics. The new theoretical calculations have been evaluated by means of low temperature laboratory plasmas experiments (see also Augsburg University contribution). In microwave discharges, the population of $n=3$ levels was obtained from emission and the $n=2$ population from absorption measurements. Figure 1 shows selected results in comparison with ADAS calculations. The latter were carried out with or without considering the re-absorption of spectral lines in these plasmas. Due to the low ionisation degree, recombination is negligible. The diffusion losses of the two me-

tastable levels were taken into account by artificial transition probabilities to the ground state. As can be seen in Fig. 1, the triplet metastable level is little influenced by optical thickness. The singlet 2p state is shifted up by three orders of magnitude due to the opacity of the corresponding resonance line and it also influences the 2s level. Similar effects are seen for $n=3$. They are less pronounced due to population paths from $n=2$ and a smaller A-value. The transition 2s-2p in the triplet is also optically thick, considerably enhancing the 2p level. A comparison with experimental results demonstrates the necessity of including opacity effects. Then, the ADAS rate coefficients can be confirmed within less than 30%. The most important remaining problem is the singlet 3s population. This is unfortunate, because lines from this levels would otherwise be best for plasma diagnostics, since they are least affected by assumptions on opacity and diffusion.

[1] Summers H P 2001, private communication

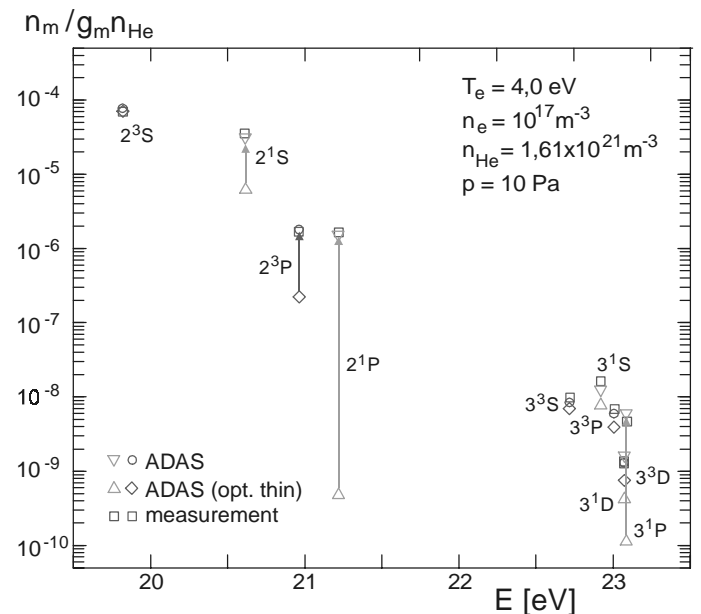


FIG. 1: Boltzmann plot of neutral helium levels. Shown are calculations using the ADAS collisional-radiative code and the latest HeI atomic data set with and without re-absorption of spectral lines in the plasma (Doppler profile, $T=500$ K). Experimental results were obtained in microwave plasmas for $n=3$ from emission and for $n=2$ from absorption studies.

EXPERIMENTAL PLASMA PHYSICS DIVISION 5 (VINETA)

(Head of Project: Prof. Dr. Thomas Klinger)

The VINETA group consists of Experimental Plasma Physics Division 5 and guests. The work is described in the VINETA report.

Experimental Plasma Physics Division 5

R. Bhattacharyay, G. Bonhomme⁴, C. M. Franck, O. Grulke,
S. Hanske, T. Kinder, T. Klinger, C. Schröder, A. Stark

Guests

R. Boswell¹, V. Naulin², E. S. Scime³

¹ ANU Canberra (Australia)

² FZ Risø (Denmark)

³ WVU Morgantown (USA)

⁴ L.P.M.I Université Henri Poincaré Nancy (France)

WENDELSTEIN 7-X CONSTRUCTION

(Dr. Manfred Wanner)

W7-X Construction Division

Engineering Team: Y. Bozhko, J. Boscary, T. Bräuer, R. Bünde, J.-H. Feist, W. Gardebrecht, H. Grote, B. Hein, F.-W. Hoffmann, H. Laqua, M. Nagel, H. Niedermeyer, J. Reich, H. Renner, K. Riße, T. Rummel, J. Schacht, F. Schauer, H. Schneider, A. Spring, K. Stache, M. Wanner, L. Wegener

Technical Team: H. Bau, A. Benndorf, A. Berg, H.-J. Bramow, R. Brockmann, A. Brückner, M. Czerwinski, H. Dutz, M. Fricke, F. Füllenbach, G. Gliege, M. Gottschewsky, S. Heinrich, A. Hölting, U. Kamionka, T. Kluck, E. Köster, C. Kopplin, U. Krybus, K. Lang, H. Lentz, B. Missal, T. Mönnich, I. Müller, F. Nankemann, A. Opitz, M. Pietsch, S. Pingel, S. Raatz, R. Rieck, U. Schultz, M. Schweitzer, K.-U. Seidler, F. Starke, H. Viebke, O. Volzke, A. Vorköper, A. Wölk

The W7-X Construction Division was supported by

Technology Division: D. Hartmann, B. Heinemann, S. Obermayer, W. Ott, R. Riedl, P. Rong, N. Rust, W. Schärlich, R. Schroeder, E. Speth, J. Wendorf, F. Wesner

Experimental Division E3: R. Brakel, V. Erckmann, F. Hollmann, L. Jonitz, H. Laqua, G. Michel, F. Purps, T. Schulz

Plasma Diagnostics Division Berlin: D. Hildebrandt, M. Laux, N. Rüter

Materials Research Division: B. Böswirth, H. Greuner, S. Kötterl, G. Matern, D. Valenza

Central Technical Services (ZTE, TD): F. Ascher, B. Brucker, H. Eixenberger, T. Franke, K. Gallowski, S. Geißler, M. Haas, R. Holzthüm, N. Jaksic, F. Kerl, R. Krampitz, A.E. Maier, J. Maier, M. Marquardt, B. Mendelevitich, M. Müller, J. Perchermeier, K. Pfefferle, G. Pfeiffer, H. Pirsch, M. Röpke, J. Sachtleben, D. Schinkel, J. Simon-Weidner, J. Stadlbauer, J. Tretter, K.J. Voigt, M. Weißgerber, M. Winkler, H. Zedler

Forschungszentrum Karlsruhe FZK (IHM, IMF I, ITP, PMW): A. Arnold, E. Borie, G. Dammertz, A. Goetz, P. Grundel, R. Heidinger, R. Heller, H. Hunger, S. Illy, M. Klenk, P. Komarek, H.-R. Kunkel, M. Kuntze, W. Leonhardt, R. Lukits, W. Maurer, D. Mellein, G. Neffe, B. Piosczyk, M. Schmid, W. Spiess, R. Spörl, M. Thumm, A. Ulbricht, R. Vincon, F. Wüchner, G. Zahn

Institut für Plasmaforschung (IPF) Stuttgart: P. Brand, G. Gantenbein, H. Hailer, W. Kasperek, M. Krämer, F. Müller, G.A. Müller, R. Munk, C. Rieper, H. Salzmann, H. Schlüter, P.G. Schüller, R. Schütz, K. Schwörer, R. Wacker

Stellarator Theory

STELLARATOR THEORY

(Head of Project: Prof. Dr. Jürgen Nührenberg)

The activity of the Stellarator Theory Division is concentrated on further development of the stellarator concept and numerical as well as analytical methods to investigate equilibrium, stability and transport problems in three-dimensional toroidal configurations.

The relevant team is:

X. Bonnin, M. Borchardt, M. Drevlak, S. Gori, R. Hatzky, R. Kleiber, A. Könies, V. Kornilov, H. Leyh, K. Matyash, N. McTaggart, P. Merkel, A. Mutzke, C. Nührenberg, A. Pulss, J. Riemann, R. Schneider, S. Sorge, R. Zille.

TOKAMAK PHYSICS

(Head of Project: Prof. Dr. S. Günter)

The aims of the activities in the tokamak physics division are twofold: On the one hand it provides theoretical support for the current tokamak activities of the IPP. On the other hand it is developing further the theoretical basis for tokamak physics. The main topics of the theoretical activities are: modelling of the scrape-off layer and divertor plasmas, investigation of MHD stability, analysis of transport properties, propagation and absorption of waves in inhomogeneous plasmas, and the simulation of the turbulent transport. The contributions described here are mostly concern with model and code developments in the stage prior to specific applications or those aspects of theory where comparison with experiments is still in the qualitative rather than the quantitative phase. That part of the scientific work which has been carried out in close collaboration with experiments is reported in the respective sections on the projects: ASDEX Upgrade, JET and ITER.

Head: S. Günter, Deputy: M. Brambilla

R. Arslanbekov, M. Apostoliceanu, G. Becker, A. Bergmann, R. Bilato, K. Borrass, D. Correa-Restrepo, D. Coster, K. Dimova, W. Feneberg, M. Götz, V. Igochine, F. Jenko, O. Kardaun, A. Kendl, J. Kim, R. Kochergov, P. Lauber, P. Martin, P. Merkel, R. Meyer-Spasche, Y. Nishimura, G. Pautasso, A. Peeters, G. Pereverzev, S. Pinches, E. Poli, S. Riondato, S. Schade, T. Schmidt-Dannert, W. Schneider, E. Schwarz, B. Scott, G. Spies, D. Strinzi, E. Strumberger, G. Tardini, H. Tasso, C. Tichmann, Q. Yu, H.-P. Zehrfeld,

Guests: C.V. Atanasiu, Institute of Atomic Physics, Romania, A. H. Boozer, Columbia University, New York, USA, P. Lalousis, IESL.FORTH, Heraklion, Greece, P. McCarthy, University College, Cork, Ireland, G. J. Miron, Institute of Atomic Physics, Romania, E. Quigley, University College, Cork, Ireland, V. Rozhansky, State Technical University, St. Petersburg, Russia, Samuli Saarelma, Helsinki University of Technology, Finland, J. Tataronis, University of Madison, USA, G.N. Throumoulopoulos, University of Ioannina, Greece, I. Veselova, State Technical University, St. Petersburg, Russia, S. Voskoboynikov, State Technical University, St. Petersburg, Russia, H. Weitzner, Courant Institute of Mathematical Sciences, New York, USA

1. Tokamak Edge Physics

D. Coster, K. Borrass, J. Kim, Y. Nishimura, V. Rozhansky*, S. O. Voskoboynikov*¹

The edge physics group has continued work on a number of fronts: continued support and development of the SOLPS suite of codes (which includes B2-Eirene), direct modelling in support of the experiment, the development of techniques for coupling the results from turbulence codes to edge transport codes and the improvement of our understanding of the edge physics.

The natural H-mode density, i.e. the plasma density evolving in an H-mode discharge without active fuelling, reaches

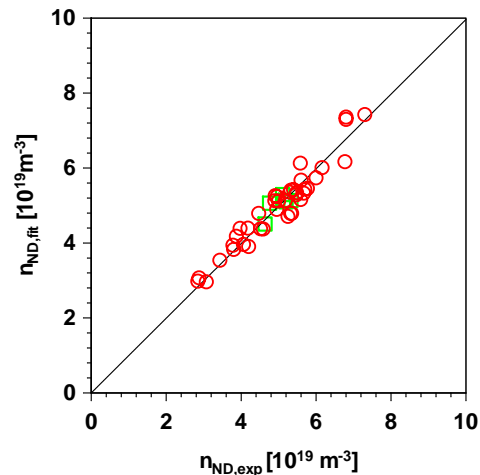


Fig.1 1.1: Density $n_{ND,fit}$ calculated from the scaling found for the natural density versus experimental natural densities $n_{ND,exp}$ from JET (circles) and ASDEX Upgrade (squares).

Greenwald fractions in JET typically higher than in ASDEX Upgrade. According to general thinking this reflects device-specific differences as regards recycling-induced fuelling and beam fuelling. A study has been performed which presents evidence for a different view, namely that at sufficiently low plasma fuelling rates any fuelling rate dependence of the plasma density vanishes and the plasma particle content is completely determined by the plasma itself. It has been shown that this limit, which would constitute an additional H-mode operational boundary, is reached in JET and ADSEX Upgrade natural density discharges and its scaling is determined, figure1.1 . The observed differences between JET and ASDEX Upgrade are found to be due to the combined effect of size and triangularity. The question, whether the gap between natural density and density limit may decrease further or even vanish in ITER (indicating a vanishing H-mode operation window), is important. The answer depends on the density limit scaling that is used for comparison. While one would be on the safe side for the Greenwald scaling, the situation would be marginal for the recently established JET-ASDEX Upgrade scaling. Extension of the empirical database on the triangularity dependences of both the natural density and the density limit, insufficient at present, is mandatory for a final clarification of this issue.

¹ * Visitors

In making predictions of the edge plasma for future devices, one large uncertainty is the value of the anomalous radial transport to use. Last year we reported the development of a scaling to experimentally determined profiles; a separate, complementary, technique is to couple the edge plasma transport code to an edge turbulence code so that the fluxes (or transport coefficients) are determined from first principles. This coupling has been performed with a 2d turbulence code (developed by Bruce Scott of the turbulence group), both directly (by alternately running the two codes) and by parametrization of the turbulence code results and then using the parametrization in the transport code to give the transport coefficients. The numerical simulation (in B2) demonstrated a new feature of spatially inhomogeneous transport coefficients that increase towards the divertor separatrix regions. The current effort focuses on the evolution of the radial electric field structures in the H-mode regimes by including turbulence suppression effects by the E_r shear.

In other work, simulations of He compression reproduced the experimental observation that only small differences were to be expected between the DivII and DivIIb divertor structures on ASDEX Upgrade, and the observation that the power asymmetry to the target reduced, or could even reverse, during ELMs.

1.2 MHD Theory Group

1.2.1 Drift Tearing Modes

Q. Yu

The non-linear MHD code in cylindrical geometry (TM code) has been generalized dealing now with two-fluid equations and thus allows model drift tearing modes.

Although previous theories have shown that the electron diamagnetic drift is stabilizing for vanishing perpendicular heat transport, it becomes destabilized as soon as a finite perpendicular heat conductivity is taken into account. Therefore, tearing modes can be driven unstable by a temperature gradient. That way, experimental observations on ASDEX Upgrade of linearly unstable tearing modes at large β -values can be explained

1.2.2 Extension of the DIVA equilibrium code

H.-P. Zehrfeld

The DIVA equilibrium code has been extended and is now capable of calculating free- and fixed-boundary axisymmetric equilibria with and without flow. For stability studies of such MHD equilibria these can be pre-calculated and stored in a generic form. For mode analysis with the CASTOR (tearing, kink), GATO (peeling) and GARBO (ballooning) codes corresponding access and evaluation interfaces have been developed and are now used routinely.

1.2.3 Application of 3D MHD codes to Tokamaks

E. Strumberger, S. Günter, P. Merkel, E. Schwarz, C. Tichmann, H.-P. Zehrfeld

A generalized version of the MFBE code called MFBE_2001 has been developed. It is able to compute magnetic fields of

finite- β equilibria with net toroidal current and general symmetry in a form suitable for field line tracing. The code system VMEC/NEMEC+MFBE_2001+GOURDON was used to study the influence of non-resonant helical fields on the tokamak magnetic field topology. An ergodization of the edge region was observed.

1.2.4 MHD Stability Analysis of Type II ELMs in ASDEX Upgrade

S. Saarelma, S. Günter

An MHD stability analysis of the type II ELM discharges on ASDEX Upgrade was conducted. This analysis was compared with an earlier analysis of type I ELMs. It was found that for the type II ELMy plasma conditions (high density, high triangularity, high safety factor at the edge, almost double null configuration), the bootstrap current driven peeling mode instability becomes more localized to the edge. This could explain the smaller ELMs in the type II regime

1.2.5 The CAS3D-G MHD Stability Code

P. Merkel, C. Nührenberg²

For the 3D CAS3D MHD stability code a generalized version of the vacuum part has been developed. The conducting wall in the vacuum region can now be multiple connected using a finite element method. The integral equation for the vacuum field is solved by a Galerkin type technique. The new version of CAS3D allows us to study wall stabilization by arbitrarily shaped conducting structures including holes, poloidal and toroidal gaps.

1.2.6 Interpretation of Experimentally Observed MHD Activity Using MHD-IC Code

V. G. Igochine, S. Günter

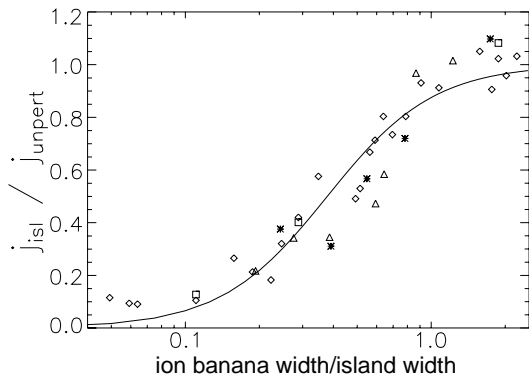
For the investigation of MHD activities inside the plasma the MHD Interpretation Code (MHD-IC) has been developed. The code uses a collection of all available information about the observed MHD activities from Mirnov coils, SXR, ECE and MSE measurements. To determine the shape of the eigenfunction of the perturbation a comparison to theoretical predictions by the non-linear resistive MHD code XTOR is used. The code has successfully been applied to different types of instabilities in conventional and advanced tokamak scenarios on ASDEX Upgrade.

1.2.7 Triggering of ITBs by fishbones

S. D. Pinches, S. Günter

Fishbones have been found to be able to trigger ITBs on ASDEX Upgrade. Using the HAGIS code which describes the non-linear interaction between MHD modes and fast particles it has been shown that fishbones generate a sheared plasma rotation by redistributing the resonant fast particles. If the fishbone repetition rate is larger than the damping rate of the poloidal plasma rotation, the generated shearing rates are

² Stellarator Theory division



1.2: Bootstrap current inside an island structure

comparable to the linear growth rates of the ITG modes, and thus should cause suppression of the turbulent transport.

1.3 Transport analysis Group

A. G. Peeters, G. Becker, A. Bergmann, O. Kardaun, G. V. Pereverzev, E. Poli, G. Tardini, M. Apostoliceanu, W. Feneberg

The group studies neoclassical as well as anomalous transport. This year the study of anomalous tokamak transport has concentrated on the comparison of theory based transport models with the observed electron transport, the evolution of the density profile and the physics of internal transport barriers. This work is described under the ASDEX Upgrade section. Below two topics (bootstrap current in island structures and linear theory of plasma instabilities) of the work on theory development are discussed in more detail.

The study of the behaviour of the bootstrap current in the presence of a magnetic island has been performed for various plasma conditions (size, isotope) using a drift kinetic description of the plasma (numerically integrated). When the ion banana width w_b is comparable to the island width W , the island is overlapped by the trapped particles and a significant current is generated inside the island. This process is not considered in the standard theoretical description of the mode. No drop of the bootstrap current is observed for $w_b/W = 1$ or for even lower values of this ratio if the density profile is flat. Moreover, the non-local nature of the process is confirmed by the fact that the value of the current is not consistent with the local pressure profile in the island. A linear scaling for the value of the poloidal β at the mode onset with the ion poloidal gyro-radius ρ_p^* can be obtained on the basis of this overlapping effect. This is consistent with the experimental observations of ASDEX Upgrade. In 2001 we have also started the calculation of the polarization current that is generated by the island rotation. So far these studies have been performed for a prescribed rotation frequency aiming at the collisionality dependence of the polarization current.

The influence of a uniform radial electric field on the linear stability of toroidal ion temperature gradient driven modes has been studied using the ballooning representation. The field rotates the modes in the poloidal direction into the region where the curvature is favourable and hence leads to stabilization. The most important result found in this study is a simple criterion for the field necessary to stabilize the mode, which states that the mode is stabilized if the rotation frequency E_r/rB is larger

than the linear growth rate of the mode. For linear modes an alternative theoretical formulation has also been developed which is described below.

A modification of the WKB method, the beam tracing has been developed and applied for solving the boundary value problem in multi-dimensionally inhomogeneous plasma. In this method, eigenfunctions are constructed as wave patterns located in the vicinity of closed ray trajectories (basis contour). The existence of such a contour can be considered as a necessary condition for an eigenmode. The implementation of the beam tracing technique to gradient-driven instabilities in a tokamak sheds new light on this type of plasma instabilities. They can be thought of as waves propagating in the purely toroidal direction (alternatively one can think of a standing wave), while interaction with a plasma defines whether such a wave absorbs or releases energy. Being in some aspects more restrictive than a similar asymptotic technique, the ballooning representation, the beam tracing can provide a solution in many cases of interest when the ballooning representation fails. An additional advantage is that the beam tracing technique is well suited for numerical treatment and results in numerical codes which can be by orders of magnitude faster than the conventional codes.

1.4 Computational Studies of Turbulence in Magnetised Plasmas

B. Scott, F. Jenko, A. Kendl, D. Strinzi, T. Schmidt-Dannert

Our studies of the low frequency fluidlike drift turbulence believed to underly anomalous transport in magnetically confined fusion experiments continue. We employ fluid models extended to capture important kinetic effects (Landau damping, finite gyroradius), and kinetic models intended to treat all phenomena at the scales of interest (1 mm to 10 cm, 10 kHz to 1 MHz). The latter models are called gyrokinetic, and we have been the first to reliably extend these to the electromagnetic, nonlinear regime.

The fluid studies are naturally less expensive and so have been used to treat a wider variety of cases. In 2001 we have studied further the way in which the drift wave turbulence in the tokamak edge interacts with zonal flows, using a newly derived energy theorem which identifies the pathways between the zonal flows, the global Alfvén oscillations which form the Pfirsch-Schlüter current system (“sidebands”), and the thermal reservoir (“background”). A toroidal coupling mechanism known as geodesic curvature acts to transfer free energy into the sidebands, which are mixed back into the turbulence by the nonlinear three-wave interactions. This serves to limit the growth of long-lived zonal flows to levels too small to strongly suppress the turbulence. The consequence is practical — this is the ultimate reason these codes run in proper flux surface geometry have never produced a self consistent sheared ExB flow layer which could represent the L-to-H confinement transition in the tokamak edge. To model the H-mode, a shear layer must not only be initialised but also artificially maintained. In practical terms, some mechanism associated with the neoclassical equilibrium is required to produce the transition, quite external to the dynamical system of the turbulence (the sections on edge modelling). Computational studies of the H-mode by other groups entail manual insertion of the pedestal by use of

a local heating profile. However, if the heating effects (e.g., ramping of the interior temperature) are properly confined to the edges of the computational domain, linear profiles for the density and temperatures always result. The actual mechanism of pedestal formation remains a goal for ongoing study, which is also being extended to stellarators through collaboration with the W7-X group in Greifswald.

A set of investigations using the fluid model for core turbulence was initiated, using the well known Cyclone Base Case from the gyrokinetic studies in the USA. Our codes are able to treat the fully electromagnetic response of the electrons, not simply the very restricted electrostatic, adiabatic electrons model. Preliminary results show that the pressure (plasma beta) gradient is typically large enough to support free energy access of the gradient by passing electrons. Large changes in the computed heat transport appear to result. This study will be a major theme for 2002, as it has obvious implications for the performance of future tokamaks. We are also addressing this situation with the kinetic model, although all research groups are finding it difficult to produce a definitive numerical scheme for the electromagnetic gyrokinetic model. The kinetic model is also being employed on the very largest computers in both the IPP and the Bavarian State Computing Centre in order to understand possible coupling between the ion- and electron-gyroradius scales of motion. It is still possible that the ‘‘ETG’’ modes that the smaller electron scales produce may be responsible for constraining the internal transport barriers addressed in the ASDEX Upgrade experimental section (sec.??).

1.5 Wave Physics Group

M. Brambilla

The efforts to improve numerical simulations of plasma heating and current drive in the Ion Cyclotron range of frequencies have been pursued. The toroidal full-wave code TORIC has been modified to allow interfacing with MHD equilibrium codes. The range of applications of TORIC has been extended to higher frequencies by taking into account damping at higher ion cyclotron harmonics, and to lower frequencies by including ion Landau and Transit Time damping.

R. Bilato, M. Brambilla

For the construction of the bounce-averaged quasilinear diffu-

sion coefficient for the electrons using the wave fields evaluated by TORIC, an algorithm has been developed which ensures that power absorption profiles predicted by the solver of the Fokker-Planck kinetic equation and by TORIC will agree. This makes the evaluation of reliable profiles of the driven current possible. Fast-Wave current drive scenarios for ASDEX Upgrade have been explored.

D. Correa-Restrepo, D. Pfirsch

Drift and gyrokinetic theories have been further investigated based on a previously derived Lagrangian for the system of Maxwell and kinetic equations, focusing in particular on the derivation of conservation laws. The method employed, contrary to other current approaches, enforces the exact gauge invariance in the definition of the approximate Lagrangian, thereby avoiding inconsistencies, in particular in the derivation of the energy-momentum tensor.

H. Tasso, G. N. Throumoulopoulos

Wall stabilization of MHD modes has been modelled by dissipative Mathieu-Hill equations. ‘‘Negative energy’’ modes are found to be stabilized by the combined action of parametric excitation and damping coefficient. The region of stability is significantly increased for the ‘‘two-step’’ Hill’s equation. This is a strong indication that the ‘‘resistive wall’’ mode could be stabilized by the joint action of a properly tailored time-dependent wall resistivity and sufficient viscous dissipation in the plasma.

Investigations of MHD equilibria with flows have been extended to take into account anisotropic resistivity, Hall term, and two-fluid theory. Many properties and exact solutions have been found. In particular, calculations of sheared flows and magnetic fields for cylindrical plasmas show good agreement with the known evidence concerning Internal Transport Barriers.

R. Meyer-Spasche, M. Götz, K. Dimova

Electron trajectories in a gyrotron were studied. Methods of optimum control were used to optimize the electron efficiency in the so-called cold-cavity approximation of gyrotron theory. The nonlinear dynamical properties of Runge-Kutta difference schemes have been further investigated, in search of difference schemes allowing for large time-steps and improving the computing efficiency for the solution of evolution equations.

TECHNOLOGY DIVISION

(Prof. Dr. Rolf Wilhelm)

The Technology Division (TE) is responsible for the development and operation of the three heating schemes employed for the present fusion experiments, ASDEX Upgrade and W7-AS. Neutral Beam Injection (NBI) and the two wave heating schemes, Ion Cyclotron Resonance Heating (ICRH) and Electron Cyclotron Resonance Heating (ECRH) for ASDEX Upgrade, and NBI and ICRH for the present Garching stellarator, W7-AS. In addition, the development and installation of long-pulse NBI and ICRH systems for the new W 7-X stellarator under construction at Greifswald are also the responsibility of the TE Division. A further R&D programme is dedicated to a RF-driven plasma source for negative-ion production for the ITER-NBI system.

Specific results of these activities are given below, while more detailed information about heating systems and results from the machines are to be found in the respective sections of this report.

1. NEUTRAL INJECTION HEATING

NI Group

1.1. Development of Negative RF Ion Sources

The development of a large-area RF source for negative-ion beam production was continued with the Type 6-1 prototype source. Although the H^- yields reported in 2000 were not exceeded, progress was made in several areas.

The long-pulse capability achieved with an internal Faraday shield was demonstrated by long-pulse operation with a duration of up to 15 s.

By changing the number of permanent magnets, the maximum field strength was varied in steps from 10 G to 80 G, corresponding to 100 Gcm to 800 Gcm when the field is integrated inwards from the plasma grid. The H^- current was found to have a broad maximum between 200 Gcm and 600 Gcm, or 20 G to 60 G, respectively.

During the discharge the source pressure drops by up to 40 %, depending on the RF power (Fig. 1). This is possibly due to heating of the neutral gas by the plasma, leading to a higher particle flow through the grids and thus a lower gas density in the source. For the stripping losses in the extraction system only the particle density is important, and so the source pressure during the pulse is the relevant value.

The maximum H^- current densities of 15 – 20 mA/cm² measured in 2000 were not exceeded in recent experiments. This is partly due to overestimation by the previous data evaluation method, which relied on extrapolation of the beam profile measured at low current densities. Comparison with the new improved analysis methodology leads to a reduction of 25% for the highest current densities.

Generally, in the RF source, the increase of the H^- yield by caesium seeding is a factor of only 1.2 to 2, which is much lower than in arc sources. A further, rather general finding, not

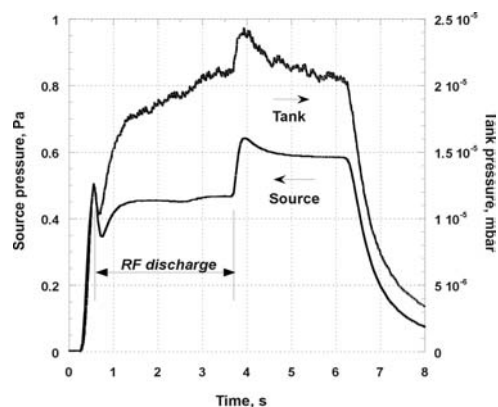


FIG. 1: Pressure in the source during 3 s 100 kW pulse with 5 s gas feed.

only in the RF source, is the unsatisfactory reproducibility with caesium. This is a strong motivation to look for alternatives. Eight different grid surface materials were therefore tested as potential options for caesium-free operation: Ge (semiconductor), C (high surface conversion rate for H^-), Al (high secondary emission), Ag, Au and Pt (low adsorption), Mo-La-alloy (low work function), and Mo as a standard material. No clear-cut conclusion can yet be drawn due to unexpected copper sputtering from the Faraday shield onto the plasma grid. To avoid this problem in future, the Faraday shield will be coated with the same material as the plasma grid. In a first experiment silver was tested in this way. The H^- currents were significantly lower than with a coating of the plasma grid only.

In Fig. 2 it is shown that, if the difference between the total extracted current I_{drain} and the electron current I_{elec} is used to calculate the H^- current density, then the value determined is much higher (12 -19 mA/cm²) as compared with 2 -5 mA/cm² from the calorimetric measurement. The current density also

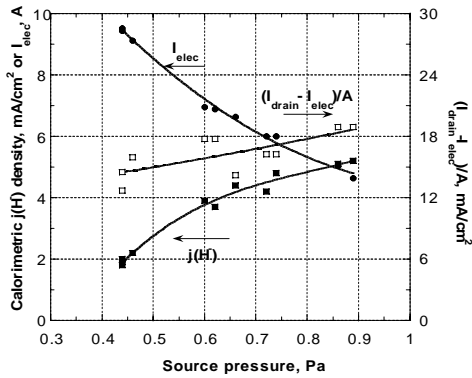


FIG. 2: H current density derived from calorimetric measurements or from the difference between I_{drain} and I_{elec} (extraction area A) and the electron current I_{elec} , and as function of the source pressure for 95 kW with argon.

shows a significantly smaller reduction at low pressures. It is known that only in RF sources does the addition of argon and other noble gases have a considerable impact on the H yield. In recent experiments 6 mA/cm² at 140 kW and 0.65 Pa with 20 % Ar were obtained as compared with 3 mA/cm² without argon. This effect may possibly be due to the higher plasma density observed in probe measurements. Another reason may be the ponderomotive ($j_{\text{RF}} \times B_{\text{RF}}$) forces in the driver, which cannot be neglected at the power level of this source. These forces may lead to energetic noble gas ions, which can enhance the generation of vibrationally excited H_2 molecules by direct collisions.

The next steps will be to improve the diagnostic system:

- laser detachment measurement of the H density,
- spectroscopic measurement of the dissociation degree and of the gas temperature,
- in-situ measurement of work function of the plasma grid.

A number of new developments are approaching completion. These include Faraday shields with different coatings, an electromagnet filter and a second prototype with two smaller drivers 14 cm in diameter. On a small test bed a RF-driven hollow cathode will be investigated. It could be a potential alternative to the inductive RF drivers.

2. ION CYCLOTRON RESONANCE HEATING

ICRH Group

Further information on ICRH and experimental results can be found in the ASDEX Upgrade and W7-X sections.

2.1 Influence of the Plasma on RF High-voltage Breakdown

Breakdown on ICRF antenna at high voltages can sometimes limit the power that can be launched into the plasma. A well-diagnosed RF probe for ASDEX Upgrade has been developed to study voltage limits of the antenna in the presence of plasma. The open end of a coaxial line represents a model of the antenna high-voltage region.

It appears that various breakdown phenomena can be considered as candidates responsible for the power limitation. Initially in experiments in the ICRH testbed the following effects were observed:

- after pumping to a pressure of 10^{-7} mbar vacuum arcs on coaxial stainless-steel electrodes were observed at voltages below 20 kV,
- the electrodes could be conditioned to a voltage of 60 kV and a pulse length of 200 ms,
- at voltages higher than 40 kV field emission dark currents were observed,
- the presence of a plasma density of 10^9 cm⁻³ produced by a large-aperture ion source did not affect voltage stand-off of the probe unless the neutral pressure of the working gas was increased, giving rise to a glow discharge,
- the critical pressure for starting glow discharges in He or air in the presence of the external plasma was about one order of magnitude lower than what is required for ignition of self-sustained glow discharges.

Secondly, the RF probe was operated as a tool to expose high RF voltages to an antenna-like electrode under real conditions of ASDEX Upgrade peripheral plasmas. H-mode discharges with a plasma shape fitted well to the ICRF antenna contour, the so-called Edge Optimized Configuration (EOC), were used. By electrode conditioning between ASDEX Upgrade discharges the voltage stand-off in vacuum was kept high and stable operation at 55 kV on the probe head for 100 ms in the discharges was achieved. However, it was observed that breakdowns often appear to be induced by ELMs.

3. ECRH ON ASDEX UPGRADE

ECRH Group (AUG)

(in cooperation with IPF Stuttgart)

Information on the ECRH system and experimental results can be found in the ASDEX Upgrade section of this report.

The application of step-tunable gyrotrons requires broadband torus windows. One option is Brewster windows. Since such a window can only transmit one polarization, internal polarizers inside the vacuum system are necessary, leading to a new optics design. Another alternative is the use of double-disc windows. They require additional tuning, but can transmit any polarization. In this case it is possible to use the existing mirror system. Figure 3 shows the calculated reflectivity of two diamond discs with a thickness of 1.797 mm and a distance of 15 mm. There are broad minima around 105 and 140 GHz, where the two discs have a resonant thickness ($3\lambda_0/2$ and $4\lambda_0/2$ at 105 and 140 GHz, respectively). Additional reflection minima between these frequencies are due to Fabry-Perot resonances. These resonance frequencies are adjustable by changing the distance between the two discs.

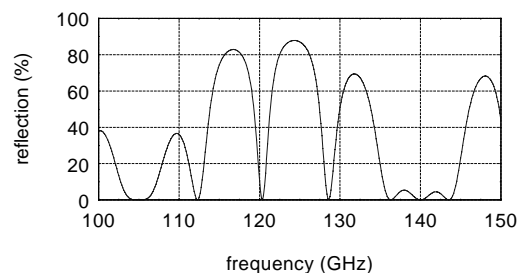


FIG. 3: Calculated reflection of a double-disc window.

SURFACE PHYSICS DIVISION

(Heads of Project: Prof. Dr. Dr. h.c. Volker Dose

Prof. Dr. Jürgen Küppers)

The surface physics division is organised in two groups. Contributions to the project "Plasma Facing Materials and Components" constitute the main activity of the Plasma Wall Interaction group and are reported under the respective project. More fundamental laboratory studies are described on the next two pages. The second group is part of the Centre for Interdisciplinary Plasma Science, and deals with fundamental plasma theory, Bayesian data analysis, and low temperature plasma surface interaction. CIPS activities are described in a separate section.

Deputy Head: E. Taglauer

Scientific Staff:

Surface Physics

R. Beikler², W. Eckstein, D. Elder⁴, K. Ertl, X. Gong⁵, S. Günter¹¹, K. Klages^{2,12}, A. Kohl², H. Knözinger¹³, K. Krieger, J.-H. Liang⁶, V. Liechtenstein⁷, Ch. Linsmeier, J. Luthin², M. Mayer, O. Ogorodnikova¹, N. Reinecke², J. Roth, K. Schmid², M. Schneider³, G. Staudenmaier, A. Tabasso¹, A. Wiltner².

CIPS / Surface Physics

I. Arkhipov⁸, M. Bauer², D. Biskamp, A. Caticha⁹, R. Fischer, K. Hallatschek, P. Giudici¹⁰, A. Golan¹⁴, F. Guglielmetti², Ch. Hopf², H. Kang¹, W. Jacob, A. von Keudell, M. Korobkov², W. von der Linden¹⁵, M. Meier², W.-Ch. Müller¹, R. Preuss, B. Racine¹, Th. Schwarz-Selinger¹, I. Sidorenko¹, U. von Toussaint¹, G. Venus, J.-S. Yoon¹, A. Zeiler.

Technical Staff (Surface Physics and CIPS)

M. Ben Hamdane, P. Böhm, J. Dorner, Th. Dürbeck, Ch. Fritsch, M. Fußeder, K. Gehringer, S. Gori, R. Hoffmann, W. Hohlenburger, A. Holzer, E. Huber, R. Lang, S. Lessmann-Bassen, P. Matern, Th. Neuner, B. Plöckl, M. Roppelt, J. Schäftner, A. Schlamp, H. Schmidl, St. Stark, R. Straßer, A. Weghorn, I. Zeising.

Post Doc

Doctoral Candidate

Undergraduate Student

Guests:

University of Toronto, Canada

Institute of Plasma Physics, Hefei, PR China

National Tsing Hua University, Hsinchu, Taiwan

Kurchatov Institute, Moscow, Russia

Russian Academy of Science, Moscow, Russia

University at Albany-SUNY, USA

Università di Pavia, Italy Collaboration with:

Synchrotron Trieste, Italy

University of Surrey, England

Ludwig-Maximilians-Universität, Munich, Germany

American University, Washington DC, USA

Technische Universität Graz, Austria

1. ION BEAM ANALYSIS METHODS

Fundamental laboratory studies on ion beam analysis methods concern the determination of scattering cross sections and the data evaluation including surface roughness.

1.1 MeV Ion Beam Analysis with Li Ions

Rutherford backscattering spectroscopy (RBS) and elastic recoil detection analysis (ERDA) with incident alpha particles are widely used techniques for elemental analysis and depth profiling of the surface layers of solids. According to theoretical considerations heavier ions such as lithium should offer several advantages over conventional RBS and ERDA, namely improved depth and mass resolution and higher sensitivity. The analytical possibilities of ^6Li and ^7Li ions were investigated experimentally. In RBS, Li ions gain only a small improvement in depth resolution owing to the degraded detector energy resolution for backscattered heavier ions, while higher sensitivity and mass resolution can be achieved. In ERDA applications for detecting hydrogen isotopes, a clear gain in depth resolution of about 50% is achieved in amorphous hydrogenated carbon multi-layers consisting of alternating layers of a-C:H and a-C:D by using Li ions instead of He.

A drawback in using Li ions is the mostly unknown backscattering cross-sections from light elements above the threshold for non-Rutherford scattering. The backscattering cross-sections for ^6Li and ^7Li ions from carbon and oxygen were determined at a scattering angle of 165° in the energy range 3–6 MeV. Above the threshold energy, the cross-sections decrease monotonically below their Rutherford values, rendering this energy range less suitable for RBS. The experimental values for the threshold energies are in good agreement with theoretical predictions by Bozoian for ^7Li , while for ^6Li the theoretical values are considerably lower than the experimental ones.

1.2 Ion Beam Analysis of Rough Thin Films

Quantitative application of MeV ion beam analysis methods is usually restricted to laterally homogeneous and smooth films. The influence of surface roughness on RBS spectra was studied experimentally by measuring the surface topography of various samples with a profiler and the corresponding RBS spectra. Measured spectra are compared with computer simulations with the SIMNRA code. In the code, rough thin films are described by a gamma distribution of film thicknesses, while rough substrates are approximated by a Lorentz distribution of local inclination angles. Correlation effects of surface roughness are neglected. Backscattering spectra obtained experimentally from long-term samples exposed to JET plasmas, limiter tiles exposed in the TEXTOR-94 tokamak, and tungsten layers deposited on JET divertor tiles show good agreement with simulation calculations. For films of high-Z elements on rough substrates multiple scattering in the film plays an additional important role. The capability of calculating surface roughness effects allows quantitative analysis of the composition, depth profile, and roughness parameters of arbitrarily rough surfaces, which are often encountered in the research of plasma-wall interaction phenomena.

2. SURFACE SCIENCE - SFB 338

Cooperation of the Surface Science group within the Sonderforschungsbereich (SFB 338: Adsorption on Solid Surfaces) was continued and terminated with its last term at the end of the year. Recent contributions include quantitative layer analysis by low-energy ion scattering (LEIS), preparation of self-organised nanostructures, and studies of the catalytic activities of rhodium model catalysts.

An advanced procedure for analysis of crystalline alloy surfaces by means of experiments and simulations was exemplified with CuAu(100). This kind of analysis is not restricted to that case but, with the necessary modifications, can be applied to other crystalline materials. In studying the surface segregation of alloys it turns out that the second layer concentration is crucial. Here oscillatory and non-oscillatory segregation profiles differ and provide information on the nature of the interatomic forces.

Evaluation of the intensity distributions from the second layer is complicated owing to focusing and neutralisation effects. Quantitative evaluation of the experimental LEIS intensities was performed by comparison with numerical simulations using the MARLOWE computer code. The necessary calibrations for scattering potentials and surface vibrational amplitudes were carried out with the pure-element samples, Cu(100) and Au(110)(1x2), as standards. For calculations of the ion scattering processes screened Coulomb potentials are used, the screening length being a critical parameter. Values slightly below the Firsov screening length were determined for 1.5 keV Na^+ scattering from Cu and Au by making use of multiple scattering intensities. In contrast to the common practice of simulating polar angle distributions for calibration, this procedure is less-time consuming and hence more accurate under fixed conditions with respect to computational effort.

The ordered CuAu(100) alloy shows nearly bulk truncation with Au termination below the critical temperature T_c of chemical ordering and exhibits strong first-layer Au segregation above T_c . The second-layer Au concentration is strongly reduced. Both first and second-layer Au concentrations do not seem to reach values of statistical equipartition even at temperatures close to the melting point. The results indicate the appearance of an oscillatory segregation profile and are in good agreement with theoretical predictions by Tersoff; see Fig. 1.

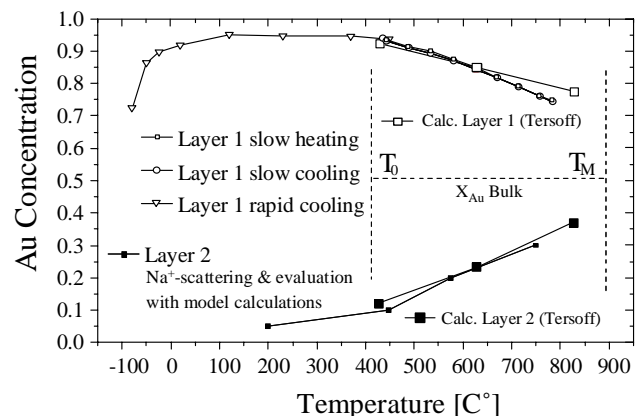


FIG. 1: Temperature dependence of the first and second atomic layer Au concentration: Experimental results and theoretical predictions by Tersoff.

MATERIALS RESEARCH DIVISION

(Prof. Dr. Dr. Hans-Harald Bolt)

The plasma-facing materials of fusion devices are subjected to complex loading conditions. In addition, the response of the materials to this environment can have a strong influence on the plasma performance of the fusion device. From the plasma a flow of ions and neutral atoms reaches the surfaces surrounding the plasma. The incident particles can lead to erosion processes on the material surfaces. Radiation from the plasma as well as the incident particles cause energy deposition on the surface of the plasma-facing component. The resulting thermomechanical loading of materials and components can limit the lifetime of the component. Excessive heat loads during operation lead to immediate destruction by melting or fracture. Furthermore, the materials can also adsorb and absorb hydrogen isotopes and eventually release fractions of the stored gas under thermal loading. This can influence the particle balance during plasma operation of the device. In addition to these fluctuations, the more resident inventory of hydrogen isotopes in a fusion device is strongly dependent on the selection of materials and should be minimised. The intense neutron irradiation of the plasma-facing materials in a fusion reactor causes nuclear activation of materials and also damage to materials, which results in degradation of dimensional stability and physical and mechanical properties. Plasma-facing materials have to be developed and optimised in order to meet these requirements as far as possible.

Since progress in plasma physics has paved the way towards the use of fusion as energy source, the issues relating to the development of materials for fusion applications call for intense effort. This entails clarification of the loading mechanisms in fusion devices and of the response of materials to these loading conditions, as a basis for the development and qualification of suitable materials.

The Materials Research Division of IPP is developing and characterising materials for plasma-facing components of fusion devices. The development of materials includes metal and ceramic coatings for plasma-facing applications as well as thin films with barrier function. The equipment and expertise comprise:

Thin-film synthesis by plasma-assisted deposition methods (PAPVD and PACVD) together with the full range of process analytical instruments; materials characterisation involving metallography and scanning electron microscopy for morphological examinations, elemental analysis (EDX), and structure and texture analyses (EBSD); structure, texture, and stress analyses by X-ray diffraction; measurement of the thermal diffusivity of materials by the laser flash method; measurement of micromechanical properties by nano- and microindentation; computational analyses of the thermomechanical behaviour of plasma-facing compounds including micromechanical modelling.

The scientific work carried out by the division is part of the “Plasma-Facing Materials and Components” project and is described in the “Projects” section of this report.

Staff

M. Balden, I. Beguiristain ³ , B. Böswirth, K. Durocher ³	1	Visiting Scientist
H. Greuner, Q. Guo ¹ , E. de Juan Pardo ² , F. Koch, S. Kötterl,	2	PhD Candidate
D. Levchuk ¹ , S. Lindig, H. Maier, K. Marx, G. Matern,	3	Graduate Student
E. Oyarzabal ³ , C. Popescu ² , O. Poznansky ¹ , S. Rolle,		
J. Schäftner, D. Valenza ² , M. Ye, J.-H. You		

CENTRE FOR INTERDISCIPLINARY PLASMA SCIENCE

(Prof. Dr. Dr. h.c. Volker Dose, IPP, Prof. Dr. Gregor Morfill, MPE)

1. PLASMA TECHNOLOGY

The Low-temperature Plasma Physics group (LTPP group) at IPP is concerned with the application of low-temperature plasmas for surface treatment, such as deposition of thin films, erosion, and surface modification. The main focus is on the investigation of plasma-surface interaction processes of hydrogen and hydrocarbon plasmas (e.g. CH_4) with hydrocarbon layers. These processes play an important role in the transport of carbon in the boundary layers of fusion experiments. The main activity in 2001 was to investigate deposition of hydrogenated carbon films from neutral radical beams in an UHV experiment and study of the synergistic interaction of argon ions and thermal hydrogen atoms during erosion of carbonaceous surfaces.

1.1 Basic Studies of Thin-film Deposition and Erosion Processes

1.1.1 Synergistic interactions of thermal radicals with C:H surfaces

Recent experiments using H and CH_3 radical beams as a model system for plasma deposition of C:H films revealed that CH_3 chemisorption at dangling bonds at the film surface is an important step for film formation. Dangling bonds are mainly created via hydrogen abstraction by incoming hydrogen. This interplay between CH_3 and H leads to a pronounced synergistic effect: the presence of H increases the effective sticking coefficient of CH_3 by up to two orders of magnitude. The cycle of hydrogen abstraction and CH_3 chemisorption implies net incorporation of two hydrogen atoms per carbon atom during steady-state growth, although the H/C ratio of the deposited layers is only ~ 1 . Dedicated experiments to verify the existence of a hydrogen elimination step were therefore conducted. The binding structure of the growing film was observed with in-situ real-time infrared reflection spectroscopy. By this technique, it was possible to prove that incorporation of carbon from the CH_3 beam into the film is a two-step process: (i) First CH_3 chemisorbs at a dangling bond at the surface forming a trihydride-terminated surface site; (ii) incoming atomic hydrogen transforms these trihydride sites into crosslinked structures such as CH_2 , thereby lowering the hydrogen content of the film. This process is self-limiting leading to a characteristic H/C ratio of 1 as a stoichiometric limit. Hydrogen elimination by atomic hydrogen is therefore a key step for C:H film growth.

1.1.2 Flux dependence, dynamics, and Bayesian parameter estimation

A rate equation model was developed which includes our knowledge that hydrogen elimination is almost as important as the chemisorption process itself. This model also correctly describes the measured dependence of the synergistic growth rate on the hydrogen flux. Our hypothesis of a partly trihydride-terminated surface during growth is further corroborated by time-resolved measurements during switching events using in-situ ellipsometry.

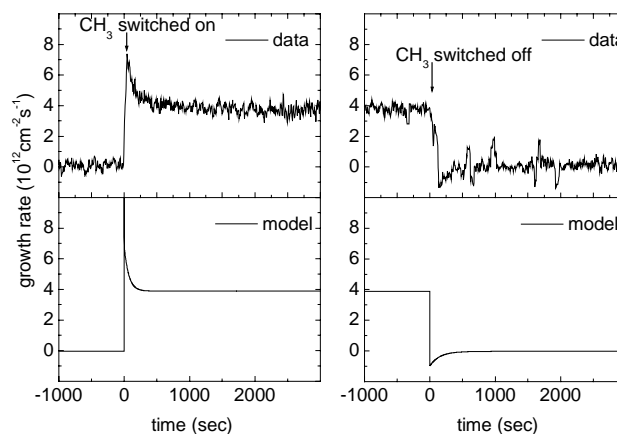


FIG. 1: Experimentally observed growth rate of C:H layers as determined by in-situ ellipsometry (upper frames) and corresponding model results (lower frames). The experiments were conducted at a constant atomic hydrogen flux. At time 0 a simultaneous flux of CH_3 radicals was switched on (left-hand side) or switched off (right-hand side).

The dynamics following the switching-on of the CH_3 flux at $t=0$ s is shown in the left part of Fig. 1. The H flux is present all the time. Immediately after the CH_3 flux is switched on, a high growth rate is observed which slowly decreases towards a steady-state value. Our model predicts two time constants: an initial large spike is caused by instantaneous consumption of dangling bonds by chemisorption. This effect is predicted to be beyond the experimental time resolution. The second time constant results from the formation of a trihydride coverage, which slows down the growth process. This is visible in the data. As soon as the CH_3 flux is switched off (right part of Fig. 1), the synergistic growth breaks down and the trihydride coverage is reduced by two processes: hydrogen elimination (observable via infrared

spectroscopy) and direct erosion of these CH_3 endgroups. The latter process is apparent in the data and predicted by the model. Five parameters describing reaction cross-sections enter into the model. A sound estimation of these parameters is achieved by following the concepts of Bayesian probability theory. The influence of experimental uncertainties with respect to both measured quantities and the input parameters is included in the algorithm. The analysis requires considerable computation effort, but yields complete probability distributions for the parameters rather than simple best estimates.

1.1.3 Synergistic erosion of C:H surfaces by energetic argon ions and thermal hydrogen atoms

Erosion of hard a-C:H films by simultaneous exposure to an Ar^+ ion beam and a beam of thermal, atomic hydrogen was investigated by in-situ real-time ellipsometry. Experiments were performed at room temperature, where erosion by atomic hydrogen is negligible. The energy of the Ar^+ ions was varied between 50 eV and 800 eV. Bombardment of the film with Ar^+ ions alone yields physical sputtering at energies higher than about 100 eV. Below that energy no physical sputtering can be observed under steady-state conditions. This is in agreement with TRIM.SP computer simulations. However, if both beams are switched on, a strong increase of the erosion rate by a factor of more than 2 is observed at an ion energy of 800 eV, and even at 50 eV substantial erosion was found, although neither ion bombardment nor atomic hydrogen leads to erosion on its own.

This effect can be explained in terms of *ion-assisted chemical erosion*: At room temperature chemical erosion by atomic hydrogen alone is negligible because one of the reaction steps – desorption of CH_3 – is a thermally-activated process effective only at temperatures above 400 K. However, with additional low-energy ion bombardment thermal activation can be replaced by physical momentum transfer to these weakly-bound end groups, thus leading to the release of CH_3 groups.

1.2 Inductively-coupled Plasma Device for In-situ Studies

A new low-temperature plasma experiment was set up. The plasma is produced by inductive coupling at a frequency of 13.56 MHz. The experiment is equipped with a number of surface and plasma diagnostics. A commercial Langmuir probe is applied to measure electron temperature and density and a plasma monitor (= energy and mass analyser) is used to determine charged and neutral fluxes reaching the substrate surfaces. Growth and erosion of layers are investigated by real-time, in-situ ellipsometry and in-situ infrared spectroscopy. First investigations will focus on deposition and erosion of hydrocarbon layers from pulsed discharges.

1.3 Exhaust-pipe Experiment

Co-deposition is a big problem for ITER or any other fusion experiment involving tritium. If plasma surface interaction produces reactive species with a low surface reaction probability

somewhere in the plasma containment, they can in principle reach any surface area of the vacuum chamber and lead to deposition of hydrogen (or deuterium and tritium) containing carbonaceous layers. For a machine operating with tritium this will lead to continuous build-up of a tritium inventory. For this effect to occur reactive species have to have a low, but not vanishing surface loss probability (P_L). P_L has to be low to enable the particle to survive many surface collisions, so that it can also reach remote areas; on the other hand, it must not be zero in order to lead finally to some film deposition. A candidate for such a species is the CH_3 radical with $P_L = 10^{-4}$ as measured in radical beam experiments. The question whether a CH_3 radical can really be transported over long distances was investigated in a dedicated test experiment.

An ECR methane plasma was applied as a source of a flux of reactive species. It is known from earlier investigations that the particle flux emanating from such a discharge comprises a wide variety of species with widely varying surface reaction probabilities. A fraction of this reactive flux was extracted from the discharge through a baffle into a stainless-steel tube (1 cm in diameter, 30 cm long). Species with a high P_L (such as ions and C_2H radicals) will deposit at the entrance of the tube and only species with a low P_L will reach the end. At the end of this tube a sniffer probe was mounted to extract a fraction of the remaining flux. It consisted of a stainless-steel pipe 70 cm long with an effective inner diameter of 3 mm. The remaining particle flux reaching the end of the sniffer probe was injected into a quadrupole mass spectrometer for mass analysis. By threshold ionisation mass spectroscopy the CH_3 radical was clearly identified as a constituent of the particle flux. This experiment proves that CH_3 radicals can survive many wall collisions (of the order of 10,000) and be transported over long distances to very remote areas of a fusion device. In future experiments the composition of the particle flux shall be examined as a function of the temperature of the tube, in order to find an optimal temperature range to minimize CH_3 migration.

2. PLASMA THEORY

2.1 Decay Properties and Statistics of Two-dimensional MHD Turbulence

In a strongly magnetised plasma turbulence dynamics is highly anisotropic, since the stiffness of the mean magnetic field prevents sharp bending so that small-scale fluctuations can only be excited perpendicularly to the mean field, making the turbulence practically two-dimensional. (In fact, 3D turbulence studies have shown that with increasing strength of the mean field statistical properties approach those observed for 2D turbulence.) The 2D approximation is very convenient for numerical studies because much higher Reynolds numbers become accessible than in fully 3D turbulence studies. Direct simulations with spatial resolutions of up to 8192^2 collocation points have been performed, which should be compared with the maximum achievable resolution of 512^3 in 3D. The results concern two different areas, viz. decay properties of integral quantities and the statistical properties of the small-scale dynamics. The turbulence

decay proceeds in a selfsimilar way characterised by invariance of the ratios of kinetic to magnetic energy, of viscous to resistive dissipation rate, and of parallel to perpendicular kinetic energy. The selfsimilarity of the decay allows one to calculate the energy decay law from the constancy of the mean-square magnetic potential. In contrast to isotropic 3D turbulence, the energy spectrum is found to agree essentially with the Iroshnikov-Kraichnan power law, but it is modified by a logarithmic factor. A rather complete description of the statistical properties is obtained from the set of scaling exponents of the structure functions. These show that MHD turbulence is significantly more intermittent in 2D than in 3D.

2.2 Scaling Laws in Two-dimensional Turbulent Convection

In the presence of a strong magnetic field convection in a stratified medium is essentially two-dimensional. The statistical properties of 2D turbulent convection were studied numerically in the Boussinesq approximation. We consider an open system with periodic boundary conditions for the fluctuations that simulate conditions in the central part of a convection zone away from boundary layers. While we find the spectra of velocity and temperature fluctuations roughly consistent with the Bolgiano-Obukhov scaling, the intermittency of the temperature fluctuations is very strong, being similar to that of passive scalar turbulence, though in thermal convection the temperature is not passive. The reason for this behaviour lies in the ramp-and-cliff structure of the temperature field, which is similar to that of a passive scalar. By contrast, the velocity fluctuations exhibit almost no intermittency.

2.3 Fast Magnetic Reconnection due to Resistivity Localisation

The effect of localising the resistivity in a small region around the X-point is studied self-consistently in the coalescence of two magnetic flux bundles. The reconnection rate is found to be almost independent of the value of the resistivity taking place in a finite-angle X-point magnetic configuration, which differs strongly from the case of a homogeneous resistivity distribution, where the reconnection process occurs in a macroscopic current sheet and the time scale strongly depends on the resistivity. The results, which agree quantitatively with a recent theory, indicate that the clue to fast reconnection dynamics is that the reconnection mechanism be localised. While such localisation does not naturally occur with collisional resistivity, it is enforced by the dispersive properties in high-beta as well as low-beta collisionless plasmas, which explains the observed fast reconnection rates observed in the latter.

2.4 Three-dimensional Particle-in-cell Simulation of Complex Plasmas

In order to achieve a fully self-consistent numerical model for simulation of complex plasmas in RF-driven discharges, a highly

efficient parallel particle-in-cell code was extended to plasmas containing dust particles. The program was designed for operation on massively parallel architectures and is at present running on Cray T3E and IBM SP systems allowing realization of up to one billion interacting particles.

To evaluate the physical influence of different hybrid approaches to dust modelling, we implemented a Yukawa system as the simplest approximation for studying the dynamics of plasma crystallisation, wave propagation, and thermodynamic properties. The abstraction level of the complex plasma model will be successively lowered by introducing an ion particle species, leading to self-consistent dust shielding and dust-dust interaction, the electrons being regarded as adiabatically adjusting to electric potential differences. This will allow comparisons between full-particle simulations and different potential-modelling approaches.

2.5 Local Anisotropy of Homogeneous Magneto-hydrodynamic Turbulence

In the wake of recent theoretical advances, homogeneous incompressible magnetohydrodynamic (MHD) turbulence with and without a mean magnetic field was studied by direct numerical simulation. As it has been argued that the presence of a magnetic field, even in a globally isotropic system, would locally introduce spatial anisotropy, we considered the two-point statistics of the turbulent fields parallel and perpendicular to the local magnetic field. It could be shown that there is indeed such statistically significant anisotropy. While the turbulence exhibits hydrodynamic features perpendicular to the local magnetic field, it shows a pronounced reduction of intermittency in the parallel direction. Interestingly, in spatially isotropic statistics the evidently different field-parallel dynamics do not dominate the overall statistical behaviour of the turbulent system, i.e. one observes Kolmogorov scaling $\sim k^{-5/3}$ of the energy spectrum in combination with statistical behaviour which is consistent with nonlinear interactions based on eddy scrambling.

Additional studies where a mean magnetic field of varying strength penetrates the fluid allowed detailed examination of the local anisotropy in the physical mechanisms underlying MHD turbulence. First theoretical results based on well-supported intermittency phenomenologies have been achieved. Work on a consistent theory for this new phenomenon is under way.

2.6 Three-dimensional Particle Simulations of Collisionless Magnetic Reconnection

Some of the most challenging problems in laboratory and space plasma physics, such as collisionless magnetic reconnection and the dynamics of collisionless shocks, require three-dimensional large-scale and high-resolution simulations, which are only feasible on massively parallel computer systems. To allow such simulations a new particle-in-cell code was developed for the Cray T3E system which treats the Poisson equation with a parallel multigrid solver and is therefore particularly well suited to computer systems with a distributed memory architecture. With this new code simulations were performed to investigate the

stability of current sheets and boundary layers which develop during magnetic reconnection of anti-parallel fields in collisionless plasmas. The strong current layers which are driven near the X-line remain surprisingly laminar, with no evidence of turbulence and associated anomalous resistivity or viscosity. Neither the electron shear flow instabilities nor kink-like instabilities which have been observed in these current layers in earlier simulations are present. The sharp boundary layers which develop between the inflow and outflow regions downstream of the X-line are unstable to the lower hybrid drift instability. The associated fluctuations, however, do not strongly impact the rate of reconnection. As a consequence, magnetic reconnection in the 3-D system remains nearly two-dimensional.

To allow even larger simulations which exceed the memory limit of the Cray T3E system, the code was ported to use MPI (Message-Passing Interface) as an architecture-independent communication scheme. In this new version the code is, in particular, ready to run on the IBM SP system. As another extension additional modules were added which allow the code to be operated in hybrid and two-fluid mode. In the hybrid mode the ions are treated as in the full-particle case, whereas the electrons are modelled as a massive fluid with isotropic pressure. The resulting Helmholtz equation is treated with a multigrid solver very similar to that introduced for the full-particle version. In two-fluid mode, finally, a Hall-MHD model is used which again contains a Helmholtz equation as in the hybrid case.

3. DATA ANALYSIS

Measured data are usually spoiled by noise. Background information necessary for the measurement descriptive model is often uncertain. A ubiquitous problem in data analysis is to identify and quantify sources of errors of a measurement system and describe the data with a model including all uncertainties in a concise formalism in order to obtain the most reliable result including its credibility. Bayesian probability theory (BPT) provides a general and consistent frame for combining various kinds of information taking into account the degree of uncertainty of data and models.

Joint automatic evaluation of experimental data from different plasma diagnostics to derive reliable spatial profiles of plasma quantities (n_e , T_e , T_i , Z_{eff} ...) suffers from a lack of systematic statistical modelling of the uncertainties involved. BPT allows a systematic combination of all information entering the measurement descriptive model that takes into account all uncertainties of the measured data, calibration measurements, physical model parameters, and measurement nuisance parameters. As a first step the validation procedure was applied to the Nd:Yag-Thomson scattering diagnostics and the Ruby-Thomson scattering diagnostics at W7-AS to obtain the most reliable n_e and T_e profiles. The results of the Nd:Yag diagnostics are consistent with the long-established ratio-evaluation data evaluation method. Systematic consideration of all raw data obtainable, in particular those data suffering from low signal levels, results in improved evaluation for weakly informative data. Sensitivity analysis of model parameters allows one to find

crucial uncertainties with an impact on diagnostic improvement. The results of the ruby diagnostics benefit from the concise formulation of the measurement descriptive model without successive analysis steps. The prospect is to combine the two diagnostics after mapping on magnetic surfaces.

Temperature measurements in tokamak edge plasmas frequently suffer from outliers of unknown origin. Such outliers have an important unwanted influence on the estimation of parameters for edge temperature model functions in conventional least-squares fits. BPT is applied to deal with such outliers and develop a robust procedure which performs highly satisfactorily.

In the analysis of the spectra recorded with mass spectrometers one has to infer the concentration of the contributing molecule species from the signal intensities in the mass channels. Though every molecule produces a particular spectrum (referred to as cracking pattern), the pattern of various species in a gas mixture may overlap and have to be disentangled. Since the data are noisy and the cracking pattern itself originates from a noisy calibration measurement, a method for decomposing mass spectra based on BPT was developed.

Given a set of spectra, the algorithm combines the measurement of the gas mixture with the result from the calibration measurements and returns the relative concentrations and the associated margin of confidence for each component of the mixture. In addition to the concentrations, such a data set allows one to derive improved values of the cracking coefficients of all contributing species, even for those components for which the set does not contain a calibration measurement. This latter feature also allows one to analyse mixtures which contain radicals in addition to stable molecules. As an example we analysed and discussed mass spectra obtained from pyrolysis of azomethane which contain the radical CH_3 apart from nitrogen and C_1 - and C_2 -hydrocarbons.

For the future this work will serve as a basis for proper analysis of vector mass spectra like hydrogen-helium gas mixtures such as arise in fusion machines.

Elastic recoil detection analysis is improved in respect of depth resolution and reliability of the measured spectra by deconvolving the measured spectra by the adaptive kernel method in the framework of BPT. The growth process of tetrahedral amorphous carbon (ta-C) was studied on deconvolved ^{13}C depth profiles including the uncertainties.

Measured spectra consisting of a collection of 'peaks' were analysed by the recently proposed reversible-jump Markov chain Monte Carlo method. The numbers of mixture components and component parameters were jointly estimated. The method was applied to data from Rutherford backscattering spectroscopy and high-resolution electron energy loss spectroscopy.

Plasma Diagnostics Division

(Head of Division: Prof. Dr. G. Fussmann)

The Plasma Diagnostics Division in Berlin is part of the Greifswald Branch of IPP. Its activities cover the WENDELSTEIN 7-AS and 7-X projects as well as the ASDEX Upgrade fusion experiment at Garching. Other research activities comprise experimental and theoretical investigations in Berlin. The topics covered are: PSI-2 plasma generator, UHV laboratory, electron beam ion trap (EBIT) experiment, and studies of edge physics and plasma-surface interaction problems. Only the results of the activities in Berlin are described in this section of the report.

P. Bachmann, C. Biedermann, W. Bohmeyer, D. Hildebrandt, B. Jüttner², H. Kastelewicz², Zh. Kiss'ovski¹, B. Koch, P. Kornejew, M. Laux, A. Markin³, D. Naujoks, R. Radtke, H.D. Reiner, A. Stareprawo, D. Sünder, U. Wenzel

1 Guest, University Sofia, Bulgaria

2 Humboldt University, Berlin

3 Guest, Ac. Sci. Institute of Chemistry Moscow, Russia

1. PSI-2 PLASMA GENERATOR

In 2001, the activities of the PSI group were concentrated on four main topics: hot-liner experiment, measurement of the Balmer spectrum, plasma flow velocities, and heat flux measurements. To understand both the formation of amorphous hydrogenated carbon layers and the process of deposition in tokamaks with ITER-like conditions, the hot-liner experiment was designed in close co-operation with the EFDA group in Garching. To produce the hydrocarbons, a heated graphite target is used (diameter 80 mm, max. target temperature 600^o C). The efficiency of hydrocarbon generation in front of the target was determined as a function of the plasma conditions: a flow from the target of more than 10¹⁸ C atoms s⁻¹ was measured. In addition, the hydrocarbons' distribution at the entrance of the hot liner was determined and modelled by Monte Carlo methods. The sticking coefficient of the hydrocarbons will be measured as a function of temperature using Si wafers and cavities attached to the inner structure of the hot liner (max. temperature 1000^o C). As a new topic the Balmer spectrum (lines and continuum) was investigated under conditions where three-body recombination prevails (Fig. 1). The results from the spectroscopic diagnostics are compared with those from Langmuir probe measurements. The aim is to resolve the discrepancy observed in tokamaks for two different methods of electron temperature diagnostics. Probe measurements in tokamaks tend to give systematically higher temperatures. Another topic was measurement of the plasma streaming velocity by means of a Mach probe. The Mach probe offers the advantage over other spectroscopic techniques (e.g. LIF) of providing good spatial resolution and easy application. An important result is that the magnetic field strength along the PSI generator has a large effect on the flow velocity. Earlier investigation of the heat flux was complemented by measuring this quantity for different orientations of the sensor surface to the magnetic field direction. Generally, the results agree fairly

well with theoretical predictions. Only the result for helium shows larger discrepancies in relation to theoretical values for the heat flux. It turns out that the difference is due to the effect of helium atoms in metastable states.

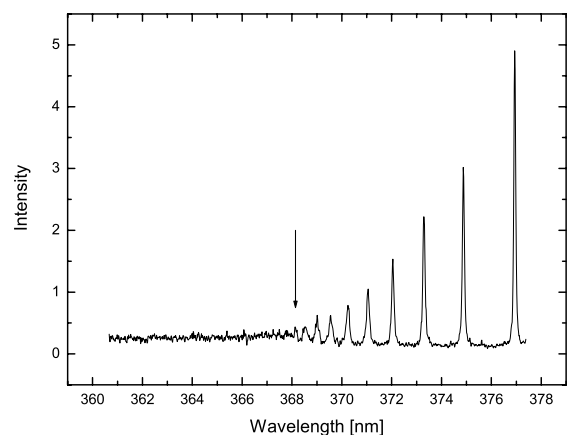


FIG. 1: Balmer spectrum of hydrogen between 364 and 380 nm. The highest series member ($n = 22$ to $n = 2$) that could be resolved in the spectrum is marked.

2. ELECTRON BEAM ION TRAP (EBIT)

The investigation of magnetic dipole radiation from highly charged tungsten in the range from 500 to 1000 Å was continued (in cooperation with the Racah Institute of Physics, Jerusalem). Many lines could be identified and marked as diagnostics for tokamak measurements. In addition, time-resolved measurements of the X-radiation produced by argon and barium were made, demonstrating for the first time sawtooth activity of the ion population in the trap.

One major topic of investigation at EBIT was high-resolution measurements of the characteristic X-ray emission from helium-like argon. Helium-like ions with a well-known level structure allow prediction of a few distinct line ratio combinations to determine the electron temperature T_e or density of the plasma. These theoretical predictions require, however, knowledge of quite a number of accurate cross-sections and need to be checked by benchmark experiments. We have investigated with EBIT the intensity ratio of individual dielectronic satellites to resonance lines for He-like Ar, since argon is an element deliberately added to tokamak plasmas for diagnostic purposes. By sweeping EBIT's electron beam over a wide range of energies

we can excite and sample the He-like Ar ions, simultaneously recording the emitted radiation with a high-resolution crystal spectrometer. Thereby, information on the different processes of resonantly excited dielectronic recombination and direct excitation can be separated into emission wavelength and excitation energy. Since the so-called j and z lines blend and can only be separated by the differential technique used for this EBIT experiment, they are usually treated together. The ratio of $j+z$ lines to the w line previously used in TFR experiments shows only a weak T_e dependence (Fig. 2). However, the strong k and w lines are particularly well suited to diagnostics because they can easily be distinguished in the X-ray spectra. Furthermore, as the graph demonstrates, the line ratio has a steep temperature dependence, which is also predicted by HULLAC calculations.

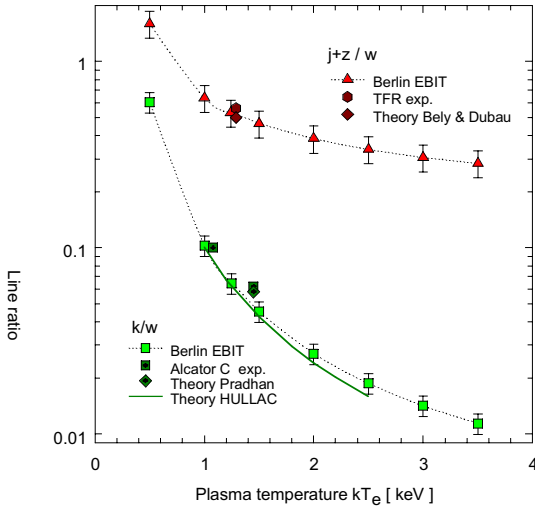


FIG. 2: Line ratios of dielectronic satellites to the w resonance line of argon. Experimental values from the Berlin EBIT are compared with measurements at tokamak facilities and calculations.

3. UHV LABORATORY

Layers of B_4C are envisaged for use as plasma-facing material for the W7-X stellarator. To investigate the properties of such layers, a movable mushroom-shaped Cu limiter was coated with a $170 \mu\text{m}$ thick B_4C film and exposed to the TEXTOR-94 plasma during 40 ohmically and NB-heated discharges. During exposure, intense light spots were observed on the limiter surface, and at the same time the current to the limiter and the infrared radiation were enhanced. Preferably, these features were detected during high-power discharges or disruptions when the position of the limiter was close to the separatrix. The spots have a lifetime of up to several seconds. Instead of moving in a retrograde direction, as expected for arcs in magnetic fields, they persist at a fixed position. Post-mortem investigations of the limiter revealed that there are craters on the B_4C layer at positions which correspond to the light spots observed in the experiment. Using laser profilometry, the diameter and depth of a single crater were measured to be 250 and $170 \mu\text{m}$, respectively. Note that the depth just corresponds to the thickness of the B_4C layer. Surface analysis using SIMS and AES revealed that the bottom of the largest craters consists entirely of substrate copper. In the re-solidified region surrounding the craters, the surface concentration of Cu was up to 8% . In order to clarify some specific aspects of the spot formation, laboratory experiments were conducted with

vacuum arc discharges. The arcs were ignited on a B_4C -coated Cu cathode in the presence of a magnetic field of 0.4 tesla. The discharge current was limited to 20 A, and the discharge duration was 1 ms. Observation of the arcs was made by means of a fast CCD camera. The arcs generated in vacuum behave similarly to the light spots observed in the tokamak experiments: on the cathode they burn through the B_4C coating, and there is hardly any change in the position of the arc as a function of time. In fact, the arc spot seemed to stay at the location of the ignition. Furthermore, the craters produced by the vacuum arcs are very similar to those found on the limiter surface. The crater depth increases with the number of arc discharges (provided the ignition takes place at the same position) and reached the thickness of the B_4C coating ($170 \mu\text{m}$) after about 10 discharges. This corresponds to a total charge transfer into the crater of approximately 70 mC. Surface profilometry revealed that only a minor part of the eroded B_4C material (less than 30%) was redeposited. In a region of about 1 mm around the craters, copper was found with surface concentrations of up to 30% . The formation of craters on plasma-facing B_4C components due to arcing and damage to the substrate can be a serious problem, in particular if the structure contains water pipes for cooling purposes.

4. THEORY AND MODELLING

The following topics were covered by the theory and plasma modelling group:

- (i) Bifurcation and chaos in radiative edge plasmas. The problem was tackled by using a periodically driven reaction-diffusion equation which resulted from the time dependent 1-D heat conduction equation. The transition to chaos by the Feigenbaum route was demonstrated. When spatial variations are included, Hopf bifurcation and intermittence phenomena also exist.
- (ii) Charge shielding in magnetised plasmas. The shielding of a test charge embedded in a magnetised plasma was investigated by means of a particle-in-cell (PIC) model. It is shown that the ratio of the gyration radius to the Debye length is the main parameter in the analysis. For small values of this parameter, plasma shielding of a test charge does not occur. For high values, the effect of the magnetic field vanishes and the electric forces dominate.
- (iii) PIC code simulations of plasmas. The PIC code, PLAS, was developed to model a plasma with a given density profile embedded in an external magnetic field. It is shown that the difference in the electron and ion gyration radii leads to charge separation resulting in the origin of an electric field. Whereas the electrons with their extremely small gyration radii stay relatively fixed at the magnetic field lines, the ions need this additional force, which ensures near equality of the electron and ion density profiles.
- (iv) B2-EIRENE modelling. Numerical calculations were made to predict the effect that a probe could have on the properties of a plasma. The probe was modelled as a ring-shaped target at floating potential embedded in a magnetised plasma. In front of the probe, the electron temperature increases along the flux tubes; the increase in temperature is typically 2 eV. Behind the probe, there is a decrease of the temperature by about the same value. The predicted effect is in qualitative agreement with a recent observation in the PSI plasma generator.

VINETA

(Head of Project: Prof. Dr. Thomas Klinger)

Members of Experimental Plasma Physics Division 5 and contributors to the project: see section “Divisions and Groups, VINETA“.

1. INTRODUCTION

The linearly magnetized helicon plasma device, VINETA, went into full operation in spring 2001. It was originally designed for conducting basic research in plasma dynamics and equipped with specialized diagnostics. The current scientific programme is project A15 in the DFG special collaborative research centre (SFB 198) “kinetics of partially ionized plasmas” at Greifswald University. The project is focused on electromagnetic plasma waves and plasma instabilities, in particular Whistler waves, Alfvén waves, and drift waves.

2. DEVICE DESIGN AND DIAGNOSTICS

The VINETA device is designed for versatile operation and maximum flexibility. It consists of four identical cylindrical modules; each of them immersed in a set of 8-10 water-cooled magnetic field coils that can be freely adjusted along the axis. The assembled device has a homogeneous magnetic field of maximum $B = 0.1$ T. If desired, axial gradients in the magnetic field can be tailored to create magnetic bottle, mirror or separatrix configurations. The total length of the VINETA device is 5m. Figure 1 shows a picture of the experiment.

VINETA is usually operated in steady state and a long, large-volume ($V = 40l$) magnetized argon plasma column with electron densities of up to 10^{19} m^{-3} is established. The electron temperature is in the range of 2-10 eV. Owing to the high efficiency of the helicon plasma source, the β -regime of *electromagnetic* drift waves ($\beta \geq m_e/m_i$) can be experimentally explored. Another consequence of the high density is that the Alfvén wave length v_A/f_{ci} is fairly low, which allows one to study compressional and torsional Alfvén waves without too strong influence of the axial boundaries.

Electrostatic probes are used for standard plasma diagnostics with high spatial and temporal resolution. Probe positioning in the plasma is done by various computer-controlled servomotor systems. Plasma wave measurements are done with HF-matched electrostatic and magnetic probes.

The latter have been carefully frequency calibrated. The ion kinetics and ion dynamics will be non-intrusively observed by laser-induced fluorescence (LIF), for which a 60 mW 661 nm cw diode laser system is already set up. Finally, the line-integrated density will be steadily monitored by a tuneable microwave interferometer, which is under construction.

FIG. 1: Full view of the VINETA device. The magnetic field coils (brown ring structures) can be adjusted along



the axis. On the right-hand side, the helicon plasma source is installed.

3. EXPERIMENTAL PROGRAMME

3.1 Whistler and Helicon Waves

Whistler waves are right-hand polarized electromagnetic waves with frequencies in the range of $\omega_{LH} \ll \omega \ll \omega_{ce}$. They are of fundamental importance in ionospheric plasma physics and radio sciences. Recently, Whistler waves received much attention in the context of non-resonant plasma wave heated discharges: Long-wavelength Whistler waves, launched in a target plasma, form eigenmodes, so-called “helicon” modes. It was discovered that helicon modes perform surprisingly efficient transfer of wave to particle energy. The actual transfer mechanism is not yet well understood. The primary goal of this research project is to investigate systematically the transition from unbounded-plasma Whistler waves to bounded-plasma helicon modes; in particular the change in dynamics and dissipation.

RF power is coupled to the plasma by a Nagoya type III double-half-turn right-helical antenna. This antenna geometry drives the $m=1$ helicon mode. Figure 2 shows radial density profiles of the three consecutive discharge modes – capacitive,

inductive, helicon - established if the RF input power is gradually increased from zero to a few kW.

by systematic investigation of the transition from electrostatic drift waves

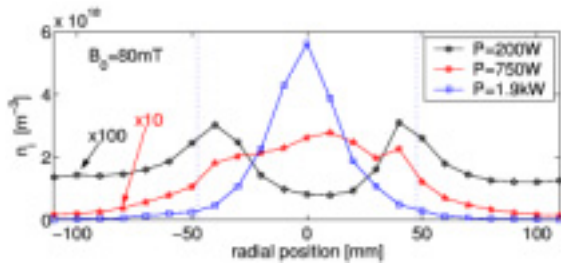


FIG. 2: Radial profiles of the plasma density for increasing RF power at $B = 80$ mT. Note the scaling factor applied to the profiles of the capacitive (black) and the inductive (red) mode. The dotted lines indicate the radial positions of the helical double-ring antenna.

Since in the capacitive mode plasma production takes place in the antenna sheaths only, a hollow profile forms. Above a certain power threshold, the discharge suddenly jumps into the inductive mode with a factor of ten higher flat-top density profiles. The sudden transition to wave-heated helicon discharge finally occurs at relatively high power. It is characterized by high plasma densities (up to 10^{19} m $^{-3}$) and a peaked density profile. In all three cases, the electron temperature remains moderate in the range 2-10 eV.

Figure 3 shows probe measurements of the poloidal plasma density profiles in the three discharge modes. The profiles are fairly axisymmetric and compatible with the conclusions drawn from Figure 2.

FIG. 3: Poloidal plasma density profiles for capacitive, inductive, and helicon discharge mode (left to right).

In progress is the investigation of electron and ion Whistler waves in a bounded cylindrical plasma. This is accomplished by axially-radially movable magnetic loop probes and by laser-induced fluorescence (LIF) techniques. The final goal is to develop a consistent picture of the dynamics of circularly polarized electromagnetic waves in a bounded, cylindrical, and magnetized plasma.

3.2 Drift-Alfvén Waves

The high density achieved in the helicon discharge mode allows one to approach the electromagnetic regime of drift waves. So-called drift-Alfvén waves (DAWs) have been thoroughly investigated in the Tokamak Theory division of IPP. However, there is still a need for well-defined experiments on DAWs. This project aims to close this gap

ELECTRON SPECTROSCOPY GROUP, FHI BERLIN

(Head of Project: Dr. Uwe Hergenhahn)

1. INTRODUCTION

The Programme of the group consists in investigating novel phenomena in photoionization and the mechanisms concerned. Such processes are important in the cold regions of fusion plasmas. The experiments are conducted with an advanced light source in the VUV and X-Ray regime: at the BESSY II synchrotron radiation storage ring in Berlin. While further pursuing our studies of high resolution molecular photoionization, we have also broadened their scope. For photoionization of chiral molecules with circularly polarized light, first reported in 2000, there are new results, and a new project on autoionization of Van der Waals clusters has been successfully initiated.

2. TECHNICAL ACHIEVEMENTS

For future experiments we are developing methods of detecting two electrons resulting from the same photoionization event in co-incidence. This necessarily requires detection systems which separately register every electron. The original readout of our hemispherical electron analyzer, in which a 10% range of the pass energy is detected by a microchannel plate via a CCD camera, was far too slow for efficient single-electron detection. We have adapted a commercially available fast position-resolving anode to our spectrometer. With this equipment we recorded the time-of-flight broadening of trajectories pertaining to equal electron kinetic energy, using a pulsed-beam mode ('single bunch') of the BESSY II storage ring. At the same time, this development has permitted us to increase the detection efficiency.

3. RESULTS

In nine weeks of synchrotron radiation beam time the following results were achieved:

3.1 Photoionization of Chiral Molecules

A chiral molecule is defined as being different from its own mirror image. The two forms of opposite handedness are called enantiomers. The optical effects of enantiomerically pure samples on light are well established, but are small (10^{-4} range). We have studied a potentially much larger effect resulting from the interference of electric dipole photoionization amplitudes. This differential effect does not lead to a net asymmetry, but to

a redistribution of the photoelectron intensity between forward and backward directions that flips sign with the helicity of the ionizing light and the handedness of the molecule. For the normalized intensity difference of the carbonyl C 1s photoelectron line of gaseous, unoriented camphor recorded with a 54.7° forward scattering geometry, we validated the measurement of an asymmetry of up to 6 % reported last year, and showed that this effect can be observed from threshold up to kinetic energies as high as 20 eV.

3.2 Experiments on Van der Waals Clusters

Intensities at BESSY II are sufficient to study directly photoionization of a free cluster beam. We produced noble gas clusters by supersonic expansion, and recorded their photoelectron spectra with a resolution vastly improved compared to earlier studies. Recently, a new type of charge transfer process has been predicted for Van der Waals clusters. This so-called 'Interatomic Coulombic Decay (ICD)' is mediated by autoionization of inner valence hole states in clusters, *i.e.* for Ne the $2s^{-1}$ state. We have tried to detect the signature of this process and indeed have observed a significant increase in the yield of low kinetic energy electrons above the Ne 2s threshold. To state definitely that this proves the existence of the ICD effect is, however, premature before further checks of the spectrometer characteristics in this energy region have been performed.

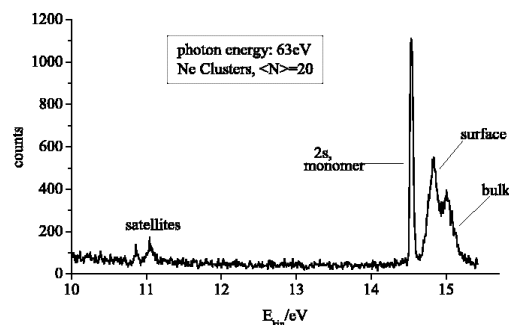


FIG. 1: Ne 2s photoelectrons from a free cluster beam. The separation of the peak into monomer, cluster surface and cluster bulk fraction can be seen with unprecedented clarity.

GARCHING COMPUTER CENTRE (RZG)

(Head: Stefan Heinzel)

RZG traditionally provides supercomputing power and archival services for IPP and other Max Planck Institutes throughout Germany. Besides operation of the systems, application support is given to Max Planck Institutes with high-end computing needs in fusion research, materials science, astrophysics, and other fields. Large amounts of experimental data from the fusion devices of IPP (ASDEX Upgrade, Wendelstein 7-AS, and, later, Wendelstein 7-X), satellite data of MPI of Extraterrestrial Physics (MPE) at the Garching site, and data from supercomputer simulations are administered and stored with high lifetimes. In addition, RZG provides network and standard services for IPP and part of the other MPIs at the Garching site. The experimental data acquisition software development group for the new Wendelstein 7-X fusion experiment and the current ASDEX Upgrade fusion experiment operates as part of RZG.

I. Ahlert, A. Altbauer, G. Bacmeister, J. Cox **, K. Desinger, R. Dohmen, S. Gross, A. Hackl, S. Heinzel, C. Hennig, A. Jacob, K. Lehnberger, H. Lederer, R. Mühlberger, K. Näckel*, W. Nagel, M. Panea-Doblado, P. Pflüger, F. Pirker, A. Porter-Sborowski, H. Reuter, S. Sagawe*, H.-G. Schätzko, R. Schmid, J. Schmidt, A. Schott, H. Schürmann*, H. Soenke, U. Schwenn, R. Tisma, S. Valet*, I. Weidl, V. Weinert

Data Acquisition Group:

P. Heimann, J. Maier, J. Reetz, M. Zilker

* IPP Greifswald ** till June 2001

1. MAJOR HARDWARE CHANGES

The massively parallel Cray T3E system (with 816 processors, 102 GB main memory, and a peak performance of 0.49 TFlop/s) is used for projects with highly scalable parallel applications that require a large main memory. For non-parallel vectorizing codes, a NEC SX-5 vector system with high single processor performance with 3 processors and 12 GB of main memory is available. Since Oct an 8-processor test system for the forthcoming new IBM supercomputer has been in operation. For high requirements in mid-range computing power, the following dedicated compute servers of client institutes of RZG have been newly installed and are being operated by RZG: SGI Origin 3400 system (12 processors, 24 GB main memory) for IPP; SUNFIRE 3800 system (8 processors US III, 32 GB main memory) for MPI of Developmental Biology; SUNFIRE V880 system (4 processors, 8 GB of main memory) for MPI of Extraterrestrial Physics.

2. DATA MANAGEMENT

2.1 Multiple-resident AFS and OpenAFS

In October 2000 AFS became an open source. This allowed RZG to bring all extensions needed in the client for MR-AFS into the OpenAFS source. The most important change is that the OpenAFS client now has large file support for AIX, LINUX, and SOLARIS. Other changes now allow the MR-AFS extensions to the "fs" command to do their RPCs via the cache manager, which is much more efficient than before /757/.

The major changes in the MR-AFS fileserver are that the old technique to store files without directory entries abusing fields in the inode has been replaced by a technique where the files are visible in the directory tree. This technique, called NAMEI interface, had first been used by Transarc (IBM) for the Linux client some years ago. The main advantage is that no special file system check program (fsck) is required any more and therefore any kind of Unix file system can be used.

A low-cost fileserver based on Intel PC hardware with RAID adapters and DIE disks has been tested. This is the same kind of server as used by CERN and DESY. The performance of this server turned out to be very good, but many disk failure problems were encountered. After replacement of all disks from a different vendor, the stability increased, but did not achieve that of the much more expensive SSA disks on IBM machines. Since this disk system could not be used for high-availability purposes, it is now used for replicated software and for replications of user home volumes. This additional backup strategy to automatically replicate the home directories every night to this stand-by server would allow recovery from the loss of a server partition in a significantly shorter time than would be required to restore the volumes from the TSM system.

2.2 Archival and Backup System

Concerning mass storage of data, a basic distinction is made between experiment-type data sets with requirements for long-time conservation and short-lifetime data of the backup type which are replaced by new versions at short intervals. For the second type, backup data, not MR-AFS was used, but the so-called “arc” software developed at RZG had been used for the most common system platforms. This system has been replaced by the commercially available product TSM (Tivoli Storage Manager, formerly ADSM) from IBM. The tape drive capacity of the TSM server, an IBM H80 machine, has been extended: three new STK 9940 drives have been added to the already existing six STK 9840 (“Eagle”) tape drives, served by the Grau/ADIC robot system and tape silo. “Arc” backup service stays in operation only for the high-performance systems Cray T3E and NEC SX-5, for which no TSM clients are available. For routinely performed backups of all other systems, TSM is now used as standard. The migration of “arc”-based archival data into the TSM system is ongoing. For TSM archival data, security against physical damage has been significantly improved: A second tape copy is being routinely generated at Leibniz Rechenzentrum München (LRZ) in downtown Munich, whereas LRZ has the option of second-tape generation and storage at RZG.

3. DEVELOPMENT FOR HIGH-END PARALLEL COMPUTING

High-performance computing is a key technology for IPP and other Max Planck Institutes. Application development and support for high-end parallel computing is of great importance for disciplines especially in the fields of plasma physics, materials science, and astrophysics. Projects to support new developments in close collaboration with the respective scientists are described in detail, as well as the preparation for a new supercomputer generation /573, 574/.

3.1 Fusion Research

3.1.1 P3D particle-in-cell code

The P3D particle-in-cell code of A. Zeiler had been highly optimized for the Cray T3E system, using the proprietary shmем library for one-sided communication. For a cooperation project with the University of Maryland, the code is to be used on a large IBM system at NERSC, Berkeley. The T3E-specific communication scheme was therefore redesigned. The hierarchical group structure for efficient I/O was adapted. The P3D code is thus also already ported to the T3E follow-up IBM system at RZG.

3.1.2 SDTrimSP code

The new standard-version SDTrimSP (static/dynamic Trim sputtering) of the generalized TRIDYN code package was further extended in cooperation with R. Schneider. New features

include implementation of particle statistics (especially tracing of particles of different classes) and a new, universal I/O interface. This allows the fine tuning of the amount and complexity of dynamically selected physical quantities such as moments of the distribution function in phase space and the energy transfer. Portability could be achieved by implementing a portable parallel random number generator.

3.1.3 Plasma edge transport EMC3 code

The combined parallel EMC3 / EIRENE code allows study of plasma transport in edge regions. The EMC3 Monte Carlo part is suited to fluid approaches (solution of Navier-Stokes-like fluid equations especially for protons and electrons), the EIRENE part (from FZ Jülich) is suited to treatment of neutral atoms or molecules (solution of the kinetic Boltzmann equations). The code had been ported to the SR8000 Hitachi system at LRZ, where 1 GB of memory is available per processor. The limited memory of 128 MB per T3E processor at RZG did not allow sufficiently large problem sizes. Attempts were made especially to further optimize the single-processor performance of the Hitachi system. The Monte Carlo part, however, appeared to be not well suited to the pseudo-vector architecture of the Hitachi system.

3.2 Materials Sciences

The new portable parallel version of the WIEN97 code package for the LAPW method (Linearized Augmented Plane Wave) /76/ was tested under production conditions on the Cray T3E system, and first implementation tests for the new IBM system were carried out. The parallelization scheme was adopted for the new WIEN2K version by the authors of the WIEN97 code.

3.3 Astrophysics

The 16-processor IBM power3 system (Nighthawk II) of MPI of Astrophysics can be considered as the predecessor system of the new IBM Power4 system (Regatta) with a similar macro architecture. On this shared memory system, for parallel processing no explicit message passing is required for communication, but the new standard for shared-memory parallel processing, the OpenMP model, can be applied. For three parallel codes based on OpenMP, scalability comparisons with an SGI Origin system revealed a higher degradation on the IBM system. For two codes, application of specific compiler options in combination with the tuning of those environment variables which are responsible for the behaviour of the multi-user interrupt handling could significantly improve the scalability. For the third code, the reduction of work per processor with an increasing number of processors turned out to be the limiting factor specifically on the IBM system: the 4-way parallelism for floating-point operations on the Power3 processor (with independent multiply/add operations on the two floating-point units) could no longer be exploited, whereas on the MIPS processors of the Origin system. 2-way parallelism for floating-point operations was the maximum anyway. By code restructuring the amount of work per processor was increased, and good scalability was achieved.

3.4 Geo Sciences / Climate Research

The ECHAM climate model codes of MPI of Meteorology are to be used by MPI of Chemistry on parallel machines at RZG. The parallel efficiency of the code is therefore of general interest, and RZG became involved in the analysis and optimization of ECHAM. Prior to the availability of the new ECHAM5 version, work was based on the ECHAM4 standard version. In close cooperation with the MPI of Meteorology, the ECHAM4 output procedure was parallelized which significantly improved the overall scalability. In a second step, this parallelization scheme was migrated to ECHAM5. Since the ECHAM4 to ECHAM5 transition was accompanied by a revised memory allocation scheme, the new output routines could only be incorporated after further modifications.

Parallelizing strategies for the new advection part in ECHAM5 were discussed with scientists from MPI of Meteorology, and the SPITFIRE option for the advection part was efficiently parallelized for distributed memory systems. The new version was developed on the Cray T3E system and ported to the IBM Power4 system. Parallel I/O and the parallel spitfire routine are now part of the new ECHAM5 standard version.

3.5 Preparing for a new supercomputer

In spring, IPP and MPG contracted IBM to deliver a follow-up system for the current Cray T3E/816 supercomputer by the end of 2001. From October on an early 8-processor test system was in operation that allowed tests on operating system features and on application level. Essential T3E production codes could be tested prior to delivery of the ordered system /573, 574/. Communication patterns used for parallel processing included: a) direct message passing with portable MPI (possible as on T3E), b) shared-memory parallel processing with portable OpenMP (not possible on T3E), c) one-sided communication with the low-level application programming interface (LAPI), IBM proprietary. Especially c) proved to be an interesting option for easy porting shmem-based T3E codes with one-sided communication. Bugs and design problems could be directly discussed and overcome with the US developers at the IBM software laboratories.

4. VECTOR COMPUTING

The 3-processor NEC SX-5 vector system is used for projects which require a fast single processor and can benefit from the vector architecture with access up to 10 GB of shared memory for a single code. A postprocessing code of MPI of Microstructure Physics for SX-5 output data could be significantly improved in vector performance. The netcdf library which supports a universal data format was implemented for usage with the ECHAM climate codes both on the SX-5 and the temporarily installed SX-4 system for MPI of Biogeochemistry. Gaussian was installed for MPI of Coal Research.

5. MULTIMEDIA

5.1 Visualization

The W7-X animations based on simulations by the stellarator theory group were selected to be shown at the "Medienfestival Bilder aus der Physik", organized by IWF (BMBF and DPG). The infrastructure and multimedia tools have also been extensively used for the colloquium of the PhD students at IPP and the annual summer university.

5.2 Video Conferencing

The IPP solution for the lecture halls at Garching and Greifswald proved to be very reliable over the last year. Rare problems arose from breakdowns of the ISDN links (approx. 10 times) and the GWiN. The VC systems together with the audio systems worked reliably, NetMeeting has more or less replaced the PowerPoint conference mode for practical reasons and is in regular use.

The present IPP infrastructure in videoconferencing (VC) has been presented together with a concept for a smooth transition from the ISDN-based standard H.320 to the IP-based H.323 in /802/. This led to an ad hoc study group from EFDA to set up a functionality requirements list for videoconferencing within a general teleconference infrastructure to support the remote participation activities of EFDA.

A H.323 concept for IPP has been worked out. This includes concrete propositions for ASDEX Upgrade, the replacements of the H.320 codecs in Greifswald and Garching, and use of the now available multipoint control units (MCU) of the DFN-Verein /802/.

6. DEVELOPMENTS IN NETWORKING

New network infrastructure was implemented at IPP. The goal was to use a cabling structure that can easily be adapted to future technologies. The data network realized was therefore based on the concept of a "collapsed backbone", consisting of switches at a few central locations which directly connect to all endpoints via links based on copper or fibre. This structure drastically enhances overall network performance, for all connections between centralized switches are now at a speed of 1 Gigabit/s (Gigabit Ethernet technology) with the option of implementing even more powerful trunks. Due to the availability of both multimode and monomode fibre optic cables between the premises it is also possible to adopt upcoming new network technologies such as 10 or 40-Gigabit Ethernet. With this structure we also improved the security and integrity of data because eavesdropping is almost impossible.

For logical security based on the functionality of the internet protocol suite TCP/IP a packet filter firewall at the access point to the internet was implemented, where all the incoming/outgoing packets are checked against a set of blocking or granting rules. Additionally all incoming electronic mail is scanned for

viruses and only clean and unobjectionable data (based on known problems) will be passed to the internal network.

During the last two years an innovative technique was built up and periodically extended for the new generation of the German science network, called G-WiN. As one out of nine, RZG is one of the core sites making up the backbone topology. A lot of the attachments to the internet for scientific and educational institutions are therefore implemented via RZG.

RZG itself also migrated to this powerful G-WiN with a speed of 155 Mbit/sec and an actual allowed incoming traffic of 6000 Mbyte/month, satisfying at the moment the need for high-bandwidth backups, which is realized for remote sites (as well as for all local machines, of course) by Tivoli Storage Manager TSM (see also 2.2)

7. PILOT PROJECTS FOR THE GERMAN GIGABIT SCIENCE NETWORK

In so-called Gigabit Testbeds (GTB), funded by the German government, pilot projects for the Gigabit Wissenschaftsnetz (GwiN) had been carried out. Results of the metacomputing project led by RZG were presented /234/. The experiences made facilitate future work with fast long-distance networks. Fast wide-area networks primarily offer chances for loosely coupled distributed applications. Tightly coupled distributed applications, however, still strongly benefit from the infrastructure of local-area networks.

8. DATA ACQUISITION AND DATA BASES FOR PLASMA FUSION EXPERIMENTS

The XDV group supports the experiments at IPP in data acquisition, archiving and processing. At the moment the data acquisition system for W7-X, which is just under construction at the institute in Greifswald, is in development. This system is responsible for archiving all diagnostic data that are produced during the long discharges of ca. 30 minutes. New procedures had to be developed to handle the huge amount of sampled data over the discharge period /595, 596, 658, 752, 872/.

Based on the experience with the first prototype of the data acquisition system proposed for W7-X, the concepts have been further developed. In addition to the continuous archiving of the sampled data, new requirements of the control system led to major extensions of the previous concepts. Both control systems of W7-X and of the ASDEX Upgrade tokamak experiment need information from distinguished diagnostic systems in "real time". The idea behind this requirement is to use the expertise of the diagnostic physicist to handle his own data and deliver meaningful values, in a physical sense, for control of the machine. To reach this objective, part of the previously introduced data streams are stripped off and processed immediately. The total concept with the extensions mentioned was verified with a second prototype.

The whole object-oriented design of the data acquisition was reviewed. The software and the corresponding objects, defining the configuration and the control parameters, were brought together and led to a global view of the total system. Development of the classes for the acquisition software and the persistent descriptor classes was started and has to be finished in the near future.

The object-oriented Objectivity database is used as data store. All measured values are archived together with the logged parameters and configuration in one database. This database contains all information that an analysis task needs for processing. The results are written to the same database by identical means. The setup parameters and configuration are stored in a second database. Some effort was expended on development of a general GUI-based object editor, which is needed for generating and editing parameter and configuration objects. The user interface for accessing database information was further developed. A whole set of new access routines for descriptor objects were implemented.

The time-measuring system of W7-X consists of a central clock and time-generating device that connects via a star-like fibre optic network to numerous slave time-capturing devices (TDC's and TTE's). Development of the hardware for the slave devices was started. Both interfaces are implemented as PCI cards. A first version of the TDC ("time to digital converter") was available for testing in the prototype system. To use the card, drivers for Windows NT and Linux had to be developed. The second improved version of the TDC is now under construction and will be available very soon. The TTE (time trigger event module) and the central timing device is being developed by the control group.

In close cooperation with the control groups of W7-X and ASDEX Upgrade, an abstraction of the real-time requirements was introduced. This "real-time data field" is a system-wide collection of data structures that in principle looks to an application like a global shared memory. The implementation of this data field will be different for W7-X and ASDEX Upgrade. W7-X intends to use the commonly available Ethernet as the transport medium. Data are transferred by means of the multicast properties of the Ethernet. ASDEX Upgrade uses special interfaces that implement the global shared memory in hardware. Implementation of the "real-time data field", as far as the diagnostic subsystems are concerned, has been started.

The second prototype also included a sample implementation of the monitoring system. The status of the experiment and the diagnostic stations will be presented during the long discharges. Distribution of the data of interest is done by means of the IP multicasting protocol, where one data stream corresponds to one IP multicast address. The data streams are reduced on the diagnostic stations and sent to one or more monitor servers. The server publishes evaluated and physically meaningful data on the net. The tasks of the monitor server have to be investigated in close cooperation with the physicists. This is also necessary for the event detection system, which was implemented only in a rudimentary form in this prototype. Further work has to be done on these subjects.

CENTRAL TECHNICAL SERVICES

(Head of Project: Dr.-Ing. Harald Rapp)

The Central Technical Services (ZTE) of Max-Planck-Institut für Plasmaphysik support the experimental divisions with the design, development, and construction of experiment components and diagnostic equipment. They also run all kinds of utilities for facility and experiment operation. The staff at Garching comprises approximately 140 craftsmen, technicians, and engineers plus 20 apprentices. At the Greifswald branch of IPP the Technical Services have rapidly developed and now have approximately 51 members.

1. MECHANICAL DESIGN AND CALCULATION

(J. Simon-Weidner)

Most of the department designs and calculates mechanical structures and components for experimental devices. Manpower was again dedicated to W7-X design with coil and vessel supports, feeds for cooling and current and in-vessel components. New activities were the supervision of construction of the vessel at the manufacturer's and construction of testing equipment for the modular coils at CEA in Saclay and coil diagnostic equipment. Other activities were contributions to ASDEX Upgrade and to high frequency heating devices and FE calculations for ITER. The commercial documentation software was replaced by a home-made solution.

1. ELECTRONICS DEVELOPMENT

(Acting: H. Rapp)

The department develops analogue and digital electronic equipment, including fast voltage switching and control devices for plasma heating systems. Successful development of a bolometer amplifier led to the production of 170 units, 70 of them for the Culham MAST tokamak. A new electronic timer was developed on the basis of special skills in the field of PLD's. Activities of the HV group were focused on system reliability and modulator development. The group assisted the Greifswald Technical Services in commissioning the new high-voltage pulse-step modulator device for plasma heating.

2. MATERIALS DEVELOPMENT

(J. Perchermeier)

The department offers services for functional surface treatment, galvanic technique, UHV plasma welding and vacuum testing, optical spectroscopy, chemical processing, including boronization and plastics technology. Special tasks were measurements of roughness and contamination of superconducting cables, vacuum tests of superconducting coil feed-throughs, killer pellet production for ASDEX Upgrade, and development of silicon carbide fibre coating. Support was given to developing plastics and insulation technology at Greifswald and supervising coil fabrication at the manufacturer's.

4. EXPERIMENTAL POWER SUPPLY

(M. Huart)

The department is responsible for supplying electric energy to the experiments. It consists of three groups for generators, high DC current, and high DC voltage. Its tasks include provision of operational support (incl. fault investigation and repair), speci-

fication and procurement of new equipment, refurbishment of old equipment, and regular maintenance. In addition, conceptual design studies are undertaken in-house. The overhaul of the EZ2 generator was completed and the generator re-assembled. The support of the EZ2 foundation slab was renewed by a set of improved spring-damper assemblies. The vibrations of the foundation slab were substantially reduced. A design study on paralleling of the EZ3 and EZ4 variable frequency grids was placed with Industry. A new 4 MVA thyristor converter was commissioned. Installation of thyristor converter No. 6, rated 2 * (1.25kV, 45kA or +/-22.5kA), started in June and was substantially completed. The control of HV modules 9-16 was upgraded to Simatic S7. Installation of two new HV outputs for the ECRH was nearly completed.

3. FACILITY OPERATION (acting: H. Rapp)

The department is charged with planning and supervising all kinds of facility installations and ensuring their maintenance. A contract for maintaining airing installations was placed and a 600 kVA diesel generator was installed. Due to the planned subway construction in front of IPP new groundwater pumping stations for experiment cooling were built. The Geographical Information System was continuously enlarged with data of all kinds of equipment.

4. WORKSHOPS (M. Keiner, W. Lösch)

The personnel and key posts were rejuvenated. Both experiments at Garching were strongly supported by mechanical and electrical manufacture and construction work. For the W7-X stellarator work-flow control at Garching was continued. Documentation of the demo cryostat was finished and forwarded to the project. Work routing and co-ordination of workshops and industry increased. The coil supports for testing at Saclay/France were completed.

5. GREIFSWALD TECHNICAL SERVICES

(G. Pfeiffer)

After finishing most of the construction work on the buildings, Technical Services were fully charged with facility operation and workshop and laboratory equipment. A major task became the installation and commissioning of the high DC voltage supply for the additional heating systems. With completion of one module the first step has nearly been completed. Technical support for stellarator experiment construction was continued with installation of platforms and the ECRH channel. Moreover, the WEGA experiment for plasma studies has been constructed and equipped with power and cooling supplies.

OFFICE OF THE DIRECTOR

(Dr. Hans-Stephan Bosch)

The Office of the Director provides the scientific management infrastructure of IPP and is responsible for project planning, information services, public relations, and general energy studies. In particular, it supports the Scientific Director in his overall responsibility for health and safety.

Scientific staff:

M. Biberacher, Dr. W. Dyckhoff, Dr. T. Farid, Dr. T. Hamacher, A. Hohaus, Dr. M. Hüls, Dr. P. Nieckchen, I. Milch, U. Schneider-Maxon, S. Richter**

**Doctoral students*

1. HEALTH AND SAFETY

The group supervises and coordinates all activities relating to industrial safety, radiation protection, laser protection, handling and transport of hazardous substances, special waste disposal, fire protection, and site supervision. In particular, it attends to safety matters which, for legal or practical reasons, cannot be delegated to the persons in charge of safety and radiation protection in the various divisions of IPP and therefore have to be supervised centrally.

Furthermore, the Health and Safety Division supports the legally responsible superiors and radiation safety officers in the execution and coordination of their duties and assists with safety organisation in the context of administrative and technical supervision of the divisions of IPP.

2. PUBLIC INFORMATION DEPARTMENT

The department informs the public on scientific research at IPP and on the latest developments in nuclear fusion research in general. This is done by providing information to the media through press releases and press conferences. In 2001 this resulted in 450 articles in German newspapers and magazines relating to IPP or fusion research. Brochures and publications for the general public and IPP's internet presentation are also provided by the Public Relations Department.

The group organises public events such as open days, public talks, and presentations at exhibitions and fairs. Special offers - tutorials and practicals - are provided for schoolchildren. A visitors service organises tours through the IPP sites at Garching and Greifswald. A quarterly newsletter in German "Energie-Perspektiven" (Energy Perspectives) is to stress the importance of energy

research in general. It is published in a printed version as well as on the internet: www.energie-perspektiven.de.

3. LIBRARY

This group runs the central libraries in Garching and in Greifswald, and oversees the smaller divisional libraries. Furthermore it provides support with respect to electronic search and retrieval of scientific literature.

4. PROJECT PLANNING

In annual programme presentations the projects and groups discuss the status and the plans of their research. Based on these data this group sets up the annual man power and budget needs as well as the medium-term planning of the institute.

5. EQUAL OPPORTUNITIES

The equal opportunities officer of IPP offers personal counselling in cases of career restraint, family care, mobbing, personal stress, sexual harassment, etc. As an important instrument in human resources development and as affirmative action, mentoring for scientists is planned to be implemented in cooperation with universities and other research institutions. Introducing the accepted strategy of gender mainstreaming will improve equal opportunity in the administration and scientific divisions. Furthermore, in 2001 we had six vacation project activities for children, two of them for girls only; a total of 70 children took part in these activities. More information at www.ipp.mpg.de/cg/.

6. ENERGY STUDIES

The energy studies supply information on the possible development of the energy system and the possible role of fusion therein.

6.1 SERF Studies

In 1997, the European Commission launched a series of studies called Socio-Economic Research on Fusion (SERF). After SERF I and II were concluded in 2001 preparation of SERF III was completed. IPP took responsibility for the macro tasks on “Long-term Energy Scenarios” and “External Costs of Fusion”. The goal of implementing a global energy model based on TIMES is to produce pictures of the future energy system – so-called scenarios - which include fusion as a major technology. TIMES is an energy model supported by the IEA to describe future energy systems. The dynamics of the system is described by a least-cost approach. In cooperation with the University of Stuttgart, the IER, the software tool is to be installed at IPP. The TIMES model describing Europe, adapted from the ECN MARKAL model, is to be further developed and used as nucleus of a global model. In cooperation with the Indian Institute of Management in Ahmedabad (IIMA) and the Netherlands centre of energy research (ECN), a study of long-term developments in the Indian energy system was launched. Results indicate that Indian energy supply is on the way to becoming very strongly dependent on coal. Fusion might play a role if reduction of greenhouse gas emission is seriously pursued.

The introduction of new electricity sources such as renewables or fusion might pose problems with their integration in the electricity network. The electricity network has to provide a reliable supply at all times at a fixed voltage and frequency. The study is being made in cooperation with the Chair of Electrical Engineering of the University of Rostock. A software tool capable of simulating the entire UCTE net is applied.

External costs are those costs incurred by an economic activity but not covered by the price paid by the consumer. In the framework of the European ExternE study a methodology was developed for application to fusion plants. The results indicate that the external costs of fusion are low.

6.2 EISS Study

Cadarache in France is one of the possible sites in Europe for ITER. A comprehensive study (www.efda.org) underlined

ADMINISTRATION AND GENERAL SERVICES

Administration and General Services is responsible for the commercial and administrative operations of IPP. In particular, these services support the scientific divisions in personnel, financial, legal, organisational and social matters as well as in procedures relating to purchasing and buildings. Control and planning are handled by the Auditing Department and the Control of W7-X project. Administration and General Services reports to the Managing Director (Dr. Karl. Tichmann) and Heads of Administration at Garching and Greifswald (Dr. Michael Winkler, Dr. Winfried König).

PERSONNEL DEPARTMENT

The personnel department is responsible for administrative matters relating to personnel. The personnel figures of the institute for 2001 were as follows (22.01.2002): Total personnel (including Greifswald and Berlin) 1069: 278 Scientists, 466 Technicians, 41 Directorate and Staff Representative Council, 37 General Services, 78 Administration, 169 other personnel.

CONTRACTS AND PURCHASING DEPARTMENT

The contracts and purchasing department is responsible for placing survey and follow-up of the relevant contracts and orders placed by IPP. In 2001, approximately 10,890 orders were made. They include complex contracts, many of which were signed after Europe-wide calls for tender. Furthermore, all export and import formalities are handled within this department: about 176 international and European shipments were carried out in 2001.

FINANCE AND ACCOUNTING DEPARTMENT

The finance and accounting department is responsible for the financial planning and all financial transactions and fiscal matters of IPP.

Total expenses in 2000:	134 MEURO
These expenses were financed as follows:	
Federal Republic of Germany, through Federal Ministry of Education and Research (BMBF)	78,5 MEURO
Bavaria	17,0 MEURO
Berlin	0,5 MEURO
Mecklenburg-Vorpommern	12,0 MEURO
EURATOM	21,0 MEURO
Other income	17,0 MEURO

SITE AND BUILDINGS DEPARTMENT

The site and buildings department is in charge of planning, construction, structural alteration and reconditioning of buildings and main service facilities. Building maintenance is also provided for the neighbouring Max Planck Institutes of

Astrophysics and Extraterrestrial Physics, the European Southern Observatory, the Greifswald branch of IPP and various guesthouses at Garching and Greifswald.

SOCIAL SERVICES DEPARTMENT

The social services department gives assistance to employees seeking housing, provides accommodation for guests in IPP residences, organizes transportation to outside locations, runs cleaning services and canteen service, supports staff in obtaining loans for the purchase of accommodation and surveys the public liability, fire and electronic insurance business of IPP.

LEGAL AND PATENT DEPARTMENT

The legal and patent department works out and controls co-operation contracts with German and foreign universities and research institutes. Concerning patent matters it attends to patent applications and supervision and licensing of patents in co-operation with Garching Innovation GmbH, a subsidiary of the Max Planck Society. In 2001 the division supervised 72 patents and similar rights.

AUDITING DEPARTMENT

The Auditing department is responsible for the auditing of workflow and proceedings within the administration of IPP with respect to their commercial efficiency and their compliance with regulations. The individual tasks are defined in an auditing plan, which is drawn up every year according to the directives of the Managing Director.

ORGANISATION DEPARTMENT

The main task of the Organisation Department is data processing for the IPP administration, i.e. coordination and development of SAP-related hardware and software, and SAP users throughout IPP as well as about 120 PC users, their workstations, software and the network in the administration. In addition, the department is in charge of organisational material such as forms and charts, organisation manuals and phonebook. Travel expense accounting was switched over to SAP in 2001.

Publications and Conference Reports

1. *Albertia**, S., *A. Arnold**, E. *Borie**, G. *Dammertz**, V. *Erckmann*, P. *Garin**, E. *Giguet**, S. *Illy**, G. *Le Cloarec**, Y. *Le Goff**, R. *Magne**, G. *Michel*, B. *Piosczyk**, C. *Tran**, M.Q. *Tran**, M. *Thumm** and D. *Wagner*: European High-Power CW Gyrotron Development for ECRH Systems. *Fusion Engineering and Design* **53**, 387-397 (2001).
2. *Alimov**, V.K., K. *Ertl* and J. *Roth*: Deuterium Retention and Lattice Damage in Tungsten Irradiated with D Ions. *Journal of Nuclear Materials* **290-293**, 389-393 (2001).
3. *Alimov**, V.K., K. *Ertl* and J. *Roth*: Deuterium Retention and Lattice Damage in Tungsten Irradiated with D Ions. *Physica Scripta* **T94**, 34-42 (2001).
4. *Allfrey**, S., A. *Bottino**, R. *Hatzky*, G. *Jost** and L. *Villard**: Characterization of Ion-Temperature (ITG) Modes in the W VII-X Stellarator Configuration. In: Proceedings of the 28th EPS Conference on Controlled Fusion and Plasma Physics, Funchal 2001, (Eds.) C.Silva, C.Varandas, D.Campbell. ECA 25A. European Physical Society, Geneva 2001, 1933-1936.
5. *Antonov**, A.N., Yu.P. *Bliokh**, O.F. *Kovpik**, E.A. *Kornilov**, M.G. *Lyubarskii**, K.V. *Matyash*, V.O. *Podobinskii**, V.G., *Svichenskii** and Ya.B. *Fainberg**: Effect of Plasma Nonlinearity on the Beam-Plasma Interaction in a Hybrid Plasma Waveguide. *Plasma Physics Reports* **27**, 251-258 (2001).
6. *Antonov**, A.N., E.A. *Kornilov**, O.F. *Kovpik**, K.V. *Matyash* and V.G. *Svichenskii**: Beam-Plasma Interaction in a Hybrid Plasma Waveguide in the Pulsed Mode of Microwave Generation. *Plasma Physics Reports* **27**, 614-618 (2001).
7. *Aquilonius**, K., B. *Hallberg**, D. *Hofman**, U. *Bergström**, Y. *Lechon**, H. *Cabal**, R.M. *Saez**, T. *Schneider**, S. *Lepicard**, D. *Ward**, T. *Hamacher* and R. *Korhonen**: Sensitivity and Uncertainty Analyses in External Cost Assessments of Fusion Power. *Fusion Engineering and Design* **58-59**, 1021-1026 (2001).
8. *Atanasiu**, C., S. *Günter*, K. *Lackner*, A. *Moraru** and A.A. *Subbotin**: Determination of the Influence of the Plasma Triangularity on the Tearing Mode Stability Parameter Δ for the ASDEX Upgrade Tokamak. In: Proceedings of the 28th EPS Conference on Controlled Fusion and Plasma Physics, Funchal 2001, (Eds.) C.Silva, C.Varandas, D.Campbell. ECA 25A. European Physical Society, Geneva 2001, 1105-1108.
9. *Baity**, F.W., G.C. *Barber**, R.H. *Goulding**, D.W. *Swain**, V. *Bobkov* and J.-M. *Noterdaeme*: The ORNL/ASDEX Upgrade RF Breakdown Tester: Results and Plans. In: Proc. 14th Topical Conference on Radiofrequency Power in Plasmas, Oxnard 2001, (Eds.) Tal Kuen Mau, J.de Grassie. AIP Conference Proceedings 595, AIP Press, Melville, NY 2001, 510-513.
10. *Balden*, M. and M. *Mayer*: Deuterium in Re-Deposited Silicon-Doped Carbon Layers and its Removal by Heating in Air. *Journal of Nuclear Materials* **298**, 225-230 (2001).
11. *Balden*, M., C. *García-Rosales**, R. *Behrisch*, J. *Roth*, P. *Paz** and J. *Etxebarria**: Chemical Erosion of Carbon Doped with Different Fine-Grain Carbides. *Journal of Nuclear Materials* **290-293**, 52-56 (2001).
12. *Balden*, M., S. *Picardle* and J. *Roth*: Mechanism of the Chemical Erosion of SiC under Hydrogen Irradiation. *Journal of Nuclear Materials* **290-293**, 47-51 (2001).
13. *Baldzuhn*, J. and A. *Werner*: Calculation of the Radial Electric Field Change during Radial Neutral Beam Injection into the Stellarator W7-AS. In: Proceedings of the 28th EPS Conference on Controlled Fusion and Plasma Physics, Funchal 2001, (Eds.) C.Silva, C.Varandas, D.Campbell. ECA 25A. European Physical Society, Geneva 2001, 1945-1948.
14. *Bao**, S., R. *Lindsay**, M. *Polcik**, A. *Theobald**, T. *Gieβel**, O. *Schaff**, P. *Baumgärtel**, R. *Terborg*, A.M. *Bradshaw*, N.A. *Booth** and D.P. *Woodruff**: Local Structure Determination for Benzene/NO Coadsorption on Ni(111) Using Scanned-Energy Mode Photoelectron Diffraction. *Surface Science* **478**, 35-48 (2001).
15. *Bartels*, H.-W.: Safety and Environmental Aspects of Fusion. In: Summer University for Plasma Physics, Garching 2001, (Eds.) A.Könies, K.Krieger. Max-Planck-Institut für Plasmaphysik, Garching 2001, 249-259.
16. *Basse*, N.P., S. *Zoletnik**, M. *Saffman**, M. *Endler* and M. *Hirsch*: Separation of L- and H-Mode Density Fluctuations in Dithering Wendelstein 7-AS Plasmas. In: Proceedings of the 28th EPS Conference on Controlled Fusion and Plasma Physics, Funchal 2001, (Eds.) C.Silva, C.Varandas, D.Campbell. ECA 25A. European Physical Society, Geneva 2001, 1941-1944.
17. *Bastasz**, R. and W. *Eckstein*: Plasma-Surface Interactions on Liquids. *Journal of Nuclear Materials* **290-293**, 19-24 (2001).
18. *Beckmann**, M. and F. *Leuterer*: Electron Cyclotron Current Drive at $w=w_c$ with X-Mode Launched from the Low Field Side. *Fusion Engineering and Design* **53**, 59-63 (2001).
19. *Behrisch*, R.: Measurements of Hydrogen Isotopes in Plasma-Facing Materials of Fusion Devices. *Physica Scripta* **T94**, 52-57 (2001).
20. *Behrisch*, R., M. *Mayer*, W. *Jacob*, W. *Assmann**, G. *Dollinger**, A. *Bergmaier**, U. *Kreissig**, M. *Friedrich**, G.Y. *Sun**, D. *Hildebrandt*, M. *Akbi**, W. *Schneider*, D. *Schleußner**, W. *Knapp** and C. *Edelmann**: Quantitative Analysis of Deuterium in Amorphous a-C:D Layers, a Round Robin Experiment. *Journal of Nuclear Materials* **281**, 42-56 (2001).
21. *Beidler*, C.D., Ya.I. *Kolesnichenko**, V.S. *Marchenko**, I.N. *Sidorenko* and H. *Wobig*: Stochastic Diffusion of Energetic Ions in Optimized Stellarators. *Physics of Plasmas* **8**, 2731-2738 (2001).
22. *Beidler*, C.D. and H. *Maaßberg*: An Improved Formulation of the Ripple-Averaged Kinetic Theory of Neoclassical Transport in Stellarators. *Plasma Physics and Controlled Fusion* **43**, 1131-1148 (2001).
23. *Beikler*, R. and E. *Taglauer*: Trajectory Resolved Analysis of LEIS Energy Spectra: Neutralization and Surface Structure. *Nuclear Instruments and Methods in Physics Research B* **182**, 180-186 (2001).
24. *Bergmann*, A., A.G. *Peeters* and S.D. *Pinches*: Guiding Center Particle Simulation of Wide-Orbit Neoclassical Transport. *Physics of Plasmas* **8**, 5192-5198 (2001).
25. *Berk**, H.L., D.N. *Borba**, B.N. *Breizmann**, S.D. *Pinches* and S. *Sharapov**: Theoretical Interpretation of Alfvén Cascades in Tokamaks with Nonmonotonic q Profiles Plasma. *Review Letters* **87**, 185003 (2001).
26. *Bessenrodt-Weberpals*, M., H. *Blank*, R. *Schneider* and A. *Könies*: Basic Plasma Physics. In: Summer University for Plasma Physics, Garching 2001, (Eds.) A.Könies, K.Krieger. Max-Planck-Institut für Plasmaphysik, Garching 2001, 23-41.
27. *Beurskens**, M., E. *Giovannozzi**, J. *Gunn**, Y. *Andrew**, M. *Brix**, J.-M. *Chareau**, K. *Erents**, C. *Gowers**, K. *Günther**, S. *Jachmich**, A. *Kallenbach*, A. *Korotkov**, E. *de la Luna**, P. *Morgan**, R. *Prentice**, M. *Proschek**, G. *Saibene**, W. *Suttrop*, J.-M.

Publications

- Traveere*, V. Tribaldos*, M. Zerbini* and EFDA-JET Work-programme Collaborators: Analysis of Plasma Edge Profiles at JET. In: Proceedings of the 28th EPS Conference on Controlled Fusion and Plasma Physics, Funchal 2001, (Eds.) C.Silva, C.Varandas, D.Campbell. ECA 25A. European Physical Society, Geneva 2001, 1229-1232.
28. Biedermann, C., T. Fuchs, G. Fußmann and R. Radtke: The Berlin Electron Beam Trap. In: Trapping Highly Charged Ions: Fundamentals and Applications, (Ed.) J.Gillaspy. Nova Science Publishers Inc., Huntington, NY 2001, 81-101.
29. Biedermann, C., R. Radtke, J.L. Schwob*, P. Mandelbaum*, R. Doron*, T. Fuchs and G. Fußmann: EUV Spectroscopy of Highly Charged Tungsten Ions Relevant to Hot Plasmas. *Physica Scripta* **T92**, 85-88 (2001).
30. Biel*, W., I. Ahmad*, C.J. Barth*, G. Bertschinger*, R. Dux, G. Fuchs*, M. von Hellermann*, H.R. Koslowski*, A. Krämer-Flecken*, M. Lehnen*, A. Marchuk*, H.J. v.d. Meiden*, J. Rapp*, B. Unterberg* and TEXTOR Team: Progress in Impurity Transport Studies on TEXTOR Using New VUV Spectrometers with High Time Resolution. In: Proceedings of the 28th EPS Conference on Controlled Fusion and Plasma Physics, Funchal 2001, (Eds.) C.Silva, C.Varandas, D.Campbell. ECA 25A. European Physical Society, Geneva 2001, 1389-1392.
31. Bilato, R., I. Pavlenko*, M. Brambilla and F. Meo: Simulation of RF Current Drive in Tokamaks in the Ion Cyclotron Frequency Range. In: Proceedings of the 28th EPS Conference on Controlled Fusion and Plasma Physics, Funchal 2001, (Eds.) C.Silva, C.Varandas, D.Campbell. ECA 25A. European Physical Society, Geneva 2001, 805-808.
32. Biskamp, D., K. Hallatschek, and E. Schwarz: Scaling Laws in Two-Dimensional Turbulent Convection. *Physical Review E* **63**, 045302 (2001).
33. Biskamp, D. and E. Schwarz: Localization, the Clue to Fast Magnetic Reconnection. *Physics of Plasmas* **8**, 4729-4731 (2001).
34. Biskamp, D. and E. Schwarz: On Two-Dimensional Magnetohydrodynamic Turbulence. *Physics of Plasmas* **8**, 3282-3292 (2001).
35. Block*, D., A. Piel*, C. Schröder* and T. Klinger: Synchronization of Drift Waves. *Physical Review E* **63**, 056401 (2001).
36. Block*, D., C. Schröder*, T. Klinger and A. Piel*: Influence of an Octupole Arrangement of Electrodes on Drift Waves. *Contributions to Plasma Physics* **41**, 455-460 (2001).
37. Bolshukhin, D., R. Neu, D. Schlögl, R. Dux and ASDEX Upgrade Team: Measurements of Spurious Impurity Concentrations in ASDEX Upgrade by X Ray Spectroscopy. *Review of Scientific Instruments* **72**, 4115-4124 (2001).
38. Bolshukhin, D., R. Neu, M.Yu. Kantor*, B. Kurzan and ASDEX Upgrade Team: Central Z_{eff} Measurements with a New PHA Diagnostic and its Further Applications on ASDEX Upgrade. In: Proceedings of the 28th EPS Conference on Controlled Fusion and Plasma Physics, Funchal 2001, (Eds.) C.Silva, C.Varandas, D.Campbell. ECA 25A. European Physical Society, Geneva 2001, 41-44.
39. Bolt, H.: Materials for Fusion. In: European White Book on Fundamental Research in Materials Science.(Eds.) M.Rühle, H.Dosch, E.J.Mittemeijer, M.H.Van de Voorde. Max-Planck-Institut für Metallforschung, Stuttgart 2001, 100-104.
40. Bonnin, X., R. Schneider, D.P. Coster, V. Rozhansky* and S. Voskoboynikov*: Electric Fields and Currents in an Island Divertor Configuration. *Journal of Nuclear Materials* **290-293**, 829-835 (2001).
41. Borchardt, M., J. Riemann, R. Schneider and X. Bonnin: W7-X Edge Modelling with the 3D SOL Fluid Code BoRiS. *Journal of Nuclear Materials* **290-293**, 546-550 (2001).
42. Bornatici*, M., R.A. Egorchenkov*, Yu.A. Kravtsov*, O. Maj* and E. Poli: Exact, Beam Tracing and Complex Geometrical Optics Solutions for the Propagation of Gaussian Electromagnetic Beams. In: Proceedings of the 28th EPS Conference on Controlled Fusion and Plasma Physics, Funchal 2001, (Eds.) C.Silva, C.Varandas, D.Campbell. ECA 25A. European Physical Society, Geneva 2001, 297-300.
43. Borrass, K.: Study of the Relation between Density and Temperature Fall-off Lengths in a Detached Divertor Plasma. *Journal of Nuclear Materials* **290-293**, 551-555 (2001).
44. Borrass, K., R.D. Monk, W. Suttrop, J. Schweinzer, J. Rapp*, J. Ongena*, G. Saibene*, L.D. Horton, V. Mertens and Contributors to the EFDA-JET Work Programme: Recent H-Mode Density Limit Studies at JET. In: Proceedings of the 28th EPS Conference on Controlled Fusion and Plasma Physics, Funchal 2001, (Eds.) C.Silva, C.Varandas, D.Campbell. ECA 25A. European Physical Society, Geneva 2001, 501-504.
45. Boscary, J., H. Greuner, F.W. Hoffmann, B. Mendelevitch, K. Pfefferle and H. Renner: Optimisation of Target Plates for the W7-X Divertor at Stationary Operation. *Fusion Engineering and Design* **56-57**, 279-283 (2001).
46. Bosch, H.-S.: Basic Nuclear Fusion. In: Summer University for Plasma Physics, Garching 2001, (Eds.) A.Könies, K.Krieger. Max-Planck-Institut für Plasmaphysik, Garching 2001, 9-22.
47. Bosch, H.-S. and A.M. Bradshaw: Kernfusion als Energiequelle der Zukunft. *Physikalische Blätter* **57**, 55-60 (2001).
48. Bosch, H.-S., W. Ullrich, D.P. Coster, O. Gruber, G. Haas, A. Kallenbach, R. Schneider, R. Wolf and ASDEX Upgrade Team: Helium Transport and Exhaust with an ITER-Like Divertor in ASDEX Upgrade. *Journal of Nuclear Materials* **290-293**, 836-839 (2001).
49. Bradshaw, A.M.: The Physics of a Lifetime: Reflections on the Problems and Personalities of 20th Century Physics by V.L. Ginzburg. *Nature* **412** (6843), 121-122 (2001).
50. Brakel, R., D. Hartmann, P. Grigull and W7-AS Team: ICRF Wall Conditioning Experiments in the W7-AS Stellarator. *Journal of Nuclear Materials* **290-293**, 1160-1164 (2001).
51. Brambilla, M.: Kinetic Wave Equations for Drift and Shear Alfvén Waves in Axisymmetric Toroidal Plasmas. *Plasma Physics and Controlled Fusion* **43**, 483-506 (2001).
52. Brambilla, M., R. Bilato and P. Bonoli*: Selfconsistent Simulation of Heating and Current Drive in Tokamak Plasma in the Ion Cyclotron Frequency Range. In: Proceedings of the 14th Topical Conference on Radiofrequency Power in Plasmas, Oxnard 2001, (Eds.) Tal Kuen Mau, J.de Grassie. AIP Conference Proceedings 595, AIP Press, Melville, NY 2001, 16-24 (2001).
53. Braun, F., F. Hofmeister, F. Wesner, W. Becker, H. Faugel, D. Hartmann and J.-M. Noterdaeme: ICRF System Enhancements at ASDEX Upgrade. *Fusion Engineering and Design* **56-57**, 551-555 (2001).
54. Brix*, M., A. Korotkov*, M. Lehnen*, P. Morgan*, K. McCormick, J. Schweinzer, D. Summers*, J. Vince* and Contributors to the EFDA-JET Work Programme: Determination of Edge Density Profiles in JET Using a 50 kV Lithium Beam. In: Proceedings of the

Publications

- 28th EPS Conference on Controlled Fusion and Plasma Physics, Funchal 2001, (Eds.) C.Silva, C.Varandas, D.Campbell. ECA 25A. European Physical Society, Geneva 2001, 389-392.
55. Bruhn*, B., A. Dinklage, B.-P. Koch* and C. Wilke*: Onset of Chaotic Wave Dynamics near the Critical Point in a Glow Discharge, Theory and Experiment. *Physics of Plasmas* **8**, 146-150 (2001).
56. Budny*, R.V., M. de Baar*, C.S. Chang*, C. Giroud*, R. Goldston*, A. Gondhalekar*, D. McCune*, M.F.F. Nave*, J.-M. Noterdaeme, J. Ongena*, F.W. Perkins*, E. Righi*, J. Strachan*, F. Suttin*, W. Suttrop, M. Valisa*, R.B. White*, K.-D. Zastrow* and Contributors to the EFDA-JET Work Programme: Comparison of Theory of ICRH-Induced Torques with Rotation Measurements in JET Plasmas. In: Proceedings of the 28th EPS Conference on Controlled Fusion and Plasma Physics, Funchal 2001, (Eds.) C.Silva, C.Varandas, D.Campbell. ECA 25A. European Physical Society, Geneva 2001, 481-484.
57. Bünde, R., M. Gottschewsky and S. Heinrich: Project Control of Wendelstein 7-X. *Fusion Engineering and Design* **58-59**, 803-808 (2001).
58. Bürbaumer*, H., R. Neu, R. Schneider, D.P. Coster, J. Stober, F. Aumayr* and H.P. Winter*: Extension of the B2-Code towards the Plasma Core for a Self-Consistent Simulation of ASDEX Upgrade Scenarios. *Journal of Nuclear Materials* **290-293**, 571-574 (2001).
59. Campbell*, D.J., R.J. Buttery*, C.D. Challis*, S. Günter and F. Nguyen*: Report on the 7th European Fusion Physics Workshop, Kloster Seeon, Germany, 8-10 December 1999. *Plasma Physics and Controlled Fusion* **43**, 603-628 (2001).
60. Campbell*, D.J., X. Garbet*, G.M.D. Hogewij*, P. Mantica*, A.G. Peeters, G. Saibene*, Y. Shimomura* and M.L. Watkins*: Report on the 8th European Fusion Physics Workshop. *Plasma Physics and Controlled Fusion* **43**, 985-1000 (2001).
61. Carlson, A.: Linearized Magnetohydrodynamic Theory of Langmuir Probes with Resistivity, Friction, and Polarization. *Physics of Plasmas* **8**, 4732-4739 (2001).
62. Carlson, A., D.P. Coster, A. Herrmann, R. Pugno, U. Wenzel and ASDEX Upgrade Team: Plasma Profiles in the Inner Divertor of ASDEX Upgrade. *Journal of Nuclear Materials* **290-293**, 575-578 (2001).
63. Chappuis*, P., E. Tsitrone*, M. Mayne*, X. Arnaud*, J. Linke*, H. Bolt, D. Petti* and J.P. Sharpe*: Dust Characterisation and Analysis in Tore Supra. *Journal of Nuclear Materials* **290-293**, 245-249 (2001).
64. Connor*, J.W., G. Bracco*, R.J. Buttery*, C. Hidalgo*, A. Jacchia*, A.G. Peeters and U. Stroth*: EU-US Transport Task Force Workshop on Transport in Fusion Plasmas, Transport Barrier Physics. *Plasma Physics and Controlled Fusion* **43**, 355-368 (2001).
65. Conway, G., C.D. Challis*, J.-M. Chareau*, T. Estrada*, J. Fessey*, N. Hawkes*, G.M.D. Hogewij*, X. Litaudon*, L. Meneses*, T. Ribeiro*, R. Sabot*, Y. Sarazin*, J. van Gorkom*, K.-D. Zastrow* and Contributors to the EFDA-JET Work Programme: Turbulence Behaviour during Electron Heated Reversed Shear Discharges in JET. In: Proceedings of the 28th EPS Conference on Controlled Fusion and Plasma Physics, Funchal 2001, (Eds.) C.Silva, C.Varandas, D.Campbell. ECA 25A. European Physical Society, Geneva 2001, 545-548.
66. Conway, G., A.G. Peeters, O. Gruber, A. Gude, S. Günter, J. Hobirk, B. Kurzan, M. Maraschek, H. Meister, H.W. Müller, T. Ribeiro*, F. Serra*, A.C.C. Sips, W. Suttrop and R. Wolf: Turbulence Reduction in Internal Transport Barriers on ASDEX Upgrade. *Plasma Physics and Controlled Fusion* **43**, 1239-1254 (2001).
67. Cordey*, J.G., D.C. McDonald*, K. Borrass, M. Charlet*, I. Coffey*, A. Kallenbach, K. Lawson*, P. Lomas*, J. Ongena*, J. Rapp*, F. Ryter, G. Saibene*, R. Sartori*, M. Stamp*, J. Strachan*, W. Suttrop, M. Valovic* and Contributors to the EFDA-JET Work Programme: Energy Confinement in Steady State ELMy H-Modes in JET. In: Proceedings of the 28th EPS Conference on Controlled Fusion and Plasma Physics, Funchal 2001, (Eds.) C.Silva, C.Varandas, D.Campbell. ECA 25A. European Physical Society, Geneva 2001, 969-972.
68. Coster, D.P., X. Bonnin, K. Borrass, H.-S. Bosch, B. Braams*, H. Bürbaumer*, A. Kallenbach, M. Kaufmann, J.W. Kim, E. Kovaltsov*, E. Mazzoli*, J. Neuhauser, D. Reiter*, V. Rozhansky*, R. Schneider, W. Ullrich, S. Voskoboinikov*, P. Xantopoulos* and ASDEX Upgrade Team: Recent Developments in Tokamak Edge Physics at Garching. In: Proceedings of the 18th Fusion Energy Conference, Sorrento 2000, IAEA, Vienna 2001, EXP4/20.
69. Coster, D.P., H.-S. Bosch, W. Ullrich and ASDEX Upgrade Team: B2-EIRENE Modelling of He Compression and Enrichment. *Journal of Nuclear Materials* **290-293**, 845-848 (2001).
70. Coster, D.P., G. Corrigan*, M. Beurskens*, K. Erents*, W. Fundamenski*, M. Stamp*, D. Reiser*, E. Tsitrone*, ASDEX Upgrade Team and Contributors to the EFDA-JET Work Programme: JET and ASDEX Upgrade Modeling. In: Proceedings of the 28th EPS Conference on Controlled Fusion and Plasma Physics, Funchal 2001, (Eds.) C.Silva, C.Varandas, D.Campbell. ECA 25A. European Physical Society, Geneva 2001, 1601-1604.
71. Counsell*, G.F., J.P. Coad*, G. Federici, K. Krieger, V. Philipps*, C.H. Skinner* and D.G. Whyte*: Towards an Improved Understanding of the Relationship between Plasma Edge and Materials Issues in a Next-Step Fusion Device. *Journal of Nuclear Materials* **290-293**, 255-259 (2001).
72. Da Silva*, F., M. Manso*, A. Silva* and ASDEX Upgrade Team: Simulation of Reflectometry Density Changes Using a 2D Full-Wave Code. *Review of Scientific Instruments* **72**, 311-314 (2001).
73. Dammertz*, G., S. Albertia*, A. Arnold*, E. Borie*, V. Erckmann, G. Gantenbein*, E. Giguet*, J.-P. Hogge*, S. Illy*, W. Kasperek*, K. Koppenburg*, H. Laqua, G. Le Cloarec*, Y. Le Goff*, W. Leonhardt*, C. Lievin*, R. Magne*, G. Michel, G. Müller*, G. Neffe*, M. Kuntze*, B. Piosczyk*, M. Schmid*, M. Thumm* and M.Q. Tran*: Development of a 140GHz, 1MW, Continuous Wave Gyrotron for the W7-X Stellarator. *FREQUENZ* **55**, 270-275 (2001).
74. Darrow*, D.S., A. Werner, A. Weller and W7-AS Team: Energetic Ion Loss Diagnostic for the Wendelstein 7-AS Stellarator. *Review of Scientific Instruments* **72**, 2936-2942 (2001).
75. D'Ippolito*, D.A., J.R. Myra*, P.M. Ryan*, E. Righi*, J.A. Heikkinen*, P. Lamalle*, J.-M. Noterdaeme and Contributors to the EFDA-JET Work Programme: Modeling of Mixed-Phasing Antenna-Plasma Interactions Applied to JET A2 Antennas. In: Proc. 14th Topical Conference on Radiofrequency Power in Plasmas, Oxnard 2001, (Eds.) Tal Kuen Mau, J.de Grassie. AIP Conference Proceedings 595, AIP Press, Melville, NY 2001, 114-117 (2001).
76. Dohmen, R., J. Pichlmeier, M. Petersen, F. Wagner and M. Scheffler: Parallel FP-LAPW for Distributed-Memory Machines. *Computing in Science & Engineering* **3**, 18-29 (2001).
77. Dose, V., J. Neuhauser, B. Kurzan, H. Murmann, H. Salzmann and ASDEX Upgrade Team: Tokamak Edge Profile Analysis Employing Bayesian Statistics. *Nuclear Fusion* **41**, 1671-1685 (2001).
78. Dose, V., R. Preuss and J. Roth: Evaluation of Chemical Erosion Data for Carbon Materials at High Ion Fluxes Using Bayesian Probability Theory. *Journal of Nuclear Materials* **288**, 153-162 (2001).

Publications

79. *Dumbrajs*, O., J.A. Heikkinen* and H. Zohm*: Electron Cyclotron Heating and Current Drive Control by Means of Frequency Step Tunable Gyrotrons. *Nuclear Fusion* **41**, 927-944 (2001).
80. *Durodié*, F., P. Lamalle*, G. Garici*, G. Amarante*, F.W. Baity*, B. Beaumont*, G. Bosia*, S. Brémond*, L. Colas*, J. Fanthome*, R. Goulding*, R. Koch*, A. Kaye*, G. Mazzone*, J.-M. Noterdaeme, Y. Pouleur*, V. Riccardo*, M. Roccella*, S. Sborchia*, A. Sibley*, P. Testoni*, P. Tigwell*, K. Vulliez* and R. Walton**: JET-EP ITER-Like ICRH Antenna. In: Proc. 14th Topical Conference on Radiofrequency Power in Plasmas, Oxnard 2001, (Eds.) Tal Kuen Mau, J.de Grassie. AIP Conference Proceedings 595, AIP Press, Melville, NY 2001, 122-125 (2001).
81. *Dux, R., C. Ingesson*, C. Giroud*, K.-D. Zastrow* and Contributors to the EFDA-JET Work Programme*: Impurity Behaviour in ITB Discharges with Reversed Shear on JET. In: Proceedings of the 28th EPS Conference on Controlled Fusion and Plasma Physics, Funchal 2001, (Eds.) C.Silva, C.Varandas, D.Campbell. ECA 25A. European Physical Society, Geneva 2001, 505-508.
82. *Eckstein, W., J.A. Stephens*, R.E.H. Clark*, J.W. Davis*, A.A. Haasz*, E. Vietzke* and Y. Hirooka** (Eds.): Particle Induced Erosion of Be, C and W in Fusion Plasmas. Part B: Physical Sputtering and Radiation-Enhanced Sublimation, Atomic and Plasma-Material Interaction Data for Fusion 7. IAEA, Vienna 2001, 188 p.
83. *Ehmler, H., K. McCormick, E. Wolfrum, P. Grigull, R. Burhenn, T. Klinger and W7-AS Team*: Carbon Density in the Wendelstein 7-AS Stellarator Measured with the High Energy Li-Beam. In: Proceedings of the 28th EPS Conference on Controlled Fusion and Plasma Physics, Funchal 2001, (Eds.) C.Silva, C.Varandas, D.Campbell. ECA 25A. European Physical Society, Geneva 2001, 2081-2084.
84. *Erckmann, V. and H.-J. Hartfuß*: Comments on the Emission and Absorption of a Magnetized Plasma in the Electron Cyclotron Range of Frequencies. *Physica Scripta* **63**, 173-175 (2001).
85. *Erckmann, V., H.P. Laqua, H. Maaßberg, J. Geiger, G. Dammertz*, W. Kasperek*, M. Thumm*, W7-X Team, W7-AS Team, W7-X Team (FZK Karlsruhe)* and W7-X Team (IPF Stuttgart)**: Electron Cyclotron Resonance Heating and EC-Current Drive Experiments at W7-AS, Status at W7-X. *Fusion Engineering and Design* **53**, 365-375 (2001).
86. *Fantz*, U., B. Heger and D. Wunderlich*: Using the Radiation of Hydrogen Molecules for Electron Temperature Diagnostics of Divertor Plasmas. *Plasma Physics and Controlled Fusion* **43**, 907-918 (2001).
87. *Fantz*, U. and S. Meir*: Diagnostics of Hydrocarbons and their Influence on Hydrogen Plasmas. In: Proceedings of the 28th EPS Conference on Controlled Fusion and Plasma Physics, Funchal 2001, (Eds.) C.Silva, C.Varandas, D.Campbell. ECA 25A. European Physical Society, Geneva 2001, 273-276.
88. *Fantz*, U., D. Reiter*, B. Heger and D.P. Coster*: Hydrogen Molecules in the Divertor of ASDEX Upgrade. *Journal of Nuclear Materials* **290-293**, 367-373 (2001).
89. *Fantz*, U., P. Starke and T. Ondak**: Diagnostics of Electron Distribution Functions in Planar ICP Sources. In: Proceedings of the 25th International Conference on Phenomena in Ionized Gases 4, Nagoya 2001, (Ed.) T.Goto. University of Nagoya 2001, 201-202.
90. *Federici, G., J.N. Brooks*, D.P. Coster, G. Janeschitz*, A.S. Kukushkin*, A. Loarte*, H.D. Pacher*, J. Stober and C.H. Wu*: Assessment of Erosion and Tritium Codeposition in ITER-FEAT. *Journal of Nuclear Materials* **290-293**, 260-265 (2001).
91. *Federici, G., C.H. Skinner*, J.N. Brooks*, J.P. Coad*, C. Grisolia*, A.A. Haasz*, A. Hassanein*, V. Philipps*, C.S. Pitcher*, J. Roth, W.R. Wampler* and D.G. Whyte**: Plasma-Material Interactions in Current Tokamaks and their Implications for Next-Step Fusion Reactors. *Nuclear Fusion* **41**, 1925-2137 (2001).
92. *Feist, J.-H., H.-J. Bramow, T. Bräuer, G. Gliege, U. Kamionka, B. Krause, M. Pieger-Frey and M. Wanner*: Quality Management for Wendelstein 7-X. *Fusion Engineering and Design* **58-59**, 809-813 (2001).
93. *Feist, J.-H. and W7-X Construction Team*: Technologies for the Fusion Experiment Wendelstein 7-X. In: Proceedings der Jahrestagung Kerntechnik, Dresden 2001, Deutsches Atomforum e.V.. INFORUM Verlags- und Verwaltungsgesellschaft mbH, Bonn 2001, 569-573.
94. *Feist, J.-H., M. Wanner and W7-X Construction Team*: Status of Wendelstein 7-X Construction. In: Proceedings of the 28th EPS Conference on Controlled Fusion and Plasma Physics, Funchal 2001, (Eds.) C.Silva, C.Varandas, D.Campbell. ECA 25A. European Physical Society, Geneva 2001, 1937-1940.
95. *Feng, Y., F. Sardei, J. Kisslinger, D. Reiter* and Yu.L. Iglikhanov*: Numerical Studies on Impurity Transport in the W7-AS Island Divertor. In: Proceedings of the 28th EPS Conference on Controlled Fusion and Plasma Physics, Funchal 2001, (Eds.) C.Silva, C.Varandas, D.Campbell. ECA 25A. European Physical Society, Geneva 2001, 1949-1952.
96. *Fischer, R. and V. Dose*: Analysis of Mixtures in Physical Spectra. In: Monographs of Official Statistics: Bayesian Methods, (Ed.) E.I.George. Eurostat, Luxembourg 2001, 145-154.
97. *Fischer, R., K.M. Hanson*, V. Dose and W. von der Linden**: Bayesian Background Estimation. In: Proceedings of the 19th International Workshop on Bayesian Inference and Maximum Entropy Methods in Science and Engineering, Boise, ID 1999, (Eds.) J.T.Rychert, G.J.Erickson, C.R.Smith. AIP Conference Proceedings 567, AIP Press, Melville, NY 2001, 193-212.
98. *Foley*, M., P.J. McCarthy*, J. Hobirk and O. Kardaun*: Expansion of ASDEX Upgrade's Real-Time Parameter Recovery Routine to Include Additional Moments in the Current Profile. In: Proceedings of the 28th EPS Conference on Controlled Fusion and Plasma Physics, Funchal 2001, (Eds.) C.Silva, C.Varandas, D.Campbell. ECA 25A. European Physical Society, Geneva 2001, 357-360.
99. *Franck*, C., T. Klinger, A. Piel* and H. Schamel**: Dynamics of Periodic Ion Holes in a Forced Beam-Plasma Experiment. *Physics of Plasmas* **8**, 4271-4274 (2001).
100. *Franke*, S., A. Dinklage, S. Solyman* and C. Wilke**: Power Loss by Resonance Radiation from a dc Neon Glow Discharge at Low Pressures and Low Currents. *Journal of Physics D* **34**, 340-346 (2001).
101. *Franke*, S., A. Dinklage and C. Wilke**: A New Method for Absolute Calibration of Laser-Induced Fluorescence Experiments. *Review of Scientific Instruments* **72**, 2048-2051 (2001).
102. *Franzen, P., S. Obermayer, J. Schäffler, A. Stäbler, E. Speth and O. Vollmer*: Beam Current Feedback Regulation of the RF Neutral Beam Sources of ASDEX Upgrade. *Fusion Engineering and Design* **56-57**, 487-491 (2001).
103. *Franzen, P., J. Sielanko*, R. Riedl and E. Speth*: An Alternative Residual Ion Dump for the ITER Neutral Beam System. *Fusion Engineering and Design* **56-57**, 511-515 (2001).
104. *Friedrich*, M., W. Pilz*, G.Y. Sun*, R.-D. Penzhorn*, N. Bekris*, R. Behrisch and C. Garcia-Rosales**: Tritium Depth Profiling by AMS in Carbon Samples from Fusion Experiments. *Physica Scripta* **T94**, 98-101 (2001).

Publications

105. *Fuchs, C. and M. Austin**: Measurements of Edge-Localized-Mode (ELM) Induced Electron Cyclotron Emission (ECE) Bursts in DIII-D. *Physics of Plasmas* **8**, 1594-1599 (2001).
106. *Fuchs, C., J. Geiger, H.-J. Hartfuß, H. Maaßberg and W7-AS Team*: Shafranov Shift in the "Electron Root" Feature at the W7-AS Stellarator. *Fusion Engineering and Design* **53**, 309-314 (2001).
107. *Fuchs, C. and H.-J. Hartfuß*: Extreme Broadband Multichannel ECE Radiometer with "Zoom" Device. *Review of Scientific Instruments* **72**, 383-386 (2001).
108. *Fuchs, C. and H.-J. Hartfuß*: Technology of the New Broadband Radiometer System. *Fusion Engineering and Design* **53**, 451-456 (2001).
109. *Fuchs, J.C., D.P. Coster, A. Herrmann, A. Kallenbach, K.-F. Mast and ASDEX Upgrade Team*: Radiation Distribution and Power Balance in the ASDEX Upgrade LYRA Divertor. *Journal of Nuclear Materials* **290-293**, 525-529 (2001).
110. *Fußmann, G., W. Bohmeyer, S. Klose and P. Kornejew*: Measurements of Parallel and Perpendicular Diffusion Coefficients in a Linear Plasma Device. In: Proceedings of the 10th International Conference on Plasma Physics, Quebec 2000. American Physical Society, College Park, MD 2001, 744-747.
111. *Gadelmeier, F., Y. Feng, P. Grigull, L. Giannone, J. Kisslinger, J. Knauer, K. McCormick, R. König, A. Werner, F. Wagner, U. Wenzel and W7-AS Team*: Conditions for Island Divertor Operation in the W7-AS Stellarator. In: Proceedings of the 28th EPS Conference on Controlled Fusion and Plasma Physics, Funchal 2001, (Eds.) C.Silva, C.Varandas, D.Campbell. ECA 25A. European Physical Society, Geneva 2001, 2085-2088.
112. *Gafert, J., W. Fundamenski*, M. Stamp*, J. Strachan* and Contributors to the EFDA-JET Work Programme*: Distribution of Carbon Impurity Sources between Low and High Field Side Measured via Zeeman-Spectroscopy in JET. In: Proceedings of the 28th EPS Conference on Controlled Fusion and Plasma Physics, Funchal 2001, (Eds.) C.Silva, C.Varandas, D.Campbell. ECA 25A. European Physical Society, Geneva 2001, 1637-1640.
113. *Gandini*, F., S. Cirant*, M. Hirsch, H.P. Laqua, S. Nowak*, A. Bruschi*, G. Granucci*, V. Erckmann, V. Mellera*, V. Muzzini*, A. Nardone*, A. Simonetto*, C. Sozzi* and N. Spinicchia**: The Detection of the Non-Absorbed Millimeterwave Power during EC Heating and Current Drive. *Fusion Engineering and Design* **56-57**, 975-979 (2001).
114. *Gandini*, F., M. Hirsch, S. Cirant*, V. Erckmann, G. Granucci*, W. Kasperek*, H.P. Laqua, V. Muzzini*, S. Nowak* and S. Radau*: Measurement of Stray EC Radiation on W7-AS Radio Frequency Power in Plasmas. In: Proceedings of the 14th Topical Conference on Radio Frequency Power in Plasmas, Oxnard, CA 2001, (Eds.) Tal Kuen Mau, J.de Grassie. AIP Conference Proceedings 595, AIP Press, Melville, NY 2001, 358-361.
115. *García-Cortes*, I., A. Loarte*, R. Balbin*, J. Bleuel, A. Chankin*, S.J. Davies*, M. Endler, K. Ereñts*, C. Hidalgo*, G.F. Matthews* and H. Thomsen*: Turbulent Transport Studies in JET Edge Plasmas in X-Point Configurations. *Journal of Nuclear Materials* **290-293**, 604-608 (2001).
116. *García-Rosales*, C. and M. Balden*: Chemical Erosion of Doped Graphites for Fusion Devices. *Journal of Nuclear Materials* **290-293**, 173-179 (2001).
117. *García-Rosales*, C., P. Paz*, J. Etxeberria*, M. Balden and R. Behrisch*: First Results on the Development of Improved Doped Carbon Materials for Fusion Applications. *Physica Scripta* **T91**, 130-133 (2001).
118. *Geier, A., R. Neu, H. Maier, K. Krieger and ASDEX Upgrade Team*: Divertor Retention for Metallic Impurities at ASDEX Upgrade. In: Proceedings of the 28th EPS Conference on Controlled Fusion and Plasma Physics, Funchal 2001, (Eds.) C.Silva, C.Varandas, D.Campbell. ECA 25A. European Physical Society, Geneva 2001, 169-172.
119. *Giroud*, C., K.-D. Zastrow*, P. Andrew*, R. Dux, P. Morgan*, M. O'Mullane*, G. Tresselt*, A.D. Whiteford* and Contributors to the EFDA-JET Work Programme*: Neon Transport in JET Plasmas Close to ITB Formation with Monotonic and Reversed q-Profiles. In: Proceedings of the 28th EPS Conference on Controlled Fusion and Plasma Physics, Funchal 2001, (Eds.) C.Silva, C.Varandas, D.Campbell. ECA 25A. European Physical Society, Geneva 2001, 549-552.
120. *Golan*, A. and V. Dose*: A Generalized Information Theoretical Approach to Tomographic Reconstruction. *Journal of Physics A* **34**, 1271-1283 (2001).
121. *Goldstraß, P., K.U. Klages and C. Linsmeier*: Surface Reactions on Beryllium after Carbon Vapor Deposition and Thermal Treatment. *Journal of Nuclear Materials* **290-293**, 76-79 (2001).
122. *Goldstraß, P. and C. Linsmeier*: Formation of Mixed Layers and Compounds on Beryllium due to C and CO Ion Bombardment. *Journal of Nuclear Materials* **290-293**, 71-75 (2001).
123. *Greuner, H., J. Glagla, O. Jandl, B. Mendelevitch, H. Renner and R. Rieck*: Concepts and Prototype Elements of Low-Z Wall Protection for the Stellarator W7-X. *Fusion Engineering and Design* **56-57**, 297-302 (2001).
124. *Grigull, P.*: First Island Divertor Experiments on W7-AS. *Stellarator News* **77**, 4-10 (2001), <http://www.ornl.gov/fed/stelnews>.
125. *Grigull, P., M. Hirsch, J. Baldzuhn, H. Ehmler, F. Gadelmeier, L. Giannone, H.-J. Hartfuß, D. Hildebrandt, R. Jaenicke, J. Kisslinger, R. König, K. McCormick, F. Wagner, A. Weller, C. Wendland and W7-AS Team*: Edge Transport Barrier Formation and ELM Phenomenology in the W7-AS Stellarator. *Journal of Nuclear Materials* **290-293**, 1009-1012 (2001).
126. *Grigull, P., K. McCormick, J. Baldzuhn, R. Burhenn, R. Brakel, H. Ehmler, Y. Feng, F. Gadelmeier, L. Giannone, D. Hartmann, D. Hildebrandt, M. Hirsch and R. Jaenicke*: First Island Divertor Experiments on the W7-AS Stellarator. *Plasma Physics and Controlled Fusion* **43**, A175-A193 (2001).
127. *Gruber, O., R. Arslanbekov, C. Atanasiu*, A. Bard, G. Becker, W. Becker, M. Beckmann, K. Behler, K. Behringer, A. Bergmann, R. Bilato, D. Bolshukhin, M. Brambilla, R. Brandenburg*, F. Braun, H. Brinkschulte, R. Brückner, B. Brüsehaber, K. Büchl, A. Buhler, H. Bürbaumer*, A. Carlson, M. Ciric, G. Conway, C. Dorn, R. Drube, R. Dux, S. Egorov, W. Engelhardt, H.-U. Fahrbach, U. Fantz*, H. Faugel, M. Foley*, P. Franzen, P. Fu*, J.C. Fuchs, J. Gafert, G. Gantenbein*, O. Gehre, A. Geier, J. Gernhardt, E. Gubanka, A. Gude, S. Günter, G. Haas, D. Hartmann, B. Heinemann, A. Herrmann, J. Hübirk, F. Hofmeister, H. Hohenöcker, L.D. Horton, L. Hu*, D. Jacobi, M. Jakobi, F. Jenko, A. Kallenbach, O. Karadaun, M. Kaufmann, A. Kendl, J.W. Kim, K. Kirov, R. Kochergov, H. Kollotzek, W. Kraus, K. Krieger, B. Kurzan, G. Kyriakakis*, K. Lackner, P.T. Lang, R.S. Lang, M. Laux, L.L. Lengyel, F. Leuterer, A. Lorenz, H. Maier, K. Mank*, M. Manso*, M. Maraschek, K.-F. Mast, P.J. McCarthy*, D. Meisel, H. Meister, F. Meo, R. Merkel, V. Mertens, J. Meskat, R.D. Monk, H.W. Müller, M. Münich, H. Murmann, G. Neu, R. Neu, J. Neuhauser, J.-M. Noterdaeme, I. Nunes*, G. Pautasso, A.G. Peeters, G. Pereverzev, S.D. Pinches, E. Poli, R. Pugno, G. Raupp, T. Ribeiro*, R. Riedl, S. Riondato, V. Rohde, H. Röhr, J. Roth, F. Ryter, H. Salzmann, W. Sandmann, S. Saarelma*, S. Schade, H.-B. Schilling, D. Schlögl, K. Schmidtman, R. Schneider, W. Schneider, G.*

Publications

- Schramm, J. Schweinzer, S. Schweizer, B.D. Scott, U. Seidel, F. Serra*, S. Sesnic*, C. Sihler, A. Silva*, A.C.C. Sips, E. Speth, A. Stäbler, K.-H. Steuer, J. Stober, B. Streibl, E. Strumberger, W. Suttrop, A. Tabasso, A. Tanga, G. Tardini, C. Tichmann, W. Treutterer, M. Troppmann, N. Tsois*, W. Ullrich, M. Ulrich, P. Varela*, O. Vollmer, U. Wenzel, F. Wesner, R. Wolf, E. Wolfrum, R. Wunderlich, N. Xantopoulos*, Q. Yu, M. Zarrabian, D. Zasche, T. Zehetbauer, H.-P. Zehrfeld, A. Zeiler and H. Zohm: Overview of ASDEX Upgrade Results. *Nuclear Fusion* **41**, 1369-1389 (2001).
128. Grulke, O., F. Greiner*, T. Klinger and A. Piel*: Comparative Experimental Study of Coherent Structures in a Simple Magnetized Torus. *Plasma Physics and Controlled Fusion* **43**, 525-542 (2001).
129. Grulke, O., T. Klinger, M. Endler, A. Piel* and W7-AS Team: Analysis of Large-Scale Fluctuation Structures in the Scrape-off Layer of the Wendelstein 7-AS Stellarator. *Physics of Plasmas* **8**, 5171-5180 (2001).
130. Günter, S., A. Gude, J. Hobirk, M. Maraschek, S. Saarelma*, S. Schade, R. Wolf and ASDEX Upgrade Team: MHD Phenomena in Advanced Scenarios on ASDEX Upgrade and the Influence of Localized Electron Heating and Current Drive. *Nuclear Fusion* **41**, 1283-1290 (2001).
131. Günter, S., A. Gude, M. Maraschek, S. Sesnic*, H. Zohm, ASDEX Upgrade Team and D.F. Howell*: High-Confinement Regime at High β_N Values due to a Changed Behaviour of the Neoclassical Tearing Modes. *Physical Review Letters* **87**, 275001 (2001).
132. Günter, S., A. Gude, M. Maraschek, S. Sesnic*, H. Zohm, ASDEX Upgrade Team, D.F. Howell*, Contributors to the EFDA-JET Work Programme and JET Task Force MHD: High Confinement Regime in the Presence of (3,2) Neoclassical Tearing Modes. In: Proceedings of the 28th EPS Conference on Controlled Fusion and Plasma Physics, Funchal 2001, (Eds.) C.Silva, C.Varandas, D.Campbell. ECA 25A. European Physical Society, Geneva 2001, 1321-1324.
133. Günter, S., K. Lackner, A. Stäbler and ASDEX Upgrade Team: Limitation of the Operational Regime due to MHD Instabilities in Conventional Scenarios on ASDEX Upgrade. *Fusion Engineering and Design* **54**, 41-47 (2001).
134. Günter, S., S.D. Pinches, G. Conway, A. Gude, J. Hobirk, M. Maraschek, A.G. Peeters, R. Wolf and ASDEX Upgrade Team: MHD Phenomena as Trigger for the Formation of Internal Transport Barriers on ASDEX Upgrade. In: Proceedings of the 28th EPS Conference on Controlled Fusion and Plasma Physics, Funchal 2001, (Eds.) C.Silva, C.Varandas, D.Campbell. ECA 25A. European Physical Society, Geneva 2001, 49-52.
135. Haasz*, A.A., J.A. Stephens*, E. Vietzke*, Eckstein, W., J.W. Davis* and Y. Hirooka*(Eds.): Particle Induced Erosion of Be, C and W in Fusion Plasmas. Part A: Chemical Erosion of Carbon-Based Materials, Atomic and Plasma-Material Interaction Data for Fusion **7**. (Ed.) IAEA, Vienna 2001, 277 p.
136. Hallatschek, K. and D. Biskamp: Transport Control by Coherent Zonal Flows in the Core/Edge Transitional Regime. *Physical Review Letters* **86**, 1223-1226 (2001).
137. Hamacher, T.: Economic and Environmental Aspects of Future Fusion Plants. In: Proceedings der Jahrestagung Kerntechnik, Dresden 2001, Deutsches Atomforum e.V.. INFORUM Verlags- und Verlagsgesellschaft mbH, Bonn 2001, 585-588.
138. Hamacher, T.: Lessons from the Development of Water Mills in the Early Middle Ages for the Future of Fusion. Lessons from History of Technology. In: Proceedings of the 28th EPS Conference on Controlled Fusion and Plasma Physics, Funchal 2001, (Eds.) C.Silva, C.Varandas, D.Campbell. ECA 25A. European Physical Society, Geneva 2001, 477-480.
139. Hamacher, T. and A.M. Bradshaw: Fusion as a Future Power Source: Recent Achievements and Prospects. In: Proceedings of the 18th World Energy Congress, Buenos Aires 2001, (Ed.) World Energy Council, London 2001, 01-06-06.
140. Hamacher, T., H. Cabal*, B. Hallberg*, R. Korhonen*, Y. Lechon*, R.M. Saez and L. Schleisner*: External Costs of Future Fusion Plants. *Fusions Engineering and Design* **54**, 405-411 (2001).
141. Hamacher, T., R. Korhonen*, K. Aquilonius*, H. Cabal*, B. Hallberg*, Y. Lechon*, S. Lepicard*, R.M. Saez*, T. Schneider* and D. Ward*: Radiological Impact of an Intense Fusion Economy. *Fusion Engineering and Design* **58-59**, 1037-1042 (2001).
142. Hamacher, T., P. Lako*, J.R. Ybema*, R. Korhonen*, K. Aquilonius*, H. Cabal*, B. Hallberg*, Y. Lechon*, S. Lepicard*, R.M. Saez*, T. Schneider* and D. Ward*: Can Fusion Help to Mitigate Greenhouse Gas Emissions? *Fusion Engineering and Design* **58-59**, 1087-1090 (2001).
143. Hamacher, T., R.M. Saez*, K. Aquilonius*, H. Cabal*, B. Hallberg*, R. Korhonen*, Y. Lechon*, S. Lepicard*, L. Schleisner*, T. Schneider* and D. Ward*: A Comprehensive Evaluation of the Environmental External Costs of a Fusion Power Plant. *Fusion Engineering and Design* **56-57**, 95-103 (2001).
144. Harmeyer, E., O. Jandl, J. Kisslinger and H. Wobig: Structural Analysis of the Helias Reactor Coil System. *Fusion Engineering and Design* **58-59**, 265-269 (2001).
145. Harmeyer, E., J. Kisslinger and H. Wobig: Some Aspects of the Coil System of a Stellarator Fusion Reactor. In: Proceedings der Jahrestagung Kerntechnik, Dresden 2001, Deutsches Atomforum e.V.. INFORUM Verlags- und Verlagsgesellschaft mbH, Bonn 2001, 589-592.
146. Hartmann, D.: Plasma Heating. In: Summer University for Plasma Physics, Garching 2001, (Eds.) A.Könies, K.Krieger. Max-Planck-Institut für Plasmaphysik, Garching 2001, 185-200.
147. Hartmann, D., M.-L. Mayoral*, J. Heikkinen*, J.-M. Noterdaeme, E. Righi*, P. Lamalle* and F. Rimini*: Coupling Resistance of the JET ICRH A2 Antennas in the Divertor Configuration Mark II GB. In: Proc. 14th Topical Conference on Radiofrequency Power in Plasmas, Oxnard 2001, (Eds.) Tal Kuen Mau, J.de Grassie. AIP Conference Proceedings 595, AIP Press, Melville,NY 2001, 130-133 (2001).
148. Hatayama*, A., H. Segawa*, N. Komatsu*, R. Schneider, D.P. Coster, N. Hayashi*, S. Sakurai* and N. Asakura*: Reversal of In-Out Asymmetry of the Particle Recycling Associated with X-Point MARFE and Plasma Detachment. *Journal of Nuclear Materials* **290-293**, 407-412 (2001).
149. Hawkes*, N., B.C. Stratton*, C.D. Challis*, G. Conway, R. de Angelis*, C. Giroud*, J. Hobirk, E. Joffrin*, P. Lomas*, P. Lotte*, J. Mailloux*, D. Mazon*, E. Rachlew*, S. Reyes-Cortes*, E. Solano* and K.-D. Zastrow*: Observation of Zero Current Density in the Core of JET Discharges with Lower Hybrid Heating and Current Drive. *Physical Review Letters* **87**, 115001 (2001).
150. Heger, B. and U. Fantz*: Modification of the Ground State Vibrational Population of Molecular Hydrogen and Deuterium by Different Wall Materials in Low Temperature Plasmas. In: Proceedings of the 28th EPS Conference on Controlled Fusion and Plasma Physics, Funchal 2001, (Eds.) C.Silva, C.Varandas, D.Campbell. ECA 25A. European Physical Society, Geneva 2001, 261-264.
151. Heger, B., U. Fantz*, K. Behringer and ASDEX Upgrade Team: Vibrational Population of the Ground State of H₂ and D₂ in the Divertor of ASDEX Upgrade. *Journal of Nuclear Materials* **290-293**, 413-417 (2001).

Publications

152. *Hergenbahn, U., O. Kugeler, A. Rüdeler*, E.E. Rennie and A.M. Bradshaw*: Symmetry-Selective Observation of the N 1s Shape Resonance in N₂. *Journal of Physical Chemistry A* **105**, 5704-5708 (2001).
153. *Herrmann, A. and ASDEX Upgrade Team*: Limitations for Divertor Heat Flux Calculations of Fast Events in Tokamaks. In: *Proceedings of the 28th EPS Conference on Controlled Fusion and Plasma Physics*, Funchal 2001, (Eds.) C.Silva, C.Varandas, D.Campbell. ECA 25A. European Physical Society, Geneva 2001, 2109-2112.
154. *Herrmann, A., A. Carlson, J.C. Fuchs, O. Gruber, M. Laux, J. Neuhauser, R. Pugno, A.C.C. Sips, W. Treutterer, W. Schneider and ASDEX Upgrade Team*: Heat Flux Decay Length in the Midplane of ASDEX Upgrade. *Journal of Nuclear Materials* **290-293**, 619-622 (2001).
155. *Hildebrandt, D., P. Grigull, K. McCormick, J. Roth, W. Schneider and W7-AS Team*: Erosion Measurements on the Inner Wall of the Stellarator W7-AS. In: *Proceedings of the 28th EPS Conference on Controlled Fusion and Plasma Physics*, Funchal 2001, (Eds.) C.Silva, C.Varandas, D.Campbell. ECA 25A. European Physical Society, Geneva 2001, 2089-2092.
156. *Hildebrandt, D., P. Wienhold* and W. Schneider*: Mixed-Material Coating Formation on Tungsten Surfaces during Plasma Exposure in TEXTOR-94. *Journal of Nuclear Materials* **290-293**, 89-93 (2001).
157. *Hirsch, M., E. Holzhauer*, J. Baldzuhn and B. Kurzan*: Doppler Reflectometry for the Investigation of Propagating Density Perturbations. *Review of Scientific Instruments* **72**, 324-327 (2001).
158. *Hirsch, M., E. Holzhauer*, J. Baldzuhn, B. Kurzan and B.D. Scott*: Doppler Reflectometry for the Investigation of Propagating Density Perturbations. *Plasma Physics and Controlled Fusion* **43**, 1641-1660 (2001).
159. *Hobirk, J., R. Wolf, O. Gruber, A. Gude, S. Günter, B. Kurzan, M. Maraschek, P.J. McCarthy*, H. Meister, A.G. Peeters, G. Pereverzev, J. Stober and ASDEX Upgrade Team*: High β_{pol} Discharges at the Greenwald Density with Mainly Non-Inductive Driven Current in ASDEX Upgrade. In: *Proceedings of the 28th EPS Conference on Controlled Fusion and Plasma Physics*, Funchal 2001, (Eds.) C.Silva, C.Varandas, D.Campbell. ECA 25A. European Physical Society, Geneva 2001, 913-916.
160. *Hobirk, J., R. Wolf, O. Gruber, A. Gude, S. Günter, B. Kurzan, M. Maraschek, P.J. McCarthy*, H. Meister, A.G. Peeters, G. Pereverzev, J. Stober, W. Treutterer and ASDEX Upgrade Team*: Reaching High Poloidal Beta at Greenwald Density with Internal Transport Barrier Close to Full Noninductive Current Drive. *Physical Review Letters* **87**, 085002 (2001).
161. *Hoffmann, D.H.H. and M. Stetter**: Interaction of Heavy Ions with Dense Plasma. In: *Summer University for Plasma Physics*, Garching 2001, (Eds.) A.Könies, K.Krieger. Max-Planck-Institut für Plasmaphysik, Garching 2001, 233-247.
162. *Hogeweyj*, G.M.D., Y. Baranov*, C.D. Challis*, G. Conway, F. Crisanti*, M. De Baar*, N. Hawkes*, F. Imbeaux*, X. Litaudon*, J. Mailloux*, F. Rimini*, S. Sharapov*, B.C. Stratton*, R. Wolf, K.-D. Zastrow* and Contributors to the EFDA-JET Work Programme*: Electron Heated Internal Transport Barriers in JET. In: *Proceedings of the 28th EPS Conference on Controlled Fusion and Plasma Physics*, Funchal 2001, (Eds.) C.Silva, C.Varandas, D.Campbell. ECA 25A. European Physical Society, Geneva 2001, 485-488.
163. *Horton, L.D. and JET Team*: Pellet Fuelling and ELMy H Mode Physics in JET. *Nuclear Fusion* **41**, 189-196 (2001).
164. *Igitkhanov, Yu.L. and G. Janeschitz**: Attenuation of Secondary Electron Emission from Divertor Plates due to Magnetic Field Inclination. *Journal of Nuclear Materials* **290-293**, 99-103 (2001).
165. *Igitkhanov, Yu.L., M. Sugihara*, O.P. Pogutse*, H.R. Wilson*, J.W. Connor*, H. Wobig, P. Grigull, M. Hirsch, G. Janeschitz*, A. Loarte*, G. Saibene*, R. Sartori*, G. Pacher* and H.D. Pacher**: A Physics Picture of Type I ELMs. In: *Proceedings of the 28th EPS Conference on Controlled Fusion and Plasma Physics*, Funchal 2001, (Eds.) C.Silva, C.Varandas, D.Campbell. ECA 25A. European Physical Society, Geneva 2001, 1693-1696.
166. *Imbeaux*, F., F. Ryter and X. Garbet**: Modelling of ECH Modulation Experiments in ASDEX Upgrade with an Empirical Critical Temperature Gradient Length Transport Model. *Plasma Physics and Controlled Fusion* **43**, 1503-1524 (2001).
167. *Ingesson*, C., J.C. Fuchs, R. Barnsley*, D.P. Coster, W. Fundamenski*, A. Huber*, G.F. Matthews*, D.C. McDonald*, F. Milani*, R. Neu, V. Philipps*, M. Stamp* and EFDA-JET Workprogramme Collaborators*: Radiation Distribution and Neutral-Particle Loss in High-Density Plasmas in the JET MKI-IGB Divertor. In: *Proceedings of the 28th EPS Conference on Controlled Fusion and Plasma Physics*, Funchal 2001, (Eds.) C.Silva, C.Varandas, D.Campbell. ECA 25A. European Physical Society, Geneva 2001, 1633-1636.
168. *Isobe*, M., S. Okamura*, K. Matsuoka*, N. Nakajima*, A. Shimizu*, S. Nishimura*, C. Suzuki*, S. Murakami*, A. Fujisawa*, C. Nührenberg and J. Nührenberg*: Neoclassical Bootstrap Current in CHS-qa Quasi-Axisymmetric Stellarator. In: *Proceedings of the 28th EPS Conference on Controlled Fusion and Plasma Physics*, Funchal 2001, (Eds.) C.Silva, C.Varandas, D.Campbell. ECA 25A. European Physical Society, Geneva 2001, 761-764.
169. *Itoh*, K., S.-I. Itoh* and L. Giannone*: Modelling of Density Limit Phenomena in Toroidal Helical Plasmas. *Journal of the Physical Society of Japan* **70**, 3274-3284 (2001).
170. *Jachmich*, S., M. Laux, M. Becoulet*, T. Eich*, A. Loarte*, G.F. Matthews*, V. Philipps*, W. Fundamenski* and M. Stamp**: Novel Method to Study SOL-Response to ELMs by Divertor Target Probes in JET. In: *Proceedings of the 28th EPS Conference on Controlled Fusion and Plasma Physics*, Funchal 2001, (Eds.) C.Silva, C.Varandas, D.Campbell. ECA 25A. European Physical Society, Geneva 2001, 1617-1620.
171. *Jacob, W.*: Plasma Technology. In: *Summer University for Plasma Physics*, Garching 2001, (Eds.) A.Könies, K.Krieger. Max-Planck-Institut für Plasmaphysik, Garching 2001, 217-231.
172. *Jacob, W., A. von Keudell, and T. Schwarz-Selinger*: ERRATUM: Infrared Analysis of Thin Films: Amorphous, Hydrogenated Carbon on Silicon. *Brazilian Journal of Physics* **31**, 109 (2001).
173. *Jaksic, N., J. Simon-Weidner and J. Sapper*: Final Structural and Mechanical Evaluation of the W7-X Magnet Support System. *Fusion Engineering and Design* **58-59**, 259-263 (2001).
174. *Jauregi*, E., D. Ganuza*, I. Garcia*, J.M. Del Rio* and T. Rummel*: Power Supply of the Control Coils of Wendelstein 7-X Experiment. *Fusion Engineering and Design* **58-59**, 79-86 (2001).
175. *Jenko, F. and W. Dorland**: Nonlinear Electromagnetic Gyrokinetic Simulations of Tokamak Plasmas. *Plasma Physics and Controlled Fusion* **43**, A141-A150 (2001).
176. *Jenko, F., W. Dorland* and G.W. Hammett**: Critical Gradient Formula for Toroidal Electron Temperature Gradient Modes. *Physics of Plasmas* **8**, 4096-4104 (2001).

Publications

177. *JET Team and A.C.C. Sips*: Internal Transport Barrier Discharges in JET and their Sensitivity to Edge Conditions. *Nuclear Fusion* **41**, 1559-1566 (2001).
178. *Johnson*, T., T. Hellsten*, M. Mantsinen*, V. Kiptily*, S. Sharapov*, J. Hedin*, J.-M. Noterdaeme, M.-L. Mayoral*, F. Nguyen* and Contributors to the EFDA-JET Work Programme*: RF-Induced Pinch of Resonant ^3He Minority Ions in JET. In: Proc. 14th Topical Conference on Radiofrequency Power in Plasmas, Oxnard 2001, (Eds.) Tal Kuen Mau, J.de Grassie. AIP Conference Proceedings 595, AIP Press, Melville, NY 2001, 102-105 (2001).
179. *Jones*, T.T.C., A. Bickley*, R. Felton*, P. Lamalle*, K. Lawson*, G.P. Maddison*, M. Mantsinen*, J.-M. Noterdaeme, S. Podda*, E. Righi*, Y. Sarazin*, A. Stäbler, A.A. Tuccillo* and Contributors to the EFDA-JET Work Programme*: Simulation of Alpha Particle Plasma Self-Heating Using ICRH under Real-Time Control. In: Proceedings of the 28th EPS Conference on Controlled Fusion and Plasma Physics, Funchal 2001, (Eds.) C.Silva, C.Varandas, D.Campbell. ECA 25A. European Physical Society, Geneva 2001, 1197-1200.
180. *Jory*, H., D. Wagner, M. Blank*, S. Chu* and K. Felch**: Compact Mode Converter System for the Cold Test of Assembled Gyrotrons. *International Journal of Infrared and Millimeter Waves* **22**, 1395-1407 (2001).
181. *Jüttner, B.*: Topical Review: Cathode Spots of Electric Arcs. *Journal of Physics D* **34**, R103-R123 (2001).
182. *Kallenbach, A., M. Beurskens*, R. Dux, K. Ereñts*, W. Fundamenski*, A. Korotkov*, B. Kurzan, H.W. Müller, J. Neuhauser, W. Sandmann, Contributors to the EFDA-JET Work Programme and ASDEX Upgrade Team*: Comparison of the H-Mode Pedestal Density and its Underlying Physics on JET and ASDEX Upgrade. In: Proceedings of the 28th EPS Conference on Controlled Fusion and Plasma Physics, Funchal 2001, (Eds.) C.Silva, C.Varandas, D.Campbell. ECA 25A. European Physical Society, Geneva 2001, 949-952.
183. *Kallenbach, A., A. Carlson, G. Pautasso, A.G. Peeters, U. Seidel, H.-P. Zehrfeld and ASDEX Upgrade Team*: Electric Currents in the Scrape-off Layer in ASDEX Upgrade. *Journal of Nuclear Materials* **290-293**, 639-643 (2001).
184. *Kang*, J.-H., R.L. Toomes*, J. Robinson*, D.P. Woodruff*, R. Terborg, M. Polcik*, J.-T. Hoefl*, P. Baumgärtel* and A.M. Bradshaw*: Local Structure of CO Coadsorbed with O on Ni(111): A Temperature-Dependent Study. *Journal of Physical Chemistry B* **105**, 3701-3707 (2001).
185. *Kasperek*, W., L. Empacher*, V. Erckmann, G. Gantenbein*, F. Hollmann, H.P. Laqua, P. Schüller*, M. Weißgerber* and H. Zohm*: Mirror Development for the 140 GHz ECRH. Transmission System on the Stellarator W7-X. *Fusion Engineering and Design* **53**, 545-551 (2001).
186. *Kendl, A.*: Gyrokinetic Analysis of Microinstabilities in a Stellarator Reactor. *Plasma Physics and Controlled Fusion* **43**, 1559-1571 (2001).
187. *Kendl, A. and B.D. Scott*: Influence of Flux Surface Shape on Microinstabilities and Turbulence. In: Proceedings of the 28th EPS Conference on Controlled Fusion and Plasma Physics, Funchal 2001, (Eds.) C.Silva, C.Varandas, D.Campbell. ECA 25A. European Physical Society, Geneva 2001, 1905-1908.
188. *Keudell, A. von, M. Meier and C. Hopf*: Fundamental Growth Mechanisms during PECVD of Carbon Thin Films. In: Proceedings of the 13th International Colloquium on Plasma Processes, Antibes 2001, (Ed.) Société Française du Vide, Paris 2001, 137-141.
189. *Keudell, A. von, T. Schwarz-Selinger and W. Jacob*: Simultaneous Interaction of Methyl Radicals and Atomic Hydrogen with Amorphous Hydrogenated Carbon Films. *Journal of Applied Physics* **89**, 2979-2986 (2001).
190. *Keudell, A. von, T. Schwarz-Selinger and W. Jacob*: Simultaneous Interaction of Methyl Radicals and Atomic Hydrogen with Amorphous Hydrogenated Carbon Films, as Investigated with Optical in situ Diagnostics. *Applied Physics A* **72**, 551-556 (2001).
191. *Keudell, A. von, T. Schwarz-Selinger, W. Jacob and A. Stevens**: Surface Reactions of Hydrocarbon Radicals: Suppression of the Re-Deposition in Fusion Experiments via a Divertor Liner. *Journal of Nuclear Materials* **290-293**, 231-237 (2001).
192. *Kim, J.W., D.P. Coster, J. Neuhauser, R. Schneider and ASDEX Upgrade Team*: ASDEX-Upgrade Edge Transport Scalings from the Two-Dimensional Interpretative Code B2.5-I. *Journal of Nuclear Materials* **290-293**, 644-647 (2001).
193. *Kirk*, A., J.-W. Ahn*, D.P. Coster, G.F. Counsell* and W. Fundamenski**: Analysis of SOL Behaviour in MAST Using an Advanced Onion-Skin Solver (OSM2). In: Proceedings of the 28th EPS Conference on Controlled Fusion and Plasma Physics, Funchal 2001, (Eds.) C.Silva, C.Varandas, D.Campbell. ECA 25A. European Physical Society, Geneva 2001, 221-224.
194. *Kiss'ovsky, Z., W. Bohmeyer and H.-D. Reiner*: Measurement of Flow Velocity in the Plasma Generator PSI-2. *Contributions to Plasma Physics* **41**, 517-523 (2001).
195. *Kittel*, M., M. Polcik*, R. Terborg, J.-T. Hoefl*, P. Baumgärtel*, A.M. Bradshaw, R.L. Toomes*, J.-H. Kang*, D.P. Woodruff*, M. Pascal*, C.L.A. Lamont* and E. Rotenberg**: The Structure of Oxygen on Cu(100) at Low and High Coverages. *Surface Science* **470**, 311-324 (2001).
196. *Kivimäki*, A., U. Hergenbahn, B. Kempgens*, R. Hentges*, M.N. Piancastelli*, K. Maier, A. Rüdell*, J.J. Tulkki* and A.M. Bradshaw*: A Near-Threshold Study of Xe 3d Photoionization. *Physical Review A* **63**, 012716 (2001).
197. *Kiviniemi*, T.P., J.A. Heikkinen*, A.G. Peeters and S.K. Sipilä**: Comparison of $E \times B$ Flow Shear in JET and ASDEX Upgrade by Monte Carlo Simulations. In: Proceedings of the 28th EPS Conference on Controlled Fusion and Plasma Physics, Funchal 2001, (Eds.) C.Silva, C.Varandas, D.Campbell. ECA 25A. European Physical Society, Geneva 2001, 1641-1644.
198. *Kiviniemi*, T.P., J.A. Heikkinen*, A.G. Peeters and S.K. Sipilä**: Monte Carlo Guiding-Centre Simulations of $E \times B$ Flow Shear in Edge Transport Barrier. *Plasma Physics and Controlled Fusion* **8**, 1103-1118 (2001).
199. *Kleiber, R.*: Resistive Drift Modes in General Geometry. *Physics of Plasmas* **8**, 4090-4095 (2001).
200. *Klinger, T., C. Schröder*, D. Block*, F. Greiner*, A. Piel*, G. Bonhomme* and V. Naulin**: Chaos Control and Taming of Turbulence in Plasma Devices. *Physics of Plasmas* **8**, 1961-1968 (2001).
201. *Klose, S., W. Bohmeyer, M. Laux, H. Meyer*, G. Fußmann and PSI-2-Team*: Investigation of Ion Drift Waves in the PSI-2 Using Langmuir Probes. *Contributions to Plasma Physics* **41**, 467-472 (2001).
202. *Koch*, B., W. Bohmeyer, G. Fußmann, P. Kornejew and H.-D. Reiner*: Energy Flux Measurements in a Steady-State Discharge at PSI-2. *Journal of Nuclear Materials* **290-293**, 653-657 (2001).
203. *Koepke*, M.E., A. Dinklage, T. Klinger and C. Wilke**: Spatiotemporal Signatures of Periodic Pulling during Ionization-Wave Mode Transitions. *Physics of Plasmas* **8**, 1432-1436 (2001).

Publications

204. Kohl, A., C. Linsmeier, E. Taglauer and H. Knözinger*: Influence of Support and Promotor on the Catalytic Activity of Rh/VO_x/SiO₂ Model Catalysts. *Physical Chemistry Chemical Physics* **3**, 4639-4643 (2001).
205. Kolesnichenko*, Ya.I., V.V. Lutsenko*, V.V., H. Wobig, Yu.V. Yakovenko* and O.P. Fesenyuk*: Alfvén Continuum and High-Frequency Eigenmodes in Optimized Stellarators. *Physics of Plasmas* **8**, 491-509 (2001).
206. Könies, A. and K. Krieger (Eds.): Summer University for Plasma Physics, Garching 2001. Max-Planck-Institut für Plasmaphysik, Garching 2001, 274 p.
207. König, R., K. McCormick, Y. Feng, S. Fiedler, P. Grigull, D. Hildebrandt, J. Kisslinger, J. Knauer, G. Kühner, D. Naujoks, J. Sallander, F. Sardei, F. Wagner, A. Werner and W7-AS Team: Island Divertor Investigations on the W7-AS Stellarator. *Journal of Nuclear Materials* **290-293**, 882-886 (2001).
208. Kornejew, P., W. Bohmeyer, H.-D. Reiner and C.H. Wu: Chemical Erosion of CFC at High Ion Flux Densities. *Physica Scripta* **T91**, 29-32 (2001).
209. Köttler, S., H. Bolt, H. Greuner, A. Huber*, J. Linke*, M. Mayer, A. Pospieszczyk*, H. Renner, J. Roth, B. Schweer*, G. Sergienko* and D. Valenza: Development of Thick B₄C Coatings for the First Wall of W7-X. *Physica Scripta* **T91**, 117-123 (2001).
210. Kraus, W., P. Franzen, B. Heinemann, E. Speth and O. Vollmer: Recent Developments of Long Pulse RF Ion Sources for NBI Systems. *Fusion Engineering and Design* **56-57**, 499-503 (2001).
211. Krieger, K.: Plasma-Wall Interaction in Fusion Devices with Magnetic Confinement. In: Summer University for Plasma Physics, Garching 2001, (Eds.) A.Könies, K.Krieger. Max-Planck-Institut für Plasmaphysik, Garching 2001, 201-216.
212. Krieger, K., H. Maier, R. Neu, V. Rohde and A. Tabasso: Plasma-Wall Interaction at the ASDEX Upgrade Tungsten Heat Shield. *Fusion Engineering and Design* **189**, 56-57 (2001).
213. Krieger, K. and J. Roth: Synergistic Effects by Simultaneous Bombardment of Tungsten with Hydrogen and Carbon. *Journal of Nuclear Materials* **290-293**, 107-111 (2001).
214. Kukushkin*, A.S., G. Janeschitz*, A. Loarte*, H.D. Pacher*, D.P. Coster, D. Reiter* and R. Schneider: Critical Issues in Divertor Optimisation for ITER-FEAT. *Journal of Nuclear Materials* **290-293**, 887-891 (2001).
215. Kukushkin*, A.S., G. Janeschitz*, A. Loarte*, H.D. Pacher*, D.P. Coster, G.F. Matthews*, D. Reiter*, R. Schneider and V. Zhogolov: Basic Divertor Operation in ITER-FEAT. In: Proceedings of the 18th Fusion Energy Conference, Sorrento 2000, IAEA, Vienna 2001, TERP/10(R).
216. Kurzan, B., H. Murmann, M. Jakobi, D. Bolshukhin and ASDEX Upgrade Team: Neutral Beam Injection Induced Anisotropy of the Electron Velocity Distribution on ASDEX Upgrade. In: Proceedings of the 28th EPS Conference on Controlled Fusion and Plasma Physics, Funchal 2001, (Eds.) C.Silva, C.Varandas, D.Campbell. ECA 25A. European Physical Society, Geneva 2001, 29-32.
217. Kurzan, B., H. Murmann, H. Salzmann and ASDEX-Upgrade-Team: Improvements in the Evaluation of Thomson Scattering on ASDEX Upgrade. *Review of Scientific Instruments* **72**, 1111-1114 (2001).
218. Labich, S., E. Taglauer and H. Knözinger*: Metal-Support Interactions on Rhodium Model Catalysts. *Topics in Catalysis* **14**, 153-161 (2001).
219. Lalouis*, P., R. Schneider and L.L. Lengyel: Cloud Drifts over Eroding Surfaces in Magnetic Field Configurations with Three Field Components. *Journal of Nuclear Materials* **290-293**, 1084-1087 (2001).
220. Lalouis*, P., H. Strauss*, W. Park* and H.-P. Zehrfeld: Simulation of Pellet Cloud Drift with Multileveled 3D Code (M3D). In: Proceedings of the 28th EPS Conference on Controlled Fusion and Plasma Physics, Funchal 2001, (Eds.) C.Silva, C.Varandas, D.Campbell. ECA 25A. European Physical Society, Geneva 2001, 705-708.
221. Lang, P.T., B. Alper*, L.R. Baylor*, M. Beurskens*, J.G. Cordey*, R. Dux, R. Felton*, L. Garzotti*, G. Haas, L.D. Horton, S. Jachmich*, T.T.C. Jones*, A. Lorenz, P. Lomas*, M. Maraschek, H.W. Müller, J. Ongena*, J. Rapp*, K.F. Renk*, M. Reich, R. Sartori*, G. Schmidt*, M. Stamp*, W. Suttrup, E. Villedieu* and Contributors to the EFDA-JET Work Programme: Optimisation of Pellet Scenarios for Long Pulse Fuelling to High Density at JET. In: Proceedings of the 28th EPS Conference on Controlled Fusion and Plasma Physics, Funchal 2001, (Eds.) C.Silva, C.Varandas, D.Campbell. ECA 25A. European Physical Society, Geneva 2001, 973-976.
222. Lang, P.T., O. Gruber, L.D. Horton, T.T.C. Jones*, A. Lorenz, M. Maraschek, V. Mertens, J. Neuhauser, G. Saibene*, H. Zohm, ASDEX Upgrade Team and Contributors to the EFDA-JET Work Programme: High Density H-Mode Operation Achieved Using Efficient Particle Refuelling by Inboard Launch of Cryogenic Pellets. *Journal of Nuclear Materials* **290-293**, 374-380 (2001).
223. Lang, P.T., A. Lorenz, V. Mertens, J.C. Fuchs, J. Gafert, O. Gehre, O. Gruber, G. Haas, M. Kaufmann, B. Kurzan, M. Maraschek, H.W. Müller, H. Murmann, J. Neuhauser, M. Reich, W. Schneider, S. Vergamota* and ASDEX Upgrade Team: Refuelling Performance Improvement by High Speed Pellet Launch from the Magnetic High Field Side. *Nuclear Fusion* **8**, 1107-1112 (2001).
224. Lang, P.T., A. Lorenz, M. Reich, R. Dux, J. Gafert, M. Mertens, H.W. Müller, J. Neuhauser, K.F. Renk* and ASDEX Upgrade Team: Performance Improvement by Advanced High Field Side Pellet Refuelling in ASDEX Upgrade. In: Proceedings of the 28th EPS Conference on Controlled Fusion and Plasma Physics, Funchal 2001, (Eds.) C.Silva, C.Varandas, D.Campbell. ECA 25A. European Physical Society, Geneva 2001, 37-40.
225. Langer, U., E. Taglauer, R. Fischer and W7-AS Team: Investigation of the Hydrogen Fluxes in the Plasma Edge of W7-AS during H-Mode Discharges. *Journal of Nuclear Materials* **290-293**, 658-662 (2001).
226. Laqua, H.P., V. Erckmann, M. Hirsch, W7-AS Team and F. Gandini*: Distribution of the ECRH Stray Radiation in Fusion Devices. In: Proceedings of the 28th EPS Conference on Controlled Fusion and Plasma Physics, Funchal 2001, (Eds.) C.Silva, C.Varandas, D.Campbell. ECA 25A. European Physical Society, Geneva 2001, 1277-1280.
227. Laqua, H.P., V. Erckmann, H. Maaßberg, W7-AS Team and ECRH-Group (IPF-Stuttgart)*: The Electron Heat Transport for High Power Electron Cyclotron Heating at the Wendelstein 7-AS Stellarator. In: Proceedings of the 28th EPS Conference on Controlled Fusion and Plasma Physics, Funchal 2001, (Eds.) C.Silva, C.Varandas, D.Campbell. ECA 25A. European Physical Society, Geneva 2001, 17-20.
228. Laqua, H., H. Niedermeyer and I. Willmann: Ethernet Based Real Time Control Data Bus. In: Proceedings of the 12th IEEE-NPSS Real Time Conference, Valencia 2001, (Eds.) E.Sanchis, A.Ferrer, V.González. University of Valencia, Valencia 2001, 1-5.

Publications

229. *Laux, M.*: Application of Triple Probes to Magnetized Plasmas. *Contributions to Plasma Physics* **41**, 510-516 (2001).
230. *Laux, M. (Ed.)*: 4th Workshop on Electrical Probes in Magnetized Plasmas, Berlin 2000. *Contributions to Plasma Physics* **41**, 434-538 (2001).
231. *Laux, M., S. Jachmich*, A. Herrmann, G.F. Matthews*, W. Fundamenski* and Contributors to the EFDA-JET Work Programme*: Particle and Power Fluxes during an ELM Observed by Probes in the Divertors of ASDEX Upgrade and JET. In: *Proceedings of the 28th EPS Conference on Controlled Fusion and Plasma Physics*, Funchal 2001, (Eds.) C.Silva, C.Varandas, D.Campbell. ECA 25A. European Physical Society, Geneva 2001, 1625-1628.
232. *Laux, M. and H. Pursch**: Sound Emission from an Arc Cathode. *IEEE Transactions on Plasma Science* **29**, 722-725 (2001).
233. *Lechon*, Y., H. Cabal*, R.M. Saez*, D. Ward*, B. Hallberg*, K. Aquilonius*, R. Korhonen*, T. Hamacher, T. Schneider* and S. Lepicard**: Exploitation and Improvement of the External Costs Assessment of Fusion Power. *Fusion Engineering and Design* **58-59**, 1027-1032 (2001).
234. *Lederer, H., K. Desinger, A.P. Seitsonen*, et al.*: Meta-computing im Gigabit-Testbed Süd und Berlin. In: *Abschlussberichte von DFN-Projekten, Digitale Bibliothek der Niedersächsischen Staats- und Universitätsbibliothek Göttingen*, 2001, 65 pp, <http://webdoc.sub.gwdg.de/ebook/ah/dfn/GTBSB-Metacomputing.pdf>.
235. *Letellier*, C., A. Dinklage, H. El-Naggar*, C. Wilke* and G. Bonhomme**: Experimental Evidence of a Torus Breakdown through a Global Bifurcation in a Glow Discharge Plasma. *Physical Review E* **63**, 042702 (2001).
236. *Letellier*, C., O. Ménard*, T. Klinger, A. Piel* and G. Bonhomme**: Dynamical Analysis and Map Modelling of a Thermionic Diode Plasma Experiment. *Physica D* **156**, 169-178 (2001).
237. *Leuterer, F.*: Plasma Waves. In: *Summer University for Plasma Physics*, Garching 2001, (Eds.) A.Könies, K.Krieger. Max-Planck-Institut für Plasmaphysik, Garching 2001, 109-120.
238. *Leuterer, F., M. Beckmann*, A. Borchegowski*, H. Brinkschulte, A.V. Chirkov*, G.G. Denisov*, L. Empacher*, F. Förster*, G. Gantenbein*, V. Illin*, W. Kasperek*, K. Kirov, F. Monaco, M. Münich, L. Popov*, P. Schüller*, K. Schwörer*, H. Schütz and V. Sigalaev**: The ECRH System of ASDEX Upgrade. *Fusion Engineering and Design* **56-57**, 615-619 (2001).
239. *Leuterer, F., M. Beckmann*, H. Brinkschulte, F. Monaco, M. Münich, F. Ryter, H. Schütz, L. Empacher*, G. Gantenbein*, W. Förster*, W. Kasperek*, P. Schüller*, K. Schwörer*, A. Borchegowski*, A. Fix*, V. Illin*, L. Popov*, V. Sigalaev* and E. Tai**: Experience with the ECRH System of ASDEX-Upgrade. *Fusion Engineering and Design* **53**, 485-489 (2001).
240. *Leuterer, F., G. Gantenbein*, S. Günter, J. Hobirk, K. Kirov, F. Ryter, R. Wolf, H. Zohm and ASDEX Upgrade Team*: ECRH Experiments in ASDEX Upgrade. In: *Proc. 14th Topical Conference on Radiofrequency Power in Plasmas*, Oxnard 2001, (Eds.) Tal Kuen Mau, J.de Grassie. AIP Conference Proceedings 595, AIP Press, Melville, NY 2001, 259-266 (2001).
241. *Leuterer, F., S. Günter, M. Maraschek, F. Ryter, W. Sutrop, R. Wolf, G. Gantenbein*, H. Zohm and ASDEX Upgrade Team*: ECRH Experiments in ASDEX Upgrade. *Fusion Engineering and Design* **53**, 277-287 (2001).
242. *Lingertat, J., M. Laux and R.D. Monk*: Narrow Power Deposition Profiles on the JET Divertor Target. *Journal of Nuclear Materials* **290-293**, 896-899 (2001).
243. *Linsmeier, C., P. Goldstraf and K.U. Klages*: ARTOSS - A New Surface Science Experiment to Study the Hydrogen Inventory in Multi-Component Materials. *Physica Scripta* **T94**, 28-33 (2001).
244. *Linsmeier, C., J. Luthin and P. Goldstraf*: Mixed Material Formation and Erosion. *Journal of Nuclear Materials* **290-293**, 25-32 (2001).
245. *Litaudon*, X, F. Crisanti*, J. Mailloux*, Y. Baranov*, E. Barbato*, V. Basiuk*, A. Becoulet*, M. Becoulet*, C.D. Challis*, G. Conway, R. Dux, R. De Angelis*, L.-G. Eriksson*, B. Esposito*, D. Frigione*, C. Giroud*, N. Hawkes*, P. Henniquin*, G. Huysmans*, F. Imbeaux*, E. Joffrin*, P. Lotte*, P. Maget*, M. Mantsinen*, D. Mazon*, D. Moreau*, F. Rimini*, Y. Sarazin*, G. Tresset*, K.-D. Zastrow*, M. Zerbini* and Contributors to the EFDA-JET Work Programme*: Towards Full Current Drive Operation in JET. In: *Proceedings of the 28th EPS Conference on Controlled Fusion and Plasma Physics*, Funchal 2001, (Eds.) C.Silva, C.Varandas, D.Campbell. ECA 25A. European Physical Society, Geneva 2001, 1313-1316.
246. *Loarte*, A., G. Saibene*, R. Sartori*, G. Janeschitz*, Yu.L. Igitkhanov, A.S. Kukushkin*, M. Sugihara*, D.P. Coster, A. Herrmann, L.D. Horton, J. Stober, N. Asakura*, K. Itami*, H. Tamai*, G.F. Matthews*, R. Schneider, D. Reiter*, A.W. Leonard* and G.D. Porter**: Predicted ELM Energy Loss and Power Loading in ITER-FEAT. In: *Proceedings of the 18th Fusion Energy Conference*, Sorrento 2000, IAEA, Vienna 2001, ITERP/11(R).
247. *Lorenz, A., P. Cierpka, C. Dorn, P.T. Lang, R.S. Lang and W. Zeidner*: Design and Implementation of a High Speed Guiding System for Inboard Pellet Refuelling. *Fusion Engineering and Design* **58-59**, 325-329 (2001).
248. *Lorenzini*, R., P.T. Lang, G. Pereverzev, C. Fuchs, J. Stober and ASDEX Upgrade Team*: Particle Transport Analysis of ELMy H-Mode Pellet Fuelled Plasma in ASDEX Upgrade. In: *Proceedings of the 28th EPS Conference on Controlled Fusion and Plasma Physics*, Funchal 2001, (Eds.) C.Silva, C.Varandas, D.Campbell. ECA 25A. European Physical Society, Geneva 2001, 33-36.
249. *Luthin, J. and C. Linsmeier*: Characterization of Electron Beam Evaporated Carbon Films and Compound Formation on Titanium and Silicon. *Physica Scripta* **T91**, 134-137 (2001).
250. *Luthin, J. and C. Linsmeier*: Influence of Oxygen on the Carbide Formation on Tungsten. *Journal of Nuclear Materials* **290-293**, 121-125 (2001).
251. *Luthin, J., H. Plank, J. Roth and C. Linsmeier*: Ion Beam-Induced Carbide Formation at the Ti-C Interface. *Nuclear Instruments and Methods in Physics Research B* **182**, 218-226 (2001).
252. *Maier, H., J. Luthin, M. Balden, J. Linke*, F. Koch and H. Bolt*: Properties of Tungsten Coatings Deposited onto Fine Grain Graphite by Different Methods. *Surface and Coatings Technology* **142-144**, 733-737 (2001).
253. *Manso*, M., P. Varela*, I. Nunes*, J. Santos*, G. Conway, M. Hirsch, S. Klenge, J. Stober, CFN/IST Reflectometry Team and ASDEX Upgrade Team*: Reflectometry in Conventional and Advanced Plasma Scenarios on ASDEX Upgrade and Perspectives for ITER. *Plasma Physics and Controlled Fusion* **43**, A73-A93 (2001).
254. *Mantica*, P., Y. Sarazin*, I. Coffey*, R. Dux, L. Garzotti*, G. Gorini*, C. Ingesson*, M. Kissick*, J.E. Kinsey*, V. Parail*, C. Sozzi*, A. Walden* and Contributors to the EFDA-JET Work Programme*: Cold Pulse Propagation Experiments in ITB Plasmas of JET. In: *Proceedings of the 28th EPS Conference on Controlled Fusion*

Publications

and Plasma Physics, Funchal 2001, (Eds.) C.Silva, C.Varandas, D.Campbell. ECA 25A. European Physical Society, Geneva 2001, 1749-1752.

255. *Mantsinen**, M., *M.-L. Mayoral**, *J. Bucalossi**, *M. de Baar**, *P. de Vries**, *A. Figueiredo**, *T. Hellsten**, *V. Kiptily**, *P. Lamalle**, *F. Meo*, *F. Milani**, *I. Monakhov**, *F. Nguyen**, *J.-M. Noterdaeme*, *Yu. Petrov**, *V. Riccardo**, *E. Righi**, *F. Rimini**, *A.A. Tuccillo**, *D. Van Eester** and *M. Zerbini**: ICRF Mode Conversion Experiments on JET. In: Proceedings of the 28th EPS Conference on Controlled Fusion and Plasma Physics, Funchal 2001, (Eds.) C.Silva, C.Varandas, D.Campbell. ECA 25A. European Physical Society, Geneva 2001, 1745-1748.

256. *Mantsinen**, M., *M.-L. Mayoral**, *E. Righi**, *J.-M. Noterdaeme*, *A.A. Tuccillo**, *M. de Baar**, *A. Figueiredo**, *A. Gondhalekar**, *T. Hellsten**, *V. Kiptily**, *K. Lawson**, *F. Meo*, *F. Milani**, *I. Monakhov**, *Yu. Petrov**, *V. Riccardo**, *F. Rimini**, *S. Sharapov**, *D. Van Eester**, *K.-D. Zastrow**, *R. Barnsley**, *L. Bertalog**, *A. Bickley**, *J. Bucalossi**, *R. Cesario**, *J.-M. Chareau**, *M. Charlet**, *I. Coffey**, *S. Conroy**, *P. de Vries**, *K. Eretns**, *L.-G. Eriksson**, *C. Gowers**, *C. Ingesson**, *N. Jarvis**, *T. Johnson**, *R. Koch**, *P. Lamalle**, *G.P. Maddison**, *J. Mailloux**, *A. Murari**, *F. Nguyen**, *J. Ongena**, *V. Parail**, *S. Popovichev**, *G. Saibene**, *F. Sartori**, *J. Strachan**, *M. Zerbini** and *Task Force H and Contributors to the EFDA-JET Work Programme*: ICRF Heating Scenarios in JET with Emphasis on ⁴He Plasmas for the Non-Activated Phase of ITER. In: Proc. 14th Topical Conference on Radiofrequency Power in Plasmas, Oxnard 2001, (Eds.) Tal Kuen Mau, J.de Grassie. AIP Conference Proceedings 595, AIP Press, Melville,NY 2001, 59-66 (2001).

257. *Maraschek*, M.E., *R.J. Buttery**, *T.C. Hender**, *O. Sauter**, *S. Cortes**, *S. Günter*, *A. Gude*, *D.F. Howell**, *P.T. Lang*, *S.D. Pinches*, *H. Zohm*, *Contributors to the EFDA-JET Work Programme and ASDEX Upgrade Team*: Density Dependence of the Onset of Neoclassical Tearing Modes in H-Mode and Pellet Refuelled Discharges on JET and ASDEX Upgrade. In: Proceedings of the 28th EPS Conference on Controlled Fusion and Plasma Physics, Funchal 2001, (Eds.) C.Silva, C.Varandas, D.Campbell. ECA 25A. European Physical Society, Geneva 2001, 1801-1804.

258. *Maruyama**, K., *W. Jacob* and *J. Roth*: Formation of Hard Amorphous Hydrogenated Carbon Films with Low Hydrogen Concentration and their Erosion in Air. Japanese Journal of Applied Physics **40**, 788-793 (2001).

259. *Matthews**, G.F., *K. Eretns**, *W. Fundamenski**, *C. Ingesson**, *R.D. Monk* and *V. Riccardo**: Divertor Energy Distribution in JET H-Modes. Journal of Nuclear Materials **290-293**, 668-672 (2001).

260. *Mayer*, M. and *M. Schneider*: Scattering Cross Sections for 6Li and 7Li Ions from Carbon below 5.5 MeV. Nuclear Instruments and Methods B **183**, 221-226 (2001).

261. *McCarthy**, P.J., *W. Suttrop*, *J. Hobirk*, *W. Schneider*, *R. Wolf* and *ASDEX Upgrade Team*: Current Density Profile Identification in the ASDEX Upgrade Pedestal Region from Kinetic and Magnetic Data Using the CLISTE Interpretative Equilibrium Code. In: Proceedings of the 28th EPS Conference on Controlled Fusion and Plasma Physics, Funchal 2001, (Eds.) C.Silva, C.Varandas, D.Campbell. ECA 25A. European Physical Society, Geneva 2001, 173-176.

262. *McCormick*, K., *P. Grigull*, *H. Ehmler*, *Y. Feng*, *G. Haas*, *J. Knauer* and *W7-AS Team*: Neutral Compression in the W7-AS Stellarator Divertor. In: Proceedings of the 28th EPS Conference on Controlled Fusion and Plasma Physics, Funchal 2001, (Eds.) C.Silva, C.Varandas, D.Campbell. ECA 25A. European Physical Society, Geneva 2001, 2097-2100.

263. *McCormick*, K., *P. Grigull*, *R. König*, *R. Burhenn*, *H. Ehmler*, *Y. Feng*, *S. Fiedler*, *L. Giannone*, *D. Hildebrandt*, *J. Knauer*, *G. Kühner*, *D. Naujoks*, *J. Sallander*, *C. Wendland* and *W7-AS Team*: On the Way to Divertor Detachment in the W7-AS Stellarator. Journal of Nuclear Materials **290-293**, 920-924 (2001).

264. *McNeely*, P., *B. Heinemann*, *W. Kraus*, *R. Riedl*, *E. Speth* and *O. Vollmer*: Recent Developments of Long Pulse RF Ion Source for NBI. Fusion Engineering and Design **56-57**, 493-498 (2001).

265. *Meier*, M. and *A. von Keudell*: Formation of Polymer-Like Hydrocarbon Films from Radical Beams of Methyl and Atomic Hydrogen. In: Proceedings of the 15th International Symposium on Plasma Chemistry, Orleans 2001, (Eds.) A.Bouchoule, J.M.Pouvesle, A.L.Thomann et al. GREMI,CNRS/University of Orleans 2001, 239-244.

266. *Meier*, M. and *A. von Keudell*: Hydrogen Elimination as a Key Step for the Formation of Polymerlike Hydrocarbon Films. Journal of Applied Physics **90**, 3585-3594 (2001).

267. *Meißen**, F., *A.J. Patchett**, *R. Imbühl** and *A.M. Bradshaw*: Novel Types of Spatio-Temporal Patterns in Catalytic CO Oxidation on a Faceted Pt(110) Surface. Chemical Physics Letters **336**, 181-186 (2001).

268. *Meister*, H., *J.C. Fuchs*, *B. Kurzan*, *K.-H. Steuer* and *ASDEX Upgrade Team*: Extension of the Z_{eff} Diagnostic at ASDEX Upgrade. In: Proceedings of the 28th EPS Conference on Controlled Fusion and Plasma Physics, Funchal 2001, (Eds.) C.Silva, C.Varandas, D.Campbell. ECA 25A. European Physical Society, Geneva 2001, 377-380.

269. *Meister*, H., *A. Kallenbach*, *A.G. Peeters*, *A. Kendl*, *J. Hobirk*, *S.D. Pinches* and *ASDEX Upgrade Team*: Measurement of Poloidal Flow, Radial Electric Field and $E \times B$ Shearing Rates at ASDEX Upgrade. Nuclear Fusion **41**, 1633-1644 (2001).

270. *Menhart**, S., *M. Proschek**, *H.-D. Falter**, *H. Anderson**, *H. Summers**, *A. Stäßler*, *P. Franzen*, *H. Meister*, *J. Schweinzer*, *T.T.C. Jones**, *S. Cox**, *N. Hawkes**, *F. Aumayr** and *H.P. Winter**: Explorative Studies for the Development of Fast He Beam Plasma Diagnostics. Journal of Nuclear Materials **290-293**, 673-677 (2001).

271. *Meo*, F., *M. Brambilla*, *R. Bilato*, *J.-M. Noterdaeme*, *F. Nguyen**, *C. Petty**, *Task Force H and Contributors to the EFDA-JET Work Programme*: Comparison of FWCD Scenarios on ASDEX Upgrade, JET and DIII-D Tokamaks. In: Proc. 14th Topical Conference on Radiofrequency Power in Plasmas, Oxnard 2001, (Eds.) Tal Kuen Mau, J.de Grassie. AIP Conference Proceedings 595, AIP Press, Melville,NY 2001, 194-197 (2001).

272. *Meskat*, J., *H. Zohm*, *G. Gantenbein**, *S. Günter*, *M. Maraschek*, *W. Suttrop*, *Q. Yu*, *H. Zohm* and *ASDEX Upgrade Team*: Analysis of the Structure of Neoclassical Tearing Modes in ASDEX Upgrade. Plasma Physics and Controlled Fusion **43**, 1325-1332 (2001).

273. *Michel*, G.: Full Performance ECRH Experiments at W7-AS. In: Proceedings of the 14th Topical Conference on Radio Frequency Power in Plasmas, Oxnard,CA 2001, (Eds.) Tal Kuen Mau, J.de Grassie. AIP Conference Proceedings 595, AIP Press, Melville,NY 2001, 354-357.

274. *Michel*, G., *H. Laqua* and *W. Kasperek**: Calorimetric Measurement of the Microwave Power Transmitted through a Diamond Window. Fusion Engineering and Design **56-57**, 655-660 (2001).

275. *Mikhailov**, M.I., *M.Yu. Isaev**, *J. Nührenberg*, *A.A. Subbotin**, *W.A. Cooper**, *M.F. Heyn**, *V.N. Kalyuzhnyj**, *S.V. Kasilov**, *V.V. Kasilov**, *W. Kernbichler**, *V.V. Nemov**, *M.A. Samitov** and *V.D. Shafranov**: Topology of Magnetic Field Strength Surfaces and Particle Confinement in Mirror-Type Stellarators. In: Proceedings of

Publications

- the 28th EPS Conference on Controlled Fusion and Plasma Physics, Funchal 2001, (Eds.) C.Silva, C.Varandas, D.Campbell. ECA 25A. European Physical Society, Geneva 2001, 757-760.
276. *Milch, I.*: Kernfusion - Stand und Perspektiven. atw - Internationale Zeitschrift für Kernenergie **46**, 691 (2001).
277. *Milch, I.*: Spulen für das Sternenfeuer. Helmholtz-Jahresheft 2001, 42-43 (2001).
278. *Milch, I.*: Status quo und Perspektiven der Fusionsforschung. Brennstoff, Wärme, Kraft **53**, 25-27 (2001).
279. *Miri*, A.M., C. Müller* and C. Sihler*: Modelling of Inrush Currents in Power Transformers by a Detailed Magnetic Equivalent Circuit. In: Proceedings of the 4th International Conference on Power Systems Transients, Rio de Janeiro 2001, (Ed.) Federal University of Rio de Janeiro 2001, 215-220.
280. *Morabito*, F.C., M. Versaci*, G. Pautasso, C. Tichmann and ASDEX Upgrade Team*: Fuzzy-Neural Approaches to the Prediction of Disruptions in ASDEX Upgrade. Nuclear Fusion **41**, 1715-1723 (2001).
281. *Moré*, S., A.P. Seitsonen*, W. Berndt* and A.M. Bradshaw*: Ordered Phases of Na Adsorbed on Pt(111): Experiment and Theory. Physical Review B **63**, 75406 (2001).
282. *Mukherjee, S., M. Balden, S. Kötterl, S. Schweizer, J. Simon-Weidner, B. Streibl and R. Uhlemann**: High-Intensity Non-Brazed Heat Shield for Safe Steady-State Operation. Fusion Engineering and Design **56-57**, 303-307 (2001).
283. *Müller, H.W., E. Wolfrum, R. Drube, J.C. Fuchs, A. Kallenbach, B. Kurzan, T. Naiser, J. Neuhauser, J. Schweinzer and ASDEX Upgrade Team*: Improved Edge Density Profile Measurements by the Li-Beam Diagnostic on ASDEX Upgrade. In: Proceedings of the 28th EPS Conference on Controlled Fusion and Plasma Physics, Funchal 2001, (Eds.) C.Silva, C.Varandas, D.Campbell. ECA 25A. European Physical Society, Geneva 2001, 421-424.
284. *Naujoks, D.*: Charge Shielding in Magnetized Plasmas. Contributions to Plasma Physics **41**, 375-386 (2001).
285. *Naujoks, D. and J.N. Brooks**: Combined Sheath and Thermal Analysis of Overheated Surfaces in Fusion Devices. Journal Nuclear Materials **290-293**, 1123-1127 (2001).
286. *Nave*, M.F.F., J. Rapp*, T. Bolzonella*, R. Dux, N. Hawkes*, S. Jamich*, H.R. Koslowski*, P. Lotte*, M. Mantsinen*, J. Ongena*, V. Parail*, J. Strachan* and Contributors to the JET-EFDA Workprogramme*: Sawtooth and Impurity Accumulation Control in JET Radiative Mantle Discharges. In: Proceedings of the 28th EPS Conference on Controlled Fusion and Plasma Physics, Funchal 2001, (Eds.) C.Silva, C.Varandas, D.Campbell. ECA 25A. European Physical Society, Geneva 2001, 961-964.
287. *Neu, R., J.C. Fuchs, G. Haas, A. Herrmann, M. Laux, J. Neuhauser, F. Ryter, H.-S. Bosch, D.P. Coster, J. Gafert, O. Gruber, A. Kallenbach, M. Kaufmann, V. Mertens, H.W. Müller, R. Pugno, V. Rohde, J. Stober, B. Streibl and ASDEX Upgrade Team*: First Characterization of the New Divertor IIB in ASDEX Upgrade. In: Proceedings of the 28th EPS Conference on Controlled Fusion and Plasma Physics, Funchal 2001, (Eds.) C.Silva, C.Varandas, D.Campbell. ECA 25A. European Physical Society, Geneva 2001, 177-180.
288. *Neu, R., K.B. Fournier*, D. Bolshukhin and R. Dux*: Spectral Lines from Highly Charged Tungsten Ions in the Soft X-Ray Region for Quantitative Diagnostics of Fusion Plasma. Physica Scripta **T92**, 307-310 (2001).
289. *Neu, R., V. Rohde, A. Geier, K. Krieger, H. Maier, D. Bolshukhin, A. Kallenbach, R. Pugno, K. Schmidtman, M. Zarrabian and ASDEX Upgrade Team*: Plasma Operation with Tungsten Tiles at the Central Column of ASDEX Upgrade. Journal of Nuclear Materials **290-293**, 206-210 (2001).
290. *Neu, R.*: Diagnostics of Fusion Plasmas. In: Summer University for Plasma Physics, Garching 2001, (Eds.) A.Könies, K.Krieger. Max-Planck-Institut für Plasmaphysik, Garching 2001, 65-80.
291. *Neumaier*, P., G. Dollinger*, A. Bergmaier*, I. Genchev*, L. Görgens*, R. Fischer, C. Ronning* and H. Hofsäuss**: High-Resolution Elastic Recoil Detection Utilizing Bayesian Probability Theory. Nuclear Instruments and Methods B **183**, 48-61 (2001).
292. *Nguyen*, F., J.-M. Noterdaeme, M.-L. Mayoral*, T. Hellsten*, M. Mantsinen*, D. Hartmann, R. de Angelis*, V. Basium*, M. de Baar*, L.-G. Eriksson*, D. Van Eester*, A. Gondhalekar*, N. Hawkes*, R. Johnsson*, P. Lamalle*, P. Lotte*, F. Meo, L. Panaccione*, A.-L. Pecquet*, S. Podda*, E. Righi*, Y. Sarazin*, O. Sauter*, T. Tala*, A. Ruccillo*, M. Zabiégo* and Contributors to the EFDA-JET Work Programme*: ICRF Current Drive Experiments on JET. In: Proceedings of the 28th EPS Conference on Controlled Fusion and Plasma Physics, Funchal 2001, (Eds.) C.Silva, C.Varandas, D.Campbell. ECA 25A. European Physical Society, Geneva 2001, 781-784.
293. *Nishijima*, D., U. Wenzel, M. Motoyama*, N. Ohno*, S. Takamura* and S.I. Krashennikov**: Evaluation of Electron Temperature in Detached Recombining Plasmas. Journal of Nuclear Materials **290-293**, 688-691 (2001).
294. *Noterdaeme, J.-M., E. Righi*, J. de Grassie*, V. Chan*, K. Kirov, P. Lamalle*, F. Meo, M.F.F. Nave*, K.-D. Zastrow* and Contributors to the EFDA-JET Work Programme*: Spatially Resolved Plasma Rotation Profiles with ICRH on JET. In: Proc. 14th Topical Conference on Radiofrequency Power in Plasmas, Oxnard 2001, (Eds.) Tal Kuen Mau, J.de Grassie. AIP Conference Proceedings 595, AIP Press, Melville, NY 2001, 98-101 (2001).
295. *Noterdaeme, J.-M., E. Righi*, J. de Grassie*, V. Chan*, M.F.F. Nave*, K.-D. Zastrow*, R.V. Budny*, R. Cesario*, A. Gondhalekar*, N. Hawkes*, T. Hellsten*, F. Meo, F. Nguyen* and Contributors to the EFDA-JET Work Programme*: Toroidal Plasma Rotation with ECRF on JET. In: Proceedings of the 28th EPS Conference on Controlled Fusion and Plasma Physics, Funchal 2001, (Eds.) C.Silva, C.Varandas, D.Campbell. ECA 25A. European Physical Society, Geneva 2001, 777-780.
296. *Nöthe*, M., U. Breuer*, F. Koch, H.J. Penkalla*, W.P. Rehbach* and H. Bolt*: Investigation of the Structure and Properties of a-C:H Coatings with Metal and Silicon Containing Interlayers. Applied Surface Science **179**, 122-128 (2001).
297. *Nührenberg, C.*: Alfvén Eigenmodes in Wendelstein 7-X - Equilibrium Properties and Spectral Gap Structure. In: Theory of Fusion Plasmas, Varenna 2000, Societa Italiana di Fisica, Bologna 2001, 313-320.
298. *Nührenberg, J., M. Drevlak, R. Hatzky, R. Kleiber, A. Könies, P. Merkel, D. Monticello*, C. Nührenberg, A. Reiman* and T.M. Tran**: Recent Developments in Theory for W7-X. In: Proceedings of the 18th Fusion Energy Conference, Sorrento 2000, IAEA, Vienna 2001, TH5/1.
299. *Nunes*, I., P. Varela*, G. Conway, F. Silva*, F. Serra*, M. Manso* and ASDEX Upgrade Team*: Absolute Calibration of Density Profiles from both O and X Mode Reflectometry on ASDEX Upgrade. In: Proceedings of the 28th EPS Conference on Controlled Fusion and Plasma Physics, Funchal 2001, (Eds.) C.Silva, C.Varandas, D.Campbell. ECA 25A. European Physical Society, Geneva 2001, 1249-1252.

Publications

300. *Ogorodnikova, O.V.*: Surface Effects on Plasma-Driven Tritium Permeation through Metals. *Journal of Nuclear Materials* **290-293**, 459-463 (2001).
301. *Ohdachi*, S., S. Yamamoto*, K. Toi*, A. Weller, R. Sakamoto*, H. Yamada*, K. Tanaka*, T. Tokuzawa*, K. Kawahata*, S. Morita*, M. Goto*, S. Sakakibara* and LHD Experimental Group*: Pellet-Induced Low Frequency Oscillations on the Large Helical Device. In: Proceedings of the 28th EPS Conference on Controlled Fusion and Plasma Physics, Funchal 2001, (Eds.) C.Silva, C.Varandas, D.Campbell. ECA 25A. European Physical Society, Geneva 2001, 1521-1524.
302. *Okamura*, S., K. Matsuoka*, S. Nishimura*, M. Isobe*, I. Nomura*, C. Suzuki*, A. Shimizu*, S. Murakami*, N. Nakajima*, M. Yokoyama*, A. Fujisawa*, K. Ida*, K. Itoh*, P. Merkel, M. Drevlak, R. Zille, S. Gori and J. Nührenberg*: Physics and Engineering Design of the Low Aspect Ratio Quasi-Axisymmetric Stellarator CHS-qa. *Nuclear Fusion* **41**, 1865-1871 (2001).
303. *Ott, W. and E. Speth*: Theory of Plasma Build-Up in Stellarators. In: Proceedings of the 28th EPS Conference on Controlled Fusion and Plasma Physics, Funchal 2001, (Eds.) C.Silva, C.Varandas, D.Campbell. ECA 25A. European Physical Society, Geneva 2001, 305-308.
304. *Pautasso, G., S. Egorov, C. Tichmann, J.C. Fuchs, A. Herrmann, M. Maraschek, K.-F. Mast, V. Mertens, J. Perchermeier, C.G. Windsor, T. Zehetbauer and ASDEX Upgrade Team*: Prediction and Mitigation of Disruptions in ASDEX Upgrade. *Journal of Nuclear Materials* **290-293**, 1045-1051 (2001).
305. *Pautasso, G., U. Seidel, O. Gruber and ASDEX Upgrade Team*: Asymmetric Halo Currents in ASDEX Upgrade Disruptions. In: Proceedings of the 28th EPS Conference on Controlled Fusion and Plasma Physics, Funchal 2001, (Eds.) C.Silva, C.Varandas, D.Campbell. ECA 25A. European Physical Society, Geneva 2001, 45-48.
306. *Paz*, P., C. García-Rosales*, J. Etxebarria*, M. Balden, J. Roth and R. Behrisch*: Development of Doped Graphites for Plasma-Facing Components. *Fusion Engineering and Design* **56-57**, 325-330 (2001).
307. *Peeters, A.G.*: Kinetic Theory. In: Summer University for Plasma Physics, Garching 2001, (Eds.) A.Könies, K.Krieger. Max-Planck-Institut für Plasmaphysik, Garching 2001, 81-93.
308. *Pereverzev, G.*: Paraxial WKB Description of Short Wavelength Eigenmodes in a Tokamak. *Physics of Plasmas* **8**, 3664-3672 (2001).
309. *Pericoli-Ridolfini*, V., S. Podda*, J. Mailloux*, Y. Sarazin*, Y. Baranov*, S. Bernabei*, R. Cesario*, V. Cocilovo*, A. Ekedahl*, K. Erents*, G. Granucci*, F. Imbeaux*, F. Leuterer, F. Mirizzi*, G.F. Matthews*, L. Panaccione*, F. Rimini*, A.A. Tuccillo* and Contributors to the EFDA-JET Work Programme*: LHCD Coupling during H-Mode and ITB in JET Plasmas. In: Proc. 14th Topical Conference on Radiofrequency Power in Plasmas, Oxnard 2001, (Eds.) Tal Kuen Mau, J.de Grassie. AIP Conference Proceedings 595, AIP Press, Melville, NY 2001, 245-248 (2001).
310. *Pinches, S.D., S. Günter, A.G. Peeters and ASDEX Upgrade Team*: Fishbone Generation of Sheared Flows in the Creation of Transport Barriers. In: Proceedings of the 28th EPS Conference on Controlled Fusion and Plasma Physics, Funchal 2001, (Eds.) C.Silva, C.Varandas, D.Campbell. ECA 25A. European Physical Society, Geneva 2001, 57-60.
311. *Pitts*, R.A., B.P. Duval*, A. Loarte*, J.-M. Moret*, J.A. Boedo*, D.P. Coster, I. Furno*, J. Horacek*, A.S. Kukushkin*, D. Reiter* and J. Rommers**: Divertor Geometry Effects on Detachment in TCV. *Journal of Nuclear Materials* **290-293**, 940-946 (2001).
312. *Poli, E., A.G. Peeters, A. Bergmann and S.D. Pinches*: Monte Carlo δf Simulations of the Bootstrap Current in the Presence of an Island. In: Proceedings of the 28th EPS Conference on Controlled Fusion and Plasma Physics, Funchal 2001, (Eds.) C.Silva, C.Varandas, D.Campbell. ECA 25A. European Physical Society, Geneva 2001, 1033-1036.
313. *Poli, E., A.G. Peeters and G. Pereverzev*: Boundary Conditions for a Gaussian Wave Beam. *Physics of Plasmas* **8**, 4325-4330 (2001).
314. *Poli, E., A.G. Peeters and G. Pereverzev*: TORBEAM, a Beam Tracing Code for Electron Cyclotron Waves in Tokamak Plasmas. *Computer Physics Communications* **136**, 90-104 (2001).
315. *Poli, E., G. Pereverzev, A.G. Peeters and M. Bornatici**: EC Beam Tracing in Fusion Plasmas. *Fusion Engineering and Design* **53**, 9-21 (2001).
316. *Pothhoff*, M., T. Wegner*, W. Nolting*, T. Schlatholter*, M. Vonbank*, K. Ertl, J. Braun* and M. Donath*: Electron-Correlation Effects in Appearance-Potential Spectra of Ni. *Physical Review B* **63**, 165118 (2001).
317. *Preuss, R. and V. Dose*: Marginalization Using the Metric of Likelihood. In: Proceedings of the 20th International Workshop on Bayesian Inference and Maximum Entropy Methods in Science and Engineering, Gif-sur-Yvette 2000, (Ed.) A.Mohammad-Djafari. AIP Conference Proceedings 568, AIP Press, Melville, NY 2001, 264-269.
318. *Preuss, R., P. Pecher and V. Dose*: Handling Discordant Data Sets. In: Proceedings of the 19th International Workshop on Bayesian Inference and Maximum Entropy Methods in Science and Engineering, Boise, ID 1999, (Eds.) J.T.Rychert, G.J.Erickson, C.R.Smith. AIP Conference Proceedings 567, AIP Press, Melville, NY 2001, 213-220.
319. *Pugno, R., A. Kallenbach, D. Bolshukhin, R. Dux, J. Gafert, R. Neu, V. Rohde, K. Schmidtman, W. Ulrich, U. Wenzel and ASDEX Upgrade Team*: Spectroscopic Investigation on the Impurity Influxes of Carbon and Silicon in the ASDEX Upgrade Experiment. *Journal of Nuclear Materials* **290-293**, 308-311 (2001).
320. *Pugno, R., K. Krieger, D.P. Coster, M. Laux, S.W. Yoon and ASDEX Upgrade Team*: Modelling of Impurities in the ASDEX Upgrade Divertor II with DIVIMP and B2-Eirene. In: Proceedings of the 28th EPS Conference on Controlled Fusion and Plasma Physics, Funchal 2001, (Eds.) C.Silva, C.Varandas, D.Campbell. ECA 25A. European Physical Society, Geneva 2001, 181-184.
321. *Puri, S.*: Tokamak Refuelling via Induced Convection. In: Proceedings of the 28th EPS Conference on Controlled Fusion and Plasma Physics, Funchal 2001, (Eds.) C.Silva, C.Varandas, D.Campbell. ECA 25A. European Physical Society, Geneva 2001, 637-640.
322. *Radtke, R., C. Biedermann, J.L. Schwob*, P. Mandelbaum* and R. Doron**: Line and Band Emission from Tungsten Ions with Charge 21+ to 45+ in the 45-79 Å Range. *Physical Review A* **64**, 012720 (2001).
323. *Reiman*, A., L. Ku, D. Monticello*, S. Hirshman*, S. Hudson*, C. Kessel*, E. Lazarus*, D. Mikkelsen*, M. Zarnstorff*, L.A. Berry*, A. Boozer*, A. Brooks*, W.A. Cooper*, M. Drevlak, E. Fredrickson*, G. Fu*, R. Goldston*, R. Hatcher*, M.Yu. Isaev*, C. Jun*, J. Lewandowski*, Z. Lin*, J.F. Lyon*, P. Merkel, M.I. Mikhailov*, W. Miner*, H. Mynick*, G. Neilson*, B.E. Nelson*, C. Nührenberg, N. Pomphrey*, M. Redi*, W. Reiersen*, P. Rutherford*, R. Sanchez*, J. Schmidt*, D. Spong*, D. Strickler*, A.A. Subbotin*, P. Valanju* and R.B. White**: Recent Advances in the Design of Quasi-Axisymmetric Stellarator Plasma Configurations. *Physics of Plasmas* **8**, 2083-2094 (2001).

Publications

324. Reiser*, D., R. Schneider, D.P. Coster, W. Ullrich and H.-S. Bosch: Helium Compression Analysis for ASDEX Upgrade with Fluid and Kinetic Codes. *Journal of Nuclear Materials* **290-293**, 953-956 (2001).
325. Ribeiro*, T., F. Serra*, G. Conway, M. Manso*, F. Ryter, L. Cupido*, B. Kurzan, A. Silva*, W. Suttrop, S. Vergamota* and ASDEX Upgrade Team: Microwave Reflectometry for Turbulence Studies on ASDEX Upgrade. *Review of Scientific Instruments* **72**, 1366-1371 (2001).
326. Rohde, V., H. Maier, K. Krieger, R. Neu, J. Perchermeier and ASDEX Upgrade Team: Carbon Layers in the Divertor of ASDEX Upgrade. *Journal of Nuclear Materials* **290-293**, 317-320 (2001).
327. Rohde, V., R. Neu, A. Geier, R. Dux, O. Gruber, A. Kallenbach, K. Krieger, H. Maier, R. Pugno and ASDEX Upgrade Team: Tungsten as First Wall Material in the Main Chamber of ASDEX Upgrade. In: *Proceedings of the 28th EPS Conference on Controlled Fusion and Plasma Physics*, Funchal 2001, (Eds.) C.Silva, C.Varandas, D.Campbell. ECA 25A. European Physical Society, Geneva 2001, 185-188.
328. Roth, J.: Synopsis of Erosion and Redeposition. *Physica Scripta* **T91**, 65-69 (2001).
329. Roth, J., K. Ertl and C. Linsmeier (Eds.): Plasma-Surface Interactions in Controlled Fusion Devices. *Proceedings of the 14th International Conference, Rosenheim 2000*. *Journal of Nuclear Materials* **290-293**, (2001) 1294 p.
330. Roth, J., U. von Toussaint, K. Schmid, J. Luthin, W. Eckstein, R.A. Zuhr* and D.K. Hensley*: Formation and Erosion of WC under W^+ Irradiation of Graphite. In: *Proceedings of the MRS Fall Meeting Solid State Chemistry of Inorganic Materials*, Boston, MA 2000, (Eds.) M.J.Geselbracht, J.E.Greedan, D.C.Johnson. *MRS Proceedings* 658, MRS, Pittsburgh, MA 2001, 05.31.1-05.31.6.
331. Rozhansky*, V., S. Voskoboynikov*, E.G. Kaveeva*, D.P. Coster, X. Bonnin and R. Schneider: Modeling of Electric Fields in Tokamak Edge Plasma and L-H Transition. In: *Proceedings of the 28th EPS Conference on Controlled Fusion and Plasma Physics*, Funchal 2001, (Eds.) C.Silva, C.Varandas, D.Campbell. ECA 25A. European Physical Society, Geneva 2001, 1457-1460.
332. Rozhansky*, V., S. Voskoboynikov*, E.G. Kaveeva*, D.P. Coster and R. Schneider: Modeling of Tokamak Edge Plasma for Discharges with Neutral Beam Injection. *Journal of Nuclear Materials* **290-293**, 710-714 (2001).
333. Rozhansky*, V., S. Voskoboynikov*, E.G. Kaveeva*, D.P. Coster and R. Schneider: Simulation of Tokamak Edge Plasma Including Self-Consistent Electric Fields. *Nuclear Fusion* **41**, 387-401 (2001).
334. Rubel*, M., P. Wienhold* and D. Hildebrandt: Fuel Accumulation in Co-Deposited Layers on Plasma Facing Components. *Journal of Nuclear Materials* **290-293**, 473-477 (2001).
335. Rummel, T. and I. Schoenewolf: Design Requirements for the Plasma Edge Control System in Wendelstein 7-X. *Fusion Engineering and Design* **58-59**, 47-51 (2001).
336. Rumov, A., D. Reiter*, S.V. Kasilov*, M.F. Heyn* and W. Kernbichler*: Monte Carlo Study of Heat Conductivity in Stochastic Boundaries: Application to the TEXTOR Ergodic Divertor. *Physics of Plasmas* **8**, 916-930 (2001).
337. Rust, N., W. Ott, C. Fuchs, A. Werner and E. Speth: Determination of Neutral-Beam Deposition Profiles with Modulation Experiments in Combination with ECRH-Heating in W7-AS. In: *Proceedings of the 28th EPS Conference on Controlled Fusion and Plasma Physics*, Funchal 2001, (Eds.) C.Silva, C.Varandas, D.Campbell. ECA 25A. European Physical Society, Geneva 2001, 1153-1156.
338. Ryter, F., C. Angioni*, M. Beurskens*, S. Cirant*, G.G. Hoang*, G.M.D. Hogewij*, F. Imbeaux*, A. Jacchia*, P. Mantica*, W. Suttrop and G. Tardini: Experimental Studies of Electron Transport. *Plasma Physics and Controlled Fusion* **43**, A323-A338 (2001).
339. Ryter, F., F. Imbeaux*, F. Leuterer, H.-U. Fahrbach, W. Suttrop and ASDEX Upgrade Team: Experimental Characterization of the Electron Heat Transport in Low-Density ASDEX Upgrade Plasmas. *Physical Review Letters* **86**, 5498-5501 (2001).
340. Ryter, F., F. Leuterer, G. Pereverzev, H.-U. Fahrbach, J. Stober, W. Suttrop and ASDEX Upgrade Team: Experimental Evidence for Gradient Length-Driven Electron Transport in Tokamaks. *Physical Review Letters* **86**, 2325-2328 (2001).
341. Ryter, F., J. Stober, A. Stäbler, G. Tardini, H.-U. Fahrbach, O. Gruber, A. Herrmann, A. Kallenbach, M. Kaufmann, B. Kurzan, F. Leuterer, M. Maraschek, H. Meister, A.G. Peeters, G. Pereverzev, A.C.C. Sips, W. Suttrop, W. Treutterer, H. Zohm and ASDEX Upgrade Team: Confinement and Transport Studies of Conventional Scenarios in ASDEX Upgrade. *Nuclear Fusion* **41**, 537-550 (2001).
342. Saarelma*, S., S. Günter, T. Kinviemi*, T. Kurki-Suonio* and ASDEX Upgrade Team: MHD Stability Analysis of Type II ELMs in ASDEX Upgrade. In: *Proceedings of the 28th EPS Conference on Controlled Fusion and Plasma Physics*, Funchal 2001, (Eds.) C.Silva, C.Varandas, D.Campbell. ECA 25A. European Physical Society, Geneva 2001, 165-168.
343. Saffman*, M., S. Zoletnik*, N.P. Basse, W. Svendsen*, G. Kocsis* and M. Endler: CO₂ Laser Based Two-Volume Collective Scattering Instrument for Spatially Localized Turbulence Measurements. *Review of Scientific Instruments* **72**, 2579-2592 (2001).
344. Saibene*, G., P. Lomas*, M. Becoulet*, R. Sartori*, A. Loarte*, R.V. Budny*, V. Parail*, K.-D. Zastrow*, M. von Hellermann*, M. Beurskens*, Y. Andrew*, A. Kallenbach, P. Hennequin*, W. Suttrop, J. Stober, S. Sharapov*, M. Zerbini* and Contributors to the EFDA-JET Work Programme: The Effect of Plasma Shape on Density and Confinement of ELMY H-Modes in JET. In: *Proceedings of the 28th EPS Conference on Controlled Fusion and Plasma Physics*, Funchal 2001, (Eds.) C.Silva, C.Varandas, D.Campbell. ECA 25A. European Physical Society, Geneva 2001, 1749-1752.
345. Salat, A. and J.A. Tatatronic*: Shear Alfvén Mode Resonances in Nonaxisymmetric Toroidal Low-Pressure Plasmas. Part 1: Mode Equations in Arbitrary Geometry. *Physics of Plasmas* **8**, 1200-1206 (2001).
346. Salat, A. and J.A. Tatatronic*: Shear Alfvén Mode Resonances in Nonaxisymmetric Toroidal Low-Pressure Plasmas. Part 2: Singular Modes in the Shear Alfvén Continuum. *Physics of Plasmas* **8**, 1207-1218 (2001).
347. Sapper, J., W. Gardebrecht, F. Kerl and I. Schoenewolf: The Layout of the Wendelstein 7-X Magnet. *Fusion Engineering and Design* **58-59**, 237-240 (2001).
348. Schacht, J., H. Niedermeyer, C. Wiencke*, J. Hildebrandt* and A. Wassatsch*: The Trigger-Time-Event System for the W7-X Experiment. In: *Proceedings of the 12th IEEE-NPSS Real Time Conference*, Valencia 2001, (Eds.) E.Sanchis, A.Ferrer, V.González. University of Valencia, Valencia 2001, 240-244.
349. Schauer, F., H. Bau, I. Bojko, R. Brockmann, J.-H. Feist, B. Hein, M. Pieger-Frey, H. Pirsch, J. Sapper, B. Sombach, J. Stadlbauer, O. Volzke, I. Wald and M. Wanner: Assembly and Test of the W7-X DEMO-Cryostat. *Fusion Engineering and Design* **56-57**, 861-866 (2001).

Publications

350. *Schauer, F. and I. Bojko*: Helium Cryogenic System for W7-X. In: Proceedings of the Satellite Workshop on Cryogenics for Large Systems, Ahmedabad 2000, (Eds.) Y.C.Saxena, C.P.Dhard, S.Das. Institute for Plasma Research, Bhat, Gandhinagar 2001, 16-27.
351. *Scheerer*, M., H. Bolt, A. Gervash*, J. Linke* and I. Smid**: The Design of Actively Cooled Plasma-Facing Components. *Physica Scripta* **T91**, 98-103 (2001).
352. *Schleisner*, L., T. Hamacher, H. Cabal*, B. Hallberg*, Y. Lechon*, R. Korhonen* and R.M. Saez**: Energy, Material and Land Requirements of a Fusion Plant. *Fusion Engineering and Design* **58-59**, 1081-1085 (2001).
353. *Schmid, K., J. Roth and W. Eckstein*: Influence of Diffusion on W Sputtering by Carbon. *Journal of Nuclear Materials* **290-293**, 148-152 (2001).
354. *Schneider, R., M. Borchardt, J. Riemann, X. Bonnin, J. Nührenberg and A. Mutzke*: Edge Modelling for W7-X. In: Proceedings of the 18th Fusion Energy Conference, Sorrento 2000, IAEA, Vienna 2001, THP1/24.
355. *Schneider*, T., S. Lepicard*, R.M. Saez*, H. Cabal*, Y. Lechon*, D. Ward*, T. Hamacher, K. Aquilonius*, B. Hallberg* and R. Korhonen**: Evaluation of Radiological and Economic Consequences Associated with an Accident in a Fusion Power Plant. *Fusion Engineering and Design* **58-59**, 1077-1080 (2001).
356. *Schneider, W., D. Hildebrandt, X. Gong, K. Krieger, R. Neu, V. Rohde, J. Roth and ASDEX Upgrade Team*: Tungsten Migration between Main Chamber and Divertor of ASDEX Upgrade. In: Proceedings of the 28th EPS Conference on Controlled Fusion and Plasma Physics, Funchal 2001, (Eds.) C.Silva, C.Varandas, D.Campbell. ECA 25A. European Physical Society, Geneva 2001, 189-192.
357. *Schröder*, C., T. Klinger, D. Block* and A. Piel**: Taming Drift Wave Turbulence. *Contributions to Plasma Physics* **41**, 455-460 (2001).
358. *Schröder*, C., T. Klinger, D. Block*, A. Piel*, G. Bonhomme* and V. Naulin**: Mode Selective Control of Drift Wave Turbulence. *Physical Review Letters* **86**, 5711-5714 (2001).
359. *Schwarz-Selinger, T., D.G. Cahill*, S.-C. Chen*, S.-J. Moon* and C.P. Grigoropoulos**: Micron-Scale Modifications of Si Surface Morphology by Pulsed-Laser Texturing. *Physical Review B* **64**, 155323 (2001).
360. *Schwarz-Selinger, T., V. Dose, W. Jacob and A. von Keudell*: Quantification of a Radical Beam Source for Methyl Radicals. *Journal of Vacuum Science and Technology A* **19**, 101-107 (2001).
361. *Schwarz-Selinger, T., R. Preuss, V. Dose and W. von der Linden**: Analysis of Multicomponent Mass Spectra Applying Bayesian Probability Theory. *Journal of Mass Spectrometry* **36**, 866-874 (2001).
362. *Schwenn, U.*: Computer Simulation of Plasmas. The Computational Stellarator. In: Summer University for Plasma Physics, Garching 2001, (Eds.) A.Könies, K.Krieger. Max-Planck-Institut für Plasmaphysik, Garching 2001, 261-274.
363. *Scott, B.D.*: An Introduction to MHD. In: Summer University for Plasma Physics, Garching 2001, (Eds.) A.Könies, K.Krieger. Max-Planck-Institut für Plasmaphysik, Garching 2001, 43-63.
364. *Scott, B.D.*: Shifted Metric Procedure for Flux Tube Treatments of Toroidal Geometry: Avoiding Grid Deformation. *Physics of Plasmas* **8**, 447-458 (2001).
365. *Sergeev*, V.Yu., V.M. Timokhin*, O.A. Bakhareva*, B.V. Kuteev*, V.A. Belopolsky*, R. Burhenn, L. Ledl and W7-AS Team*: Studies of C-Pellet Ablation Cloud Structure on Wendelstein 7-AS Stellarator. In: Proceedings of the 28th EPS Conference on Controlled Fusion and Plasma Physics, Funchal 2001, (Eds.) C.Silva, C.Varandas, D.Campbell. ECA 25A. European Physical Society, Geneva 2001, 1953-1956.
366. *Sihler, C., P. Fu*, M. Huart, B. Streibl and W. Treutterer*: Paralleling of Two Large Flywheel Generators for the Optimisation of the ASDEX Upgrade Power Supply. *Fusion Engineering and Design* **58-59**, 41-45 (2001).
367. *Sihler, C., M. Huart, B. Streibl, D. Hrabal* and H. Schmitt**: Transient Performance of Vacuum-Switched Static VAR Compensators Optimised for Large Inductive Loads. In: Proceedings of the 4th International Conference on Power Systems Transients, Rio de Janeiro 2001, (Ed.) Federal University of Rio de Janeiro 2001, 481-486.
368. *Silva*, A., L. Cupido*, M. Manso*, S. Vergamota*, I. Nunes*, J. Santos*, F. Serra*, V. Grossmann*, G. Conway and ASDEX Upgrade Team*: Advances in Microwave Reflectometry on ASDEX Upgrade. In: Proceedings of the 28th EPS Conference on Controlled Fusion and Plasma Physics, Funchal 2001, (Eds.) C.Silva, C.Varandas, D.Campbell. ECA 25A. European Physical Society, Geneva 2001, 1297-1300.
369. *Silva*, A., M. Manso*, S. Vergamota*, L. Cupido*, L. Meneses*, I. Nunes* and ASDEX Upgrade Team*: Performance of the Microwave Reflectometry Diagnostic for Density Profile Measurements on ASDEX Upgrade. *Review of Scientific Instruments* **72**, 307-310 (2001).
370. *Simintzis*, C., G.N. Throumoulopoulos*, G. Pantis* and H. Tasso*: Analytic Magnetohydrodynamic Equilibria of a Magnetically Confined Plasma with Sheared Flows. *Physics of Plasmas* **8**, 2641-2648 (2001).
371. *Simon-Weidner, J. and N. Jaksic*: Safety Margins of the W7-X Plasma Vessel for the Static Case. *Fusion Engineering and Design* **58-59**, 881-886 (2001).
372. *Snead*, L.L. and M. Balden*: Reordering and Crystallisation of Silicon Carbide by Neutron Irradiated. *Materials Research Society Symposium Proceedings* **650**, R5.1.1-6 (2001).
373. *Snell*, G., U. Hergenbahn, N. Müller*, M. Drescher*, J. Viehhaus*, U. Becker* and U. Heinzmann**: Study of Xenon 4d, 5p, and 5s Photoionization in the Shape-Resonance Region Using Spin-Resolved Electron Spectroscopy. *Physical Review A* **63**, 032712 (2001).
374. *Spies, G.O., D. Lortz and R. Kaiser**: Relaxed Plasma-Vacuum Systems. *Physics of Plasmas* **8**, 3652-3663 (2001).
375. *Stan-Sion*, C., R. Behrisch, J.P. Coad*, U. Kreissig*, F. Kubo*, V. Lazarev*, S. Lindig, M. Mayer, E. Nolte*, A. Peacock*, L. Rohrer* and J. Roth*: Hydrogen Isotope Depth Profiling in Carbon Samples from the Erosion Dominated Inner Vessel Walls of JET. *Journal of Nuclear Materials* **290-293**, 491-495 (2001).
376. *Stober, J., C. Fuchs, O. Gruber, M. Kaufmann, B. Kurzan, F. Meo, H.W. Müller, R. Ryter and ASDEX Upgrade Team*: Dependence of the Density Shape on the Heat Flux Profile in ASDEX Upgrade High Density H Modes. *Nuclear Fusion* **41**, 1535-1538 (2001).
377. *Stober, J., M. Maraschek, G. Conway, O. Gruber, A. Herrmann, A.C.C. Sips, W. Treutterer, H. Zohm and ASDEX Upgrade Team*: Type II ELMy H-Modes on ASDEX Upgrade with Good Confinement at High Density. *Nuclear Fusion* **41**, 1123-1134 (2001).
378. *Stober, J., H. Zohm, O. Gruber, A. Herrmann, M. Kaufmann, M. Maraschek, F. Meo, A.C.C. Sips, W. Treutterer and ASDEX Upgrade Team*: Optimization of Confinement, Stability and Power Exhaust of

Publications

the ELMy H-Mode in ASDEX Upgrade. *Plasma Physics and Controlled Fusion* **43**, A39-A53 (2001).

379. *Streibl, B., A. Kaltenberger, H. Kollotzek, K. Mattes, V. Rohde, G. Schall and K. Schindler*: Operational Behaviour of the ASDEX Upgrade In-Vessel Cryo Pump. *Fusion Engineering and Design* **56-57**, 867-872 (2001).

380. *Stroth*, U.*: Experimental Results from Stellarators. In: Summer University for Plasma Physics, Garching 2001, (Eds.) A.Könies, K.Krieger. Max-Planck-Institut für Plasmaphysik, Garching 2001, 143-165.

381. *Stroth*, U., K. Itoh*, S.-I. Itoh*, H.-J. Hartfuß, H. Laqua, ECRH-Team and W7-AS Team*: Internal Transport Barrier Triggered by Neoclassical Transport in W7-AS. *Physical Review Letters* **86**, 5910-5913 (2001).

382. *Strumberger, E., H.-P. Zehrfeld, S. Günter and ASDEX Upgrade Team*: Stability Studies of Ideal Plasma Flow Equilibria. In: Proceedings of the 28th EPS Conference on Controlled Fusion and Plasma Physics, Funchal 2001, (Eds.) C.Silva, C.Varandas, D.Campbell. ECA 25A. European Physical Society, Geneva 2001, 1909-1912.

383. *Subbotin*, A.A., M.I. Mikhailov*, J. Nührenberg, M.Yu. Isaev*, W.A. Cooper*, M.F. Heyn*, V.N. Kalyuzhnyj*, S.V. Kasilov*, W. Kernbichler*, V.V. Nemov*, M.A. Samitov* and V.D. Shafranov**: Optimization of N=6 Helias-Type Stellarator. In: Proceedings of the 28th EPS Conference on Controlled Fusion and Plasma Physics, Funchal 2001, (Eds.) C.Silva, C.Varandas, D.Campbell. ECA 25A. European Physical Society, Geneva 2001, 1973-1976.

384. *Suttrop, W., R.V. Budny*, J.G. Cordey*, C. Gowers*, M. Mantsinen*, G.F. Matthews*, H. Nordman*, V. Parail*, J. Rapp*, J. Storr*, J. Strachan*, J. Weiland*, K.D. Zanzrow* and Contributors to the EFDA-JET Work Programme*: Effect of Heat Flux and Density Variation on Electron Temperature Profiles in JET ELMy H-Modes. In: Proceedings of the 28th EPS Conference on Controlled Fusion and Plasma Physics, Funchal 2001, (Eds.) C.Silva, C.Varandas, D.Campbell. ECA 25A. European Physical Society, Geneva 2001, 989-992.

385. *Svensson*, J., M. von Hellermann* and R. König*: Direct Measurement of JET Local Deuteron Densities by Neutral Network Modelling of Balmer Alpha Beam Emission Spectra. *Plasma Physics and Controlled Fusion* **43**, 389-403 (2001).

386. *Tabasso, A., H. Maier, J. Roth, K. Krieger and ASDEX Upgrade Team*: Studies of Tungsten Erosion at the Inner and Outer Main Chamber Wall of the ASDEX Upgrade Tokamak. *Journal of Nuclear Materials* **290-293**, 326-330 (2001).

387. *Tardini, G., A.G. Peeters, G. Pereverzev, F. Ryter and ASDEX Upgrade Team*: Theory Based Modelling of EC Heated Discharges. In: Proceedings of the 28th EPS Conference on Controlled Fusion and Plasma Physics, Funchal 2001, (Eds.) C.Silva, C.Varandas, D.Campbell. ECA 25A. European Physical Society, Geneva 2001, 685-688.

388. *Terborg, R., M. Polcik*, R.L. Toomes*, P. Baumgärtel*, J.-T. Hoefl*, A.M. Bradshaw and D.P. Woodruff**: Photoelectron Diffraction Determination of the Local Adsorption Geometry of CO on Cu(210). *Surface Science* **473**, 203-212 (2001).

389. *Thomsen, H., M. Endler, J. Bleuel, A. Chankin* and G.F. Matthews**: Parallel Correlation Studies of Fluctuations and the Impact of Perturbations in the Magnetic Configuration. *Contributions to Plasma Physics* **41**, 530-536 (2001).

390. *Thomsen, H., M. Endler and M. Schubert*: Modification of the Turbulence in the Plasma Boundary of the Wendelstein 7-AS Stellarator Using Electric Probes. *Czechoslovak Journal of Physics* **51**, 1079-1086 (2001).

391. *Thomsen, H., M. Endler, M. Schubert and W7-AS Team*: Modification of the Turbulence in the Plasma Boundary of the Wendelstein 7-AS Stellarator Using Electric Probes. In: Proceedings of the 28th EPS Conference on Controlled Fusion and Plasma Physics, Funchal 2001, (Eds.) C.Silva, C.Varandas, D.Campbell. ECA 25A. European Physical Society, Geneva 2001, 2093-2096.

392. *Throumoulopoulos*, G.N. and H. Tasso*: Axisymmetric Equilibria of a Gravitating Plasma with Incompressible Flows. *Geophysical and Astrophysical Fluid Dynamics* **94**, 249-262 (2001).

393. *Throumoulopoulos*, G.N. and H. Tasso*: On Resistive Magneto-hydrodynamic Equilibria of an Axisymmetric Toroidal Plasma with Flow. *Journal of Plasma Physics* **64**, 601-612 (2001).

394. *Toi*, K., S. Ohdachi*, S. Yamamoto*, S. Sakakibara*, H. Yamada*, A. Weller, K.W. Watanabe*, Y. Narushima*, K. Narihara*, K. Tanaka*, I. Yamada*, T. Tokuzawa*, S. Masuzaki*, S. Morita*, M. Goto*, J. Li, K. Kawahata*, N. Ohyaibu* and LHD Experimental Group*: Characteristics of MHD Instabilities Excited in the Core and Edge Regions of the LHD Plasmas. In: Proceedings of the 28th EPS Conference on Controlled Fusion and Plasma Physics, Funchal 2001, (Eds.) C.Silva, C.Varandas, D.Campbell. ECA 25A. European Physical Society, Geneva 2001, 1517-1520.

395. *Toussaint, U. von, R. Fischer and V. Dose*: Bayesian Analysis of Ion Beam Diagnostics. In: Proceedings of the 20th International Workshop on Bayesian Inference and Maximum Entropy Methods in Science and Engineering, Gif-sur-Yvette 2000, (Ed.) A.Mohammad-Djafari. AIP Conference Proceedings 568, AIP Press, Melville, NY 2001, 615-624.

396. *Tuccillo*, A.A., Y. Baranov*, E. Barbato*, P. Bibet*, C. Castaldo*, R. Cesario*, V. Cocilovo*, F. Crisanti*, R. De Angelis*, A. Ekedahl*, A. Figueiredo*, M. Graham*, G. Granucci*, D. Hartmann, J.A. Heikkinen*, T. Hellsten*, F. Imbeaux*, T.T.C. Jones*, T. Johnson*, K. Kirov, P. Lamalle*, M. Laxaback*, F. Leuterer, X. Litaudon*, P. Mage*, J. Mailloux*, M. Mantsinen*, M.-L. Mayoral*, F. Meo, I. Monakhov*, F. Nguyen*, J.-M. Noterdaeme, V. Pericoli-Ridolfini*, S. Podda*, L. Panaccione*, E. Righi*, F. Rimini*, Y. Sarazin*, A. Sibley*, A. Stäbler, T. Tala*, D. Van Eester* and Contributors to the EFDA-JET Work Programme*: Recent Heating and Current Drive Results on JET. In: Proc. 14th Topical Conference on Radiofrequency Power in Plasmas, Oxnard 2001, (Eds.) Tal Kuen Mau, J.de Grassie. AIP Conference Proceedings 595, AIP Press, Melville, NY 2001, 209-216 (2001).

397. *Valenza, D., H. Iida*, R. Plenteda* and R.T. Santoro**: Proposal of Shutdown Dose Estimation Method by Monte Carlo Code. *Fusion Engineering and Design* **55**, 411-418 (2001).

398. *Valovic*, M., J. Rapp*, J.G. Cordey*, D.C. McDonald*, L. Garzotti*, A. Kallenbach, M.A. Mahdavi*, J. Ongena*, V. Parail*, G. Saibene*, R. Sartori*, M. Stamp*, O. Sauter*, J. Strachan*, W. Suttrop and Contributors to the EFDA-JET Work Programme*: Long Time-Scale Density Peaking in JET. In: Proceedings of the 28th EPS Conference on Controlled Fusion and Plasma Physics, Funchal 2001, (Eds.) C.Silva, C.Varandas, D.Campbell. ECA 25A. European Physical Society, Geneva 2001, 957-960.

399. *Varela*, P., M. Manso*, G. Conway, C. Fuchs, B. Kurzan, H.W. Müller, W. Suttrop and ASDEX Upgrade Team*: Density Pedestal Measurements with Microwave Reflectometry on ASDEX Upgrade. In: Proceedings of the 28th EPS Conference on Controlled Fusion and Plasma Physics, Funchal 2001, (Eds.) C.Silva, C.Varandas, D.Campbell. ECA 25A. European Physical Society, Geneva 2001, 193-196.

Publications

400. *Varela*, P., M. Manso*, S. Vergamota*, V. Grossmann*, J. Santos* and ASDEX Upgrade Team*: Assessment of Density Profile Automatic Evaluation from Broadband Reflectometry Data. *Review of Scientific Instruments* **72**, 315-319 (2001).
401. *Vasquez-Borucki*, S., C.A. Achete* and W. Jacob*: Hydrogen Plasma Treatment of Poly(Ethylene Terephthalate) Surfaces. *Surface and Coatings Technology* **138**, 256-263 (2001).
402. *Veselova*, I.Y., I.Y. Senichenkov*, H.-P. Zehrfeld, R. Schneider, P.T. Lang, A. Lorenz, M. Reich and L.L. Lengyel*: Effect of grad(B)-Induced Drift on the Ablation History of Pellets: Results of Scenario Calculations. In: *Proceedings of the 28th EPS Conference on Controlled Fusion and Plasma Physics*, Funchal 2001, (Eds.) C.Silva, C.Varandas, D.Campbell. ECA 25A. European Physical Society, Geneva 2001, 701-704.
403. *Viljoen*, E.C., E. Taglauer and J. du Plessis**: A Novel Method to Determine the Ion Sputter Coefficient of Dilute Segregating Impurities. *Nuclear Instruments and Methods in Physics Research B* **179**, 512-520 (2001).
404. *Voitsenya*, V.S., A.F. Bardamid*, V.N. Bondarenko*, W. Jacob, V.G. Konovalov*, S. Masuzaki*, O. Motojima*, D.V. Orlinskij*, V.L. Poperenko*, I.V. Ryzhkov*, A. Sagara*, A.F. Shtan, S.I. Solodovchenko* and M.V. Vinnichenko**: Some Problems Arising due to Plasma-Surface-Interaction for Operation of the In-Vessel Mirrors in a Fusion Reactor. *Journal of Nuclear Materials* **290-293**, 336-340 (2001).
405. *Vollmer, O., B. Heinemann, W. Kraus, P. McNeely, R. Riedl, E. Speth, R. Trainham* and R. Wilhelm*: Progress in the Development of a Large RF Negative Ion Source for Fusion. *Fusion Engineering and Design* **56-57**, 465-470 (2001).
406. *Volpe, F.*: Electron Bernstein Emission Diagnostic of Electron Temperature Profiles at W7-AS Stellarator. In: *Proceedings of the 28th EPS Conference on Controlled Fusion and Plasma Physics*, Funchal 2001, (Eds.) C.Silva, C.Varandas, D.Campbell. ECA 25A. European Physical Society, Geneva 2001, 1329-1332.
407. *Volpe, F., H.P. Laqua and W7-AS Team*: Electron Bernstein Emission Electron Temperature Profile Diagnostic at the W7-AS Stellarator. *Stellarator News* **77**, 1-4 (2001), <http://www.ornl.gov/fed/stelnews>.
408. *Wanner, M., J.-H. Feist, H. Renner, J. Sapper, F. Schauer, H. Schneider, V. Erckmann, H. Niedermeyer and W7-X Team*: Design and Construction of Wendelstein 7-X. *Fusion Engineering and Design* **56-57**, 155-162 (2001).
409. *Wegener, L., J.-H. Feist, J. Sapper, F. Kerl and F. Werner*: Final Design and Construction of the Wendelstein 7-X Coils. *Fusion Engineering and Design* **58-59**, 225-230 (2001).
410. *Weller, A., M. Anton, J. Geiger, M. Hirsch, R. Jaenicke, A. Werner, C. Nührenberg, E. Sallander, D.A. Spong* and W7-AS Team*: Survey of Magnetohydrodynamic Instabilities in the Advanced Stellarator Wendelstein 7-AS. *Physics of Plasmas* **8**, 931-956 (2001).
411. *Wendt*, M., T. Klinger, C. Franck* and A. Piel**: Localization of the High Frequency Field in a Beam-Plasma Diode due to Density Gradients. *Physica Scripta* **63**, 62-69 (2001).
412. *Wenmin*, W., J. Roth, S. Lindig and C.H. Wu*: Blister Formation of Tungsten due to Ion Bombardment. *Journal of Nuclear Materials* **299**, 124-131 (2001).
413. *Wenzel, U., D.P. Coster, A. Kallenbach, H. Kastelewicz, M. Laux, H. Maier, R. Schneider and ASDEX Upgrade Team*: In-Out Asymmetry of Divertor Temperatures in Tokamaks. *Nuclear Fusion* **41**, 1695-1701 (2001).
414. *Wenzel, U., M. Laux, R. Pugno and K. Schmidtman*: Extinction of CD Band Emission in the Divertor of ASDEX Upgrade. *Journal of Nuclear Materials* **290-293**, 352-355 (2001).
415. *Werner, A., A. Weller, D.S. Darrow* and W7-AS Team*: Fast Ion Losses in the W7-AS Stellarator. *Review of Scientific Instruments* **72**, 780-783 (2001).
416. *Wienhold*, P., H.G. Esser*, D. Hildebrandt, A. Kirschner*, M. Mayer, V. Philipps* and M. Rubel**: Investigation of Carbon Transport in the Scrape-off Layer of TEXTOR-94. *Journal Nuclear Materials* **290-293**, 362-366 (2001).
417. *Wienhold*, P., M. Rubel*, M. Mayer, D. Hildebrandt, W. Schneider and A. Kirschner**: Deposition and Erosion in Local Shadow Regions of TEXTOR-94. *Physica Scripta* **T94**, 141-145 (2001).
418. *Wiltner, A., A. Rosenhahn*, J. Schneider*, C. Becker*, P. Pervan*, M. Milun*, M. Kralj* and K. Wandelt**: Growth of Copper and Vanadium on a Thin Al₂O₃-Film on Ni₃Al(111). *Thin Solid Films* **400**, 71-75 (2001).
419. *Wobig, H.*: Introduction to Stellarator Physics. In: *Summer University for Plasma Physics*, Garching 2001, (Eds.) A.Könies, K.Krieger. Max-Planck-Institut für Plasmaphysik, Garching 2001, 121-142.
420. *Wolf, R.*: Experimental Results in Tokamak Physics. In: *Summer University for Plasma Physics*, Garching 2001, (Eds.) A.Könies, K.Krieger. Max-Planck-Institut für Plasmaphysik, Garching 2001, 167-183.
421. *Wolf, R.C., Y. Baranov*, C. Giroud*, M. Mantsinen*, D. Mazon*, K.-D. Zastrow*, N. Hawkes*, T. Hellsten*, J. Hobirk, M. Laxaback*, J.-M. Noterdaeme, F. Rimini*, A. Stäbler, F. Ryter, J. Stober, H. Zohm, ASDEX Upgrade Team and Contributors to the EFDA-JET Work Programme*: Influence of Electron Heating on Confinement in JET and ASDEX Upgrade Internal Transport Barrier Plasmas. In: *Proceedings of the 28th EPS Conference on Controlled Fusion and Plasma Physics*, Funchal 2001, (Eds.) C.Silva, C.Varandas, D.Campbell. ECA 25A. European Physical Society, Geneva 2001, 513-516.
422. *Wolf, R., J. Hobirk, G. Conway, O. Gruber, A. Gude, S. Günter, K. Kirov, B. Kurzan, F. Leuterer, M. Maraschek, P.J. McCarthy*, H. Meister, G. Pereverzev, E. Poli, F. Ryter, W. Treutterer, Q. Yu and ASDEX Upgrade Team*: Performance, Heating and Current Drive Scenarios of ASDEX Upgrade Advanced Tokamak Discharges. *Nuclear Fusion* **41**, 1259-1271 (2001).
423. *Yamada-Takamura*, Y., F. Koch, H. Maier and H. Bolt*: Characterisation of α -Phase Aluminium Oxide Films Deposited by Filtered Vacuum Arc. *Surface and Coatings Technology* **142-144**, 260-264 (2001).
424. *You, J.-H. and H. Bolt*: Analysis of Singular Interface Stresses in Dissimilar Material Joints for Plasma-Facing Components. *Journal of Nuclear Materials* **299**, 1-8 (2001).
425. *You, J.-H. and H. Bolt*: Analytical Method for Thermal Stress Analysis of Plasma-Facing Materials. *Journal of Nuclear Materials* **299**, 9-19 (2001).
426. *Yu, Q., S. Günter and K. Lackner*: Stabilizing Effect of a Non-resonant Helical Field on Neoclassical Tearing Modes. In: *Proceedings of the 28th EPS Conference on Controlled Fusion and Plasma Physics*, Funchal 2001, (Eds.) C.Silva, C.Varandas, D.Campbell. ECA 25A. European Physical Society, Geneva 2001, 1093-1096.

Publications

427. *Zarrabian, M., A. Kallenbach, K. Behringer, A. Carlson, J. Gafert and G. Haas*: Determination of Hydrocarbon Impurity Influxes, Photon Efficiencies and Chemical Sputtering Yield in ASDEX Upgrade. *Physica Scripta* **T91**, 43-47 (2001).

428. *Zehetbauer, T., G. Pautasso, C. Tichmann, S. Egorov, A. Lorenz, V. Mertens, G. Neu, G. Raupp, W. Treutterer, D. Zasche and ASDEX Upgrade Team*: Real-Time Disruption Handling at ASDEX Upgrade. *Fusion Engineering and Design* **56-57**, 721-725 (2001).

429. *Zille, R., J. Nührenberg and S. Gori*: Stellarator Optimizations at 4 and 3 Periods. In: *Theory of Fusion Plasmas, Varenna 2000*, Societa Italiana di Fisica, Bologna, 2000, 393-400.

430. *Zohm, H.*: Tokamaks: Equilibrium, Stability and Transport. In: *Summer University for Plasma Physics, Garching 2001*, (Eds.) A.Könies, K.Krieger. Max-Planck-Institut für Plasmaphysik, Garching 2001, 95-107.

431. *Zohm, H., G. Gantenbein*, A. Gude, S. Günter, F. Leuterer, M. Maraschek, J. Meskat, W. Suttrop, Q. Yu, ASDEX Upgrade Team and ECRH Team*: Neoclassical Tearing Modes and their Stabilization by Electron Cyclotron Current Drive in ASDEX Upgrade. *Physics of Plasmas* **8**, 2009-2016 (2001).

432. *Zohm, H., G. Gantenbein*, A. Gude, S. Günter, F. Leuterer, M. Maraschek, J. Meskat, W. Suttrop, Q. Yu, ASDEX Upgrade Team and ECRH Team*: The Physics of Neoclassical Tearing Modes and their Stabilization by ECCD in ASDEX Upgrade. *Nuclear Fusion* **41**, 197-202 (2001).

433. *Zuhr*, R.A., J. Roth, W. Eckstein, U. von Toussaint and J. Luthin*: Implantation, Erosion, and Retention of Tungsten in Carbon. *Journal of Nuclear Materials* **290-293**, 162-165 (2001).

Diploma Theses

434. *Beguiristain Repáraz, I.*: Investigation of the Influence of Substrate Temperature and Bias Voltage on the Crystal Structure of Vacuum Arc Deposited Al₂O₃ Coatings. Universidad de Navarra, San Sebastián 2001.

435. *Durocher, K.*: Deuterium Retention in Doped Graphites. Ecole Nationale Supérieure de Chimie, Paris 2001.

436. *Götz, M.*: Optimierung der Lösungen einer Differentialgleichung zur Beschreibung eines Gyrotrons. TU München 2001.

437. *Schneider, M.*: Bestimmung des Wirkungsquerschnittes von 7Li an Kohlenstoff sowie von 6Li an Kohlenstoff, Sauerstoff und Aluminium für die RBS-Analyse im Energiebereich unter 6 MeV. FH München 2001.

Doctoral Theses

438. *Beikler, R.*: Untersuchung der Oberflächensegregation geordneter Legierungen mittels Ionenstreuung am Beispiel CuAu(100). Universität München 2001.

439. *Geier, A.*: Aspekte des Verhaltens von Wolfram im Fusionsreaktor ASDEX Upgrade. TU München 2001.

440. *Grulke, O.*: Investigation of Large-Scale Spatiotemporal Fluctuation Structures in Magnetized Plasmas. Universität Kiel 2001.

441. *Kang, H.*: Structure and Magnetism in Ultra-Thin Fe_x Co_{1-x}-Films. Universität Bayreuth 2001.

442. *Kleberg, I.*: Dynamik von kathodischen Brennflecken im externen Magnetfeld. Humboldt-Universität Berlin 2001.

443. *Luthin, J.*: Untersuchungen zur chemischen Wechselwirkung bei der Bildung von Kohlenstoff-Mischsystemen. Universität Bayreuth 2001.

444. *Reinecke, N.*: Adsorbatinduziert selbstorganisierende Nanostrukturen auf Cu(111)-Oberflächen. Universität Bayreuth 2001.

445. *Schade, S.*: MHD Stability of ASDEX Upgrade and Textor-94 Advanced Scenarios. Universität Rostock 2001.

446. *Schmid, K.*: Untersuchung der Temperaturabhängigkeit der Erosion von Wolfram durch Kohlenstoff. Universität Bayreuth 2001.

Habilitations

447. *Schneider, R.*: Plasma Edge Physics for Tokamaks. Universität Greifswald 2001.

448. *Suttrop, W.*: Physics of Edge Operational Limits and their Effect on Tokamak Confinement. Universität Bayreuth 2001.

Patents

449. *Biedermann, C., R. Radtke and S. Deuchler*: Bestrahlungseinrichtung mit einem hochflexiblen Membranbalg. Antrag auf internationale vorläufige Prüfung der PCT-Anmeldung EP00/11207: Juli 2001. Erteilung des deutschen Patents Nr. DE 199 62 198.5: 13.12.2001.

450. *Gehring, K.*: Vitondichtungen. Freigabe des deutschen Gebrauchsmusters Nr. 29519 353.0: 6.11.2001.

451. *Haas, G.*: Heisskathoden-Ionisationsmanometer II. Erteilung des japanischen Patents Nr. 4-05639: 6.4.2001. Einzahlung der 2. Verlängerungsgebühr für das USA-Patent Nr. 5 300 890: August 2001. Verlängerung des deutschen Gebrauchsmusters 9305441: April 2001.

452. *Kasperek*, W. and G. Müller**: Wellenzahl-Spektrometer. Freigabe des europäischen Patents Nr. EP 209727: 20.3.2001.

453. *Mast, K.-F., G. Schramm and M. Münch*: Folienmanometer. Veröffentlichung der japanischen Patentanmeldung Nr. 2001-517313: 2.10.2001. Erteilung des europäischen Patents Nr. EP 0968407 B1: 24.10.2001.

454. *Probst, F.*: Dichtung für Hochvakuumgefäß. Freigabe des deutschen Patents 19713975.2: 20.3.2001.

455. *Schacht, J. and H. Niedermeyer*: Verfahren und Vorrichtung zum Synchronisieren und Steuern von technischen Systemen. Unbeschränkte Inanspruchnahme der Erfindung: 18.4.2001. Patentanmeldung Nr. 101341946: 13.7.2001.

456. *Steinberger, J.*: UHV-Vielfachdurchführung für Mantelthermoelemente. Patentanmeldung Nr. 10114336.2: 23.3.2001.

457. *Weber, G.*: Vakuum-Stromdurchführung. Freigabe des deutschen Patents P 4212859.5: 20.3.2001.

458. *Wilhelm, R., W. Möller and R. Hytry*: PECVD-Innenbeschichtung. Freigabe des europäischen Patents Nr. 0568049: 20.2.2001.

459. *Wittenbecher, K.*: Verfahren und Vorrichtung zur Frequenzmultiplikation und -division. Freigabe des deutschen Patents 19810576: 30.10.2001.

460. *Wittenbecher, K., P. Turba and K. Klaster*: Lichtschranke mit hoher Störsicherheit. Verlängerung des deutschen Gebrauchsmusters: Juli 2001.

Lectures

461. *Bachmann, P.*: Chaos im Plasma. Lange Nacht der Wissenschaften, Berlin 2001.
462. *Bachmann, P.*: Chaos im Plasma. Rotary Club, Berlin 2001.
463. *Bachmann, P.*: Chaos in 1d Radiative Edge Plasmas. 8th Workshop on Plasma Edge Theory, Helsinki 2001.
464. *Bachmann, P.*: Chaos in 1d Radiative Edge Plasmas. Zinnowitz Theory Meeting, Zinnowitz 2001.
465. *Bakhareva*, O.A., V.M. Timokhin*, B.V. Kuteev*, R. Burhenn and W7-AS Team*: Studies of C-Pellet Ablation Cloud Structure on W7-AS. 28th Zvenigorod Conference on Plasma Physics and Controlled Fusion, Zvenigorod 2001.
466. *Balden, M., C. Garcia-Rosales*, J. Etxeberria* and J. Roth*: Chemical Erosion and Morphological Changes of Carbide-Doped Graphites by Deuterium Bombardment. 10th International Conference on Fusion Reactor Materials, Baden-Baden 2001.
467. *Balden, M., L.L. Snead*, H. Wang*, J. Strizak* and A.M. Williams**: Thermal Conductivity of Tensile Tested SiC_f/SiC Composites. 10th International Conference on Fusion Reactor Materials, Baden-Baden 2001.
468. *Basse, N.P., P.K. Michelsen*, S. Zoletnik*, M. Saffman*, M. Endler and M. Hirsch*: Spatial Distribution of Turbulence in the Wendelstein 7-AS Stellarator. 25th International Conference on Phenomena in Ionized Gases, Nagoya 2001.
469. *Basse, N.P., S. Zoletnik*, M. Saffman*, G. Antar* and P.K. Michelsen**: Temporal Separation of Turbulent Time Series: Measurements and Simulations. 9th European Fusion Theory Conference, Helsingor 2001.
470. *Bäumel, S.*: Development of a mm-Wave Imaging System for W7-AS. Verhandl. DPG (VI) **36**, 157, P4.2 (2001).
471. *Bäumel, S., E. Martines*, M. Endler and H.-J. Hartfuß*: 2D ECE Diagnostics on the W7-AS Fusion Experiment. Workshop "Simulation of Plasma Turbulence and Comparison with Experiment", Kiel 2001.
472. *Behringer, K.*: Einführung in die Plasmaspektroskopie. Vorlesung, Universität Augsburg, WS 2001/2002.
473. *Behringer, K.*: Interpretation der Linienstrahlung von Wasserstoff in Helium in Labor- und Divertorplasmen. Berliner Seminar über Plasmaphysik, IPP Berlin 2001.
474. *Behringer, K.*: Spektroskopie von Nichtgleichgewichtsplasmen. Vorlesung, Universität Augsburg, SS 2001.
475. *Behringer, K., U. Fantz* und T. Hamacher*: Physikalische Grundlagen der Energiewandlung und Verteilung. Seminar, Universität Augsburg, SS 2001, WS 2001/2002.
476. *Behringer, K., M. Stritzker*, U. Fantz* und H. Schreck**: Diagnostik von Niederdruckplasmen als industrielle Schlüsseltechnologie. Seminar, Universität Augsburg, SS 2001, WS 2001/2002.
477. *Behrisch, R.*: Contribution of Different Erosion Processes to the Material Release from the Vessel Walls of Fusion Devices during Plasma Operation. 8th Workshop on Plasma Edge Theory, Helsinki 2001.
478. *Behrisch, R.*: Das Problem der Plasma-Wand-Wechselwirkungen bei der kontrollierten thermonuklearen Fusion. Physikalisches Kolloquium, TU Dresden 2001.
479. *Beidler, C.D., E. Harmeyer, F. Herrnegger, J. Kisslinger, Yu.L. Igitkhanov and H. Wobig*: Stellarator Fusion Reactors - An Overview. 12th International Toki Conference on Plasma Physics and Controlled Nuclear Fusion, Toki-City 2001.
480. *Beidler, C.D., J. Kisslinger, E. Harmeyer, F. Herrnegger, Yu.L. Igitkhanov and H. Wobig*: Power Balance in Helias Reactors. Workshop of Innovative Concepts and Theory of Stellarators, Kiev 2001.
481. *Beikler, R.*: Surface Segregation of Ordered Alloys Studied by Low-Energy Ion Scattering - the Example CuAu. 3rd International Workshop on Surface and Interface Segregation, Porquerolles 2001.
482. *Beikler, R. und E. Taglauer*: Trajektorienaufgelöste Analyse von LEIS - Intensitätsverteilungen. Verhandl. DPG (VI) **36**, 332, O5.5 (2001).
483. *Berger*, M., U. Fantz* and K. Behringer*: Investigations of Excitation Transfer in He/He/Ar-Plasmas by Absorption Spectroscopy. Verhandl. DPG (VI) **36**, 171, P10.23 (2001).
484. *Bergmann, A., E. Poli and A.G. Peeters*: Monte Carlo δf Calculation of the Neoclassical Ion Current in a Rotating Island. 9th European Fusion Theory Conference, Helsingor 2001.
485. *Bessenrodt-Weberpals, M.*: Astrophysikalische Plasmen. Vorlesung, Universität Düsseldorf, SS 2001.
486. *Bessenrodt-Weberpals, M.*: Einführung in die Astrophysik. Vorlesung, Universität Düsseldorf, WS 2000/2001.
487. *Bessenrodt-Weberpals, M.*: Physikerinnen in Dual-Career Couple. Deutsche Physikerinnentagung, Dresden 2001.
488. *Bessenrodt-Weberpals, M.*: Work-Life Balancing. Wissenschaftsdialog FUTUR des BMBF, Berlin 2001.
489. *Beyer*, H., W. Bohmeyer, P. Kornejew, H.-D. Reiner and G. Fußmann*: Comparison of Different Beam Sources for the Helium Beam Diagnostics. ECAMP VII, Berlin 2001. Verhandl. DPG (VI) **36**, 177, P12.16 (2001).
490. *Biedermann, C., G. Fußmann, P. Mandelbaum*, R. Radtke and J.L. Schwob**: EUV Spectroscopy of Highly Charged Tungsten Ions Relevant to Hot Plasmas. ECAMP VII, Berlin 2001. Verhandl. DPG (VI) **36**, 69, A10.24 (2001).
491. *Bindemann, T., C. Fuchs, H.-J. Hartfuß and M. Hirsch*: Robust Line Density Measurement at W7-AS Using a Cotton-Mouton Polarimeter. International Conference on Advanced Diagnostics for Magnetic and Inertial Fusion, Varenna 2001.
492. *Bolshukhin, D., R. Neu, R. Dux and A. Kallenbach*: Determination of Z_{eff} from Central Bremsstrahlung in ASDEX Upgrade Discharges. Verhandl. DPG (VI) **36**, 153, P1.4 (2001).
493. *Bolt, H.*: Adaptation of Materials to Complex Environments. EU-Workshop on Strategies for Future Areas of Basic Materials Science, Stuttgart 2001.
494. *Bolt, H.*: Dünne Schichten. Vorlesung, TU München, SS 2001.
495. *Bolt, H.*: Materials for Fusion Energy Systems. Plenary Lecture, Materials Week, München 2001.
496. *Bolt, H.*: Oberflächentechnologie. Vorlesung, TU München, WS 2001/2002.
497. *Bolt, H.*: Plasma-Facing and High Heat Flux Materials - Introduction. Plenary Discussion Session on Role of Materials in the

Lectures

Development of Fusion Energy, 10th International Conference on Fusion Reactor Materials, Baden-Baden 2001.

498. *Bolt, H., V. Barabash, G. Federici, J. Linke*, A. Loarte*, J. Roth and K. Sato**: Plasma-Facing and High Heat Flux Materials - Needs for ITER and Beyond. 10th International Conference on Fusion Reactor Materials, Baden-Baden 2001.

499. *Bosch, H.-S.*: Alpha Particle Physics in Fusion Plasmas - from Plasma Heating to Helium Ash. Seminar "New Trends in Plasma Physics", Garching 2001.

500. *Bosch, H.-S.*: Heliumtransport und Heliumabfuhr in Divertor-tokamaks. Kolloquium IPP, Forschungszentrum Jülich 2001.

501. *Bosch, H.-S.*: Probleme und Möglichkeiten unserer zukünftigen Energieversorgung. Starnberger Kunstkreis BUZENTAUR, Starnberg 2001.

502. *Bosch, H.-S.*: Zum Stand der Fusionsforschung. Workshop "Moderne Energien - Fusionsenergie", Messe Hannover 2001.

503. *Bradshaw, A.M.*: Wohin führt uns die Kernfusionsforschung? Kolloquium, Universität Münster 2001.

504. *Bradshaw, A.M.*: Wohin führt uns die Kernfusionsforschung? Kolloquium, Universität Ulm 2001.

505. *Brakel, R.*: Experimental Results from Stellarators. Summer University for Plasma Physics, IPP Garching 2001.

506. *Brambilla, M.*: Numerical Simulation of IC Heating and Current Drive in Tokamak Plasmas. CEA Cadarache 2001.

507. *Brambilla, M.*: Numerical Simulation of IC Heating and Current Drive in Tokamak Plasmas. CNR Milano 2001.

508. *Bürbaumer*, H., R. Schneider, X. Bonnin, D.P. Coster, F. Aumayr* und H.P. Winter**: Investigation of the Detachment Front of ASDEX-Upgrade L-Mode Discharge 11276 Using the New Method for Grid Refinement in B2 Plasma Edge Simulation Code. 28th EPS Conference on Controlled Fusion and Plasma Physics, Funchal 2001.

509. *Burhenn, R., L. Giannone, H. Hacker, L. Ledl, A. Weller, C. Wendland, G. Kocsis*, Z. Zoletnik*, W7-AS Team, NBI Group and ECRH Group*: Investigations on Impurity Ion Behaviour in the Stellarator W7-AS. 1st Hungarian Plasma Physics Workshop, Budapest 2001.

510. *Conway, G., B. Kurzan, B.D. Scott, E. Holzhauer*, S. Klenge, W. Suttrop, M. Kaufmann, F. Jenko, F. Serra*, T. Ribeiro*, H. Zohm, ASDEX Upgrade Team and CFN Reflectometry Group*: Fluctuation and Reflectometer Simulation Studies on ASDEX Upgrade. 5th International Reflectometer Workshop, NIFS, Nagoya 2001.

511. *Cowers*, C., C.J. Barth*, R. Behn*, M. Beurskens*, B. Kurzan, P. Nielsen*, R. Pasqualotto*, M. Peres Alonso*, F. Orsitto*, J. Sanchez*, M. Walsh*, D. Wilson* and Contributors to the EFDA-JET Work Programme*: High Resolution Thomson Scattering on JET - an Assessment of the Feasibility. International Conference on Advanced Diagnostics for Magnetic Inertial Fusion, Varenna 2001.

512. *Dinklge, A.*: Nichtgleichgewichtsphysik in Glimmentladungen. Kolloquiumsvortrag, IPF Stuttgart 2001.

513. *Dose, V.*: Bayes und die Analyse physikalischer Daten. Kolloquium, Universität Erlangen 2001.

514. *Dose, V.*: Bayes und die Analyse physikalischer Daten. Kolloquium, Universität Greifswald 2001.

515. *Dose, V.*: Quantitative Analysis of Multicomponent Mass Spectra. 19th International Workshop on Maximum Entropy and Bayesian Methods, Baltimore, MD 2001.

516. *Düchs, D.*: Flüssigkeitsmodelle in der Plasmaphysik; mathematische Struktur der Gleichungssysteme. Vortrag, TU Darmstadt 2001.

517. *Düchs, D.*: Necessary and Possible "Pre-ITER" Fusion Research. 4th Symposium on Current Trends in International Fusion Research: Review and Assessment, Washington, D.C. 2001.

518. *Düchs, D.*: Plasmen als Strahlungsquellen Vorlesung, Ruhr-Universität Bochum, SS 2001.

519. *Düchs, D.*: Randschichten von heißen Plasmen; moderne Theorien und Messergebnisse. Vorlesung, Ruhr-Universität Bochum, WS 2000/2001.

520. *Düchs, D.*: Wechselwirkung von Teilchen in Plasmen. Vorlesung, Ruhr-Universität Bochum, WS 2001/2002.

521. *Dux, R.*: Plasmaphysik und Fusionsforschung I. Vorlesung, Universität Augsburg, WS 2000/2001.

522. *Dux, R.*: Plasmaphysik und Fusionsforschung II. Vorlesung, Universität Augsburg, SS 2001.

523. *Dux, R., K.-D. Zastrow*, C. Giroud*, ASDEX Upgrade Team and Contributors to the EFDA-JET Work Programme*: Transport and Accumulation of Impurities in JET and ASDEX Upgrade Advanced Scenarios. International Workshop on Physics of Internal Transport Barriers, Edge Pedestal, and Steady State Operation in Tokamaks, IPP Garching 2001.

524. *Ehmeler, H.*: Measurement of the C⁶⁺ Density in the Edge Region of the W7-AS Stellarator. Verhandl. DPG (VI) **36**, 157, P4.1 (2001).

525. *Endler, M.*: Physikalische Grundlagen und Techniken. Seminar "Energie", Universität Greifswald, WS 2000/2001.

526. *Endler, M.*: Turbulenz und Transport in Stellaratoren und Tokamaks. Physikalisches Kolloquium, Universität Greifswald 2001.

527. *Endler, M., J. Bleuel, O. Grulke, H. Niedermeyer, U. Pfeiffer, M. Schubert, H. Thomsen and W7-AS Team*: The Spatial Structure of Edge Fluctuations in the Wendelstein 7-AS Stellarator. Workshop "Simulation of Plasma Turbulence and Comparison with Experiment", Kiel 2001.

528. *Ertl, K. and J. Roth*: Analysemöglichkeiten an einem 3MV-Tandembeschleuniger. IPP Greifswald 2001.

529. *Fantz*, U. and K. Behringer*: Physik III: Atom- und Molekülphysik. Vorlesung, Universität Augsburg, WS 2001/2002.

530. *Fantz*, U., P. Starke and T. Ondak**: Diagnostics of Electron Distribution Functions in Planar ICP Sources. 25th International Conference on Phenomena in Ionized Gases, Nagoya 2001.

531. *Feng, Y., F. Sardei, J. Kisslinger, D. Reiter* and Yu.L. Igitkhanov*: Island Divertor Transport Modelling and Comparison with Experiment. 8th Workshop on Plasma Edge Theory, Helsinki 2001.

532. *Feng, Y., F. Sardei, J. Kisslinger, D. Reiter* and Yu.L. Igitkhanov*: Numerical Studies on Impurity Transport in the W7-AS Island Divertor. IAEA Technical Committee Meeting on Divertor Concepts, Aix-en-Provence 2001.

533. *Fischer, R.*: Datenanalyse mit der Bayesschen Wahrscheinlichkeitstheorie. Kolloquium, Abteilung 6 "Ionisierende Strahlung", Forschungszentrum Rossendorf 2001.

534. *Fischer, R.*: Rekonstruktion der Energieverteilung der Elektronen aus optischen Messungen. Seminar Niedertemperaturplasmaphysik, Universität Greifswald 2001.

Lectures

535. *Fischer, R.*: ROSAT All-Sky Survey Data Analysis with Bayesian Probability Theory. CIPS Workshop Datenanalyse, Schloß Ringberg 2001.
536. *Fischer, R.*: Tiefenprofile und Auflösungsgrenzen bei beschleunigergestützter Festkörperanalytik. 11. Tagung Festkörperanalytik, Chemnitz 2001.
537. *Fischer, R. and V. Dose*: Physical Mixture Modeling with Unknown Number of Components. 19th International Workshop on Maximum Entropy and Bayesian Methods, Baltimore, MD 2001.
538. *Fischer, R. and V. Dose*: Reversible Jump MCMC Mixture Modeling in Physics. Mixtures 2001, Hamburg 2001.
539. *Fischer, R., J.-S. Yoon, S. Gori, V. Dose, A. Dinklage, J. Knauer and C. Wendland*: Thomson Scattering Profile Reconstruction with Bayesian Probability Theory. Workshop on W7-X Data Validation, IPP Greifswald 2001.
540. *Fournier*, K.B., R. Neu, D. Bolshukhin, R. Dux, A. Geier and ASDEX Upgrade Team*: Soft X-Ray Emission Spectra from Highly Charged Tungsten Ions as a Quantitative Diagnostic of Fusion Plasma. Bulletin of the American Physical Society **46** (8), 267 (2001).
541. *Franzen, P.*: RF Sources at IPP Garching. Neutral Beam Injection Seminar of Large Helical Device, Toki 2001.
542. *Franzen, P., J. Sielanko*, B. Heinemann, R. Riedl and E. Speth*: An Alternative Residual Ion Dump for the ITER Neutral Beam System. Coordinating Committee on Neutral Beams Meeting, Forschungszentrum Jülich 2001.
543. *Franzen, P. and E. Speth*: What is the Optimum Pressure of the ITER Source? Coordinating Committee on Neutral Beams Meeting, Cadarache 2001.
544. *Franzen, P. and E. Speth*: What is the Optimum Pressure of the ITER Source? ITER NBI Review Meeting, Naka 2001.
545. *Franzen, P., E. Speth and NI Group*: Development of an RF Source for ITER NBI. ITER NBI Review Meeting, Naka 2001.
546. *Fußmann, G.*: Atomic Physics with an EBIT Trap. Racah Institute, University of Jerusalem 2001.
547. *Fußmann, G.*: Challenging Problems in Plasma Physics. Weizmann Institute of Science, Rehovot 2001.
548. *Fußmann, G.*: Einführung in die Plasmaphysik (Plasmaphysik I). Vorlesung, Humboldt-Universität Berlin, SS 2001.
549. *Fußmann, G.*: Highly Charged Ions in an Electron-Beam-Ion-Trap (EBIT). ECAMP VII, Berlin 2001. Verhandl. DPG (VI) **36**, 38, AMPD9.3 (2001).
550. *Fußmann, G.*: Investigation of Highly Charged Ions in an EBIT. 1st IAEA Research Coordination Meeting on "Atomic and Molecular Data for Fusion Plasma Diagnostics", Vienna 2001.
551. *Fußmann, G.*: Plasmaphysik und Fusionsforschung (Plasmaphysik II), Vorlesung, Humboldt-Universität Berlin, WS 2001/2002.
552. *Gadelmeier, F.*: The Power Balance in W7-AS Plasmas Bounded with Divertor Modules by Means of Calorimetry and Bolometry. Verhandl. DPG (VI) **36**, 161, P8.5 (2001).
553. *García-Rosales*, C., E. Oyarzabal*, J. Etxebarria*, M. Balden, S. Lindig and R. Behrisch*: Improvement of the Thermomechanical Properties of Fine Grain Graphite by Doping with Different Carbides. 10th International Conference on Fusion Reactor Materials, Baden-Baden 2001.
554. *Gavrilin*, A.V., J.R. Miller*, F. Schauer and S.W. Van Sciver**: Comparative Analysis of Design Options for Current Leads for Wendelstein 7-X Magnet System. 17th International Conference on Magnet Technology, Geneva 2001.
555. *Geier, A., R. Neu, H. Maier, K. Krieger and ASDEX Upgrade Team*: Divertor Retention and Penetration Probabilities for Tungsten at ASDEX Upgrade. Verhandl. DPG (VI) **36**, 161, P8.6 (2001).
556. *Geier, A., R. Neu, H. Maier, K. Krieger and ASDEX Upgrade Team*: Divertorrückhaltevermögen und Eindringwahrscheinlichkeiten für Wolfram an ASDEX Upgrade. Verhandl. DPG (VI) **36**, 161, P8.6 (2001).
557. *Golan, A. and V. Dose*: Tomographic Reconstruction from Noisy Data. 19th International Workshop on Maximum Entropy and Bayesian Methods, Baltimore, MD 2001.
558. *Grigull, P.*: First Island Divertor Experiments on the W7-AS Stellarator. Plasma-Kolloquium, IPF, Universität Stuttgart 2001.
559. *Grigull, P., K. McCormick, R. Burhenn, R. Brakel, H. Ehmler, Y. Feng, F. Gadelmeier, L. Giannone, D. Hildebrandt, R. Jaenicke, J. Kisslinger, T. Klinger, J. Knauer, R. König, G. Kühner, R. Narayanan, D. Naujoks, H. Niedermeyer, E. Pasch, N. Rust, F. Sardei, F. Wagner, A. Weller, U. Wenzel and W7-AS Team*: The Impact of the New Island Divertor on the Plasma Performance in the W7-AS Stellarator. 12th International Toki Conference on Plasma Physics and Controlled Nuclear Fusion, Toki-City 2001.
560. *Gruber, O.*: Current ASDEX Upgrade Programme and Technical Possibilities. ASDEX Upgrade Programme Workshop, Garching 2001.
561. *Gruber, O. and ASDEX Upgrade Team*: Recent Results on High Performance Steady-State Discharges in ASDEX Upgrade. Joint Meeting of DOE/JAERI Technical Planning of Tokamak Experiments FP1/1 and IEA Co-operation of Large Tokamak Facilities W27, Naka 2001.
562. *Gruber, O. and ASDEX Upgrade Team*: Status, Plans and Current Drive Issues in ASDEX Upgrade. JT60-U Seminar, JAERI, Naka 2001.
563. *Gruber, O., J. Stober and ASDEX Upgrade Team*: Steady Power Exhaust with High Confinement Type-II ELMs on ASDEX Upgrade. 13th International Expert Group Workshop on MHD, Disruptions and Plasma Control, Funchal 2001.
564. *Gulke, O.*: Fluctuation Induced Transport in a Simple Magnetized Torus. Verhandl. DPG (VI) **36**, 173, P11.13 (2001).
565. *Gulke, O., T. Klinger, M. Endler and A. Piel**: Conditional Averaging of Fluctuations in the SOL of the Stellarator W7-AS. Verhandl. DPG (VI) **36**, 161, P8.2 (2001).
566. *Günter, S.*: Die Energie der Sterne. Urania, Berlin 2001.
567. *Günter, S.*: Neuere Entwicklungen in der Fusionsforschung - Der Weg zu einem kompakten, stationären Fusionsreaktor. Kolloquium, Universität Bremen 2001.
568. *Günter, S.*: The Role of MHD Stabilities in Tokamaks. 11th Conference on Plasma Physics and Applications, Constanta 2001.
569. *Günter, S., A. Gude, K. Lackner, M. Maraschek, Q. Yu, H. Zohm, ASDEX Upgrade Team, R.J. La Haye* and J.T. Scotville**: The Influence of Helical Perturbation Fields on Neoclassical Tearing Modes (NTMs). Bulletin of the American Physical Society **46** (8), 102 (2001).

Lectures

570. *Günter, S., A. Gude, M. Maraschek, S. Sesnic*, H. Zohm, ASDEX Upgrade Team, D.F. Howell*, Contributors to the EFDA-JET Work Programme and JET Task Force MHD: High Confinement Regime in the Presence of (3,2) Neoclassical Tearing Modes.* 13th International Expert Group Workshop on MHD, Disruptions and Plasma Control, Funchal 2001.
571. *Günter, S., A. Gude, M. Maraschek, S. Sesnic*, H. Zohm, ASDEX Upgrade Team, D.F. Howell*, Contributors to the EFDA-JET Work Programme and JET Task Force MHD: Stabilization of Neoclassical Tearing Modes by Nonresonant External Helical Fields.* 13th International Expert Group Workshop on MHD, Disruptions and Plasma Control, Funchal 2001.
572. *Günter, S., K. Lackner, M. Maraschek, Q. Yu, R.J. La Haye* and J.T. Scotville*:* Influence of Non-Resonant Perturbations on NTMs and Rotation. APS-MHD-Workshop, San Diego, CA 2001.
573. *H. Lederer:* Nachfolgebeschaffung zum Cray T3E Hochleistungsrechner der MPG. Herbsttreffen des Arbeitskreises Supercomputing des ZKI, Konrad-Zuse-Zentrum für Informationstechnik, Berlin 2001.
574. *H. Lederer:* Der neue IBM SP Hochleistungsrechner der MPG. 18. DV-Treffen der Max-Planck-Institute, Göttingen 2001.
575. *Hamacher, T.:* Energie für das 21. Jahrhundert. Bundesökologietreffen der Studenten, Augsburg 2001.
576. *Hamacher, T.:* Fusion as Future Power Source, Prospects and Recent Achievements. World Energy Congress, Buenos Aires 2001.
577. *Hamacher, T.:* The Fusion Programme. Summer University for Plasma Physics, IPP Garching 2001.
578. *Hamacher, T.:* Introduction to Fusion. Workshop on Long Term Energy Scenarios for India, Ahmedabad 2001.
579. *Hamacher, T.:* Long Term Energy Scenarios for India Including Fusion. 28th EPS Conference on Controlled Fusion and Plasma Physics, Funchal 2001.
580. *Hamacher, T.:* Ökonomie und Umwelteigenschaften der Fusion. KTG Frühjahrstagung 2001.
581. *Hamacher, T.:* Very Long Energy and Environmental Modelling. Brüssel 2001.
582. *Hamacher, T.:* Was können wir aus der Entwicklung der Wassermühle im frühen Mittelalter über die Zukunft der Energieversorgung lernen? Verhandl. DPG (VI) **36**, 477, AKE3.3 (2001).
583. *Hamacher, T.:* Zukünftige Energietechniken. Gemeinsames Kolloquium des IPP-Greifswald und der Universität Rostock 2001.
584. *Harmeyer, E., J. Kisslinger, A. Wiczorek* and H. Wobig:* Superconducting Coil Systems for a Stellarator Fusion Reactors. 17th International Conference on Magnet Technology, Geneva 2001.
585. *Hartfuß, H.-J.:* Boundary/Divertor Diagnostics. W7-X Divertor Symposium, Greifswald 2001.
586. *Hartfuß, H.-J.:* Diagnostics of Fusion Plasmas. Summer School, International Max-Planck-Research-School, Greifswald 2001.
587. *Hartfuß, H.-J.:* Diagnostic System for the W7-X Stellarator. International Conference on Advanced Diagnostics for Magnetic and Inertial Fusion, Varenna 2001.
588. *Hartfuß, H.-J.:* Hochtemperatur Plasmadiagnostik. Vorlesung, Universität Greifswald, WS 2000/2001.
589. *Hartfuß, H.-J.:* Hochtemperatur Plasmadiagnostik. Vorlesung, Universität Greifswald, WS 2001/2002.
590. *Hartfuß, H.-J.:* Plasmaphysik mit Mikrowellen. Physikalisches Kolloquium, Universität Rostock 2001.
591. *Hartfuß, H.-J.:* Temperature Fluctuation Measurements. Tutorial Lecture, International Max-Planck-Research-School, Greifswald 2001.
592. *Hartmann, D.:* Stellarators. Vortrag, Carolus Magnus Summer School, Bad Honnef 2001.
593. *Hartmann, D. and F. Wesner:* Physics Aspects of ICRH on W7-X. Coordinating Committee on Fast Wave, Greifswald 2001.
594. *Heger, B., U. Fantz* and K. Behringer:* Electron Density Dependence of He-Line Ratios in Microwave Plasmas. Verhandl. DPG (VI) **36**, 167, P9.23 (2001).
595. *Heimann, P.:* The Data Acquisition System of W7X. 3rd IAEA Technical Committee Meeting on Control, Data Acquisition, and Remote Participation for Fusion Research, Padova 2001.
596. *Heimann, P.:* Datenerfassung bei W7X. Universität Rostock 2001.
597. *Hergenhahn, U.:* Altes und neues von der K-Schalen-Photoionisation kleiner Moleküle. Seminar des Arbeitskreises Theoretische Chemie, Universität Heidelberg 2001.
598. *Hergenhahn, U.:* Continuum Structures in Molecular Photoionization. 13th Conference on Vacuum Ultraviolet Physics, Trieste 2001.
599. *Hergenhahn, U.:* High-Resolution Molecular Photoionization at X1B. National Synchrotron Light Source, Brookhaven National Laboratory, Brookhaven, NY 2001.
600. *Hergenhahn, U.:* Symmetry-Selective Observation of the N 1s Shape-Resonance in N₂. ECAMP VII, Berlin 2001. Verhandl. DPG (VI) **36**, 147, MO13.4 (2001).
601. *Hergenhahn, U.:* Two Lectures on Fundamentals of and Current Problems in Molecular Photoionization. 3^{ème} Cycle Interuniversitaire en Physique Atomique et Moléculaire, Université de Liège 2001.
602. *Herrmann, A.:* Energy and Particle Fluxes to Main Chamber and Divertor during Type I ELMs. 9th European Fusion Physics Workshop, Saariselkä 2001.
603. *Herrmann, A.:* Leistungsdichtebestimmung für burstartige Ereignisse in Fusionsmaschinen. Verhandl. DPG (VI) **36**, 175, P12.1 (2001).
604. *Herrnegger, F.:* Stellarator Fields with Small PS Current at Small Rotational Transform. Workshop of Innovative Concepts and Theory of Stellarators, Kiev 2001.
605. *Herrnegger, F. and J. Kisslinger:* On the Concept of Breeding Blanket in a Helias Reactor. Workshop of Innovative Concepts and Theory of Stellarators, Kiev 2001.
606. *Hildebrandt, D., M. Laux, J. Sachtleben and W7-X Divertor Team:* Divertor Operational Diagnostics for W7-X. Status Meeting on the Wendelstein 7-X Divertor and the First Wall, Greifswald 2001.
607. *Hildebrandt, D. and W. Schneider:* Stöchiometrieuntersuchungen von B₄C nach Plasmaexposition. Workshop "Borcarbid als Wandmaterial für W7-X", Berlin 2001.
608. *Horton, L.D.:* Energy and Particle Losses from the Main Plasma. 9th European Fusion Physics Workshop, Saariselkä 2001.
609. *Horton, L.D., ASDEX Upgrade Team and JET-Team:* High Density H-Mode Operation in ASDEX Upgrade and JET. International Workshop on Physics of Internal Transport Barriers, Edge Pedestal and Steady State Operation in Tokamaks, Garching 2001.

Lectures

610. *Jacob, W.*: Ion-Driven Surface Reactions during Growth and Erosion of Hydrocarbon Films. Seminar, CNRS PHASE, Strasbourg 2001.
611. *Jacob, W.*: Was passiert an der Oberfläche bei der Plasmadeposition von amorphen Kohlenwasserstoffschichten. Kolloquium, Institut für Oberflächenmodifizierung, Leipzig 2001.
612. *Jacob, W. and B. Racine*: Stöchiometrie, Struktur und Stress von plasmadeponierten a-C:H-Schichten. VIII. Erfahrungsaustausch "Oberflächentechnologie mit Plasmaprozessen", Mühlleithen 2001.
613. *Jakobi, M., B. Kurzan, H. Murmann, J. Neuhauser and ASDEX Upgrade Team*: Measurement of Fast Local Changes in Electron Temperature and Density by Thomson Scattering at ASDEX Upgrade. Bulletin of the American Physical Society **46** (8), 252 (2001).
614. *Jaksic, N. and J. Simon-Weidner*: Strukturanalyse des W7-X Magnet Systems. Ingenieur-Wissenschaftliches Kolloquium, Universität Rostock 2001.
615. *Joffrin*, E., R. Wolf, B. Alper*, Y. Baranov*, A. Becoulet*, C.D. Challis*, M. De Baar*, C. Giroud*, C. Gowers*, N. Hawkes*, T.C. Hender*, M. Maraschek, D. Mazon*, V. Parail*, K.-D. Zastrow* and Contributors to the EFDA-JET Work Programme*: Similar Advanced Tokamak Experiments in JET and ASDEX Upgrade. 28th EPS Conference on Controlled Fusion and Plasma Physics, Funchal 2001.
616. *Johnson*, T., T. Hellsten*, M. Mantsinen*, C. Ingesson*, V. Kiptily*, T. Bergkvist*, S. Conroy* J. Hedin*, M.-L. Mayoral*, F. Nguyen*, J.-M. Noterdaeme, S. Sharapov* and Contributors to the EFDA-JET Work Programme*: Experimental Evidence for RF-Induced Transport of Resonant ³He-Ions in JET. 7th IAEA Technical Committee Meeting on Energetic Particles in Magnetic Confinement Systems, Gothenburg 2001.
617. *Kasilov*, S.V., D. Reiter*, A.M. Runov, W. Kernbichler* and M.F. Heyn**: Heat Conductivity in the Vicinity of Rational Magnetic Surfaces in Ergodic Divertors. IAEA Technical Committee Meeting on Divertor Concepts, Aix-en-Provence 2001.
618. *Kaufmann, M.*: Einführung in die Plasmaphysik und Fusionsforschung II. Vorlesung, Universität Bayreuth, SS 2001.
619. *Keudell, A. von*: Artificial Plasmas: Understanding Thin Film Growth Processes. FOM-Institute Rijnhuizen, Nieuwegein 2001.
620. *Keudell, A. von*: Artificial Plasmas: Understanding Thin Film Growth Processes. International Seminar on New Trends in Plasma Physics, Garching 2001.
621. *Keudell, A. von*: Artificial Plasmas: Understanding Thin Film Growth Processes. Kolloquium, Technische Universität Chemnitz 2001.
622. *Keudell, A. von*: Elementarmechanismen der plasmagestützten Schichtabscheidung. 10. Bundesdeutsche Fachtagung Plasmatechnologie, Greifswald 2001.
623. *Keudell, A. von*: Oberflächenreaktionen von Kohlenwasserstoffradikalen. DFG Sonderforschungsbereich, Kolloquium, Universität Karlsruhe 2001.
624. *Keudell, A. von*: Surface Processes during Thin Film Growth. Summerschool "Low Temperature Plasma Physics", Bad Honnef 2001.
625. *Keudell, A. von, M. Meier and C. Hopf*: Fundamental Growth Mechanisms during PECVD of Carbon Thin Films. Colloquium International des Plasmas, Antibes 2001.
626. *Keudell, A. von, M. Meier, C. Hopf, T. Schwarz-Selinger and W. Jacob*: A-C:H Growth Mechanism. Diamond 2001, Budapest 2001.
627. *Kisslinger, J., C.D. Beidler, E. Harmeyer, F. Herrnegger and H. Wobig*: Modular Coil Systems of Advanced Stellarator Reactors. Workshop of Innovative Concepts and Theory of Stellarators, Kiev 2001.
628. *Kleiber, R.*: Department of Electrical Engineering and Computer Sciences. University of California, Berkeley, CA 2001.
629. *Kleiber, R.*: Global Resistive Drift Ballooning Modes in General Geometry. International Sherwood Fusion Theory Conference, Santa Fe, CA 2001.
630. *Kleiber, R.*: Magnetic Fusion Energy Research Group. Lawrence Livermore National Laboratory, Livermore 2001.
631. *Kleiber, R.*: Resistive Drift Modes in General Geometry. Institute for Electromagnetic Field Theory and Plasma Physics, Chalmers University, Göteborg 2001.
632. *Kleiber, R.*: Theory of Fusion Plasmas. International Max-Planck-Research-School, Greifswald 2001.
633. *Klinger, T.*: International Max-Planck-Research-School on Bounded Plasmas. CPT-Sektionssitzung der MPG, Berlin 2001.
634. *Klinger, T.*: Laboratory Observation of Periodic Ion Holes. International Symposium PLASMA 2001 on Research and Applications of Plasmas, Warsaw 2001.
635. *Klinger, T.*: The Large Helicon Plasma Device VINETA. Workshop "Simulation of Plasma Turbulence and Comparison with Experiment", Kiel 2001.
636. *Klinger, T.*: Observation and Modelling of Periodic Ion Holes. Royal Institute of Technology, Alfvén Laboratory, Stockholm 2001.
637. *Klinger, T.*: Overview over Bifurcation Phenomena in Simple Plasma Diodes. International Workshop on Bifurcation Phenomena in Plasmas, Interdisciplinary Graduate School of Engineering Sciences, Kyushu University, Fukuoka 2001.
638. *Klinger, T.*: Physik für Mediziner und Zahnmediziner. Grundvorlesung, Universität Greifswald, WS 2000/2001.
639. *Klinger, T.*: Physik für Mediziner und Zahnmediziner. Proseminar, Universität Greifswald, WS 2000/2001.
640. *Klinger, T.*: Physikalisches Praktikum für Mediziner. Praktikumsvorlesung, Universität Greifswald, WS 2000/2001.
641. *Klinger, T.*: Plasmadynamik: Wellen und Instabilitäten im Weltraum, Experiment und Anwendung. Mathematisch-Technisches Kolloquium, Rhein-Ahr-Campus, Remagen 2001.
642. *Klinger, T.*: Plasmaentladungen und Modellierung. Vorlesung, Universität Greifswald, WS 2000/2001.
643. *Klinger, T.*: Plasmaentladungen und Modellierung. Vorlesung, Universität Greifswald, WS 2001/2002.
644. *Klinger, T.*: Plasmawellen und -instabilitäten. Vorlesung, Universität Greifswald, SS 2001.
645. *Klose, S.*: Investigation of MHD-Instabilities in W7-AS. Verhandl. DPG (VI) **36**, 161, P8.4 (2001).
646. *Klose, S., A. Weller, A. Werner, P. Schötz and H. Greve*: X-Ray Multi Camera Tomography System of Wendelstein 7-X. International Conference on Advanced Diagnostics for Magnetic and Inertial Fusion, Varenna 2001.
647. *Koch, F., Y. Yamada-Takamura*, I. Beguiristain Repáraz, H. Maier and H. Bolt*: Deposition, Characterisation and Application of Alumina Coatings as Hydrogen Permeation Barriers. 10th International Conference on Fusion Reactor Materials, Baden-Baden 2001.

Lectures

648. *Kolesnichenko*, Ya.I., V.V. Lutsenko*, H. Wobig and Yu.V. Yakovenko**: Alfvén Instabilities Caused by Circulating Energetic Ions in Optimized Stellarators. Workshop of Innovative Concepts and Theory of Stellarators, Kiev 2001.
649. *Kolesnichenko*, Ya.I., V.V. Lutsenko*, H. Wobig and Yu.V. Yakovenko**: Core-Localized Alfvén Eigenmodes in Stellarators. Workshop of Innovative Concepts and Theory of Stellarators, Kiev 2001.
650. *Kolesnichenko*, Ya.I., V.V. Lutsenko*, H. Wobig and Yu.V. Yakovenko**: Effect of Destabilized Alfvén Eigenmodes on Alpha Particles in a Helias Reactor. Workshop of Innovative Concepts and Theory of Stellarators, Kiev 2001.
651. *Könies, A.*: CAS3D-K: A Three Dimensional Kinetic MHD Stability Code. 7th IAEA Technical Committee Meeting on Energetic Particles in Magnetic Confinement Systems, Göteborg 2001.
652. *Könies, A.*: Kinetic Expansion of the Three-Dimensional Ideal MHD Stability Code CAS3D. Workshop of Innovative Concepts and Theory of Stellarators, Kiev 2001.
653. *König, R., P. Grigull, K. McCormick, Y. Feng, J. Kisslinger, A. Komori*, S. Masuzaki*, K. Matsuoka*, T. Obiki*, N. Ohyaib*, H. Renner, F. Sardei, F. Wagner and A. Werner*: The Divertor Program in Stellarators. IAEA Technical Committee Meeting on Divertor Concepts, Aix-en-Provence 2001.
654. *König, R., P. Grigull, K. McCormick, U. Wenzel, Y. Feng, F. Gadelmeier, L. Giannone, D. Hildebrandt, J. Kisslinger, F. Wagner, A. Werner and W7-AS Team*: Investigation of the Route to Partial Detachment on W7-AS. 28th EPS Conference on Controlled Fusion and Plasma Physics, Funchal 2001.
655. *Kraus, W., P. McNeely, A. Entsheva, C. Hu, P. Franzen, B. Heinemann, R. Riedl, E. Speth, O. Vollmer and R. Wilhelm*: Status and Plans on BATMAN. Coordinating Committee on Neutral Beams Meeting, Forschungszentrum Jülich 2001.
656. *Krieger, K., A. Geier, X. Gong, H. Maier, V. Rohde, J. Roth, W. Schneider and AUG Team*: Einsatz von Wolfram für Wandkomponenten in Fusionsmaschinen. Physikalisches Seminar, Universität Greifswald 2001.
657. *Krieger, K., X. Gong, M. Balden, D. Hildebrandt, H. Maier, V. Rohde, J. Roth, W. Schneider and ASDEX Upgrade Team*: Erosion and Migration of Tungsten Employed at the Central Column Heat Shield of ASDEX Upgrade. 10th International Conference on Fusion Reactor Materials, Baden-Baden 2001.
658. *Kühner, G., J. Reetz, P. Heimann, S. Heinzel, C. Henning, H. Kroiss, J. Maier and M. Zilker*: A Flexible Method for System Configuration and Operation Scheduling. 3rd IAEA Technical Committee Meeting on Control, Data Acquisition, and Remote Participation for Fusion Research, Padova 2001.
659. *Kurzan, B., H. Murmann, D. Bolshukhin, M. Jakobi and ASDEX Upgrade Team*: Determination of the Electron Density and Mean Energy for Anisotropic Velocity Distributions by Thomson Scattering. International Conference Advanced Diagnostics for Magnetic and Inertial Fusion, Varenna 2001.
660. *Kurzan, B., H. Murmann and M. Jakobi*: Evaluation of Thomson Scattering Data on ASDEX Upgrade. Workshop on W7-X Data Validation, Greifswald 2001.
661. *Kurzan, B., H. Murmann, M. Jakobi, D. Bolshukhin, W. Suttrop and ASDEX Upgrade Team*: Detection of Neutral Beam Generated Suprathermal Electrons by Thomson Scattering on ASDEX Upgrade. Verhandl. DPG (VI) **36**, 162, P8.7 (2001).
662. *Lang, P.T., ASDEX Upgrade Team and Contributors to the EFDA-JET Work Programme*: High Field Side Pellet Refuelling for High Density Tokamak Operation. 18th Annual Meeting of Japan Society of Plasma Science and Fusion Research, Fukuoka 2001.
663. *Laqua, H.P.*: Elektron-Bernstein-Wellen. Kolloquiumsvortrag, IPF, Universität Stuttgart 2001.
664. *Laqua, H.P.*: Elektron-Bernstein-Wellen. Physikalisches Kolloquium, Universität Konstanz 2001.
665. *Laqua, H.P.*: Fusionsplasmen. Vorlesungsreihe zur Plasmatechnologie, Fachhochschule Stralsund, WS 2001/2002.
666. *Laux, M.*: Kernfusion. Bertolt-Brecht-Gymnasium, Dresden 2001.
667. *Laux, M.*: Kernfusion. Marie-Curie-Gymnasium, Ludwigsfelde 2001.
668. *Laux, M.*: Sonography as a New PSI Diagnostic. FZ Seibersdorf 2001.
669. *Laux, M.*: Test of B4C Covered Limiters in Textor. B4C-Workshop, Berlin 2001.
670. *Laux, M., S. Jachmich*, A. Herrmann, T. Eich* and EFDA-JET Team*: ELMs Observed at the Targets of an Axisymmetric Divertor. IAEA-Conference/TCM-Workshop, Aix-en-Provence 2001.
671. *Leuterer, F., M. Beckmann*, H. Brinkschulte, K. Kirov, F. Monaco, M. Münich, F. Ryter, H. Schütz, L. Empacher*, G. Gantenbein*, W. Förster*, W. Kasperek*, P. Schüller*, K. Schwörer*, A. Borchegowski*, V. Illin*, L. Popov* and V. Sigalaev**: The ECRH System of ASDEX Upgrade. 28th EPS Conference on Controlled Fusion and Plasma Physics, Funchal 2001.
672. *Leuterer, F., K. Kirov, M. Münich, F. Monaco, F. Ryter, H. Schütz, R. Wolf and H. Zohm*: Experience with the ECRH System of ASDEX Upgrade and Recent Results. 13th Joint Russian-German Workshop on ECRH and Gyrotrons, Greifswald 2001.
673. *Lingertat, J., D. Aßmus, M. Otte and H. Scholz*: The WEGA Stellarator. International Symposium PLASMA 2001 on Research and Applications of Plasmas, Warsaw 2001.
674. *Linsmeier, C.*: New Perspectives in Surface Science. ESF Network on Atomic Layer Epitaxy, Florenz 2001.
675. *Linsmeier, C.*: Reaktion und Diffusion ultradünner Kohlenstoff-Filme auf Be, Si, Ti und W. Humboldt-Universität Berlin 2001.
676. *Linsmeier, C., P. Goldsträß and J. Luthin*: Chemical Reactions at Fusion First Wall Materials. Gordon Conference on Chemical Reactions at Surface, Ventura, CA 2001.
677. *Linsmeier, C., A. Kohl, E. Taglauer and H. Knözinger**: Influence of Support and Promotor on the Catalytic Activity of Rh/VO_x/SiO₂ Model Catalysts. Europacat V, Limerick 2001.
678. *Linsmeier, C., A. Kohl, E. Taglauer and H. Knözinger**: Influence of Support and Promotor on the Catalytic Activity of Rh/VO_x/SiO₂ Model Catalysts. 6th Workshop Gas-Surface Interactions, Reinischkogel 2001.
679. *Lotter*, A., U. Fantz* and K. Behringer*: Absorption Measurements in Helium and Argon Plasmas. Verhandl. DPG (VI) **36**, 171, P10.24 (2001).
680. *Maier, H., J. Luthin, M. Balden, J. Linke*, V. Rohde, H. Bolt and ASDEX Upgrade Team*: Development of Tungsten Coated First Wall and High Heat Flux Components for Application in ASDEX Upgrade. 10th International Conference on Fusion Reactor Materials, Baden-Baden 2001.

Lectures

681. *Maier, J.*: Some Realtime Aspects of the W7X DAQ System and Continuous Data Archiving in an Object Database. 3rd IAEA Technical Committee Meeting on Control, Data Acquisition, and Remote Participation for Fusion Research, Padova 2001.
682. *Mantsinen*, M., M.-L. Mayoral*, V. Kiptily*, S. Sharapov*, A. Bickley*, M. de Baar*, L.-G. Eriksson*, T. Hellsten*, K. Lawson*, F. Nguyen*, J.-M. Noterdaeme, E. Righi*, A.A. Tuccillo*, M. Zerbini* and Contributors to the EFDA-JET Work Programme*: Alpha Particle Physics Studies on JET with ICRH-Accelerated ⁴He Beam Ions. 7th IAEA Technical Committee Meeting on Energetic Particles in Magnetic Confinement Systems, Gothenburg 2001.
683. *Matsuoka*, K., S. Okamura*, S. Nishimura*, M. Isobe*, C. Suzuki*, A. Shimizu*, A. Fujisawa*, K. Ida*, T. Minami*, H. Iguchi*, Y. Yoshimura*, M. Osakabe*, I. Nomura*, S. Murakami*, M. Yokoyama*, N. Nakajima*, T. Hayashi*, K. Itoh*, P. Merkel, M. Drevlak, C. Nührenberg, S. Gori, R. Zille and J. Nührenberg*: Physics Design of CHS-qa Based on CHS Experiments. Workshop of Innovative Concepts and Theory of Stellarators, Kiev 2001.
684. *Mayer, M.*: Characterisation of Tungsten Layers and Status of Long Term Samples. 2nd European Workshop on the Characterisation of First Wall Materials, Culham 2001.
685. *Mayer, M.*: RBS an rauhen Oberflächen. Hahn-Meitner-Institut, Berlin 2001.
686. *Mayer, M.*: Status of Tasks JWO-FT-3.4 (Deposition and Erosion Studies) and JWO-FT-3.8 (W-Coated Divertor Tiles). Kick-off Meeting Fusion Technology Tasks, Karlsruhe 2001.
687. *Mayer, M., A. Pospieszczyk*, P. Wienhold* and M. Laux*: Erste Ergebnisse zu Erosion und Redeponierung am B4C Testlimiter in TEXTOR. Arbeitstreffen über Borcarbid als Wandmaterial für W7-X, Berlin 2001.
688. *Mayer, M., J. Roth and K. Ertl*: Rutherford Backscattering Spectroscopy and Elastic Recoil Detection Analysis with Lithium Ions - The Better Alternative to Helium? 15th International Conference on Ion Beam Analysis, Cairns 2001.
689. *McCormick, K.*: Status and Results of Divertor Experiments on W7-AS. 1st Hungarian Plasma Physics Workshop, Budapest 2001.
690. *Meier, M.*: Elementare Mechanismen der Wechselwirkung von CH₃ und H mit Kohlenwasserstoff-Filmen. Lehrstuhlseminar (Prof. G. Wachutka), TU München 2001.
691. *Meier, M.*: Mechanismen der Schichtabscheidung mit CH₃ und H. Arbeitsgruppenseminar, Technische Universität Chemnitz 2001.
692. *Meier, M.*: Prozesse beim Schichtwachstum mit Kohlenwasserstoffradikalen. Studien-/Arbeitsgruppenseminar (Prof. M. Donath), Universität Münster 2001.
693. *Meier, M. and A. von Keudell*: Erosion von Kohlenwasserstoffschichten durch Methylradikale. 10. Bundesdeutsche Fachtagung Plasmatechnologie, Greifswald 2001.
694. *Meier, M. and A. von Keudell*: Mechanismen beim synergetischen Wachstum von CH₃ mit H. VIII. Erfahrungsaustausch Oberflächentechnologie mit Plasmaprozessen, Mühlleithen 2001.
695. *Meier, M., T. Schwarz-Selinger, W. Jacob and A. von Keudell*: Eliminierung von Wasserstoff beim Wachstum polymerartiger Kohlenwasserstoffschichten. 10. Bundesdeutsche Fachtagung Plasmatechnologie, Greifswald 2001.
696. *Meir, S., U. Fantz* and K. Behringer*: Determination of Atomic Hydrogen Fluxes and Reflection Coefficients in ICP-Discharges. Verhandl. DPG (VI) **36**, 175, P12.3 (2001).
697. *Mertens, V.*: Overview of Methods to Avoid Disruptions. 9th European Fusion Physics Workshop, Saariselkä 2001.
698. *Meyer-Spasche, R.*: Instabilitäten und Bifurkationen bei Taylor-Couette-Strömungen. Workshop Strukturbildung und Stabilität in rotierenden Systemen, Brandenburgische TU Cottbus 2001.
699. *Meyer-Spasche, R.*: Nonlinear Dynamics of Numerical Methods/Dynamik und Numerik. Vorlesung, TU München, SS 2001.
700. *Meyer-Spasche, R.*: Spektren und Pseudospektren - Theorie, Numerik und Anwendungen. Vorlesung, TU München, WS 2001/2002.
701. *Mikhailov*, M.I., M.Yu. Isaev*, J. Nührenberg, A.A. Subbotin*, W.A. Cooper*, M.F. Heyn*, V.N. Kalyuzhnyj*, S.V. Kasilov*, V.V. Kasilov*, W. Kernbichler*, V.V. Nemov*, M.A. Samitov* and V.D. Shafranov**: The Alpha-Particle Confinement in Zero and Finite Beta-Mirror-Type Stellarators. Workshop of Innovative Concepts and Theory of Stellarators, Kiev 2001.
702. *Milch, I.*: Energie aus Kernfusion. KBS-Gesprächsabend, Mainz 2001.
703. *Mück, A., H. Zohm, W. Kasperek* and C. Forest**: An Antenna for Electron Bernstein Heating of the Pegasus Spherical Tokamak. Verhandl. DPG (VI) **36**, 163, P8.18 (2001).
704. *Müller, W.-C.*: Large-Eddy Simulations of Magnetohydrodynamic Turbulence. Plasmaphysik-Seminar, Ruhr-Universität Bochum 2001.
705. *Müller, W.-C. and D. Biskamp*: Alfvén Waves versus Fluid Swirls: Who Wins in MHD Turbulence? Space Plasma Simulation - 6th Int. School/Symposium JSSS-6. 2001, MPE Garching 2001.
706. *Müller, W.-C. and D. Biskamp*: The Local Anisotropy of MHD Turbulence. MHD-Tag 2001, Ruhr-Universität Bochum 2001.
707. *Müller, W.-C. and D. Corati**: Dynamic Gradient-Diffusion Models for Magnetohydrodynamic Turbulence. Europhysics Conference on Computational Physics, Aachen 2001.
708. *Müller, W.-C. and D. Corati**: New Approach towards Subgrid Modeling in Magnetohydrodynamic Turbulence. DLES4 Workshop - Direct/Large-Eddy Simulations in Fluid Turbulence. University of Twente, Enschede 2001.
709. *Müller, W.-C., R. Grappin* and D. Biskamp*: Energy Dynamics in Magnetohydrodynamic Turbulence. CIAS Workshop - Space Plasma Phenomena at the Collisional/Non-Collisional Interplay. Observatoire de Paris-Meudon, Paris 2001.
710. *Nagel, M. and F. Schauer*: Thermohydraulic Behavior of the Wendelstein 7-X Magnet System. 17th International Conference on Magnet Technology, Geneva 2001.
711. *Naiser, T., H.W. Müller and E. Wolftrum*: Recent Progress in the Lithium-Beam Diagnostic for Tokamak Edge Plasmas. Verhandl. DPG (VI) **36**, 178, P12.18 (2001).
712. *Naujoks, D.*: Computer-Simulation in der Plasmaphysik. Vorlesung, Humboldt-Universität Berlin, WS 2001/2002.
713. *Naujoks, D.*: Does the Diamagnetic Drift Exist? 8th International Workshop on Plasma Edge Theory in Fusion Devices, Helsinki 2001.
714. *Naujoks, D.*: Electric Confinement of Ions in Fusion Experiments. ECAMP VII, Berlin 2001. Verhandl. DPG (VI) **36**, 153, P1.2 (2001).
715. *Neu, R.*: Plasmaphysik und Fusionsforschung. Vorlesung, Universität Tübingen, SS 2001.

Lectures

716. Neu, R., J.C. Fuchs, G. Haas, A. Herrmann, A. Kallenbach, M. Laux, J. Neuhauser, F. Ryter, J. Gafert, O. Gruber, M. Kaufmann, B. Kurzan, V. Mertens, H.W. Müller, V. Rohde, A.C.C. Sips, J. Stober, B. Streibl, W. Treutterer and ASDEX Upgrade Team: Properties of the New Divertor IIB in ASDEX Upgrade. IAEA-Conference/TCM-Workshop, Aix-en-Provence 2001.
717. Niedner, S., A. Kendl, C. Lechte*, B.D. Scott and U. Stroth*: Mikrostruktur der Turbulenz in magnetisierten Plasmen. Verhandl. DPG (VI) **36**, 168, P10.1 (2001).
718. Nishimura, Y., D.P. Coster, J.W. Kim and B.D. Scott: ASDEX Upgrade Edge Transport Studies by Turbulence and Braginskii Divertor Transport Codes. 8th International Workshop on Plasma Edge Theory in Fusion Devices, Helsinki 2001.
719. Nishimura, Y., D.P. Coster and B.D. Scott: Effect of Neoclassical Electric Field on the Tokamak Edge Turbulence. Bulletin of the American Physical Society **46** (8), 188 (2001).
720. Noterdaeme, J.-M.: About Bananas and Potatoes or on the Importance of Fast Particle Orbits in ICRH. Invited Talk at the Thesis Defence of J. Hedin. Royal Institute of Technology, Stockholm 2001.
721. Noterdaeme, J.-M.: The ASDEX Upgrade Antennas. JET-EP ICRH Antenna Design Review Meeting, Cadarache 2001.
722. Noterdaeme, J.-M.: Comments on the JET-EP ICRH Design. JET-EP ICRH Design Team Meeting, Cadarache 2001.
723. Noterdaeme, J.-M.: Progress of Task Force H for 2002 on JET. Coordinating Committee on Fast Wave, Greifswald 2001.
724. Noterdaeme, J.-M.: Recent Results from Heating and Current Drive Experiments on JET. International Workshop on Physics of Internal Transport Barriers, Edge Pedestal, and Steady State Operation in Tokamaks, IPP Garching 2001.
725. Noterdaeme, J.-M.: Report on EFDA-JET Physics Activity of Task Force H. Coordinating Committee on Fast Wave, Cadarache 2001.
726. Noterdaeme, J.-M.: Report on the JET-EP-ICRH Design Team Meeting with Emphasis on 3dB Couplers and Transmission Line. Coordinating Committee on Fast Wave, Greifswald 2001.
727. Noterdaeme, J.-M. and ICRH Group: Experience from the ASDEX and ASDEX Upgrade ICRF Systems with Emphasis on the Antenna. Workshop on RF Technology, Oxnard, CA 2001.
728. Noterdaeme, J.-M. and ICRH Group: Topics for Cooperation Between AUG and Tore Supra in the ICRF Area. Workshop on International Cooperation on Tore Supra, Cadarache 2001.
729. Noterdaeme, J.-M., E. Righi* and Task Force H: Plasma Rotation with ICRF. 3rd Task Force H Meeting, Cadarache 2001.
730. Noterdaeme, J.-M., Task Force H and Contributors to the EFDA-JET Work Programme: Overview of Some of the ICRH Related TF-H Results on JET. Meeting of the ITER Expert Group on Fast Particles, Heating and Steady State Operation, Garching 2001.
731. Noterdaeme, J.-M., Task Force H and Contributors to the EFDA-JET Work Programme: Task Force H-Results and Future Activities. 9th European Fusion Physics Workshop, Saariselkä 2001.
732. Nührenberg, J.: Development of Optimized Stellarator Lines. Workshop of Innovative Concepts and Theory of Stellarators, Kiev 2001.
733. Nührenberg, J.: Stellaratortheorie. Universität Greifswald, WS 2001/2002.
734. Nührenberg, J.: Theorie der Hochtemperaturplasmen. Universität Greifswald, SS 2001.
735. Obst, B.: High Resolution Photoelectron Spectroscopy of the Scandium 2p-3d Excitation. ECAMP VII, Berlin 2001. Verhandl. DPG (VI) **36**, 136, MO9.1 (2001).
736. Ogorodnikova O.V.: A Model for the Steady State Plasma - and Gas - Driven Hydrogene Isotope Permeation through Multi-Layer Metal. 10th International NATO Advanced Research Workshop on Hydrogen Isotope Recycling at Plasma-Facing Materials in Fusion Reactors, Argonne, IL 2001.
737. Ogorodnikova, O.V.: Trapping Effect in Hydrogen Retention in Metals. 10th International NATO Advanced Research Workshop on Hydrogen Isotope Recycling at Plasma-Facing Materials in Fusion Reactors, Argonne, IL 2001.
738. Pautasso, G.: Session Leader and Introduction to Disruptions. 9th European Fusion Physics Workshop, Saariselkä 2001.
739. Pautasso, G., S. Egorov, Y. Nakamura, M. Bakhtiari*, G. Mank*, K.H. Finken*, A. Savtchikov*, O. Gruber, V. Mertens, V. Rohde, R.R. Khayrutdinov* and V.E. Lukash*: Mitigation of Disruptions in Present Machines (and ITER). 9th European Fusion Physics Workshop, Saariselkä 2001.
740. Pautasso, G., U. Seidel, O. Gruber, V. Riccardo*, W. Schneider, E. Strumberger and H.-P. Zehrfeld: About Asymmetries of the Halo Current and the Role of $q(\psi)$. 13th International Expert Group Workshop on MHD, Disruptions and Plasma Control, Funchal 2001.
741. Pautasso, G., C. Tichmann, E. Wolfrum and T. Naiser: Einsatz neuronaler Netze bei Plasmaexperimenten. Kolloquium, Universität Rostock 2001.
742. Pedemonte*, L., G. Bracco*, R. Tartarek*, R. Beikler, E. Taglauer, K. Brüning* and W. Heiland*: The Structure and the Disordering Mechanism of Ag (110). 19th International Conference on Atomic Collisions in Solids, Paris 2001.
743. Poli, E.: Beam Tracing for Electron Cyclotron Waves. Kolloquium, IPP, Forschungszentrum Jülich 2001.
744. Poli, E.: Geometrische Optik und Beugungseffekte. Vorlesung, University of Pavia, WS 2000/2001.
745. Poli, E.: Monte Carlo δf Simulation of the Bootstrap Current in the Presence of a Magnetic Island. Kolloquium, FOM-Institute Rijnhuizen, Nieuwegein 2001.
746. Poli, E., A.G. Peeters, A. Bergmann, S. Günter and S.D. Pinches: Monte Carlo δf Simulation of Neoclassical Processes in a Tokamak with a Perturbed Magnetic Equilibrium. 9th European Fusion Theory Conference, Helsingor 2001.
747. Preuss, R.: Bayesian Analysis of Cell Migration. CIPS Workshop Datenanalyse, Schloß Ringberg 2001.
748. Preuss, R.: Bayessche Datenanalyse: Verbindungsglied zwischen Modellhypothese und experimentellen Daten. Symposium zu Trends in der Zell- und Kardiovaskulären Physiologie, Dresden 2001.
749. Preuss, R.: Bayesscher Modellvergleich mittels thermodynamischer Integration. Freiburger Zentrum für Datenanalyse und Modellbildung, Freiburg 2001.
750. Preuss, R., H. Kang, T. Schwarz-Selinger and V. Dose: Quantitative Analysis of Multicomponent Mass Spectra. 19th International Workshop on Maximum Entropy and Bayesian Methods, Baltimore, MD 2001.
751. Raupp, G., K. Behler, G. Neu, W. Treutterer, D. Zasche, T. Zehetbauer and ASDEX Upgrade Team: Integrating Discharge Control and Data Acquisition at ASDEX Upgrade. 3rd IAEA Technical Committee Meeting on Control, Data Acquisition, and Remote Participation for Fusion Research, Padova 2001.

Lectures

752. *Reetz, J.*: Video Data Acquisition and Processing at W7X. 3rd IAEA Technical Committee Meeting on Control, Data Acquisition, and Remote Participation for Fusion Research, Padova 2001.
753. *Reich, M., P.T. Lang, R. Dux, A. Lorenz, V. Mertens, H.W. Müller, J. Neuhauser, K.F. Renk* and ASDEX Upgrade Team*: Compound Pellets for Improved Tokamak Plasma Refuelling. *Verhandl. DPG (VI)* **36**, 153, P1.3 (2001).
754. *Reinecke, N. und E. Taglauer*: Adsorbatinduzierte Nanostrukturen auf Cu (11n)-Oberflächen. *Verhandl. DPG (VI)* **36**, 397, O39.2 (2001).
755. *Renner, H., J. Boscary, H. Greuner, H. Grote, F.W. Hoffmann, J. Kisslinger, E. Strumberger and B. Mendelevitich*: Divertor Concept for the W7-X Stellarator and Mode of Operation. IAEA Technical Committee Meeting on Divertor Concepts, Aix-en-Provence 2001.
756. *Rennie, E.E.*: High Resolution Gas Phase Molecular Spectroscopy Using Synchrotron Radiation as the Ionisation Source. Physical Chemistry Seminar, University of Ottawa 2001.
757. *Reuter, H.*: Update on Shared Storage Systems: OpenAFS, MR-AFS, Castor, DataGrid. 3rd IAEA Technical Committee Meeting on Control, Data Acquisition, and Remote Participation for Fusion Research, Padova 2001.
758. *Richter, S.*: Analyse und Modellierung urbaner Energiesysteme als ein Ansatzpunkt zur Emissionsreduktion von Klimagasen. Sitzung der Fachkommission CO₂-Minderungskonzept der Stadt Augsburg 2001.
759. *Richter, S.*: Untersuchungen zukünftiger urbaner Energiesysteme am Beispiel der Stadt Augsburg. Stadtwerke Augsburg 2001.
760. *Roth, J., M. Mayer and O.V. Ogorodnikova*: Deuterium Retention in W for Different Surface Conditions. IAEA Advising Committee for T Inventory in Fusion Devices, Vienna 2001.
761. *Rummel, T., O. Gaupp*, G. Lochner* and J. Sapper*: Quench Protection for the Superconducting Magnet System of Wendelstein 7-X. 17th International Conference on Magnet Technology, Geneva 2001.
762. *Runov, A.*: E3D - Towards Stellarator Applications. IEA-DED and IEA-TEXTOR Workshop, Forschungszentrum Jülich 2001.
763. *Runov, A., S.V. Kasilov*, J. Riemann, M. Borhardt, D. Reiter* and R. Schneider*: Benchmark of the 3-Dimensional Plasma Transport Codes E3D and BoRis. 8th International Workshop on Plasma Edge Theory in Fusion Devices, Helsinki 2001.
764. *Rust, N. and NI-Team*: Recent Results from W7-AS with NBI. Coordinating Committee on Neutral Beams Meeting, Forschungszentrum Jülich 2001.
765. *Ryter, F.*: Experimental Studies of Electron Transport Results from ASDEX Upgrade and Proposals for Tore Supra. Tore Supra Kick-off Workshop, Cadarache 2001.
766. *Ryter, F.*: Possible Identity Confinement Experiments between FTU and other Tokamaks. FTU Programme Workshop, Frascati 2001.
767. *Ryter, F. (for the ASDEX Upgrade Team)*: Recent Development of Threshold and Confinement in ASDEX Upgrade. 1st International Tokamak Physics Activity Meeting on Burning Plasma Transport, NIFS, Toki 2001.
768. *Ryter, F. and ASDEX Upgrade Team*: Influence of Sawteeth and GAPBOT on Power Threshold in ASDEX Upgrade. Confinement Database and Modeling Workshop, Lausanne 2001.
769. *Ryter, F. and ASDEX Upgrade Team*: Pedestal Data from ASDEX Upgrade for the International Confinement Database. Confinement Database and Modeling Workshop, Lausanne 2001.
770. *Ryter, F., H.-U. Fahrbach, A. Gude, R. Neu, V. Rohde, J. Stober and ASDEX Upgrade Team*: Survey of H-Mode Transition and Confinement from ASDEX Upgrade H-Mode Standard Shot. IAEA Technical Committee Meeting Workshop on H-Mode Physics and ITB Physics, Toki 2001.
771. *Ryter, F. and H-Mode Data Base Working Group*: Proposals for Transport Studies in FTU Summary and Discussion. FTU Programme Workshop, Frascati 2001.
772. *Ryter, F. and H-Mode Data Base Working Group*: Status of the International Global Database for the Power Threshold. 1st International Tokamak Physics Activity Meeting on Burning Plasma Transport, NIFS, Toki 2001.
773. *Ryter, F. and H-Mode Data Base Working Group*: Status of the International Threshold Database and Analyses. Confinement Database and Modeling Workshop, Lausanne 2001.
774. *Ryter, F. and H-Mode Threshold Database Group*: Progress of the International H-Mode Threshold Database Activity. IAEA Technical Committee Meeting Workshop on H-Mode Physics and ITB Physics, Toki 2001.
775. *Ryter, F., F. Leuterer, K. Kirov, F. Monaco, M. Munich, A.G. Peeters, G. Pereverzev, H. Schütz, J. Stober, W. Suttrop, G. Tardini, ASDEX Upgrade Team and ECRH Group (IPF Stuttgart)**: Transport Studies with ECRH in ASDEX Upgrade. 13th Russian-German Workshop on ECRH and Gyrotrons (STC-Meeting), Greifswald 2001.
776. *Ryter, F., F. Leuterer, K. Kirov, A.G. Peeters, G. Pereverzev, A.C.C. Sips, W. Suttrop, G. Tardini, R. Wolf, ASDEX Upgrade Team and ECRH Group (IPF Stuttgart)**: Electron Heat Transport in ASDEX Upgrade: Stiffness and ITBs. FTU Programme Workshop, Frascati 2001.
777. *Ryter, F., F. Leuterer, K. Kirov, A.G. Peeters, G. Pereverzev, J. Stober, W. Suttrop, G. Tardini and ASDEX Upgrade Team*: Untersuchung des Elektronenwärmetransports mit ECRH an ASDEX Upgrade. Kolloquium, IPF Stuttgart 2001.
778. *Ryter, F., E. Righi*, J.G. Cordey* and Contributors to the EFDA-JET Work Programme*: Threshold in JET Using He⁴ Isotope. Confinement Database and Modeling Workshop, Lausanne 2001.
779. *Ryter, F., G. Tardini, J. Stober, F. Leuterer, A.G. Peeters, W. Suttrop and ASDEX Upgrade Team*: Studies of Electron Transport in ASDEX Upgrade. Confinement Database and Modeling Workshop, Lausanne 2001.
780. *Salewski*, K.-D. and M. Endler*: Physik-Praktikum für Biochemiker und Geologen. Universität Greifswald, SS 2001.
781. *Sardei, F.*: Magnetohydrodynamik. Vorlesung, Universität der Bundeswehr München, FT 2001.
782. *Sardei, F.*: Rechneranwendungen in der Fluidodynamik. Vorlesung, Universität der Bundeswehr München, WT 2000/2001.
783. *Sardei, F., Y. Feng and J. Kisslinger*: Divertor Physics Modelling for W7-AS. W7-X Divertor Symposium, Greifswald 2001.
784. *Schacht, J. and H. Niedermeyer*: Das Trigger-Time-Event-System für die W7-X-Experimentsteuerung. 10. Symposium "Maritime Elektronik", Rostock 2001.
785. *Schacht, J., H. Niedermeyer, C. Wiencke*, J. Hildebrandt* and A. Wassatsch**: The Trigger-Time-Event System for the W7-X Experiment. 3rd IAEA Technical Committee Meeting on Control, Data

Lectures

Acquisition and Remote Participation for Fusion Research, Padova 2001.

786. *Schild*, T., D. Bouziat*, P. Bredy*, G. Dispau*, A. Donati*, P. Fazilleau*, L. Genini*, M. Jacquemet*, B. Levesy*, F. Molinié*, J. Sapper, C. Walter*, M. Wanner and L. Wegener:* Overview of a New Test Facility for the W7-X Coil Acceptance Tests. 17th International Conference on Magnet Technology, Geneva 2001.

787. *Schmid, K. and J. Roth:* Comparison of Surface Modification and Erosion of High-Z Metals due to Carbon Ion Implantation. International Conference on Surface Modification of Material by Ion Beams, Marburg 2001.

788. *Schmidt*, G., M. Stamp* and P.T. Lang:* Initial Pellet Spectrometer Results from JET. Bulletin of the American Physical Society **46** (8), 153 (2001).

789. *Schneider, R.:* Comparison of Island and Axisymmetric Divertor. IAEA Technical Committee Meeting on Divertor Concepts, Aix-en-Provence 2001.

790. *Schneider, R.:* Computational Physics. Vorlesungen, Universität Greifswald, WS 2000/2001.

791. *Schneider, R.:* Computersimulationen in der magnetischen Fusion. Fachschaftstagung "Computational Physics des Cusanuswerks", Marienburg, Zell an der Mosel 2001.

792. *Schneider, R.:* Edge Physics in Fusion Plasmas. Vorlesungen, Universität Greifswald, WS 2001/2002.

793. *Schneider, R.:* Evidence for Shoulder Recycling. Meeting on Edge, SOL and Divertor Plasma Turbulence and Transport, Fairbanks 2001.

794.

Laboratory Reports

Internal Laboratory Reports

- IPP 1/328 *Bosch, H.-S. (Ed.): ASDEX Upgrade Results, Publications and Conference Contributions Period 1/00 to 2/01.*
- IPP II/3 *Bosch, H.-S. (Ed.): ASDEX Upgrade Results, Publications and Conference Contributions Period 1/00 to 2/01.*
- IPP III/268 *Beidler, C.D., E. Harmeyer, F. Herrnegger, Yu.L. Igithkanov, A. Kendl, J. Kisslinger, Ya.I. Kolesnichenko*, V.V. Lutsenko*, C. Nührenberg., I.N. Sidorenko, E. Strumberger, H. Wobig and Yu.V. Yakovenko*.: The Helias Reactor 4/18.*
- IPP III/269 *Kolesnichenko*, Ya.I., V.V. Lutsenko*, H. Wobig and Yu.V. Yakovenko*.: Circulating-Particle-Induced Alfvén Instabilities in Optimized Stellarators and Losses of Alpha Particles in a Helias Reactor.*
- IPP 5/92 *Scott, B.D.: Low Frequency Fluid Drift Turbulence in Magnetised Plasmas.*
- IPP 5/93 *Pfirsich*, D. and D. Correa-Restrepo: New Method of Deriving Local Energy and Momentum-Conserving Maxwell-Collisionless Drift-Kinetic and Gyrokinetic Theories I.*
- IPP 5/94 *Bosch, H.-S. (Ed.): ASDEX Upgrade Results, Publications and Conference Contributions Period 1/00 to 2/01.*
- IPP 5/95 *Kendl, A.: Drift Wave Instability and Turbulence in Advanced Stellarator Configurations.*
- IPP 5/96 *Kendl, A.: Kugelblitz und Kaltfusion: Argumente und Referenzen zu parawissenschaftlichen Themen.*
- IPP 5/97 *Schade, S.: MHD Stability of ASDEX Upgrade and Textor-94 Advanced Scenarios.*
- IPP 8/17 *Bachmann, P.: Chaos in 1d Radiative Edge Plasmas.*
- IPP 8/18 *Naujoks, D.: Ion Confinement in a Linear Plasma Column.*
- IPP 9/127 *Kang, H.: Structure and Magnetism in Ultra-Thin Fe_x Co_{1-x}-Films.*
- IPP 9/128 *Federici, G., C.H. Skinner*, J.N. Brooks*, J.P. Coad*, C. Grisolia*, A.A. Haasz*, A. Hassanein*, V. Philipps*, C.S. Pitcher*, J. Roth, W.R. Wampler* and D.G. Whyte*.: Plasma-Material Interactions in Current Tokamaks and their Implications for Next-Step Fusion Reactors.*
- IPP 9/129 *Luthin, J.: Untersuchungen zur chemischen Wechselwirkung bei der Bildung von Kohlenstoff-Mischsystemen.*
- IPP 9/130 *Reinecke, N.: Adsorbate-Induced Self-Organising Nanostructures on Cu(11n)-Surfaces.*
- IPP 10/17 *Bosch, H.-S. (Ed.): ASDEX Upgrade Results, Publications and Conference Contributions Period 1/00 to 2/01.*
- IPP 10/18 *Fantz*, U. and D. Wunderlich: Anwendung und Erweiterung des Stoss-Strahlungsmodells für H₂ und H.*
- IPP 10/19 *Geier, A.: Aspekte des Verhaltens von Wolfram im Fusionsexperiment ASDEX Upgrade.*
- IPP 12/1 *Schneider, R.: Plasma Edge Physics for Tokamaks.*

External Laboratory Reports

- EU TASK DV7a/
ITER TASK EU-
T438 *Alessandrini*, C., G. Maddaluno*, G. Giacomi* and W. Bohmeyer: Report on Deuterium Desorption of W-1% La203 Samples after Exposure in Plasma Generator. ENEA, Frascati.*

Index

Author Index

- Achete*, C.A. 401
Ahmad*, I. 30
Ahn*, J.-W. 193
Akbi*, M. 20
Albertia*, S. 1, 73
Alessandrini*, C. EU TASK DV7a/ITER TASK EU-T438
Alimov*, V.K. 2, 3
Allfrey*, S. 4
Alper*, B. 221, 615
Amarante*, G. 80
Anderson*, H. 270
Andrew*, P. 119
Andrew*, Y. 27, 344
Angioni*, C. 338
Antar*, G. 469
Anton, M. 410
Antonov*, A.N. 5, 6
Aquilonius*, K. 7, 141, 142, 143, 233, 355
Arnaud*, X. 63
Arnold*, A. 1, 73
Arslanbekov, R. 127
Asakura*, N. 148, 246
Assmann*, W. 20
Aßmus, D. 673
Atanasiu*, C. 8, 127
Atsumi*, H. 806
Aumay*, F. 58, 270, 508
Austin*, M. 105
- Bachmann, P. 461, 462, 463, 464, IPP 8/17
Baity*, F.W. 9, 80
Bakhareva*, O.A. 365, 465
Bakhtiari*, M. 739
Balbin*, R. 115
Balden, M. 10, 11, 12, 116, 117, 252, 282, 306, 372, 466, 467, 553, 657, 680, 806, 827
Baldzuhn, J. 13, 125, 126, 157, 158
Bao*, S. 14
Barabash, V. 498
Baranov*, Y. 162, 245, 309, 396, 421, 615, 870
Barbato*, E. 245, 396
Barber*, G.C. 9
Bard, A. 127
Bardamid*, A.F. 404
Barnsley*, R. 167, 256
Bartels, H.-W. 15
Barth*, C.J. 30, 511
Basiuk*, V. 245
Basium*, V. 292
Basse, N.P. 16, 343, 468, 469
Bastasz*, R. 17
Bau, H. 349
Bäumel, S. 470, 471
Baumgärtel*, P. 14, 184, 195, 388
Baylor*, L.R. 221
Beaumont*, B. 80
Becker*, C. 418, 863, 864
Becker, G. 127
Becker*, U. 373
Becker, W. 53, 127
Beckmann*, M. 18, 238, 239, 671
Becoulet*, A. 245, 615, 870
Becoulet*, M. 170, 245, 344
Beguiristain Repáraz, I. 434, 647
Behler, K. 127, 751
- Behn*, R. 511
Behringer, K. 127, 151, 427, 472, 473, 474, 475, 476, 483, 529, 594, 679, 696, 809
Behrisch, R. 11, 19, 20, 104, 117, 306, 375, 477, 478, 553
Beidler, C.D. 21, 22, 479, 480, 627, IPP III/268
Beikler, R. 23, 438, 481, 482, 742, 819
Bekris*, N. 104
Belopolsky*, V.A. 365
Berger*, M. 483
Bergkvist*, T. 616
Bergmaier*, A. 20, 291
Bergmann, A. 24, 127, 312, 484, 746
Bergmann*, K. von 863, 864
Bergström*, U. 7
Berk*, H.L. 25
Bernabei*, S. 309
Berndt*, W. 281
Berry*, L.A. 323
Bertalog*, L. 256
Bertschinger*, G. 30
Bessenrodt-Weberpals, M. 26, 485, 486, 487, 488, 797
Beurskens*, M. 27, 70, 182, 221, 338, 344, 511
Beyer*, H. 489
Bibet*, P. 396
Bickley*, A. 179, 256, 682
Biedermann, C. 28, 29, 322, 449, 490
Biel*, W. 30
Bilato, R. 31, 52, 127, 271
Bindemann, T. 491
Biskamp, D. 32, 33, 34, 136, 705, 706, 709
Blank*, M. 180, 848
Blank, H. 26
Bleuel, J. 115, 389, 527
Bliokh*, Yu.P. 5
Block*, D. 35, 36, 200, 357, 358
Bobkov, V. 9
Boedo*, J.A. 311
Bohmeyer, W. 110, 194, 201, 202, 208, 489, EU TASK DV7a/ITER TASK EU-T438
Bojko, I. 349, 350
Bolshukhin, D. 37, 38, 127, 216, 288, 289, 319, 492, 540, 659, 661
Bolt, H. 39, 63, 209, 252, 296, 351, 423, 424, 425, 493, 494, 495, 496, 497, 498, 647, 680, 827, 828, 829, 871
Bolzonella*, T. 286
Bondarenko*, V.N. 404
Bonhomme*, G. 200, 235, 236, 358
Bonnin, X. 40, 41, 68, 331, 354, 508, 795
Bonoli*, P. 52
Booth*, N.A. 14
Boozer*, A. 323
Borba*, D.N. 25
Borchardt, M. 41, 354, 826
Borchegowski*, A. 238, 239, 671
Borhardt, M. 763
Borie*, E. 1, 73
Bornatici*, M. 42, 315
Borrass, K. 43, 44, 67, 68, 795
Boscary, J. 45, 755
Bosch, H.-S. 46, 47, 48, 68, 69, 287, 324, 499, 500, 501, 502, IPP 1/328, IPP II/3, IPP 5/94, IPP 10/17
Bosia*, G. 80
Bottino*, A. 4
Bouziat*, D. 786
Braams*, B. 68
Bracco*, G. 64, 742

Index

- Bradshaw, A.M. 14, 47, 49, 139, 152, 184, 195, 196, 267, 281, 388, 503, 504
Brakel, R. 50, 126, 505, 559
Brambilla, M. 31, 51, 52, 127, 271, 506, 507
Bramow, H.-J. 92
Brandenburg*, R. 127, 862
Bräuer, T. 92
Braun, F. 53, 127
Braun*, J. 316
Bredy*, P. 786
Breizmann*, B.N. 25
Brémond*, S. 80
Breuer*, U. 296
Brinkschulte, H. 127, 238, 239, 671
Brix*, M. 27, 54
Brockmann, R. 349
Brooks*, A. 323
Brooks*, J.N. 90, 91, 285, IPP 9/128
Brückner, R. 127
Bruhn*, B. 55
Brüning*, K. 742
Bruschi*, A. 113
Brüsehaber, B. 127
Bucalossi*, J. 255, 256
Büchl, K. 127
Budny*, R.V. 56, 295, 344, 384
Buhler, A. 127
Bünde, R. 57
Bürbaumer*, H. 58, 68, 127, 508
Burhenn, R. 83, 126, 263, 365, 465, 509, 559, 824
Buttery*, R.J. 59, 64, 257
- Cabal*, H. 7, 140, 141, 142, 143, 233, 355
Cahill*, D.G. 359
Campbell*, D.J. 59, 60
Carlson, A. 61, 62, 127, 154, 183, 427
Castaldo*, C. 396
Causey*, R.A. 806
Cesario*, R. 256, 295, 309, 396
Challis*, C.D. 59, 65, 149, 162, 245, 615, 870
Chan*, V. 294, 295
Chang*, C.S. 56
Chankin*, A. 115, 389
Chappuis*, P. 63
Chareau*, J.-M. 27, 65, 256
Charlet*, M. 67, 256
Chen*, S.-C. 359
Chirkov*, A.V. 238
Chu*, S. 180, 848
Cierpka, P. 247
Cirant*, S. 113, 114, 338
Ciric, M. 127
Clark*, R.E.H. 82
Coad*, J.P. 71, 91, 375, IPP 9/128
Cocilovo*, V. 309, 396
Coffey*, I. 67, 254, 256
Colas*, L. 80
Connor*, J.W. 64, 165
Conroy*, S. 256, 616
Conway, G. 65, 66, 127, 134, 149, 162, 245, 253, 299, 325, 368, 377, 399, 422, 510
Cooper*, W.A. 275, 323, 383, 701, 810
Corati*, D. 707, 708
Cordey*, J.G. 67, 221, 384, 398, 778
Correa-Restrepo, D. IPP 5/93
Corrigan*, G. 70
Cortes*, S. 257
- Coster, D.P. 40, 48, 58, 62, 68, 69, 70, 88, 90, 109, 148, 167, 192, 193, 214, 215, 246, 287, 311, 320, 324, 331, 332, 333, 413, 508, 718, 719, 795
Counsell*, G.F. 71, 193
Cowers*, C. 511
Cox*, S. 270
Crisanti*, F. 162, 245, 396
Cupido*, L. 325, 368, 369
- Da Silva*, F. 72
Dammertz*, G. 1, 73, 85
Darrow*, D.S. 74, 415, 857
Davies*, S.J. 115
Davis*, J.W. 82, 135
De Angelis*, R. 149, 245, 292, 396
De Baar*, M. 56, 162, 255, 256, 292, 615, 682
De Grassie*, J. 294, 295
De la Luna*, E. 27
De Vries*, P. 255, 256
Del Río*, J.M. 174
Denisov*, G.G. 238
Desinger, K. 234
Deuchler, S. 449
Dinklage, A. 55, 100, 101, 203, 235, 512, 539
D'Ippolito*, D.A. 75
Dispau*, G. 786
Dohmen, R. 76
Dollinger*, G. 20, 291
Donath, M. 316
Donati*, A. 786
Dorland*, W. 175, 176
Dorn, C. 127, 247
Doron*, R. 29, 322
Dose, V. 77, 78, 96, 97, 120, 317, 318, 360, 361, 395, 513, 514, 515, 537, 538, 539, 557, 750
Drescher*, M. 373
Drevlak, M. 298, 302, 323, 683
Drube, R. 127, 283
Du Plessis*, J. 403
Düchs, D. 516, 517, 518, 519, 520
Dumbrajs*, O. 79
Durocher, K. 435
Durodié*, F. 80
Duval*, B.P. 311
Dux, R. 30, 37, 81, 119, 127, 182, 221, 224, 245, 254, 286, 288, 319, 327, 492, 521, 522, 523, 540, 753
- Eckstein, W. 17, 82, 135, 330, 353, 433
Edelmann*, C. 20
Egorchenkov*, R.A. 42
Egorov, S. 127, 304, 428, 739
Ehmler, H. 83, 125, 126, 262, 263, 524, 559
Eich*, T. 170, 670
Ekedahl*, A. 309, 396
El-Naggar*, H. 235
Empacher*, L. 185, 238, 239, 671
Endler, M. 16, 115, 129, 343, 389, 390, 391, 468, 471, 525, 526, 527, 565, 780, 822, 823, 862
Engelhardt, W. 127
Entscheva, A. 655
Erckmann, V. 1, 73, 84, 85, 113, 114, 185, 226, 227, 408
Erents*, K. 27, 70, 115, 182, 256, 259, 309
Eriksson*, L.-G. 245, 256, 292, 682
Ertl, K. 2, 3, 316, 329, 528, 688
Esposito*, B. 245
Esser*, H.G. 416
Estrada*, T. 65
Etxeberria*, J. 11, 117, 306, 466, 553

Index

- Fahrbach, H.-U. 127, 339, 340, 341, 770
Fainberg*, Ya.B. 5
Falter*, H.-D. 270
Fanthome*, J. 80
Fantz*, U. 86, 87, 88, 89, 127, 150, 151, 475, 476, 483, 529, 530, 594, 679, 696, 809, IPP 10/18
Faugel, H. 53, 127
Fazilleau*, P. 786
Federici, G. 71, 90, 91, 498, IPP 9/128
Feist, J.-H. 92, 93, 94, 349, 408, 409
Felch*, K. 180, 848
Felton*, R. 179, 221
Feng, Y. 95, 111, 126, 207, 262, 263, 531, 532, 559, 653, 654, 783
Fenstermacher*, M.E. 826
Fesenyuk*, O.P. 205
Fessey*, J. 65
Fiedler, S. 207, 263
Figueiredo*, A. 255, 396
Finken*, K.H. 739
Fischer, R. 96, 97, 225, 291, 395, 533, 534, 535, 536, 537, 538, 539
Fix*, A. 239
Foley*, M. 98, 127
Forest*, C. 703
Förster*, F. 238, 671
Förster*, W. 239
Fournier*, K.B. 288, 540
Franck*, C. 99, 411
Franke*, S. 100, 101
Franzen, P. 102, 103, 127, 210, 270, 541, 542, 543, 544, 545, 655
Fredrickson*, E. 323
Friedrich*, M. 20, 104
Frigione*, D. 245
Fu*, G. 323
Fu*, P. 127, 366
Fuchs, C. 105, 106, 107, 108, 248, 337, 376, 399, 491
Fuchs*, G. 30
Fuchs, J.C. 109, 127, 154, 167, 223, 268, 283, 287, 304, 716
Fuchs, T. 28, 29
Fugueiredo*, A. 256
Fujisawa*, A. 168, 302, 683
Fundamenski*, W. 70, 112, 167, 170, 182, 193, 231, 259
Furno*, I. 311
Fußmann, G. 28, 29, 110, 201, 202, 489, 490, 546, 547, 548, 549, 550, 551

Gadelmeier, F. 111, 125, 126, 552, 559, 654
Gafert, J. 112, 127, 223, 224, 287, 319, 427, 716
Gandini*, F. 113, 114, 226
Gantenbein*, G. 73, 127, 185, 238, 239, 240, 241, 272, 431, 432, 671
Ganuza*, D. 174
Garbet*, X. 60, 166
García*, I. 174
García-Cortes*, I. 115
García-Rosales*, C. 11, 104, 116, 117, 306, 466, 553
Gardebrecht, W. 347, 849
Garici*, G. 80
Garin*, P. 1
Garzotti*, L. 221, 254, 398
Gaupp*, O. 761
Gavrilin*, A.V. 554
Gehre, O. 127, 223
Gehringer, K. 450
Geier, A. 118, 127, 289, 327, 439, 540, 555, 556, 656, IPP 10/19
Geiger, J. 85, 106, 410
Geigl*, M. 862
Genchev*, I. 291
Genini*, L. 786
Gernhardt, J. 127

Gervash*, A. 351
Giacomi*, G. EU TASK DV7a/ITER TASK EU-T438
Giannone, L. 111, 125, 126, 169, 263, 509, 559, 654
Gießel*, T. 14
Giguet*, E. 1, 73
Giovannozi*, E. 27
Giroud*, C. 56, 81, 119, 149, 245, 421, 523, 615
Glagla, J. 123
Gliège, G. 92
Golan*, A. 120, 557
Goldston*, R. 56, 323
Goldstraß, P. 121, 122, 243, 244, 676
Gondhalekar*, A. 56, 256, 292, 295
Gong, X. 356, 656, 657
Görgens*, L. 291
Gori, S. 302, 429, 539, 683
Gorini*, G. 254
Gorkom*, J. van 65
Goto*, M. 301, 394
Gottschewsky, M. 57
Götz, M. 436
Goulding*, R.H. 9, 80
Gowers*, C. 27, 256, 384, 615
Graham*, M. 396
Granucci*, G. 113, 114, 309, 396
Grappin*, R. 709
Greiner*, F. 128, 200
Greuner, H. 45, 123, 209, 755, 827, 828, 829
Greve, H. 646
Grigoropoulos*, C.P. 359
Grigull, P. 50, 83, 111, 124, 125, 126, 155, 165, 207, 262, 263, 558, 559, 653, 654, 855
Grisolia*, C. 91, IPP 9/128
Grossmann*, V. 368, 400
Grote, H. 755
Gruber, O. 48, 66, 127, 154, 159, 160, 222, 223, 287, 305, 327, 341, 376, 377, 378, 422, 560, 561, 562, 563, 716, 739, 740, 825, 870
Grulke, O. 128, 129, 440, 527, 564, 565, 862
Gubanka, E. 127
Gude, A. 66, 127, 130, 131, 132, 134, 159, 160, 257, 422, 431, 432, 569, 570, 571, 770
Gunn*, J. 27
Günter, S. 8, 59, 66, 127, 130, 131, 132, 133, 134, 159, 160, 240, 241, 257, 272, 310, 342, 382, 422, 426, 431, 432, 566, 567, 568, 569, 570, 571, 572, 746, 870
Günther*, K. 27

Haas, G. 48, 127, 221, 223, 262, 287, 427, 451, 716
Haasz*, A.A. 82, 91, 135, IPP 9/128
Hacker, H. 509
Hallatschek, K. 32, 136
Hallberg*, B. 7, 140, 141, 142, 143, 233, 355
Hamacher, T. 7, 137, 138, 139, 140, 141, 142, 143, 233, 352, 355, 475, 575, 576, 577, 578, 579, 580, 581, 582, 583
Hammett*, G.W. 176
Hanson*, K.M. 97
Harmeyer, E. 144, 145, 479, 480, 584, 627, IPP III/268
Hartfuß, H.-J. 84, 106, 107, 108, 125, 381, 471, 491, 585, 586, 587, 588, 589, 590, 591, 857
Hartmann, D. 50, 53, 126, 127, 146, 147, 292, 396, 592, 593
Hassanein*, A. 91, IPP 9/128
Hatayama*, A. 148
Hatcher*, R. 323
Hatzky, R. 4, 298
Hawkes*, N. 65, 149, 162, 245, 270, 286, 292, 295, 421, 615, 870
Hayashi*, N. 148
Hayashi*, T. 683
Hedin*, J. 178, 616

Index

- Heger, B. 86, 88, 150, 151, 594
Heikkinen*, J.A. 75, 79, 147, 197, 198, 396
Heiland*, W. 742
Heimann, P. 595, 596, 658
Hein, B. 349
Heinemann, B. 127, 210, 264, 405, 542, 655
Heinrich, S. 57
Heinzel, S. 658
Heinzmann*, U. 373
Hellermann*, M. von 30, 344, 385
Hellsten*, T. 178, 255, 256, 292, 295, 396, 421, 616, 682
Hender*, T.C. 257, 615
Hennequin*, P. 344
Henning, C. 658
Henniquin*, P. 245
Hensley, D.K. 330
Hentges*, R. 196
Hergenahn, U. 152, 196, 373, 597, 598, 599, 600, 601
Herrmann, A. 62, 109, 127, 153, 154, 231, 246, 287, 304, 341, 377, 378, 602, 603, 670, 716
Herrnegger, F. 479, 480, 604, 605, 627, IPP III/268
Heyn*, M.F. 275, 336, 383, 617, 701, 810
Hidalgo*, C. 64, 115
Hildebrandt, D. 20, 125, 126, 155, 156, 207, 263, 334, 356, 416, 417, 559, 606, 607, 654, 657, 796, 858
Hildebrandt*, J. 348, 785
Hirooka*, Y. 82, 135
Hirsch, M. 16, 113, 114, 125, 126, 157, 158, 165, 226, 253, 410, 468, 491
Hirshman*, S. 323
Hoang*, G.G. 338
Hobirk, J. 66, 98, 127, 130, 134, 149, 159, 160, 240, 261, 269, 421, 422, 870
Hoefl*, J.-T. 184, 195, 388
Hoffmann, D.H.H. 161
Hoffmann, F.W. 45, 755
Hofman*, D. 7
Hofman*, G. 828, 829
Hofmeister, F. 53, 127
Hofsäss*, H. 291
Hogeweyj*, G.M.D. 60, 65, 162, 338
Hogge*, J.-P. 73
Hohenöcker, H. 127
Hollmann, F. 185
Holzhauer*, E. 157, 158, 510
Holzthüm, R. 849
Hopf, C. 188, 625, 626
Horacek*, J. 311
Horton, L.D. 44, 127, 163, 221, 222, 246, 608, 609
Howell*, D.F. 131, 132, 257, 570, 571
Hrabal*, D. 367
Hu, C. 655
Hu*, L. 127
Huart, M. 366, 367
Huber*, A. 167, 209
Hudson*, S. 323
Huysmans*, G. 245
Hytry, R. 458

Ida*, K. 302, 683
Igitkhanov, Yu.L. 95, 164, 165, 246, 479, 480, 531, 532, , IPP III/268
Iguchi*, H. 683
Iida*, H. 397
Illin*, V. 238, 239, 671
Illy*, S. 1, 73
Imbeaux*, F. 162, 166, 245, 309, 338, 339, 396
Imbihl*, R. 267
Ingesson*, C. 81, 167, 254, 256, 259, 616

Isaev*, M.Yu. 275, 323, 383, 701, 810
Isobe*, M. 168, 302, 683
Itami*, K. 246
Itoh*, K. 169, 302, 381, 683
Itoh*, S.-I. 169, 381

Jacchia*, A. 64, 338
Jachmich*, S. 27, 170, 221, 231, 670
Jacob, W. 20, 171, 172, 189, 190, 191, 258, 360, 401, 404, 610, 611, 612, 626, 695
Jacobi, D. 127
Jacquemet*, M. 786
Jaenicke, R. 125, 126, 410, 559
Jakobi, M. 127, 216, 613, 659, 660, 661
Jaksic, N. 173, 371, 614, 804, 849
Jamich*, S. 286
Jandl, O. 123, 144
Janeschitz*, G. 90, 164, 165, 214, 215, 246
Jansen*, F. 862
Jarvis*, N. 256
Jauregi*, E. 174
Jenko, F. 127, 175, 176, 510
Joffrin*, E. 149, 245, 615, 870
Johnson*, T. 178, 256, 396, 616
Johnsson*, R. 292
Jones*, T.T.C. 179, 221, 222, 270, 396
Jory*, H. 180, 848
Jost*, G. 4
Jun*, C. 323
Jüttner, B. 181

Kaiser*, R. 374
Kallenbach, A. 27, 48, 67, 68, 109, 127, 182, 183, 269, 283, 287, 289, 319, 327, 341, 344, 398, 413, 427, 492, 716
Kaltenberger, A. 379
Kalyuzhnyj*, V.N. 275, 383, 701, 810
Kamionka, U. 92
Kang, H. 441, 750, IPP 9/127
Kang*, J.-H. 184, 195
Kantor*, M.Yu. 38
Kardaun, O. 98, 127
Kasilov*, S.V. 275, 336, 383, 617, 701, 763, 810
Kasilov*, V.V. 275, 701
Kasperek*, W. 73, 85, 114, 185, 238, 239, 274, 452, 671, 703
Kastelewicz, H. 413
Kaufmann, M. 68, 127, 223, 287, 341, 376, 378, 510, 618, 716
Kaveeva*, E.G. 331, 332, 333, 795
Kawahata*, K. 301, 394
Kaye*, A. 80
Kempgens*, B. 196
Kendl, A. 127, 186, 187, 269, 717, IPP III/268, IPP 5/95, IPP 5/96
Kerl, F. 347, 409, 849
Kernbichler, W. 275, 336, 383, 617, 701, 810
Kersten*, H. 862
Kessel*, C. 323
Keudell, A. von 172, 188, 189, 190, 191, 265, 266, 360, 619, 620, 621, 622, 623, 624, 625, 626, 693, 694, 695
Khayrutdinov*, R.R. 739
Kim, J.W. 68, 127, 192, 718, 795
Kiniviemi*, T. 342
Kinsey*, J.E. 254
Kiptily*, V. 178, 255, 256, 616, 682
Kirk*, A. 193
Kirov, K. 127, 238, 240, 294, 396, 422, 671, 672, 775, 776, 777, 870
Kirschner*, A. 416, 417, 858
Kissick*, M. 254
Kisslinger, J. 95, 111, 125, 144, 145, 207, 479, 480, 531, 532, 559, 584, 605, 627, 653, 654, 755, 783, IPP III/268

Index

- Kiss'ovsky, Z. 194
Kittel*, M. 195
Kivimäki*, A. 196
Kiviniemi*, T.P. 197, 198
Klages, K.U. 121, 243
Klaster, K. 460
Kleberg, I. 442
Kleiber, R. 199, 298, 628, 629, 630, 631, 632
Klunge, S. 253, 510
Klinger, T. 35, 36, 83, 99, 128, 129, 200, 203, 236, 357, 358, 411, 559, 565, 633, 634, 635, 636, 637, 638, 639, 640, 641, 642, 643, 644
Klose, S. 110, 201, 645, 646
Knapp*, W. 20
Knauer, J. 111, 207, 262, 263, 539, 559
Knözinger*, H. 204, 218, 677, 678
Koch*, B. 202
Koch*, B.-P. 55
Koch, F. 252, 296, 423, 647, 811
Koch*, R. 80, 256
Kochergov, R. 127
Kocsis*, G. 343, 509
Koepke*, M.E. 203
Kohl, A. 204, 677, 678
Kolesnichenko*, Ya.I. 21, 205, 648, 649, 650, IPP III/268, IPP III/269
Kollotzek, H. 127, 379
Komatsu*, N. 148
Komori*, A. 653
Könies, A. 26, 206, 298, 651, 652
König, R. 111, 125, 207, 263, 385, 559, 653, 654, 855
Kononov*, V.G. 404
Koppenburg*, K. 73
Korhonen*, R. 7, 140, 141, 142, 143, 233, 355
Kornejew, P. 110, 202, 208, 489
Kornilov*, E.A. 5, 6
Korotkov*, A. 27, 54, 182
Koslowski*, H.R. 30, 286
Kötterl, S. 209, 282, 827, 828, 829
Kovaltsov*, E. 68
Kovpik*, O.F. 5, 6
Kralj*, M. 418, 863, 864
Krämer-Flecken*, A. 30
Krames*, B. 862
Krasheninnikov*, S.I. 293
Kraus, W. 127, 210, 264, 405, 655
Krause, B. 92
Kravtsov*, Yu.A. 42
Kreissig*, U. 20, 375
Krieger, K. 71, 118, 127, 206, 211, 212, 213, 289, 320, 326, 327, 356, 386, 555, 556, 656, 657
Kroiss, H. 658
Ku, L. 323
Kubo*, F. 375
Kuduk*, R. 857
Kugeler, O. 152
Kühner, G. 125, 207, 263, 559, 658
Kukushkin*, A.S. 90, 214, 215, 246, 311
Kuntze*, M. 73
Kurki-Suonio*, T. 342
Kurzan, B. 38, 66, 77, 127, 157, 158, 159, 160, 182, 216, 217, 223, 268, 283, 325, 341, 376, 399, 422, 510, 511, 613, 659, 660, 661, 716, 870
Kuteev*, B.V. 365, 465, 824
Kyriakakis*, G. 127
Lackner, K. 8, 127, 133, 426, 569, 572
Lako*, P. 142
Lalousis*, P. 219, 220
Lamalle*, P. 75, 80, 147, 179, 255, 256, 292, 294, 396
Lamont*, C.L.A. 195
Lang, P.T. 127, 221, 222, 223, 224, 247, 248, 257, 402, 662, 753, 788
Lang, R.S. 127, 247
Langer, U. 225
Laqua, H. 73, 228, 274, 381
Laqua, H.P. 85, 113, 114, 185, 226, 227, 407, 663, 664, 665
Laux, M. 127, 154, 170, 201, 229, 230, 231, 232, 242, 287, 320, 413, 414, 606, 666, 667, 668, 669, 670, 687, 716
Lawson*, K. 67, 179, 256, 682
Laxaback*, M. 396, 421
Lazarev*, V. 375
Lazarus*, E. 323
Le Cloarec*, G. 1, 73
Le Goff*, Y. 1, 73
Lechon*, Y. 7, 140, 141, 142, 143, 233, 355
Lechte*, C. 717
Lederer, H. 234, 573, 574
Ledl, L. 365, 509
Lehnen*, M. 30, 54
Lengyel, L.L. 127, 219, 402
Leonard*, A.W. 246
Leonhardt*, W. 73
Lepicard*, S. 7, 141, 142, 143, 233, 355
Letellier*, C. 235, 236
Leuterer, F. 18, 127, 237, 238, 239, 240, 241, 309, 339, 340, 341, 396, 422, 431, 432, 671, 672, 775, 776, 777, 779, 870
Levesy*, B. 786
Lewandowski*, J. 323
Lievin*, C. 73
Lin*, Z. 323
Linden*, W. von der 97, 361
Lindig, S. 375, 412, 553
Lindsay*, R. 14
Lingertat, J. 242, 673
Linke*, J. 63, 209, 252, 351, 498, 680
Linsmeier, C. 121, 122, 204, 243, 244, 249, 250, 251, 329, 674, 675, 676, 677, 678
Litaudon*, X. 65, 162, 245, 396
Loarte*, A. 90, 115, 165, 170, 214, 215, 246, 311, 344, 498
Lochner*, G. 761
Lomas*, P. 67, 149, 221, 344
Lorenz, A. 127, 221, 222, 223, 224, 247, 402, 428, 753
Lorenzini*, R. 248
Lortz, D. 374
Lotte*, P. 149, 245, 286, 292
Lotter*, A. 679
Lukash*, V.E. 739
Luthin, J. 244, 249, 250, 251, 252, 330, 433, 443, 676, 680, IPP 9/129
Lutsenko*, V.V. 205, 648, 649, 650, IPP III/268, IPP III/269
Lyon*, J.F. 323
Lyubarskii*, M.G. 5
Maaßberg, H. 22, 85, 106, 227, 867
Maddaluno*, G. EU TASK DV7a/ITER TASK EU-T438
Maddison*, G.P. 179, 256
Maget*, P. 245, 396
Magne*, R. 1, 73
Mahdavi*, M.A. 398
Maier, H. 118, 127, 212, 252, 289, 326, 327, 386, 413, 423, 555, 556, 647, 656, 657, 680, 811
Maier, J. 658, 681
Maier, K. 196
Mailloux*, J. 149, 162, 245, 256, 309, 396
Maj*, O. 42

Index

- Mandelbaum*, P. 29, 322, 490
Mank*, K. 127, 739
Manso*, M. 72, 127, 253, 299, 325, 368, 369, 399, 400
Mantica*, P. 60, 254, 338
Mantsinen*, M. 178, 179, 245, 255, 256, 286, 292, 384, 396, 421, 616, 682
Maraschek, M. 66, 127, 130, 131, 132, 134, 159, 160, 221, 222, 223, 241, 257, 272, 304, 341, 377, 378, 422, 431, 432, 569, 570, 571, 572, 615, 870
Marchenko*, V.S. 21
Marchuk*, A. 30
Martines*, E. 471
Maruyama*, K. 258
Mast, K.-F. 109, 127, 304, 453
Masuzaki*, S. 394, 404, 653
Matsuoka*, K. 168, 302, 653, 683
Mattes, K. 379
Matthews*, G.F. 115, 167, 170, 215, 231, 246, 259, 309, 384, 389
Matyash, K.V. 5, 6
Mayer, M. 10, 20, 209, 260, 375, 416, 417, 684, 685, 686, 687, 688, 760, 827, 858
Mayne*, M. 63
Mayoral*, M.-L. 147, 178, 255, 256, 292, 396, 616, 682
Mazon*, D. 149, 245, 421, 615
Mazzoli*, E. 68
Mazzone*, G. 80
McCarthy*, P.J. 98, 127, 159, 160, 261, 422
McCormick, K. 54, 83, 111, 125, 126, 155, 207, 262, 263, 559, 653, 654, 689, 855
McCune*, D. 56
McDonald*, D.C. 67, 167, 398
McNeely, P. 264, 405, 655
Meiden*, H.J. v.d. 30
Meier, M. 188, 265, 266, 625, 626, 690, 691, 692, 693, 694, 695
Meir, S. 87, 696
Meisel, D. 127
Meißen*, F. 267
Meister, H. 66, 127, 159, 160, 268, 269, 270, 341, 422, 870
Mellera*, V. 113
Ménard*, O. 236
Mendelevitch, B. 45, 123, 755
Meneses*, L. 65, 369
Menhart*, S. 270
Meo, F. 31, 127, 255, 256, 271, 292, 294, 295, 376, 378, 396
Merkel, P. 298, 302, 323, 683
Merkel, R. 127
Mertens, V. 44, 127, 222, 223, 224, 287, 304, 428, 697, 716, 739, 753, 825
Meskat, J. 127, 272, 431, 432
Meyer*, H. 201
Meyer-Spasche, R. 698, 699, 700
Michel, G. 1, 73, 273, 274
Michelsen*, P.K. 468, 469
Mikhailov*, M.I. 275, 323, 383, 701, 810
Mikkelsen*, D. 323
Milani*, F. 167, 255, 256
Milch, I. 276, 277, 278, 702
Miller*, J.R. 554
Milun*, M. 418, 863, 864
Minami*, T. 683
Miner*, W. 323
Miri*, A.M. 279
Mirizzi*, F. 309
Molinié*, F. 786
Möller, W. 458
Monaco, F. 238, 239, 671, 672, 775
Monakhov*, I. 255, 256, 396
Monk, R.D. 44, 127, 242, 259
Monticello*, D. 298, 323
Moon*, S.-J. 359
Morabito*, F.C. 280
Moraru*, A. 8
Moré*, S. 281
Moreau*, D. 245
Moret*, J.-M. 311
Morgan*, P. 27, 54, 119
Morita*, S. 301, 394
Motojima*, O. 404
Motoyama*, M. 293
Mück, A. 703
Mukherjee, S. 282
Müller, C. 279
Müller*, G. 73, 452
Müller, H.W. 66, 127, 182, 221, 223, 224, 283, 287, 376, 399, 711, 716, 753
Müller*, N. 373
Müller, W.-C. 704, 705, 706, 707, 708, 709
Münch, M. 453
Münich, M. 127, 238, 239, 671, 672, 775
Murakami*, S. 168, 302, 683
Murari*, A. 256
Murmman, H. 77, 127, 216, 217, 223, 613, 659, 660, 661
Muroga*, T. 811
Mutzke, A. 354
Muzzini*, V. 113, 114
Mynick*, H. 323
Myra*, J.R. 75
Nagel, M. 710
Nahrihara*, K. 394
Naiser, T. 283, 711, 741
Nakajima*, N. 168, 302, 683
Nakamura, Y. 739
Narayanan, R. 559
Nardone*, A. 113
Narushima*, Y. 394
Naujoks, D. 207, 263, 284, 285, 559, 712, 713, 714, 855, IPP 8/18
Naulin*, V. 200, 358
Nave*, M.F.F. 56, 286, 294, 295
Neffe*, G. 73
Neilson*, G. 323
Nelson*, B.E. 323
Nemov*, V.V. 275, 383, 701, 810
Neu, G. 127, 428, 751
Neu, R. 37, 38, 58, 118, 127, 167, 212, 287, 288, 289, 290, 319, 326, 327, 356, 492, 540, 555, 556, 715, 716, 770, 796
Neuhauser, J. 68, 77, 127, 154, 182, 192, 222, 223, 224, 283, 287, 613, 716, 753
Neumaier*, P. 291
Nguyen*, F. 59, 178, 255, 256, 271, 292, 295, 396, 616, 682
Niedermeyer, H. 228, 348, 408, 455, 527, 559, 784, 785
Niedner, S. 717
Nielsen*, P. 511
Nishijima*, D. 293
Nishimura*, H. 811
Nishimura*, S. 168, 302, 683
Nishimura, Y. 718, 719
Nolte*, E. 375
Nolting*, W. 316
Nomura*, I. 302, 683
Nordman*, H. 384
Noterdaeme, J.-M. 9, 53, 56, 75, 80, 127, 147, 178, 179, 255, 256, 271, 292, 294, 295, 396, 421, 616, 682, 720, 721, 722, 723, 724, 725, 726, 727, 728, 729, 730, 731
Nöthe*, M. 296
Nowak*, S. 113, 114

Index

- Nührenberg, C. 168, 275, 297, 298, 323, 410, 683, 701, 732, 810, IPP III/268
Nührenberg, J. 298, 302, 354, 383, 429, 683, 733, 734
Nunes*, I. 127, 253, 299, 368, 369
- Obermayer, S. 102
Obiki*, T. 653
Obst, B. 735
Ogorodnikova, O.V. 300, 736, 737, 760
Ohdachi*, S. 301, 394
Ohno*, N. 293
Ohyabu*, N. 394, 653
Okamura*, S. 168, 302, 683
O'Mullane*, M. 119
Ondak*, T. 89, 530, 809
Ongena*, J. 44, 56, 67, 221, 256, 286, 398
Orlinskij*, D.V. 404
Orsitto*, F. 511
Osakabe*, M. 683
Ott, W. 303, 337
Otte, M. 673
Oyarzabal*, E. 553
- Pacher*, G. 165
Pacher*, H.D. 90, 165, 214, 215
Panaccione*, L. 292, 309, 396
Pantis*, G. 370, 803
Parail*, V. 254, 256, 286, 344, 384, 398, 615
Park*, W. 220
Pascal*, M. 195
Pasch, E. 559
Pasqualotto*, R. 511
Patchett*, A.J. 267
Pautasso, G. 127, 183, 280, 304, 305, 428, 738, 739, 740, 741
Pavlenko*, I. 31
Paz*, P. 11, 117, 306
Peacock*, A. 375
Pecher, P. 318
Pecquet*, A.-L. 292
Pedemonte*, L. 742
Peeters, A.G. 24, 60, 64, 66, 127, 134, 159, 160, 183, 197, 198, 269, 307, 310, 312, 313, 314, 315, 341, 387, 484, 746, 775, 776, 777, 779, 870
Penkalla*, H.J. 296
Penzhorn*, R.-D. 104
Perchermeier, J. 304, 326
Peres Alonso*, M. 511
Pereverzev, G. 127, 159, 160, 248, 308, 313, 314, 315, 340, 341, 387, 422, 775, 776, 777
Pericoli-Ridolfini*, V. 309, 396
Perkins*, F.W. 56
Pervan*, P. 418, 863, 864
Petersen, M. 76
Petrov*, Yu. 255, 256
Petti*, D. 63
Petty*, C. 271
Pfefferle, K. 45
Pfeiffer, U. 527
Pfirsch*, D. IPP 5/93
Philipps*, V. 71, 91, 167, 170, 416, IPP 9/128
Piancastelli*, M.N. 196
Picarle, S. 12
Pichlmeier, J. 76
Pieger-Frey, M. 92, 349
Piel*, A. 35, 36, 99, 128, 129, 200, 236, 357, 358, 411, 565
Piltz*, W. 104
Pinches, S.D. 24, 25, 127, 134, 257, 269, 310, 312, 746
Piosczyk*, B. 1, 73
- Pirsch, H. 349
Pitcher*, C.S. 91, IPP 9/128
Pitts*, R.A. 311
Plank, H. 251
Plenteda*, R. 397
Podda*, S. 179, 292, 309, 396
Podobinskii*, V.O. 5
Pogutse*, O.P. 165
Polcik*, M. 14, 184, 195, 388
Poli, E. 42, 127, 312, 313, 314, 315, 422, 484, 743, 744, 745, 746, 870
Pomphrey*, N. 323
Poperenko*, V.L. 404
Popov*, L. 238, 239, 671
Popovichev*, S. 256
Porter*, G.D. 246
Pospieszczyk*, A. 209, 687, 827
Potthoff*, M. 316
Pouleur*, Y. 80
Prentice*, R. 27
Preuss, R. 78, 317, 318, 361, 747, 748, 749, 750
Probst, F. 454
Proschek*, M. 27, 270
Pugno, R. 62, 127, 154, 287, 289, 319, 320, 327, 414
Puri, S. 321
Pursch*, H. 232
- Quaas*, M. 862
- Rachlew*, E. 149
Racine, B. 612
Radau, S. 114
Radtke, R. 28, 29, 322, 449, 490
Rapp*, J. 30, 44, 67, 221, 286, 384, 398
Raupp, G. 127, 428, 751, 825
Redi*, M. 323
Reetz, J. 658, 752
Rehbach*, W.P. 296
Reich, M. 221, 223, 224, 402, 753
Reiersen*, W. 323
Reiman*, A. 298, 323
Reinecke, N. 444, 754, IPP 9/130
Reiner, H.-D. 194, 202, 208, 489
Reiser*, D. 70, 324
Reiter*, D. 68, 88, 95, 214, 215, 246, 311, 336, 531, 532, 617, 763
Renk*, K.F. 221, 224, 753
Renner, H. 45, 123, 209, 408, 653, 755
Rennie, E.E. 152, 756
Reuter, H. 757
Reyes-Cortes*, S. 149
Ribeiro*, T. 65, 66, 127, 325, 510
Riccardo*, V. 80, 255, 256, 259, 740
Richter*, A. 862
Richter, S. 758, 759
Rieck, R. 123
Riedl, R. 103, 127, 264, 405, 542, 655
Riemann, J. 41, 354, 763, 826
Righi*, E. 56, 75, 147, 179, 255, 256, 292, 294, 295, 396, 682, 729, 778
Rimini*, F. 147, 162, 245, 255, 256, 309, 396, 421
Riondato, S. 127
Robinson*, J. 184
Roccella*, M. 80
Rognlien*, T.D. 826
Rohde, V. 127, 212, 287, 289, 319, 326, 327, 356, 379, 656, 657, 680, 716, 739, 770, 796
Röhr, H. 127
Rohrer*, L. 375

Index

- Rommers*, J. 311
Ronning*, C. 291
Röpcke*, J. 862
Rosenhahn*, A. 418, 863, 864
Rotenberg*, E. 195
Roth, J. 2, 3, 11, 12, 78, 91, 127, 155, 209, 213, 251, 258, 306, 328, 329, 330, 353, 356, 375, 386, 412, 433, 466, 498, 528, 656, 657, 688, 760, 787, 828, 829, IPP 9/128
Rozhansky*, V. 40, 68, 331, 332, 333, 795
Rubel*, M. 334, 416, 417, 858
Ruccillo*, A. 292
Rüdel*, A. 152, 196
Rummel, T. 174, 335, 761
Runov, A. 336, 617, 762, 763
Rust, N. 337, 559, 764
Rutherford*, P. 323
Ryan*, P.M. 75
Ryter, F. 67, 127, 166, 239, 240, 241, 287, 325, 338, 339, 340, 341, 376, 387, 421, 422, 671, 672, 716, 765, 766, 767, 768, 769, 770, 771, 772, 773, 774, 775, 776, 777, 778, 779
Ryzhkov*, I.V. 404
- Saarelma*, S. 127, 130, 342
Sabot*, R. 65
Sachtleben, J. 606
Saez*, R.M. 7, 140, 141, 142, 143, 233, 355
Saffman*, M. 16, 343, 468, 469
Sagara*, A. 404
Saibene*, G. 27, 44, 60, 67, 165, 222, 246, 256, 344, 398
Sakakibara*, S. 301, 394
Sakamoto*, R. 301
Sakurai*, S. 148
Salat, A. 345, 346
Salewski*, K.-D. 780
Sallander, J. 207, 263, 410
Salzmann, H. 77, 127, 217
Samitov*, M.A. 275, 383, 701, 810
Sanchez*, J. 511
Sanchez*, R. 323
Sandmann, W. 127, 182
Santoro*, R.T. 397
Santos*, J. 253, 368, 400
Sapper, J. 173, 347, 349, 408, 409, 761, 786, 849
Sarazin*, Y. 65, 179, 245, 254, 292, 309, 396
Sardei, F. 95, 207, 531, 532, 559, 653, 781, 782, 783
Sartori*, F. 256
Sartori*, R. 67, 165, 221, 246, 344, 398
Sato*, K. 498
Sauter*, O. 257, 292, 398
Savtchkov*, A. 739
Sborchia*, S. 80
Schacht, J. 348, 455, 784, 785
Schade, S. 127, 130, 445, IPP 5/97
Schaff*, O. 14
Schäffler, J. 102
Schall, G. 379
Schamel*, H. 99
Schauer, F. 349, 350, 408, 554, 710
Scheerer*, M. 351
Scheffler, M. 76
Schild*, T. 786
Schilling, H.-B. 127
Schindler, K. 379
Schlatholter*, T. 316
Schleisner*, L. 140, 143
Schleußner*, D. 20
Schlögl, D. 37, 127
Schmid, K. 330, 353, 446, 787
- Schmid*, M. 73
Schmidt*, G. 221, 788
Schmidt*, J. 323
Schmidtman, K. 127, 289, 319, 414
Schmitt*, H. 367
Schneider, H. 408
Schneider*, J. 418, 863, 864
Schneider, M. 260, 437
Schneider, R. 26, 40, 41, 48, 58, 68, 127, 148, 192, 214, 215, 246, 324, 331, 332, 333, 354, 402, 413, 447, 508, 763, 789, 790, 791, 792, 793, 794, 795, 826, IPP 12/1
Schneider*, T. 7, 141, 142, 143, 219, 233, 355
Schneider, W. 20, 127, 154, 155, 156, 223, 261, 356, 417, 607, 656, 657, 740, 796, 858
Schober*, C. 797
Schoenewolf, I. 335, 347
Scholz, H. 673
Schötz, P. 646
Schramm, G. 127, 453
Schreck*, H. 476
Schröder*, C. 35, 36, 200, 357, 358
Schubert, M. 390, 391, 527, 798, 799, 800, 822, 823
Schüller*, P. 185, 238, 239, 671
Schütz, H. 238, 239, 671, 672, 775
Schwarz, E. 32, 33, 34
Schwarz-Selinger, T. 172, 189, 190, 191, 359, 360, 361, 626, 695, 750, 801
Schweer*, B. 209
Schweitzer, J. 44, 54, 127, 270, 283
Schweizer, S. 127, 282
Schwenn, U. 362, 802
Schwob*, J.L. 29, 322, 490
Schwörer*, K. 238, 239, 671
Scott, B.D. 127, 158, 187, 363, 364, 510, 717, 718, 719, IPP 5/92
Scotville*, J.T. 569, 572
Segawa*, H. 148
Seidel, U. 127, 183, 305, 740
Seitsonen*, A.P. 234, 281
Senichenkov*, I.Y. 402
Sergeev*, V.Yu. 365
Sergienko*, G. 209, 827
Serra*, F. 66, 127, 299, 325, 368, 510
Sesnic*, S. 127, 131, 132, 570, 571
Shafranov*, V.D. 275, 383, 701, 810
Sharapov*, S. 25, 162, 178, 256, 344, 616, 682
Sharpe*, J.P. 63
Shimizu*, A. 302, 683
Shimomura*, Y. 60
Shtan, A.F. 404
Sibley*, A. 80, 396
Sidorenko, I.N. 21, 867, IPP III/268
Sielanko*, J. 103, 542
Sigalae*, V. 238, 239, 671
Sihler, C. 127, 279, 366, 367
Silva*, A. 72, 127, 325, 368, 369
Silva*, F. 299
Simintzis*, C. 370, 803
Simonetto*, A. 113
Simon-Weidner, J. 173, 282, 371, 614, 804
Sipilä, S.K. 197, 198
Sips, A.C.C. 66, 127, 154, 177, 341, 377, 378, 716, 776, 805
Skinner*, C.H. 71, 91, IPP 9/128
Skokov*, V.G. 824
Smid*, I. 351
Snead*, L.L. 372, 467, 806
Snell*, G. 373
Solano*, E. 149
Solodovchenko*, S.I. 404

Index

- Solyman*, S. 100
Sombach, B. 349
Sonnenfeld*, A. 862
Sozzi*, C. 113, 254
Speth, E. 102, 103, 127, 210, 264, 303, 337, 405, 542, 543, 544, 545, 655, 807, 808
Spies, G.O. 374
Spinicchia*, N. 113
Spong*, D.A. 323, 410
Stäbler, A. 102, 127, 133, 179, 270, 341, 396, 421
Stadlbauer, J. 349
Stamp*, M. 67, 70, 112, 167, 170, 221, 398, 788
Stan-Sion*, C. 375
Starke, P. 89, 530, 809
Steffen*, H. 862
Steinberger, J. 456
Stephens*, J.A. 82, 135
Stetter*, M. 161
Steuer, K.-H. 127, 268
Stevens*, A. 191
Stober, J. 58, 90, 127, 159, 160, 246, 248, 253, 287, 340, 341, 344, 376, 377, 378, 421, 563, 716, 770, 775, 777, 779, 870
Stockhausen*, G. 862
Storrs*, J. 384
Strachan*, J. 56, 67, 112, 256, 286, 384, 398
Stratton*, B.C. 149, 162
Strauss*, H. 220
Streibl, B. 127, 282, 287, 366, 367, 379, 716
Strickler*, D. 323
Stritzker*, M. 476
Strizak*, J. 467
Stroth*, U. 64, 380, 381, 717
Strumberger, E. 127, 382, 740, 755, IPP III/268
Subbotin*, A.A. 8, 275, 323, 383, 701, 810
Sugihara*, M. 165, 246
Summers*, D. 54
Summers*, H. 270
Sun*, G.Y. 20, 104
Suttin*, F. 56
Suttrop, W. 27, 44, 56, 66, 67, 127, 221, 241, 261, 272, 325, 338, 339, 340, 341, 344, 384, 398, 399, 431, 432, 448, 510, 661, 775, 776, 777, 779
Suzuki*, A. 811
Suzuki*, C. 168, 302, 683
Svendsen*, W. 343
Svensson*, J. 385
Svichenskii*, V.G. 5, 6
Swain*, D.W. 9

Tabasso, A. 127, 212, 386
Taglauer, E. 23, 204, 218, 225, 403, 482, 677, 678, 742, 754, 812, 813, 814, 815, 816, 817, 818, 819
Tai*, E. 239
Takamura*, S. 293
Tala*, T. 292, 396
Tamai*, H. 246
Tanaka*, K. 301, 394
Tanga, A. 127
Tardini, G. 127, 338, 341, 387, 775, 776, 777, 779, 870
Tartarek*, R. 742
Tasso, H. 370, 392, 393, 803, 820
Tatatronis*, J.A. 345, 346
Terborg, R. 14, 184, 195, 388
Testoni*, P. 80
Theobald*, A. 14
Thomsen, H. 115, 389, 390, 391, 527, 821, 822, 823
Throumoulopoulos*, G.N. 370, 392, 393, 803, 820
Thumm*, M. 1, 73, 85

Tichmann, C. 127, 280, 304, 428, 741
Tigwell*, P. 80
Timokhin*, V.M. 365, 465, 824
Toi*, K. 301, 394
Tokuzawa*, T. 301, 394
Toomes*, R.L. 184, 195, 388
Toussaint, U. von 330, 395, 433
Trainham*, R. 405
Tran*, C. 1
Tran*, M.Q. 1, 73
Tran*, T.M. 298
Traveere*, J.-M. 27
Tresset*, G. 119, 245
Treutterer, W. 127, 154, 160, 341, 366, 377, 378, 422, 428, 716, 751, 825
Tribaldos*, V. 27
Troppmann, M. 127
Tsitrone*, E. 63, 70
Tsois*, N. 127
Tuccillo*, A.A. 179, 255, 256, 309, 396, 682
Tulkki*, J.J. 196
Turba, P. 460

Uhlemann*, R. 282
Uhrlandt*, D. 862
Ullrich, W. 48, 68, 69, 127, 319, 324
Ulrich, M. 127
Umansky*, M.V. 826
Unterberg*, B. 30

Valanju*, P. 323
Valenza, D. 209, 397, 827, 828, 829
Valisa*, M. 56
Valovic*, M. 67, 398
Van Eester*, D. 255, 256, 292, 396
Van Sciver*, S.W. 554
Varela*, P. 127, 253, 299, 399, 400
Vartolomei*, V. 862
Vasquez-Borucki*, S. 401
Vergamota*, S. 223, 325, 368, 369, 400
Versaci*, M. 280
Veselova*, I.Y. 402
Viefhaus*, J. 373
Vietzke*, E. 82, 135
Viljoen*, E.C. 403
Villard*, L. 4
Villedieu*, E. 221
Vince*, J. 54
Vinnichenko*, M.V. 404
Voitsenya*, V.S. 404
Vollmer, O. 102, 127, 210, 264, 405, 655
Volpe, F. 406, 407, 830, 831, 832, 833, 834, 835
Volzke, O. 349
Vonbank*, M. 316
Voskoboynikov*, S. 40, 68, 331, 332, 333, 795
Vulliez*, K. 80

Wagner, D. 1, 111, 125, 180, 559, 836, 837, 838, 839, 840, 841, 842, 843, 844, 845, 846, 847, 848
Wagner, F. 76, 207, 653, 654
Wald, I. 349
Walden*, A. 254
Walsh*, M. 511
Walter*, C. 786
Walton*, R. 80
Wampler*, W.R. 91, IPP 9/128
Wandelt*, K. 418, 863, 864
Wang*, H. 467

Index

- Wanner, M. 92, 94, 349, 408, 786, 849
Ward*, D. 7, 141, 142, 143, 233, 355
Wassatsch*, A. 348, 785
Watanabe*, K.W. 394
Watkins*, M.L. 60
Weber, G. 457
Wegener, L. 409, 786, 849
Wegner*, T. 316
Weiland*, J. 384
Weißgerber*, M. 185
Weller, A. 74, 125, 301, 394, 410, 415, 509, 559, 646, 850, 851, 852, 853, 854, 857
Wendland, C. 125, 263, 509, 539
Wendt*, M. 411
Wenmin*, W. 412
Wenzel, U. 62, 111, 127, 293, 319, 413, 414, 559, 654, 855
Werner, A. 13, 74, 111, 207, 337, 410, 415, 646, 653, 654, 856, 857
Werner, F. 409
Wesemann, A. 862
Wesner, F. 53, 127, 593
White*, R.B. 56, 323
Whiteford*, A.D. 119
Whyte*, D.G. 71, 91, IPP 9/128
Wieczorek*, A. 584
Wiencke*, C. 348, 785
Wienhold*, P. 156, 334, 416, 417, 687, 858
Wiese*, R. 862
Wilhelm, R. 405, 458, 655, 859, 860, 861
Wilke*, C. 55, 100, 101, 203, 235, 862
Williams*, A.M. 467
Willmann, I. 228
Wilson*, D. 511
Wilson*, H.R. 165
Wiltner, A. 418, 863, 864
Windsor, C.G. 304
Winter*, H.P. 58, 270, 508
Wittenbecher, K. 459, 460
Wobig, H. 21, 144, 145, 165, 205, 419, 479, 480, 584, 627, 648, 649, 650, 865, 866, 867, IPP III/268, IPP III/269
Wolf, R. 48, 66, 127, 130, 134, 159, 160, 162, 240, 241, 261, 420, 421, 422, 615, 672, 776, 868, 869, 870
Wolfrum, E. 83, 127, 283, 711, 741
Woodruff*, D.P. 14, 184, 195, 388
Wu, C.H. 90, 208, 412
Wunderlich, D. 86, IPP 10/18
Wunderlich, R. 127
Xantopoulos*, N. 127
Xantopoulos*, P. 68
Yakovenko*, Yu.V. 205, 648, 649, 650, IPP III/268, IPP III/269
Yamada*, H. 301, 394
Yamada-Takamura*, Y. 423, 647
Yamamoto*, S. 301, 394
Ybema*, J.R. 142
Yokoyama*, M. 302, 683
Yoon, J.-S. 539
Yoon, S.W. 320
Yoshimura*, Y. 683
You, J.-H. 424, 425, 871
Yu, Q. 127, 272, 422, 426, 431, 432, 569, 572
Zabiégo*, M. 292
Zanstrow*, K.D. 384
Zarnstorff*, M. 323
Zarrabian, M. 127, 289, 427
Zasche, D. 127, 428, 751
Zastrow*, K.-D. 56, 65, 81, 119, 149, 162, 245, 256, 294, 295, 344, 421, 523, 615
Zehetbauer, T. 127, 304, 428, 751
Zehrfeld, H.-P. 127, 183, 220, 382, 402, 740
Zeidner, W. 247
Zeiler, A. 127
Zerbini*, M. 27, 245, 255, 256, 344, 682
Zhogoloev, V. 215
Zilker, M. 658, 872
Zille, R. 302, 429, 683
Zohm, H. 79, 127, 131, 132, 185, 222, 240, 241, 257, 272, 341, 377, 378, 421, 430, 431, 432, 510, 569, 570, 571, 672, 703, 873, 874, 875, 876, 877, 878
Zoletnik*, S. 16, 343, 468, 469
Zoletnik*, Z. 509
Zuhr*, R.A. 330, 433

Index

Teams

ASDEX Upgrade Team: R.Arslanbekov, C.Atanasiu*, W.Becker, G.Becker, K.Behler, K.Behringer, A.Bergmann, R.Bilato, D.Bolshukhin, K.Borrass, B.Braams*, M.Brambilla, F.Braun, A.Buhler, A.Carlson, G.Conway, D.P.Coster, R.Drube, R.Dux, S.Egorov*, T.Eich, K.Engelhardt, H.-U.Fahrbach, U.Fantz*, H.Faugel, M.Foley*, P.Franzen, J.C.Fuchs, J.Gafert, G.Gantenbein*, O.Gehre, A.Geier, J.Gernhardt, O.Gruber, A.Gude, S.Günter, G.Haas, D.Hartmann, B.Heger*, B.Heinemann, A.Herrmann, J.Hobirk, F.Hofmeister, H.Hohenöcker, L.D.Horton, V.Igochine, D.Jacobi, M.Jakobi, F.Jenko, A.Kallenbach, O.Kardaun, M.Kaufmann, A.Keller, A.Kendl, J.-W.Kim, K.Kirov, R.Kochergov, H.Kollotzek, W.Kraus, K.Krieger, B.Kurzan, P.T.Lang, P.Lauber, M.Laux, F.Leuterer, A.Lohs, A.Lorenz, C.Maggi, H.Maier, K.Mank, M.-E.Manso*, M.Maraschek, K.-F.Mast, P.McCarthy*, D.Meisel, H.Meister, F.Meo, R.Merkel, D.Merkel, V.Mertens, F.Monaco, A.Mück, H.W.Müller, M.Münich, H.Murmann, Y.-S.Na, G.Neu, R.Neu, J.Neuhauser, J.-M.Noterdaeme, I.Nunes*, G.Pautasso, A.G.Peeters, G.Pereverzev, S.D.Pinches, E.Poli, M.Proschek*, R.Pugno, E.Quigley*, G.Raup, T.Ribeiro*, R.Riedl, S.Riondato, V.Rohde, J.Roth, F.Ryter, S.Saarelma*, W.Sandmann, S.Schade, H.-B.Schilling, W.Schneider, G.Schramm, S.Schweizer, B.D.Scott, U.Seidel, F.Serra*, S.Sesnic*, C.Sihler, A.Silva*, A.C.C.Sips, E.Speth, A.Stäbler, K.-H.Steuer, J.Stober, B.Streibl, E.Strumberger, W.Suttrop, A.Tabasso, A.Tanga, G.Tardini, C.Tichmann, W.Treutterer, M.Troppmann, P.Varela*, O.Vollmer, D.Wagner, U.Wenzel, F.Wesner, R.Wolf, E.Wolfrum, E.Würsching, Q.Yu, M.Zarrabian, D.Zasche, T.Zehetbauer, H.-P.Zehrfeld, H.Zohm.

ECRH Group (AUG): F.Leuterer, K.Kirov, F.Monaco, F.Ryter, H.Schütz, D.Wagner.

ECRH Group (W7-AS): L.Empacher*, V.Erckmann, G.Gantenbein*, F.Hollmann*, J.Hofner*, W.Kasperek*, H.Laqua, G.Michel, F.Nohe, F.Purps, P.G.Schüller*, K.Schwörer

ICRH Group: W.Becker, V.Bobkov, F.Braun, H.Faugel, D.Hartmann, F.Hofmeister, F.Meo, J.-M.Noterdaeme, S.Puri, J.Wendorf, F.Wesner, E.Würsching.

NI Group: M.Bandyopadhyay, A.Entscheva, P.Franzen, B.Heinemann, C.Hu, M.Kick, W.Kraus, P.McNeely, S.Obermayer, W.Ott, F.-P.Penningsfeld, F.Probst, R.Riedl, N.Rust, W.Schärich, R.Schroeder, A.Stäbler, R.Süß, O.Vollmer.

NI Team (W7-AS): W.Ott, F.Probst, R.Riedl, N.Rust, W.Schärich, E.Speth, R. Süß

Threshold Database Group: T.N.Carlstrom*, J.G.Cordey*, J.C.DeBoo*, S.J.Fielding*, T.Fukuda*, M.Greenwald*, Y.Kamada*, O.Kardaun, S.M.Kaye*, Y.Miura*, M.Mori*, Y.Martin*, T.Matsuda*, E.Righi*, F.Ryter, M.Sato*, J.A.Snipes*, J.Stober, T.Takizuka*, H.Tamai*, K.Thomsen*, K.Tsuchiya*, M.Valovic*.

W7-AS Team: T.Andreeva, S.Bäumel, J.Baldzuhn, C.Beidler, T.Bindemann, R.Brakel, R.Burhenn, A.Dinklage, A.Doddy, H.Ehmler, M.Endler, K.Engelhardt, V.Erckmann, Y.Feng, C.Fuchs, F.Gadelmeier, J.Geiger, L.Giannone, P.Grigull, O.Grulke, H.Hacker, E.Harmeyer, H.-J.Hartfuß, D.Hartmann, F.Hernegger, M.Hirsch, E.Holzhauser*, K.Horvath, Yu.L.Igitkhanov, R.Jaenicke, F.Karger, M.Kick, J.Kisslinger, T.Klinger, S.Klose, J.Knauer, R.König, H.Kroiss, G.Kühner, A.Kus, H.Laqua, J.Lingertat, R.Liu, H.Maaßberg, N.B.Marushchenko, K.McCormick, G.Michel, R.Narayanan, U.Neuner, S.Niedner, M.Otte, M.G.Pacco-Düchs, E.Pasch, E.Polunovsky*, N.Ruhs, J.Saffert, F.Sardei, F.Schneider, M.Schmidt, M.Schubert, J.Svensson, H.Thomsen, Y.Turkin, F.Volpe, F.Wagner, A.Weller, A.Werner, C.Wiechmann, H.Wobig, E.Würsching, D.Zimmermann.

W7-X Team: H.Bau, A.Benndorf, A.Berg, Y.Bozhko, J.Boscary, T.Bräuer, H.-J.Bramow, R.Brockmann, A.Brückner, R.Bünde, M.Czerwinski, H.Dutz, J.-H.Feist, M.Fricke, F.Füllenbach, W.Gardebrecht, G.Gliege, M.Gottschewsky, H.Grote, B.Hein, S.Heinrich, A.Höltling, F.-W.Hoffmann, U.Kamionka, T.Kluck, E.Köster, C.Kopplin, U.Krybus, K.Lang, H.Laqua, H.Lentz, B.Missal, T.Mönnich, I.Müller, M.Nagel, F.Nankemann, H.Niedermeyer, A.Opitz, M.Pietsch, S.Pingel, S.Raatz, J.Reich, H.Renner, R.Rieck, K.Riße, R.Rummel, J.Schacht, F.Schauer, H.Schneider, U.Schultz, M.Schweitzer, K.-U.Seidler, A.Spring, K.Stache, F.Starke, H.Viecke, O.Volzke, A.Vorköper, M.Wanner, L.Wegener, A.Wölk.

Contributors to the EFDA-JET Work Programme: S.Alberti*, S.Allfred*, B.Bagatin*, Y.Baranov*, E.Barbato*, P.Barker*, R.Barnsley*, P.Bayetti*, L.Baylor*, B.Beaumont*, A.Becoulet*, M.Becoulet*, A.C.Bell*, M.Beldishevski*, S.Bernabei*, L.Bertalot*, B.Bertrand*, M.Beurskens*, P.Bibet*, A.Bickley*, M.Biggi*, T.Bolzonella*, A.Bondeson*, W.Bongers*, K.Borrass, D.Borba*, G.Bosia*, G.Bracco*, J.Bradshaw*, F.Braun, S.Bremond*, P.D.Brennan*, M.Bright*, F.Briscoe*, M.Brix*, A.Brusci*, J.Brzozowski*, J.Bucalossi*, R.Budny*, P.Buratti*, R.Buttery*, T.Budd*, A.Buhler, D.Campbell*, D.C.Campling*, P.Card*, P.Carman*, L.Carraro*, C.Castaldo*, R.Cesario*, C.Challis*, A.Chankin*, P.Chappuis*, M.Charlet*, S.Ciattaglia*, S.Cirant*, D.Ciric*, P.Coad*, P.Coates*, V.Cocilovo*, S.Cooper*, I.Coffey*, S.Conroy*, G.Conway*, G.Cordey*, G.Corrigan*, S.Cortes*, D.Coster*, G.Cottrell*, G.Counsel*, M.Cox*, R.Cox*, S.J.Cox*, F.Crisanti*, B.Crowley*, L.Cupido*, R.Cusack*, S.Dalley*, C.Damiani*, D.Darrow*, J.Davis*, N.Davies*, R.De Angelis*, P.De Antonis*, M.De Baar*, O.De Barbieri*, R.Bartimoro*, C.De Benedetti*, J.DeGrassie*, E.De la Luna*, R.F.Denyer*, P.De Vries*, A.Dines*, J.A.Dobbing*, L.Doceu*, J.Doncel*, A.Donne*, S.Dorling*, V.Drozdov*, O.Dumbrajs*, P.Dumortier*, A.Durocher*, F.Durodié*, B.Duval*, R.Dux, T.Edlington*, D.Edwards*, M.Edwards*, P.Edwards*, T.Eich*, A.Ekedah*, D.Elbeze*, C.Elsmore*, B.Ellingboe*, B.Elzendoorn*, K.Erents*, L.Eriksson*, G.Eriksson*, B.Esposito*, G.Esser*, T.Estrada*, M.Evrard*, C.Ewart*, J.Farthing*, D.Fasel*, A.Fasoli*, R.Felton*, J.Fessey*, P.Finburg*, K.-H.Finken*, C.Fleming*, P.Franz*, D.Frigione*, C.Fuchs, C.Fuchs, T.Fukuda*, K.Fullard*, W.Fundamenski*, F.Gabriel*, J.Gafert, I.Garcia-Cortes*, L.Garzotti*, E.Gauthier*, J.Gedney*, S.Gerasimov*, A.Geraud*, G.Gervasini*, P.Ghendrih*, R.Giannella*, R.D.Gill*, C.Gimblett*, E.Giovannozzi*, C.Giroud*, D.Godden*, P.Gohil*, A.Gondhalekar*, A.Goodyear*, G.Gorelenkov*, G.Gorini*, C.Gormezzano*, R.Goulding*, C.Gowers*, G.Granucci*, D.Gregoratto*, S.Griph*, C.Grisolia*, A.Gude, S.Günter, K.Günther*, C.Guérin*, R.Guirlet*, J.Gunn*, G.Haas, L.Hackett*, R.Handley*, J.Harling*, J.Harrison*, D.Hartmann, T.Hatae*, N.Hawkes*, I.Hayward*, J.Hedin*, J.Heikinen*, P.Hellingman*, T.Hellsten*, O.Hemming*, R.Hemsworth*, T.Hender*, M.Henderson*, P.Hennequin*, A.Herrmann, C.Hidalgo*, D.Hillis*, T.Hoang*, F.Hoekzema*, F.Hofmann*, C.Hogan*, C.Hogben*, D.Hogewey*, T.Hope*, L.D.Horton, J.Hosea*, A.J.Hoskins*, S.Hotchin*, M.Hough*, W.Houlberg*, J.How*, D.Howell*, A.Huber*, Z.Hudson*, H.Hume*, F.Hurd*, I.Hutchinson*, T.Hutter*, G.Huysmans*, F.Imbeaux*, L.C.Ingesson*, S.Jachmich*, G.Jackson*, J.Jacquinot*, O.N.Jarvis*, R.Jaspers*, A.Jaun*, E.Joffrin*, M.Johnson*, R.Johnson*, E.Jones*, T.Jones*, T.Jonsson*,

Index

C.Jupen*, A.Kallenbach, J.Kallne*, S.Karttunen*, W.Kasperek*, A.Kaye*, D.Kelliher*, N.Kidd*, V.Kiptily*, P.Knight*, S.Knipe*, R.Koch*, A.Korotkov*, H.R.Koslowski*, O.Kruijt*, T.Kurki Suonio*, K.Lackner, R.LaHaye*, P.Lamalle*, G.Land*, P.T.Lang, M.Laux, C.Laviron*, K.Lawson*, E.Lazzaro*, M.Leigheb*, C.Lescure*, F.Leuterer, J.Likonen*, K.Lingier*, J.B.Lister*, X.Litaudon*, B.Lloyd*, T.Loarer*, A.Loarte*, P.Lomas*, P.Lotte*, A.Loving*, R.Lucock*, A.Maas*, P.Macheta*, G.Maddaluno*, G.Maddison*, P.Maget*, R.Magne*, J.Mailloux*, D.Mank*, E.Manso*, P.Mantica*, M.Mantsinen*, M.Maraschek, M.Marinucci*, P.Marmillod*, L.Marrelli*, J.S.Marsh*, D.Martin*, P.Martin*, K.-F.Mast, G.Mathews*, M.Mayoral*, D.Mazon*, G.Mazzone*, E.Mazzucato*, K.McClements*, K.McCormick, P.McCullen*, D.McDonald*, A.Meigs*, W.Melissen*, L.Meneses*, F.Meo, P.Mertens*, V.Mertens, A.Messiaen*, R.Middelton*, F.Milani*, S.Mills*, F.Mirizzi*, P.Monier-Garbet*, R.Monk, P.Moreau*, D.Moreau*, P.Morgan*, W.Morris*, G.Müller, A.Murari*, F.Nave*, R.Nazikian*, G.Neill*, J.D.Neilson*, R.Neu, G.J.Newbert*, F.Nguyen*, Per Nielson*, H.Nordman*, K.Norman*, J-M.Noterdaeme, S.Nowak*, M.T.Ogawa*, M.O'Mullane*, J.Ongena*, F.Orsitto*, D.Pacella*, L.Panaccione*, V.Paral*, R.Pasqualotto*, P.Pale*, J.Pamela*, B.Patel*, A.T.Peacock*, R.J.H.Pearce*, A-L.Pecquet*, R.D.Penzhorn*, M.Peres Alonso*, G.Pereverzev, A.Perevezentsev*, V.Pericoli*, J.-P.Perin*, S.Peruzzo*, V.Philipps*, M.Pick*, S.D.Pinches, B.Piosczyk*, S.Pitcher*, R.Pitts*, A.Pochelon*, S.Podda*, S.Popovichev*, C.Portafaix*, A.Pospieszczyk*, R.Prins*, R.Prentice*, M.Proschek*, M-E.Puiatti*, K.Purahoo*, E.Rachlew*, M.Rainford*, J.Rapp*, D.Reiser*, T-M.Ribeiro*, V.Riccardo*, E.Righi*, F.G.Rimini*, M.Riva*, D.Robinson*, D.Robson*, M.Rochella*, L.Rodriguez*, A.Rolfe*, M.Rubel*, F.Ryter, F.Sabathier*, R.Sabot*, G.Saibene*, S.Sakurai*, J-F.Salavy*, J.Sanchez*, D.Sands*, Y.Sarazin*, F.Sartori*, F.Sattin*, O.Sauter*, C.Sborchia*, F.Scaffidi-Argentina*, J.Schlosser*, W.Schmidt*, B.Schweer*, J.Schweitzer, J-L.Segui*, G.Sergienko*, F.Serra*, S.Sharapov*, S.R.Shaw*, K.Shimizu*, A.Sibley*, M.Siegrist*, C.-A.Silva*, P.G.Smith*, J.Snipes*, E.Solano*, C.Sozzi*, T.Spelzini*, J.Spence*, E.Speth, A.Stäbler, R.Stagg*, M.Stamp*, D.Starkey*, A.Stephen*, A.Sterk*, J.Stober, D.Stork*, J.Strachan*, K.Stratton*, D.Summers*, E.Surrey*, W.Suttrop, F.Tabares*, J.Tait*, S.Takeji*, T.Tala*, A.Talbot*, D.Tampucci*, N.Tartoni*, G.Telesca*, A.O.Terrington*, D.Testa*, P.Testoni*, P.Thomas*, H.Thomsen, K.Thomsen*, M.Thumm*, P.Tigwell*, J.Todd*, M.Tokar*, M.Q.Tran*, J-M.Travere*, V.Tribaldos*, E.Tsitrone*, A.Tuccillo*, O.Tudisco*, V.Udintsev*, B.Unterberg*, M.P.Valetta*, M.Valisa*, M.Valovic*, T.Van der Grift*, D.Van Eester*, J.Van Gorkorm*, A.Verhoeven*, E.Villedieu*, M.Von Helleman*, K.Vulliez*, A.Waldon*, M.L.Watkins*, M.J.Watson*, M.Way*, J.Weiland*, E.Westerhof*, B.Weyssow*, M.Wheatley*, L.Widdershoven*, P.Wienhold*, C.Wilson*, D.Wilson*, R.Wilson*, B.Willis*, R.Wolf, J.S.Yorkshades*, C.Young*, D.Young*, I.Young*, K.Young*, M.Zabiego*, P.Zanca*, K-D.Zastrow*, M.Zerbini*, W.Zwingman*.

LEHRSTUHL FÜR EXPERIMENTELLE PLASMAPHYSIK DER UNIVERSITÄT AUGSBURG

(Prof. Dr. Kurt Behringer)

PLASMA EDGE DIAGNOSTICS

(K. Behringer, U. Fantz, B. Heger, S. Meir, P. Starke, D. Wunderlich, M. Berger, J. Günther)

In continuation to the work of the previous years, the experimental investigations are focused on spectroscopic diagnostics of atomic and molecular low pressure plasmas. The application of the diagnostic methods to the plasma edge of fusion experiments is in close co-operation with the Experimental Plasma Physics Division E4.

1. Atomic Spectroscopy

The data base of neutral helium was experimentally checked by a comparison of results of the collisional-radiative model ADAS with measured population densities of the excited states in the main quantum numbers $n=2$ to $n=4$ in the singlet and the triplet system (see E4 contribution, which discusses also discrepancies in absolute populations). As diagnostic line for T_e measurements the He line at 728nm (3^1S-2^1P transition) was identified. Furthermore, it has been found that the line ratio 668nm/728nm ($3^1D-2^1P/3^1S-2^1P$) is sensitive on n_e variations as shown in Fig. 1, whereas the other examples are almost independent of n_e for the parameters of the microwave discharge. It has to be pointed out that the line ratio 501nm/728nm (3^1P-

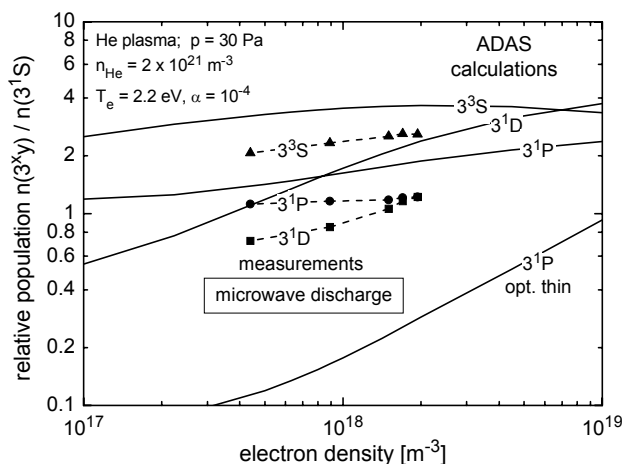


FIG. 1: Electron density dependence of measured population ratios of helium (3^1P , 3^1D , $3^3S/3^1S$) in comparison with ADAS.

$2^1S/3^1S-2^1P$) is very sensitive on the opacity of resonance lines at low T_e and is therefore an indicator whether opacity plays a role in the investigated plasma. These identifications of diagnostic lines for T_e , n_e and opacity in laboratory plasmas are transferable to plasma edge diagnostics by using a thermal helium beam.

2. Molecular Spectroscopy

The acquisition of a spectroscopic system, which enables a recording of the whole visible spectral range (300-750nm) with a spectral resolution of 25 pm, allows measurements of molecular spectra (H_2 , CH , C_2) simultaneously with atomic lines in the same line of sight. Furthermore, the small size and robust construction of the system favour a mobile usage at different plasma discharges. This Echelle system (ESA3000) is maintained in Augsburg, which implies the check at laboratory experiments and the absolute calibration. First measurements were carried out in the divertor of ASDEX Upgrade to demonstrate the possible operating conditions. Figure 2 shows an example spectrum of the wavelength region around the CH band, commonly used for erosion measurements of carbon materials. Typical integration time is 100 ms and, either one survey spectra per discharge can be obtained, or a sequence of spectra with reduced wavelength range. It is intended to

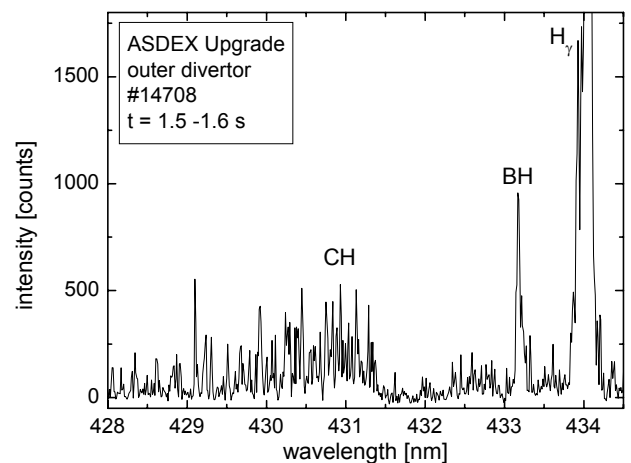


FIG. 2: Example spectra of the mobile spectroscopic system (ESA3000) for use at different plasma experiments.

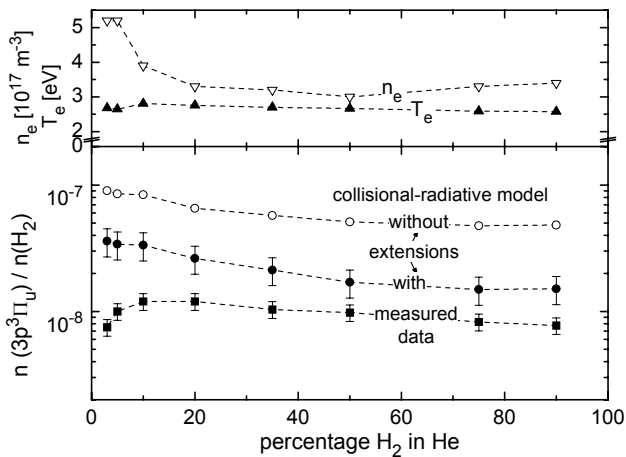


FIG. 3: Comparison of measured population densities of the upper Fulcher state of H_2 with calculations from the CR-model using the plasma parameters n_e and T_e as input parameter.

measure CH and C_2 emission simultaneously during gas puffs of methane and C_2H_2 gases to determine the D/XB ratios for flux measurements. In a similar manner, molecular hydrogen fluxes are determined and the corresponding (S+D)/XB ratio will be measured at different plasma parameters. Furthermore, measurements at W7-AS are planned. For a characterisation of negative ion sources first measurements were carried out at the inductively coupled plasma of the neutral injection group at the IPP.

On the basis of measured molecular radiation and comparisons with predicted radiation from a collisional-radiative (CR) model for molecules (see annual report 2000, university contributions), the interpretation of molecular spectra of hydrogen has made progress. The deviations between calculated and measured population densities of almost a factor of ten were reduced by extending the underlying CR-model (Fig. 3). Here, the important reactions of dissociative attachment from electronically excited states and the quenching of the metastable state in the triplet system of the molecule have been identified to reduce the population density even in the low pressure plasmas. As a next step the remaining discrepancy has to be clarified and the extrapolation of

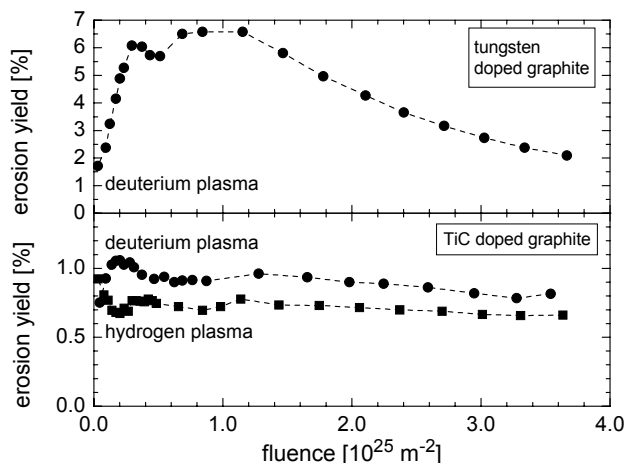


FIG. 4: Erosion yields as a function of the incoming hydrogen flux times exposure time (fluence) of TiC and tungsten doped graphite measured in an ICP discharge.

calculations to plasma parameters of the plasma edge of fusion experiments has to be checked experimentally.

3. Plasma Wall Interaction

As in the last years, chemical erosion of carbon materials have been investigated in a HF-discharge in hydrogen and deuterium, separately. In co-operation with the group of material research at the IPP doped graphite materials were exposed to the plasma. The time resolved intensities of CH (CD) and C_2 emission bands were converted to carbon fluxes by using time integrated weight loss measurements. The erosion yields depending on the fluence (atomic hydrogen flux times exposure time) are shown in Fig. 4. The decrease with increasing fluence point out reduced erosion yields by covering the graphite with the remaining dopand which reduces the effective carbon surface.

The influence of various materials on the atomic hydrogen density above an additional surface in the plasma have been measured. The atomic density decreases with steel, copper and graphite in comparison with the density without a probe in the plasma, whereas a strong enhancement (factor of 2) was measured in case of aluminum.

Publications

U. Fantz, H. Paulin: *Chemical Erosion of Carbon at Low Temperatures and Low Ion Energies*, Physica Scripta T91 (2001) 43-46

U. Fantz, B. Heger and D. Wunderlich: *Using the Radiation of Hydrogen Molecules for Electron Temperature Diagnostics of Divertor Plasmas*, Plasma Phys. Contr. Fusion **43** (2001) 907-918

P. Scheubert, U. Fantz, P. Awakowicz and H. Paulin: *Experimental and Theoretical Characterization of an ICP Source*, J. Appl. Phys. **90** (2001) 587-598

U. Fantz, P. Starke and T. Ondak: *Diagnostics of Electron Distribution Functions in Planar ICP Sources*, Proc. of XXV ICPIG **4** (2001) 201-202

P. Scheubert, P. Awakowicz and U. Fantz: *Characterization of an ICP source: Electron Density Profiles in He, Ar and H_2/He* , Proc. of Frontiers in Low Temp. Plasma Diagnostics IV (2001)

Oral Presentations

U. Fantz: *Atom- und Molekülspektroskopie an Wasserstoffplasma*, Berliner Seminar, Humboldt-Universität zu Berlin, Mai 2001

U. Fantz: *Diagnostics of Hydrogen Plasmas and Plasma Wall Interaction in Low Pressure Discharges*, CIPS Colloquium (Centre for Interdisciplinary Plasma Science), Garching, Juni 2001

U. Fantz: *Diagnostikmethoden für die Elektronenenergieverteilungsfunktion in planaren ICPs*, Workshop zu induktiv gekoppelten Niederdruckplasmen, Bad Tölz, Juli 2001

U. Fantz: *Hydrogen Molecules in the Divertor of ASDEX Upgrade: Measurements and Calculations*, CRP on Data for Molecular Processes in Edge Plasmas, IAEA Vienna, Okt. 2001

**LEHRSTUHL FÜR EXPERIMENTALPHYSIK III
DER UNIVERSITÄT BAYREUTH**

(Prof. Dr. Jürgen Küppers)

Elementary Reactions Of Hydrogen Atoms with Adsorbates and Solid Surfaces

(J. Biener, C. Lutterloh, D. Kolovos-Vellianitis, Th. Zecho, A. Dinger, B. Brandner)

Cooperation between IPP and the University of Bayreuth is concentrated on investigating fusion-relevant plasma-wall interaction processes. Accordingly, the hydrogen atom surface chemistry on possible reactor wall materials is the primary research topic.

A considerable fraction of the species impinging on the first wall of a fusion experimental vessel are neutrals and ions in the energy range below a kinetic energy of about 10 eV. These particles are not capable of causing physical sputtering, but can induce several processes, such as chemical erosion, abstraction etc, which contaminate the plasma. It is therefore desirable to understand the elemental processes and mechanisms of these processes. Recent work of the IPP/UBT collaboration was concentrated on investigating these issues. Since low-energy ions are neutralised in the immediate vicinity of a substrate by resonance neutralisation, it is sufficient to study the low-energy atom-surface interaction. For experimental reasons, the work utilised only thermal atoms with energies in the 0.1 eV range.

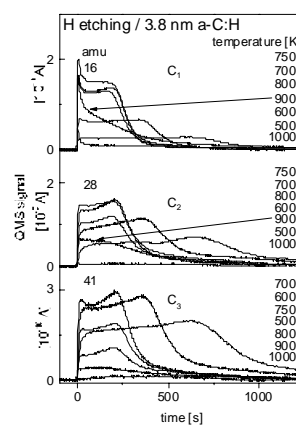
Siliconisation is a widely used technique to cover the first wall with a thin Si:H layer prior to performing plasma discharges. Due to the fact that current plasma vessels cannot reach UHV, a substantial fraction of the Si:H will be oxidised. But by the action of a dense hydrogen boundary plasma the oxidised amorphous Si film may be hydrogenated back and then exhibit a reasonably clean Si surface.

The existence of a near-unity coverage of SiH₃ on Si surfaces was recently reported. It is therefore a concern that a high coverage of SiH₃ on the Si-coated wall may lead to significant Si erosion through the H + SiH₃ → SiH₄ reaction. A high SiH₃ coverage would cause chemical erosion of Si in a H-rich environment to be a factor of about 10 bigger than erosion of Si by H deduced from laboratory experiments.

To investigate this, the saturation coverage of SiH₃ on Si was determined by exposing disilane to Si surfaces. In contrast to the literature, it was found that the maximum coverage of SiH₃ on Si is only about 0.15. Accordingly, SiH₃-covered Si surfaces should not exhibit enhanced chemical erosion as compared with Si. Through an in-situ comparison it was confirmed that upon H admission the silane erosion yield at SiH₃-covered Si surfaces is the same as the yield at Si.

Our new facilities for in-situ mass spectroscopy product measurements while admitting a flux of H atoms in the 10¹³ to 10¹⁶ s⁻¹cm⁻² range at a surface enables us to study product distribution during chemical erosion. This was applied to erosion of thick a-C:H layers deposited on a Pt carrier. The H fluxes employed were sufficient to completely erode few nm thick layers in up to 1000 s. The product kinetics of C₁ (methane) to C₆ (benzene, cyclohexane) and C₇ (xylol) product molecules were recorded as a function of time at constant T (figure 1) or while ramping the temperature up.

FIG.1 Product kinetics in the C₁, C₂, and C₃ channels during eroding of 3.8 nm thick C:H films at various temperatures with a H flux of 10¹⁶ s⁻¹cm⁻². The H flux was started at t=0 s.



The results from these measurements were compared with data obtained through temperature-activated film erosion (without an acting H flux).

As expected, film erosion while admitting H produces substantially more hydrocarbons, especially higher hydrocarbons. However, even with the H flux acting, C₁ and C₂ represent the dominating erosion products, about 85%. Only 2% of the erosion yield is due to C₄ and higher hydrocarbons. The product-specific erosion

maxima are located between 600 K and 900 K, similar to the erosion maxima determined for purely thermal erosion. The occurrence of unsaturated hydrocarbons (C_nH_m with double bonds) as products is in accordance with an erosion mechanism proposed by us a few years ago: H-induced erosion of hydrogenated carbon is connected with the formation of a radical C either on the surface or in the erosion product.

Since it is known that ordered graphite (HOPG) exhibits a very small H erosion yield, we investigated whether high-temperature annealed a-C:H displays also this feature. One would expect that in H-depleted a-C:H the structural transition of the carbon network towards higher cross-linking of the small graphitic clusters leads to a reduction of the erosion yield. However, it was observed that annealing to 800 K did not alter the erosion of a-C:H as compared with not-annealed films. Only the product distribution was affected. One has therefore to conclude that during erosion of amorphous carbon, annealed or non-annealed and H-rich or H-depleted, the acting H flux "prepares" the target in a state which only slightly depends on the initial target condition. Only if by annealing the above-mentioned cross-linking approaches the graphite limit, can one expect substantially reduced erosion. The annealing temperatures needed are very high, in excess of 2000 K, and cross-linking is a slow process.

Reactions of H atoms with adsorbates (O, Si, H) on various metal surfaces were also investigated and confirmed the dominance of hot-atom mediated processes, for which we recently provided a consistent kinetic model.

Publications:

A. Dinger, C. Lutterloh, and J. Küppers
Interaction of hydrogen atoms with Si(111) surfaces:
adsorption, abstraction, and etching.
J. Chem. Phys. 114 (2001) 5338

S. Wehner, Th. Zecho, and J. Küppers
Kinetics of the reaction of adsorbed hexamethyldisilane on
C/Pt(111) surfaces with D atoms: Si-Si bond-breaking.
J. Phys. Chem. B 105 (2001) 1799

Th. Zecho, B. Brandner, J. Biener, and J. Küppers
UHV study of hydrogen atom induced etching of amorphous
hydrogenated silicon thin films.
J. Phys. Chem. B 105 (2001) 3502

D. Kolovos-Vellianitis, Th. Kammler, and J. Küppers
Interaction of gaseous hydrogen atoms with oxygen covered
Cu(100) surfaces.
Surf. Sci. 482-485 (2001) 166

A. Dinger, C. Lutterloh, and J. Küppers
Phenomenology of the ∇ -hydrogen state on Si(110) surfaces.
Surf. Sci. 482-485 (2001) 227

C. Lutterloh, A. Dinger, and J. Küppers
Abstraction of ∇ -deuterium on Si(110) surfaces with H

atoms.
Surf. Sci. 482-485 (2001) 233

Th. Zecho, B. Brandner, J. Biener, and J. Küppers
Hydrogen induced chemical erosion of a-C:H thin films:
Product distribution and temperature dependence.
J. Phys. Chem. B 105 (2001) 6194

Th. Kammler and J. Küppers
The kinetics of the reaction of gaseous hydrogen atoms with
oxygen on Cu(111) surfaces towards water.
J. Phys. Chem. B 105 (2001) 8369

D. Kolovos-Vellianitis, Th. Kammler, Th. Zecho, and J.
Küppers
Abstraction of Si and SiH_x ($x=1,2,3$) adsorbed on Cu(100)
surfaces with gaseous H (D) towards silane.
Surf. Sci. 491 (2001) 17

C. Lutterloh, M. Wicklein, A. Dinger, J. Biener, and J.
Küppers
Thermal stability and hydrogen abstraction of silyl groups on
Si(100) surfaces.
Surf. Sci., in press

Th. Zecho, B. Brandner, J. Biener, and J. Küppers
Hydrogen induced chemical erosion of a-C:H thin films:
structure and reactivity.
J. Phys. Chem. B 106 (2002) 610

J. Biener, E. Lang, C. Lutterloh, and J. Küppers
Reactions of gas-phase H atoms with atomically and
molecularly adsorbed oxygen on Pt(111) surfaces.
J. Chem. Phys. 116 (2002) 3063

J. Biener, C. Lutterloh, M. Wicklein, A. Dinger, and J.
Küppers
Thermal stability and hydrogen atom induced etching of
amorphous hydrogenated silicon thin films.
J. Phys. Chem. submitted

A. Dinger, C. Lutterloh, and J. Küppers
Interaction of hydrogen atoms with Si(110) surfaces:
adsorption, abstraction, and etching.
Surf. Sci. submitted

Doctoral thesis:

Th. Zecho: Thermische Zersetzung und H-induzierte Erosion
dünner a-C:H Schichten.
Dissertation Universität Bayreuth, July 2001

Diploma theses:

M. Wicklein: Untersuchungen an der Si(100)-Oberfläche:
Wechselwirkung mit Disilan und amorphe Si:H Filme,
Diplomarbeit Universität Bayreuth, March 2001

E. Lang: Wechselwirkung thermischer Wasserstoffatome mit
auf Pt(111) adsorbiertem Sauerstoff, Diplomarbeit
Universität Bayreuth, March 2001

ERNST-MORITZ-ARNDT-UNIVERSITÄT GREIFSWALD
LEHRSTUHL FÜR EXPERIMENTELLE PHYSIK II

(Prof. Dr. Rainer Hippler)

PLASMA DEPOSITION OF METAL-CONTAINING AMORPHOUS HYDROCARBON FILMS

(D.Rohde, M. Balden, H. Kersten, W. Jacob; R. Hippler)

The cooperation of the MPI-IPP and the University of Greifswald concentrates on investigating fusion-relevant plasma wall interaction processes.

Plasma enhanced techniques for the deposition of thin solid films have received considerable interest in the past decades. Of special importance are metal-containing amorphous hydrocarbon films (e.g., a-C:H:Mo, a-C:H:Ti), which are under consideration for a number of applications in wear protection, surface coating, fusion research, etc. The technological interest is triggered by a broad range of technologically useful properties which are intermediate between diamond, graphite, and hydrocarbon polymers. Moreover, hydrocarbon films play a significant role in today's thermonuclear fusion experiments either as protective coating of the first wall of fusion reactors or as non-desired by-products in form of re-deposited C:H-layers from previously eroded carbon and abundantly available hydrogen [1-5].

Titanium and molybdenum doped amorphous hydrogenated carbon films were deposited by means of magnetron sputtering. The doping material (Ti, Mo) was magnetron sputtered in a reactive gas atmosphere consisting of a mixture of argon and methane, the latter contributes to the layer growth. The goal of this work is to find useful correlations between the plasma parameters (electron temperature, electron density and energy influx) and the layer properties of the deposited films. Mass spectrometry was employed to control the particle fluxes, the reactive gas, the sputter products and the gas crack patterns. X-ray photoelectron spectroscopy (XPS) measurements were used to investigate the film

properties and the chemical composition of the deposited layers.

Thin films were deposited in an argon atmosphere with different discharge power and reactive gas admixture (CH_4). Figure 1 shows a typical XPS spectrum of a molybdenum-containing a-C:H film. The spectra were fitted with Lorentzian-type curves and from the peak areas the concentration of the fractions of metallic (Mo), oxidised (MoO_2 , MoO_3), and carbonised (Mo_2C) molybdenum were determined. In addition, since the hydrogen fraction of the films cannot be determined in this way, the elemental composition was determined by means of electric recoil detection analysis.

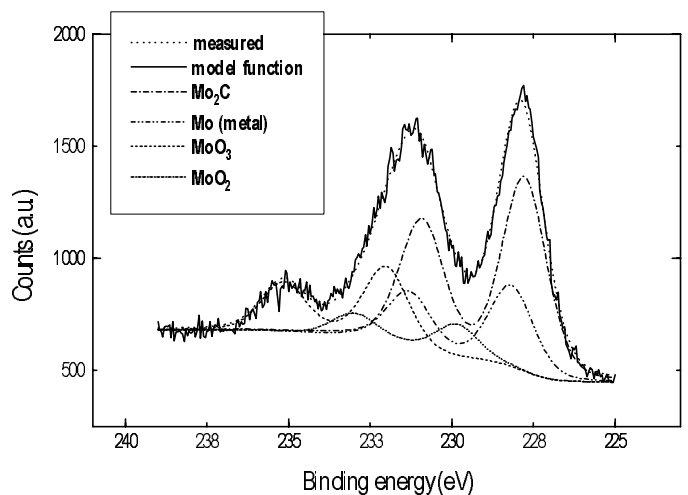


Fig. 1: XPS spectra of a molybdenum containing amorphous hydrocarbon film and its deconvolution into different contributions.

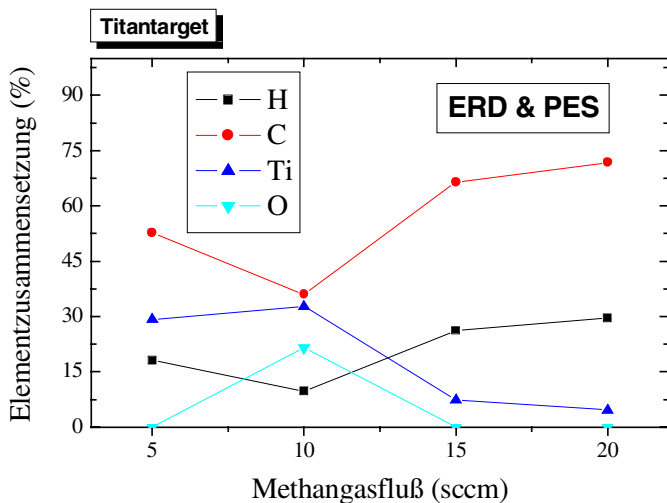


Fig. 2: Composition of a titanium containing amorphous hydrocarbon film versus methane gas flow.

Results of such an ion beam analysis are displayed in Figure 2. The analysis shows that the carbon content increases with increasing methane gas flow (Fig. 2). At the same time the metal (Ti) content decreases. The origin of oxygen in the deposited film is not yet clear since no oxygen was admitted during the deposition process.

First studies of the erosion behaviour of metal-doped amorphous carbon layers due to irradiation with 30 eV deuterium ions were performed on the High Current Source at IPP, Garching. Weight loss measurements and mass spectroscopy confirm the expected decrease of the erosion yield of doped carbon compared with pure carbon materials with increasing deuterium fluence. The fluence necessary to reduce the yield of a 7 at% Ti-doped layer to 50% of the initial value was 10^{22} D/m², i.e. several orders of magnitude lower than for conventionally doped carbon materials. Applying ex-situ analysis (XPS) the titanium enrichment for this 7 at% Ti layer was determined to be 0.44 Ti per C atom. Only a portion of the titanium formed carbide; the largest amount was found to be metallic or oxidised.

These layers are excellent test material for fundamental investigations of the influence of dopants on the processes of chemical erosion, especially for atomic and very low energy (<10 eV) hydrogen.

References

- [1] G. Federici, C.H. Wu, J. Nucl. Mater. 207 (1993) 62.
- [2] J. Winter, Plasma Phys. Contr. Fusion 38 (1996) 1503.
- [3] A. Annen, A. von Keudell, W. Jacob, J. Nucl. Mater. 231 (1996) 151.
- [4] W. Wang, W. Jacob, J. Roth, J. Nucl. Mater. 245 (1997) 66.
- [5] A. Schüler, R. Gampp, P. Oelhafen, Phys. Rev. B 16 (1999) 164-169.

Publications:

D. Rohde, H. Kersten, W. Jacob, R. Hippler: „Plasma deposition of titanium- and molybdenum-containing a-C:H-films“, in preparation

D. Rohde, P. Pecher, H. Kersten, W. Jacob, R. Hippler
The energy influx during plasma deposition of amorphous hydrogenated carbon films
Surface and Coatings Techn. 149, 206 (2002)

INSTITUT FÜR EXPERIMENTELLE UND ANGEWANDTE PHYSIK DER CHRISTIAN-ALBRECHTS-UNIVERSITÄT ZU KIEL

(Head of Project: Prof. Dr. Ulrich Stroth)

Cooperation with IPP on the fields plasma turbulence in toroidally confined plasmas and comparison with numerical turbulence simulations as well as diagnostic development for turbulence measurements.

1. THE PROJECT TJ-K

(N. Krause, C. Lechte, S. Niedner, J. Stöber, R. F. Greiner)

The torsatron TJ-K is operated with a low-temperature plasma at typical electron temperatures of 10 eV and densities of up to $6 \cdot 10^{18} \text{ m}^{-3}$ at a heating frequency of $f = 27.12 \text{ MHz}$. The objectives of the experiment are to carry out studies on turbulent transport and plasma waves. Although the magnetic configuration is that of a fusion experiment, the plasma parameters are considerably reduced. This allows Langmuir and magnetic pick-up probe access in the plasma core. Turbulence measurements are compared with drift-wave simulations and wave field measurements with cylindrical models for helicon waves.

2. HELICON WAVE STUDIES

In the described parameter range the right-handed helicon wave can propagate in the plasma. The wave is coupled to the plasma with a double-half-turn Nagoya-type-III antenna. The antenna is electrically insulated and placed inside the vacuum chamber. Experiments were carried out to measure the dispersion relation and the two dimensional magnetic wave field. The dispersion relation relates the density increase with B to the wavelength. In a toroidal plasma an integer number of wavelength must fit in one toroidal circumference: $2\pi R = N\lambda$. Discontinuities in the density evolution and phase occur due to changes in the toroidal wave number from N to $N+1$. The *blue core*, which is characteristic for high-density helicon sources, is only observed at high neutral gas pressures of about 10^{-2} mbar. In this case, the wave is toroidally damped strongly, the plasma becomes inhomogeneous. Wave field measurements were carried out in the poloidal plasma cross-section. The phase between radial and poloidal wave components is 90° , as expected for right handed polarized waves. The wave fields were compared with a cylindrical model, which gives analytic solutions (bessel functions in radial direction) as a function of the poloidal mode number. The measured wave field could be qualitatively reproduced by a superposition of 30% of $m=0$ and 70% of $m=+1$. These are the first systematic studies of helicon waves in a toroidal geometry.

3. TURBULENCE STUDIES

Turbulence simulations were carried out with the drift-Alfvén code DALF. The dimensionless parameters which govern the fluid equations are similar to those in the fusion plasma scrape-off layer. Poloidal wave number (k) resolved cross-phase spectra between density and potential fluctuations are relevant to disentangle different turbulence driving mechanisms. With parallel dynamics turned off, phases of $\pi/2$ are found for all wavelengths (MHD turbulence). In the pure drift-wave case, with magnetic curvature neglected but parallel dynamics taken into account, the phases are around zero. Transport, which is concentrated in the transition from injection to inertia region of the spectra, increases with resistivity. At realistic TJ-K parameters with both effects included, a drift-wave like result is found. Since experimental k spectra are not available yet, comparison with experimental cross-phase spectrum are done in frequency space. In a range from 10 to 500 kHz the cross phases are close to zero. This is consistent with the simulations. The measured spectra are typical for plasma turbulence. The slopes in the inertial region are somewhat lower than in the simulation. Measured and simulated PDFs for density and potential are Gaussian, while the transport PDF is peaked. Hence, the statistical features agree reasonably well with simulations of drift wave turbulence. More advanced studies like the comparison of wavelength spectra or the effect of Reynolds stress on transport are planned for the near future. The spatial structure was investigated by correlation measurements between a movable array and a fixed probe. Large events of 5 cm size and 80 μs duration were found, which is smaller than in the simulations. The motion is in the electron diamagnetic drift direction and coincides with the flux surfaces. The density-density and density-potential correlations are between 70% and 90%, respectively. This is less than that observed over longer distances in W7-AS. It has to be investigated, whether this is due to the strong local shear in TJ-K.

TECHNISCHE UNIVERSITÄT MÜNCHEN
LEHRSTUHL FÜR MESSSYSTEM- UND SENSORTECHNIK

(Prof. Dr.-Ing. Alexander W. Koch)

The cooperation IPP – Technische Universität München is concentrated on the development of speckle- measurement techniques to detect arc traces, deformation, erosion, surface roughness, surface structure and surface contour in the divertor region of experimental fusion devices. The optical method is superior to any mechanical method with respect to data acquisition time and non-perturbing measurement.

SPECKLE-INTERFEROMETRY IN VIBRATING ENVIRONMENTS

(A. Meixner, P.Evanschitzky, A.W. Koch)

The Speckle-Interferometry is a well known technique for measuring contours and deformations of technical surfaces at a high precision. One major disadvantage of interferometric measurements in general is the enormous susceptibility of the whole setup to vibrations during and between several exposures. For this reason, an interferometer was developed which is capable of recording all necessary data simultaneously during one laser shot. Thus a contour measurement of moving or vibrating objects becomes possible.

In most interferometers the measurement object has to be included in the setup itself. Such a kind of setup is not capable to investigate different areas of large and fixed objects like the divertor region of a fusion device. Therefore the aim of the development is a dynamic sensor-head which is separated from all bulky parts like powerful laser-sources and PCs.

The contour measurement in general requires two single interferograms of different wavelengths. The sensitivity of this kind of measurement depends on the so called synthetic wavelength λ_{synth} which can be calculated out of the two single wavelengths λ_1 and λ_2 and the angle Θ between surface and direction of observation as can be seen in equation (1):

$$\lambda_{synth} = \frac{\lambda_1 \cdot \lambda_2}{2 \cdot |(\lambda_1 - \lambda_2)| \cdot \cos \Theta} \quad (1)$$

In order to avoid disturbances caused by vibrations of the environment it essential to get these two wavelength data simultaneously. For these purposes the interferometer is supplied with several wavelengths at the same time. The two superposed interferograms are separated by interference filters situated in front of two cameras recording exactly the same image. (See Fig. 1). A superposition of different wavelengths of a coherent multiline Ar - ion laser is passed to the setup by an optical fiber as can be seen at the bottom left of Fig. 1. This multiline beam is divided in a reference beam and an object beam by beam-splitter 1. These two beams are expanded separately in order to be able to vary the illuminated area on the measurement object without influencing the reference beam. The object beam is passed to the measurement object by two mirrors. The surface of the object is imaged by a system of two lenses which operate as a zoom objective and allow to vary both

measurement distance and area. The scattered light from the surface is superposed by the reference beam by beam splitter 2. With beam splitter 3, the emerging interferogram is directed to two separate cameras. An optical bandpass-filter in front of each camera selects one single wavelength in each case.

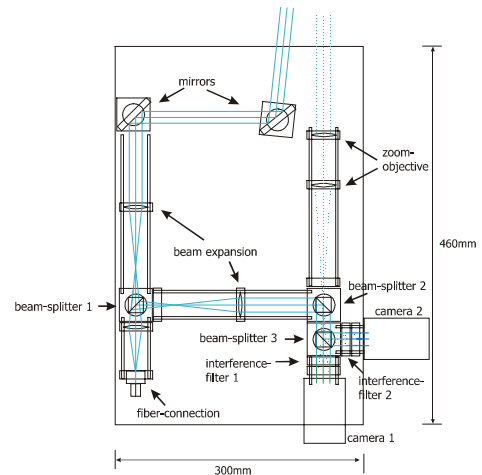


FIG. 1: Sensor-Head

The complete interferometer is integrated in a dynamic sensorhead separated both from the laser-source and from the PC. Fig. 2 shows an example of a measurement result with this sensor head.

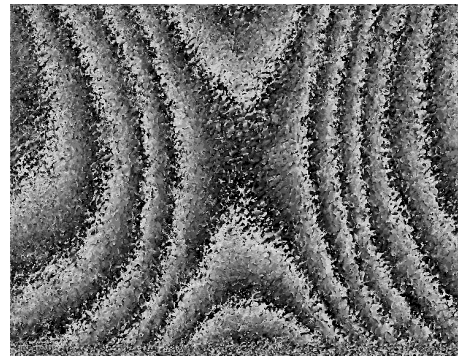


FIG. 2: result of a measurement of a saddle like contour on an aluminium plate; synthetic wavelength 24 μm ; measurement area: 12 mm x 8 mm

INSTITUT FÜR PLASMAFORSCHUNG (IPF) DER UNIVERSITÄT STUTTGART

(Prof. Dr. U. Schumacher)

For almost three decades, Max-Planck-Institut für Plasmaphysik (IPP) at Garching and Institut für Plasmaforschung (IPF) at University of Stuttgart are collaborating closely on developments, measurements, and interpretations of heating and diagnostic systems. The main topics of the co-operation are application of microwave heating, current drive, and diagnostics - mainly for W7-X, ASDEX Upgrade and W7-AS - and contributions to emission and absorption spectroscopy for bulk and divertor plasma diagnostics.

1. PLASMA HEATING

(W. Kasparek, P. Brand¹⁾, G. Gantenbein, H. Hailer, E. Holzhauser, S. Klänge, H. Kumric, J. P. Meskat²⁾, G. A. Müller, B. Plaum, P. G. Schüller³⁾, K. Schwörer, R. Wacker)

¹⁾ since May 1, 2001

²⁾ until January 31, 2001

³⁾ until November 30, 2001

In collaboration with IPP Garching, FZK Karlsruhe, and IAP Nizhny Novgorod.

The investigation of the application of electron cyclotron resonance heating (ECRH) to fusion plasmas was continued. On the technical side, work on the ECRH system of W7-X formed the major part. Nevertheless, the supporting aid for W7-AS and ASDEX Upgrade was kept on. In addition, studies of the MHD stability of high- β discharges in ASDEX Upgrade and the use of ECRH / ECCD to control instabilities continued to be a major issue. Moreover, general developments in the field of millimetre wave technology as well as the study of microwaves as a plasma diagnostic tool are reported here.

1.1 Electron cyclotron resonance heating (ECRH)

1.1.1 ECRH on W7-AS

Technical support of the ECRH system on W7-AS was continued. The generator as well as the transmission system could be maintained at a high level of reliability. Plasma experiments with ECRH were performed using four gyrotrons at 140 GHz and one at 70 GHz, each of them delivering 0.5 MW.

1.1.2 ECRH system for ASDEX Upgrade

The existing ECRH system on ASDEX Upgrade (four gyrotrons, 0.5 MW each) will be extended by four gyrotrons delivering 1 MW output power each. The new system will be used to optimise the confinement and stability of plasma operation by flexible deposition of the RF power. A special feature of the system is that the gyrotrons will be operated at different fre-

quencies. First it is planned to install a pair of tubes operating at 104 GHz and 140 GHz. In a second step an additional pair of gyrotrons will be installed operating at various frequencies in the range 114 – 140 GHz (step-tuneable gyrotrons).

In co-operation with the ECRH group at ASDEX Upgrade, IPF designed a system for broadband RF power transmission from the gyrotrons to the tokamak. Components for corrugated waveguides were designed at IPF and ordered from industry. Special parts of the waveguide system were developed and manufactured at IPF. A beam waveguide system with individual mirrors (matching optics) will be used to couple the free-space gyrotron output radiation to the HE₁₁ waveguide.

Since the foreseen pulse lengths will be up to 10 s, cooling of the components is an essential issue. Thermo-mechanical calculations were performed and resulted in a simple and compact design which does not require an extensive cooling system.

The development of polarisers which allow broadband transmission at high power levels was started. First measurements using a preliminary design show sufficient bandwidth.

1.1.3 ECRH system for W7-X

Work on the 140 GHz, 10 MW CW ECRH system for the stellarator W7-X continued. IPF has taken responsibility for the quasi-optical transmission lines as well as for the development of the acceleration voltage modulator, the thyatron crowbars and cathode heater supplies for the depressed collector gyrotrons which are under development at FZK Karlsruhe.

1.1.3.1 Multi-beam transmission system

In 2001, the prototype transmission system was further improved, and some water-cooled mirrors finally envisaged for the transmission system in Greifswald were implemented. With these components, various tests on integration into the system, thermo-mechanical properties as well as steering of the mirrors by PLC could be performed. Furthermore, two water-cooled mirrors were tested in the gyrotron test stand at FZK under high-power conditions (until now up to 740 kW, with pulse lengths up to 100 s) without exhibiting any problems. These mirrors are equipped with a grating coupler, a waveguide coupler integrated into the surface of a mirror, as well as sensors

for calorimetric measurement of millimetre wave absorption. They were used to optimise the beam and power diagnostics of the CW ECRH system on W7-X.

Investigations of the deformation of mirrors and polarisers were continued. It turned out, that deformation under application of a heat load equivalent to the absorbed power from a 1 MW millimetre wave beam was in the tolerable range for all components. (The maximal change of the surface curvature was 0.001 m^{-1} .)

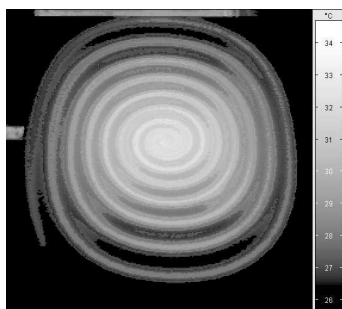
The main work concentrated on the detailed design, specifications, and supervision of the industrial mass fabrication of mirrors and other components for the ECRH system at IPP Greifswald. (For reference, confer the CAD drawing in Fig. 1.2 of IPF Annual Report 2000). The mirrors and holders of type M3 were designed and completed with the exception of the surface. The mounting frames for 10 matching optics of type M1 and M2 together with 22 polarisers and 10 switching mirrors were built by industry and FZK. These components as well as the beam conditioning optics are now ready to be installed. The design of the beam combining and distribution optics type M4/M12 was completed, four units are on order now.

Two prototypes for the water-cooled mirrors of the multi-beam waveguide (MBWG) were built, and, after some problems with the bonding between stainless-steel body and copper surfaces as well as with the surface quality, finally passed the acceptance test. An example for the test of one of the cooling channels by thermography is shown in Fig. 1.1. At the end of the year, the order for series production of 12 MBWG mirrors (M5 – M11) could be placed with industry.

Absolute power measurements and absorption of MW CW gyrotron power will be necessary in the ECRH-system of W7-X during conditioning and test operation of the gyrotrons by matched loads. At the test stand of the TTE 1 MW test-gyrotron ("Maquette tube") at FZK, the maximum output power was limited to 0.64 MW due to arcing in the load (Calabazas Creek Research, Inc., USA). Therefore, as an immediate measure IPF designed and built a copper cone reflector with optimised surface structure which replaced the plane rotatable reflector in the load. As a result it was possible to extend the maximum power level to 1.05 MW with a pulse length of 5 s. Generally it turned out that further work has to be done to improve this load for application to the gyrotrons of the next development step.

The IPF development of a short-pulse calorimeter (1 MW, 0.5 s) which will be installed on W7-X near the output window of each gyrotron was continued. Due to the lack of a supplier for an appropriate cylinder of silicon nitride in this load the design was revised for use of a quartz cylinder. This change possibly will lead to a small reduction in the prospected pulse length.

FIG. 1.1: Thermal image of the mirror surface illustrating the (warm) cooling water channel situated below the surface.



1.1.3.2 Voltage regulator for gyrotron power control and tube protection

The output power of a gyrotron depends on the electron beam energy. In a gyrotron with a voltage depressed collector the output power depends sensitively on the beam accelerating voltage between cathode and resonator body, whereas the decelerating voltage between body and collector has its main influence on the power efficiency of the tube.

The experience obtained with the first prototype of a 140 GHz, 1 MW CW gyrotron from THALES shows that the tube can operate with a poorly stabilised voltage of about 50 kV between cathode and collector whereas the voltage between cathode and body must be highly stable for constant output power. Due to the quality of the electron beam only a very small fraction of the electrons is collected by the body section. Therefore, a medium power HV-amplifier whose output is connected between body and collector is sufficient for stabilisation and control of the accelerating voltage.

In contrast to the HV high power source for the gyrotrons on W7-AS consisting of a classical transformer with rectifier and an additional tetrode for HV switch on-off and voltage regulation, the HV high power (65 kV, 50 A) source for the gyrotrons on W7-X consists of individual 1 kV DC sources connected in series via semiconductor switches. The number of connected sources determines the output voltage of the HV-supply. The speed of voltage control is governed by the switching cycle at a frequency of 100 kHz. This type of HV-source (pulse-step modulator, PSM) was realised by THALES, France. First tests for system approval are under way.

Due to the necessity of an output filter for suppression of the switching frequency consisting of reactive elements where electrical energy is stored, an adapted protective system has to be designed which limits the amount of energy released in a short circuit by arcing in the gyrotron load. A crowbar circuit with a thyatron and snubbers was simulated by PSpice. The circuit elements depend on the final design of the PSM and are presently adapted to the changed specifications.

Owing to the residual noise from the PSM high voltage source, the design of the HV-amplifier for accelerating voltage regulation has to be revised for a higher regulation speed and slew rate of the amplifier output voltage. Different circuit designs are compared by PSpice simulation of the amplifier which will be realised in semiconductor and tube technology.

1.1.4 ITER contributions

In 2001, work on an ITER-relevant concept of remotely steerable antennas based on the imaging properties of a four-wall corrugated square wave guide was continued. Measurements were performed to confirm calculations showing that the low-loss integration of mitre bends into the antenna (e.g. for neutron screening) is possible provided that the position of such "dog-legs" is optimised. For this case, the usable steering range of the antenna is at least $\varphi = \varphi_0 \pm 10^\circ$ similar to the straight antenna.

An essential issue of this antenna is the transmission loss. For the straight remote-steering antenna, the efficiency (including scanning mirror, coupling loss to the waveguide as well as mode conversion and ohmic loss in the guide) can be ap-

proximated by $\eta = 0.98 - 0.005 \cdot \varphi [^\circ] \pm 0.05$ in the relevant steering range. At present, a separate measurement of the ohmic loss and the characterisation of a full antenna mock-up including steering mirror, vacuum window, and mitre bends is in progress.

1.2 MHD stability studies

The gradients of the toroidal current density and the plasma pressure in a tokamak can drive MHD modes. These modes may limit the energy content of magnetically confined fusion plasmas and may lead in some cases to a complete loss of confinement. Basically it is possible to avoid these modes by operating the machine at sufficiently small values of the plasma pressure which of course is in contradiction to the requirement of maximum fusion power. Therefore, possibilities have to be explored to control or prevent such instabilities. In the case of the so-called neoclassical tearing modes (NTM) these instabilities are associated with the development of magnetic islands with a relatively small width. Thus, a well localised power deposition is required to influence the current distribution within the islands. Electron cyclotron current drive (ECCD) or electron cyclotron resonance heating (ECRH) are excellent candidates to stabilise NTMs since they enable flexible and narrow deposition of the RF power in the plasma. On the tokamak ASDEX Upgrade we use both ECRH and ECCD to study MHD stability of fusion plasmas.

1.2.1 Active control of neoclassical tearing modes using ECRH / ECCD on ASDEX Upgrade

Recent experiments on the stabilisation of NTMs in ASDEX Upgrade showed that ECCD can suppress the $m = 3, n = 2$ tearing mode. To extend the accessible parameter space on ASDEX Upgrade it is planned to use additional neutral beam heating to increase the value of β and to stabilise simultaneously the $3 / 2$ tearing mode using ECCD.

In some discharges the occurrence of the $2 / 1$ NTM was a serious problem and led in many cases to a dramatic deterioration of the confinement. First considerations have been undertaken to use ECRH/ECCD for this experimental scenario.

The first experiments to control NTMs on ASDEX Upgrade were performed using phased injection of the RF power into the O-point of the island. Although these experiments were successful it could be shown that in the plasma parameter range of ASDEX Upgrade the more simple DC-scheme is also possible. However, for larger machines like JET or ITER, the DC operation may not stabilise NTMs. Therefore, preparations were made to resume AC operation.

1.3 General developments in millimetre wave technology

1.3.1 Investigations of materials for in-vessel components and absorbers

To get exact data on heat loads under millimetre wave irradiation, the absorption of plane ground samples made from

materials relevant for ECRH systems was studied. These materials include copper and aluminum used for reflecting surfaces in mirrors and mitre bends etc. as well as stainless steel, molybdenum alloy (TZM), tungsten and graphite, which are used in vacuum for antennas and vessel walls. The measurement technique is based on the comparison of the quality factor of a two-mirror reference resonator with the quality factor of a three-mirror resonator having identical dimensions and including the mirror to be tested.

In **Table 1.1**, the measuring results are summarised. A typical finding is that the ohmic loss of metal samples with grinding quality is about 15% higher than predicted by theory due to surface roughness. For graphite tiles with tungsten coating the measurements support the assumption, that very thin coatings (thickness $0.9 \mu\text{m}$) suffer from porosity leading to an increase of the losses by more than 50%.

Material (plane ground sample)	Measured loss at perp. incidence [%]	Theoretical loss at perp. incidence [%]
Copper	0.115 ± 0.005	0.103
Copper, quartz-coated	0.134 ± 0.003	
Aluminium alloy AlMgCuPb	0.20 ± 0.003	0.163
Molybdenum alloy TZM	0.246 ± 0.003	0.208
Stainless steel (1.4301)	0.702 ± 0.003	0.674
Graphite + tungsten coat., $10 \mu\text{m}$	0.229 ± 0.004	0.185 (pure W)
Graphite + tungsten coat., $3.8 \mu\text{m}$	0.245 ± 0.008	0.185 (pure W)
Graphite + tungsten coat., $0.9 \mu\text{m}$	0.298 ± 0.005	0.185 (pure W)
Graphite EK98	4.8 ± 0.1	3

TABLE 1.1: Measured and theoretical loss for perpendicular incidence of various plane samples of microwave reflecting materials. The errors represent the standard deviation of the mean value of seven measurements.

To study the reflection loss at 140 GHz of in-vessel materials (like TZM-alloy and stainless steel, with copper as a reference) at high temperatures, measurements with a two-mirror resonator set-up in an oven were performed in the temperature range $30 - 600 \text{ }^\circ\text{C}$. The apparatus is described in the 1999 and 2000 Annual Reports. Results for reflective properties are as follows: The absorption increases with temperature according to the increase of the ohmic resistivity of the samples under test. No anomalies were found. A small discrepancy (15%) to theory can again be explained by surface roughness.

1.3.2 Design of components for oversized waveguide systems

The existing computer codes for numerical optimisation and design of overmoded waveguide systems (based on scattering matrix method, coupled wave equations and simulated annealing) were further improved. The development focuses on calculations of far field patterns radiated from waveguide antennas based on the mode mixtures generated in the corrugated or smooth waveguide structures. The programs use analytic formulas and are suitable for both cylindrical and rectangular waveguides. In addition, the implementation of optimisation algorithms for waveguide structures with varying diameter (tapers, mode converters, horn antennas) is in progress.

For the next step of ECRH on ASDEX Upgrade when 140 GHz microwave power will be injected into the plasma calculations of mode mixtures for optimum coupling and narrow power deposition have been discussed. Broadband converters for $HE_{11} + HE_{12}$ mode mixtures with quasi-rectangular power distribution on the aperture are under design.

1.3.3 Microwave beam propagation and diagnostics

Computer programs for analysing measured patterns of microwave beams and for calculating beam propagation were developed further and applied to actual problems like beam analysis at the test mirror waveguide for W7-X and beam calculations for ASDEX Upgrade.

1.3.4 Alignment of beam waveguides for non-stationary targets

In collaboration with the National Institute for Fusion Science, Japan, the problem of alignment control of beam waveguides was investigated. Especially the movement of large fusion experiments (W7-X, LHD) during cool-down and magnetisation requires remote alignment of at least two mirrors in front of the vacuum barrier windows. Four methods to generate appropriate signals for re-alignment were studied, and the most promising versions (which use the high-power millimetre wave beam itself, in contrast to others requiring a separate alignment beam) were tested: A grating coupler, which produces an image of the main beam is not very sensitive to spurious modes contained in the main beam; however, the alignment has to be performed by scanning a single maximum. A mirror equipped with four waveguide couplers delivers separate signals for spatial and angular alignment, and, as it applies nulling of an interference minimum, it is adapted best to automated re-alignment systems. Low- and high-power tests confirm the simulations, showing that a precision for the mirror orientation of about ± 0.1 degrees can be achieved. If in addition the differential power signal of a coupler pair is used, such an integrated direction-finding antenna could be used for automatic spatial and angular re-alignment.

1.4 Millimetre wave diagnostics

1.4.1 Doppler reflectometer for density fluctuation and plasma rotation studies

Doppler reflectometry is a new diagnostic method for the investigation of propagating density perturbations. It probes the plasma by a microwave signal with a line of sight which is non-perpendicular with respect to the reflecting layer. The diagnostic selects density perturbations with finite wave number k_{\perp} in the reflecting layer defined by the tilt angle. Criteria were developed to optimise the antenna spot size with respect to plasma curvature effects in order to obtain maximum k-resolution. From the Doppler shift of the returning microwave the propagation velocity of the selected density perturbations v_{\perp} can be directly obtained. Numerical studies were continued in 2001 using numerically calculated drift wave turbulence (B. Scott).

1.4.2 Microwave reflectometry on W7-AS

The 2000-2002 experimental campaign of W7-AS comprises the first island divertor operation as well as externally triggered radial electric fields. For this campaign fast changes in the radial profile of turbulence level and propagation velocity must be diagnosed. Until end of 2001, a multi-channel Doppler reflectometer with four channels was installed (plus two channels under construction), which simultaneously probes densities between 0.4 and $5.8 \times 10^{19} \text{ m}^{-3}$. The reflectometers use a common antenna with gaussian antenna characteristics and a fixed tilt angle of $+14$ deg with respect to the normal onto the reflecting layer. A second symmetric antenna with -14 deg allows differential measurements if the orientation of the cutoff layer changes with the magnetic configuration. Values of up to 10 MHz were observed for the Doppler frequency shift which correspond to a poloidal velocity of up to 70 km/s. Analogue spectrum analysis with high temporal and dynamic resolution is used. In cases where a comparison of the poloidal propagation velocity of the turbulence with the results from radial electric field measurements (CRX spectroscopy) were available agreement was found within the error bars of the diagnostics.

1.4.3 Microwave reflectometry on ASDEX Upgrade

The optimised O- and X-Mode antennas together with the improved receiver module of the Doppler reflectometer now allow measurements of rotation velocities v_{\perp} perpendicular to the magnetic field. An example for a rotation velocity profile is given in **Fig. 1.2**.

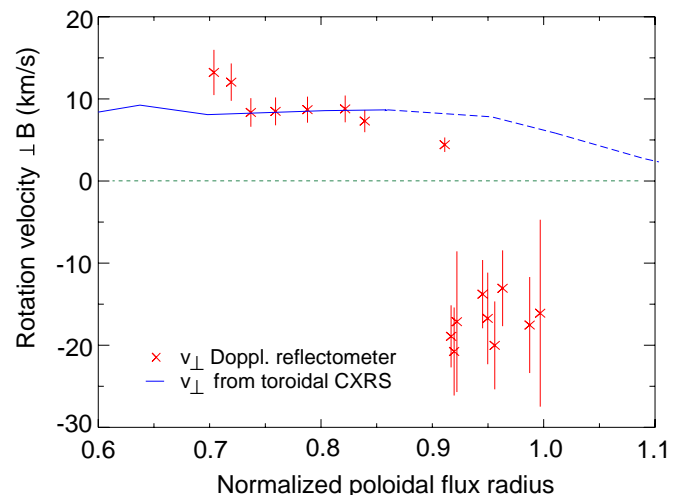


FIG. 1.2: ASDEX Upgrade shot #14147. Comparison of measured rotation velocity profiles perpendicular to \vec{B} .

In this particular shot only toroidal rotation velocities from the CXRS diagnostic were available. For $\rho_{\text{pol}} < 0.85$, where the poloidal component of v_{\perp} can be neglected, there is good agreement between the two diagnostics.

Although in the H-mode barrier the density fluctuations are strongly reduced, the scattered microwave power is sufficient to allow rotation velocity measurements. Since the new antennas have small divergence, measurements are no longer restricted

to the plasma edge. The accessible radial region where rotation velocities can be determined now extends to a normalised flux radius of $\rho_{\text{pol}} \approx 0.6$.

The k -selectivity of the antenna system with respect to fluctuations is calculated by numerical modelling of the Doppler reflectometer experiment using a 2D full wave code (B. Kurzan). In principle, the comparison of this k -selectivity with the measured k -spectrum yields the k -spectrum of density fluctuations, e.g. **Fig 1.3**. The spectrum shows a steep decay with about k^{-6} for $k \geq 2 \text{ cm}^{-1}$, in reasonable agreement with expectations from theory.

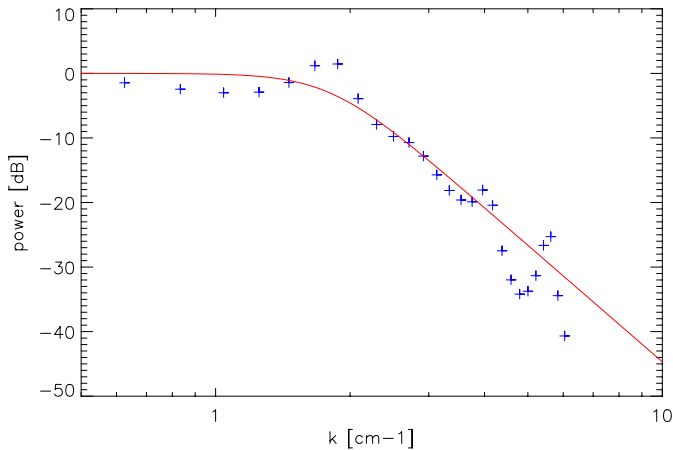


FIG. 1.3: The k -spectrum of fluctuations, calculated for ASDEX Upgrade H-mode shot #14147 with $\rho_{\text{pol}} \approx 0.85$.

1.4.4 Collective Thomson Scattering (CTS) using microwaves

This project is continued together with the IAP Nizhny Novgorod within the framework of "Kinetic stability analysis of distribution functions". As radiation sources the ECRH gyrotrons are used. The CTS diagnostic serves to measure the velocity distribution function of ions and the propagation of plasma waves in the frequency range of ion-cyclotron harmonics, and the LH-frequency (up to 1.3 GHz).

During a brief campaign the LH-instability was studied in detail. In some cases side bands from cyclotron harmonics were found. In addition, broadband magnetic antennas are used to measure magnetic fluctuations up to 1 GHz. The results will be compared with predictions from kinetic theory in the framework of a PhD thesis carried out jointly at IAP and IPP.

1.5 WEGA

The revision and improvement of the Gourdon code were continued. With respect to the imminent magnetic field measurements on WEGA special adjustments were applied to this code. Especially, a subroutine allowing better approximation of the real geometry of the helical windings of WEGA has been integrated. Examples for data sets were set up and hints about the application of the code were provided.

Meanwhile the computational power of personal computers is sufficient to run programs like the Gourdon code. This code was made portable by replacing system-dependent functions and by emulating the graphics routines called from the RZG GGLIB1 library by equivalent routines in Fortran source code. Gourdon code versions were run on PCs in Fortran 90 under Windows NT and in GNU FORTRAN 77 under Linux.

2. PLASMA EDGE DIAGNOSTICS

(U. Schumacher, I. Altmann, G. Dodel, K. Hirsch, J. Krüger¹⁾, P. Lindner¹⁾, B. Roth, K. Schmidtman²⁾, J. Schneider, R. Stirn¹⁾, and A. Tawfik)

¹⁾ since April 1, 2001

²⁾ until January 31, 2001

2.1 Developments for spectroscopic measurements of plasma parameters in the divertor of ASDEX Upgrade

The determination of spatially resolved temperature and density profiles of hydrogen isotopes, wall materials and impurities are the goal of this project.

Laser induced fluorescence (LIF) is an established method in plasma physics to determine atomic and molecular species by spatially and spectrally resolved measurements, which also allow to measure the velocity distribution of the species.

Preparatory work for such experiments in a small scale device was started to qualify the laser system, the frequency conversion and the wavelength tuning as well as the detection system. In a first laboratory experiment the applicability of LIF using fibre optics was analysed.

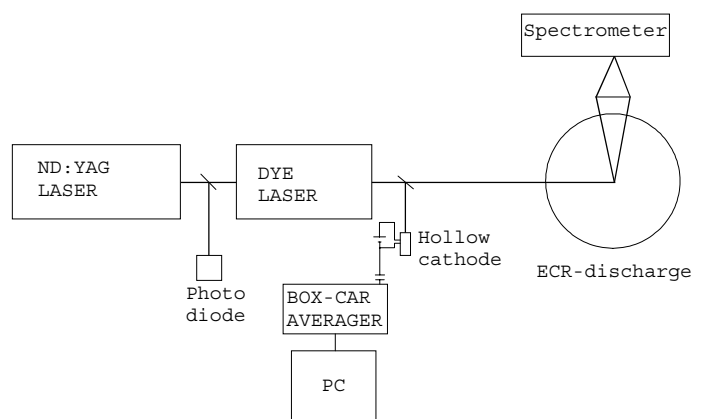


FIG. 2.1: Experimental set up of the LIF diagnostics.

Figure 2.1 shows the experimental set up of the laboratory version of the LIF diagnostics. A frequency doubled Nd:YAG-Laser ($\lambda = 532 \text{ nm}$, $\tau_{\text{pulse}} = 7 \text{ ns}$) is used as a pump laser for the dye laser. The spectral ranges of the system depend on the applied dye. The first measurement was done with the DCM dye with a specified spectral range between 600-660 nm.

The opto-galvanic effect on a Neon filled hollow cathode lamp is used to calibrate the dye laser wavelength by tuning with the grating. This effect is due to absorption of light which increases neon ionisation resulting in an increased lamp current. The change of the current signal is detected via capacitive coupling. As an example a measured signal is shown in **Fig. 2.2**. The negative signal occurs when the ionisation probability of the excited state is lower than that of the ground state.

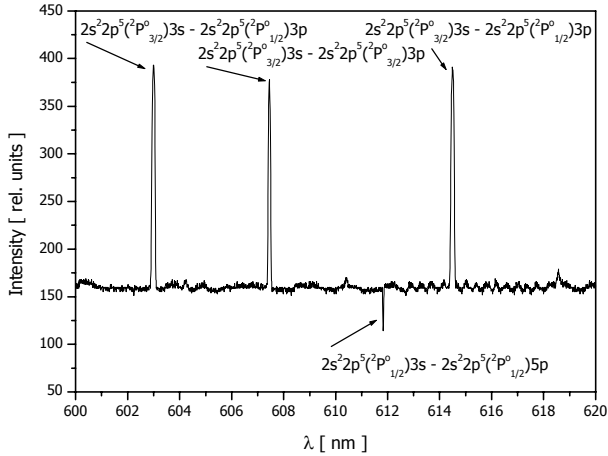


FIG. 2.2: Opto-galvanic signal from a Neon filled hollow cathode lamp.

To complete the experimental set up with the laser system and the detection system an ECR discharge is used. **Figure 2.3** shows an LIF-Signal of neon at 618 nm in an ECR discharge at $p = 7$ mbar and $P_{\text{ECR}} = 200$ W.

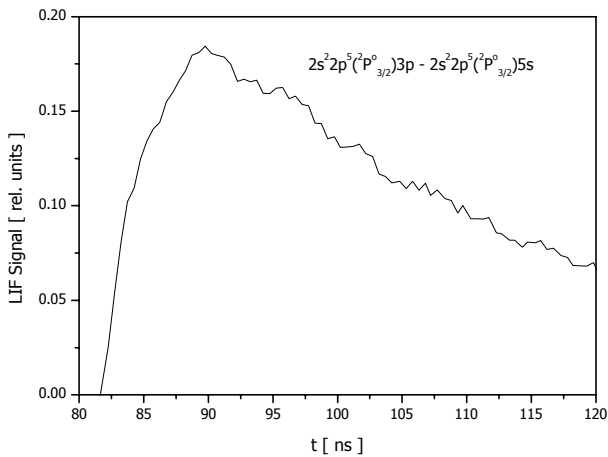


FIG. 2.3: LIF signal of neon at $\lambda = 618$ nm from which $A_{ik} = 3.47 \times 10^{-7} \text{ s}^{-1}$ is deduced.

The first test of the power load for the fibre at $\lambda = 532$ nm shows that the specification of the maximum power load of 1 GW/cm^2 will be achieved. The tests at 656 nm are in preparation. Calculations show that with a power density of 1 GW/cm^2 the LIF signal should be 10 times greater than the noise and consequently should be detectable.

2.2 Erosion studies from emission and absorption spectroscopy

The determination of erosion mechanisms and erosion rates as a function of the plasma parameters is of major importance not only for tests of thermal protection materials for reusable space transportation systems but also for plasma facing components in thermonuclear fusion devices. Plasma jets interacting with targets of the material in question are applied for these measurements and material tests. One of the methods is to study the erosion of a C/C-SiC target in such a plasma jet by high resolution emission and absorption spectroscopy of Si I resonance spectra of the multiplet lines at 251 nm and the singlet lines at 263 nm, 288 nm, or 390 nm, respectively. The silicon is eroded by the plasma jet and forms a disc like radiating cloud in front of the target.

The experimental set up was further improved to allow measurement of the axial line intensity profiles in front of the sample surface simultaneously up to a distance of 8 mm and hence determination of the silicon ground state density profile and the electron temperature profile. **Figure 2.4** shows an example of measured axial line intensity profiles of Si I at $\lambda = 251$ nm and $\lambda = 288$ nm.

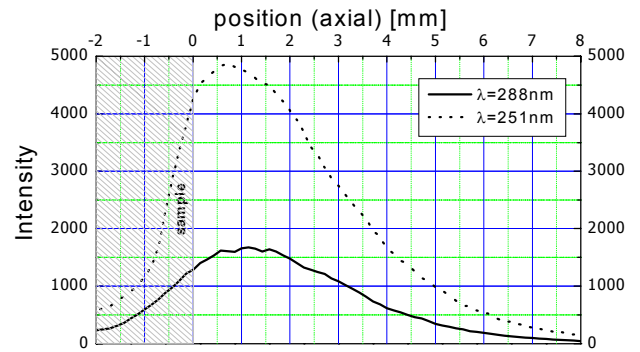


FIG. 2.4: Axial line intensity profiles of Si I in front of the sample surface.

In addition to the determination of the spatial distribution of the ground state density of silicon from the line ratios of the Si I multiplet at 251 nm the determination of electron temperature distribution from the line intensity ratios of different energy levels (251/263/288/390 nm) was started. The electron collisional excitation coefficients corresponding to the relevant energy levels were calculated in cooperation with H.P. Summers, Strathclyde University (Scotland), using modelling of the Si atom with the R-matrix method especially for low energies near threshold. Together with the collisional radiative model and the ADAS data source the populations of the energy levels relevant for the line ratios were calculated as a function of electron density and electron temperature (cf **Fig. 2.5**).

From the measured line ratios of Si I lines (after relative calibration) the electron temperature was determined (cf **Fig. 2.6**). In a few mm distance from the front of the sample surface the electron temperature is in good agreement with laser Thomson scattering results. The experiments show that self absorption is of significant influence.

In a further step the influence of self absorption has to be calculated by ratios within the Si I multiplet at $\lambda = 251$ nm.

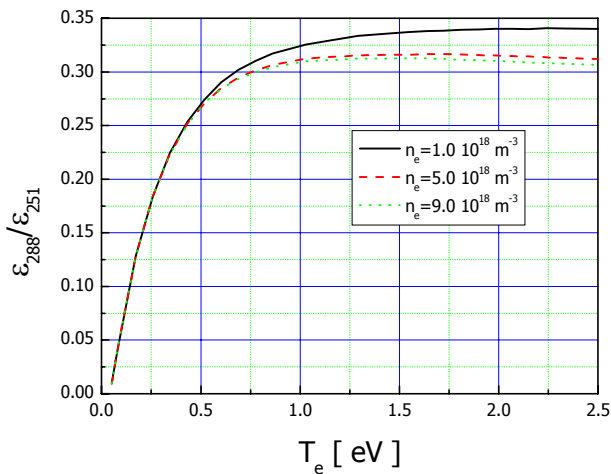


FIG. 2.5: Calculated emissivity ratios for different electron densities.

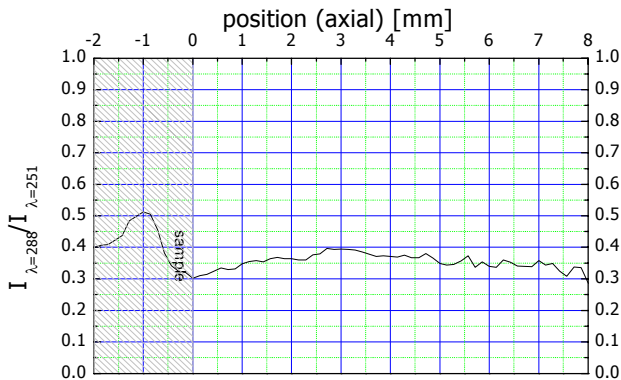


FIG. 2.6: Measured axially resolved intensity ratios of Si I in front of the sample surface.

PUBLICATIONS, CONFERENCE REPORTS, DIPLOMA THESIS, DOCTORAL THESES, AND SEMINAR TALKS

PUBLICATIONS

Alberti, S., A. Arnold, E. Borie, G. Dammertz, V. Erckmann, P. Garin, E. Giguet, S. Illy, G. LeCloarec, Y. Le Goff, R. Magne, G. Michel, B. Piosczyk, C. Tran, M.Q. Tran, M. Thumm, and D. Wagner: European high-power CW gyrotron development for ECRH systems. *Fusion Eng. and Design* **53** (2001) 387-397.

Chirkov, A.V., G.G. Denisov, W. Kasperek, D. Wagner, G. Gantenbein, H. Haug, and F. Hollmann: Simulation and experimental study of a remote steering system for ECRH/ECCD antenna beams. *Fusion Eng. and Design* **53** (2001) 465-474.

Dammertz, G., S. Alberti, A. Arnold, E. Borie, V. Erckmann, G. Gantenbein, E. Giguet, J.-P. Hogge, S. Illy, W. Kasperek, K. Koppenburg, H. Laqua, G. Le Cloarec, Y. Le Goff, W. Leonhardt, Ch. Lievin, R. Magne, G. Michel, G. Müller, G. Neffe, M. Kuntze, B. Piosczyk, M. Schmid, M. Thumm, and M.Q. Tran: Development of a 140 GHz, 1 MW, continuous wave gyrotron for the W7-X stellarator. *Frequenz* **55** (2001) 270-275.

Empacher, L. and W. Kasperek: Analysis of a multiple-beam waveguide for free-space transmission of microwaves. *IEEE Trans. Antennas Propagat.* **AP-49** (2001) 483-493.

Erckmann, V., H.P. Laqua, H. Maassberg, J. Geiger, G. Dammertz, W. Kasperek, M. Thumm, W7-X and W7-AS teams IPP, W7-X team FZK, and W7-X team IPF: Electron cyclotron resonance heating and EC-current drive experiments at W7-AS, status at W7-X. *Fusion Eng. and Design* **53** (2001) 365-375.

Fernandez, A., W. Kasperek, K. Likin, and R. Martin: Design of the upgraded TJ-II quasi-optical transmission line. *Int. J. Infrared Millimeter Waves* **22** (2001) 649-660.

Hirsch, M., E. Holzhauser, J. Balduhn, B. Kurzan, and B. Scott: Doppler reflectometry for the investigation of propagating density perturbations. *Plasma Phys. Control. Fusion* **43** (2001) 1641-1660.

Kasperek, W., D. Arz, L. Empacher, V. Erckmann, G. Gantenbein, F. Hollmann, P.G. Schüller, K. Schwörer, and M. Weissgerber: Performance of the 140 GHz prototype transmission system for ECRH on the stellarator W7-X. *Fusion Eng. and Design* **56-57** (2001) 621-626.

Kasperek, W., L. Empacher, V. Erckmann, G. Gantenbein, F. Hollmann, H.P. Laqua, P.G. Schüller, M. Weissgerber, and H. Zohm: Mirror development for the 140 GHz ECRH transmission system on the stellarator W7-X. *Fusion Eng. and Design* **53** (2001) 545-551.

Kasperek, W., L. Empacher, V. Erckmann, G. Gantenbein, F. Hollmann, P.G. Schüller, K. Schwörer, and M. Weissgerber: The multi-beam transmission system for 140 GHz electron cyclotron heating on the stellarator W7-X: Concept, design and first tests. *Frequenz* **55** (2001) 263-269.

Kasperek, W., A. Fernandez, F. Hollmann, and R. Wacker: Measurement of ohmic loss of metallic reflectors at 140 GHz by a 3-mirror resonator technique. *Int. J. Infrared and Millimeter Waves* **22** (2001) 1695-1707.

Leuterer, F., M. Beckmann, A. Borchegowski, H. Brinkschulte, A. Chirkov, G. Denisov, L. Empacher, W. Förster, G. Gantenbein, V. Illin, W. Kasperek, K. Kirov, F. Monaco, M. Münich, L. Popov, F. Ryter, P.G. Schüller, K. Schwörer, and H. Schütz: Experience with the ECRH system of ASDEX Upgrade. *Fusion Eng. and Design* **56-57** (2001) 615-619.

Leuterer, F., M. Beckmann, H. Brinkschulte, F. Monaco, M. Münich, F. Ryter, H. Schütz, L. Empacher, G. Gantenbein, W. Förster, W. Kasperek, P. Schüller, K. Schwörer, A. Borchegowski, A. Fix, V. Illin, L. Popov, V. Sigalaev, and E. Tai: Experience with the ECRH system of ASDEX Upgrade. *Fusion Eng. and Design* **53** (2001) 485-489.

Meskat, J.P., H. Zohm, G. Gantenbein, S. Günter, M. Maraschek, W. Suttrop, Q. Yu, and ASDEX Upgrade team: Analysis of the structure of neoclassical tearing modes in ASDEX Upgrade. *Plasma Phys. Control. Fusion* **43** (2001) 1325-1332.

Michel, G., H.P. Laqua, and W. Kasperek: Calorimetric measurement of the microwave power transmitted through a diamond window. *Fusion Eng. and Design* **56-57** (2001) 655-660.

Plaum, B., D. Wagner, W. Kasperek, and M. Thumm: Optimisation of oversized waveguide components using a genetic algorithm. *Fusion Eng. and Design* **53** (2001) 499-503.

Schumacher, U.: Status and problems of fusion reactor development. *Naturwissenschaften* **88** (2001) 102-112.

Verhoeven, A.G.A., F.J. v. Amerongen, H. Bindslev, W.A. Bongers, P. Hellingman, B.S.Q. Elzendoorn, W. Kooijman, O.G. Kruijt, G. Land, W. Melissen, A.B. Sterk, S. Alberti, D. Fasel, M. Henderson, P. Marmillod, Q. Tran, J.A. Hoekzema, A. Brusci, S. Cirant, W. Kasperek, G. Müller, B. Piosczyk, M. Thumm, A. Fernandez, K. Likin, A. Kaye, C. Fleming, C. Damiani, J. Pamela, and E. Solano: The ECRH system for JET-EP. *Proc. 9th Int. Conf. Displays and Vacuum Electronics, Garmisch-Partenkirchen, Germany, ITG-Fachbericht* **165** (2001) 345-350.

Zohm, H., G. Gantenbein, A. Gude, S. Günter, F. Leuterer, M. Maraschek, J. Meskat, W. Suttrop, Q. Yu, ASDEX-Upgrade Team, and ECRH group (AUG): Neoclassical tearing modes and their stabilisation by electron cyclotron current drive in ASDEX Upgrade. *Physics of Plasmas*, **8** (2001) 2009-2016.

Zohm, H., G. Gantenbein, A. Gude, S. Günter, F. Leuterer, M. Maraschek, J. Meskat, W. Suttrop, Q. Yu, ASDEX-Upgrade Team, and ECRH group (AUG): The physics of neoclassical tearing modes and their stabilisation by ECCD in ASDEX Upgrade. *Nuclear Fusion*, **41** (2001) 197-202.

CONFERENCE REPORTS

Jahrestagung Kerntechnik, Dresden (Germany), March 2001

Dammertz, G., V. Erckmann, G. Gantenbein, W. Kasperek, H.P. Laqua, G. Müller, and M. Thumm: Electron cyclotron resonance heating for the stellarator Wendelstein 7-X. Proc. of Jahrestagung Kerntechnik 2001, Dresden (Germany) pp. 575-579.

2nd Symp. on Atmospheric Reentry Vehicles and Systems, Arcachon (France), March 26-29, 2001

Hirsch, K., I. Altmann, G. Bauer, B. Roth, D. Schinköth, J. Schneider, U. Schumacher, and A. Tawfik: Investigation of C/C-SiC Heat Shield Materials with and without Oxidation Protection Layer - High Temperature Emergency Behaviour, Paper 14-9-P

ECAMP VII and Spring Meeting of DPG Section Plasma Physics, Berlin, April 2-6, 2001

Feichtinger, J., S. Quell, J. Schneider, A. Schulz, M. Walker, U. Schumacher und J. Wunderlich: Entkeimung von Materialien mit Mikrowellen-erzeugten Niederdruckplasmen, Verhandl. DPG (VI) 36, 154, P 2.1 (2001)

Quell, S., J. Feichtinger, J. Schneider, A. Schulz, M. Walker und U. Schumacher: Spektroskopische Analyse mikrowellen-erzeugter Niederdruckplasmen, Verhandl. DPG (VI) 36, 169, P 10.12 (2001)

Hirsch, K., I. Altmann, G. Bauer, T. Kollermann, B. Roth, D. Schinköth, J. Schneider, U. Schumacher, and A. Tawfik: Development and Investigation of Erosion Protection Layers for Heat Shields of Re-Entry Space Vehicles, Verhandl. DPG (VI) 36, 177, P 12.13 (2001)

Altmann, I., S. Quell, K. Hirsch, B. Roth, J. Schneider, and U. Schumacher: In Situ Determination of Erosion Rates by Application of Emission and Absorption Spectroscopy, Verhandl. DPG (VI) 36, 177, P 12.14 (2001)

Tawfik, A., S. Quell, K. Hirsch, B. Roth, J. Schneider, and U. Schumacher: Time Correlated Measurements of Spectra from Process and Beam Plasmas in the Range from 240 to 1000 nm, Verhandl. DPG (VI) 36, 177, P 12.15 (2001)

2nd IEEE International Vacuum and Electronics Conference, Nordwijk (Netherlands), April, 2001

Giguet, E., S. Alberti, A. Arnold, E. Borie, F. Bouquay, G. Dammertz, C. Darbos, V. Erckmann, S. Illy, W. Kasperek, G. Le Cloarec, Y. Le Goff, W. Leonhardt, C. Liévin, R. Magne, G. Michel, G. Müller, B. Piosczyk, M. Schmid, M. Thumm, and M.Q. Tran: High-power CW gyrotron development for ECRH Systems. Conference Proceedings, pp. 325-326.

8th EPS Conference on Controlled Fusion and Plasma Physics, Madeira (Portugal), June 18-22, 2001

Hirsch, M., E. Holzhauser, J. Balduhn, B. Kurzan, and B. Scott: Doppler reflectometry for the investigation of propagating density perturbations. Abstracts of Invited and Contributed Papers, P. 112.

Maraschek, M., H. Zohm, G. Gantenbein, G. Giruzzi, S. Günter, F. Leuterer, J. Meskat, Q. Yu, ASDEX Upgrade Team, and ECRH-Group (AUG): Stabilisation of neoclassical tearing modes in ASDEX Upgrade with ECRH. Abstracts of Invited and Contributed Papers, P. 14.

2001 IEEE Antennas and Propagation Society International Symposium, Boston, USA, July 8-13, 2001

Kasperek, W., L. Empacher, V. Erckmann, G. Gantenbein, F. Hollmann, P.G. Schüller, K. Schwörer, M. Weißgerber: Performance of the 140 GHz prototype transmission system for ECRH on the stellarator W7-X. Conf. Digest, Vol.1, ISBN 0-7803-7070-8, 296-299.

13th Joint Russian German Meeting on ECRH and Gyrotrons, Greifswald (Germany), July 16-21, 2001

Gantenbein, G., H. Hailer, and W. Kasperek: On the design of the multi-frequency ECRH system on ASDEX-Upgrade.

Gantenbein, G., H. Hollmann, W. Kasperek, P.G. Schüller, K. Schwörer, and M. Weissgerber: Status of the transmission system for ECRH on W7-X.

Kasperek, W., A.V. Chirkov, G.G. Denisov, G. Gantenbein, H. Hollmann, B. Plaum, S. Kuzikov, and D. Wagner: Experimental results from a remote steering antenna based on a 4-wall corrugated square waveguide.

Klunge, S.: News from Doppler reflectometry on ASDEX Upgrade.

Plaum, B.: Optimisation of broadband waveguide components – a comparison between a genetic algorithm and simulated annealing.

Schwörer, K. and P.G. Schüller: Developments for dummy loads and calorimetric loads for W7-X.

Wacker, R., H. Hailer, and W. Kasperek: Measurement of dielectric properties of SiN samples and reflection coefficients from metals at temperatures up to 600 °C.

Ringberg-Seminar, IPP Bereich Technologie, July 23-27, 2001

Gantenbein, G.: On the design of the multi-frequency ECRH system of ASDEX Upgrade.

26th International Conference on Infrared and Millimeter Waves, Toulouse, France, September 10-14, 2001.

Dammertz, G., S. Alberti, E. Borie, V. Erckmann, E. Giguet, S. Illy, K. Koppenburg, M. Kuntze, H.P. Laqua, Y. Le Goff, W. Kasperek, W. Leonhardt, G. Michel, G. Müller, B. Piosczyk, M. Schmid, M. Thumm, and M.Q. Tran: Advanced high-power gyrotron for the W7-X stellarator. Conference Digest.

Hailer, H., W. Kasperek, and R. Wacker: Measurement of dielectric properties of ceramics and reflection coefficients of metals in the 140 GHz range at high temperatures. Conference Digest.

Fernandez, A., K. Likin, F. Hollmann, W. Kasperek, and R. Martin: Cold test of upgraded TJ-II transmission line. Conference Digest.

Ogawa, I., T. Idehara, Y. Mitake, K. Yamada, H. Nozu, R. Pavlichenkov, and W. Kasperek: A system converting the output radiation of a gyrotron into a gaussian beam. Conference Digest.

Plaum, B.: Numerical optimisation of broadband waveguide bends. Conference Digest.

Verhoeven, A.G.A., H. Bindslev, W.A. Bongers, P. Hellingman, B.S.Q. Elzen-doorn, K. Kamp, W. Kooijman, O.G. Kruijt, J. Maagdenberg, W. Melissen, A. Putter, A.B. Sterk S. Alberti, D. Fasel, M. Henderson, P. Marmillod, Q. Tran, J.A. Hoekzema, A. Fernandez, K. Likin, A. Brusci, S. Cirant, W. Kasperek, G. Müller, B. Piosczyk, R. Heidinger, M. Thumm, A. Kaye, C. Fleming, C. Damiani, J. Pamela, and E. Solano: The ECRH system for JET. Conference Digest.

DIPLOMA THESIS

Quell, S.: Spektroskopische Analyse von Mikrowellen-erzeugten Plasmen, Universität Stuttgart, August 2001

DOCTORAL THESES

Meskat, J. P.: Untersuchung der Struktur und Dynamik magnetischer Inseln im Tokamak ASDEX Upgrade. Universität Stuttgart, April 24, 2001

Nguyen, T. K.: Kohärente Strahlung eines räumlich modulierten Elektronenstrahls in einem mit inhomogenem Plasma gefüllten Wellenleiter, Universität Stuttgart, November 12, 2001

Plaum, B.: Optimierung von überdimensionierten Hohlleiterkomponenten. Universität Stuttgart, February 14, 2001

Schinköth, D.: Laser-Streu-Diagnostik im Vergleich mit Emissionsspektroskopie an einem Freistrahplasma. Universität Stuttgart, Januar 19, 2001

SEMINAR TALKS

Gantenbein, G.: Influence of ECRH on MHD (Status and Plans). National Institute for Fusion Science, Plasma Heating Division, Toki (Japan), January 25, 2001

Gantenbein, G.: Low-power measurements of the multi-beam waveguide system. National Institute for Fusion Science, Plasma Heating Division, Toki (Japan), January 25, 2001

Gantenbein, G.: Low-power measurements of the multi-beam waveguide system. Fukui University, FIR Center (Japan), February 2, 2001

Kasperek, W.: Activities at IPF Stuttgart in high-power millimeter wave transmission for electron cyclotron heating systems. National Institute for Fusion Science, Microwave Seminar, Toki (Japan), August 24, 2001

Kasperek, W.: Development of transmission technology for ECRH/ECCD on W7-X and ITER. Fukui University (Japan), November 9, 2001

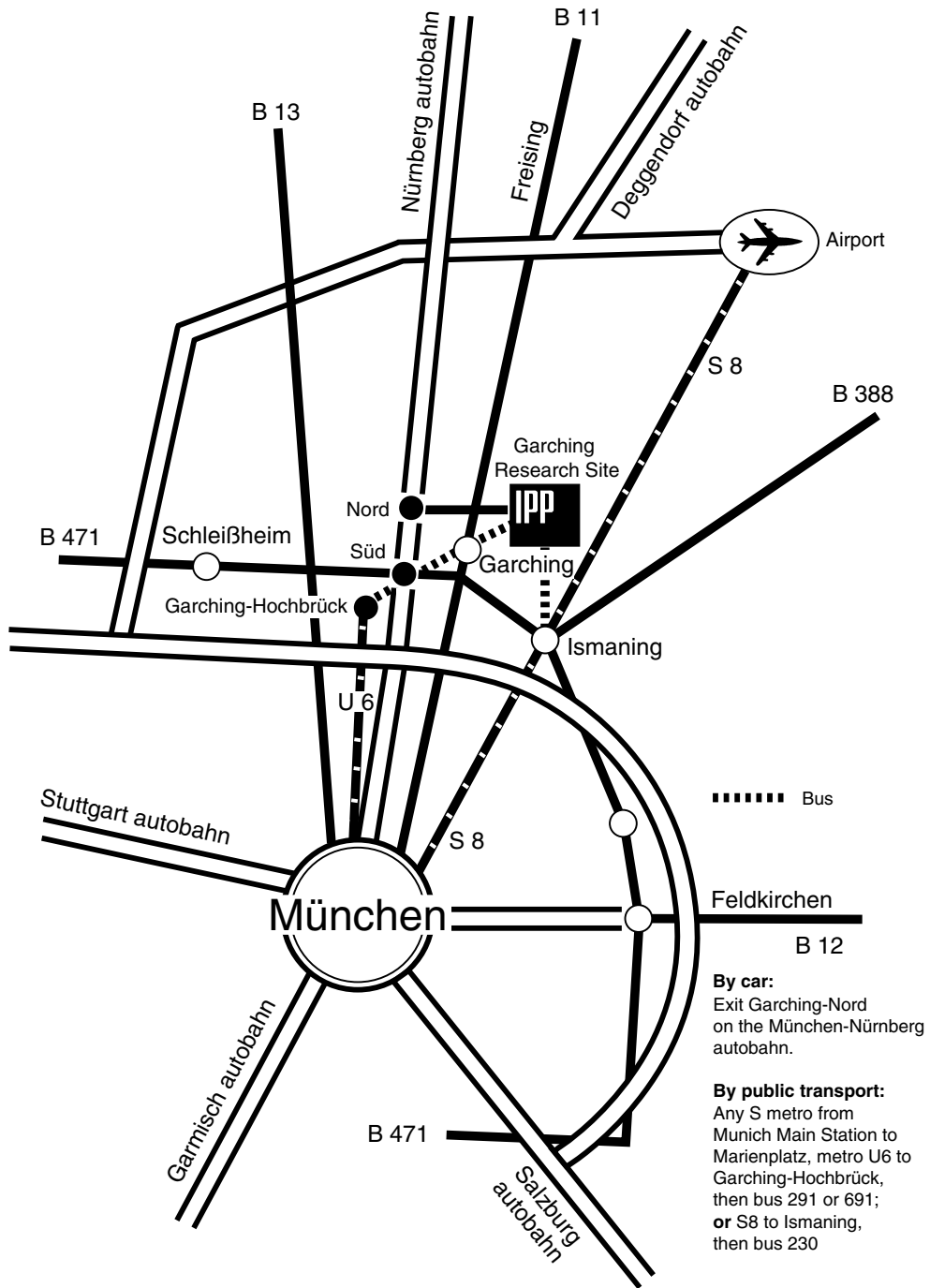
Müller, G. A.: Micro- and millimetre wave processing of ceramics – studies on transfer of a new technology from lab to industry. Fukui University (Japan), March 8, 2001

Schumacher, U.: Stand und Perspektiven der Entwicklung des Fusionsreaktors, ZES-Konferenz, Stuttgarter Energie-Impulse, September 26, 2001

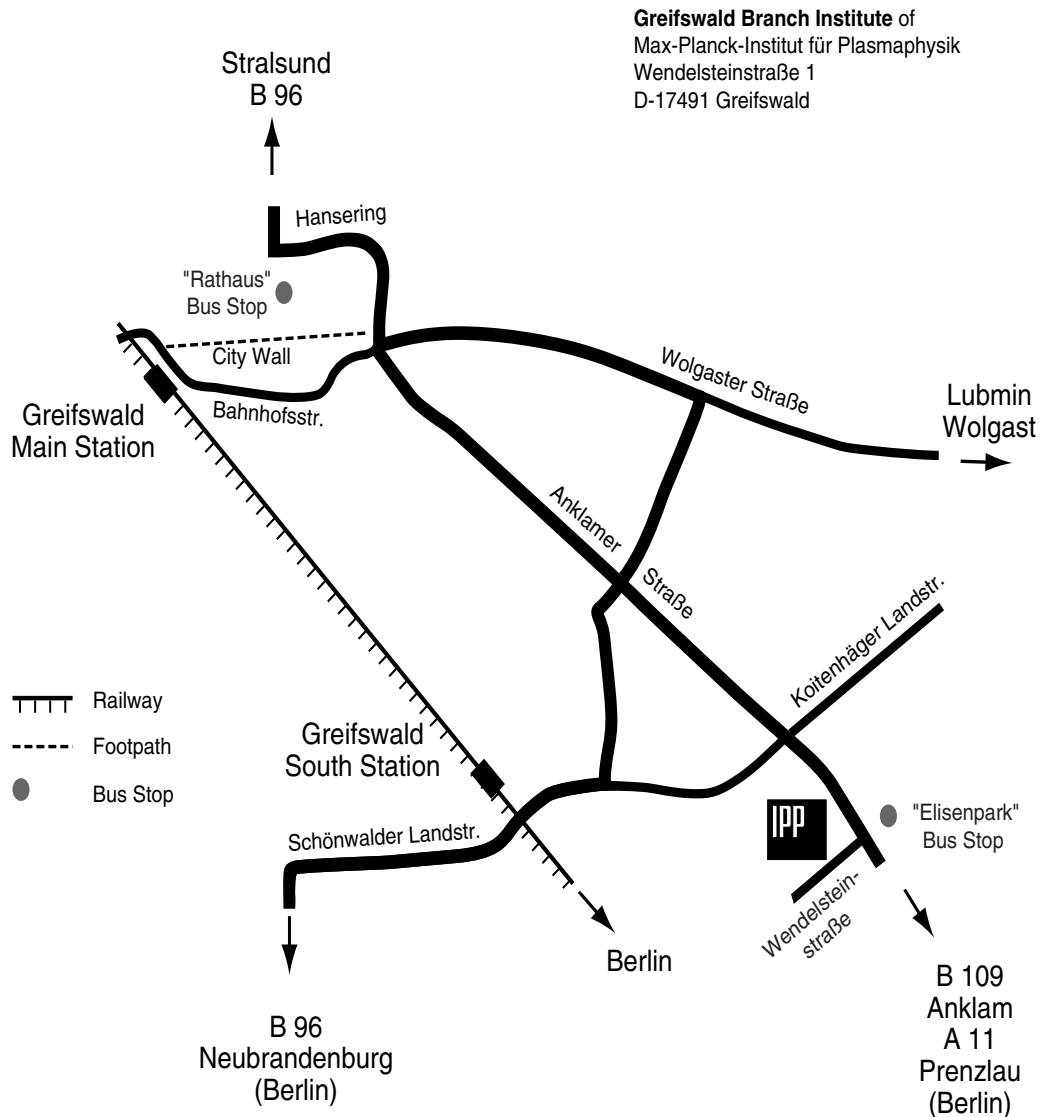
Schumacher, U.: Das 'Sonnenfeuer auf Erden' als Option für die langfristige Energieversorgung. Universität Stuttgart, Sonntagsmatinée, October 21, 2001

Schumacher, U.: Magnetischer Einschluß heißer Plasmen, GSI-Seminar, Gesellschaft für Schwerionenforschung (GSI), Darmstadt, December 4, 2001

How to reach Max-Planck-Institut für Plasmaphysik (IPP)



How to reach Greifswald Branch Institute of Max-Planck-Institut für Plasmaphysik



By air:

Via Berlin: from Berlin Tegel Airport by bus No. X9 to Zoologischer Garten, by train to Greifswald
Via Hamburg: from the airport to Main Railway Station, by train to Greifswald.

By car:

Via Berlin, Neubrandenburg to Greifswald **or** via Hamburg, Lübeck, Stralsund to Greifswald, in Greifswald follow the signs "Max-Planck-Institut".

By bus:

From Greifswald Railway Station walking distance of 10 minutes to the "Rathaus" (Town Hall). Then from "Rathaus's" stop by bus No. 2 or 3 to the "Elisenpark's" stop.